

Boletín de

ISSN 0210-6558

la Sociedad Española de

Mineralogía

Una revista europea de Mineralogía, Petrología,
Geoquímica y Yacimientos Minerales

Directora: P. Fenoll Hach-Alí



Volumen 18-1, 1995

Abstracts of the
XIII ECROFI Conference
(European Current Research
on Fluid Inclusions)
Sitges, June 21-23, 1995

Publicado por la Sociedad Española de Mineralogía con la colaboración de
la Secretaría de Estado para Universidades e Investigación

Alenza, 1 - 28003 MADRID

Boletín de la Sociedad Española de Mineralogía

Vol 18-1

Periodicidad anual

ISSN 0210-6558

XIII ECROFI Symposium

(European Current Research on Fluid Inclusions)

Sitges, June 21-23, 1995

Volumen 18-1, 1995

(Abstracts)

**Publicado por la Sociedad Española de Mineralogía,
con la colaboración de
la Secretaría de Estado para Universidades e Investigación**

**Sociedad Española de Mineralogía
Alenza, 1 - 28003 Madrid**

**XIII ECROFI Conference
(European Current Research on Fluid Inclusions)**

Sitges, June 21-23, 1995

ORGANIZING COMMITTEE

**Carlos Ayora
Institut de Ciències de la Terra, CSIC**

**Angels Canals
Dpt. de Cristal·lografia, Mineralogia i Dipòsits Minerals, Universitat de Barcelona**

**Javier García-Veigas
Serveis Científic-Tècnics, Universitat de Barcelona**

**Esteve Cardellach
Dpt. de Geologia, Universitat Autònoma de Barcelona**

COLLABORATORS

**Dionisio Cendón
Institut de Ciències de la Terra, CSIC**

**David Arcos
Dpt. de Cristal·lografia, Mineralogia i Dipòsits Minerals, Universitat de Barcelona**

**Jordi Trilla
Dpt. de Cristal·lografia, Mineralogia i Dipòsits Minerals, Universitat de Barcelona**

SPONSORSHIP

Sociedad Española de Mineralogía

Dirección General de Ciencia y Tecnología (DGCYT), Ministerio de Educación y Ciencia de España

Comisió Interdepartamental per a Ciència i Tecnologia (CIRIT), Generalitat de Catalunya

Consejo Superior de Investigaciones Científicas (CSIC)

Universitat de Barcelona

Excm Ajuntament de Sitges

LINKAM Scientific Instruments Ltd.

Empresa Nacional de Residuos Radiactivos (ENRESA)

BOLETIN DE LA SOCIEDAD ESPAÑOLA DE MINERALOGIA

Volume 18-1, 1995

INDEX

AISSA M., RAMBOZ C., BENY C. AND PASCAL M. L. GENESIS OF SN-W SKARNS AT HIGH TEMPERATURE, LOW FO ₂ AND HYPOGENE CONDITIONS, AND LATE BORON METASOMATISM AT EL HAMMAM (CENTRAL MOROCCO).....	1
ALFONSO, P. AND MELGAREJO, J.C. THE CAP DE CREUS RARE ELEMENT PEGMATITE FIELD (CATALONIA, SPAIN): MODEL OF CRISTALLIZATION.	4
ANDERSEN, T. AND BURKE, E.A.J. HYDROCARBON INCLUSIONS IN SHOCKED QUARTZ FROM GRADNOS IMPACT BRECCIA, SOUTH NORWAY.....	7
ARCOS, D., SOLER, A. AND DELGADO, J. FLUID BEHAVIOR IN THE GOLD-SKARN DEPOSIT OF CARLES (NW SPAIN).....	8
ARNAUD F., BOULLIER A.M. AND BURG J.P. FLUID CIRCULATION WITHIN THRUSTING SHEAR ZONES IN A SCHIST SEQUENCE (CEVENNES, SE FRENCH MASSIF CENTRAL): A FLUID INCLUSION STUDY IN QUARTZ LENSES.....	10
AYORA, C., GARCIA-VEIGAS, J., ORTI, F. AND ROSELL, L. THE CHEMICAL COMPOSITION OF THE MIOCENE OCEAN: FLUID INCLUSION IN SALT FROM LORCA BASIN (SE SPAIN).....	11
AYT OUGOUGDAL, M., CATHELINÉAU, M., PIRONON, J., BOIRON, M.C., BANKS, D. and YARDLEY, B. SALT-RICH AND ORGANIC-RICH FLUID MIGRATION IN THE RHINE GRABEN TRIASSIC SANDSTONES (SOULTZ DEEP DRILLING).....	13
BAKKER, R.J. THE APPLICATION OF A COMPUTERISED AND OPTIMISED CLATHRATE STABILITY MODEL TO FLUID INCLUSION STUDIES.....	15
BANERJEE, A. INVESTIGATION OF FLUID INCLUSIONS IN EMERALDS OF DIFFERENT GEOLOGICAL ORIGINS BY MICROCHEMICAL AND IR-REFLEXION-SPECTROSCOPY.	18
BANKS, D.A., GIULIANI, G., CHEILLETZ, A. and RUEDA, F. CHEMISTRY AND SOURCE OF THE FLUIDS IN THE COLOMBIAN EMERALD DEPOSITS.....	20
BARAKAT, A., CATHELINÉAU, M., CANALS, M., BOIRON, M.C., DURISOVA, J. and BANKS, D. 3D RECONSTRUCTION AND PVTX CONDITIONS OF MICROFISSURAL FLUID MIGRATION AND EXTENSIONAL VEIN FORMATION : EXAMPLES OF MOKRSKO (BOHEMIA) AND MALPICA-TUY SHEAR ZONE GRANITES (GALICIA)	22
BENCHEKROUN, F. and MOINE, B. FLUID INCLUSIONS AND PROCESS OF GOLD PRECIPITATION IN THE SALSIGNE DEPOSIT (MONTAGNE NOIRE, FRANCE).....	24
BODNAR, R.J. SYNTHETIC FLUID INCLUSION STUDIES OF PHASE EQUILIBRIA AND PVT PROPERTIES IN THE H ₂ O-CO ₂ -NaCl SYSTEM.....	26
BOIRON, M.C., DUBESSY, J., MOISSETTE, A., GEERTSEN, C., BANKS, D.A., PRIETO, A.C., LACOUR, J.L. and MAUCHIEN, P. ELEMENTAL ANALYSIS OF INDIVIDUAL AQUEOUS INCLUSIONS. PART I: NEW DEVELOPMENTS USING MICRO LASER ABLATION OPTICAL EMISSION SPECTROSCOPY (MLA-OES).....	28
BROWN, P.E., HAGEMANN, S.G. GEOBAROMETRY AND DEPTH RELATIONS IN ARCHEAN LOBE-GOLD DEPOSITS.....	30
BROWN, P.E., HAGEMANN, S.G. FLUID INCLUSION DTA REDUCTION AND INTERPRETATION USING Macflincor ON THE MACINTOSH	32
CATHELINÉAU, M., AYT OUGOUGDAL, M., BANKS, D., LESPINASSE, M., BOIRON, M.C. and B. POTY, B. FLUID INPUTS AND MASS TRANSFER DURING ALPINE BRITTLE DEFORMATION OF THE MONT-BLANC GRANITE.....	36
CHUPIN, V.P. and CHUPIN, S.V. MELT INCLUSIONS IN ZIRCON FROM ARCHEAN ROCK: PETROLOGICAL SIGNIFICANCE AND RESULTS OF STUDY.....	38
CHUPIN, V.P.; SMIRNOV, S.Z.; KUZMIN, D.V. and TITOV, A.V. EVOLUTION OF FLUORINE AND OTHER VOLATILES DURING THE CRYSTALLIZATION OF RARE-METAL GRANITOID AND ONGONITE MELTS: THE STUDY OF MELT AND FLUID INCLUSIONS.....	39
CHUPIN, V.P. and TOMILENKO, A.A. MELT FLUID INCLUSIONS IN HIGH-PRESSURE MINERALS (KYANITE, GARNET, QUARTZ): FEATURES OF STUDY AND INTERPRETATIONS.....	41

CLINE, J.S., HOFSTRA, A.H., LANDIS, G.P. and ALLERTON, S. VOLATILE COMPOSITIONS OF FLUID INCLUSIONS FROM A CARLIN-TYPE GOLD DEPOSIT: GETCHELL, NEVADA, USA.....	41
COELHO C.E.S., RAMBOZ C. and BENY C. CONTRASTED POLYPHASE HISTORY OF GOLD MOBILIZATION AT FAZENDA BRASILEIRO AND FAZENDA MARIA PRETA, RIO ITAPICURU GREENSTONE BELT; THE ROLE OF EARLY HYDROTHERMALISM, ORGANIC MATTER, DUCTILE-BRITTLE DEFORMATION AND TEMPERATURE.	43
COETZEE, D.S. and KALBSKOPF, S. THRUST ASSOCIATED GOLD MINERALIZATION IN AN ARCHAEOAN AURIFEROUS QUARTZ-CARBONATE VEIN SYSTEM AT THE EERSTELING GOLD MINE, SOUTH AFRICA.	46
COETZEE, D.S. and VAN DEN KERKHOF, A.M. FLUID INCLUSIONS AND CATHOLUMINESCENCE OF MALTZ REEF QUARTZ VEINS: EERSTELING GOLD MINE, PIETERSBURG GREENSTONE BELT, SOUTH AFRICA.	48
COX, W.; RANKIN, A. and ALDERTON, D. LATE-STAGE FLUID EVOLUTION MODEL FOR EXTENSIVE KAOLINIZATION AND RELATED FERRUGINOUS LODE FORMATION IN SOUTH-WEST ENGLAND.....	50
CRISPINI L., FREZZOTTI M.L., CATHELINAEU M. SYNTECTONIC CO ₂ -H ₂ O FLUIDS IN EXTENSIONAL VEINS IN METASEDIMENTS OF THE VOLTRI GROUPS (NW ALPS).....	52
DE VIVO, B., TÖRÖK, K. and LIMA, A. MAGMATIC SILICATE/SALINE/CO ₂ IMMISCIBILITY: OTHER EVIDENCE FROM PONZA ISLAND, PONTINE ARCHIPELAGO, ITALY.	54
DIAMOND, L.W. ISOCHORIC PATHS IN MULTICOMPONENT FLUIDS AND THE INTERPRETATION OF FLUID INCLUSIONS.....	56
DOBES, P. and DUBESSY, J. FLUID EVOLUTION IN BITUMEN-RICH FORMATIONS OF THE VOLCANO-SEDIMENTARY COMPLEX OF THE BARRANDIAN UPPER PROTEROZOIC (CZECH REPUBLIC).	58
DOBES, P., DUBESSY, J. and KOTKOVA, J. FLUID INCLUSION RECORD IN HIGH GRANULITES OF NORTHERN BOHEMIA (CZECH REPUBLIC).	60
DORIA, A.; NOGUEIRA, P.; CATHELINAEU, M. and NORONHA, F. FLUID/DEFORMATION RELATIONSHIPS IN CONSTRAINED LITHOFACIES: AN INTEGRATED FLUID INCLUSION STUDY OF NORTHERN PORTUGAL Au-QUARTZ VEINS.	62
DOUMBIA, S., GAGNY, C. and MARIGNAC, Ch. LATE MAGMATIC OVERPRESSURING IN LEUCOGRANITE MAGMAS; THE LAYERED PEGMATITE OF RIBEIRA (NE PORTUGAL).....	64
DUBESSY, J., BAKKER, R., FRANTZ, J. and ZHANG, Y. HIGH TEMPERATURE RAMAN SPECTROSCOPIC STUDY OF H ₂ O-CO ₂ -CH ₄ MIXTURES IN SYNTHETIC FLUID INCLUSIONS USING THE LABRAM SPECTROMETER (DILOR) SOME FIRST INSIGHTS ON MOLECULAR INTERACTIONS	66
DURISOVA, J., STRNAD, L., BOIRON, M.C. and PERTOLD, Z. CHARACTER OF PALEOFLUIDS IN GOLD-BEARING QUARTZ VEINS IN GNEISSES OF THE MOLDAUNABIAN ZONE: THE KASPERSKÉ HORY GOLD DEPOSIT (CZECH REPUBLIC).	68
EDON M., RAMBOZ C., VOLFINGER M., CHOI C.G. and ISABELLE D. PIXE EVIDENCES FOR DEEP METAL-RICH EVAPORITIC FLUID EMISSION AT THE OXFORDIAN SEA-BOTTOM (SE BASIN, FRANCE)	70
ENNACIRI, A., BARBANSON, L. and TOURAY, J.C. ORE FORMING BRINES FROM THE Co - As DISTRICT OF BOU AZZER (ANTI-ATLAS, MOROCCO) : A FLUID INCLUSIONS STUDY.	73
FANLO, I. and FERNANDEZ-NIETO, C. HYDROTHERMAL FLUID EVOLUTION IN THE F-Pb-(Zn) MINERALIZATION OF PARZAN (BIELSA MINING DISTRICT, CENTRAL SPANISH PYRENEES).	76
FIRDAOUS, K., BOULLIER, A.M., BOIRON, M.C. and ROBERT, F. NATURE OF FLUID INCLUSIONS AND EVIDENCE FOR P.V.T.X EVOLUTION OF HYDROTHERMAL SOLUTIONS IN GOLD-QUARTZ VEINS IN THE ARCHAEOAN ABTIBI GREENSTONE BELT, QUEBEC.....	78
FREZZOTTI, M.L., BURKE, E.A.J. and GHEZZO, C. CO/CO ₂ FLUID INCLUSIONS IN ALUMINOUS METASEDIMENTARY XENOLITHS IN SILICEOUS LAVAS FROM MT.AMIATA (TUSCANY, ITALY).	80
FUERTEB, M., MARTIN-IZARD, A. and MANGAS, J. FLUID INCLUSIONS IN QUARTZ, BERYL AND APATITE FROM THE FORCAREY-SUR PEGMATITE FIELD (SPAIN).....	82

GARCIA, E., LOPEZ-GÓ, J.A., VINDEL, E. and BOIRON, M.C. FLUID MIGRATION IN MICROFISSURED GRANITES: A FLUID INCLUSION STUDY OF W-Sn VEINS IN THE SPANISH CENTRAL SYSTEM.	84
GARCIA-VEIGAS, J., AYORA, C., ORTI, F., ROSELL, L., ROUCHY, J.M. and LUGLI, S. THE MESSINIAN SALT FROM THE MEDITERRANEAN: SOLUTE CONCENTRATION OF FLUID INCLUSIONS IN HALITE FROM THE CENTRAL SICILY BASIN.	86
GIORGETTI G., FREZZOTTI M.L., CAROSI R., MECCHERI M. and TOURET J.L.R. CARBONIC FLUID EVOLUTION IN SYNTECTONIC VEINS IN METAPELITES AND MARBLES FROM PRIESTLY FORMATION (CENTRAL VICTORIA LAND, ANTARCTICA)	88
GLEESON, S.A. and WILKINSON, J.J. ICP-AES ANALYSIS OF FLUID INCLUSIONS II: COMPARISON WITH OTHER TECHNIQUES.	90
GRISHINA, S. and KNIPPING, B.J. FLUID INCLUSIONS IN EVAPORITES - SOME IMPLICATIONS ON DISPOSAL OF HIGH-LEVEL RADIOACTIVE WASTES.	91
GUILHAUMOU, N., CORDON, S., DURAND, C. and SOMMER, F. P-T CONDITIONS OF SILICIFICATION IN DIAGENETIC SANDSTONES FROM THE BRENT FORMATION OF DUNBAR (NORTH SEA).	93
HÉBERT, R., ROBERTS, S., SANDERSON, D.J., SOLDEVILA, J. and GUMIEL, P. AMPHIBOLITE-FACIES METAMORPHIC FLUID AND STRUCTURAL CONTROLS ON GOLD DEPOSITION: THE TOMIÑO GOLD DEPOSIT (GALICIA, NW SPAIN).	95
HEIN, U.F., SCHÖTTLER, T. and BEHR, H.J. CH ₄ -RICH INCLUSIONS IN SYNKINEMATIC VEINLETS ALONG THE VARISCAN FRONT OF CENTRAL EUROPE.	97
HERMS, P., APPEL, P., MÖLLER, A. and SCHENK, V. AN ANTICLOCKWISE P-T PATH OF THE ULUGURU GRANULITE COMPLEX, TANZANIA, AS RECORDED BY FLUID INCLUSIONS.	99
HURAI, V. and SIMON, K. LARGE-SCALE AND LOCAL FLUID MIGRATION DURING METAMORPHISM: EVIDENCE FROM H, O, C ISOTOPE COMPOSITION AND Na/Ca RATIO OF THE INCLUSION FLUIDS.	101
HURAIOVA, M., KONECKNY, P. and HURAI, V. VOLATILES IN MANTLE-DERIVED MAGMA CHAMBRES IN THE CRUST: EVIDENCE FROM FLUID INCLUSIONS IN ANORTHOCLASITE AND TRONDHJEMITE XENOLITHS FROM LATE TERTIARY ALKALINE BASALTS (WESTERN CARPATHIANS).	102
ISTRATE, G. and ALTHAUS, E. FLUID-ABSENT AND CARBONIC FLUID GRANULITE METAMORPHISM IN GRENVILLE PROVINCE, ADIRONDACK AND ONTARIO.	104
KODERA, P. FLUID EVOLUTION AT THE VHYNE-KLOKOC IRON SKARN DEPOSIT (WESTERN CARPATHIANS, SLOVAKIA).	106
KONECKNY, P., SIMON, K., HURAIOVA, M. and HURAI, V. SILICATE MELTS IN ANORTHOCLASITIC MELTS AND TRONDHJEMITIC XENOLITHS HOSTED BY LATE TERTIARY ALKALI BASALTS.	108
KOVALEVICH, V.M. and PERYT, T.M. CHEMISTRY OF FLUID INCLUSIONS IN THE WERRA (ZECHSTEIN, UPPER PERMIAN) HALITE OF NORTH POLAND.	110
KOVALEVICH, V.M. and PETRICHENKO, O.Y. FLUID INCLUSIONS IN HALITE FROM PARATETHYS MIOCENE EVAPORITES AND THE PROBLEMS OF THEIR CHEMICAL COMPOSITION INTERPRETATION.	112
KUZMIN, D.V., TITOV, A.V. and CHUPIN, V.P. TEMPERATURES OF CRYSTALLIZATION AND VOLATILES OF A-TYPE MAGMAS (ON INCLUSIONS IN MINERALS OF ALKALI GRANITES OF BRYANSKII MASSIF AND THEIR VOLCANIC COMAGMATITES, WEST TRANSBAIKALIA).	114
LEGENDRE, O. and GIRARD, J.P. CONSTRAINTS ON TEMPERATURES OF QUARTZ AND CARBONATE CEMENTATION IN THE MIDDLE JURASSIC OSEBERG RESERVOIR (NORTHERN NORTH SEA) DERIVED FROM FLUID INCLUSIONS.	116
LEOST, I., RAMBOZ, C., MOSSMANN, J.R. and BRIL, H. FLUID PALAEOCIRCULATIONS IN A PASSIVE MARGIN OF THE SOUTH EAST BASIN OF FRANCE. PRELIMINARY RESULTS OF FLUID INCLUSIONS AND STABLE ISOTOPES IN THE MORTE MERIE-1 BOREHOLE (ARDECHE).	118
LINNEN, R.L., KEPPLER, H. and STERNER, S.M. HIGH TEMPERATURE FTIR MEASUREMENTS OF SYNTHETIC H ₂ O-CO ₂ FLUID INCLUSIONS IN THE ONE-PHASE FIELD. .	121
LIRA, R.; MARTINEZ, E. and GOMEZ, G.M. FLUID INCLUSION STUDIES ON SKARN HELVITES FROM CORDOBA PROVINCE, CENTRAL ARGENTINA.	123

LU, Ch. and MISRA, K.C. GEOCHEMISTRY AND SOURCES OF CO ₂ -BEARING HYDROTHERMAL FLUIDS AT THE PALEOZOIC BREWER GOLD HYDROTHERMAL SYSTEM, SOUTH CAROLINA, U.S.A.....	125
LÜDERS, V. and PFLUGBEIL, B. FLUID INCLUSION STUDIES IN WOLFRAMITE AND SULPHIDES - APPLICATIONS OF INFRA-RED MICROSCOPY.....	128
MAINERI, C. and LATTANZI, P. IMMISCIBILITY PHENOMENA IN THE GIGLIO ISLAND PLUTON, SOUTHERN TUSCANY ITALY.....	130
MANGAS, J. and GOMEZ-FERNANDEZ, F. GEOLOGICAL AND FLUID INCLUSION CHARACTERISTICS OF THE Zn Pb CARBONATE HOSTED MINERALIZATIONS IN THE S.E. AREA OF PICOS DE EUROPA (NORTHERN SPAIN).....	132
MARESCOTTI P. and GIORGETTI G. FLUID-MINERAL EQUILIBRIUM IN ANTITAXIAL QUARTZ VEIN SYSTEM IN MANGANESE-ORE FROM VAL GRAVEGLIA (NORTHERN APENNINES, ITALY).....	133
MARTIN-ROMERA, C., VINDEL, E., LOPEZ-GO, J.A. and CATHELINEAU, M. RELATIONSHIPS BETWEEN FLUID MIGRATION AND REGIONAL STRESS FIELD IN MINERALIZED PEGMATITES: AN EXAMPLE FROM THE SPANISH CENTRAL SYSTEM.	135
MEERE, F.A. and BANKS, D.A. UPPER CRUSTAL FLUID MIGRATION DURING AN OROGENIC CYCLE: AN EXAMPLE FROM THE VARISCIDES OF SOUTH WEST IRELAND.	137
MELFOS, V. and VAVEDELIS, M. FLUID INCLUSION STUDIES ON THE PORPHYRY TYPE Cu-Mo(±Au) MINERALIZATION IN MARONIA AREA, THRACE COUNTRY, GREECE.....	139
MESA, M., LOREDO, J. and GARCIA-IGLESIAS, J. FLUID INCLUSIONS STUDY IN QUARTZ RELATED TO THE AURIFEROUS GOLD MINERALIZATION OF LA GRUEBA, ASTURIAS, NORTHERN SPAIN.	142
MOISSETTE A., SHEPHERD T.J. and CHENERY S.R. ELEMENTAL ANALYSIS OF INDIVIDUAL AQUEOUS FLUID INCLUSIONS. PART II: CALIBRATION STRATEGIES FOR THE OPTIMISATION OF LASER ABLATION ICP-MS (LAMP-ICP-MS).....	144
MOORE, S.L.O. and SPENCER, R.J. A SUMMARY OF THE DOLOMITIZATION HISTORY OF THE PIKA AND ELDON FORMATIONS, YOHO NATIONAL PARK, B.C., CANADA.....	145
MORITZ, R. and GHAZBAN, F. FLUID EVOLUTION AND GOLD MINERALIZATION IN THE PRECAMBRIAN BASEMENT OF THE ZAGROS BELT AT MUTEH, ESFAHAN PROVINCE, IRAN.....	147
MOURA, A.J.; NORONHA, F. & FERREIRA, A. FLUIDS FROM THE RUBANE AND FISSURAL ORES OF THE CORVO OREBODY, NEVES-CORVO MINE, PORTUGAL.....	149
MUCHEZ, PH., SLOBODNIK, M., VIAENE, W.A. and KEPPENS, E. GEOCHEMICAL CONSTRAINTS ON THE ORIGIN AND MIGRATION OF PALAEOFLUIDS AT THE NORTHERN MARGIN OF THE VARISCAN FORELAND SOUTHERN BELGIUM.....	151
MULLIS J. PT-TIME-PATH, FLUID EVOLUTION AND CRYSTAL GROWTH IN THE AAR- AND GOTTHARD MASSIFS DURING LATE PLATE COLLISION AND EXHUMATION OF THE CENTRAL ALPS.....	153
MUNOZ M., NESBITT R.W. and POLVE M. R.E.E. ICP-MS ANALYSES OF FLUID INCLUSIONS WITHIN FLUORITE FROM SOUTHWESTERN MASSIF CENTRAL (FRANCE); CONTRIBUTION TO THE CHARACTERIZATION OF BRINE EVOLUTION.....	154
MURPHY, P.J. and ROBERTS, S. OBSERVATIONS ON THE MELTING AND NUCLEATION BEHAVIOUR OF CLATHRATES IN MULTIVOLATILE FLUID INCLUSIONS.....	156
MUTEMERI, N., BLENKINSOP, T. and TOURET, J.L.R. FLUID INCLUSION EVIDENCE FROM TWO GENERATIONS OF QUARTZ-VEINS IN THE ARCHAIC GOLD-BEARING VENUS SHEAR ZONE OF THE ARCTURUS MINE, ZIMBABWE.....	158
NADEN, J., LENG, M.L., CHELIOTIS, Y. and ELIOPOULOS, D. PRECIOUS AND BASE METAL MINERALISATION, LESVOS ISLAND, GREECE.....	160
NOGUEIRA, P. and NORONHA, F. "PLANIP" A COMPUTER PROGRAM FOR THE STUDY OF FLUID INCLUSION PLANES.....	162
NORONHA, F., VINDEL, E., LOPEZ-GO, J.A., DORIA, A., BOIRON, M.C. and CATHELINEAU, M. FLUID EVOLUTION ASSOCIATED WITH W(Sn)-SULPHIDE-QUARTZ-VEIN IN THE IBERIAN PENINSULA.....	164
O REILLY, C., GALLAGHER, V. and FEELY, M. CHARACTERIZATION OF FLUID INCLUSIONS IN W-Sn-SULPHIDE MINERALIZATION HOSTED BY CALEDONIAN MICROTONALITES ON THE SE MARGIN OF THE LEINSTER GRANITE, IRELAND.....	166

ORPHANIDIS I., PASCAL M.L., RAMBOZ C., OUDIN E. and THISSE Y. MECHANISM OF BARITE AND ANHYDRITE COPRECIPITATION AT TEMPERATURES AROUND 400°C IN THE SUBSEAFLOOR OF SW BASIN, ATLANTIS II DEEP (CENTRAL RED SEA).....	168
ORTEGA, L., SIERRA, J., OYARZUN, R. and LUNAR, R. THE EPITHERMAL MANTO GOLD DEPOSITS FROM ANDACOLLO (CHILE).....	170
PANIAGUA, A., LOREDO, J. and GARCIA-IGLESIAS, J. EPITHERMAL CARBONATE-HOSTED Au-Cu-Ni-Co MINERALIZATION AT THE VILLAMANIN AREA (CANTABRIAN ZONE, N SPAIN): FLUID INCLUSION STUDY VERSUS PARAGENETIC AND SULFUR ISOTOPIC DATA.....	172
PANINA, L.I. DIFFERENTIATION AND FRACCIONATION PROCESSES OF MELTS DURING FORMATION OF LAYERED PLUTONS OF HIGH-POTASSIC ALKALINE ROCKS.....	174
PETRICHENKO, O.Y. and KOVALEVICH, V.M. HYDROCARBON INCLUSIONS IN HALITE OF EVAPORITE DEPOSITS OF EAST EUROPE.....	176
PETROV, P.P. and RANKIN, A.H. DISTRIBUTION OF SECTORIAL PRIMARY FLUID INCLUSIONS AND SULPHIDE ORE MINERALS IN EPITHERMAL QUARTZ CRYSTALS FROM BULGARIA: A MANIFESTATION OF GRAVITATIONAL CRYSTALLIZATION PROCESSES?.....	178
PETKE, Th. and DIAMOND, L.W. Rb-Sr DATING OF SPHALERITE BASED ON FLUID INCLUSION-HOST MINERAL ISOCHRONS: SYSTEMATICS AND AGE SIGNIFICANCE.....	179
PETKE, Th., FREI, R., KAMENSKY, I. L., KRAMERS, J. D., TOLSTIKHIN, I. N. and VILLA, I. M. U, He AND Ar ISOTOPE SYSTEMATICS IN FLUID INCLUSIONS OF VEIN-GOLD, QUARTZ AND CARBONATES FROM BRUSSON, VAL D'AYAS (NW ITALY): (U+Th)/He DATING OF GOLD and ISOTOPIC TRACING.....	181
PHILIPPOT P., CHEVALLIER P. and GIBERT F. SYNCHROTRON X-RAY FLUORESCENCE ANALYSIS OF INDIVIDUAL FLUID INCLUSION: ($K\alpha/K\beta$) _i USED AS A CORRECTION TERM FOR CONCENTRATION ESTIMATES.....	183
PINTEA, I. FLUID INCLUSIONS EVIDENCE FOR LIQUID MAGMATIC IMMISCIBILITY BETWEEN HYDROUS SALT MELT AND SILICATE MELT AS P RIMARY SOURCE OF ORE METALS IN PORPHYRY COPPER SYSTEMS FROM APUSENY MOUNTAINS (ROMANIA).....	184
PINTO-COELHO, C., CHAROY, B. and RONCHI, L.H. PRIMARY AQUO-CARBONIC FLUID INCLUSIONS IN ALKALI FELDSPARS FROM THE SERRA BRANCA GRANITE (GOIÁS STATE-CENTRAL BRAZIL).....	186
PIRONON, J., GRISHINA, S and MAZUROV, M. ON THE ORIGIN OF MOLECULAR NITROGEN IN SALT DEPOSITS : THE EXAMPLE OF LENA-TUNGUSSKA OIL-BEARING REGION (SIBERIA).....	188
POULSEN, T. FLUID EVOLUTION DURING FORMATION OF THE IVIGTUT CRYOLITE DEPOSIT, SOUTH GREENLAND: EVIDENCE FROM FLUID INCLUSION.....	190
POUTIAINEN, M. MAGMATIC VERSUS METAMORPHIC FLUIDS IN THE SILIJÄRVI CARBONATITE COMPLEX, EASTERN FINLAND: A FLUID INCLUSION STUDY OF ZIRCON AND APATITE.....	192
PRIETO, M., PANIAGUA, A. and MARCOS, C. FORMATION OF PRIMARY FLUID INCLUSIONS BY INFLUENCE OF THE HYDRODYNAMIC ENVIRONMENT.....	194
PROSPERT, C. and BIINO, G.G. FLUID-ROCK INTERACTIONS IN THE POLYMETAMORPHIC METASEDIMENTARY ROCKS OF THE SILVRETTA THRUST SHEET (EASTERN ALPS).....	196
QUILEZ, E., MORALES, S., BOIRON, M.C., CATHELINEAU, M., VINDEL, E. and LOPEZ-GARCIA, J.A. FLUID INCLUSION STUDIES AND GEOCHEMICAL FEATURES OF THE FORMATION OF W-Mo-SHULPHIDES FROM CABEZA LIJAR ORE DEPOSITS (SPANISH CENTRAL SYSTEM).....	198
RAMAMBAZAFY A., RAKOTONDRAZAFY M., MOINE B. and CUNNEY M. CO ₂ -RICH FLUIDS, GRANULITE FACIES METAMORPHISM AND METASOMATISM IN SOUTH-EAST MADAGASCAR.....	200
RANKIN, A.H. FLUID INCLUSION EVIDENCE FOR MINERAL TRANSPORT AND ACCUMULATION BY BUBBLE FLOTATION IN NATURAL FLUID SYSTEMS.....	202
RENAC C., RAMBOZ C. and MOSSMANN J.R. EPIGENETIC FILLINGS AND LOCAL FLUID INFLEXES AT THE BOTTOM OF BAL BOREHOLE.....	203
REUTEL, C., LUDERS, V., BOTH, P. and IDIZ, E.P. GAS MIGRATION AND ACCUMULATION ALONG LINEAMENT STRUCTURES - LOWER SAXONY BAS IN (NW GERMANY).....	205

RHEDE, D. and THOMAS, R. MICROPROBE ANALYSIS OF SILICATE MELT INCLUSIONS IN QUARTZ FROM "STOCKSCHEIDER" PEGMATITE AT EHRENFRI EDERSDORF, ERZGEBIRGE, GERMANY.....	207
ROEDDER, E. MAGMATIC PROCESSES AS VIEWED FROM FLUID INCLUSION STUDIES.....	209
RONCHI, LH., FOGACA, A.C.C., FUZIKAWA, K., GIULIANI, G. and PIMENTA, M. FLUID INCLUSIONS ASSOCIATED TO GOLD QUARTZ VEINS IN DIAMANTITA AND COSTA SENA, MINAS GERAIS, BRAZIL: A COMPARATIVE STUDY.....	210
RUGGIERI, G. and GIANELLI, G. FLUID INCLUSIONS AND ISOTOPE DATA FROM A PHREATIC BRECCIA OF THE MONTEVERDI 5A WELL (LARDERELLO GEOTHERMAL FIELD, ITALY).....	212
RYAN, C.G. DEVELOPMENTS OF PIXE AND THE PROTON MICROPROBE AND THE NON-DESTRUCTIVE ANALYSIS OF FLUID INCLUSIONS IN MINERALS.....	214
SCAMBELLURI, M., PHILIPPOT, P. and PENNACCHIONI, G. HIGH-SALINITY BRINES IN ECLOGITIZED METABASITES AS THE RESULT OF ROCK HYDRATATION DURING HIGH PRESSURE METHAMORPHISM (MT. EMILIUS AUSTRALPINE UNIT, ITALIAN WESTERN ALPS).....	216
SCAMBELLURI, M., ROBBIANO, A. and PICCARDO, G.B. HIGH-PRESSURE VEINING AND FLUID INCLUSIONS IN AN ALPINE ECLOGITIZED PERIDOTITE: RECYCLING OF OCEANIC FLUIDS?.....	218
SCHALAMUK, I.A., RIOS, F.J., FUZIKAWA, K. and PIMENTA, M.A. FLUID INCLUSION STUDIES IN EPITHERMAL AURIFEROUS-QUARTZ DEPOSITS OF MACIZO DEL DESEADO, SANTA CRUZ, ARGENTINA.....	220
SCHMIDT MUMM, A., BLENKINSOP, T. and OBERTHÜR, T. GOLD MINERALIZATION AND REGIONAL FLUID MOBILIZATION DURING THE EBURNEAN CRUSTAL CONSOLIDATION IN GHANA, WEST AFRICA.....	222
SCHMIDT MUMM, A., BLENKINSOP, T., OBERTHÜR, T. and WEISER, T. THE MINERALIZATION AT THE VICEROY GOLD MINE, HARARE-BINDURA GREENSTONE BELD, ZIMBABWE.....	224
SCHMIDT MUMM, A., LEHNER, C., SAWATZKI, J. and IDIZ, E. GAS ANALYSIS IN FLUID INCLUSIONS BY NIR FT RAMAN SPECTROSCOPY.....	226
SEMIANI, A., BOIRON, M.C. and MARIGNAC, CH. FLUID EVOLUTION IN A MINERALIZED SHEAR-ZONE: GOLD DEPOSITS OF TIREK AND AMESMESSA (HOGGAR, ALGERIA).....	228
SHARYGIN, V.V. CRISTALIZATION CONDITIONS OF HAUYNE PHONOLITES OF LAAHER SEE VOLCANO (E.EIFEL, W. GERMANY).....	230
SHARYGIN, V.V. and STOPPA, F. Zr-Ti-BEARING DISILICATES FROM INCLUSIONS IN MINERALS OF PEGMATOID VENANZITE (PIAN DI CELLE VOLCANO, SAN VENANZO, ITALY).....	232
SHEPHERD, T.J., CHENERY, S.R. and MOISSETTE, A. LASER ABLATION ICP-MS ANALYSIS OF SINGLE INCLUSIONS IN EVAPORITE MINERALS.....	234
SLABY, E, KOZLOWSKI, A., CZERWOSZ, E., DIDUSZKO and BANERJEE, A. INVESTIGATION OF SYNTHETIC FLUID INCLUSIONS IN HYDROTHERMAL ANALCIMES.....	235
SMITH, M.P. MODELLING OF FLUID EVOLUTION ON THE BASIS OF CRUSH LEACH ANALYSES OF FLUID INCLUSIONS FROM THE CLIGGA HEAD GREISEN RELATED Sn-W DEPOSIT, S.W.ENGLAND.....	237
SPENCER, R.J., ROBERTS, S.M. and YANG, W. PALEOCLIMATE DATA FROM FLUID INCLUSIONS IN SALT: EXAMPLES FROM THE QAIDAM BASIN, CHINA, AND DEATH VALLEY, UNITED STATES.....	239
SZABÓ, C.S. and BODNAR, R.J. CARBON DIOXIDE, SILICATE MELT AND SULFIDE MELT INCLUSIONS IN MANTLE METASOMATIZED PERIDOTITE XENOLITHS FROM THE NÓGRÁD-GÓMÖR VOLCANIC FIELD, NORTHERN HUNGARY/SOUTHERN SLOVAKIA.....	240
TALNIKOVA, S., BARASHLOV, Y. and PANKOV, V. FLUID COMPONENT IN YAKUTIAN DIAMONDS OF DIFFERENT PARAGESESIS.....	242
TOMILENKO, A.A.; CHEPUROV, A.I. and SHEBANIN, A.P. CRYOMETRIC STUDIES OF FLUID INCLUSIONS IN NATURAL DIAMONDS.....	244
TOMILENKO, A.A. and KOVYAZIN, S.V. INTERACTION OF MELT INCLUSION SUBSTANCE AND HOST SYNTHETIC PERICLASE ON HEATING.....	246

TÖRÖK, K. <i>CaCl₂-RICH FLUID INCLUSIONS IN THE GARNET BEARING GNEISS OF THE KO-HEGY QUARRY, SOPRON (W-HUNGARY)</i>	248
TOURET, J.L.R. <i>BRINES IN GRANULITES: THE OTHER FLUID</i>	250
TRITTLA, J., CANALS, A., BANKS, D. and CARDELLACH, E. <i>EVAPORITE-RELATED FLUIDS AND ORE DEPOSITION DURING MESOZOIC RIFTING IN EASTERN AND NORTHEASTERN SPAIN</i>	252
VAN DEN KERKHOFF, A.M. and GRANTHAM, G.H. <i>THE CHARNOKITIZATION AT NICHOLSON'S POINT, NATAL METAMORPHIC PROVINCE, SOUTH AFRICA: THE ROLE OF FLUIDS</i>	254
VARELA, M.E., BJERG, E.A. and LABUDIA, C.H. <i>FLUID INCLUSION EVOLUTION IN UPPER MANTLE XENOLITHS FROM PATAGONIA, ARGENTINA</i>	256
VARELA, M.E. and GREGORY, D.A. <i>FLUID CIRCULATION PATH IN A VOLCANIC-HOSTED POLYMETALLIC DEPOSITS, ANGELA MINE ARENTINA</i>	258
VAVEDELIS, M., SCHMIDT-MUMM, A. and MELFOS, V. <i>MICROTHERMOMETRIC INVESTIGATIONS IN THE Bi-Te-Ag BEARING Cu-MINERALIZATION OF PANAGIA AREA, THASOS ISLAND, GREECE</i>	261
VELASCO, F., TORNOS, F., PESQUERA, A., and PEÑA, A. <i>METAMORPHIC HYDROTHERMAL FLUIDS IN TONALITE-HOSTED COPPER-GOLD VEIN MINERALIZATION. MINA SULTANA (CALA, HUELVA, SPAIN)</i>	263
VITYK, M. and BODNAR, R. J. <i>EXPERIMENTAL RE-EQUILIBRATION OF SYNTHETIC FLUID INCLUSIONS: POTENTIAL EFFECTS OF TIME AND LOADING RATES</i>	265
VOLLBRECHT, A., SCHILD, M., REUTEL, CH., SIEGESMUND, S., CHLUPAC, T. and WEIB, T. <i>HEALED MICROCRACKS IN GRANITES FROM THE HDR DRILLHOLE EPS-1, SOULTE-SOUS-FOR TS. - PALEOSTRESS, PALEOFLUIDS AND CRACK-RELATED VP-ANISOTROPY</i>	267
WILKINSON, J.J., GLEESON, S.A. and COLES, B. <i>ICP-AES ANALYSIS OF FLUID INCLUSIONS I: RECENT DEVELOPMENTS AND APPLICATIONS</i>	269
ZACHARIAS, J., PUDILOVA, M., PERTOLD, Z., PERTOLDOVA, J., BENDL, J. and WILKINSON, J. <i>FLUID CHARACTERISTICS OF VARISCAN PORPHYRY GOLD SYSTEM: AN EXAMPLE FROM BOHEMIAN MASSIF, CZECH REPUBLIC</i>	270
ZAW, K. <i>GEOLOGY AND FLUID INCLUSION MICROTHERMOMETRY OF GRANITIC PEGMATITES IN MYANMAR: RELATIONSHIPS WITH W-Sn VEIN MINERALISATION</i>	272
ZIEMANN, M. and THOMAS, R. <i>THERMOBAROMETRIC AND MICRO-RAMAN INVESTIGATIONS ON FLUID AND MELT INCLUSIONS IN SILLIMANITE FROM REINBOLT HILL / EAST-ANTARCTICA</i>	274
ZIMMERMANN, H. <i>FLUID INCLUSION ANALYSIS OF HALITE FROM THE SOLAR SALTWORK OF INAGUA, BAHAMAS</i>	275
ZIMMERMANN, H. <i>FLUID INCLUSION STUDIES OF MESSINIAN EVAPORITES FROM SICILY -PRELIMINARY RESULTS</i>	276
ZIMMERMANN, J.L., GIULIANI G. and CHEILLETZ, A. <i>QUADRUPOLEAR MASS SPECTROMETRIC STUDY OF FLUIDS IN GEMS: AN APPLICATION TO COLOMBIAN EMERALDS</i>	277
ZINCHUK, I.M., BAGATAJEV, R.M., VISHTALIUK, S.D. and SVOREN, J.M. <i>THE VOLATILES IN MINERAL-FORMING FLUIDS OF MYKYTIVKA Sb-Hg DEPOSIT</i>	279
ZINCHUK, I.M., KALYUZHNY, V.A., PLATONOVA, E.L. and MUROMTSEVA, A.O. <i>THE PARAMETERS OF MIGRATION OF HYDROCARBONS IN LVIV- VOLYN COAL BASIN OF UKRAINE</i>	281
ZINCHUK, I.M. and VISHTALIUK, S.D. <i>THE GASES OF INCLUSIONS IN SANDSTONES MINERALS OF DONETS BASIN</i>	283
VIGGIANO, J.C. <i>FLUID INCLUSIONS STUDIES IN MEXICAN GEOTHERMAL FIELDS: AN UNDERESTIMATED MATTER</i>	286
SRIKANTAPPA, C., LAKSHMEESHA, B. and RAIKH, M. <i>SHEAR RELATED GOLD MINERALIZATION DURING RETROGRESSION OF THE NILGIRI GRANULITES, SOUTH INDIA</i>	288
CHAREF, A. and SHEPPARD, S.M.F. <i>THE RELATIONSHIPS BETWEEN DIAPIR AND DIAPIRIC ORE DEPOSITS IN TUNISIA AS DEDUCED FROM FLUID INCLUSIONS</i>	290

MORALES, S., QUILEZ, E. and FENOLL HACH-ALI, P. THE EVOLUTION OF POLYSALINE FLUIDS DURING THE ORE GENESIS OF THE HYDROTHERMAL DEPOSITS AT AGUILAS-SIERRA ALMAGRERA (SE SPAIN).....	292
MORALES, S., BARBANSON, L., FENOLL HACH-ALI, P. and TOURAY, J.C. THE STRATABOUND Zn-Pb-(Ge-F) CERRO DEL TORO ORE DEPOSIT (ALPUJARRIDE CARBONATE FORMATION, BETIC CORDILLERA, SOUTHERN SPAIN): MINERALOGY AND FLUID INCLUSION STUDIES.....	294
<i>Autor Index</i>	299
<i>Normas de presentación de manuscritos</i>	303
<i>Ficha de Inscripción S.E.M.</i>	307

GENESIS OF Sn-W SKARNS AT HIGH TEMPERATURE, LOW fO_2 AND HYPOGENE CONDITIONS, AND LATE BORON METASOMATISM AT EL HAMMAM (CENTRAL MOROCCO)

AISSA M. (1,2), RAMBOZ C. (1), BENY C. (1,3) and PASCAL M. L. (1)

(1) CRSCM, 1A rue de la Férollerie, 45071 Orléans Cedex 02-France

(2) Faculté des Sciences, B.P. 4010 Beni M'hamed Meknès-Maroc

(3) BRGM, DR/GPC, BP 6009, 45071-Orléans-la Source

GEOLOGICAL SETTING OF THE SKARNS

The El Hammam district, located 60 km SW of Meknes, in the NE margin of the Hercynian Central Morocco, not only hosts a major fluorite mine but also sub-economic tin-tungsten and boron-bearing skarns [1]. The skarns consist of isolated lenses aligned along a NE-SW trend in the calc-silicate metamorphic schists. They are interpreted to have formed under the metasomatic influence of a hidden granitic pluton of variscan age. Three distinct parageneses are recognized:

1- Tungsten-bearing skarns, of restricted extent, are mainly found in the most metamorphosed part of the pelitic series. They consist of pyroxene bands replacing the feldspar-pyroxene-bearing hornfelses. Large -or medium- grained pyroxenites contain scheelite with accessory titanite, K-feldspar, plagioclase, idocrase, epidote and sulfides. Their W-content ranges up to 1.4 wt % WO_3 .

2- Tin-bearing skarns, which cover a larger, several km-wide, area, are found in the highly to moderately metamorphosed schists. The skarns are preferentially formed at the expense of the wollastonite-rich calc-silicate rocks. Andradite and malayaite are the main Sn-bearing minerals. The stannian andradite is all the greener as its tin-content is higher (up to 5.6 wt.% SnO_2). These skarns show a zonation depending on the nature of the replaced calc-silicate bands:

* outer zone 1: zoned pyroxene, malayaite, plagioclase and quartz,

* zone 2: Sn-andradite, malayaite and diopside, with or without relic wollastonite,

*inner zone: Mn-hedenbergite and malayaite.

3- Boron-bearing skarns contain axinite and datolite, depending on whether the replaced rock is more calcic or pelitic. They locally contain epidote, calcite, quartz, and rare tourmaline. They are late and overprint earlier formed W-Sn-bearing skarns. The axinite can be Sn-rich (up to 3.5 wt.% SnO_2).

FLUID INCLUSION STUDY

In order to reconstruct the metasomatic evolution of these skarns, fluid inclusions (FI) are examined in the characteristic minerals of all three different stages (namely, pyroxenes, garnets, axinite, quartz and calcite). The main results are the following:

Results

1-Scheelite-bearing skarns, FI have been studied in pyroxenes (hed₆₅₋₇₀, diop₃₀₋₃₅) and metamorphic grossularite:

*remnant of metamorphic grossular garnet. FI analyzed in these relic garnet are CH_4 -rich, gas-dominant and water-poor. Measured clathrate melting temperatures are between 1.5° and 12.5°C. FI bulk homogenize either to the vapour in the range 370° to 410°C or to the liquid at $T = 425$ °C,

**ferrosalite pyroxene*. Two main FI types have been recognized:
-CH₄-rich aqueous fluid inclusions often show euhedral negative crystal shapes and a high homogeneous vapour filling (>70 % of bulk volume). They have a low salinity (1.5 wt % NaCl equiv) and bulk homogenize to the vapour between 380° and 400 °C. Only CH₄ has been detected by Raman microspectrometry. Clathrate melting temperatures between -2° and 3°C fix P_{CH₄} = 25 - 30 bars.

- Aqueous fluid inclusions have a variable liquid filling between 10 and 90 vol.% and contain no detectable volatile species. Homogenization temperatures to vapour or to liquid vary from 420° to 130 °C, with a correlative salinity increase of 2 to 8 wt % NaCl equiv. Besides these regular shaped-inclusions, pyroxenes also contain large, 40 to 50 µm-long, FI with complex shapes. These have a variable salinity (3 to 18 wt % NaCl equiv) and homogenize to the liquid in the range 260° - 310 °C.

2- Malayaite-bearing skarns: Three types of minerals are studied:

**Diopside from Sn-garnet skarns* (diop₈₅₋₉₅, hed₅₋₁₅): it contains highly saline fluid inclusions, with up to 5 or 6 daughter salt crystals (bulk salinity 40 to 55 wt % NaCl equiv). They all homogenize to the liquid phase between 400° and > 570°C.

**zoned garnets* (Sn-andradite: and₆₀₋₇₀, Sn-and₀₋₁₀, gross₁₅₋₄₀) typically trap in their core an early dense brine (40 wt % NaCl equiv.). Traces of CH₄ are occasionally detected. Measured homogenization temperatures to the liquid by vapour disappearance are between 450° and 510°C. By contrast, FI trapped in the mineral rims contain a low salinity aqueous fluid (3 wt % NaCl equiv.) and homogenize either to the liquid or to the vapour phase in the range 400°-230°C.

**hedenbergite* (hed₆₅₋₇₀, diop₃₀₋₃₅): in contrast to the diopside-hosted FI, FI in hedenbergite are rarer and smaller (<12µm). They have a low salinity (3.5 to 15 wt % NaCl equiv) and homogenize to the liquid or the vapour at lower temperatures (between 375° and 400°C).

3- Boron-bearing skarns only contain aqueous FI with a low to moderate salinity (6 - 13 wt % NaCl equiv), and which homogenize to the liquid or the vapour between 330° and 380°C.

Interpretations and conclusions

Sn-W stage. Previous interpretations of field and mineralogical data suggested that the W-skarns formed at P≤2kb and 525°<T<580°C and were overprinted by the Sn-bearing skarns [1]. Present fluid and mineralogical studies show the following: (1) The trapping of low density aquo-carbonaceous fluids contemporaneous with dense hypersaline brines fixes a lithostatic P regime for the Sn-W stages. (2) The isochore representative of the brine in the core of Sn-garnets [2] intersects the isochore of the H₂O-CH₄-bearing vapour [3] from the W-stage at ≈ 570°C and 1.2 kb. This pressure is a maximum value for the W-stage to remain colder or at most, in thermal equilibrium, with the Sn-stage. (3) The fO₂-conditions of the W-stage, fixed by fluid compositions, become closer to the graphite-fluid equilibrium as the fluid pressure approaches ≈1kb (fO₂ ≈10⁻²⁵ bar at 500°C) : hence a lithostatic pressure ≈1kb and a temperature of 500°C are inferred for the W mineralization. (4) At P ≈1kb, the Sn-skarn formed between 570° and 630°C, consistent with T-estimates based on the titanite-content of malayaite [4]. (4) The fluid responsible for the Sn-metasomatism has characteristic features of fluids derived from hypogene magmatic intrusions [5]: dense multicationic brine, trapping P≤1kb and fO₂ ≈Ni-NiO indicated by malayaite stability [6].

Retrograde evolution. Primary FI in Sn-garnet rims and hedenbergite in Sn-skarns, secondary FI in W-skarns, and all the boron-stage mark the retrograde evolution of the system. The development of boron

metasomatism and of rock-fracturing suggests a transition from lithostatic to hydrostatic pressure regime. It corresponds to the influx of colder low salinity aqueous fluids, with a drop of both P and T to \approx 250-280 bar and 370°-420°C, respectively.

Bibliography:

- [1] SONNET & VERKAEREN 1989, Econ. Geol. v.84;
- [2] BODNAR 1994, GCA v.58;
- [3] KRADER & FRANCK 1989, Ber. Bunsenges. Phys. Chem. 91;
- [4] TAKENOUCI 1971, Min. Deposita v.6;
- [5] LINNEN & WILLIAM JONES 1993, Archiwum Mineral.XLIX,
- [6] AÏSSA & PASCAL 1995, submitted to V.M.Goldschmidt Conf.

**THE CAP DE CREUS RARE ELEMENT PEGMATITE FIELD (CATALONIA, SPAIN):
MODEL OF CRISTALLIZATION**

ALFONSO, P. & MELGAREJO, J.C.

Departament de Cristal·lografia, Mineralogia i Diposits Minerals,
Universitat de Barcelona. C/ Martí i Franquès s/n, 08028
Barcelona, Spain.

In the Cap de Creus a pegmatitic field occurs within medium to high-grade metamorphic rocks. In addition to microcline-rich, barren pegmatites (type I), three pegmatite types have been established according to the clasification of Cerny (1992), based on mineralogical and internal structure criteria: beryl-columbite type (type II), beryl-columbite-phosphate type (type III), and albite type (type IV). All these types are genetically related.

All the pegmatites are concentrically zoned. This zoning reflects the sequence of early pegmatite crystallization. From outer to innermost parts there can be distinguished: border, wall, intermediate zones and core. In addition, vein fillings occur, which represent late hydrothermal events: cleavelandite veins in type II and III, quartz-muscovite veins in type III and IV, and last phosphate veins in type IV. The fluid responsible of the formation of the albite veins reacts with the preexisting zones and produces albitization.

Fluid inclusions have been studied in all the types and zones. Host minerals were quartz, beryl, albite, montebrasite and berlinite.

Microcline pegmatites. Only secondary fluid inclusions have been observed in them.

Beryl-columbite pegmatites contain two kinds of fluid inclusions: (1) H₂O-salts-CO₂-N₂ and (2) H₂O-salts. The first coexist with melt inclusions in beryl from the intermediate zones. This fact suggests that the intermediate zones in beryl-columbite pegmatites were formed during an unmixing stage between granitic magma and hydrothermal fluids. The isochores obtained from these inclusions, combined with the diagram of the Al₂SiO₅ polimorphs, indicate that beryl from the first intermediate zones formed between 570-600°C and 3-3,4 Kb. Group (2) occur in the replaced units, and represent late hydrothermal fluids that replaced the above units. Th L-V ranges between 210-290°C. They contain muscovite, calcite and apatite as trapped solids, and the last reflects high PO₄²⁻ activity in this pegmatitic episode. These fluids produce beryl and chrysoberyl replacement for herderite.

Beryl-columbite-phosphate pegmatites contain the following kinds of inclusions: (1) H₂O-salts-CO₂-(N₂), (2) H₂O-CO₂, (3) H₂O-salts, (4) H₂O-salts-CO₂-(N₂), (5) H₂O-salts-other vapours, (6) CO₂-(N₂)-(CH₄).

Fluid inclusions (1) occur in the intermediate zones. Melt inclusions have been observed in one sample associated to this type of inclusions. Th L-V ranges between 380° and >550°C. They are hypersaline (up to 46 wt% NaCl eq.), and contain muscovite, FeCl₂, calcite and, probably, kutnohorite. Hence, this zone formed similarly as above. The hydrothermal fluid (1) unmixed in two. The first one, represented by inclusions (2), is CO₂-rich, salts-poor (3-6 wt% NaCl

eq.). These fluid inclusions occur in the quartz from the core of the pegmatite. They contain some solids: calcite, barite, siderite, muscovite. These inclusions homogenize to vapour, then, to avoid the errors in the observation of that change, it has been calculated by a graphic method that relates the volume of CO_2 , X_{CO_2} , CO_2 density and Th L-V, obtaining a temperature of 380°C . This fluid probably generated the quartz core. The other unmixed fluid (3) is aqueous saline (23-35 wt% NaCl eq.), and fluid inclusions are very rich in trapped solids: muscovite, calcite, forroditite, apatite and, possibly, kutnohorite. Th L-V is comprised between 230° and 300°C . This fluid generated the cleavelandite veins and the related albitizations, as well as the replacement of beryl for hurlbutite. Moreover, this saline fluid concentrated all the rare elements, alternatively to that which formed the quartz core: Nb-Ta oxide minerals are highly concentrated in albite veins, and practically absent in the quartz core.

Later, a hydraulic decompression took place and quartz-muscovite veins formed. The fluid inclusions trapped at this stage (4) are more saline (37-39 wt% NaCl eq.). Trapped solids include muscovite and sparse carbonates. Th L-V is comprised between 280 and 290°C . These fluids produce a sparse crystallization of cassiterite.

Finally, inclusions (5) occur in replaced units, and contain the highest salinities: up to 43 wt% NaCl eq, and silvite crystals are widespread, indicating K enrichment in these late fluids. Th L-V is comprised between 160 - 200°C . The vapour phase contains CO_2 and the high fluorescence emitted by Raman spectroscopy here indicates that there are more constituents, probably organic compounds. These are solid-rich inclusions: muscovite, calcite, ferrian calcite, sphalerite, apatite. They represent the fluid responsible for the formation of the late hydrothermal veins: sulphide veins, quartz-actinolite veins, and late apatite veins.

Moreover, an ubiquitous group of apparently monophasic fluid inclusions (6) exists, with different characteristics depending on the zone: in the intermediate zones, Th is 15 - 18°C ; in the core, 10 - $12,5^\circ\text{C}$; in the albitization replacements, 1 - 7°C ; and, in the quartz muscovite veins, -5 to 1°C . These inclusions are related to the continuous aqueous and CO_2 -rich vapour unmixing phenomena along the pegmatite crystallization.

Albite pegmatites display the next kinds of inclusions: (1) H_2O -salts, (2) CO_2 - (N_2) - (CH_4) , (3) H_2O -salts- CO_2 - (N_2) - (CH_4) , (4) CO_2 .

The first (1) represent the fluid that formed the intermediate zones. Melt inclusions were not found. The salinity is comprised between 35-39 wt% eq. Th is comprised between 270 and 350°C . Trapped solids are muscovite, calcite, kutnohorite and FeCl_2 .

Fluid inclusions (2) occur in the quartz core and in the quartz-muscovite veins. They are CO_2 -rich (H_2O <10% vol), also N_2 (10-15%) and CH_4 (2-4%) are present. CO_2 homogenizes into liquid from 9 to 12°C . Carbonates sparsely occur as trapped solids. In some quartz-muscovite veins these fluid inclusions have graphite as a trapped solid.

Fluid inclusions (3) are saline, up to 40 wt%. Graphite also has been found within them, other trapped solids are muscovite, calcite, and ferrian calcite. Their homogenization temperature ranges from 280 and 290°C .

In the quartz-muscovite veins, inclusions (2) coexist with inclusions (3). The presence of graphite indicates reduction conditions at this stage. According to the coexistence of inclusions (2) and (3), a temperature between 280 - 290°C and pressure of 1,5-1,8 Kb were obtained for the formation of the quartz muscovite veins. These veins contain the highest concentration in Sn, Ta, and REE

minerals in all the pegmatitic field.

Fluid inclusions (4) also occur in quartz-muscovite veins. They are dense (Th -12 to -4°C). They are probably related to late trapping of metamorphic fluids.

HYDROCARBON INCLUSIONS IN SHOCKED QUARTZ FROM GARDNOS IMPACT BRECCIA, SOUTH NORWAY

ANDERSEN, T. (1) & BURKE, E.A.J. (2)

(1) Mineralogical-Geological Museum, Sars Gate 1, N-0562 Oslo, Norway
(2) Faculty of Earth Sciences, Free University, Amsterdam, The Netherlands

The Gardnos breccia in the Hallingdal area, South Norway, has recently been recognized as a meteorite impact structure of latest Proterozoic or early Phanerozoic age (Naterstad & Dons, 1991). The meteorite is thought to have hit in a shallow sea, penetrating through a thin layer of carbon-rich sediment and into a basement dominated by quartzite and metasedimentary gneisses of pre-1100 Ma age. In the late Silurian, the impact structure was overrun by Caledonian nappes, causing minor deformation in the impact breccia and its surrounding basement. The overburden has largely been removed by Quaternary glacial erosion, so that parts of the impact structure are now well exposed.

Shocked quartzite from the central part of the Gardnos breccia is impregnated by fine-grained carbonaceous material, giving a nearly black colour in hand specimen. Micro Raman spectroscopy shows this material to consist of poorly crystalline graphite. Planar fractures, typical of shocked quartz, are outlined by graphite inclusions and by trails of secondary fluid inclusions. The fluid inclusions consist of methane, with minor carbon dioxide ($X_{CH_4} \geq 96$ mole percent). The inclusions show H1 and S2 type of microthermometric behaviour, H1 inclusions showing a peak of homogenization temperatures to liquid at -100 °C., which corresponds to isochore pressure of ca. 2.5 kbar at 500 °C and ca. 4.3 kbar at 1000 °C. Such trapping conditions cannot be related to the extreme pressures encountered during the impact. On the other hand, PT conditions along the methane isochore can easily have been attained during Caledonian metamorphism, presumably at $T < 500$ °C. In this process, methane was formed in-situ by reaction between graphite and water, and was trapped as the partly open planar fractures healed.

The hydrocarbon-rich fluid inclusions in shocked quartz from the Gardnos breccia are thus only indirectly related to processes during the meteorite impact, and not at all to hydrocarbons of a deep (mantle) origin.

Reference:

- Naterstad, J. and Dons, J.A. 1991: Meteoritnedslag i Hallingdal: Nytt om Gardnosbreksjen (abstract, in Norwegian). Geonytt 18, No.1 p. 39.

FLUID BEHAVIOR IN THE GOLD-SKARN DEPOSIT OF CARLÉS (NW SPAIN).

ARCOS, D.; SOLER, A. & DELGADO, J.

Dept. de Cristal·lografia, Mineralogia i Dipòsits Minerals.
Universitat de Barcelona. Martí i Franqués s/n. 08028 Barcelona
SPAIN.

The gold-bearing skarn deposit of Carlés is located in the NW of the Iberian Peninsula related to a granodiorite intrusion. This granodiorite is one of a group of small intrusive bodies emplaced in the Cantabrian Zone, which is the outermost zone of the Iberian Massif (Hercynian orogen).

There are four different types of mineralization related to the granodiorite of Carlés. Two of them developed on the granodiorite itself and the other two on the marbles that host the granodiorite body.

A brief description, including the main characteristics of each mineralization follows. On the marbles a skarn-type mineralization is developed (1), with a well defined metasomatic column where the ore mineralization is placed interstitially and in veins that crosscut the metasomatic column. The ore mineralization is mainly characterized by copper sulfides with gold associated, and quartz, K-feldspar and calcite as gangue minerals. The other mineralization developed on the marbles (2) is made up by ferro-actinolite and arsenopyrite, which replace marbles near the contact with the skarn mineralization. There are also minor amounts of quartz, calcite and pyrrhotite. The mineralizations developed over the granodiorite are a K-feldspar alteration (3) with the ore mineralization emplaced in veins, and a sericitic greisen (4). The first is characterized by an important K-feldspar alteration associated with the veins, which are made up of quartz, calcite and copper sulfides with gold associated. This mineral association is similar to the ore found in the skarn-type mineralization. The greisen mineralization is characterized by an intense alteration of the granodiorite to an assemblage of sericite and quartz. The ore mineralization is found in masses of arsenopyrite, pyrite, pyrrhotite, quartz and calcite of metric scale associated with the greisen alteration.

Fluid inclusions in quartz crystals of each type of mineralization have been studied. Quartz from K-feldspar alteration and skarn-type mineralization contain fluid inclusions of the same type at room temperature. They are three-phase fluid inclusions made up by: an aqueous fluid solution, a vapor bubble and a halite crystal as a daughter mineral; some of these fluid inclusions also have a K-feldspar crystal, trapped during their formation. The ferro-actinolite-arsenopyrite mineralization that replaces marbles and the greisen-type mineralization both have quartz crystals with the same type of fluid inclusion, which consists, at room temperature, of three phases: a liquid aqueous solution, a carbonic liquid and a carbonic vapor bubble. In some cases, we found quartz crystals from the skarn mineralization and the K-feldspar alteration containing both types of fluid inclusion: high salinity and CO₂-rich.

From the microthermometric study carried out with a Linkam stage, we recorded halite dissolution temperatures in high salinity fluid inclusions, ranging from 265°C to 410°C, whereas total homogenization temperatures (by bubble disappearance) range from 500°C to 265°C. The good correlation between halite dissolution and total homogenization temperatures indicates that this fluid is nearly saturated in NaCl at the temperature range of total homogenization. This means that salinity is about 48 wt% eq. NaCl between 500°C and 375°C and decrease along the NaCl saturation curve to 35 wt% eq. NaCl at 265°C. No CO₂ phases were detected in these high salinity fluid inclusions.

CO₂-bearing fluid inclusions have CO₂ melting temperatures ranging from -57°C to -66°C, which are lower than that for pure CO₂, indicating the presence of other gases such as CH₄ and N₂. CO₂ homogenization is to the vapor phase in a temperature range from +26°C to +20°C. These data together with the CO₂ volume fraction observed in these fluid inclusions (between 0.25 and 0.55), suggest an X_{CO₂} between 0.03 and 0.15, assuming that these fluid inclusions belong to the H₂O-CO₂-NaCl system. Total homogenization temperatures range from 390°C to 340°C to vapor and from around 340°C to 320°C to liquid, whereas some fluid inclusions homogenize by meniscus disappearance around 345°C, indicating a critical behavior of the fluid. This evolution suggests that small variations in the composition of the system could have an important effect on the locus of the critical point and therefore on the type of total homogenization of these fluid inclusions, i.e., the addition of small quantities of CH₄.

From Raman spectroscopy we have detected no CO₂ in high salinity fluid inclusions, suggesting a very low X_{CO₂}, whereas analyses of CO₂-bearing fluid inclusions show that gases are mainly CO₂, with minor CH₄ and N₂, ranging from 1 to 12% and from 0 to 8% of the total gases respectively.

All these data suggest that a high salinity fluid with very low X_{CO₂} has suffered an unmixing process by which a fluid, mainly water with small amounts of CO₂ and CH₄, was separated from it. This process took place in an open system, where the high salinity fluid was responsible for the formation of the ore in the skarn and K-feldspar alteration, whereas the CO₂-CH₄-bearing fluid formed the ore in the greisen and in the ferro-actinolite-arsenopyrite replacement.

FLUID CIRCULATION WITHIN THRUSTING SHEAR ZONES IN A SCHIST SEQUENCE (CÉVENNES, SE FRENCH MASSIF CENTRAL): A FLUID INCLUSION STUDY IN QUARTZ LENSES

ARNAUD F. (1), BOULLIER A.M. (1) and BURG J.P. (2)

(1) CRPG 15 rue Notre Dame des Pauvres 54501 Vandoeuvre-les-nancy CEDEX

(2) Geologisches Institut, ETH Zentrum, Sonneggstrasse, 5, 8092 Zürich, Suisse.

E-mail: florence@crpg.cnrs-nancy.fr

In most zones of imbricate schists shear zones are underlined by quartz lenses that result from circulation of SiO₂-rich fluids during deformation. Such lenses have been studied in the quartz-pelitic schists of the Cévennes area. The main structures are:

- a low angle, north-dipping regional S1 slaty-cleavage.
- 100 m thick shear zones characterized by superposed cleavages, polyphase folding, a strong stretching lineation (l) and numerous quartz veins.

These structures result from a Variscan shear deformation in low grade metamorphic conditions. The shear zones produced stacking of the lithological sequence and correspond to S-SEward thrusts. Quartz lenses concentrated in shear zones were formed during progressive shear. Most of them are parallel to the regional cleavage S1 and are locally folded or may be stretched and sheared. Some of them are parallel to the local S2 cleavage and/or to the main shear planes.

According to the type of fluid inclusion (F.I.), the orientation of FI planes and the microthermometric and Raman data, different types of fluid inclusions have been identified (see figure in page 297):

- primary CO₂-CH₄-N₂-H₂O inclusions in albite and CO₂-H₂O inclusions in apatite
- Lc1: CO₂-N₂-H₂O±CH₄ F.I. planes sub-parallel to S1 and to l
- Lc2: CO₂-N₂-H₂O±CH₄ F.I. planes sub-perpendicular to S1 with variable orientations to l.
- L1: H₂O±N₂±CH₄ F.I. planes sub-perpendicular to S1 with variable orientations to l.
- F.I. planes sub-perpendicular to S1 and to l which have different compositions: Vc1: CO₂-N₂±CH₄±H₂O, Vc2: CH₄-N₂±H₂O±CO₂ and L2: H₂O±N₂±CH₄

The cleavage associated to the thrust zones is deformed by a granodiorite pluton. However, the F.I. planes keep the same orientation with respect to S1. Therefore fluid inclusion trapping predates the granodiorite and is related to the circulation of earlier metamorphic fluids. The geometric relationship between the different types of F.I. indicate a relative chronology as follows: (1) primary F.I. in apatite and albite, (2) Lc1 which may be contemporaneous with lens opening, (3) Lc2 (4) L1 and (5) Vc1, Vc2 and L2 which have the same orientation.

These preliminary results show variations in F.I. compositions which may be interpreted as resulting from the evolution of the metamorphic fluid during the shear event. The large variation in composition of the Vc1-Vc2-L2 F.I. could be interpreted as an heterogeneous trapping of a single H₂O-CO₂-N₂-CH₄ parent fluid.

This work is supported by the BRGM.

THE CHEMICAL COMPOSITION OF THE MIOCENE OCEAN: THE INTERPRETATION OF FLUID INCLUSION IN SALT FROM LORCA BASIN (SE SPAIN)

AYORA, C. (1), GARCIA-VEIGAS, J. (2), ORTI, F (3) & ROSELL, L, (3)

(1) Institut de Ciències de la Terra, CSIC, Martí i Franquès s/n., E-08028 Barcelona

(2) Serveis Científic-Tècnics, Univ. Barcelona, Martí i Franquès s/n., E-08028 Barcelona

(3) Dpt. de Geoquímica, Petrologia i Prospecció Geològica, Univ. Barcelona, Martí i Franquès s/n., E-08028 Barcelona

The chemical composition of the ocean in the Phanerozoic is assumed to be very close to present seawater. This assumption is mainly based on the mineral record of marine evaporite sequences and on a few data on the chemical composition of the brines trapped in halite (Holland et al., 1986). However, detailed compilation of marine evaporites show that the sequences following the expected evaporation path of present seawater are the exception rather than the rule. Indeed, most of fossil evaporites do not contain Mg-K sulfates and belong to the so-called 'sulfate-depleted' trend (Hardie, 1990). Does the composition of ancient oceans vary with regards to present seawater?, or are changes due to the evolution of the brine in the evaporite basin?. Based on the accurate chemical analysis of individual fluid inclusions in halite crystal Kovalevich (1990) confirms that the differences in the mineral sequences are due to variations in the mother brine, which are in turn attributed to differences in Ca and SO₄-content of the ocean water

The Lorca basin is a representative example of a Miocene western Mediterranean basin. The outcropping sedimentary sequence is formed by: 1) a basal member of lutites with sandstones, gypsum and limestone lenses; 2) an evaporite member made up of a massive halite and a gypsum unit; 3) an upper clastic member. The halite unit does not outcrop but has been intersected by two drillcores.

The Drillcore #4 intersected 235 m of halite from the center of the basin, although the lower 54 m section is not available. The Drillcore #5 intersected 49 m of the base of the halite unit. The sequence of drillcore #5 belongs to the margin of the basin and is unconformably overlain by the gypsum unit. The difference in thickness of the two halite sequences is interpreted as being due to differential subsidence, with the area of drillcore #5 remaining emerged during formation of most of halite in the depocenter.

The mineralogical record and the textures allow us to correlate the sequence of drillcore #5 with that of the lower part of drillcore #4 (below 193 m). The evolution of Br content of the brine confirms the correlation between the upper part of drillcore #5 (<137 m) with the lower part of drillcore #4 (>139m).

Primary fluid inclusions trapped in halite have been analyzed by Cryo-SEM-EDS. According to solute proportions in fluid inclusions from drillcore #5, the halite was precipitated in an open basin with a major inflow very close in composition to present day seawater. However, the fluid inclusions from drillcore #4 shows SO₄-contents distinctly lower than expected from the simple evaporation of present day seawater. The inflow of a CaCl₂-bearing brine to the basin is a more likely process to account for sulfate depletion, as suggested by the solute proportions analyzed in fluid inclusions. The Neogene faults that

limit the basin may have played an important role in differential subsidence of the central part of the basin, and in the change in the hydrological regime.

Therefore, the systematic analyses of primary fluid inclusions, in the Messinian basin of Lorca, suggests that rather than a different chemical composition of the past ocean, the differences found in mineralogical record and in fluid inclusions are due to chemical changes within the evaporite basin.

References:

- Hardie, L.A. (1990) The roles of drifting and hydrothermal CaCl₂ brines in the origin of potash evaporites: an hypothesis. *Am. Jour. Sci.*, 290: 43-106.
- Holland, H.D.; Lazar, B. & McCarafferey, M. (1986) Evolution of the atmosphere and oceans. *Nature*, 320: 27-33.
- Kovalevich, V.M. (1990) Phanerozoic evolution of Ocean Water Composition. *Geochemistry International*, 256. 20-27

Acknowledgements: This work has been carried out in the framework of the DGICYT PB90-0485 and PB93-0165 projects.

SALT-RICH AND ORGANIC-RICH FLUID MIGRATION IN THE RHINE GRABEN TRIASSIC SANDSTONES (SOULTZ DEEP DRILLING)

AYT OUGOUGDAL, M.(1), CATHELINÉAU, M.(1), PIRONON, J.(1), BOIRON, M.C.(1), BANKS, D.(2), YARDLEY, B.W.D.(2)

(1)CREGU, BP 23, 54501 - Vandoeuvre-lès-Nancy, France,

(2)Leeds University, Woodhouse Lane, LEEDS LS29JT, UK

Self sealing of open microstructures characterizes the sedimentary formations as well as the granitic basement of the Rhine continental rift basin in the region of Soultz (HDR Soultz-sous-Forêts drillhole, Rhine graben, France), which is currently submitted to active fluid migration.

A detailed petrographic and microthermometric study of trapped paleofluids in the sedimentary formations (veins filled by quartz or barite, healed microfissures, authigenic quartz overgrowths in sandstones) reveals a significant fluid migration in the Triassic sediments and downward fluid movements towards the basement.

The coarse-grain Triassic sandstones have undergone dissolution and precipitation of quartz, coupled to the development of overgrowths around the detrital quartz grains. Careful observation of quartz overgrowths by SEM-CL in samples from 1038.9, 1053.0 and 1065 meters depth reveals the presence of both primary inclusions and secondary inclusions distributed along trails. Thus, in sandstones, the sequence of fluid trapping is the following : i) primary inclusions in quartz overgrowths, and quartz veinlets ii) secondary inclusions in FIP crosscutting the quartz overgrowth, ii) primary and pseudo-secondary fluid inclusions in barite veins crosscutting the cemented sandstones

Microscopic observations and microthermometric studies have demonstrated the presence of two types of fluids related to the recent to modern circulations :

Hydrocarbon fluids

Fluid inclusions are scattered in barite crystal among the aqueous primary fluid inclusions. They have been distinguished thanks to observations under UV illumination. They are biphasic inclusions and contain sometimes bitumen. Vapor phase is highly variable in the 40- 80 vol.% range.

Melting temperature of hydrocarbon phase is around -70°C which indicate that hydrocarbons are mostly nonane - octane species. Homogenization temperature (Th) are relatively high (up to 200°C) but problems of leakage along mineral cleavage prevent any Th measurements.

Infra-red spectroscopy has been carried out on the different fluid inclusion phases (liquid, vapor and solid). Analyses of liquid and vapor phases confirm the presence of aliphatic hydrocarbons which are formed by 6 to 8 carbons. This estimation has been obtained by calculation of the CH₂/CH₃ area ratio. Traces of CH₄ have been detected in vapor phase. IR spectra of solid phase show the presence of aliphatic CH (corresponding to alkyl chains with 8 to 16 carbons), aromatic CH and OH groups. CO₂ is detected in all inclusion phases.

Gas chromatography performed on organic matter from microfissures

has shown that the most abundant species are composed of 13 to 16 carbons (tridecane to hexadecane).

Aqueous fluids

Three groups of fluids have been distinguished on the basis of the microthermometric data:

- aqueous fluids observed in healed microcracks as fluid inclusion planes in quartz, having salinity in the 17-20wt% eq. NaCl range and Th between 150 and 190°C.

- primary fluid inclusions in barite and in quartz overgrowth which display lower salinity about 7-10 wt% eq. NaCl and Th in the 120-130°C range. These data show that fluid related to diagenesis and barite crystallization in veinlets belongs to the same event of fluid circulation.

- some fluid inclusions with distinct microthermometric characteristics have been observed in fluid inclusion planes in quartz grains. Salinity is relatively high around 25 wt% eq. NaCl and Th is about 100°C.

The large variations of salinities suggest a mixing process between convected low salinity fluids (less than 5 wt% eq. NaCl) and brines, indicating active fluid movements between the sedimentary formation, the basement, and the surface.

This conclusion is confirmed by the study of Br/Cl ratios in trapped fluids by using crush-leach procedures. Results show that the barite fluids are characterized by a relatively wide range of Br/Cl ratios from 0.03 to 0.08 indicating the contribution of a Br enriched end-member in fluids percolating the sediments. Such values are higher than that compared to the mixed fluids from the present day reservoir, or trapped within the granite.

The overall data indicate that the movements of the saline and HC bearing fluids were limited to specific episodes of fluid circulation. This stage may correspond to the main stage of oil production, and happens later than the cementation of the sandstones, but prior to the recent hydrothermal circulation.

However, the lack of high salinity fluids and HC inclusions in the deep granite levels indicate that fluid movements were limited at that stage to the Trias formations and to the fractured top part of the granite basement.

The generalized fluid movements under the present day gradients imply probably convection cells and a fluid mixing of meteoric and saline waters at greater scale than during the past.

THE APPLICATION OF A COMPUTERISED AND OPTIMISED CLATHRATE STABILITY MODEL TO FLUID INCLUSION STUDIES

BAKKER, Ronald J.

CREGU, BP 23, 54500 Vandœuvre-lès-Nancy, France

Microthermometric analysis, i.e. measurement of temperatures of noticeable phase changes, is a first approach to identify the fluid in inclusions. In inclusions that contain both water and gases like CH₄, CO₂, and N₂, a gas hydrate (clathrate) will be present near the freezing-point of pure water. Clathrate is a solid compound with an ice-like structure that contains mainly water and up to 15 mole% gas. The exact melting conditions of a clathrate gives important information for the interpretation of inclusion composition and density. However, these conditions may be difficult to estimate because both clathrates and ice may occur in a similar temperature range, and can easily be mistaken. Furthermore, metastable phase relations are usually present in inclusions that contain solid compounds, and may mask true phase transitions.

Several classical clathrate models are available to predict stability conditions, and which involve many chemical/physical parameters. These models are applicable to specific conditions that confine only a small part of the total range of clathrate stability conditions. A major shortcoming of these models is that a complete set of most accurate values for its parameters was never used. Furthermore, the mystification in clathrate modelling is increased by the lack of some fundamental thermodynamic principles, like fixed standard conditions. So much the worse, a thorough error analysis was not revealed in most publications. Consequently, calculated conditions may differ up to 10% from experimental data, and extrapolated results are even less accurate.

A new modified clathrate stability model is presented here, to eliminate the previously mentioned defects, and which gives a complete and accurate description of the H₂O-CO₂-CH₄-N₂-NaCl-KCl-CaCl₂ fluid system between 253-293 K and 0-200 MPa. This model handles the thermodynamics of aqueous solutions (solubility of gases, osmotic coefficients); equations of state for calculating fugacities and liquid-vapour equilibria; thermodynamic properties of clathrates and pure H₂O; molecular potentials. In electrolyte-free systems, the model is able to reproduce all available data within 2% accuracy. In salt-bearing systems, clathrate stability conditions are calculated within 5% accuracy of experimental data, and are valid up to eutectic compositions.

The calculations of clathrate stability conditions and fluid inclusion salinity and density are rather complex and a time consuming practise. Therefore, a computer program in C++ language has been developed to handle the complex calculation method, which includes several numerical approximations. Known properties of each phase that is present during clathrate melting (e.g. clathrate, aqueous solution, non-aqueous vapour bubble) are introduced during input procedures of the program (Fig.1a). The results of Raman spectroscopic analysis are introduced to characterise the composition of the non-aqueous phase. A clathrate melting

temperature is a prerequisite to calculate anything at all. Additionally, either the salinity of the aqueous phase or the density of the non-aqueous phase are required to calculate the composition and molar volume of individual phases. Similar to the method of DUBESSY et al. (1992), both the properties of individual phases and the total fluid inclusion are obtained from the final melting temperature of ice and an estimation of the relative volume fractions. The volume fractions are always required for the calculation of the properties of the total fluid inclusions. Calculated properties of each phase are displayed during the output procedure of the program (Fig.1b). The error analysis is displayed as a range of values, because the deviation from mean values is not symmetrical.

This work is financially supported by the network HCM, CEE-DG XII-G, contract CT 930198 - PL 922279: Hydrothermal/Metamorphic water rock interactions in crystalline rocks, a multi disciplinary approach based on paleofluid analysis.

Ref.

DUBESSY J, THIERY R, and CANALS M (1992) *Eur. J. Mineral.*, **4**, 873-884.

Fig.1. An example of the input (a) and output (b) screen for a H₂O-CO₂-NaCl-rich fluid inclusion. The clathrate melting temperature is 276.1 (\pm 0.2) °C. The density of the CO₂-rich phase is obtained from its homogenisation temperature (270.5 \pm 0.1 °C). The volume fractions of the non-aqueous phase is estimated at 0.5 with a 10% error.

The fluid system H₂O-CO₂-CH₄-N₂-NaCl-KCl-CaCl₂ between 253-293 K and 0-200 MPa

a)

THE CLATHRATE

What is the final Clathrate Melting Temperature (< 292.57 K)?

T (K) = 276.1

abs. error = 0.2

Which other phases are present at final clathrate melting?

(0) Unknown

(1) H₂O(sol) + CO₂(vap)

(2) H₂O(sol) + H₂O(liq) + CO₂(vap) = Q1

(3) H₂O(liq) + CO₂(vap)

(4) H₂O(liq) + CO₂(liq) + CO₂(vap) = Q2

(5) H₂O(liq) + CO₂(liq)

0

THE AQUEOUS PART

Which salt is present? (0) none

(1) NaCl

(2) KCl

(3) CaCl₂ 1

What is the salinity of the aqueous part?

(this value is based on gas-saturated solutions)

(0) Unknown

(1) Value in Molality

(2) Value in Weight % 0

What is the Final Ice melting temperature (unknown = 0)

T (K) = 0

THE NON-AQUEOUS PART

Raman Spectroscopy: what is the composition of the non-aqueous part?

x(CO₂) = 1 abs. error = 0

x(CH₄) = 0

x(N₂) = 0

What is the Volume Fraction of non-aqueous part at room T (unknown = 0)?

Fraction (between 0 and 1) = 0.5

abs. error = 0.05

What is the density of the non-aqueous part?

(0) Unknown

(1) Value in cc/mol

(2) Value in g/cc

(3) From homogenisation temperature

3

Th CO₂ (K) = 270.5

abs. error = 0.1

mode of homogenisation (v/l)

1

b)

CLATHRATE Melting in the presence of H₂O(liq) + CO₂(liq)

At 276.1 K (± 0.2) and 7.7105 MPa (7.7873 - 7.6335)

Q2 conditions : 275.8896 K and 3.7446 MPa

x(CO₂) is undefined (0.1363 at Q2)

x(CH₄) = 0

x(N₂) = 0

AQ. SOLUTION Vm = 17.9146 cc/mol (17.9125 - 17.9168)

a(H₂O) = 0.9319 (0.9331 - 0.9368)

x(CO₂) = 0.025 (0.0251 - 0.0249)

x(Salt) = 0.0413 (0.0404 - 0.0423)

Molality = 2.3938 mol/kg (2.3373 - 2.4499)

NON-AQ. PHASE Vm = 46.6736 cc/mol (46.7021 - 46.6453)

x(CO₂) = 1

x(CH₄) = 0

x(N₂) = 0

Th = 270.5 K (± 0.1)

TOTAL FI Vm = 32.2941 cc/mol (33.7468 - 30.8446)

x(H₂O) = 0.6747 (0.6362 - 0.7098)

x(CO₂) = 0.2954 (0.3363 - 0.2581)

x(CH₄) = 0

x(N₂) = 0

x(Salt) = 0.0299 (0.0275 - 0.0322)

WARNINGS : metastable absence of clathrate during homogenisation of CO₂

INVESTIGATION OF FLUID INCLUSION IN EMERALDS OF DIFFERENT GEOLOGICAL ORIGINS BY MICROCHEMICAL ANALYSIS AND IR-REFLEXION-SPECTROSCOPY

BANERJEE, A.

Institut für Geowissenschaften-Edelsteinforschung, Johannes Gutenberg-Universität Mainz, D 55099 Mainz, Germany

Inclusions in emeralds have been used for many years for the identification of their geological origins. According to DEER and others (1962) all natural emeralds contain water in varying amounts. The purpose of the present investigation was to compare the amounts of water contained in the emeralds of different geological origins by microchemical analysis and to characterize the fluid inclusions in the emeralds by ir-spectroscopy. Moreover, the amount of nitrogen contained in the emeralds was also studied by chemical means.

Chemical analysis :

14 samples of emeralds from different sources were analysed according to a method developed by DINDORF (1995) in which the amounts of the fluids in question are measured on the basis of the thermal conductivity of the gases produced by the combustion of the samples. The amount of a sample needed for the investigation is about 10 mg. The results of the qualitative analysis of the emeralds are as follows (Table 1).

Table 1

No.	Origin	Water (wt%)
1.	Colombia (Muzo)	1.022
2.	Colombia (Chivor)	1.475
3.	Brasil (Carnaiba)	2.079
4.	Brasil (Itabira)	1.935
5.	Brasil (Capoeirana)	1.985
6.	Brasil (St.Terezinha)	2.421
7.	Malagesy Rep.	1.647
8.	Nigeria	0.585
9.	Nigeria	0.990
10.	Zimbabwe	2.016
11.	Zimbabwe	2.088
12.	Zambia (Kafubu)	2.610
13.	Zambia (Kafubu)	2.690
14.	S.Afr. (Transval)	2.529

The present investigation shows that the emeralds from different sources contain different amounts of water according to the conditions of their genesis. SILWA and NGULUWE (1984) had found striking similarities between the geological settings of the occurrences of emerald in Zimbabwe, Zambia and South Africa. According to the present investigation emeralds of these origins have relatively higher water contents in comparison to the Colombian and Nigerian emeralds, which were deposited under different conditions. Furthermore, nitrogen was identified in the Colombian emeralds by the present investigation. This result is in accord with those of DELE-DUBOIS and others (1980).

IR-spectroscopy:

As it has been proved by ir-spectroscopic investigation, the fluid inclusions in the emeralds under investigation can be classified in three groups as follows :

1. inclusions containing only water, identified by the sharp absorption band at or near 1641 cm^{-1} .

2. inclusions containing both water, identified by the absorption band at or near 1641 cm^{-1} and other fluids, e.g. hydrocarbons, identified by the absorption band at 1460 cm^{-1} , which occurs due to a C - H stretching vibration.

3. inclusions containing only hydrocarbons and no water.

References :

DEER, W.A.; HOWIE, R.A. and ZUSSMAN, I. (1962) : *Rock-Forming Minerals*, London, pp 256-267.

DINDORF, W. (1995) : Personal communication

DELE-DUBOIS, M.L.; DHAMELINCOURT, P and SCHUBNEL, H.-J. (1980) : *Rev. Gemmologie*, June, pp 11-14.

SILWA, A.S. and NGULUWE, C.A. (1984). *Precambrian Research*, 25, pp 213 - 228.

CHEMISTRY AND SOURCE OF THE FLUIDS IN THE COLOMBIAN EMERALD DEPOSITS.

BANKS, D.A.(1), GIULIANI, G.(2) CHEILLETZ, A.(3) & RUEDA, F.(4)

(1) Department of Earth sciences , University of Leeds, Leeds, U.K.

(2) ORSTOM et CRPG, BP 20, 54501 Vandoeuvre, France.

(3) ENSG et CRPG, BP 20, 54501 Vandoeuvre, France.

(4) MINERALCO, S.A., calle 32,N° 13-07, AE 17878, Bogota, Colombia.

The emerald deposits of Colombia are located in two narrow belts within the Eastern Cordillera where intense hydrothermal alteration of the enclosing black shales has occurred. Emeralds are contained in calcite - dolomite veins and breccias together with albite, quartz, fluorite, baryte, pyrite and REE-carbonates. Originally thought of as related to magmatic fluids (Oppenheim, 1948), more recent work has shown that the origin of the deposits is due to interactions of connate or basinal formation waters with the black shales (Medina, 1970; Giuliani et al, 1992). Evaporitic sulphate, reduced to sulphide by thermochemical reduction with organic matter in the shales, has been shown to be the cause of the large amount of pyrite (Ottaway et al, 1994; Giuliani et al, 1995). The intense reaction released Cr, V, Be, REE etc. into solution later to be redeposited as vein minerals (Giuliani et al, 1993). Microthermometry of primary inclusions in emerald, quartz and fluorite has shown that the fluid inclusions have a salinity of c. 40 wt% eq. NaCl and may contain significant amounts of Ca, K, Fe and Mn. Daughter minerals such as halite, calcite, dolomite, parisite, siderite, pyrite sphalerite and silicates have been identified (Kozlowski et al, 1988; Giuliani et al, 1993). This study concentrates on the fluids in emerald, quartz and fluorite from the deposits of Yacopi, Coscuez, Cincho and Pava, in the western zone, and Aranado, Chivor and Guali in the east. The aim is to determine the composition of the fluids, their likely origin and to discuss the processes which led to emerald precipitation.

Here we provide analyses of the fluids in the three minerals determined using the crush-leach technique detailed in Yardley et al (1993) on single emerald crystals and bulk samples of between 0.5 and 1g. The samples we have studied all come from the final stage of mineralisation when emerald was precipitated together with fluorite, while the majority of the quartz was later. There is no systematic difference in samples from the eastern or western zones. There are high levels of all the elements observed by microprobe and SEM. However the inclusions in quartz do have greater concentrations of Ca, Ba, Li, Fe, Mn, Pb, Zn, Cu and Br whereas the emeralds have greater Na, Mg and SO₄. There are clear positive correlations between Ca and Fe and most of the elements only Na and Be are negatively correlated with Ca and Fe.

Using chloride and bromide it is possible to determine the origin of the fluids as they are conservative in solution and are not affected by water-rock interactions. There is a large range in Cl/Br ratios (~15,000 to 700) while the salinity remains almost constant. Emeralds and fluorites (which precipitate contemporaneously) have the highest ratios, consistent with the dissolution of pure halite (Cl/Br=10,000) as the source of the

high salinity. The lower Cl/Br ratios of the quartz hosted fluids are similar to those obtained from dissolution of halite containing some residual bittern and are similar to those of the Salton Sea and some metal rich oilfield brines. The range of Cl/Br ratios and the positive correlation of I with Br is indicative of mixing of two distinct fluids with different origins.

On the basis of the halogens we suggest that there were two distinct fluids present: Fluid E (inclusions in emerald and fluorite) was relatively oxidising and dominated by Na, Cl and SO₄ with low levels of other cations. Fluid Q (inclusions in quartz) was more reduced and dominated by Na, Ca, Cl with high levels of Fe, Pb, Zn, Ba, Sr etc. but with little SO₄ or F. The trends exhibited by these elements indicate that mixing appears to have taken place during mineral precipitation. We suggest that fluid E reacted with the black shales causing bleaching by the thermochemical reduction of organic matter by SO₄ to produce reduced sulphur and CO₂ and to release metals such as Cr, V, Be etc into solution. When this modified, liquid-rich, fluid reacted with fluid Q, which was high in Ca and transition metals, minerals were precipitated (pyrite, fluorite, parisite, calcite and dolomite).

Of particular interest is the transport and deposition of Be to form the emeralds. Be was released from the shales during bleaching (Giuliani et al, 1993) and Ottaway et al (1994) suggested that it was transported as -OH complexes, however given the abundant fluorite and parisite it is more likely that highly stable BeF₂ complexes or less stable fluoroberyllates (Beus, 1966), were involved. The negative correlation of Be with Fe indicates the highest concentrations were in the low-Ca fluid. Reaction with the high-Ca fluid caused precipitation of fluorite and parisite and hence destabilised the Be-F complexes, depositing emeralds.

Our data shows that the 2 fluids responsible for the unique emerald mineralisation in Colombia had different sources but were both derived from dissolution of evaporite sequences. The subsequent modification of the fluid chemistry by water-rock interactions and mixing of the fluids was responsible for the deposition of emerald and the other vein minerals. The constancy of element ratios from deposits which are c. 80 km apart indicates that the hydrothermal system was widespread.

References

- Beus, A.A. 1966. *Geochemistry of Beryllium*. London: W.H.Freeman.
Bohlke, J.K. & J.J. Irwin. 1992. Laser microprobe analyses of Cl, Br, I and K in fluid inclusions: *Geochim. Cosmochim. Acta.* 56: 203-225.
Giuliani, G., S.M.F. Shepperd & Cheillettz, A. 1982. *C.R. Acad.Sci. Paris* 314: 269-274.
Giuliani, G., A. Cheillettz, S.M.F. Shepperd & C.Arboleda. 1993a. 2nd Biennial SGA Meeting:105-108. Rotterdam: Balkema.
Giuliani, G., A. Cheillettz, J. Dubessy & C. Rodriguez. 1993b. *Proc. 8th IAGOD Symposium*: 159-168.
Giuliani, G., A. Cheillettz, C. Arboleda, V. Carrillo, F. Rueda & J.H. Baker. 1995. *Eur. J. Mineral.* 7: 151-165.
Kozłowski, A., P. Metz & H.A.E. Jaramillo. 1988. *N. Jb. Mineral. Abh.* 159: 23-49.
Medina, L.F. 1970. *Manizales Econimas*: 10-20.
Ottaway, T.L., F.J. Wicks, L.T. Bryndzia & E.T.C. Spooner. 1994. *Nature*, 369: 552-554.
Yardley, B.W.D., D.A. Banks, S.H. Bottrell & L.W. Diamond. 1993. *Min. Mag.* 57: 407-422.

3D RECONSTRUCTION AND PVTX CONDITIONS OF MICROFISSURAL FLUID MIGRATION AND EXTENSIONAL VEIN FORMATION : EXAMPLES OF MOKRSKO (BOHEMIA) AND MALPICA-TUY SHEAR ZONE GRANITES (GALICIA)

BARAKAT, A.(1), CATHELINEAU, M.(1), CANALS, M.(1), BOIRON, M.C.(1), DURISOVA, J.(2), BANKS, D.(3)

(1)GS CNRS-CREGU, BP 23, 54501 - Vandoeuvre-les-Nancy, France

(2)Czech Geological Survey, Praha, Czech Republic

(3)Leeds University, Woodhouse Lane, LEEDS LS2 9JT, UK

Study of 3D geometry characteristics and PVTX conditions of fluid migration in crystalline rocks shows that the migration of fluids equilibrated with metamorphic host rocks may occur through dense and regular networks of extensional structures (veinlets and microfissure networks with regular spacing). New developments in the analysis of fluid inclusions in relation with their host structures (3D reconstruction of connected vein or fluid inclusion plane (FIP) networks, permeability tensor estimation) yield to a rather complete description of fluid migration parameters, and relationships between stresses and fluid pressure, this giving strong constraints on the model of fluid circulation and ore formation in the case of deposits.

New methodological developments concern the estimation of migration parameters using a probabilistic approach of the connectivity between FIP, and a fractal description of microfracture populations. Systematic 3D measurements of FIP are carried out on each sample using a Universal stage and an Image Analyser, after a detailed study of fluid inclusion using optical and scanning electron microscopy (SEM cathodoluminescence imaging). Characterization of P-T-V-X features of percolating fluids is then obtained through a multidisciplinary study of fluid inclusions (microthermometry, Raman spectroscopy, bulk ion chemistry using crush-leach procedures).

EXAMPLE OF MOKRSKO-CELINA

The Mokrsko-Celina gold ore zone is an east-west-trending dilatation fracture zone, several hundred meters thick that is developed at the contact between the amphibole-biotite granodiorite metamorphosed volcano-sedimentary rocks of the Jilové belt (Moravek, 1984, 1989). The dense network of parallel quartz veinlets penetrating the apparently unaltered biotite-amphibole bearing granodiorite represents the most characteristic structure of the deposit. However, at the microscopic scale, the ore zones are characterized by the following succession of fluid events :

i) the formation of the EW macroscopic extensional fractures filled by quartz. The preferential orientation of quartz veinlets is E-W ($N90^{\circ}E \pm 10^{\circ}$) with a "subvertical" dip (range of 80 to 90° S). These quartz veinlets display all characteristics of extensional veins, especially no shearing, no displacement in any direction. Therefore they may be considered as mode I structures which give the orientation of the main local stress plane. The quartz veins vary in thickness (from less than 7 mm up to 0.5 m thick) and in frequency (up to 100 in 1 m). Their special feature is the ratio length/ width which reaches values higher than 100. Fluids migrating in the forming fissure interact with the host rock forming new mineral assemblages depending on the nature of the crosscut mineral (microcline, amphibole II and biotite II, arsenopyrite (Au?), quartz). They contain primary inclusions ($CO_2-CH_4 \pm N_2-H_2O-NaCl$ fluids linked to the first stage of veinlet infilling (mineralizing event

with quartz-arsenopyrite (Au)). Minimal trapping temperatures (Th) are around $330 \pm 20^\circ\text{C}$.

ii) *the formation and healing of EW and NS-N30°E FIP networks*

Strong micro-fissuration affects both the veins and the host granodiorite. EW fissures are filled by authigenic minerals (chlorite-dolomite-adularia). In magmatic quartz grain from the granodiorite and in quartz veinlets, fissures are mostly subEW FIP (N80-N90°E, dip : 70 to 90) FIP network is dominated by H₂O-CO₂-CH₄ inclusions displaying lower densities than the early fluids. The two families of FIP indicate a rather strong difference in the regime of deformation with time, and could attest of at least two major stages of brittle deformation, and fluid migration. The dominant direction of microfissures (FIP and carbonate cracks) is N0- to 30°E, is clearly later than the EW FIP. NS FIP contain mostly H₂O-NaCl inclusions displaying low salinity aqueous fluids. Minimal trapping temperature (Th) is in the range of 140 to 300°C (modes at 200°C, 290°C) and salinities in the range of 1 to 9 wt. % eq. NaCl. The study of F.I., FIP by FIP, shows clearly an evolution of the Th-Tm ice pairs, attesting to a progressive decrease in salinity of the fluids correlatively to a decrease of the minimal trapping temperature. Each crack exhibit well defined features, but the successive healing of the cracks give the record of progressive evolution of the fluid chemistry entering in the fissural open space. Trapped fluids in specific networks of healed or sealed microfissures at Mokrsko show that a significant fluctuation in the fluid density occurred in the system, and FI may be considered as excellent markers of pressure changes. Considering a high temperature for the first stage (biotite-amphibole stability), the pressure would have reached 2.7 Kb at a temperature of 450°C (considered as the minimal temperature for the stability of biotite), but have probably fluctuated below this maximum (lithostatic value) down to 2.0 Kb. During the second stages (EW FIP), the fluid density attest a general decrease of the pressure down to 1.0 -1.5 Kb.

OTHER EXAMPLES AND MODELS OF FLUID MIGRATION

The study of Au concentratiois at Tomino and Corcoesto (Galicia) shows that fluid migration in syntectonic Hercynian granites display similarities to that shown on the Mokrsko example. Milky quartz veins and veinlets post-dating early subsolidus alterations form as regular networks of extensional veins displaying a rather high angle with the foliation plane related to the earlier ductile deformation. C-H-O-(N) fluids of metamorphic derivation are found in the surroundings of the early milky quartz veins, trapped under pressures above 1Kb (frequently in the 2-4 kb range) and temperatures of 350° to 450°C. They may be extremely enriched in CH₄ and N₂, indicating mixing with fluids produced by the devolatilization of nearby C-rich units (Tomino, for instance). Due to repeated tectonic reactivation, early milky quartz veins are strongly affected by late brittle deformation under similar stress conditios which result in the reopening of the structure, formation of hyaline quartz from C-H-O-(N) fluids under pressures from 0.5 to 2.0 Kb depending on the localities. A renewal of tectonic reactivation under quite different P-T conditions resulted in the main stage of gold ore deposits formation. Fluids are generally aqueous, have relatively low salinities and chemical features of fluids equilibrated with crustal series, after downward infiltration from surficial levels. Statistical description of the FIP networks, including a fractal approach, shows that the microfissural permeability may be described from the quantitative parameters of each FIP family (dip, strike, width, spacing) using the same approach than for fault or joint sets using the percolation theory.

FLUID INCLUSIONS AND PROCESS OF GOLD PRECIPITATION IN THE SALSIGNE DEPOSIT (MONTAGNE NOIRE, FRANCE)

BENCHEKROUN, F. & MOINE, B.

Laboratoire de Minéralogie, URA 67 du CNRS, 39 Allées Jules-Guesde, 31000 Toulouse, France.

It is now established that the Salsigne gold and sulfides deposit was produced by a late Hercynian hydrothermal activity. Very similar ores occur within the autochthonous schistes X ("3a-2x" ore; Nesplier; Nartau...) and a thrusting Cambrian unit ("mine traditionnelle"). Gold is generally considered to have been introduced at a late stage into early sulfides-rich bodies, mainly consisting of arsenopyrite, pyrrhotite and pyrite [1; 2]. Fluid inclusions have been studied in quartz from the schistes X ores. Three main successive families of fluids of contrasted features have been observed.

I) An early family of H_2O-CO_2-NaCl (CH_4, N_2) F.I. exhibits very variable values of X_{CO_2} as well as bulk density. All these inclusions occur along sealed microfractures (pseudosecondary and secondary F.I.) with often no evidence of their relative chronology. Five types of F.I. have been distinguished which can be interpreted as stemming from the same original fluid but trapped under different P-T conditions.

1) The original fluid (1) is represented by the F.I. with the highest water content ($0.6 < X_{H_2O} < 0.9$) and relatively high density which show no evidence of post-trapping alteration. This fluid was probably connected with the early arsenopyrite-bearing paragenesis. For a temperature of 450°C deduced from the mineral compositions [2], the isochores indicate relatively high pressures (fig. 1): 2.5-3.2 kbar (lithostatic P) at Nesplier and about 6.0 kbar (supralithostatic P) along the major "3a-2x" shear zone and at Nartau.

2) F.I. of similar composition but with a lower density indicate significant drops in pressure within the single phase region.

3) Contemporaneous F.I. with highly variable X_{CO_2} and density probably derived from fluid (1) by unmixing and heterogeneous trapping as the result of a drop in both T and P. 4) Contemporaneous F.I., some H_2O -rich (4a; X_{H_2O} approx. 1), others CO_2 -rich (4b; X_{CO_2} approx. 1), can be ascribed to the unmixing of fluid (1) and homogeneous trapping.

Finally, very small F.I. consisting of dense CO_2 are contemporaneous with a few type (1) ones. They occur in highly deformed quartz and probably derived from fluid (1) by leakage of H_2O accompanied by volume reduction or readjustment to higher pressure.

II) The second family consists of $H_2O-NaCl$ fluids of relatively low salinity (5 wt % NaCl). It is connected with the late Bi-Au paragenesis mainly observed along the fractures cross-cutting the early quartz and sulfide bodies. The conditions of precipitation of gold and accompanying minerals were about 250°C for low values of pressure (a few ten or hundred of bars; fig.1).

III) Very late $H_2O-NaCl-CaCl_2$ fluids of intermediate to high salinity, trapped along several families of sealed microfractures are probably connected with the Trias-Lias distension.

Modeling of gold deposition by the $H_2O-NaCl$ fluid within the sulfide-rich bodies has been performed using the EQ3/6 software package (work in collaboration with G. Berger). It has been shown that a decrease in both H_2S activity and oxygen fugacity due to the alteration of pyrrhotite and bismuth into pyrite and bismuthinite, respectively, can explain the precipitation of gold from an aqueous solution where the gold-bearing complexes are mainly $Au(HS)^0$, $Au(HS)^{2-}$ and $HAu(HS)_2^0$ (fig. 2).

[1] Cathelineau et al. (1993) Eur. J. Min., 5, 107-121; [2] Lescuyer et al. (1993) Chr. Rech. Min., 512, 3-73.

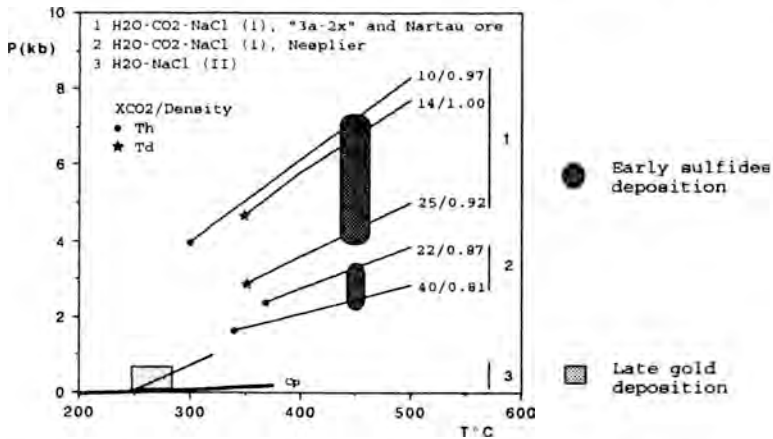


Fig.1-Isochores for the fluids related to sulfides and gold deposition, respectively (Th:homogenization T,Td:decrepitation T,Cp:critical point)

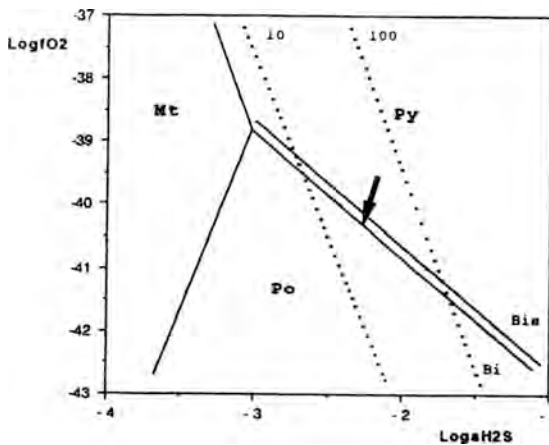


Fig.2- Decrease in fO_2 , a_{H_2S} and gold solubility (dotted curves labelled in ppb) related to the alteration of pyrrhotite (Po) into pyrite (Py). T = 250°C P = 40 bar (Mt: magnetite, Bi: bismuth, Bis: bismuthinite)

SYNTHETIC FLUID INCLUSION STUDIES OF PHASE EQUILIBRIA AND PVT PROPERTIES IN THE H₂O-CO₂-NaCl SYSTEM

BODNAR, R. J.

Fluids Research Laboratory, Department of Geological Sciences,
Virginia Tech, Blacksburg, VA 24061, USA e-mail: bubbles@vt.edu

Phase equilibria and PVT data for the H₂O-CO₂-NaCl system are used to interpret a broad range fluid inclusion types containing both saline brines and volatiles. Until relatively recently the experimental database for this important fluid system was limited to a restricted range of PTX conditions. During the past few years, however, a considerable amount of new information on this system has been published. Much of this work has included development of predictive models or equations of state describing the physical and thermodynamic properties of H₂O-CO₂-NaCl. In this presentation, recent experimental data obtained using the synthetic fluid inclusion technique are summarized.

Sternner and Bodnar (1991) used synthetic fluid inclusions to determine the P-T location of the solvus and the isochores for compositions in the H₂O-CO₂ binary from 400° to 700°C and from 2 - 6 kb. Excess molar volumes calculated from these data show minor (mostly positive) deviations from ideality, with excess volumes increasing both above and below 3 kb. Isochores determined in this study are generally in good agreement with those predicted from published equations of state at low pressure, but show increasing disagreement at higher pressure. The location of the solvus predicted by the synthetic fluid inclusions is in good agreement with data of Todheide and Franck (1963) and Takenouchi and Kennedy (1964) at low CO₂ concentrations. At higher CO₂ concentrations, the solvus determined from synthetic fluid inclusions agrees with that of Todheide and Franck (1963) but shows significant departure from that of Takenouchi and Kennedy (1964).

Phase equilibria and PVTX properties within the ternary have recently been studied by Kotel'nikov and Kotel'nikova (1990) Frantz et al. (1992), Shmulovich and Plyasunova (1993), and Schmidt et al. (1995). All of these studies document the significant increase in pressure along the solvus as NaCl is added to H₂O-CO₂, and studies of immiscible fluids confirm the strong partitioning of NaCl into the H₂O-rich fluid, as suggested by numerous studies of medium and high grade metamorphic rocks. Based on results obtained from synthetic fluid inclusions, Schmidt et al. (1995) calculated PVT data for a constant composition of 40±0.1 wt.% NaCl and 5±0.15 mole% CO₂ (both relative to H₂O) using data from synthetic fluid inclusions. The slopes of the iso-Th lines decrease from 29.5 bars/°C for Th of 400°C, to 6.4 bars/°C for Th of 600°C. Calculated molar volumes for 40 wt.% NaCl + 5 mole% CO₂ solutions at 2 and 4 kbar show trends that are similar to those of other compositions in the ternary system H₂O-CO₂-NaCl at the same pressures and temperatures. Schmidt et al. (1995) reported that all excess volumes for this composition are negative over the P-T range of the experiments, and lie between the values for the compositions H₂O - 5 mole% CO₂ and H₂O - 40 wt.% NaCl.

Diamond (1992) used synthetic fluid inclusions to determine the dissociation temperature of the carbon dioxide clathrate in NaCl + KCl aqueous solutions. These results were used to develop empirical equations to calculate salinities of aqueous inclusions based on low temperature microthermometric behavior.

- DIAMOND, L. W. (1992) Stability of CO₂ clathrate hydrate + CO₂ liquid + CO₂ vapour + aqueous KCl-NaCl solutions: Experimental determination and application to salinity estimates of fluid inclusions. *Geochim. et Cosmochim. Acta*, 56, 273-280.
- FRANTZ, J. D., POPP, R. K., and HOERING, T. C. (1992) The compositional limits of fluid immiscibility in the system H₂O-NaCl-CO₂ as determined with the use of synthetic fluid inclusions in conjunction with mass spectrometry. *Chem. Geol.*, 98, 237-255.
- KOTEL'NIKOV, A. R. and KOTEL'NIKOVA, Z. A. (1990) The phase state of the H₂O-CO₂-NaCl system examined from synthetic fluid inclusions in quartz. *Geokhimiya*, no. 4, 526-537 (in Russian).
- SCHMIDT, C., ROSSO, K. M. and BODNAR, R. J. (1995) Synthetic fluid inclusions. XIII: Experimental determination of the PVTX properties in the system (H₂O + 40 wt.% NaCl) - CO₂ at elevated temperatures and pressures. *Geochim. et Cosmochim. Acta*, (in press).
- SHMULOVICH, K. I. and PLYASUNOVA, N. V. (1993) Phase equilibria in ternary systems formed by H₂O and CO₂ with CaCl₂ or NaCl at high T and P. *Geochemistry International*, 30, 53-71.
- STERNER, S. M. and R. J. BODNAR (1991) Synthetic fluid inclusions. X. Experimental determination of P-V-T-X properties in the CO₂-H₂O system to 6 kb and 700°C. *American Journal of Science*, 291, 1-54.
- TAKENOUCHI, S. and KENNEDY, G. C. (1964) The binary system H₂O-CO₂ at high temperatures and pressures. *American Journal of Science*, 262, 1055-1074.
- TÖDHEIDE, K. and FRANCK, E. U. (1963) Das Zweiphasengebiet und die kritische Kurve im System Kohlendioxid-Wasser bis zu Drucken von 3,500 bar. *Zeitschrift für Physikalische Chemie Neue Folge*, 37, 387-401 (in German).

ELEMENTAL ANALYSIS OF INDIVIDUAL AQUEOUS INCLUSIONS. PART I: NEW DEVELOPMENTS USING MICRO LASER ABLATION OPTICAL EMISSION SPECTROSCOPY (MLA-OES)

BOIRON, M.C. (1), DUBESSY, J. (1), MOISSETTE, A. (1), GEERTSEN, C. (2), BANKS, D.A. (3), PRIETO, A.C. (4), LACOUR, J.L. (5), MAUCHIEN, P. (5)

- (1) CREGU, BP 23 - 54501 - Vandoeuvre-lès-Nancy Cedex, France
- (2) Pechiney, Centre de Recherche de Voreppe, BP27, 38340 Voreppe, France
- (3) Department of Earth Sciences, University of Leeds, UK
- (4) Mineralogy and Crystallography, University of Valladolid, Spain
- (5) LSLA, CEN Saclay, 91191 - Gif-sur-Yvette Cedex, France

Fluid inclusions, as relics of paleo-fluids, can be used as markers of past fluid-rock interactions if the chemical composition of the included fluid is known with a sufficient accuracy to serve as an input in computer code modelling equilibria between fluid phase and rock mineral. Recent developments in the ion analysis of individual inclusions using a prototype apparatus of Micro-Laser Ablation Optical Emission Spectroscopy (MLA-OES) shows that accurate estimations of ratios between major ions will soon be possible.

LA-OES is based on a time-resolved analysis of the emission from atoms present in a plasma produced by a laser pulse. The wavelengths of the emitted line are characteristic of the atomic electronic levels, which allows identification of the emitting atoms. This technique has already been investigated on solids and on Ca-Mg-Cl aqueous solutions either free or included in synthetic fluid inclusions (Boiron et al., 1991). In solids, the reproducibility of the net intensity of the emission line has been shown to be around 10% and the limit of detection was around 1 ppm for most elements which are sensitive to this method.

The radiation used is the 266 nm radiation provided by a pulsed (5 ns) Nd-YAG laser, since plasma using UV radiation of this wavelength has been proven to give better analytical results (Geersten et al., 1994). The laser is focused on the inclusion and the emitted signal is analyzed by a spectrometer with a 200 nm spectral range. In the first step, the ablation process of the quartz matrix has been studied. Ablation is obtained in quartz crystal from an energy pulse above a few μJ . The diameter of the crater does not increase significantly for energy in the range of 30-120 μJ per pulse and is around 5 μm . The depth of the ablated crater is 0.3 μm (Figure 1). Some fractures identified only by Scanning Electron Microscope (SEM) of less than 0.5 μm large may form inside the crater and extend a few μm from the crater.

Synthetic fluid inclusions containing Na, K, Ca, Mg and Li, have been prepared by hydrothermal synthesis for the investigation of the analytical potential and for the calibration of this method. Compositions of the solutions to be trapped as fluid inclusions are analyzed before and after experiments. Small pieces of quartz are crushed and the released solutions are analyzed to control the composition of the trapped fluids using crush leach procedure (Banks and Yardley, 1992).

The investigated elements are Na and K radiating respectively at 589 nm (the unresolved doublet) and (766.5 nm and 769.9 nm) (Figure 2). From the intensity obtained on a single laser shot from a 10 x 10 x 10 μm inclusion, the limits of detection are estimated to be around 20 ppm for Na and 100 ppm for K. The ablation is strongly localized, and does not vaporize the fluid of the opened inclusions

since it was possible to record spectra even after 20 laser shots in the same inclusion. The reproductibility of the intensity ratio between the K and Na line is around 20 %. However, results obtained on solids have shown a reproductibility of the absolute intensity of a single line to be 10 % (Geertsen and Mauchien, to be published), indicating that improvements in the methodology for fluid inclusion analysis would probably increase the reproductibility.

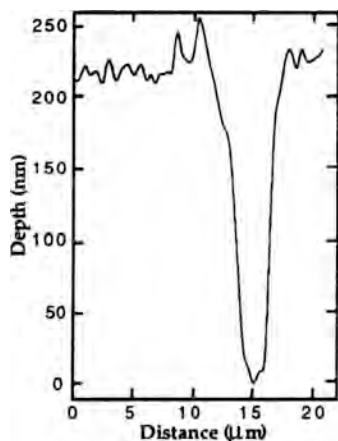


Figure 1 : Depth profile of ablation crater produced by a single laser shot.

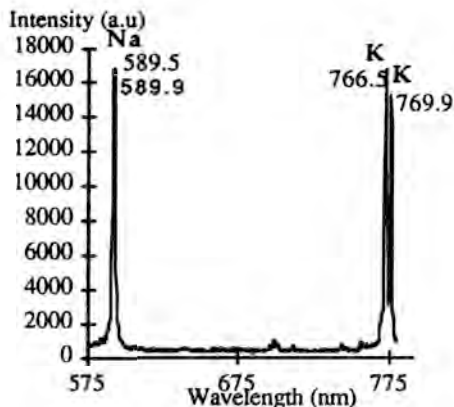


Figure 2 : Emission spectrum of Na and K obtained from a single laser shot on a synthetic fluid inclusion (K + Na = 1 molal and Na/K = 0.1).

MLA-OES appears to be a powerful localized analytical method for trace elements at the ppm level. Alkaline, calco-alkaline elements, metal elements and REE are good candidates for this method but Cl, S bearing species and oxygen cannot be identified. MLA-OES will complement usefully LA-ICP-MS analysis and vice versa, since they give the best accuracy for complementary elements.

Acknowledgements : This work has been supported by the EC programe BCR, Measurement and Testing " Study of Emission Spectroscopy on Laser Produced Plasma for Localized Multielement Analysis in Solids with Surface Imaging" and by the EC - HCM network "Hydrothermal/Metamorphic Water-Rock Interactions in Crystalline Rocks : a Multidisciplinary Approach based on Palaeofluid Analysis".

BANKS D.A and YARDLEY B.W.D., *Geochim. Cosmochim. Acta*, 56, 245-248.
BOIRON M.C. et al., 1991, *Geochim. Cosmochim. Acta*, 55, 917-923.
GEERTSEN C. et al., 1994, *J. A. A. S.*, 9, 17.

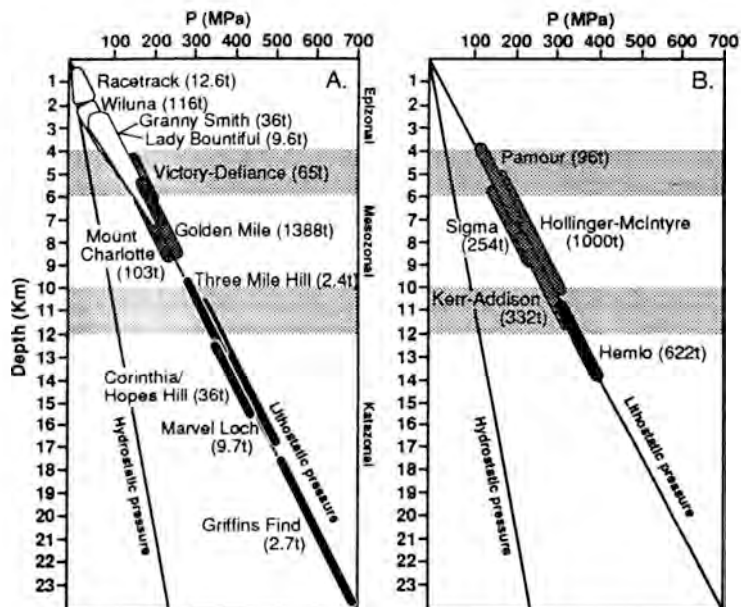
GEOBAROMETRY AND DEPTH RELATIONS IN ARCHEAN LODE-GOLD DEPOSITS

BROWN, P.E. and HAGEMANN, S.G.

The University of Wisconsin-Madison, Department of Geology and Geophysics, Madison, WI 53706, USA
pbrown@geology.wisc.edu

The depth of mineralization for Archean lode-gold deposits from the Yilgarn Craton in Australia and the Superior Province in Canada has been estimated from published data and new fluid inclusion measurements (Fig. 1). Lithostatic pressure conditions were assumed for meso- and katazonal deposits, whereas a mixed litho-hydrostatic pressure gradient was assigned to epizonal deposits. Geological evidence (brittle structural style) and isotopic and fluid inclusion evidence for incursion of surface waters (Hagemann et al., 1994) supports the possibility of a transient hydrostatic pressure gradient during mineralization in the epizonal deposits. For deeper deposits (> 5 km) lithostatic fluid pressures are assumed based on the lack of evidence for surface water influx and hydrodynamic considerations such as the total load of rocks overlying the deposits.

Fig.1 Pressure-depth conditions of Archean epizo- and katazonal lode-gold deposits from the Western Australian Yilgarn Craton (A) and Superior Province in Canada (B). Depths for deposits were estimated using ranges of pressures from isochores. Lithostatic and hydrostatic lines assume pressure gradients of 33 and 100 m/MPa. Note that for the epizonal gold deposits, pressures may vary between litho- and hydrostatic values; for meso- and katazonal deposits constant lithostatic pressures are assumed. The ranges given indicate the uncertainties of estimation. The gray bands indicate the assumed transition zone between the different crustal levels.



The calculated P-depth relations shown in Figure 1A display a continuum of pressure and depths for the formation of lode-gold deposits in Western Australia. These range from shallow, epizonal levels (<1 to 1.5 kbar at ~6 km depth e.g. Wiluna), to mesozonal (1.5 to 4 kbar at 6 to 12 km depth e.g. Mt Charlotte), to deep,

katazonal deposits (>4 kbar at >12 km depth e.g. Griffins Find). Available geobarometric data for lode-gold deposits from the Superior Province greenstone belts in Canada, in contrast, display a distinct clustering of pressure and depths of formation at the mesozonal level (1.5 to 3.0 kbar at >6 km to <12 km depth).

This study confirms earlier fluid inclusion investigations (Hagemann and Ridley, 1993) which presented P-d data that constrained the hypothesis that Archean lode-gold deposits in Western Australia formed over a remarkable range of crustal depths (Groves et al., 1991). In fact it appears that, at least in Western Australia, these deposits are hosted from epi- to katazonal depth levels and therefore contrast to other ore deposit classes, such as VMS and MVT deposits, that form only at shallow crustal levels near the seafloor, or within the top 5 km of the crust, respectively.

When comparing the depth ranges of Western Australian lode-gold deposits with deposits from the Superior Province it is obvious that the latter deposits cluster at mid-crustal levels between 4 and 12 km, except Hemlo which formed at katazonal levels of about 10 to 14 km depth. Interestingly neither the top (i.e. epizonal depths) nor the bottom (katazonal) of the crustal section appears to be represented. One reason for the apparent disparity between the two Archean terrains might be the lack of detailed fluid inclusion studies, hence lack of geobarometric data, conducted in deep and shallow level deposits. Indeed, several well known deposits such as East Main River and Red Lake lack reliable geobarometric data. These deposits are described as being situated in amphibolite facies host rocks with gold mineralization broadly syn- to peak-metamorphic. Consequently they could be classified as katazonal deposits. Conversely, geological constraints, such as structural setting and low temperature ore minerals, argue for a shallow crustal level setting (epizonal) for the Ross Mine in Ontario. However, even though there are possible examples of epi- and katazonal gold deposits in the Superior province, there are still significantly more deposits situated at mesozonal levels.

The apparent lack of giant lode-gold deposits at epi- and katazonal depth levels could be related to a variety of factors, for instance the: (1) lack of exploration in higher and lower grade metamorphic terrains due to specific exploration (genetic) models, (2) lack of exposure of lower and higher crustal rocks due to possible erosion and burial of these crustal sections, respectively, and (3) less favorable transport and precipitation mechanisms for gold at deep crustal levels.

References

- Groves D.I., Barley M.E., Cassidy K.F., Hagemann S.G., Ho S.E., Hronsky J.M.A., Mikucki E.J., Mueller A.G., Mcnaughton N.J., Perring C.S., and Ridley J.R. 1991 In *Proceedings of Brazil Gold'91, An International Symposium on the Geology of Gold*, (ed. E. A. LADEIRA) *Belo Horizonte (1991) Balkeema, Rotterdam*, 299-306.
- Hagemann, S.G. and Ridley, J.R. 1993. Hydrothermal fluids in epi- and katazonal crustal levels in the Archaean; implications for P-T-X-t evolution of lode gold mineralisation. *Australian Geological Survey Organization Record 1993/54*, 123-130.
- Hagemann, S.G., Brown, P.E., Groves, D.I., Ridley, J.R. and Valley, J.V. 1994 The Wiluna lode-gold deposits, Western Australia: Surface water influx in a shallow level Archean lode-gold system (abstr.). 12 Austr. Geol. Congress, Perth, 160-161.

FLUID INCLUSION DATA REDUCTION AND INTERPRETATION USING MacFlinCor ON THE MACINTOSH

BROWN, P.E. and HAGEMANN, S.G.

The University of Wisconsin-Madison, Department of Geology and Geophysics, Madison, WI 53706, USA
pbrown@geology.wisc.edu

MacFlinCor was developed to process laboratory data gathered on fluid inclusions and to calculate P-T isochores for geologically important fluids composed of H₂O, CO₂, CH₄, N₂, and salts (Brown and Hagemann 1994; 1995). Within the program, interactive diagrams are available to describe those chemical systems which cannot be adequately constrained numerically. The user can choose from among multiple published equations of state describing fluid behavior and can easily compare the results obtained by using different equations. Once the basic fluid parameters are established, the program allows the data to be manipulated to permit the determination of, for example, P-T conditions or the evaluation of pressure corrections.

MacFlinCor was developed in HyperCard™ which operates on the model of index cards with each card providing an entry in a simple but powerful database. This approach is ideal for working with fluid inclusions because each "card" in a data "stack" can be used to record all the information about a single inclusion. Nine of the 41 cards are tailored to specific chemical systems for which sufficient experimental data is available to attempt to

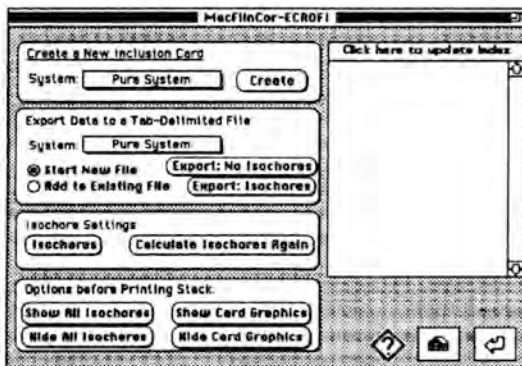


Fig. 1 Initial Index card of a newly created data stack.

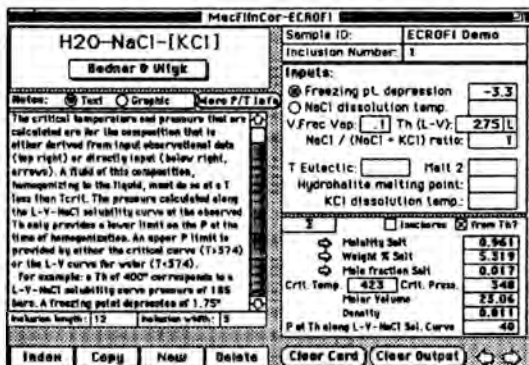


Fig. 2 Card for the system H₂O-NaCl-[KCl].

to the chosen chemical system grayed out (Fig. 3). Below this is a

interpret laboratory observations on individual fluid inclusions. These cards serve as templates that are created and copied automatically from MacFlinCor into a user's data stack by clicking "Create" on the Index card (Fig. 1).

Each of the data cards (eg. Fig. 2) has essentially the same screen layout. In the upper left corner, a popup menu permits the choice of an equation of state for the chemical system at hand. This list of equations is the same on most of the cards with those that are not applicable

large area designed for two purposes. The first use is as a notebook for recording observations in the laboratory during heating and freezing runs. Secondly, clicking on the "Graphic" button above the text box causes the text to be temporarily hidden and to be replaced by a white board upon which simple sketches of the inclusion in question, its relationship to fractures and other inclusions, and



Fig. 3 Equations of State.

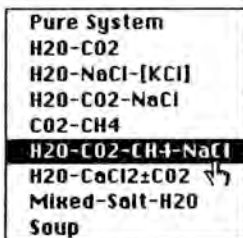


Fig. 4 Systems menu.

other data can be recorded. HyperCard provides a set of drawing tools that are adequate for simple illustrative purposes. This graphic becomes a permanent part of the data record for an inclusion.

The most complicated system that can be approximately modeled using experimental phase equilibria ($H_2O-CO_2-CH_4-NaCl$) can be accessed from the popup menu (Fig. 4) on the Index card. The output area on Figure 5 presents data for both the aqueous and carbonic phases as well as the bulk inclusion. It is not possible to calculate numerically the methane content of the carbonic phase in an inclusion - this must be done graphically. Therefore upon clicking the " Σ " button, the user is taken, in this example, to an

interactive figure in the MacFlinCor stack that has been modified from Thiéry et al. (1994). This figure permits the bulk molar volume and XCH_4 in the carbonic phase to be derived from microthermometric data. The bulk density allows the reasonably well known isochores for pure CO_2 to be applied to the mixed CO_2-CH_4 system. On returning from the CO_2-CH_4 card, the remaining calculations are automatically made on the data card.

Returning to the Index Card, a list of data cards present in the stack can be made on the right hand portion of the card (Fig. 1). Data from the stack can be exported to a tab delimited file which can be read and manipulated by spreadsheet or statistical programs.

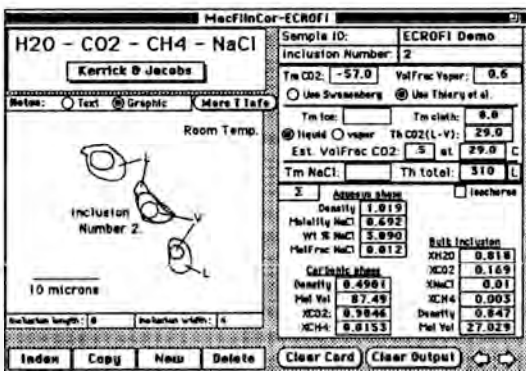


Fig 5 Data card for inclusion fluids in the system $H_2O-CO_2-CH_4-NaCl$.

References

Brown, P.E. and Hagemann, S.G. (1994) MacFlinCor: A computer program for fluid inclusion data reduction and manipulation. In De Vivo and Frezzotti (eds) Fluid Inclusions in Minerals: Methods and Applications, VPI Press, 231-250.

Brown, P.E. and Hagemann, S.G. (1995) The program MacFlinCor and its application to geobarometry in Archean lode-gold deposits. *Geochim. Cosmochim. Acta* (in press).

Thiéry R., Kerkhof A.M. Van Den and Dubessey J. (1994) vX properties of CH_4-CO_2 and CO_2-N_2 - Modeling for fluid inclusions ($T < 31^\circ C$, $P < 400$ bar). *European J. Mineral.* v. 6, 753-771.

FLUID INPUTS AND MASS TRANSFER DURING ALPINE BRITTLE DEFORMATION OF THE MONT-BLANC GRANITE

CATHELINEAU, M.(1), AYT OUGOUGDAL, M.(1), BANKS, D.(2), LESPINASSE, M.(1), BOIRON, M.C.(1) and POTY, B.(1)

(1)CREGU, BP 23, 54501 - Vandoeuvre-lès-Nancy, France,

(2)Leeds University, Woodhouse Lane, LEEDS LS29JT, UK

Study of fluid migration in crystalline rocks is frequently restricted to regions where clear evidences of water-rock interactions, e.g. the crystallization of authigenic or metamorphic minerals along fluid flow paths, especially macroscopic fractures. This is especially the case for the study of alpine fluids which are linked to nappe carriage, overthrusting, and retrograde metamorphism. Such fluids have been predominantly studied in the euhedral quartz crystals from the alpine clefts. The objective of this work was : i) to describe the fluid migration outside major channels, and to determine if the microfissural permeability around the cleft networks has played a significant role in the fluid transfer, and then : ii) to obtain additional constraints on the source of waters implicated in the strong water-rock interaction processes which affected the granites.

Methodology

Oriented blocks of granites, altered granites (quartz depleted granites) and cleft infillings have been sampled in the Mont Blanc granite (Argentières glacier) as well as euhedral quartz types from various localities in the massif (Col des Cristaux, Les Mottets, Pointe Kurtz, Pointe Hellbronner). Some comparisons are made with samples from the Grimsel zone (Aar, Switzerland), and La Gardette (Bourg d'Oisans, France). The relative chronology between fluid inclusions, the genetic relationships between a given fluid event and the quartz healing (FIP) or crystallization (new growth zones in euhedral crystals) has been studied with respect to the 3D geometric features of their host micro to macrostructures by using optical and scanning electron microscopy (SEM cathodoluminescence imaging). Characterization of P-T-V-X features of percolating fluids was obtained through a multidisciplinary study of fluid inclusions (microthermometry, quantitative in-situ analysis of gas and molecular species contents by Raman spectroscopy and FT-IR). The determination of the bulk ion chemistry was done using crush-leach procedures combined micro analysis of the leachates.

Geometry of the fluid migration

In the Mt Blanc granite, strong water rock interactions are exemplified by a complete dissolution (episyenites) of the granite quartz and redeposition of the transported silica, as euhedral quartz and silicates (albite, adularia, chlorite) in nearby fractures displaying (or not) quartz dissolution textures at their edges. This process occurs along subhorizontal extensional vein networks formed under ductile/ brittle conditions at the end of the main compressional alpine event.

Fluids migrate not only in the sealed veins, but in healed cracks within the granite (fluid inclusion planes (FIP)) attesting the existence of a significant microfissural permeability in the whole granite mass. At Pointe Kurtz, main EW FIP are subhorizontal (0-30° N) and parallel to the main extensional vein, and associated

to a complex network of FIP (NW-SE, large range of dip). These FIP contain fluids displaying the same features as those observed in the main infillings of the tension gashes. Thus, it is clear that the transfer of silica which is extracted during the quartz dissolution process without any alteration of the other granite minerals is mainly linked to connected microcrack networks in the wall-rock of the main fractures.

Fluid chemistry

Originally the fluids were aqueous, with a salinity of 5.7-12.6 wt.% eq. NaCl. Th range from 150 to 220°C in the euhedral quartz crystals, and are around 150°C in NW-SE FIP and 210°C in NS FIP networks at Pointe Kurtz. Tm-Th plot shows an evolution in the Tm-Th pairs. Values are nearly constant within specific FIP networks or cleft localities. However, the whole data shows an evolution from the lowest Tm (-4°C) corresponding to the lowest Th around 150°C, to the highest Th-Tm pairs (230°C, -7°C). Thus, the Th fluctuations cannot only be explained easily as markers of P fluctuation, but must also reflect some mixing and/ or cooling of the circulating fluids.

The presence of a low density CO₂ component accompanied by small amounts of N₂, and sometimes CH₄ (in the case of La Gardette for instance) is common as shown by FT-IR analysis, and in some instances by Raman spectroscopy. It indicates the input of volatiles from external sources, mostly during the crystallization of the late assemblages (amethyst quartz, ankerite-phengite).

Cation chemistry

The main analyzed cations are Na, K, Ca, Mg, Sr, Fe, Mn. The ratio K/Na is rather constant for most of the early quartz generations, and equal to 0.15 ± 0.01 , confirming earlier result obtained on greater size sample (Poty and Stalder, 1974). This ratio may indicate a temperature of around $400^\circ\text{C} \pm 50^\circ\text{C}$ using the Na-felspar/microcline geothermometer. The Na/K(at.) ratio is significantly different in samples displaying inclusions with detectable CO₂ (even only detected by FTIR). This is particularly the case for amethyst quartz in Mont Blanc, and La Gardette samples, with K/Na ratios around 0.10 ± 0.02 . The Mg/Ca (at.) ratio is in the range of 0.01 to 0.1, Sr/Ba(at.) is in the range of 0.5 to 2.8 and Fe/Mn (at.) from 2 to 30.

Anion chemistry to

The halogen chemistry (Br/Cl and I/Cl ratios) data documents the interactions between the fluids and the basement rocks, and may indicate a mixing of two different fluids. Parts of the Br/Cl (wt) ratio values are in the range of 0.0020/ 0.0025, but others close to the sea water ratio. Br/Cl ratio increases with salinity up to 0.0049 (at la Gardette), thus implying that the saline fluid component is enriched in Br, and could correspond to fluids equilibrated with sediments. The Cl/ SO₄ (at.) ratio displays a rather wide range from 5 to 320, which could indicate the local involvement of sulfate from the host rocks.

The data obtained at the scale of the studied alpine clefts seem rather similar indicating that fluids have similar sources (the surrounding metamorphic series) and produce the same effects on granites at the scale of the alpine belt. However, the data obtained on leachates give further constraints on the model of mass transfer and equilibria between percolating fluids and the granites, and argue in favour of more complex processes (mixing) than originally thought.

MELT INCLUSIONS IN ZIRCON FROM ARCHEAN ROCKS: PETROLOGICAL SIGNIFICANCE AND RESULTS OF STUDY.

CHUPIN V.P. & CHUPIN S.V.

Institute of Mineralogy and Petrography, Universitetsky pr.3, 630090 Novosibirsk, Russia.

The results of inclusion study have shown that primary rocks (protoliths) of ancient gneisses were intensively transformed under high-temperature metamorphism (especially under granulite metamorphism). Rock-forming minerals of enderbite- and charnockite gneisses contain only fluid inclusions. Likely, only ancient cores of zircon are restite (non-altered) mineral of protoliths. They contain preserved primary melt inclusions. The study of latter inclusions permits to evaluate the origin of ancient zircon and make possible to recognize the nature of protoliths of gneisses, composition of magmas as well as characteristic features of primary-crustal magmatism in the early stages of the Earth's continental crust formation (Chipin et al., 1993; Chupin et al., 1994).

Primary melt inclusions in zircon cores are glassy. The glass in these inclusions were determined by means of an optic method and by the analyzing chemical composition and Raman spectra of unheated inclusions. The presence of glassy inclusions indicates fast cooling of melts. It is characteristic of volcanic and subvolcanic rocks.

The study revealed magmatic, perhaps, subvolcanogenic nature of protoliths of tonalite (3,33 Ga) and charnockite (about 3,3 Ga) gneisses of the Aldan shield and the Uivak trondhjemite gneiss (3,73 Ga) of the Canadian shield. Protoliths of enderbite gneisses (>3,3 Ga) of the Anabar shield were likely to be of volcanogenic origin.

In some analyses of glass of inclusions from the cores of zircon from enderbite gneiss of the Anabar shield and from the Uivak gneiss of the Canadian shield essentially sodium trachyandesite (about 57 wt.% SiO₂) and trachybasaltic composition of melt were obtained. These melts from which the earlier cores of zircon were crystallized are supposed to characterize the primary basic substratum being a source of tonalite-trondhjemite magmas.

Essentially sodium trachyandesite (62,3 wt.% SiO₂) composition was obtained from glass of inclusions from zircon of tonalite gneiss and potassium-sodium rhyodacite composition - from zircon of charnockite gneiss of Aldan shield. It is possible that these compositions reflect the composition of initial magmas from which gneiss's protoliths were crystallized.

By results of melt inclusions investigations, geochronological and geological data it is supposed that protoliths of tonalite and charnockite gneisses had common or close (in time) source of initial magmas. Probably these protoliths were united magmas series and potassium acid rocks were formed on the early stages of the Aldan shield's continental crust formation.

Melt inclusions in zircon from archean pararocks of South Africa were also studied: OGQ quartzites from the Witwatersrand

deposit, paragneisses of Singelel, and quartzites from the Limpopo belt. It was established that zircons from OGQ quartzites were crystallized from tonalite-trondhjemite (with a low content of Cl - < 0,10 wt. %) and K-sodium rhyodacite (with a high content of Cl - 0,4-0,6 wt.%) melts. Zircons from the paragneiss were crystallized from K-sodium rhyodacite melts (with elevated content of Cl - 0,11-0,49 wt.%). Zircons from quartzites of the Limpopo belt were crystallized from trondhjemite and K-sodium rhyolite magmas of the S-type (with a low content of Cl - 0,07-0,09 wt. %). These data confirm the conclusions of E.S.Barton et al. (1989) that the rocks of tonalite-trondhjemite composition were one of sources for the Witwatersrand sediments.

We express our thanks to A.B.Kotov, L.M.Stepanyuk, D.Bridgwater and J.M.Barton for the collection of zircons.

References:

- Chupin, V.P., Tomilenko, A.A., Chupin, S.V. (1993). Geology and Geophysics (in Russian), 12, 116-131.
Chupin, V.P., Chupin, S.V., Pospelova, L.N., et al. (1994). Dokladi Akademii Nauk, v.338, N 6, 806-810.
Barton, E.S., Compston, W., Williams, I.S., et al. (1989). Economic Geology. v.84, 2012-2019.

EVOLUTION OF FLUORINE AND OTHER VOLATILES DURING THE CRYSTALLIZATION OF RARE-METAL GRANITOID AND ONGONITE MELTS: THE STUDY OF MELT AND FLUID INCLUSIONS

CHUPIN, V.P., SMIRNOV, S.Z., KUZMIN, D.V. & TITOV, A.V.

Institute of Mineralogy and Petrography, Universitetskii pr.3, 630090, Novosibirsk, Russia.

Melt and syngenetic fluid inclusions in quartz, zircon and topaz of lithium-fluorine granitoids of the Bazardarin polyphase massif (South-Eastern Pamir) and ongonites of the Ary-Bulak stock (Eastern Transbaikalia) have been studied. Crystallized melt inclusions are inherent to the minerals of granitoids of Bazardarin massif. For minerals from the ongonites of the Ary-Bulak stock glassy and partially crystallized inclusions are usual. The composition of fluid phase in melt inclusions and fluid ones have been studied by Raman spectroscopy and freezing stage. Water content in melt inclusions has been determined by calculation method. The major elements, F and Cl contents in glasses of heated melt inclusion have been analyzed by electron microprobe. The temperature range of crystallization has been determined by means of homogenization temperatures of primary melt inclusions.

Data obtained allow to establish fluorine, chlorine and other volatiles evolution during the crystallization both of leucocratic magma and ultra fluorine (ongonite) melts. The enrichment in H₂O, F, and Na is characteristic of the differentiates of Bazardarin polyphase massif. The sequence of phases is: granites of the first phase (820°C, <4 wt.% of H₂O) --> leucogranites of the main phase (750°C, about 0.5 wt.% F and 4-5 wt.% H₂O) --> leucogranites of additional intrusion phase (730°C, about 0.5 wt.% F and about 5-6 wt.% H₂O) --> topaz-bearing aplites (650°C, 1.1 wt.% F and 9-10 wt.% H₂O) --> topaz-protolithionite granites (660°C, 1.2 wt.% F and 8-11 wt.% H₂O) --> ongonites (700°C, 1.9 wt.% F and 6-7 wt.% H₂O). Melt and syngenetic fluid inclusions in quartz of granites, aplites and pegmatites contain CO₂ and fewer amounts of N₂ and CH₄ along with H₂O. Inclusions in quartz of ongonites contain N₂ and CH₄ in addition to H₂O. It is shown that initial melts of Ary-Bulak stock ongonites were richer in F (about 3 wt.%) and higher in temperature (up to 1000°C) than liquids of the Bazardarin massif ongonites (700-670°C) and topaz-bearing granites (about 660°C). High-temperature (up to 1000°C) water-poor (less than 2 wt.% H₂O) melt inclusions in quartz of Ary-Bulak ongonites contain N₂ and trace amounts of CO₂. The later melt inclusions (Th=) contain only low-density CO₂. Fluid inclusions syngenetic to the later melt ones contain CO₂+H₂O solution of low density.

The specific residual melts depleted in SiO₂ (up to 60-62 wt.%) and enriched in F and other volatiles were formed during crystallization of rare-metal ultra fluorine magmas of both massifs. The high F-contents in initial ongonitic melt is suggested to be responsible for considerable temperature interval of magmatic crystallization of the Ary-Bulak massif ongonites (from about 1000° to 500°C for quartz and up to 450°C for topaz).

MELT AND FLUID INCLUSIONS IN HIGH-PRESSURE MINERALS (KYANITE, GARNET, QUARTZ): FEATURES OF STUDY AND INTERPRETATION.

CHUPIN V.P. & TOMILENKO A.A.

Institute of Mineralogy and Petrography, Universitetsky pr.3, 630090 Novosibirsk, Russia.

High-pressure minerals expand at reduced pressures. Thus, the sizes of inclusions increases (especially in quartz) and their density decreases. These phenomena influence the homogenization temperatures (Thom.) of inclusions. On heating in standard stages (at 1 atm.) Thom of melt inclusions may be higher than their preservation temperatures (for volatile-saturated melts). The negative temperature correction for melt inclusions in quartz of migmatites of granulite facies (pressure 5-7 kbar) reaches 30-50°C (Tomilenko, Chupin, 1983).

For melt inclusions trapped at higher pressures (about 15 kbar) this correction may be 200°C and more. These data were obtained when studying melt inclusions in kyanite, garnet, quartz and sanidine from low-crust (pressure about 15 kbar) granulites from xenoliths in alkali-basaltoid explosion pipe, Eastern Pamir (Chupin, et al. 1993). The phase composition in quartz: glass + heterogeneous fluid bubble + crystalline phases. The fluid bubble consists of carbon dioxide with a density 0,3 g/cm³ (data of cryometric and Raman-spectroscopy analyses). On heating to 800°C in a standard stage (at 1 atm), separation of additional carbon dioxide bubbles occurs and their density increases up to 0,8 g/cm³. The concentration of carbon dioxide reached 1,5 wt.% (calculated data). At 1 atm inclusions do not homogenize even at 1300°C. However, they homogenize at 1050°C when the external pressure is 12 kbar (the experiments were carried out by A.D. Babansky in the IGEM of the RAS, Moscow on the device of cylinder-piston type).

Results of these studies showed that: a) Thom of melt inclusions in high-pressure minerals might be considerably higher than their preservation temperatures. To estimate their true Thom, it was necessary to perform the experiments at pressures similar to natural ones; b) the appearance of additional bubbles of carbon dioxide in inclusions and the decrease in its density is of great importance in calculation of carbon dioxide concentration in the melt and estimation of pressure. If the density of carbon dioxide is taken as 0,3 g/cm³, then the calculation will yield a reduced (2,5-3 times) content of carbon dioxide in melt inclusions.

The volumetric effect of compression of minerals is needed to be taken into account when determining the density of fluid inclusions in high-pressure minerals. The density of such inclusions at 1 atm is essentially lower than at their preservation temperatures. This phenomenon has been studied experimentally. Phase transformations in fluid inclusions in quartz were observed when the pressure was increased from 1 atm to 50 kbar. The experiments were performed at room temperature at high-pressure device with diamond anvil cell for optic, X-ray and Raman-spectroscopic studies (Belitsky et al., 1992). An increase in the density of carbon dioxide inclusions from 0,60 to 0,75 g/cm³

was found when pressure increased up to 18 kbar. A solid phase (ice or crystal hydrate) appears in water-salt inclusions (gas + liquid) at pressure of about 20 kbar and the bubble disappears - at pressure about 30 kbar.

References

- Tomilenko A.A., Chupin V.P. (1983). Thermobarogeochemistry of metamorphic complexes. Nauka, Novosibirsk, (in Russian):200 p.
Chupin V.P., Tomilenko A.A., Chupin S.V. (1993). Geology and Geophysics (in Russian), 34(12):116-131.
Belitsky I.A. et al. (1992). Phys. Chem. Minerals, 18:497-505.

VOLATILE COMPOSITIONS OF FLUID INCLUSIONS FROM A CARLIN-TYPE GOLD DEPOSIT: GETCHELL, NEVADA, USA

CLINE, J.S. (1), HOFSTRA, A.H. (2) LANDIS, G.P. (2) and ALLERTON, S. (2)

(1) Department of Geoscience, University of Nevada, Las Vegas, Nevada, USA 89154-4010

(2) U.S. Geological Survey, MS-973, Box 25046, Denver, Colorado, USA 80225

Increased production of gold from Carlin-type deposits has made Nevada the world's second leading gold producer. These deposits are generally large-tonnage, low-grade, low-sulfide, epigenetic, replacement deposits hosted in carbonate sedimentary rocks. Gold occurs as discrete, disseminated micron and sub-micron grains, often associated with arsenic-rich pyrite and marcasite. Alteration is characterized by decarbonatization, silicification, argillization and sulfidation. Despite much study, both the age of mineralization and physico-chemical environment of ore formation are controversial.

The Getchell deposit is hosted in Cambrian and Ordovician limestones and shales along a series of anastomosing, north-striking, east-dipping normal faults. The fault zone lies along the NE margin of a large Mesozoic (94 Ma) granodiorite pluton. Locally the pluton contains milky quartz veins with sericitic alteration envelopes. Much of the gold is produced from replacement ores along and within the fault zone. The Getchell deposit is unusual in that it also contains a coarse-grained, open-space-filling ore assemblage that precipitated within the fault zone. Euhedral minerals from this assemblage are divided into 3 stages: ore-stage quartz, fluorite, orpiment, pyrite, marcasite, and gold; late-ore-stage realgar, calcite, barite, marcasite, and gold; and post-ore calcite.

The volatile compositions of fluid inclusions in these minerals were analyzed quantitatively using a quadrupole mass spectrometer. Analyzed samples include Mesozoic quartz veins in and outside the deposit; ore-stage quartz, fluorite, and orpiment; late ore-stage realgar, calcite, and barite; and post-ore calcite. Most samples were incrementally heated and gases from individual inclusions or inclusion planes were released by decrepitation and analyzed. Orpiment and realgar were crushed and a bulk fluid was analyzed.

Calibration studies have shown that the amount of H₂O measured from small inclusions is low owing to adsorption of H₂O onto surfaces inside the mass spectrometer during analysis. H₂O measurements from larger inclusions, with signal to noise (SN) ratios > 5, are accurate because the amount of H₂O lost by adsorption is negligible relative to the amount of water in the inclusion. Losses by adsorption for most other gases analyzed are negligible for gas concentrations large enough to be detected. The results from Getchell samples support these observations as analyses of larger inclusions tend to record higher H₂O contents. Large inclusions (SN > 5) were relatively common in fluorite, realgar, calcite, and orpiment and, with the exception of fluorite, yield consistent results. Most inclusions in quartz were small, and have highly variable H₂O contents; a few large inclusions present in Mesozoic quartz and ore-stage quartz yield reliable results. Analyses from 26 samples are tabulated below.

Data as range of values in mole percent

Sample	H ₂ O	CO ₂	N ₂	H ₂ S	Σ HC	±trace
MzQ-away from ore*	73-90	9-24	0-3			
MzQ-away from ore	81-82	15-16	1-3		tr	
MzQ-away from ore	15-57	35-77	2-7		0.1-0.4	
MzQ-near ore*	0-95	0-62	0-15	0-9	0-56	H ₂
MzQ-near ore*	1-100	0-91	0-20	0-2	0-33	
MzQ(?) -mineralized*	1-96	0.2-15	0-13	0-4.2	0-87	H ₂
Q-ore stage	88-97	2-11	0.2-0.6	0.1-0.2		HC, H ₂
Q-ore stage (?)*	80-100	0-16.5	0-2.3	0.1-0.4	0-1.4	
Q-jasperoid*	96-100	0-4				N ₂
Fl-ore stage	75-89	11-25		0.1-0.4	tr	HF
Fl-ore stage	3-91	7-89	0.2-8	0.1-1	tr	HF, H ₂
Orp-ore stage?	44-61	30-45	2-4	0.2-0.4	4.5-8	SO ₂
Rlg-late ore stage	95-99	1-4	0-0.3	0-0.9	0-3	HF, H ₂
Cc-late ore stage	96-99	1-3	0-0.9	0-0.1	tr	
Cc-late ore stage	72-91	9-22	0-3.6	0-0.2	0.6-5.6	
Bar-late ore stage	No inclusion bursts					
Cc-post ore	97.5-99.5	0.5-2.5				

* SN < 5; probably low H₂O analyses

Inclusions in pre-ore Mesozoic quartz veins (MzQ) have a wide variety of compositions and variable H₂O-gas ratios. Generally H₂O or CO₂ are dominant; however, CH₄ is dominant in many inclusions. Minor to trace N₂ and H₂S were detected in most inclusions.

Most inclusions in ore-stage minerals are water-dominant. CO₂ is the major gas and minor H₂S is ubiquitous. Minor to trace CH₄, short chain hydrocarbons (SCHC), and N₂ may be present. The presence of both H₂O- and CO₂-dominant inclusions in fluorite (Fl) may indicate fluid immiscibility or inclusion necking. Immiscibility is substantiated by petrographic observation of two-phase liquid-rich and two- and three-phase vapor-rich inclusions. Inclusion fluids released from orpiment (Orp) by crushing contain sub equal H₂O and CO₂ with minor N₂, CH₄, SCHC, and H₂S. The near equivalence of H₂O and CO₂ in bulk analyses may indicate the presence of H₂O-dominant and CO₂-dominant inclusions. Inclusion fluids in late ore-stage realgar (Rlg) and calcite (Cc) are H₂O-dominant and contain minor CO₂ and small amounts of N₂, HC, and ubiquitous H₂S. Late ore-stage minerals generally have lower CO₂ concentrations than ore-stage minerals, although one calcite sample had relatively high CO₂. No inclusions were detected in barite (Bar). Post-ore inclusions in calcite are water dominant.

The ore fluid is H₂O-dominant with major CO₂ and ubiquitous, minor H₂S, and was capable of producing observed mineral and alteration assemblages. The low homogenization temperatures (<260°C), moderate pH (4-6) and consistent H₂S concentrations (10⁻¹ to 10⁻² molal) in ore stage fluids suggest that gold was transported as a bisulfide complex. The high CO₂ concentrations promoted decarbonatization of the host rocks, increased rock permeability, and exposed iron. Sulfidation of iron in host rocks may account for much of the gold in the replacement ores. The open-space-filling assemblage quartz-fluorite-orpiment-realgar indicates that cooling played a role in gold deposition; however, the presence of gas-dominant inclusions suggests that effervescence may have been important also.

CONTRASTED POLYPHASE HISTORY OF GOLD MOBILIZATION AT FAZENDA BRASILEIRO AND FAZENDA MARIA PRETA, RIO ITAPICURU GREENSTONE BELT: THE ROLE OF EARLY HYDROTHERMALISM, ORGANIC MATTER, DUCTILE-BRITTLE DEFORMATION AND TEMPERATURE.

COELHO C.E.S. (1,2), RAMBOZ C. (2) and BENY C. (3)

(1) Departamento Nacional da Produção Mineral, Brazil; (2) CRSCM/CNRS, 1A rue de la Férellerie, F45071 Orléans cedex 2; (3) BRGM, DR/GPC, BP 6009 F45060 Orléans

Fazenda Brasileiro (FB) and Fazenda Maria Preta (FMP) gold mining districts are located in the Early Proterozoic Rio Itapicuru greenstone belt (RIGB), which lies in the northeastern part of the precambrian Sao Francisco Craton (Bahia State, Brazil). Structural studies in the field and at the micrometer scale show that both mineralized districts were emplaced during the greenschist facies ductile/brittle deformation.

Structural settings of the gold mineralizations.

-The FMP district in the northern part of the RIGB, consists of four parallel N-S-trending shear zones (D1 stage), which are hosted in andesites interlayered with pyroclastics, sediments, dioritic and dacitic intrusions. Mineralized shear veins, rarely extensional, are mainly found at lithological contacts which concentrate the shear deformation.

-The FB Mine is situated 100 km south of the FMP district, in a 8 km-wide E-W shear zone in the mafic-felsic domain at the southern end of the RIGB. The D1-dominant event corresponds to a transcurrent dextral ductile shearing. Later D2 deformation corresponds to a ductile-brittle northward thrusting event. Hydraulic fracturing, hydrothermal alteration, concordant and discordant mineralized vein formation at FB is mainly syn-D2 [1].

Polyphased hydrothermal history of the gold mineralizations.

Early hydrothermal metamorphism H1.

Petrography. In the FB mine area, 3 main lithological facies have been identified ([1] and this work). (i) organic-rich acidic tuffs (CLXv), (ii) chlorite-magnetite schists which mainly host the mineralization (XM); (iii) sulphide-rich quartz-albite altered rocks (SUF), which result from the alteration (sulphidation) of the XM schists around mineralized concordant and discordant quartz veins.

Fluid inclusion (FI) and Raman spectrometric (RS) studies. The quartz porphyroclasts and pods from XM and CLXv predating the D1-related metamorphic schistosity S1 are called generation Qo. Quartz Qo from both facies contains liquid-dominant FI with abundant complex Ca-Mg-Fe-Mn carbonates. Organic-rich quartz pods specific of CLXv contain additional halite-saturated type S FI, vapour-rich type V FI which are CO₂-CH₄-bearing, and mixed type VS FI. They contain abundant 'semi-graphite-like' particles, either scattered or along trails. RS also reveals the presence of relic carbonaceous matter attached on early carbonate micro-solids from quartz pods. Preliminary measurements show bulk homogenization temperatures by halite melting =250°C.

Interpretation. At FB, all the porphyroclasts in the XM and CLXv facies, which predate S1, are related to an early syngenetic hydrothermal event H1 : quartz Qo, albite, apatite, marcassite, pyrite, pyrrhotite from both facies; magnetite, rare sphalerite in the XM schists; hematite, leucoxene and rutile in the CLXv facies.

We thus confirm in FB mine area the M1 early hydrothermal metamorphism identified by Silva [2] in the northern part of the RIGB. In felsic rocks, early hydrothermalism is marked by the following: (1) maturation of interstratified organic matter to 'semi-graphite'; (2) oxidation of the wall-rock (hematitization, oxidation of organic carbon to CO₂ and carbonates, as confirmed by isotopic data [3]), which are related to long-duration boiling of the CO₂-CH₄ saline fluids, with transient halite saturation; (3) gold pre-concentration, as shown by inframicroscopic gold particules adsorbed on semi-graphite. Abundant precipitation of Fe-Mn-carbonates in the CLXv facies, the presence of minor sphalerite show that the early hydrothermal fluids were metal-bearing. In the XM schists, the growth of magnetite phenoclasts predating S1 instead of hematite indicates that the early hydrothermal fluids became rock-dominated as they circulated in the XM facies, their fO₂ being buffered by Fe²⁺-bearing minerals from the wall-rock. At FMP, the widespread occurrence of hematite and 'anthracite-like' particles in the carbonaceous schists from the wall-rock of the vein system confirms a pervasive oxidation of the pile related to stage H1.

-Mechanism of vein opening during prograde metamorphism. Mineralized quartz at FMP and FB characteristically contain primary water-deficient (≤1mole%) CO₂-CH₄-bearing FI with trapped anthracite-like carbon compounds. Their composition in the C-O-H system consistently shows that, rather than being leaked aqueous FI, they record the primary mechanism of quartz vein opening and filling: the combustion of early-formed 'semi-graphite' or 'anthracite', which favoured the disappearance of the metastable hematite-carbon association inherited from stage H1. At FB, temperature was high enough to allow a near complete disappearance of earlier-formed hematite. At FB, the P-T conditions of vein opening fixed by FI data are ≈400°C-500°C, 2 to 3.5 kb, with fO₂ overpassing the upper stability limit of carbon ≈2 10⁻²⁵ bar. At FMP, the widespread persistence of the metastable carbon-hematite association in the wall-rock, the coexistence in vein quartz of primary water-dominant CO₂-CH₄-bearing FI with water-free C-bearing FI suggests that temperature only transiently reached the blocking T of the 'graphite-fluid' equilibrium ≈ 400°C. This is confirmed by the fact that the isochores representative of cogenetic H₂O-rich and H₂O-poor FI intersect at ≈350°C, 2kb. Gold was probably introduced in the vein system at FB and FMP attached on carbon compounds and freed as carbon volatilized. This is confirmed by the reported presence of gold particles in H₂O-poor FI at FMP [3].

-Ductile, ductile-brittle evolution. At FMP, quartz vein fabric study points out limited recrystallization textures and widespread microfracturing processes [4]. Cogenetic secondary H₂O-rich and H₂O-poor FI underlining μm- to cm-long cracks in quartz show that P-T-fO₂ conditions did not significantly change during later brittle-ductile, brittle evolution of the vein system. At FB on the contrary, abundant primary and secondary H₂O-dominant CO₂±CH₄±N₂-bearing FI, obliterating the relic early C-bearing FI, favoured quartz recrystallization and widespread wall-rock alteration. Their representative isochores imply a fluid pressure increase, which could be related to the late D2 thrusting of the Barrocas dome. The presence of sphene in the SUF facies fixes the conditions of quartz-recrystallization and mineralisation at FB at T=500°C and P=4.5 kb. Larger economic gold mineralization at FB than at FMP can thus be attributed to higher temperatures: it enhanced degassing and hence, particulate gold transport into the vein system, then it increased later gold solubilization [5]. Besides, a longer-lived evolution in

the ductile-brittle transition regime at FB probably favoured abrupt gold deposition by allowing transient boiling (as shown by late hematite) or reaction of the Au-bearing solutions at the surface of the broken sulfides (arsenopyrite).

Bibliography.

- [1]REINHARD & DAVISON, 1990, Econ. Geol., v.85, 952;
- [2]SILVA; 1984, see reference in [1];
- [3]XAVIER, 1991, Unpub. Ph.D Thesis, Southampton;
- [4]COELHO, 1994, unpubl. Ph.D Thesis, Orléans;
- [5]GIBERT ET AL., 1993, Procceding of the 4th International Symposium on hydrothermal reactions, Nancy.

THRUST ASSOCIATED GOLD MINERALIZATION IN AN ARCHAEOAN AURIFEROUS QUARTZ-CARBONATE VEIN SYSTEM AT THE EERSTELING GOLD MINE, SOUTH AFRICA

COETZEE, D.S. (1) & KALBSKOPF, S. (2).

(1) Department of Materials Technology, Technikon Pretoria, Private Bag X680, Pretoria, 0001, South Africa.

(2) P O Box 6084, Pietersburg North, 0750, South Africa.

INTRODUCTION

The farm Eersteling ("first born") situated in the 3 000 My old Pietersburg greenstone belt is the site of the first goldfield in the RSA. The history of this goldfield was discussed by Baines (1877), Willemse (1938), Balpin (1965) and De Jong (1986). Edward Button discovered alluvial gold and an Au-bearing quartz reef in 1871 which he named the Natalia Reef, and which is today known as the Maltz Reef and he erected the first crushing and milling plant in South Africa in 1873. Between 1900 and 1980 the large number of claim owners (\pm 100) seriously hampered the activities around Eersteling. Nevertheless, at least 320 kg of Au was produced between 1906 and 1937 (Willemse, 1938). After a series of transactions the Eersteling Gold Mining Company was founded in 1986 and began operations in January 1987.

REEF LITHOLOGIES

The gold mineralization in the vicinity of Eersteling typically occurs in quartz-carbonate vein systems within coupled shear zones. Two major mineralized settings occur. They are the Pienaar, Doreen and Girlie Reefs within east-west trending shear zones, and the Maltz, Dog and other unnamed reefs within Riedal shear zones trending roughly ENE oblique between the Doreen and Pienaar Reefs in the south and north respectively.

The Maltz Reef is a typical mesothermal shear zone hosted, quartz-carbonate lode gold deposit clearly showing evidence of brittle and ductile deformation. The pervasive carbonate alteration of the wall rocks is regarded as pre-vein-quartz formation, while a second carbonatization event accompanied the introduction of Au, As, S and K coupled with shearing and brecciation of quartz giving rise to pay shoots. Fine-grained tourmaline is also associated with gold concentrations in the vein-wall rock boundaries and carbonated aureole. Further hydrothermal fluid pulses have superimposed significant barren ferroan dolomite and calcite veining in places.

QUARTZ VEIN FORMATION & FLUID INCLUSIONS

Quartz vein formation succeeded the initial phase of carbonitization in the Maltz shear zone. The quartz vein (20 cm - 2m wide), which dominates the Maltz Reef, was initially a poorly mineralized pale cloudy variety and was subsequently considerably modified by tectonism. This quartz vein currently grades from the barren unaltered variety to laminated, ribbon textured and brecciated mineralized varieties, often containing coarse free Au.

Fluid inclusions observed in undeformed, moderately deformed and highly deformed vein-quartz have clearly different typologies

and modes of occurrence. These differences have been carefully studied in order to characterize the mineralizing fluid phase (Coetzee and van den Kerkhof, this volume).

ORE MINERALOGY AND GOLD DISTRIBUTION

The fact that gold and sulphides are not disseminated throughout the vein, but that they are rather confined to fractures and laminae suggest that sulphidation post-dates vein-quartz formation. Pyrite is the principal sulphide mineral, and mostly occurs as approximately 2 mm diameter euhedral crystals in the vein-quartz and in the carbonated wallrock. Other common sulphide assemblages are tetrahedrite-chalcopyrite-galena-arsenopyrite-sphalerite in the central payshoots, and bismuth-cosalite-bismuthinite-joseite in the western half of the mine. Abundant molybdenite over the western half of the mine does not correlate significantly with gold.

Approximately 55% of all known gold occurrences are attached to or included in pyrite as less than 2 to 50 μm diameter blebs. Lesser amounts of Au occur in association with the other two sulphide assemblages. It, however, is significant to note that all samples from the Maltz Reef that contain tetrahedrite, also carry good Au-values. Tetrahedrite can therefore clearly be associated with the mineralizing fluid phase.

Fairly common pyrrhotite-chalcopyrite mineralization is associated with late stage thrusting but is not auriferous.

The bulk of the Au is confined to elliptical pay shoots pitching at 30° to the W and WNW, parallel to the intersection of the shear foliation with the reef. These pay shoots parallel the trend of recumbent folds indicating that the principal stress emanated from the N and NNE. About 70% of the Au in the Maltz Reef is associated with quartz which appears to have responded to stress in a brittle manner.

References

- Baines, T., 1877. The Gold Regions of South Eastern Africa. Edward Stanford, Charing Cross, London, 240 pp.
- Balpin, T.V., 1965. Lost trials of The Transvaal. T.V. Bulpin, Cape Town, 474 pp.
- Byron, C.L. and Barton, J.M., 1990. The setting of mineralization in a portion of the Eersteling Goldfield, Pietersburg granite-greenstone terraine, South Africa. S.Afr. J. Geol., 93 (3) 463-472.
- Kalbskopf, S. and Barton, J.M., 1993. The Geology of the Maltz Reef at the Eersteling Gold Mine. Extended Abstracts : 16th International Coll. on African Geol.
- Willemsse, J., 1938. The field occurrences south-west of Pietersburg. Ball. geol. Surv. S.Afr., 12, 33pp.

FLUID INCLUSIONS AND CATHODOLUMINESCENCE OF MALTZ REEF QUARTZ VEINS: EERSTELING GOLD MINE, PIETERSBURG GREENSTONE BELT, SOUTH AFRICA.

COETZEE, D.S. (1) & VAN DEN KERKHOF, A.M. (2).

(1) Department of Materials Technology, Technikon Pretoria, Private Bag X680, Pretoria, 0001, South Africa.

(2) I.G.D.L., University of Göttingen, 3 Goldschmidtstrasse, D - 37 077, Göttingen, Germany.

The Eersteling gold mine is situated in greenschist-amphibolites of the Eersteling Formation (Pietersburg Greenstone Belt), South Africa. The Maltz Reef represents a typical mesothermal shear zone in which gold is hosted in quartz-carbonate vein systems. The Maltz Reef is dominated by vein quartz which varies from massive unmineralized to highly brecciated mineralized varieties. Shearing, accompanied by different stages of carbonate crystallization, was responsible for the different vein-quartz varieties within the Maltz Reef. **Optical cathodoluminescence (CL)** distinguishes at least six visible geological activities: (1) an early stage fluid inflow related to quartz deformation, (2) recrystallization and fluid infiltration, (3) fluid migration in micro-crack systems, (4) fluid flow and carbonate introduction, (5) a late stage shearing and/or brecciation, and (6) hydrothermal quartz vein filling showing primary growth zonation (no fluid inclusions). Scanning electron microscope (SEM) CL textures also indicate widespread decrepitation of fluid inclusions and a late, superimposed pattern of healed microfractures characterized by very small ($<3\mu\text{m}$) fluid inclusions.

Fluid inclusions in least deformed vein quartz (massive to slightly recrystallized) which usually shows blue CL are of three types: (1) Oversaturated liquid-rich aqueous fluid inclusions containing 1, 2 or 3 (most frequently 2) daughter crystals (LVSS), which occur in irregular clusters. SEM analyzes of decrepitates show Na-Ca-K-Cl compositions; daughter crystals are halite and carbonate. L-V-homogenization temperatures (T_h) of LVSS-type fluid inclusions are between 110 and 150°C. The halite daughter crystals show dissolution temperatures in the range of 170-300°C, always above LV-homogenization. In many inclusions showing 1 solid phase, due to metastability halite does not nucleate at room temperature and appears after freezing. The carbonate crystals are rounded and partly dissolved during cooling as a result of retrograde solubility and clearly grow larger on warming. Carbonate dissolution must be higher than the decrepitation temperature at 480-520°C and cannot be measured. The strongest transposed inclusions which have higher T_h show evidence of partial water leakage. Temperature of eutectic melting (T_e) during freezing experiments has been observed at temperatures well below the eutectic temperatures of Na and K in a number of inclusions. This significantly depressed T_e can be ascribed to the presence of CaCl_2 in the system, and confirms the SEM-observation. (2) Undersaturated liquid-rich aqueous fluid inclusions (LV) along healed cracks exhibit strong variation in salinity from the saturation point to almost pure water. These inclusions homogenize between about 110°C (high salinity) and 170°C (low salinity). Primary LV-aqueous inclusions in carbonate veinlets have salt

content of ± 10 eq.wt.% NaCl and homogenize at 110-180°C (typically at ± 110 -120°C). (3) Few mixed H₂O (brines) - CO₂ inclusions (LLV) occur mainly in quartz showing little or no secondary changes. Assuming a geothermal gradient of 29°C and $d = 2,65\text{g.cm}^{-3}$ fluid trapping must have been from 300°C at $\pm 2,5$ kbar to 180°C at $\pm 1,5$ kbar.

Fluid inclusions in moderately deformed quartz (visibly recrystallized) contain undersaturated aqueous inclusions (mostly 8-18 eq.wt.% NaCl), which occur as either small clusters with Th around 140°C, or very tiny inclusions (1-2 μm) for which no microthermometric data is available.

Highly deformed quartz (sheared, greenish-grey, translucent quartz) is the only quartz variety in which visible gold is sometimes present. It is therefore thought that gold came in during brecciation. Vast numbers of very small fluid inclusions (<1 μm) in highly deformed quartz are responsible for its translucent appearance. The extremely small size of these fluid inclusions made it impossible to collect any quantitative microthermometric data for these inclusions. Qualitatively, however, no phase changes could be observed during freezing runs to temperatures as low as -170°C. Single-phase inclusions observed here are therefore interpreted as empty cavities of inclusions destroyed by shearing.

Carbonic fluid inclusions (LLV) were only observed in a single sample (20/5W-FW), showing little deformation. This contradicts the observation in gold-bearing vein-quartz which in general contains abundant CO₂. Calcite, however, is present in almost all the studied vein-quartz samples from Eersteling, which may imply that all the CO₂ which was present could have been consumed during the process of carbonization to form calcite. Carbonate inclusions are mainly associated with the oversaturated fluid inclusions. Seen the widespread occurrence of SSLV inclusions in the least deformed quartz and the consistency of phase volumes (notably of the solids) the carbonate inclusions are supposed to be trapped during an early stage of fluid evolution and at least in part be real daughter crystals. During secondary processes like partial water leakage out of fluid inclusions salinity may have increased (up to ± 38 eq.wt.% NaCl). It can therefore be concluded that the final equilibration of the fluid inclusions must post-date an early carbonitization event. The gradual lower salinities of fluid inclusions in the higher (moderately) deformed quartz are supposed to present a mixing trend with meteoric water. The latest recognizable hydrothermal stage resulted in (non-deformed) carbonate veins which are associated with low-salinity fluid inclusions (10 eq.wt.% NaCl) homogenizing at 150°C and probably trapped at 250°C and 2 kbar. Lower salinities of fluids in higher deformed quartz (sometimes containing free Au) are favourable for gold transport.

LATE-STAGE FLUID EVOLUTION MODEL FOR EXTENSIVE KAOLINIZATION AND RELATED FERRUGINOUS LODGE FORMATION IN SOUTH-WEST ENGLAND.

COX, W. (1), RANKIN, A. (1) & ALDERTON, D. (2).

(1) School of Geological Sciences, Kingston University, Kingston-upon-Thames, Surrey, U.K.

(2) Department of Geology, Royal Holloway, University of London, Egham, Surrey, U.K.

The Cornubian metallogenic province of S.W. England has long been identified as a classic example of granite related mineralization. Emplacement of a series of granite plutons during the closing stages of the Hercynian Orogeny was associated with main-stage hydrothermal activity during which high temperature Sn-Cu-W mineralization was developed. The subsequent ingress of lower temperature, late-stage fluids of diverse origin, is widely believed to have played a dominant role in both the economic kaolinization of the granite masses and the genesis of spatially related epithermal Fe(\pm U) veins (Alderton & Rankin, 1983). This paper examines the PVTX characteristics, provenance and migration pathways utilised by such late-stage fluids and attempts to evaluate any genetic link between the processes of kaolinization and ferruginous vein formation.

To address these issues, current research has focused principally upon the St. Austell region of S.W. England, where a large number of ferruginous veins are spatially associated with an extensively kaolinized granite pluton that constitutes one of the most important areas of china clay production in the world. In particular, studies have concentrated upon the Goonbarrow china clay workings, where crustiform, north-south oriented quartz-hematite veins are exposed within the pit. To date, a combination of petrographic, microstructural and fluid inclusion techniques have been employed on variably altered granites and iron vein samples.

Detailed studies of secondary fluid inclusions in granite quartz reveal that the intensity of kaolinization correlates with the abundance of dilute, low to moderate temperature fluids (T_h 70-200°C, <1-10wt% NaCl eq.). This evidence indicates that kaolinization was achieved by the late-stage influx of meteoric waters through a consolidated and essentially cooled granite. Pervasive alteration was achieved by focusing fluid flow along microfractures in the granite and it will be argued that this micropermeability was primarily developed during the earlier episode of main-stage hydrothermal activity.

Analysis of primary inclusions in vein quartz from Goonbarrow and elsewhere, indicate that the veins were precipitated by basinal brines (T_h 100-150°C, 24wt% NaCl eq., T_e <45°C). These brines were probably tapped from compacting offshore sedimentary basins via major NW-SE wrench faults that transect the Cornubian peninsula and have already been proposed as base metal (Pb-Zn) mineralizing agents in S.W. England (Alderton, 1978). "Primary" inclusions of a dilute fluid are believed to represent subsequent recrystallization and/or flushing through of the original inclusion contents by a later low salinity, "kaolinizing" fluid.

The observed disposition of ferruginous lodes around the heavily kaolinized St. Austell granite has been promoted as evidence in favour of a common genetic association between kaolinization and Fe-vein formation (Jackson et al., 1989). It is speculated that iron released from the deferruginization of granitic biotite during argillic alteration was precipitated in dilatant N-S structures, within and adjacent to the kaolinized granite pluton.

Although iron may have been directly sourced from the granites, fluid inclusion evidence from this study suggests that the lodes were not precipitated from dilute, kaolinizing fluids charged with Fe, Si, and U, but basinal brines. This evidence, therefore is at variance with the previously accepted model invoking a common fluid source for both kaolinization and iron vein formation.

References:

Alderton, D.H.M. 1978. Fluid inclusion data for lead-zinc ores from South-west England. *Trans. Instn. Min. Metall.*, 87, B132-5.

Alderton, D.H.M. & Rankin, A.H. 1983. The character and evolution of hydrothermal fluids associated with the kaolinized St. Austell granite. *J. Geol. Soc. London*, 140, 297-309.

Jackson, N.J., Willis-Richards, J., Manning, D.A.C. & Sams, M.S. 1989. Evolution of the Cornubian Ore Field, S.W. England, part II: Mineral deposits and ore-forming processes. *Econ. Geol.*, 84, 1101-33.

SYNTECTONIC CO₂-H₂O FLUIDS IN EXTENSIONAL VEINS IN METASEDIMENTS OF THE VOLTRI GROUPS (NW ALPS).

CRISPINI L. (1), FREZZOTTI M.L. (2), CATHELINÉAU M. (3)

- (1) Dip. Scienze Terra, Corso Europa 26, I-16132 Genova.
(2) Dip. Scienze Terra, Via delle Cerchia 3, I-53100 Siena.
(3) C.R.E.G.U., B.P.23, F-54501 Vandoeuvre les Nancy.

The Voltri Group is a metaophiolitic complex at the SE margin of the Western Alps, composed mainly of serpentinites with metagabbros and eclogitic bodies, metasediments (Schistes Lustrés) with metabasites, and lherzolites with minor pyroxenite and dunite bodies. The massif was involved in the Alpine subduction events, and it underwent different degrees of metamorphic re-equilibration under HP-LT (Eclogitic / Blueschists facies) conditions, followed by decompressional steps, down to Greenshist facies conditions (Cortesogno et al., 1977). The metamorphic evolution of this complex has been reconstructed in the femic and ultrafemic rock associations, whereas the relationships between deformation and metamorphism are poorly constrained in the metasediments, because of the absence of suitable mineralogic assemblages.

Fluid inclusion studies have been performed in syntectonic extensional quartz-veins in the metasediments of the Voltri Group, to characterize the synmetamorphic fluid composition. Study veins pertain to three distinct generations of folds, that formed during the retrograde evolution (Crispini, 1995). F1 and F2 folds are tight to isoclinal shear folds with a pervasive schistosity, parallel to the axial plane, developed in the ductile field. F3 folds overprint F1 and F2 folds; they are gentle to open parallel folds; a rough disjunctive cleavage, probably developed at the ductile-brittle transition is often present. Veins are variably deformed, and veins of set 1 are folded and boudinated.

Euhedral quartz grains (5 - 10 mm), growing perpendicular to the vein walls, characterize vein set 1 and 2; grains usually show heterogeneous intracrystalline plastic deformation and dynamic recrystallization, occurring at the transition between the field of grain boundary migration and of subgrain rotation. Veins of set 3 are always recrystallized; they consist of minute quartz grains (30 - 40 μ m) with granoblastic textures and repeated microfractures.

Different types of aqueo-carbonic fluid inclusions are observed in each vein set. The relative chronology between fluid trapping, quartz growth or deformation has been studied with respect to the geometric features of the host micro- to macrostructures. The used methodology has consisted in studying fluid inclusions and their host microstructural domains in quartz veins with the help of observations carried out by using optical and scanning electron microscopy (back scattered electron mode, cathodoluminescence imaging). In addition, systematic 3D measurements of microfracture network geometry are carried out in each sample using an image analyser to depict palaeo-fluid pathways during the brittle deformation of the extensional veins. Quartz microstructures and fluid inclusion distribution allow to distinguish different generations of fluid inclusions, in order of decreasing ages: A: inclusions present isolated or in small clusters within single quartz grains; B: inclusions occurring along quartz grain

boundaries; C inclusions along healed fractures. As fluid inclusions in vein set 1 and 2 resulted to have the same distribution, composition, and densities, these two vein set will be discussed together.

Vein set 1 and 2: the oldest aqueo-carbonic inclusions (type A1 and A2) are water dominated at room temperature ($\text{CO}_2=20-40\%$ tot.vol.). Temperature of melting (T_m) for the carbonic part of the fluid are recorded at -56.9°C . Temperatures of homogenization (T_{hL}) are recorded between 7.5 and 20.9°C . Clathrate melting occurs at $\approx 7^\circ\text{C}$. The fluid composition results 8 CO_2 , $90 \text{ H}_2\text{O}$, 2 NaCl in mole%, with densities between 0.75 and 0.87 g/cm^3 . Inclusions delineating subgrain boundaries (type B1 and B2) are CO_2 dominated ($\text{CO}_2=70-80\%$ tot.vol.). $T_m \text{ CO}_2$ are around -56.6°C , with T_{hL} between 22.3 and 26.1°C . Clathrate melting occurs at $\approx 8^\circ\text{C}$. Fluid composition is 37 CO_2 , $62 \text{ H}_2\text{O}$, 1 NaCl in mole%, with densities between 0.30 and 0.60 g/cm^3 . Late trail-bound aqueo-carbonic inclusions (type C1 and C2) with extremely variable $\text{H}_2\text{O}/\text{CO}_2$ ratios are also observed in early vein sets.

Vein set 3: isolated aqueo-carbonic inclusions are CO_2 dominated at room temperature (type A3). $T_m \text{ CO}_2$ are around -56.6°C , with T_{hL} between 23.2 and 27°C . Clathrate melting occurs at $\approx 7^\circ\text{C}$. Fluid composition is 23 CO_2 , $76 \text{ H}_2\text{O}$, 1 NaCl in mole%. The fluid density is $\approx 0.25 \text{ g/cm}^3$.

Isochores distribution in the P-T space gives a better definition of the retrograde P-T path followed by the Voltri Group metasediments, and of the relationships between the late stages of deformation. Type A1 and A2 aqueo-carbonic fluids in vein sets 1 and 2, have compositions and densities consistent with Green-schist facies conditions ($P=5-6 \text{ kbar}$; $T=350^\circ\text{C}$). For these fluids we propose a pseudo-isochoric ("sensu" Touret, 1992) retrograde evolution, that is in agreement with a development of the F1-F2 folds under very similar P-T conditions, during progressive and continuous deformational events. The oldest aqueo-carbonic fluids in late set 3 veins (type A3), can be related to the late stages of circulation of type B1 and B2 fluids in the early veins.

References

- CORTESOGNO C. et al. (1977) - Journ. Geol. 85, 255-277.
CRISPINI L. (1995) - Ph.D. Thesis, Genova (Italy) 116 pp.
TOURET J.L.R. (1992) - Terra Nova, 4, 87-98.

MAGMATIC SILICATE/SALINE/CO₂ IMMISCIBILITY: OTHER EVIDENCE FROM PONZA ISLAND, PONTINE ARCHIPELAGO, ITALY.

DE VIVO, B. (1), TOROK, K. (2), LIMA, A. (1)

(1) Dipartimento di Geofisica e Vulcanologia, Largo S. Marcelino 10, 80138 Napoli, Italy.

(2) Department of Petrography and Geochemistry, Eotvos Univ., H-1088 Budapest, Muzeum KRT4/A, Hungary.

Ponza, one of the islands of the Pontine Archipelago is located in the Gulf of Gaeta. This area is part of the Tyrrhenian volcanism of the Roman alkaline province.

Fluid inclusions were measured from a foid bearing syenite xenolith entrained in trachite. The foid bearing syenite consists of potash feldspar, clinopyroxene, amphibole, biotite, nozean and accessory sphene, opaques and apatite. Most of the inclusions were observed in potash feldspar, but rarely they were found in amphibolite as well. Potash feldspars are sometimes crowded with inclusions. Most of the inclusions do not exceed 40-50 microns in size, but some of the vapour and vapour dominated ones can be as big as 200 microns.

The measured inclusions can be divided into three categories:

1. One-phase vapour, or silicate melt inclusions. One phase vapour inclusions are the biggest in size; they can be as big as 200 microns. The ragged walls of the vapour inclusions indicate some trapped silicate melt.

2. Two-phase inclusions: a) Vapour-dominated, vapour + liquid aqueous inclusions with a small amount of CO₂ in most cases. The presence of the carbon dioxide was proved by the formation of the CO₂ clathrate on cooling. Homogenization of the inclusions always occurred to the vapour phase between 359 and 424°C. Salinities vary from 2.9 to 8.5 wt% NaCl equivalent. b) Silicate melt + vapour inclusions. The silicate melt was mostly colourless, transparent, but in some cases it has been observed pale brown, devitrified glass as well. The ratio between the vapour and silicate melt is highly variable, indicating dishomogeneous trapping of these two phases.

3. Three phase and multiphase inclusions. Hypersaline aqueous inclusions sometimes with up to 8 or more solid phases. Isotropic, cubic daughter minerals (up to 5 in one inclusion), are soluble in water on heating; they are thought to be NaCl, and possibly KCl. The birefringent phases may or may not dissolve on heating. Some inclusions contain acicular minerals (up to 3), which seem to be isotropic, or slightly birefringent. The acicular phase is soluble on heating and this is the last to dissolve and the first to reappear on cooling down after homogenization. The opaque phase is rather an accidentally trapped mineral, because it is absent from most of the inclusions. Some hypersaline inclusions may contain a small amount of silicate melt as well.

SEM analyses revealed the existence of Na, K, Ca chlorides; Ca, K sulphates; Fe-Mn oxides (or hydroxides), pyrite and potash feldspar as daughter and accidentally trapped minerals in the multiphase hypersaline inclusions.

Hypersaline inclusions occur in clusters together with vapour/silicate melt inclusions in both textural position, but there was no significant difference in homogenization temperature or in salinity. Melting of the NaCl daughter crystals occur between 459 and 536°C which means a salinity range from 54 to 65 wt% NaCl equivalent. The last phase transition is the homogenization of the vapour bubble

between 640 and 755°C.

Though the evidence for immiscibility between the silicate melt and the hydrosaline melt is not as spectacular as in the similar alkali syenite xenolith of the Ventotene island (De Vivo et al., in press), it is quite clear that the associated aqueous hypersaline/vapour/silicate melt inclusions unmixed at magma conditions at subvolcanic level. The vapour rich aqueous +/- CO₂ inclusions are the trace of a later high temperature hydrothermal fluid.

References:

De Vivo, B., Torok, K., Ayuso, R.A., Lima, A., Lirer, L. Fluid inclusion evidence for magmatic silicate/saline/CO₂ immiscibility and geochemistry of alkaline xenoliths from Ventotene island (Italy). *Geochim. Cosmochim. Acta* (in press).

ISOCHORIC PATHS IN MULTICOMPONENT FLUIDS AND THE INTERPRETATION OF FLUID INCLUSIONS

DIAMOND, L.W.

Mineralogisch-petrographisches Institut, University of Bern,
Baltzerstr. 1, CH-3012 Bern, Switzerland (larryn@mpi.unibe.ch)

Fluid inclusions in minerals are usually considered in the context of a simple thermodynamic model which states that their bulk compositions and total volumes are fixed as constants during initial fluid entrapment. Hence in the ideal case, fluid inclusions are constrained to follow isochoric-isoplethic paths through P-T space, both in nature and during microthermometry. In an influential paper on the systematics arising from the ideal isochoric-isoplethic model, Pichavant *et al.* (1982, p.7-8) claimed to prove by phase-rule analysis that isochoric paths may transect a given phase boundary only once.

Their generalisation is potentially very powerful. First, it would allow natural fluid inclusions which deviate from ideal behaviour to be recognized unequivocally during microthermometry. For example, if a vapour bubble disappears upon heating and then reappears upon further heating, it follows that the inclusion must have leaked or stretched in the laboratory. Thus Pichavant *et al.* (1982) discredited reports in the literature (summarised by Roedder, 1984, p.51-52) of reversible bubble reappearances in natural fluid inclusions. Second, the generalisation could be of practical use in experimentally mapping out phase diagrams. Once the intersection temperature of an isochore on a phase boundary has been measured and its slope is known, extrapolation of the isochore through P-T space would constrain the locus of the phase boundary at all other conditions. Hence by implication, the experimental work on CO₂-H₂O-NaCl fluids by Frantz *et al.* (1992) could not be correct.

In the present communication it will be shown that the generalisation of Pichavant *et al.* (1982) is false. The implications for fluid inclusion interpretation are therefore reconsidered, both with respect to reconstructing geological environments of paleo-fluid activity, and with respect to microthermometric analysis.

The deduction of Pichavant *et al.* (1982) regarding the general nature of isochoric paths is based on an erroneous application of the phase rule. They reasoned that because (1) ideal fluid inclusions constitute univariant conditions (lines in P-T projection), (2) univariant phase equilibria are also lines in P-T projection, and (3) the phase rule is derived from a set of linear thermodynamic equations, (4) it follows that fluid inclusion trajectories can intersect univariant phase equilibria only once. However, thermodynamic variance does not constrain the curvature of univariant conditions in P-T space, and hence multiple intersections between the same univariant curves are not excluded *a priori*. In fact, there is no general thermodynamic reason why an ideal fluid inclusion trajectory cannot intersect the same equilibrium phase boundary many times. For specific chemical systems, the occurrence of multiple intersections depends on the molecular interactions between components. Thus it can be predicted only by a complete

equation of state which takes account of these interactions, and it can be verified only by empirical observation (P-V-T-X experiments).

A growing body of evidence from fluid inclusions and from synthetic isochoric systems suggests that multiple intersections indeed occur and are important for the understanding of natural, multicomponent fluids ($c \geq 2$), particularly with regard to the extent of immiscibility at elevated P-T conditions. For example, Figure 1 shows a P-T projection of a hypothetical isopleth in a volatile-bearing, saline aqueous system (based in part on data in Frantz et al., 1992). The fine line passing through points 1-3 represents an isochoric path. Fluid inclusions trapped on the isochore above point 3 would show homogenisation by vapour expansion at point 1, followed by reappearance of the liquid at point 2, followed by disappearance of the liquid again at point 3. Such a phase diagram could explain some of the unusual observations reported in the literature (Roedder, 1984, p.51-52).

Cases such as Figure 1 cannot be interpreted in the same way as fluid inclusions with only one intersection of an immiscibility boundary. If an assemblage of fluid inclusions with the depicted V-X properties shows petrographic evidence for homogeneous trapping, there is no way to deduce from the inclusion data alone, whether the fluid was trapped on the isochore between points 1 and 2, or above point 3. Conversely, if petrography indicates heterogeneous trapping, microthermometry does not yield a unique formation temperature. There are 3 possible P-T points of entrapment (1, 2 and 3) and these could be distinguished only by examining the P-V-T-X properties of cogenetic inclusions which trapped the conjugate immiscible fluid.

The consequence for microthermometry is that reproducibility and reversibility are the only criteria available to substantiate unusual phase transitions. Artefacts of non-ideal behaviour are still possible, however, and the feasibility of suspected phase equilibria must be checked against experimental P-V-T-X data.

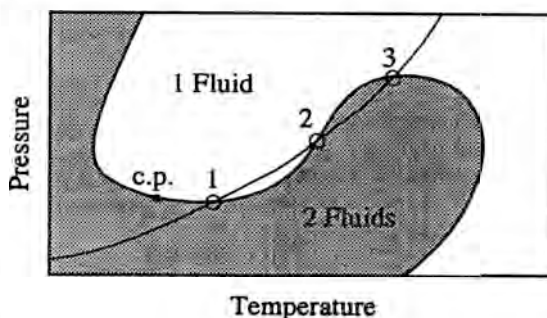


Figure 1

Temperature

PICHAVANT M., RAMBOZ C., and WEISBROD A. (1982) *Chemical Geology* 37, 1-27.

ROEDDER E. (1984) Fluid inclusions. Vol.12. *Reviews in Mineralogy*, Mineralogical Society of America.

FRANTZ J. D., POPP R. K., and HOERING T. C. (1992) *Chemical Geology* 98, 237-255.

FLUID EVOLUTION IN BITUMEN-RICH FORMATIONS OF THE VOLCANO-SEDIMENTARY COMPLEX OF THE BARRANDIAN UPPER PROTEROZOIC (CZECH REPUBLIC)

DOBES, P. (1) & DUBESSY J. (2)

(1) Czech Geological Survey, Klarov 3, 118 21 Prague 1, Czech Republic

(2) CREGU, GS-CNRS 77, BP 23, F-54501 Vandoeuvre-lés- Nancy Cedex, France

The volcano-sedimentary complex of the Barrandian Upper Proterozoic is part of the Bohemium that is a Cadomian unit incorporated in the Palaeozoic mobile zone within the region of low-grade metamorphism of the Central European Variscides (Zoubek et al. 1988).

It includes slates, siltstones and greywackes accompanied by cherts, conglomerates, tuffaceous agglomerates, tuffs and tuffites. The volcanite complex includes tholeiitic basalts and basaltic andesites with the marginal parts of the unit containing calc-alkalic volcanites.

The rocks underwent submarine basalt-sediment-water interaction producing solid bitumen resembling poorly ordered graphite under temperatures of 350-400 °C (pyrolysis and the thermal effect of basalt extrusion on the organic matter of sediments, Kribek et al. 1993). The sub-sea floor metamorphism gave rise to spherical structures of bitumen under temperatures of 200 °C (the later alteration of basaltic andesite by hydrothermal solutions under the conditions of limited miscibility of gaseous and liquid products, Kribek et al. 1993). The area was successively affected by the Cadomian metamorphism of zeolite facies and the beginning of greenschist facies.

To aid in the interpretation of fluid evolution in carbon-rich formations of low-grade metamorphic terrains fluid inclusions in bitumen-rich inter-pillow fillings of pillow lavas of the spilitized basaltic andesites and in younger oblique quartz - calcite - axinite veins from the Mitov locality (30 km SE of Plzen) were studied by optical microthermometry and micro-Raman spectrometry.

The inter-pillow matter consists of quartz, calcite, solid bitumens, chlorite ± pyrite. Calcite of concentric texture growing on lava pillows represents the initial stage of formation of the inter-pillow matter. Primary inclusions in calcite contain water solution with low salinity ($c < 10$ wt. % NaCl equiv.) and homogenization temperatures between 225 and 315 °C with most values in the range of about 250 °C.

The majority of the inter-pillow matter is dark-coloured quartz and coarse-grained calcite with an admixture of organic matter with H₂O-rich or CH₄-rich inclusions or inclusions with their mixture. Either H₂O or CH₄ predominates (up to 94 mole %) in inclusions. Methane (the density of CH₄ = 0.162 - 0.363 g/cm³) contains of about 3 mole % of CO₂ and 1 mole % of N₂ + H₂S. Water-rich inclusions have low salinity between 1 and 7 wt. % NaCl equiv. and Th in the interval of 135-207 °C. The inclusions are

believed to be trapped under the conditions of immiscibility of water solution and methane. The homogenization temperatures of H₂O-rich inclusions are in this case considered to be the temperatures of trapping of inclusions and thus the pressure of trapping (derived from the crossing of the isochores of CH₄-rich and H₂O-rich inclusions) corresponds to 50 to 100 MPa.

Quartz, calcite and axinite of the oblique veins contain H₂O-rich inclusions with temperatures of homogenization from 190 to 270 °C and variable salinity from 1 to 23 wt. % NaCl equiv. Only rarely do secondary H₂O-CO₂ inclusions with variable content of both phases (the density of gaseous phase = 0.615 - 0.741 g/cm³, admixture of CH₄ up to 20 mole %) and low salinity occur in vein quartz.

The fluid inclusion study suggests that the relics of fluids of various stages of the basalt-sediment-water interaction were trapped in the inter-pillow matter. Formation of the concentric calcite (Th to 315 °C) probably corresponds to the initial stage of basalt-water interaction, whereas dark-coloured quartz and calcite formed during successive circulation of water solution rich in SiO₂ and methane (together with organic matter) under lower temperatures of about 200 °C and pressures of about 100 MPa. The pressure could have oscillated because of the production of large amounts of gas. Gradual cooling and crystallization of quartz could have produced the organic spherical structures (Kribek et al. 1993). Low content of CO₂ and N₂ in inclusions indicates a reducing environment during the water-rock interaction.

On the other hand, formation of the oblique veins with axinite was probably connected with other types of fluids: the presence of fluid with CO₂ gives evidence of changes in the oxidation state in the rock environment and the infiltration of high salinity fluids took place at the end of crystallization of the vein filling.

References

- Kribek B., Holubár V., Parnell J., Pouba Z., Hladíková J. (1993): Interpretation of thermal mesophase in vanadiferous bitumens from Upper Proterozoic lava flows (Mítov, Czechoslovakia).- In: Parnell J., Kucha H., Landais P. (eds.): Bitumens in ore deposits, 61-77, Spec. Publ. n. 9 of SGA. Springer-Verlag. Berlin.
- Zoubek V., Cogné J., Kozhoukharov D., Krautner H.G. (1988): Precambrian in younger fold belts.- Wiley and Sons. Chichester.

FLUID INCLUSION RECORD IN HIGH-PRESSURE GRANULITES OF NORTHERN BOHEMIA (CZECH REPUBLIC)

DOBES, P. (1), DUBESSY J. (2) & KOTKOVA J. (1)

(1) Czech Geological Survey, Klarov 3, 118 21 Prague 1, Czech Republic
(2) CREGU, GS-CNRS 77, BP 23, F-54501 Vandoeuvre-lés-Nancy Cedex, France

In northern Bohemia granulites occur in the Eger crystalline complex in the vicinity of the boundary of two regional geological units (Saxothuringicum and Bohemicum). They are associated with orthogneisses and migmatites. Apart from prevailing acid and subacid rock compositions with mineral assemblage Q-Kf-Pl-Gt-Ky \pm Bt \pm Mu, pyroxene granulites (Gt-Cpx) and basic amphibole-bearing rocks (Gt-Hb-Bt-Ky-Pl) occur in minor amounts. Felsic garnet-kyanite bearing lithologies are interpreted to be derived from igneous precursors. Textural features (occurrence of varieties with relatively coarse-grained texture), modal composition, upper crustal geochemical signatures (undepleted with respect to LILE and REE elements) and P-T conditions of the metamorphic peak (up to 17 kb and ~ 800 °C) indicate melting at high P-T conditions giving rise to these granulites (Kotkova 1993).

The granulites experienced polyphase metamorphism and deformation. P-T conditions of granulite metamorphism were determined at 15-17 kb, 750-800 °C (Granulite stage I). The reconstructed P-T-t path for these rocks is characterized by initial isothermal decompression, followed by cooling during a slow decrease of pressure (Granulite stage II 13-14 kb / 800 °C, Amphibolite stage 10-11 kb / 750 °C). Late hydration characterizes the final stage of the evolution (up to 4-5 kb and 600 °C, Kotkova 1993).

Fluid inclusions in quartz were studied by optical microthermometry and micro-Raman spectroscopy from various types of granulites (granulite xenoliths, undeformed granulites, foliated granulites) to characterize the fluid phase in individual stages of the rock evolution. Regardless of the type of granulite, fluid inclusions were found mostly in quartz porphyroblasts and were distributed virtually only on planes or trails along healed fractures. Several types of inclusions showing large differences in composition and density were distinguished:

1. $\text{CO}_2 \gg \text{N}_2 > \text{CH}_4$, water-free inclusions composed of $\text{CO}_2 = 84 - 89$ mole %, $\text{N}_2 = 8 - 15$ mole % and $\text{CH}_4 = 1 - 3$ mole %. $T_m\text{CO}_2$ was measured between -59.5 and -60.9 °C, $\text{ThCO}_2 = -9.1$ to 2.0 °C, the density of inclusions corresponds to 0.82 to 0.95 g/cm³.
2. $\text{CO}_2 > \text{N}_2 \gg \text{CH}_4$, water-free inclusions consisted of $\text{CO}_2 = 51-65$ mole %, $\text{N}_2 = 33-47$ mole % and $\text{CH}_4 = 1-2$ mole %. $T_m\text{CO}_2$ was observed in the range from -60.0 to -60.7 °C, $\text{ThCO}_2 = -5.5$ to -6.6 °C, only in a few inclusions Th (V) of N_2+CH_4 phase occurred between -145.8 and -146.3 °C. The density of inclusions is in the interval 0.30 - 0.68 g/cm³.
3. CO_2 -rich inclusions without detectable H_2O , with $T_m\text{CO}_2 = -57.1$ to -57.8 °C, $\text{ThCO}_2 = 13.6$ to 30.9 °C, density was established to be between 0.48 and 0.84 g/cm³.
4. Low density CO_2 inclusions, vapour-rich only or with up to 30 vol. % of H_2O , $T_m\text{CO}_2 = -58.0$ to -60.3 °C, ThCO_2 (V) = 2.6 to 30.8 °C. The density of CO_2 was estimated as 0.11 - 0.41 g/cm³. $T_m \text{CO}_2$ clathrate = 8.7 to 9.2 °C, corresponding to low salinity from 1.6 to 2.6 wt. % NaCl

equiv.

5. Low density N_2 - CH_4 inclusions, vapour-rich only or with up to 20 vol. % of H_2O . Th (V) was observed between -108.0 and -143.5 °C, corresponding to density from 0.039 to 0.104 g/cm³. The vapour-rich inclusions are composed of $40.3 - 73.7$ mole % of N_2 and $26.3 - 60.0$ mole % of CH_4 .

6. H_2O -rich inclusions. At least three generations of H_2O -rich inclusions were found in the samples. The inclusions with low Th (138 to 192 °C and 187 to 274 °C) have higher salinity from 4.03 to 6.30 wt. % NaCl equiv. and conversely, the inclusions with high Th (346 to 389 °C) have very low salinity between 0.18 and 2.57 wt. % NaCl equiv.

CO_2 -rich inclusions (type 1-3) and H_2O -rich inclusions form the separate trails or planes, whereas the common occurrence of CO_2^V or N_2 - CH_4 and H_2O -rich inclusions with Th of about 170 °C or water-vapour phase mixtures is obvious. These inclusions were probably trapped under the conditions of immiscibility of water and vapour phase but the contribution of stretching or leakage of inclusions cannot be excluded.

Based on the distribution and the P-T path of fluid inclusion isochores it is apparent that the trapping conditions of inclusions do not correspond to the peak of granulite-facies metamorphism. Fluid inclusions are thought to be trapped during the late stage of granulite evolution under the conditions of brittle deformation, probably under the conditions of greenschist facies metamorphism.

The data suggests that the P-T-t path of granulite rocks is a result of crustal thickening and subsequent tectonic uplift during orogenic collapse following plate collision (Kotkova 1993). P-T trajectory, reconstructed from the fluid inclusion data, is convex towards the T axis, i.e. the trapping of inclusions was probably connected with the decompression regime of the late stage of the tectonic uplift of granulite bodies. Since fluid inclusions correspond to the peak of metamorphism neither in granulite xenoliths nor in undeformed relics of granulite rocks it is suggested that granulites formed under high-pressure low- CO_2 virtually fluid-free environment.

References

Kotkova J. (1993): Tectonometamorphic history of lower crust in the Bohemian Massif - example of north Bohemian granulites.- Czech Geological Survey Special Papers, 2. Prague.

FLUID/DEFORMATION RELATIONSHIPS IN CONTRASTED LITHOLOGIES: AN INTEGRATED FLUID INCLUSION STUDY OF NORTHERN PORTUGAL Au-QUARTZ VEINS

DORIA, A. (1), NOGUEIRA, P. (1), CATHELINÉAU, M. (2) & NORONHA, F. (1)

(1) Centro de Geologia, Faculdade de Ciências U.P., Pr. Gomes Teixeira. 4050 Porto, Portugal

(2) CREGU, BP 23, 54501 VANDOEUVRE-LES-NANCY Cedex France

Northern Portugal is known by its gold potential since Pre-Roman times. Retrograde metamorphism stages affecting the Hercynian basement is responsible for significant mass transfer in close relation with deformational events. Thus, numerous quartz veins occur in contrasted lithological contexts, and sometimes host gold concentrations. This is the case of quartz veins or lenses from the metamorphic series from Vila Pouca de Aguiar area or from Grovelas granites. P-V-T-X conditions of the multistage fluid circulation in these contexts have been investigated as a function of the deformational stages.

Vila Pouca de Aguiar (VPA) is a gold district hosted by metasediments of upper Ordovician to lower Silurian age, characterized by several different lithologies, namely chlorite phyllites, quartzites, acid metavolcanics, calc-silicate and Cr-rich terms affected by three hercynian deformation phases (D1, D2 and D3) followed by a brittle phase (D4). In VPA the mineralized structures are quartz veins which occur in fracture systems related to D3-phase (σ_1 NE-SW): N0°E to N20°W-subvertical at Jogadouro (JOG), N40°E to N50°E-subvertical at Vale de Egua (VE) and N120°E-subvertical at Argeriz (ARGZ). In the latter example the quartz veins are associated with tin aplitic-pegmatite veins near the contact with two-mica syntectonic granites.

Grovelas (Gro) is a gold-bearing quartz veins are hosted by hercynian biotitic granites late-tectonic relatively to D3 phase, and affected by D4 stage. The mineralized structures are quartz veinlets striking N40°E to N60°E-subvertical. Both areas are affected by the late-hercynian brittle D4 phase (σ_1 N-S).

Microthermometric studies, Raman analyses and bulk compositions calculations of fluid inclusions have been carried out in order to establish a P-T-V-X reconstruction of the fluid migration. The study of fluid inclusions has been carried out as a function of the sequence of deformation, and related quartz crystallization or healing.

Five main types of host macro- to micro structures for fluid inclusions are distinguished:

-(i) unherited quartz filling structures ante-D4 phase, observed in metamorphic series, and partially recrystallized;

-(ii) earlier milky quartz, the main infilling of the D4 structures;

-(iii) clear quartz resulting from the recrystallization of former milky and associated with arsenopyrite; it can be noted that at Grovelas, veinlets composed of almost exclusively arsenopyrite (< 5 mm in thickness) are frequently observed;

-(iv) an hyaline quartz, sometimes euhedral, associated with late sulphides;

-(v) healed microstructures which may be related to stages iii), iv) or later stages.

In mineralized structures, arsenopyrite and pyrite are the most abundant sulphides. Gold occurs always as late particles inside arsenopyrite, pyrite or in the interface between these sulphides, and sometimes associated with the late assemblages: sulphosalts such as Pb-Ag-Sb-Cu-Te (VE), Bi-Ag-Pb-Sb (ARGZ), Bi-Pb-Ag-Te (JOG and GRO), and/or bismuth and bismuthinite.

Several types of fluids, have been recognized as a function of the host rocks and host structures: H₂O-CO₂ inclusions (Lc-w) displaying dense volatile phase (T_HCO₂ (L/V -> L)) is one of the main FI types and is characteristic of the early milky quartz; ii) Vc-w two or three phase inclusions with lower density volatile phase (T_HCO₂ (L/V -> V)); iii) Vm-w two phase inclusions with a dominating CH₄ vapour phase, mostly observed in metamorphic environments; iv) Lw-(c) aqueous two phase water-rich inclusions with a very low density CO₂(CH₄); v) Lw H₂O-NaCl two phase inclusions (mostly in FIP).

The fluid composition from both systems evolved from C-H-O-(N) dense fluids trapped under pressures above 1 Kb and temperatures of 350° to 450°C to progressive diluted fluids which are enriched in CH₄ and N₂ mainly when metamorphic series are present (VPA). The later fluids, associated with main gold mineralization, are dominantly aqueous with low salinities, and trapped under low temperatures (180° to 250°C) and low pressures (hydrostatic pressures).

The general fluid evolution in terms of composition and P-T conditions is rather similar in the two studied zones. It can be emphasized that a great part of the metamorphic fluid stages have been hidden in the ante-D₄ macrostructures by the recrystallization or later deformation. The main difference between metasediment (Vila Pouca de Aguiar) and granite (Grovelas) hosted quartz veins, is the nature of the earliest preserved record of the percolating fluids. They display higher content of CH₄ in VPA fluids probably linked to specific oxydo-reduction processes in C-rich environments and a more ubiquitous presence of H₂S in Grovelas fluids; this difference is interpreted as resulting from the interaction between the fluid and the host rock. However, the late fluid stages are ubiquitous, and display the same features in both zones, and attest of a significant microfissural fluid migration during late deformational stages characterized by the lack of significant quartz deposition.

Acknowledgments: This work has been carried out through the HCM network (Hydrothermal/metamorphic water rock interactions in crystalline rocks: a multidisciplinary approach based on palaeofluid analysis). This work has also been supported by the cooperation CNRS- JNICT. P.Nogueira work benefits from a grant of JNICT - "Programa Ciência": BD-2028/92.

LATE MAGMATIC OVERPRESSURING IN LEUCOGRANITE MAGMAS: THE LAYERED PEGMATITE OF RIBEIRA (NE PORTUGAL)

DOUMBIA, S.(1), GAGNY, C.(2), MARIGNAC, CH.(3)

(1) Département Sciences de la Terre, Université Orléans, France

(2) Laboratoire de Pétrologie, UHP-Nancy 1, France

(3) CRPG-CNRS, Nancy, France

INTRODUCTION

The studied quartz came from a sample of a layered pegmatite, enclosed in a leucogranite (endogranite) cupola with Sn-W mineralization at Ribeira (NE Portugal). The sample (fig. 1) comprises two sets: a layered set, with quartz and aplite 1, overprinted by another set with quartz and aplite 2. The layered part displays an alternation of milky quartz layers and aplite 1 layers; quartz crystals show a palissadic structure, with growth zones and automorphic terminations covered by aplite material and delineated by quartz strips ("ribbon quartz").

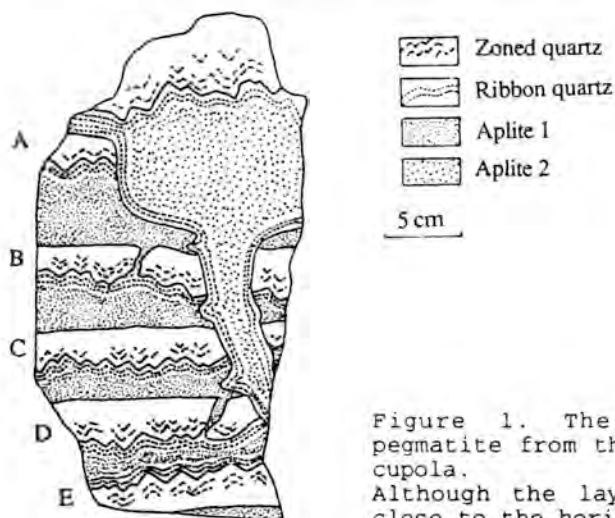


Figure 1. The sample of layered pegmatite from the Ribeira leucogranite cupola.

Although the layering is known to be close to the horizontal, "up" and "down" could not be determined for that sample.

FLUID INCLUSIONS

Fluid inclusions (f.i.) were studied in a quartz from the C layer displaying a complex internal structure : a core (QI), with plastic deformation texture; and growth zones (QII), delineated by rims of aplitic material. In both QI and QII are included minute crystals of K-feldspar, either isolated or in rows. Both QI and QII are recrystallized: the whole quartz consists of 2-3 individuals, with denticulate boundaries, reminiscent of a "Dauphiné twin".

In QI, most f.i. are large decrepitated (exploded) 2-phase (aqueous) inclusions (DPI f.i.), together with small 2-phase (aqueous) inclusions containing a minute K-feldspar prism (Sk f.i.), which are therefore considered primaries. DPI and Sk f.i. have

similar T_{mi} (-3.6 to -4.4 for DPI; -4° to -6.2 for Sk), but Sk have more dispersed Th (280°-400°C) than DPI (290°-330°C). Other f.i. are small 2-phase secondaries, with low salinity (T_{mi} between -1° and -2°C) and variable Th (280°-400°C).

In QII, are mainly found hypersaline halite-containing f.i. (Sh) and numerous secondaries organized into densely spaced planes of inclusions. Sh f.i. display no change at temperatures up to 500°C. Secondaries are low salinity (T_{mi} in the -1° to -2°C range) low Th (150°-250°C) f.i.

There are also quite rare 1-phase (carbonic) inclusions, with a few non-CO₂ component (T_{mCO_2} between -58.3° and -57.9°C), and similar Th_{CO_2} , either in the liquid (Cl f.i.; 19.2°C) or in the vapour (Cv f.i.; 19.7°C) phase. These Cl and Cv f.i. are either disseminated or located at the boundary between large K-feldspar inclusions and the host quartz; they thus appear to be primaries in the QII.

INTERPRETATION

The Sh and C(v,l) f.i. are considered to result of the unmixing of a L1 magmatic fluid during the growth of QII, whereas the DPI and Sk are considered to be representatives of the unmixed L1 magmatic fluid. As a consequence, the trapping pressure during the QI growth is estimated at ca. 3 to 3.5 kbar, whereas QII growth would have taken place under quickly decreasing pressures, down to 0.75 Kbar, thus explaining: (i) the unmixing of L1 fluid; (2) the coexistence in a very restricted space of both high (Cl) and low (Cv) carbonic inclusions; and (iii) the decrepitation of former L1 inclusions trapped in QI, due to internal overpressure, the Sk being the only to escape, due to their small size.

The layered pegmatite record the repetitive occurrence of a cycle of quartz growth from a magma, in the presence of exsolved magmatic fluid, under successively high (up to 3 to 3.5 kbar) and low (down to lithostatic, at 0.75 kbar) pressure, due to the successive building up of that pressure by the exsolved magmatic fluid and releasing by the escape of the fluid out of the magmatic system.

HIGH TEMPERATURE RAMAN SPECTROSCOPIC STUDY OF H₂O-CO₂-CH₄ MIXTURES IN SYNTHETIC FLUID INCLUSIONS USING THE LABRAM SPECTROMETER (DILOR) SOME FIRST INSIGHTS ON MOLECULAR INTERACTIONS

DUBESSY, J.(1), BAKKER,R.(1), FRANTZ, J.(2), ZHANG, Y.(3).

(1)CREGU, BP-23, 54501-Vandoeuvre-lès Nancy Cedex, France

(2)Geophysical Laboratory, CIW, NW, 20015-1305, Washington DC, USA

(3)Institute of Geology, P.O. Box 9825, Beijing 100029, China

Fluid inclusions are single phase at temperature above the bulk homogenization temperature (Th). Raman spectra obtained from this phase should provide the bulk fluid composition allowing its molar volume calculation. However, the stretching band of H₂O is extremely sensitive to molecular interactions (1). The addition of other components such gases or ions, specially Cl⁻, will a priori modify the band shape and Raman scattering cross section of the stretching vibration mode of H₂O. Therefore, an experimental investigation of the Raman spectrum of H₂O-CO₂-CH₄-system is necessary for the evaluation of the feasibility of the determination of bulk fluid composition from Raman spectra above Th. In addition, this work addresses the validation of synthetic fluid inclusion technique for the study of the vibrational properties and the molecular interactions of complex fluids in the C-O-H system.

Synthetic fluid inclusions in the H₂O-CO₂ system have been prepared by the classical technique (2) and those in the H₂O-CO₂-CH₄-system by the gas loading technique (3,4). Heating of the inclusions was carried out using the Chaix-Mecca stage attached to the stage of the microscope of the highly luminous Labram spectrometer (Dilor).

Fluid inclusion compositions, molar volume (Vm) and Th are:

sample	X(CO ₂)	X(CH ₄)	X(H ₂ O)	Vm(cm ³ /mole)	Th(°C)
COH94	.055	.057	.888	29.5	328(L)
1B	.4725	.000	.5275	47.78	355(L)
5A	.711	.000	.289	52.3	308(V)
2A	.111	.000	.889	71.17	360(V)
COH99	.055	.105	.840	47.78	355(V)

1)CH₄ Raman spectrum. The wavenumber and FWHH of the symmetric stretching band of CH₄ is constant along an isochore ($v_l=2911\text{cm}^{-1}$). There is only 1 cm^{-1} of difference between spectra of samples COH94 and COH99. This indicates that CH₄ molecules are poorly sensitive to variations in molecular interactions in these P-T conditions.

2)Fluids with liquid-like fluid density.

H₂O Raman spectrum. The bending mode of water around 1600 cm^{-1} is weak and could not be studied for the used integration time. The stretching band of water (3200-3600 cm^{-1}) is very sensitive to both the composition, density and to the temperature (T) of the fluid. The wavenumber at maximum intensity of the band (v_{max}) is always below 3590 cm^{-1} and slightly increases only by a few cm^{-1} for increasing T. This behaviour is identical for a water-dominant fluid (X(gas)/X(H₂O)=0.13: #COH94) and equal gas-water concentrations (X(gas)/X(H₂O)=0.90:#1B). For pure water, it has been demonstrated that v_{max} does not depend on T above 250 °C at fixed density (1). The full width at half maximum (FWHH) of the band decreases with

increasing T for each inclusion. The high concentration of gas ($X(\text{CO}_2) = 0.4725$, # COH94) does not produce any shift of ν_{max} to higher frequency and any narrowing of the band by comparison with #1B. Therefore, molecular interactions (hydrogen bonds) between water molecules still exist in a fluid with a water/gas ratio =1 at T up to 430 °C.

CO₂ Raman spectrum. The CO₂ bands of the Fermi doublet does not vary in frequency as a function of temperature, composition and density. Only a small increase in intensity of the hot band with T is noticed. The CO₂ Fermi diad is much more complicated in presence of H₂O compared to its spectrum when pure at the same T. Only the first hot bands are well resolved. The third hot band is identifiable only in the high frequency component of the diad. For #1B, decomposition of the CO₂ Raman spectrum into bands, with a 75 % lorentzian shape, shows that the low frequency component of the Fermi diad contains two bands (the fundamental and the first hot band) and the high frequency part contains 3 components. The 3rd component is characterised by constant frequency ($\nu = 1401 \text{ cm}^{-1}$) and FWHH (= 33 cm^{-1}) with increasing T. It still remains unexplained, although it could be interpreted as a result of the H₂O-CO₂ interactions. For # COH94, 3 band components are identified for the low frequency part, and 4 components for the high frequency part.

3) Fluids with vapour like density. *H₂O Raman spectrum.* ν_{max} of the H₂O band is higher than 3600 cm^{-1} , like for pure water fluids with a density lower than the critical density. At similar gas concentrations, ν_{max} increases and FWHH decreases for increasing ν_m as it has been found for pure H₂O (1). ν_{max} increases and FWHH decreases with increasing gas concentration for similar ν_m . This shows that gas molecules strongly weaken hydrogen bonds between water molecules, a feature that is not observed for fluids with a liquid-like density.

CO₂ Raman spectrum. The CO₂ spectra are similar to the spectra obtained for liquid like density fluids, with a large band at the foot of the high frequency diad component.

4) Intensity analysis. The ratio of integrated area of H₂O and CO₂ bands normalised to the composition is constant with increasing T for a given fluid inclusion at constant ν -x properties. However, for vapour like density, the ratio varies from 0.3 to 0.5 depending on the ν -x properties. For liquid-like density, this ratio is much less sensitive to the composition and the molar volume. The bending mode of H₂O is known to be less sensitive to molecular interactions than the stretching mode (5). Further investigations should be focused to this vibrational mode for analytical purpose, but this requires a very sensitive and luminous spectrometer such as the Labram model.

References.

- (1)-Frantz J, Dubessy J, Mysen B. (1993). Chem. Geol., 106, 9-26.
- (2)-Bodnar R. and Sterner S. (1987). In: G.C. Ulmer and H.L. Barnes (eds). Wiley-Intersciences, pp. 423-457.
- (3)-Frantz J, Zhang Y.G., Hoering T. (1989). Chem. Geol., 7, 57-70.
- (4)-Zhang Y.G. and Frantz J (1992). Chem. Geol., 100, 51-72.
- (5)-Ratcliffe C., Irish D. (1982). J. Phys. Chem., 86, 4897-4905.

Acknowledgements. The authors greatly acknowledge the Dilor company for having permitted them to work with the "Labram" spectrometer in their application laboratory. This work has been supported for J.D. by PICS 192, for R.B by network HCM (CEE-DG XII, contract 930198-PL922279).

CHARACTER OF PALEOFLUIDS IN GOLD-BEARING QUARTZ VEINS IN GNEISSES OF THE MOLDAUBIAN ZONE: THE KASPERSKÉ HORY GOLD DEPOSIT (CZECH REPUBLIC)

DURISOVA, J.(1), STRNAD, L.(2), BOIRON, M.C.(3) & PERTOLD, Z.(2)

(1) Czech Geological Survey, Klarov 3, 11821 Praha 1, Czech rep.

(2) Institute of Geochemistry, Mineralogy and Mineral Resources, Charles University, Albertov 6, Praha 2, Czech Republic

(3) CREGU. BP 23, 54501, Vandoeuvre-les-Nancy Cedex, France

The Kasperske Hory ore deposit is located in amphibolite facies gneisses of the high grade Moldanubicum terrane in the SW part of the Bohemian Massif. The gold (and scheelite) mineralization is confined to a retrograde EW trending shear zone (several tens of km long and up to two km wide) which affected the amphibolite facies rocks (600-650°C and 480-540 MPa - Pertoldova et al. 1990). The shear zone formed during the uplift of the Moldanubicum which was accompanied by postkinematic granite emplacement (330-300 Ma). Gold of high fineness (960/1000) occurs in quartz lodes of complicated morphology and different orientation (Puncochar et al. 1993).

The aim of the fluid inclusion study was to characterize fluids linked to the formation of gold-bearing quartz lodes (veins) hosted by biotite paragneisses, quartzites and calc-silicate rocks and to correlate these fluids with the tectonic and metamorphic evolution. A detailed tectonic study of host rocks and quartz lodes preceded the fluid inclusion study. The lodes follow mainly structures developed in a brittle-ductile regime of deformation: reactivated S_{1,2} foliation (NW-SE with moderate dip to N), C planes (shear bands trending EW with steeply N dipping), and dilation fractures (extension veins-Ex) frequently of box-like shape. Samples were taken from the Nadeje mine intersecting the shear zone. Fluids inclusions (F.I.) were studied in quartz using microthermometry (Chaixmecca heating-freezing stage) and by Raman spectroscopy analysis on selected F.I.. Orientations of fluid inclusion planes (F.I.P.) were studied in three oriented samples representing the main structural quartz vein types (S, C and Ex veins).

Fluid inclusions in quartz are similar in all structural types of veins. They are present in large numbers, however their size (<5 µm) and multistage quartz deformation and recrystallization (with F.I.decrepitation and refilling) make observations difficult. Quartz grains are intersected by networks of healed microcracks decorated by F.I.. Three types of F.I. based on microthermometric data and confirmed by micro-Raman analysis were identified:

(i) CO₂ rich inclusions: they occur mostly in clusters or in short nonpenetrative healed cracks in quartz grains (early F.I.). The CO₂ rich phase is liquid (T_mCO₂ varies from -65,3 to -56,8°C) with an admixture of CH₄ (1-18 mole%) and N₂ (0-15 mole%). Most inclusions seem to be monophasic at room temperature (water phase invisible), two phase inclusions were observed in quartz from dilation structures (H₂O phase up to 40 vol.%). The H₂O phase in these F.I. is 3 to 9 wt.% NaCl equiv. solution. F.I. usually decrepitate before homogenisation (Th 214 to 315°C). Density of the CO₂ rich phase varies considerably in the range 0,39-0,99 g/cm³

(ThCO₂ between -25,5 and +22,0°C) and this is probable due to variations in pressure. The highest densities have been found in shear veins (C structures) indicating pressure up to 0,32 GPa at 350, whereas inclusions in quartz from extension veins indicate a significantly lower pressure (0,15 GPa). The great pressure difference (about 0,1 GPa) has been documented also between F.I. in the same sample (in C veins). These P values were calculated using the data on composition-molar volumes of monophase CO₂ rich inclusions (water phase invisible) assuming 10 vol.% of H₂O phase. If leakage of water from these F.I. took place in the early ductile deformation stage (Bakker and Jansen 1994), the actual pressures could have been higher.

(ii) H₂O inclusions: this type follows F.I.P. across several quartz grains (late F.I.). Inclusions contain low saline solutions (2-8 wt.% NaCl equiv.) and homogenize from 160 to 280°C.

(iii) N₂ rich inclusions: these one-phase gaseous inclusions (Th -142 to -132°C to gas) occur along F.I.P., some of them are of the same orientation as the H₂O inclusions. Nitrogen prevails (68 mole%) over methane (25 mole%) and carbon dioxide (7 mole%), density of the admixture is very low (0,08 g/cm³) indicating very low pressure (25 MPa at 300 assuming presence of 5 vol.% of invisible H₂O phase in F.I.).

There is geological evidence of shear deformation and contemporaneous vein formation. Considering that retrograde mineral assemblages in host gneisses (biotite, muscovite, chlorite) were formed at temperatures around 400°C then the contemporaneous CO₂ rich inclusions provide a pressure constrain between 0,4 and 0,16 GPa. It follows that the shear zone and the quartz veins originated at considerable depths (13 - 6 km under lithostatic pressure). Nevertheless, the CO₂ rich fluids being apt to volume increase during decompression probably caused fluid overpressures in the shear zone and helped the mechanics of dilation in sense of Cathelineau et al. (1993). It is not clear if gold precipitated from CO₂ rich or from later H₂O solutions. The study of orientation of F.I.P. in vein quartz has not shown clear relation to the main geological structures. This is in agreement with the late origin of H₂O and N₂rich F.I. which could represent unmixing events in a late brittle regime.

References:

- Bakker R.J., Jansen J.B. (1994): Contrib. Mineral. Petrol 116, 7-20
Cathelineau et al. (1993): Eur. J. Mineral., 5, 107-121
Pertoldova J. et al. (1990): Proceedings of the 8th IAGOD Symposium, Ottawa, A 155
Puncochar M. et al. (1993): Unpublished final report on exploration of Au-W ores in the Kasperske Hory district, Geofond. Praha. (In Czech)

PIXE EVIDENCES FOR DEEP METAL-RICH EVAPORITIC FLUID EMISSION AT THE OXFORDIAN SEA-BOTTOM (SE BASIN, FRANCE)

EDON, M.(1), RAMBOZ, C.(1), VOLFINGER, M(1), CHOI, C.G.(2), ISABELLE, D.(2)

(1).CNRS-CRSCM, 1A rue de la Férollerie, F-45071 Orléans,

(2).CERI, 3A rue de la Férollerie, F-45071 Orléans.

In the SE basin of France, hypersaline and carbonic fluid inclusions (FI), in neofomed and diagenetic quartz from Triassic diapirs, were recently reinterpreted as representative of elevated P-T trapping conditions (≥ 1.8 kbars, $\geq 160^{\circ}$ - 400° C), reached at the faulted Triassic basement [1]. These record repetitive decompression proces related to regional tectonics [1]. At the basin center, metallogenic evidences suggest that evaporitic fluids are locally responsible of metal mobilization [2,3] but still now, no direct geochemical results confirm this hypothesis. Analytical developments in Proton Induced X-ray Emission (PIXE) now allow to obtain elementary concentrations on microvolumes. This technique, based on the analysis of emitted X-rays during irradiation of a sample by a protonic beam, constitutes a major progress to FI interpretations as direct, non-destructive and quantitative analysis. This is particularly suited to estimate ore metal concentrations [4]. PIXE analyses were performed at the CERI laboratory (CNRS, Orléans, France). Be or Al filter (138 and 104 μ m, respectively) in front of a Si(Li) detector were used to attenuate the X-radiation of light elements and the background due to the 'bremsstrahlung' and the Compton diffusion. The effect of the attenuation of X-radiation through the sample is important to consider for the concentration calculation and the possibility to detect the elements. Thus, the thickness of hosted quartz upon the selected FI has to be known precisely. For example, to detect Cl, the maximal depth of FI has to be less than 20 μ m. In detail, the GUPIX program [5] used for the X-ray spectra treatment calculates the atom quantity involved in the irradiated microvolume. For each analysis, one FI was oriented so its larger lenght be parallel to that of the protonic beam. This procedure allows to determine FI composition minimising hosted-mineral contribution and background. Our objective is to characterize the metallogenic potential of evaporitic fluids by PIXE analyses on FI in quartz from Triassic diapirs and on internal minerals in septarized nodules from oxfordian black marls (SE basin, France), related to deep evaporitic injections during early diagenesis [3]. East of one Triassic diapir (Beauvoisin site), Oxfordian black marls locally show carbonated association, or pseudobioherms, constituted of argileous-carbonated nodules, septarized or not, ammonoids, large bivalves and other non-building organisms. Inside septarized nodule, various minerals (calcites, celestite, barito-celestite, saddle dolomite) occupy the central cavity and non-opened veins towards external parts of the nodule.

Cl, Ti, Cu and Zn were detected in one secondary carbonic and hypersaline FI in evaporitic quartz. Salinity being determined by microthermometry, and maximal dissolved CO₂ concentration being known at 25°C [6], the fluid composition at 25°C can be calculated: 78.09 H₂O-1.60 CO₂-20.30 NaCl (wt %). The fluid density is estimated to be ~ 1.19 g.cm³ [7]. Thus the elementary ratio of Zn, Cu, and Ti

relative to Cl are known (Zn/Cl=0,0116, Cu/Cl=0,0217, Ti/Cl=0,0235) and concentrations can be calculated relatively to that of Cl: Zn=1400±300, Cu=2700±320, Ti=2900±370 (ppm). Note that hosted quartz is devoid of any trace elements.

For each studied internal crystallizations from Beauvoisin nodules, zones without FI were selected. Barito-celestites contain Cu in addition to Sr and Ba. Calcite is enriched in Sr, Fe and Mn. Saddle dolomite shows Fe, Sr, Mn, Cr, Zn and Cu.

Fluid chemistry. Even if Ca was not detected by PIXE in FI from evaporitic quartz, its presence is known by low eutectic temperature values (--50°C) and EDS spectrometry analyses [1]. In similar FI, previous SEM-EDS analyses [3] did not detect Zn and Ti, and only have suspected Cu. Rutile was not optically recognized in these FI, and thus we can suspect the presence of Ti chloride as already measured in such saline and carbonic fluids using PIXE [8].

Fluid source. A recent geochemical study on Oxfordian Beauvoisin nodules demonstrates that internal minerals precipitated from mixing of a 'marine' fluid and a hot, reduced, 'hydrothermal' fluid of evaporitic source [3]. The presence of Cu and ±Zn detected by PIXE, in both FI from evaporitic quartz and mineral matrix from Beauvoisin nodules, confirm this hypothesis. The absence of Zn in barito-celestites and of any metal in calcite probably reflects various mixing between the marine end-member, devoid of any metal, and the metal-rich evaporitic one. Besides, ICP/MS analyses performed on this calcite type display anormal Sr concentrations (≥10000 ppm) and Sr/Ca ratios at least 2 time higher than biogenic and inorganic calcites [9]. These results also attest the injection of an evaporitic fluid during early diagenesis of Oxfordian marls.

Metal source. PIXE results attest metal mobilization by evaporitic fluids at the Oxfordian. Evidences for two younger halokinesis during 'pyrénéo-provençale' and alpine tectonics were previously demonstrated [1,10,11]. Besides, Pb-Zn-Cu-Ba veins in the SE basin, relatively related to Tertiary, attest later metal mobilization always in relation with evaporitic fluid circulation [2,3]. However, source of metal is still unknown. Only few Pb isotopic data suggest that part of Pb could have a deeper source: Pb-Zn veins localized just upon major basement faults display more radiogenic Pb compositions than stratiform ore deposits [12,13]. Note that part of the CO₂ trapped in hypersaline FI in evaporitic quartz was related to a thermal anomaly in the Triassic faulted basement [14]. This part of carbonic component was interpreted as representative of a deeper source and as the probable heat vector and so it confirms deeper fluid circulation [14].

Hence, the systematic association metal-evaporitic fluids is either demonstrated by in situ analyses on FI and on minerals or by mineralogical evidences. These results open new research perspectives, in particular for the comprehension of metal mobilization process and the identification of metal sources or of potential metallic reservoirs. In this context, the metallic importance classically attributed to black marls [15] have to be revised.

References

- [1] EDON *et al.*, 1994. *Eur.J.Mineral.*, 6, 855-872.
- [2] MOËLO & LÉVY, 1976. *Bull.Soc.fr.Minéral.Cristallogr.*, 99, 38-49.
- [3] EDON, 1993. Thèse Univ. Orléans, 305 p.
- [4] RYAN *et al.*, 1991, *Nucl.Instr. and Method*, In Physics Research B54, 292-297.
- [5] MAXWELL *et al.*, 1989, *Nucl.Instr. and Method*, In Physics Research

B43, 218.

- [6]MALININ & KUROVSKAYA, 1975. Transf. from *Geokhimiya*, 4, 547-550.
- [7]WOLF et al., 1976, In: Lide, Handbook of chemistry and physics, CRC Press.
- [8]ANDERSON et al. 1989. *Economic Geology*, 84, 924-939.
- [9]RENARD, 1985. Thèse Univ. Paris VI. Doc BRGM n°85.
- [10]BELLON & PERTHUISOT, 1980.*C.R.Acad.Sci.*, Paris, 290, 1241-1244.
- [11]DARDEAU & GRACIANSKY de, 1990. *Bull.Centres Rech.Explor.Prod.Elf-Aquitaine*, 14, 110-151.
- [12]MARCOUX, 1987.Thèse Univ. Clermont-Ferrand, Doc. BRGM n°117.
- [13]Le GUEN et al., 1992.
- [14]EDON, RAMBOZ & GABBLE, 1995. *C.R.Acad.Sci. Paris*, (in press).
- [15]ARTRU, 1968. *Bull.Centre Rech.Explor.Prod. Elf-Aquitaine*, 2, 83-100.

ORE FORMING BRINES FROM THE Co - As DISTRICT OF BOU AZZER (ANTI-ATLAS, MOROCCO) : A FLUID INCLUSIONS STUDY

ENNACIRI, A., BARBANSON, L. and TOURAY, J.C

Equipe Ressources, Environnement et Matériaux (EREM),
URA 1366 du CNRS - ESEM - Université d'Orléans
Rue Léonard de Vinci, 45 072 Orléans Cedex 2, France

The Bou Azzer - El Graara area is located in the central part of the Anti-Atlas (Morocco), 300 km to the east of Agadir. It has been described as an eburnean basement overthrust during the major pan-african deformation by an ophiolitic complex. These formations were unconformably overlain by a volcanic and sedimentary infra Cambrian - Cambrian cover (Leblanc, 1975).

Since 1930, the Bou Azzer district has produced about 1000 tons of cobalt by year either from veins or from "contact deposits" (Ennaciri et al, 1995). At the district scale, the more complete mineral paragenesis may be described as following : 1) Ni diarsenides (rammelsbergite, pararammelsbergite); 2) Co diarsenides (safflorite, clinosafflorite); 3) triarsenides (skutterudite); 4) Fe diarsenides (löllingite); 5) sulfo-arsenides (arsenopyrite); 6) sulfides and sulfosalts (chalcopyrite, molybdenite, sphalerite, tetradrite,...). Western deposits may be distinguished from Central and Eastern ones by higher Co and Au and lower Ni contents. The mineralization stage is presumably late hercynian in age.

Fluid inclusions have been studied in quartz and calcite grown either at the mineralization or during a late stage. About 50 doubly polished wafers with thickness spanning from 0,25 to 0,70 mm have been prepared in quartz and calcite from 30 samples. A total of 720 fluid inclusions have been studied in samples from 5 occurrences (Mechoui, Bou Azzer mine at the West of the district; Bouismas and Tamdrost at the center; Ait Ahmane at the East).

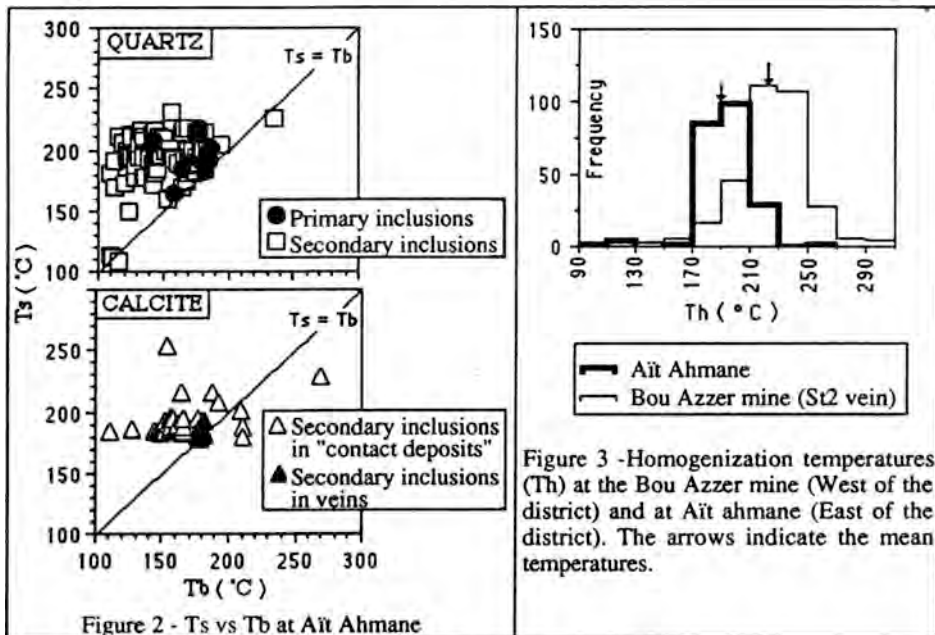
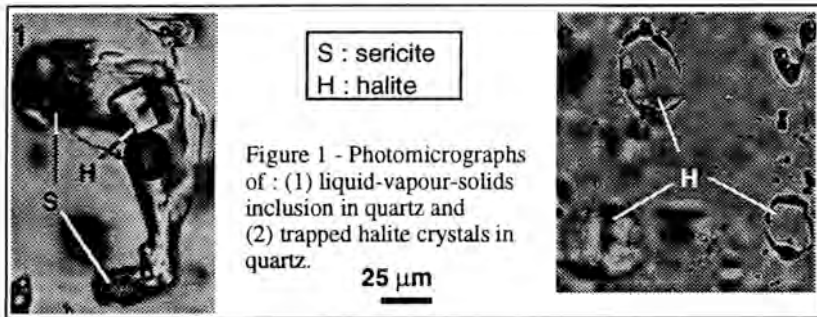
Excepting metastable inclusions, primary and secondary fluid inclusions in quartz and calcite (size in the range 10 to 50 μm) display a halite daughter crystal (fig.1). Identified trapped phases (optical microscopy, SEM-EDS, Raman microprobe) are muscovite or sericite, feldspars (albite or K-feldspar) and barite. SEM analyses of evaporated brines from broken inclusions indicate trapped solutions belonging to the system $\text{H}_2\text{O} - \text{NaCl} - \text{CaCl}_2$, with additional KCl and BaCl_2 . Minor amounts of N_2 and CH_4 have been detected by Raman microprobe in the bubbles.

During heating runs (fig.2), the gas bubble disappears at T_b , usually before the halite daughter crystal with dissolves at T_s (total homogenization). For 700 determinations, there is no systematic variation between early quartz and late calcite as well as between primary and secondary inclusions. Apparently a unique ore forming brine, with slightly variable characters was involved at a 50 Km scale. From additional freezing data and using the approach of Williams-Jones and Samson (1990), the following compositions are derived : Equivalent weight salinities ($\text{NaCl} \% + \text{CaCl}_2\%$) : 36 to 40%, $\text{CaCl}_2/\text{NaCl}$ weight ratio : 1 to 1,3. Eventually, there is a significant T_b shift with lower values in the Western part of the district (fig.3)..

At Ait Ahmane, the presence of trapped halite crystals in quartz (fig.1) suggest that at some times brines were at saturation with

NaCl. Accordingly one has then $T_s = T_f$ (Touray, 1970). Usually, brines were probably undersaturated and T_f higher than T_s . Temperature variations at constant pressure may then explain the T_b scattering. Isochore slopes have been extrapolated from Zhang and Frantz (1987) to 18 ± 2 bar / °C. The hypothesis of an isochoric evolution between T_b and T_s at Ait Ahmane lead to an upper estimation of Pf at about 1 Kb. With reference to Roedder and Bodnar (1980) and neglecting P_{gases} (from CH₄ and N₂) an actual pressure of $0,8 \pm 0.2$ Kb may be guessed.

With regard to mineral paragenesis and fluid inclusions data, Co-As ore deposits from the Bou Azzer district appear very similar to the well known mines of Cobalt, Ontario, Canada (Marshall et al 1993). An important question to be adressed is the origin of the brines, wich cannot derive from the solubilization of ancient evaporites (Touray, 1970). At a regional scale, higher erosion may be suspected in the Western part of the district, wich suggest that the Eastern and Central part of the district of Bou Azzer have a higher economic potential.



References

- ENNACIRI A., BARBANSON L. and TOURAY J. C. (1995) - Mineralized hydrothermal solution cavities in the Co-As Ait Ahmane mine (Bou Azzer, Morocco). *Mineralium Deposita*, in press.
- LEBLANC M. (1975) - Ophiolites précambriennes et gîtes arseniés de cobalt (Bou Azzer, Maroc). *Thèse Doct. d'Etat, Univ. Paris VI et Notes et Mem. Serv. Geol. Maroc n° 280* (1981).
- ROEDDER E. and BODNAR R. J. (1980) - Geologic pressure determination from fluid inclusion studies. *Ann. Rev. Earth Planet. Sci.*, 8, p. 263-301.
- TOURAY J. C. (1970) - Analyse thermo-optique des familles d'inclusions à dépôts salins (principalement halite). *Bulletin suisse de Min. et Pétro.*, 50/1, p. 67-79.
- WILLIAMS-JONES A. E. and SAMSON I. M. (1990) - Theoretical estimation of halite solubility in the system NaCl - CaCl₂ - H₂O : Applications to fluid inclusions. *Canad. mineral.*, 28, p. 299-304.
- ZHANG Y.-G. and FRANTZ J. D. (1987) - Determination of the homogenization temperatures and densities of supercritical fluids in the system NaCl-KCl-CaCl₂-H₂O using synthetic fluid inclusions. *Chemical Geology*, 64, p. 335-350.

HYDROTHERMAL FLUID EVOLUTION IN THE F-Pb-(Zn) MINERALIZATION OF PARZAN (BIELSA MINING DISTRICT, CENTRAL SPANISH PYRENEES).

FANLO, I. & FERNANDEZ-NIETO, C.

Dep. Cristalografía y Mineralogía. Universidad de Zaragoza.

The Parzán mine is located in the northernmost end of Huesca province. From the geological viewpoint, the investigated deposit is situated in the Pyrenean Axial Zone. In the study area, the later zone are marked by Devonian and Carboniferous detrital and carbonate rocks which were folded and metamorphosed during the Hercynian Orogeny. These Palaeozoic rocks were intruded by the late-kinematic Bielsa granite (298±10 My). The Mesozoic sequences that exhibit a hiatus comprising Jurassic and Lower Cretaceous, overlies an erosive discordance above the paleozoic materials. The Alpine Orogeny gave rise big south-directed overthrusts.

The Parzán deposit is a single vein enclosed between the Bielsa granite and Triassic red bed sequence. The vein is an open-space filling of a steeply dipping and E-W fracture whose length and width vary between 800 and 900 m and between 2 and 4 m, respectively. Vein-wall rock contacts are sharp and occasionally brecciated. Phyllic alteration has been observed in the granite hanging wall. The mineral assemblage mainly consists of fluorite and galena, and minor siderite, pyrite, sphalerite, chalcopyrite and quartz. Paragenetically later, dolomite and barite occur. A supergenic assemblage consisting of cerusite, anglesite, covellite, malachite, azurite and goethite are also observed.

The fluorite is mostly massive, coarsely crystalline and yellow-orange in colour. In spite of their translucent appearance, it can be occasionally observed transparent crystals. Even though the above fluorite structure is the most often one, fluorite also exhibit banded fabrics in the core of the vein and brecciated fabrics near the vein boundaries. It is worthy to note that only one fluorite sample contains euhedral crystals.

To characterize the composition and temperature of the fluids from which fluorite was precipitated, the fluid inclusion study was undertaken using microthermometry and cryogenic scanning electron microscopy. A suite of samples were collected from 7 profiles located at different vein levels. Each profile consists of three samples: two from the north and south rims and one from the core. A total of 1,160 fluid inclusions in fluorite and 40 in quartz were studied. A number of inclusions occur as small groups and rarely isolated and the remainder occur in relatively wide bands associated with healed fractures. Inclusions shapes may vary from negative crystals to regular and dimensions range from 5 to 20 μm . The fluid inclusions are consistently simple two-phase liquid-vapor inclusions, with vapor bubbles generally occupying less than 15-20 vol % of the inclusion, with no daughter minerals or separate CO₂ phase at room temperature and during freezing experiments. Approximate eutectic melting temperatures between -45° and -65°C suggest complex solutions with significant CaCl₂ content. Final ice melting temperatures (T_m ice) ranged from -7.3°

to -22.1°C and their salinities, estimated for the system NaCl-H₂O, between 10.8 and 24.1 wt % eq. NaCl (Fig. 1A). In samples of quartz this values ranged from -16.1° to -20.5°C, and between 19.7 and 23.0 wt % eq. NaCl. Final hidrohalite melting temperatures (T_{mh}) were determined for 21 fluid inclusions of fluorite and these ranged from -25.6° to -21.3°C. Homogenization temperatures in fluorite (T_h) ranged from 117°C to 195°C and in quartz samples between 179.9°C and 199.5°C (Fig. 1B).

The above results indicate that, in general, the salinity increases from lower profiles to higher ones of Parzán vein (Table 1). On the other hand, samples located in the north rim exhibit highest salinities than those samples located in the southern rim while the lowest salinity is distributed between samples from core and south rim of the vein. With regard to the homogenization temperatures, it was observed a decreasing trend from the lower levels of the vein to the shallower ones. In addition, fluorites situated close to the north rim (granitic host rock) never show a higher temperature than the samples take from the core and the south rim (sandstones host rock) of the same profile.

The Cryo-SEM-EDS study performed in the fluorite inclusions indicates that the more abundant components in the mineralizing fluids are Na, Ca and Cl, whereas K appears as a minor component. The CaCl₂/NaCl ratio vary between 0.65 and 1.

Although as a first approach the microthermometrical data could be interpreted as a result of fluid mixing process, geological (vein display neither vertical nor lateral zonation) and geochemical (the absence of any correlation between T_h and T_{mi} along with REE and stable and Sr isotopes evidences) as well as statistical model lead to reject the later hypothesis.

From the above, it follows that Ca-bearing brines, mobilized during the post-hercynian times through faults, were responsible for the formation of the studied deposit. These fluids show, if we considered all the vein profiles, a trend from a initial stage with a middle salinity and high temperatures to a final stage with increase of the salinity and decrease of the temperature. However, there are variations of the salinity and T_h data for studied samples in a same profiles, which could indicate that homogeneous solutions entered in several pulses during the successive movements in the fracture re-openings. These variations of composition, concentration, temperature and pressure in the mineralizing fluids were the principal factors from which Parzán vein was precipitated.

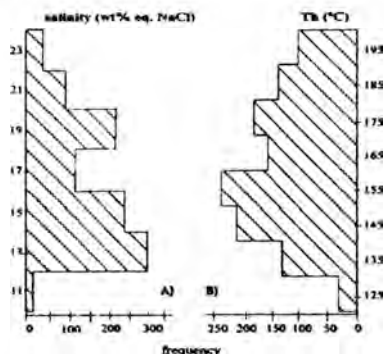


Figure 1: Microthermometric data of fluorites from Parzán: A) salinity and B) T_h.

profile	salinity		T _h	
	range	mean	range	mean
P1	-8 to -20	15.6	141 to 194	172.6
P2	-8 to -18	16.5	153 to 197	176.4
P3	-7 to -20	18.5	121 to 189	164.0
P4	-9 to -17	16.5	122 to 186	159.9
P5	-11 to -22	21.2	126 to 187	153.5
P6	-10 to -20	19.2	122 to 196	152.7
P7	-11 to -20	19.6	117 to 155	141.0

Table 1: Microthermometric results from Parzán vein.

NATURE OF FLUID INCLUSIONS AND EVIDENCE FOR P.V.T.X EVOLUTION OF HYDROTHERMAL SOLUTIONS IN GOLD-QUARTZ VEINS IN THE ARCHAIC ABITIBI GREENSTONE BELT, QUEBEC.

FIRDAOUS, K. (1), BOULLIER, A.M. (1), BOIRON, M.C. (2) and ROBERT, F. (3)

(1) CRPG - CNRS, BP 20, F-54501 Vandoeuvre-lès-Nancy cedex.

(2) CREGU, BP 23, F-54501 Vandoeuvre-lès-Nancy cedex.

(3) Geological Survey of Canada, 601 Booth St., Ottawa Ont. K1A 0E8.

The mesothermal gold-quartz vein deposits of the Archaic Abitibi Subprovince (Canada) have been interpreted in terms of ancient fault-valve (Sibson et al., 1988). Growth and deformation textures in the veins provide evidence for generally lithostatic but fluctuating fluid pressures and for cyclic stress reversals during vein formation and are consistent with such a fault-valve model (Boullier and Robert, 1992).

A fluid inclusion study has been undertaken on the gold-quartz-tourmaline-carbonate-pyrite veins (extensional and fault veins) from Sigma and Dumont-Bras d'Or (Quebec) in order to determine the P-V-T-X properties of vein-forming fluids and to estimate the amplitude of the fluid pressure fluctuations.

Fluid inclusions show three modes of occurrence in quartz: healed microcracks, three-dimensional clusters and along grain boundaries in plastically deformed quartz. Fluid inclusions in healed microcracks are secondary relative to the host crystal but the development of these microcracks and the trapping of the fluids are considered to be an integral part of the cyclic development of the veins.

Four types of fluids have been recognized from microthermometric studies and Raman spectroscopy for one sample from a fault vein and three samples from extensional veins (figure 1):

- aquocarbonic fluid (10 to 85 %vol. CO₂, -63.7°C<TfCO₂<-56.7°C, -49.2°C<ThCO₂<+30.9°C, 211.5°C<TH<425°C, 1 %eq.wt NaCl<salinity<6 %eq.wt NaCl, 5 mol.%<CH₄+N₂<30 mol.%, 0.47 g/cm³<density<1.0 g/cm³);
- carbonic fluid (-63°C<TfCO₂<-56.7°C, -49.2°C<ThCO₂<+28.8°C, 5 mol.%<CH₄+N₂<30 mol.%, 0.52 g/cm³<density<1.03 g/cm³);
- aqueous fluid (10 to 60% vol. vapour H₂O, ±NaCl solid, 78°C<Th<380°C, 0.5% eq.wt NaCl<salinity<34% eq.wt NaCl, 0.58 g/cm³<density<1.26 g/cm³);
- CH₄-N₂-rich fluid (20 to 75% vol. vapour CH₄+N₂, 10.6°C<Tfc<15.2°C, 326°C<TH<393.7°C), 20 mol.%<CH₄<72 mol.%, 28 mol.%<N₂<80 mol.%. Such fluid has been only observed in extensional veins.

In all extensional veins examined, healed microcracks contain different fluid inclusion types depending on their orientations: CO₂-CH₄-(N₂) and H₂O-CO₂-NaCl-CH₄-(N₂) fluid inclusions occur in subhorizontal planes, parallel to the vein walls, whereas H₂O-NaCl-CaCl₂ fluid inclusions occur in subvertical planes, perpendicular to the vein walls. In fault veins, the separation of fluid inclusion types in microcracks of different orientations is not as pronounced.

Microthermometric and Raman data may be interpreted by the trapping of two immiscible fluids (a carbonic-rich and a water-rich fluid) from a parent H₂O-CO₂-CH₄-(N₂)-low salinity metamorphic fluid during the formation of the vein. Calculated isochores for these aquocarbonic and carbonic fluids (figure 2) indicate Pf fluctuations

between 100 and 300 MPa in extensional veins and between 100 and 200 MPa in the fault vein at 350°C. These data are consistent with the fault-valve model (Sibson et al., 1988) which implies fluid pressure drops related to seismic activity.

It should be noted that two groups of H₂O-NaCl fluid inclusion have to be distinguished : those with T_h>200°C, and those with T_h<180°C. Inclusions of the high temperature group are interpreted to result from unmixing of the parent H₂O-CO₂-CH₄-(N₂)-low salinity and by mechanical separation from the coexisting carbonic phase due to their different wetting properties. The composition of low temperature aqueous fluid is similar to Canadian Shield basement brines that percolated down the crust, and which may have been trapped in latest open vertical vertical microcracks. Their P-T trapping conditions are between 120 to 160°C and 80 to 150 Mpa.

BOULLIER and ROBERT, 1992. *J. Struct. Geol.*, 1992, 14, 161-179.
 DUBESSY et al., 1992. *Eur. J. Miner.*, 1992, 4, 873-884.
 SIBSON et al., 1988. *Geology*, 1988, 16, 551-555.
 THIÉRY et al., 1994. *Eur. J. Miner.*, 1994, 6, 753-771.

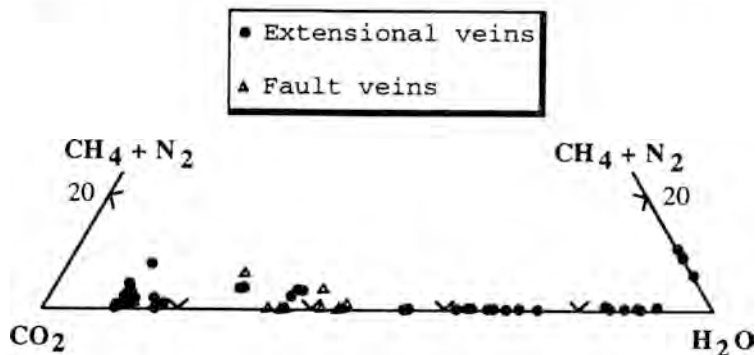


Figure. 1. Bulk-composition obtained from laser Raman spectroscopy of carbonic, aquocarbonic and CH₄-N₂-rich fluids in the extensional and fault veins.

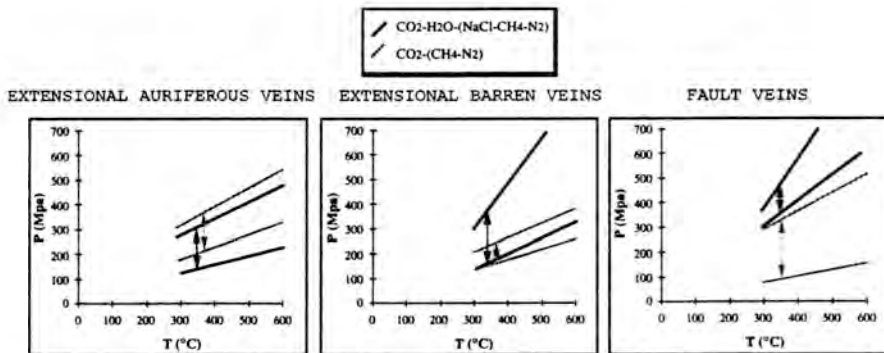


Figure. 2. P-T diagram showing calculated isochores for selected CO₂-rich and H₂O-CO₂ fluid inclusion planes. The isochores were calculated with the computer code (Dubessy et al., 1992 and Thiery et al., 1994) in the H₂O-CO₂-NaCl-(CH₄-N₂) system. Arrows show the range in fluid pressure at a temperature of 350°C.

CO/CO₂ FLUID INCLUSIONS IN ALUMINOUS METASEDIMENTARY XENOLITHS IN SILICEOUS LAVAS FROM MT. AMIATA (TUSCANY, ITALY).

FREZZOTTI, M.L. (1), BURKE, E.A.J. (2), GHEZZO, C. (1).

- (1) Dipartimento di Scienze della Terra, Via delle Cerchia, 3
53100 Siena, Italy
- (2) Instituut voor Aardwetenschappen, Vrije Universiteit,
De Boelelaan 1085, 1081 HV Amsterdam, The Netherlands.

Carbon monoxide individual natural fluid inclusions have been reported only once, by Bergman and Dubessy (1984) in a composite peridotite xenolith from the Lunar Crater Volcanic field, Nevada, U.S.A.

CO/CO₂ inclusions have been observed in aluminous metasedimentary xenoliths in rhyodacitic lavas from Mt. Amiata. These xenoliths record complex processes of magma-rock interactions and show a composite zoned pattern. Petrographic investigations (Van Bergen, 1984) revealed a sequence of zones from the cores of the xenoliths towards the enclosing lavas:

- Core: sanidine, spinel, biotite, plagioclase, andalusite, sillimanite, corundum, Fe-Ti oxides and graphite.
- Plagioclase zone: plagioclase (>90%), subordinate biotite or orthopyroxene, relict spinel. Locally some glass may be observed.
- Brown glass zone (rare): brownish glass with phenocrysts of plagioclase and/or biotite.
- Clinopyroxene zone (rare): clinopyroxene phenocrysts embedded in a fine-grained groundmass of pyroxene, sanidine, biotite and minor glass.

According to Van Bergen (1984) quartz-poor muscovite-biotite schists are considered to be the most likely parent rocks of the xenoliths.

The host lavas are K-rich rhyodacites which consist of plagioclase, K-feldspar, orthopyroxene, diopside, augite, biotite and ilmenite phenocrysts enclosed in a glassy matrix, with common perlitic cracks and spherulitic textures.

Two different types of fluid inclusions occur in the newly formed minerals in the different zones of the xenoliths:

- 1) Pure CO₂ inclusions occur in the most external zones with very low contents of graphite, observed both by Van Bergen and by us in plagioclase and orthopyroxene.
- 2) CO/CO₂ inclusions occur in sanidine in the cores with higher contents of graphite.

These CO/CO₂ inclusions in the newly formed sanidine crystals are isolated large (up to 30 μm) monophase vapour inclusions, occupying up to 5 vol-% of the crystals. During freezing runs initial melting was observed at about -59.5°C and final melting occurred between -57.7 to -57.0°C. Homogenization, always to the vapour (L+V->V), was recorded only in a few inclusions between 18.5 and 26°C. Raman analyses (with prolonged measurement times because of extremely low densities) of the inclusions with the lowest melting point give a composition of 8 to 10 mole-% CO and 92 to 90 mole-% CO₂. Because of the paucity of PVTX data for the liquid vapour equilibrium in the system CO/CO₂ it is not possible to determine the bulk molar volume from these results.

Van Bergen (1984) proposed that the pure CO₂ inclusions in the rims of the metasedimentary xenoliths from Mt. Amiata were formed by oxidation of graphite at contact-metamorphic conditions, as he observed a decrease of the abundance of graphite from the cores towards the host lavas. Temperatures in the cores were much lower, around 350-400°C (obtained from graphite peak ratios in Raman spectra). The resulting lower oxygen fugacity conditions failed to oxidize the graphite completely and caused CO/CO₂ fluids.

References:

- BERGMAN, S.C. & DUBESSY, J. (1984) CO₂-CO fluid inclusions in a composite peridotite xenolith: implications for upper mantle oxygen fugacity. *Contributions to Mineralogy and Petrology*, 85, 1-13.
- VAN BERGEN, M.J. & BARTON, M. (1984) Complex interaction of aluminous metasedimentary xenoliths and siliceous magma; an example from Mt. Amiata (Central Italy). *Contributions to Mineralogy and Petrology*, 86, 374 - 385.

FLUID INCLUSIONS IN QUARTZ, BERYL AND APATITE FROM THE FORCAREY-SUR PEGMATITE FIELD (SPAIN)

FUERTES, M (1); MARTIN-IZARD, A(1); MANGAS, J(2)

(1) Department of Geology. University of Oviedo. 33005 Oviedo, Spain

(2) Department of Physic. University of Las Palmas, Tafira. 35080 Gran Canaria, Spain

The Forcarey-Sur pegmatite field is located between the towns of Cerdedo and Avion in northwestern Spain. In this area there are several north-south-trending pegmatitic and pegmoaplitic outcrops which are contained within a narrow belt of metasedimentary rocks (Paraño Group). The pegmatite field is associated with two-mica or muscovite peraluminous synkinematic granites which are affected by the third tectonic phase of the Hercynian Orogeny and crop out to the west of the pegmatites.

The pegmatites and pegmoaplitic of the Forcarey-Sur pegmatite field belong to the LCT (Cherny, 1993) family, and within this to the rare-elements type. These rocks have a number of field, mineralogical, textural and geochemical characteristics which allow them to be divided into five different groups (A, B, C, D and E) (Fuertes et al. 1994). These groups occur in such a way that the degree of differentiation increases progressively from the west to the east; the least developed pegmatites (groups A and B) being found nearest to the western granite complex, and the most developed ones (group E) furthest from it. The most fractionated pegmatites (groups D and E) contain Sn-Nb-Ta in the form of columbite, tantalite and tantaliferous cassiterite. This mineralization appears in replacement aplitic units of albite-rich pegmoaplitic.

The fluid-inclusion study was undertaken using microthermometry on quartz, beryl and apatite from a replacement aplitic unit of a pegmatite of the group E. This aplitic unit is rich in cassiterite and columbite-tantalite. The number of inclusions studied is 60 in quartz, 50 in beryl and 30 in apatite.

Based on the estimated composition on the trapped fluid using microthermometric data only one type of inclusion fluid has been defined: complex aqueous inclusions ($H_2O-NaCl-CH_4-CO_2$). These inclusions show two phases at room temperature. CH_4 homogenisation can not be observed and its presence has been detected by formation of hydrate, which melts above 10° ($10.8^\circ C$ to $16^\circ C$). CO_2 nucleation temperature ($-105^\circ C$ / $-118^\circ C$) was observed in ten inclusions and CO_2 melting temperature was measured in three inclusions ($-60.7^\circ C$, $-60^\circ C$, $-59^\circ C$). These nucleation and melting temperatures are consistent with the presence of CH_4 . The fact that CO_2 and CH_4 phase transitions can not be observed is probably due to their low density.

The temperature of initial melting of ice, where measurable, was generally close to the eutectic for the system $NaCl-H_2O$ ($-20.8^\circ C$; Potter & Brown, 1977). These results suggest that the aqueous solutions contain mainly Na in solution, and belong to the $H_2O-NaCl$ system. The exclusion of NaCl from the clathrate lattice results in artificially high salinities in the aqueous phase of the inclusions while CH_4 hydrate is present. Thus, measurement of the melting point of ice yields falsely high values of wt.% eq. NaCl. Although the use of wt.% eq. NaCl in such inclusions seems inappropriate, the salinity based on final ice melting with reference to the system $H_2O-NaCl$ (Potter et al., 1978) has been estimated.

Based on volumetric relations and homogenization temperatures three subtypes of inclusions have been distinguished:

Subtype IA. These inclusions are scarce, they appear isolated or in groups, and are interpreted as primary. The morphology of the inclusions is variable, commonly being elongated or subhedral negative crystal. The size of

the inclusions ranges between 4 and 10 μ m. These inclusions show Vg/Vt ratio of about 50%-80% and homogenisation temperatures between 360°C and 370°C (in the gas or critical state and two inclusions in the liquid state). This degree of variability in the pattern of homogenisation can be explained by small differences in the bulk composition of the fluid because these inclusions don't present characteristic of boiling process. The final ice melting temperature ranges between -1.8°C and -3°C (3.05 - 4.94 Wt. % eq. NaCl).

Subtype IB. These inclusions are the most abundant in quartz and beryl. They appear commonly in parallel planes, and are interpreted as secondary or pseudosecondary. Inclusions morphology is varied, being irregular or subhedral negative crystal. The size of the inclusions ranged from 4 to 12 μ m. The vapour phase occupies 20%-30% and homogenisation temperatures range between 270°C and 345°C in the liquid state. The final ice melting temperature ranges between -0.8°C and -3.8°C (1.39 - 6.14 Wt. % eq. NaCl).

Inclusions in apatite are included in this subtype. They are found distributed in healing fractures or isolated. Inclusions in fractures have negative crystal morphology, size ranged from 7 to 10 μ m and the vapour phase occupies between 10% to 20%. Isolated inclusions are irregular to rectangular form, sizes varying between 15 μ m and 20 μ m and the vapour phase occupies between 30% to 40%. The homogenisation temperatures range between 273°C and 310°C in the liquid state. The final melting temperature of ice values ranges between -2.2°C and -3.9°C (3.69 - 6.29 Wt. % eq. NaCl).

Subtype IC. These inclusions are more abundant in beryl than quartz. They appear distributed in healing fractures. Inclusions morphology is varied, being irregular, elongated or subhedral negative crystal, and are interpreted as secondary. The size of the inclusions ranged from 4 to 10 μ m. The vapour phase occupies 5%-10% and homogenisation temperatures range between 200°C and 247°C in the liquid state. The final melting temperature of ice values ranges between -1.1°C and -1.9°C (1.90 - 3.21 Wt. % eq. NaCl).

The microthermometric data are summarised in Table 1.

HOST MINERAL	INCLUSION TYPE	Vg/Vt	Th °C	N°	T _{mice} °C	T _{mCO₂} °C	T _{mhydr.} °C
QUARTZ	IA	50-75%	360L 365 to 370G 365 to 370C	10	-2.1 to -3	-60	13.4 to 13.8
	IB	20-30%	270 to 345L	43	-1.8 to -3.8	-59 to -60.7	10.8 to 16
	IC	5-10%	230 to 245L	7	-1.1 to -2.1		10.8 to 11
BERYL	IA	70-80%	360 to 370G 362C	7	-1.8 to -2	-	11 to 12.4
	IB	20-40%	270 to 328L	23	-0.8 to -1.8		11.2 to 12.4
	IC	5-10%	200 to 247L	18	-1.1 to -1.9		11.2 to 13
APATITE	IA	5-10%		20	-2.2 to -3.9	-	-
	IB	30-40%	273 to 310L	10			

From the above microthermometric data clearly no significant differences exist among the fluid inclusion populations in quartz, beryl and apatite. Three discontinuous trapping stages of fluid inclusions can be distinguished with progressively lower homogenization temperatures. Only one fluid composition has been approximated, a low-salinity aqueous fluid with CH₄ and CO₂. This fluid may have been responsible for the albitic metasomatism of the pegmatitic body and associated Sn-Nb-Ta mineralization. Fluids with similarity composition has been described in fluid inclusions from metasomatic minerals in border unit of The Tanco zoned granitic pegmatite (Thomas et al., 1990).

Bibliographic references

- CERNY, P. (1993). Ore deposit models vol II. Geoscience Canada, 29-48.
 FUERTES, M. & MARTÍN-IZARD, A. (1994): *Boll. Soc. Esp. Min.* 17, 51-63.
 POTTER, R. W. & BROWN, D.L. (1977): *U.S. Geological Survey Bulletin*, 1421-C.
 POTTER, R.W.; CLYNNE, M.A.; BROWN, D.L. (1978): *Econ. Geol.* 76, 284-285.
 THOMAS, A.V.; PASTERIS, J.D.; BRAY, C.J.; SPOONER, E.T.C. (1990): *Geochimica et Cosmochimica Acta* 54, 559-573.

This paper was supported by grants from CICYT GBD 91/1077

FLUID MIGRATION IN MICROFISSURED GRANITES: A FLUID INCLUSION STUDY OF W-Sn VEINS IN THE SPANISH CENTRAL SYSTEM

GARCIA, E.(1), LOPEZ-G^a, J.A.(1), VINDEL, E.(1), & BOIRON, M.C.(2)

(1) Dpto. de Cristalografía y Mineralogía. Univ. Complutense. 28040 Madrid, Spain

(2) CREGU, BP 23, 54501 Vandoeuvre-Les-Nancy, Cedex France.

The geometry of the ore fluid migration was investigated in the (W-Sn) mineralized granites from the Spanish Central System. In the San Rafael deposit, ductile-brittle N40-60°E striking structures host W-bearing quartz veins (Q1), and are then affected by brittle deformation at the origin of a second type of vein striking N20-30°E (Q2). 3-D characterization of microstructural markers has been carried out using an optical microscope and image analyser (Lapique et al, 1988).

Characterization of fluids in FIP

Based on microthermometry and Raman microprobe analysis and textural relationships, five types of fluid inclusions V1c-w, V2c-w, Lw1 and Lw2 have been distinguished. (Table below) (C=carbonic phase; W=water; L=Liquid; V=vapour).

	Lw-s	V1c-w	V2c-w	Lw1	Lw2
Tm CO ₂ (°C)	--	-56.7 to -58.2	-56.7 to -59.2	--	--
Tm H ₂ O (°C)	--	--	--	-2.3 to -5.8	-1.5 to -3.2
Tm cl (°C)		6.5 to 9.3	6.4 to 10.7	--	--
Th CO ₂ (°C)		14.5 to 29	--	--	--
Th Tot (°C)	200 to 400	350 to 410 (V)	340 to 385 (V)	260 to 370 (L)	160 to 250 (L)
Orienta tion	N40-50°E N80-90°E N140-150°E	N50-70°E N20-30°E	N50-70°E N20-30°E	N50-70°E N20-30°E	N140-160°E N-S E-W

V1c-w fluid inclusions exhibit three phases at room temperature and critical homogenization are frequent around 350-410°C. Lw-s inclusions exhibit three phase at room temperature (L+V+S) and their salinity is in the range of 31 to 48 W% eq NaCl. V1c-w and Lw1 inclusions occur isolated, associated as primary inclusions parallel to growth planes of quartz. This two

types of inclusions could represent gas-rich and liquid-rich unmixed from a same fluid. Precipitation of wolframite can be related to this immiscibility phenomenon around 365° to 400°C and 150 MPa.

Geometry of fluid migration

Relationships between the geometry of the fluid inclusion planes (FIP) and the nature of the fluid have been established. Seven oriented blocks have been collected from the vein to the host granite on a distance of 40 m. away. Fluid inclusions have been systematically studied in healed microcracks (350-400 measured FIP in each wafer or thin section).

Lw-s inclusions are scarce, however, they are found also also in N40-50°E, N80-90°E and N140-150°E FIP and could represent the earliest fluid stages as in other W-veins hosting granites from the Spanish Central System.

Aqueous-carbonic fluids NaCl-H₂O-CO₂-(CH₄), V1c-w and V2c-w, and aqueous NaCl-H₂O inclusions Lw1, display preferential orientations N50-70°E and 20-30°E. With the distance to the veins, CO₂ contents decrease, and CH₄ and H₂O contents increase.

Aqueous NaCl-H₂O inclusions Lw2 (2.5-6.5 W% eq. NaCl) are trapped along the preferential direction: N140-160E, N-S and E-W. These directions show the lowest homogenization temperature and are exclusively characterized by aqueous inclusion planes.

Interpretation

Fluid trapping occurred in the San Rafael granites by means of a complex succession of opening and reopening of microfracture network. NE-SW ductile-brittle cracks contains quartz-wolframite, are thus connected with FIP bearing low density carbonic aqueous(0.3-0.7) fluids, and high density aqueous fluids (0.8-1.0). A later drop in XCO₂ is recorded in N140-160°E, N-S and E-W FIP. The replacement of wolframite by scheelite and sulphide deposition can be related with this stage.

A latest fluid is represented by small aqueous inclusions with relatively low Th. crosscutting along N-S, E-W, NE-SW and NW-SE all the precedent fluid inclusion planes.

References:

Lapique, F., Champenois, M & Cheilletz, A. Bull. Mineral 6 (1988). 258-263.

Acknowledgements: This work has been carried out through the Joule project N°JOU-CT93-0318 (CEE-DG XII-G) "Fluid behaviour in the upper crystalline crust: A multidisciplinary approach".

THE MESSINIAN SALT FROM THE MEDITERRANEAN: SOLUTE CONCENTRATION OF FLUID INCLUSIONS IN HALITE FROM THE CENTRAL SICILY BASIN

GARCIA-VEIGAS, J.(1), AYORA, C.(2), ORTI, F.(3), ROSELL, L.(3), ROUCHY, J.M.(4), LUGLI, S.(5)

(1) Serveis Científico-Tècnics, Univ. Barcelona, Martí i Franquès s/n., E-08028 Barcelona

(2) Institut de Ciències de la Terra, CSIC, Martí i Franquès s/n., E-08028 Barcelona

(3) Dpt. de Geoquímica, Petrologia i Prospecció Geològica, Univ. Barcelona, Martí i Franquès s/n., E-08028 Barcelona

(4) Lab. de Géologie, Muséum Nationale d'Histoire Naturelle, CNRS UA 723, Rue de Buffon, F-75005 Paris

(5) Dpto. di Scienze della Terra, Univ. Modena, S. Eufemia 19, I-41100 Modena

Deep boreholes and seismic profiles have defined three major stratigraphic units forming the Messinian evaporites: 1) Lower sulfates and marls, 2) Salt layer, 3) Upper sulfates, marls and salt lenses. Seismic data also demonstrates the existence of an unconformity between the top of the Salt layer and the Upper evaporites.

Extensive sedimentological and geochemical studies have been performed in the Messinian evaporites in recent past, but very little concerns the Salt layer. We present here the first systematic study of a Salt layer sequence from Caltanissetta Trough in Central Sicily. The study is mainly based on the evolution of the solute concentration in brines trapped as primary inclusions in halite. The solute content in the fluid inclusions have been compared with the result of the numerical simulation of evaporation processes in different scenarios of an open basin.

The results of bromine analysis in the bulk trapped fluid clearly differentiate between two units in the Salt Member: a lower unit including the kainite beds, which shows contents that increase towards the potash zone reaching a maximum of 150 ppm, and an upper unit in which contents decrease towards the top attaining values below 13 ppm. Low values, in general under 70ppm, suggest salt recycling by normal or only slightly concentrated seawater.

The results of fluid inclusion microanalysis by Cryo-SEM-EDS also record the same two saline units. The lower one is characterized by concentrated brines (high Mg, low Na contents), whereas the upper unit shows less concentrated brines (lower Mg, higher Na). In the lower unit the chemical evolution model that best matches the contents analyzed in fluid inclusions is the evaporation of seawater recharge without polyhalite precipitation, in which a small amount of CaCl_2 brine replaces an equal volume of seawater inflow. It follows that polyhalite inhibition to crystallize as a primary mineral plays an important role in the formation of economic deposits of kainite. In the upper unit the chemical evolution model that best reproduces the salinity decrease found in the fluid inclusions is the evaporation of seawater inflow saturated in halite (salt-recycling).

Thus, the geochemical study of halite samples confirms the marine origin of the mother brines and their relation ship to the SO_4 -rich evaporation trend with the inflow of seawater slightly modified by a CaCl_2 -rich inflow. In particular, the microanalysis of fluid inclusions demonstrates that the salt dissolution and reprecipitation which occurred towards the top of the Saline Member in the Caltanissetta Basin originally attributed to a

meteoric water influence was due to the inflow of seawater into the basin. Therefore, the very low bromine contents found at the top of the saline sequence do not really imply any significant contribution of continental waters.

A comparison with the marginal Lorca Basin (SE Spain), where locally also a thick Saline Unit deposited from marine waters in Messinian times, is of much interest. In this basin the elementary analysis of the solid phase shows a similar event of salt dissolution-reprecipitation at the top of the halite sequence. However, in this case, the study of fluid inclusions clearly reveals the Mg, K and SO₄-poor character of the brine with respect to normal marine waters at the top of the sequence due to the meteoric origin of the inflow waters. Thus, the Lorca Basin was isolated from the sea and evolved into desiccation under the influence of continental waters at the end of the saline deposition.

The same conclusion cannot be reached in the Caltanissetta Basin by studying samples available to us. Probably, a differentiated structural history has resulted in such diversified evaporitic records for both basins. This fact deserves to be taken into account when interpreting the significance of the sharp stratigraphic boundary recorded between the Salt Layer and the Upper Evaporite of the Messinian throughout the central parts of the Mediterranean Basin. For this interpretation it is not necessary to assume non-marine water inflow.

Acknowledgements: This work has been carried out in the framework of the DGICYT PB90-0485 and PB93-0165 projects.

CARBONIC FLUID EVOLUTION IN SYNTECTONIC VEINS IN METAPELITES AND MARBLES FROM PRIESTLY FORMATION (CENTRAL VICTORIA LAND, ANTARCTICA)

GIORGETTI G. (1), FREZZOTTI M.L. (1), CAROSI R.(2), MECCHERI M.(1), TOURET J.L.R.(3)

(1)Dip. Scienze della Terra, Università di Siena, Via delle Cerchia 3, I-53100 Siena, Italy.

(2)Dip. Scienze della Terra, Università di Pisa, Via S. Maria 53, 56100, I-Pisa, Italy.

(3) Faculteit der Aardwetenschappen, De Boelelaan 1085, 1081 HV Amsterdam, The Netherlands.

A fluid inclusion study was performed in four quartz veins occurring in low/medium grade metamorphic rocks of Priestly Formation, Wilson Terrane (O'Kane Canyon area, central Victoria Land, Antarctica); the Priestly Formation is constituted by graphite-bearing phyllites and metasiltsites interbedded with metarenites, impure marbles, and metacalcarenites. The Terrane was affected by a high T/low P metamorphism during the Cambro-Ordovician Ross orogeny; the metamorphic grade increases eastwards from lower greenschist facies to upper amphibolite facies conditions.

The structural frame consists of well developed, isoclinal to sub-isoclinal, similar upright folds with a pervasive axial plane schistosity; during the main metamorphic-tectonic event, a system of syntectonic veins developed: they are parallel to the regional foliation and sometimes boudinated. From a detailed observation of mineral assemblages in and out of the veins, it can be inferred that they were initially formed very close from the peak conditions and progressively filled during the retrograde evolution of the metamorphic complex. Veins are mostly constituted by quartz crystals (with minor calcite) showing variable degrees of recrystallization.

Objectives of the present study were the characterization of the fluids circulating at the peak of metamorphism and the reconstruction of overall fluid evolution during the retrograde path of this formation.

MR17 and MR18 veins (1/2cm in thickness) were sampled in a C-bearing metapelite, consisting of quartz+biotite+muscovite+feldspar and belonging to the upper greenschist facies; MR22 and MR25 veins (3/4cm in thickness) were sampled in a carbon-bearing marble constituted by carbonate+quartz+tremolite+diopside which experienced a higher metamorphic grade (lower amphibolite facies).

Fluid inclusion data: MR17, MR18 veins contain a single population of $\text{CO}_2+\text{H}_2\text{O}+\text{CH}_4(\pm\text{N}_2)$ fluid inclusions, with constant composition and density; these occur in clusters or short, regular intracrystalline trails and they show little or no evidence of "decrepitation".

Veins in marble: at least two episodes of fluid trapping have been recognized. i) Early $\text{CO}_2+\text{H}_2\text{O}+\text{CH}_4(\pm\text{N}_2)$ fluids, occurring in isolated inclusions or in intracrystalline trails; ii) Carbonic inclusions (with variable $\text{CO}_2/\text{H}_2\text{O}$ ratio) and aqueous inclusions associated in clusters or trails, with strong evidence of "decrepitation".

P,T interpretation: both types of vein constrain the retrograde P,T path of the formation, which appears to be more complex at higher metamorphic grade.

Fluids in MR22/25 (higher metamorphic grade) have followed a multistage P,T path evolution: early fluids ($\text{CO}_2+\text{H}_2\text{O}+\text{CH}_4\pm\text{N}_2$) were probably in equilibrium with the metamorphic assemblage at peak conditions. Then the rocks cooled isobarically leading to inclusion

decrepitation, requilibration at higher density, possible fluid immiscibility and, in many inclusions, selective H₂O leakage. All this evolution did occur at a local scale, without large movements of the fluid masses. Fluids in veins MR17/18 were trapped at lower temperature (below 400°C). Their preservation, and the fact that they were trapped in a single episode indicate that from this temperature downwards, the region did experienced an isochoric P,T path.

ICP-AES ANALYSIS OF FLUID INCLUSIONS II: COMPARISON WITH OTHER TECHNIQUES

GLEESON, S.A. & WILKINSON, J.J.

Fluid Processes Research Group, department of Geology, Imperial College of Science, Technology and Medicine, Prince Consort Road, London SW7 2BP, U.K.

A range of techniques are available for bulk analysis of solutes in fluid inclusions. However, relatively few comparisons between several different techniques have been made in the past. This study compares the results obtained from standard microthermometry, decrepitation linked ICP-AES (D-ICP), crush/leach ICP-AES (CL-ICP), crush/leach ion chromatography (CL-IC) and laser ablation ICP-AES on primary fluid inclusions in zoned quartz crystals.

Microthermometric analyses on vein quartz have shown the mineralising fluids to be highly saline NaCl-CaCl₂ dominated brines, typical of modern day formation waters (Carpenter et al.) and many Mississippi Valley type deposits (Roedder 1967). Analyses of bulk leachates by ion chromatography and ICP-AES give comparable results for the major elements (Na, Ca, K). However, the two analytical techniques correlate less well for elements which are close to the detection limits of ion chromatography analysis, e.g. Sr. This is probably due to the large uncertainty on values near background.

The discrepancy between the crush-leach and decrepitation analyses is more problematic. When the major, minor and trace elements normalised to sodium are considered, crush-leach data is much less reproducible than D-ICP. A comparison of the two techniques shows that crush-leach generally gives slightly higher values, but this relationship shows no apparent systematic bias. Occasionally crush-leach ICP and IC analyses give much higher, anomalous values than D-ICP that cannot be accounted for mechanisms such as preferential adsorption of multivalent ions (Bottrell et al., 1988). An alternative explanation is that these data may be due to contamination by dissolved microscopic solid phases; siderite, anhydrite, K-mica, sphalerite, galena are known to occur in the veins and, although not generally observed in the samples analysed, they may have contributed to anomalous Fe, Mn, Ca, K in the crush-leach data set.

This study highlights some of the problems encountered during bulk analyses of fluid inclusions. Preliminary data suggest that care must be taken when choosing samples for crush-leach analyses as microscopic solid phases in quartz may give anomalous results.

References: BOTTRELL, S.H., YARDLEY, B.W.D. & BUCKLEY, F. (1988). *Bull. Mineral.*, **111**, 279-290. CARPENTER A.B., TROUT M.L. & PICKETT E.E. (1974). *Econ. Geol.* **69**, 1191-1206. ROEDDER E. (1967). In *Genesis of Stratiform lead-zinc-barite-fluorite deposits: a symposium* (ed. J.S. BROWN), *Econ. Geol. Monogr.* **3**, 349-362.

FLUID INCLUSIONS IN EVAPORITES - SOME IMPLICATIONS ON THE DISPOSAL OF HIGH-LEVEL RADIOACTIVE WASTES

GRISHINA, S. (1) & KNIPPING, B.J. (2)

(1) Institute of Mineralogy and Petrography, Universitetsky pr. 3, 630090 Novosibirsk, Russia

(2) Institute of Mineralogy and Mineral Resources, Adolph-Roemer-Str. 2A, 38678 Clausthal, Germany

Slow decay and long lifetime of high-level radioactive waste command the use of storage procedures that will demonstrably provide the required level of environmental safety over geological timescales. Unfortunately though, experiments that reliably model the possible long-term behaviour of fluid phases in evaporites after disposing of the radioactive waste are not feasible on the required timescale. However, it is possible to look at similar processes in nature and use them as natural analogues. These experiments - carried out by nature - will supplement data from short-term experiments and mathematical models.

Basalt intrusions in evaporites can be used as natural analogues for the disposal of heat-producing radioactive wastes in evaporites. Among other geochemical parameters mainly the study of single fluid inclusions in salt minerals gives information on several relevant aspects, for example

- evolution of fluid chemistry caused by increased temperatures,
- extent of fluid migration in a temperature field,
- extent of thermal alteration of the salt rocks.

Thus fluid inclusions are studied in two different geological settings of basalt intrusions in evaporites:

- i) Basaltic sills of up to 300 m thickness intruded in Cambrian chloride-type evaporites in the Siberian platform (Russia).
- ii) Basaltic dykes of mostly < 3 m thickness intruded in Permian sulfate-type potash deposits of the Werra-Fulda potash region (Germany).

The evaporites have in both cases undergone intense mineral reactions and material transports. Rock alteration and gas accumulation obviously related to the basalt intrusion were documented both in Siberia (Pavlov 1975) and Germany (Knipping 1989). The flat shape of the basaltic sills on the Siberian Platform enabled a description of the fluid chemistry as a function of distance from the intrusions, based on fluid inclusion studies (Grishina et al. 1992). A clear zonation of inclusion associations in the vicinity of the sills was found. Apart from the host rock composition (e.g., Knipping & Herrmann 1985) the metamorphism could clearly be recognised by different inclusion characteristics like brine concentration, CO₂/H₂O ratio, CO₂ density, associated mineral inclusions and organic compounds. The extent of the thermal influence of the intrusions is visually marked by the disappearance of (primary) chevron structures in the salt minerals, which occur at a four times greater distance above than below the basaltic sills. It may indicate mainly thermal metamorphism below the intrusion and intense upward directed fluid migration above the intrusion. To verify this a quantitative investigation combined with subsequent modelling of the solution

composition concerning the major components, Br, Rb, and Li will be done.

Only a minor amount of studied halite samples from the German Werra-Fulda potash region contain water-free liquid-CO₂ inclusions. Those preliminary results confirm the relative importance of fluid migration processes (solution metamorphism) compared to thermal metamorphism.

References:

- Grishina, S.; Dubessy, J.; Kontorovich, A.; Pironon, J. (1992): Inclusions in salt beds resulting from thermal metamorphism by dolerite sills (eastern Siberia, Russia). - *Eur.J.Mineral.*, 4, 1187-1202.
- Knipping, B. (1989): Basalt Intrusions in Evaporites. - *Lecture Notes in Earth Sciences*, vol. 24, 132 pp., Berlin-Heidelberg-New York (Springer).
- Knipping, B.; Herrmann, A.G. (1985): Mineralreaktionen und Stofftransporte an einem Kontakt Basalt - Carnallitit im Kalisalzhorizont Thüringen der Werra-Serie des Zechsteins. - *Kali und Steinsalz*, 9, H. 4: 111-124.
- Pavlov, D.I. (1975): Magnetite ore-forming by Cl-bearing brines. *Nauka*, Moscow, 286.

P-T CONDITIONS OF SILICIFICATION IN DIAGENETIC SANDSTONES FROM THE BRENT FORMATION OF DUNBAR (NORTH SEA).

GUILHAUMOU, N.(1), CORDON, S.(1), DURAND, C.(2) and SOMMER, F.(3)

(1) Ecole Normale Supérieure, Laboratoire de Géologie, URA 1316 du CNRS, 24 rue Lhomond, 75230 Paris Cedex 05.

(2) Institut Français du Pétrole, BP 311, 92306, Rueil Malmaison

(3) TOTAL France, Domaine de Bauplan, 78470 Saint Remy les Chevreuses.

The Brent Province, in the North Sea, is the largest hydrocarbon reserve of North-western Europe. Its reservoirs belong to the Brent Group sandstones, deposited in the middle Jurassic. Important illitization and silicification have drastically reduced their permeability and porosity. P-T conditions of the silicification can be derived from fluid inclusions formed during overgrowth development. In the case of the Great Alwyn area, inclusions from such occurrences have been studied a lot, but two points remain questionable : the possibility of a resetting of the inclusions and the interpretation of homogenization temperatures in terms of trapping temperatures. The pressure correction strongly depends on the fluid system and, in Alwyn area, it can vary between 0 and 15 to 30°C whether the authors have considered the aqueous system contains methane or not. Nevertheless, methane presence have never been verified analytically. Thus, trapping temperatures remain uncertain and a debate still subsists over the possibility to account for other geochemical markers to constrain fluid circulation models.

In this study, Raman microanalyses were performed on single aqueous inclusions representative of quartz overgrowth conditions. The samples have been cut off in cores from different levels of the Tarbert (latest formation of the Brent Group) in four wells of Dunbar field (South Alwyn, East Shetland Basin), in the Frontal Panel and West Flank. Overgrowths are intensively developed and euhedral. Two types of fluid inclusions related to diagenesis are distinguished within a quartz grain :

a-type : Biphase inclusions (generally smaller than 5 μm), in growth bands at the boundary between the detrital grain and the overgrowth. Aqueous inclusions are mostly liquid (nearly 90 %).

b-type : Biphase inclusion trails cross-cutting the detrital grain and connecting with a-type. Aqueous inclusions display highly variable phase ratios.

In both type of trails, water and hydrocarbon-bearing inclusions often coexist.

SEM-cathodoluminescence is used to distinguish detrital grain from overgrowths. It also allows to observe fluid circulation in cracks at the beginning of the silicification within the detrital grains that has formed b-type fluid inclusions during healing. These observations suggest that a-type and b-type fluid inclusions are contemporaneous of the early stage of the silicification.

Microthermometric study of a-type aqueous inclusions leads to homogenization temperatures between 105 and 110°C in the four wells and ice melting temperatures between -1.5 and -3°C.

Raman microspectrometric analyses were performed on aqueous inclusions hosted in quartz overgrowth using 30 to 45 μm -thick polished sections. We used a confocal laser Raman Dilor spectrometer. Raman spectra obtained on the gas phase of both a-type

and b-type fluid inclusions show systematically a narrow band, near $2914,5 \pm 0,5 \text{ cm}^{-1}$ attributed to gaseous methane. CO_2 and heavier hydrocarbons are not detected in analytical conditions of analysis. Methane has been detected in every tested sample of the four wells. The analysis success is attributed partly to the confocal system. When in use, it improves the lateral resolution, the depth of the analyzed field and the axial resolution, and this leads to better signal / noise ratio. The inclusion signal is less disturbed by its environment and by the epoxy : indeed, the epoxy spectrum has C-H vibrations between 2850 and 3200 cm^{-1} , overlapping with the interval of the main methane vibration band.

The remarkable stability of CH_4 stretching band position, involving nearly identical pressure conditions, supports the hypothesis of a- and b-type fluid inclusion contemporaneity. These inclusions, which belong to the same fluid system, show a progressive evolution from essentially liquid inclusions (a) to highly gaseous inclusions (b). Both contain methane, which indicates that the fluid was saturated with methane. These analytical results allow to derive P-T conditions of the beginning of siliceous overgrowth crystallisations. Since the brines entrapped are in the methane-saturated $\text{H}_2\text{O}-\text{NaCl}$ ($\pm\text{KCl}$) system homogenization temperatures should be considered as very close to trapping temperatures. Homogenization temperatures display between 105 and 110°C for all samples which can be then interpreted as the temperature existing at the beginning of the silicification. Salinities display between 2.5 and $4 \text{ wt}\%$ equ NaCl . The temperatures are 15 to 20°C lesser than current formation temperatures, this seems to disagree with a present resetting of the inclusions. An internal pressure value of 90 bars can be derived from the Raman band position of CH_4 at room temperature. The calculation of molar volumes using Peng Robinson equation of state allows to determine a real pressure value at time of entrapment. This leads to P-T conditions allowing to emplace the beginning of main siliceous overgrowth at a burial depth in agreement with basin modelling.

AMPHIBOLITE-FACIES METAMORPHIC FLUID AND STRUCTURAL CONTROLS ON GOLD DEPOSITION: the Tomiño gold deposit (Galicia, NW Spain).

HÉBERT, R.(1), ROBERTS, S.(1), SANDERSON, D.J.(1), SOLDEVILA, J.(2) and GUMIEL, P.(3)

(1) Department of Geology, University of Southampton, Southampton SO17 1BJ, UK.

(2) Department of Geology, Universitat Autònoma de Barcelona, 08193 Barcelona, Spain.

(3) ITGME, Rios Rosas 23, 28003 Madrid, Spain)

The Tomiño gold deposit occurs within the Monteferro-El Rosal shear zone (Galicia, NW Spain). It is hosted by a series of E-W trending quartz veins within the Urgal granite which intruded the Monteferro-El Rosal metasedimentary formation. This study focuses on the characterization of the fluids responsible for gold mineralization and on the constraints they provide on the timing of the mineralization with respect to the geological history of the region.

The major phase of deformation occurred during the Variscan orogeny and affected all of the formations in the studied area. It is characterized by an intense ductile deformation which occurred during an amphibolite facies regional metamorphism.

Quartz veins are widespread in the studied area and two distinct sets can be observed. The first one consists primarily of syn-foliation N-S trending veins or pods within the Monteferro-El Rosal formation. Their synkinematic and metamorphic nature, with respect to peak metamorphism is suggested by the presence of occasional andalusite porphyroblasts. The second set are gold-bearing E-W oriented quartz veins occurring in the Urgal granite. Both vein sets contain two fluid types: an aqueous-carbonic and an aqueous fluids.

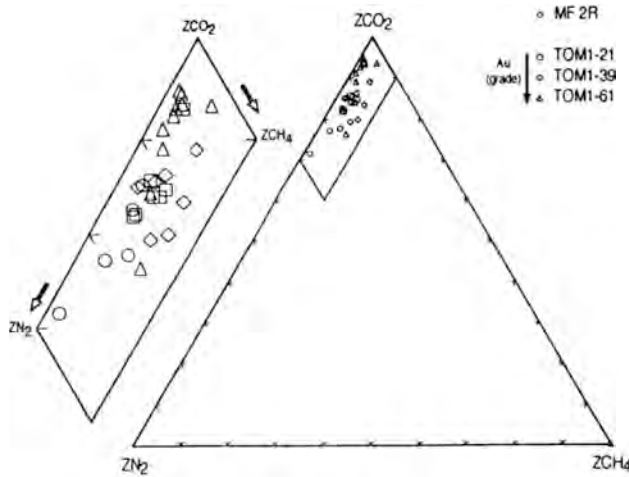
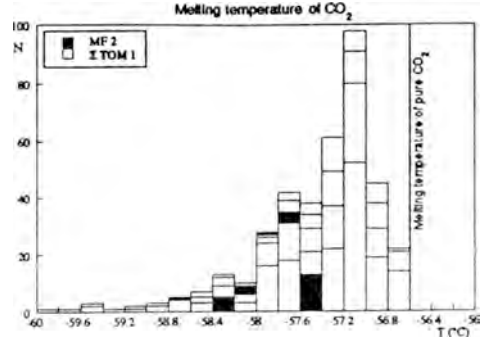
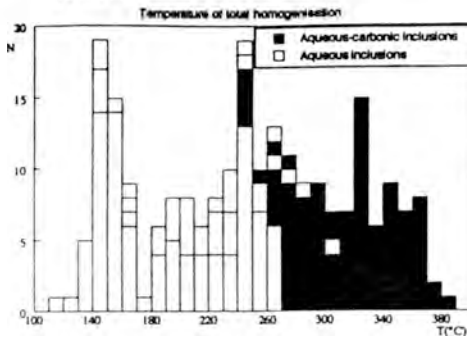
The results of microthermometry and Raman spectroscopy analyses on the vein sets are presented. These data have been used to estimate a bulk composition of the fluid, to estimate P-T conditions of the trapping of fluids, and also to propose a genetic model for the Tomiño gold deposit. Both sets of veins contain the same types of fluid:

The first is an aqueous-carbonic fluid with low salinity (< 6 wt% NaCl equivalent) and a volatile phase CO₂-dominated (CO₂ 72-95-CH₄ 0.5-7.5-N₂ 1-27 molar fraction). The N₂ molar proportion of the gaseous phase, which is generally higher than CH₄, appears to decrease as the gold grade increases. Bulk composition of the fluid is primarily H₂O (70 to 96 molar %) and CO₂ (2 to 30 molar %), that leads to a bulk density varying between 0,4 and 0,95 g.cm⁻³ depending on the degree of fill of the inclusion. The second type of fluid is an aqueous fluid with a low-salinity (2-8 Wt % NaCl equiv.).

The conditions of trapping, as determined by the intersection of the P-T conditions of metamorphism and the isochores of the fluid, are estimated at around 3-4,5 kbar and 500±50 °C.

These data suggest that the Tomiño Gold deposit was generated by metamorphic fluids. These fluids have been channeled within opening E-W fractures in the Urgal granite during ductile regional deformation. These channels may have caused local reductions in pressure which favoured the mineralization of gold and sulphides. The release of pressure, as the fractures opened in the granite, may have induced an unmixing process which favoured the gold precipitation. This phenomena could also explain the observed

correlation between gold grade and degree of fill of the aqueous-carbonic inclusion. The greater the unmixing (the more phase separation), the lower the degree of fill and the higher the gold grade.



Molar proportions of CO₂, CH₄ and N₂ within the volatile phase of aqueous-carbonic inclusions

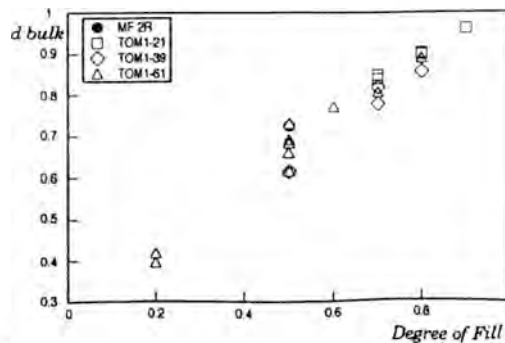


Diagram d_{bulk} / Degree of fill showing the evolution of the degree of fill and the bulk density with respect to the gold grade

CH₄-RICH INCLUSIONS IN SYNKINEMATIC VEINLETS ALONG THE VARISCAN FRONT OF CENTRAL EUROPE.

HEIN, U.F. (1), SCHÖTTLER, T. (1) & BEHR, H.J. (1).

Institut für Geologie und Dynamik der Lithosphäre, Goldschmidtstr. 3, D-37077 Göttingen.

The Variscan front of Central Europe is well exposed along the Faille-du-Midi system in Belgium, where the external Variscan slate belt (Renohercynian zone) is thrust over its autochthonous foreland. This front has been investigated for large-scale orogeneously defluidization channels from Charleroi/Belgium in the West to the Aachen Thrust/Germany (140 Km). Major channels, which would be monitored by hydrothermal mineralization f.e., are absent. But throughout the stratigraphic sequence (Ordovician to Upper Carboniferous pelites, psammities and carbonate rocks) minor quartz and carbonate mineralization occurs in shear veinlets and ruptures, which are syn- to late-kinematic with respect to folding and thrusting and are part of the local Variscan tectonic setting.

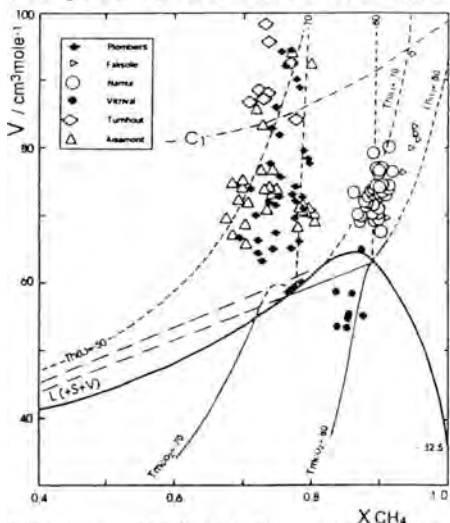


Fig.1: Individual inclusions plotted by their microthermometric data in a V-X diagram of the system CH₄-CO₂ after Thiéry et al. 1994.

Throughout the studied localities early quartz and carbonate veinlets contain fluid inclusions which can be related to veinlet formation. They may be affected by multiple deformation processes leading to secondary changes as partial leakage. Two types of early co-genetic inclusions occur:

*Two-phase aqueous inclusions with $T_e \geq -22^\circ\text{C}$ and $-3^\circ\text{C} < T_{m,ICE} < 0.5^\circ\text{C}$ contain Na-dominated low-salinity solutions. They homogenize to liquid at $112^\circ\text{C} < Th_{(L+L)} < 205^\circ\text{C}$ with variable ranges at the individual localities. Their gas bubbles are CH₄-saturated as verified by Raman analysis.

* Monophase CH₄-rich inclusions commonly exhibit CO₂-melting ($-106^\circ\text{C} < T_{m,CO_2} < -62^\circ\text{C}$) before homogenizing to liquid and in a few cases critical ($-83^\circ\text{C} < Th_{(L+L)} < -47^\circ\text{C}$). Only in inclusions from one locality

(Vitrival / Belgium) partial CH_4 homogenization occurred before CO_2 - "melting" (sublimation). Microthermometric data result in compositions of $0.63 < X_{\text{CH}_4} < 0.95$ with two maxima at $X_{\text{CH}_4} = 0.73$ and $X_{\text{CH}_4} = 0.88$ respectively (Fig. 1), which is in good agreement with Raman analysis. Neither pure CH_4 inclusions have been detected nor any traces of higher hydrocarbons in the CH_4 -rich inclusions. For the above compositions molar volumes of $50 \text{ cm}^3\text{Mol}^{-1} < V < 100 \text{ cm}^3\text{Mol}^{-1}$ can be deduced (Fig. 1). Locally, late euhedral quartz is developed in open vugs of the veinlets which hosts primary monophase CH_4 -rich inclusions, too. They show the same succession of phase transitions, i.e. CO_2 -melting ($-84^\circ\text{C} < T_{m\text{CO}_2} < -72^\circ\text{C}$) but homogenize to vapor ($-77^\circ\text{C} < T_{h(LV-W)} < -52^\circ\text{C}$). Extrapolation of melting- or homogenization-isotherms in the V-X diagram (Fig.1) would result in molar volumes of $\approx 200 \text{ cm}^3\text{mole}^{-1}$ and above and compositions which equal the gas inclusions in early quartz.

The gas inclusions are interpreted as relics of dry gas which was generated during burial of adjacent coal-bearing strata and expelled along newly forming migration pathways during deformation and tectonic stacking. Thus, their composition reflects the generation temperature. By their textures the cogenetic aqueous and gas inclusions were trapped from heterogeneous $\text{H}_2\text{O}-\text{CH}_4$ mixtures and permit the reconstruction of maximum P-T reconstructions for individual localities. Trapping temperatures hardly exceed 200°C (Fig.2) which is in good agreement with independent "thermometers" as CAI-values and coalification data. Varying trapping pressures of $0.4 \text{ kbar} < p < 1.4 \text{ kbar}$ reflect local tectonic overstacking better than the depth of burial. A local-scale fluid flow must have occurred during folding and thrusting along the Faille du Midi, since gases of equal composition are found in all stratigraphic members from Silurian to Upper Carboniferous. This fluid flow followed local geothermal gradients of up to $60^\circ\text{C}/\text{km}$ (Fig.2) along the Variscan front.

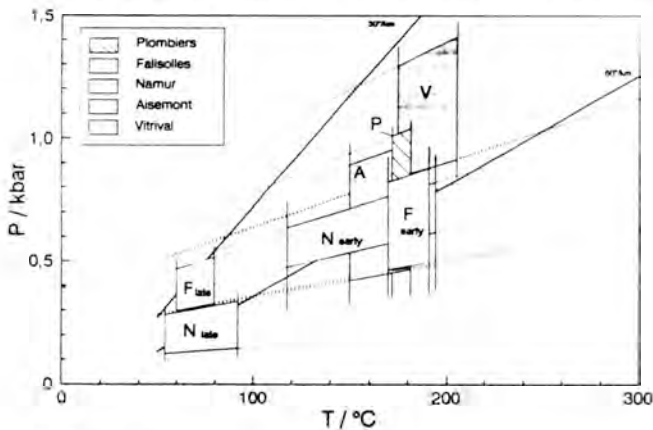


Fig. 2: P-T variation for individual localities (dotted lines: CH_4 (- CO_2) isochores).

References:

- Helsen, S. (1993) Ann. Soc. géol. Belg. 115: 135-143.
 Galimov, E.M. (1988) Chemical Geology 71: 77-95.
 Jüntgen, H., Klein, J. (1975) Erdöl und Kohle 28: 65-73.
 Schöttler, T. (1994) Diploma Thesis, 98 p., Univ. Göttingen.
 Thiéry, T. Van den Kerkhof, A.M., Dubessy, J. (1994) Eur. J. Mineral. 1994/6: 753-771.

AN ANTICLOCKWISE P-T PATH OF THE ULUGURU GRANULITE COMPLEX, TANZANIA, AS RECORDED BY FLUID INCLUSIONS

HERMS, P., APPEL, P., MÖLLER, A. & SCHENK, V.

(Mineralogisch-Petrographisches Institut, Christian-Albrechts-Universität, Kiel, Olshausenstr. 40, D-24098 Kiel, Germany)

Fluid inclusion investigations were carried out on granulite-facies rocks of the Uluguru Mountains of Tanzania, which are part of the Mozambique mobile belt. Metamorphism took place under high-pressure granulite-facies conditions (8-10 kbars) during the Pan-African orogeny (Möller et al., 1994). Recent petrological investigations of Appel et al. (1993) verify an anticlockwise P-T path for this terrane. The aim of the fluid inclusion studies is to constrain the anticlockwise P-T path and to characterize the metamorphic fluid at different P-T stages. Samples have been selected in that way that they contain mineral associations which equilibrated at different stages of the P-T path.

Fluid inclusions which represent Stage I of the prograde P-T path are supposed to occur in quartz included in garnet porphyroblasts in a metapelite. Protected against later deformation primary fluid inclusions of CO₂-rich and CO₂-N₂ composition have been preserved in the armoured quartz grains. Early quartz crystals enclosed by the growing garnet have CO₂-N₂ inclusions whereas quartz formed during garnet growth have pure CO₂ inclusions.

During the prograde pressure increase (Stage II) some of the primary fluid inclusions leaked or imploded and mixing of CO₂-rich and N₂-rich fluids occurred. The fluid inclusions re-equilibrated to lower N₂ compositions and higher fluid densities. CO₂-N₂ inclusions with uniform low N₂ contents presumably formed after high-temperature deformation and recrystallization of the matrix quartz near to the peak of granulite-facies metamorphism.

Stage III of the P-T path is characterized by isobaric cooling at high pressures and is represented by garnet growth on posttectonic veins in a two-pyroxene granulite. Fluid inclusions are CO₂-rich (<0.5 mole% N₂) and have very high densities (1.15 g/cm³). The isochores for these inclusions mark the end of the isobaric cooling path before tectonic uplift and decompression.

Stage IV is characterized by the retrograde uplift with strong decompression. Most of the inclusions decrepitated or re-equilibrated at this stage. Liberated CO₂-N₂ fluids in graphite containing metapelites must have changed their composition to N₂-CH₄ during cooling in a closed system if water was present and with graphite stable. Fluid inclusions in the metabasite remained CO₂-rich and only re-equilibrated to lower densities. Seldom H₂O-NaCl-(MgCl₂-CaCl₂) inclusions of low densities are found.

Local shear zones transformed the pyroxene granulite into biotite-hornblende-scapolite gneiss. The matrix quartz in this gneiss contains CO₂-N₂ inclusions with 14-18 mole% nitrogen and low-density N₂-CH₄ inclusions indicating temperatures below 500°C. Water-rich fluid inclusions of low salinity (about 5 wt% NaCl equivalents) are rare and formed at very low temperatures and pressures.

In conclusion, fluid inclusion investigations on the specifically

selected samples verify nicely the different P-T stages and thus confirm an anticlockwise P-T path for the Uluguru metamorphic terrane.

References:

- Appel, P., Möller, A., Schenk, V., Muhongo, S. (1993): Granulite facies metamorphism and P-T evolution in the Mozambique Belt of Tanzania. In: Thorweihe and Schandelmeier (eds): *Geosc. Res. Northeast Africa*, Balkema, 171-175.
- Möller, A., Mezger, K., Schenk, V. (1994): U-Pb dating of metamorphic minerals: Age of metamorphism and cooling history of Panafrikan granulites and early Proterozoic eclogites in Tanzania. *Beihefte zum European Journal of Mineralogy*, 6, 182.

**LARGE-SCALE AND LOCAL FLUID MIGRATION DURING METAMORPHISM:
EVIDENCE FROM H, O, C ISOTOPE COMPOSITION AND Na/Ca RATIO OF THE
INCLUSION FLUIDS**

HURAI, V. (1) & SIMON, K. (2)

(1) Dionyz Stúr Institute of Geology, 817 04 Bratislava, Slovak Republic

(2) Geochemisches Institut, Georg August Universität, Goldschmidtstr. 1, 37077 Göttingen, Germany

Chemical and isotopic records obtained from fluid inclusions indicate two contrasting fluid regimes during metamorphism of the Veporicum crystalline complexes in the Western Carpathians. The high-temperature fissures (450-500°C) have probably formed near to or below peak metamorphic conditions during the Hercynian orogeny in a closed system, in which aqueous solutions have been in chemical and isotopic equilibrium with surrounding, mostly granitoid rocks. This is corroborated by narrow ranges of Na/Ca ratios in individual fluid inclusions, and by uniform δD and $\delta^{18}O$ values (-59 ± 5 ‰ and $7-7.5$ ‰, SMOW, respectively).

The extension-related Alpine quartz, precipitating in vertically-dipping veins and mylonitic shear zones at temperatures mostly between 330-380°C, exhibits signatures of the large-scale fluid migration, resulting in much larger compositional and isotopic variability of the inclusion fluids.

Carbon isotope composition of the inclusion CO_2 varies between -7.7 to -11.9 ‰, PDB in both types of metamorphic quartzes. These values have been interpreted to reflect partial influence of the carbon dioxide liberated by decomposition of organic matter in underlying metasediments. Fixed $\delta^{13}C$ values of the inclusion CO_2 are believed to corroborate the concept of Hercynian granitoid napes in the crystalline basement of the Western Carpathians.

VOLATILES IN MANTLE-DERIVED MAGMA CHAMBRES IN THE CRUST: EVIDENCE FROM FLUID INCLUSIONS IN ANORTHOCLASITE AND TRONDHJEMITE XENOLITHS FROM LATE TERTIARY ALKALINE BASALTS (WESTERN CARPATHIANS)

HURAI, M. (1), KONECNY, P. (2) & HURAI, V. (2)

(1) Dept. of Mineralogy and Petrology, Comenius University, 84215 Bratislava, Slovak Republic

(2) Dionyz Stúr Institute of Geology, 81704 Bratislava, Slovak Republic

A variety of exotic xenoliths comprising the compositional range from basic to acidic rocks has been ejected in explosive products of the late Tertiary basaltic volcanism, decorating the northern margin of Pannonian Basin. Mineral composition of these rocks as well as compositional, REE and microthermometry data on intergranular and inclusion silicate melts are documented elsewhere (Konecny et al., this volume). This contribution is focused on fluid inclusions in the rock-forming quartz and plagioclase, as well as those trapped in the vesicular glass adhering grain boundaries of the rock-forming minerals.

Primary twophase melt and mostly monophase CO₂-rich inclusions arise in both rock types in variable proportions: the carbon dioxide inclusions are abundant in the trondhjemites and sparse in anorthoclasites, while the opposite is true for the melt inclusions. One trondhjemite sample (KP-30) contains three phase CO₂+H₂O inclusions with 0-25 vol. % of the aqueous phase, indicating water oversaturated crystallization conditions. Water, however, predominates over CO₂ vapour in isolated vesicles observed in the intergranular melts from trondhjemites. The vesicles in melt pockets of the anorthoclasite xenoliths are absent from any discernible aqueous phase.

Aqueous inclusions occur also in quartz and plagioclase hosted, carrousel resembling inclusions, consisting of rounded core of the host mineral encompassed by a ring of vitreous silicate phase connected by a conduit with the intergranular melt. The vitreous phase occasionally contains several vapour bubbles, some of them filled with aqueous fluid. An intimate genetic relationship between the intergranular melts and the carrousel resembling inclusions is documented by consistent salinities of their aqueous fluids. The interstitial melt-hosted vesicles as well as the carrousel resembling inclusions are believed to have formed during explosion, when isothermal decompression has led to significant volume expansion of the rock-forming minerals and viscous residual melt. Consequently, the aqueous phase in the vesicles as well as in the carrousel type inclusions possibly represents the equilibrium water initially dissolved in the interstitial melt at higher pressures and liberated during explosion and concomitant pressure drop.

Melting temperatures and densities of primary CO₂ inclusions are summarized in Table I. together with the formation PT conditions, inferred from homogenization temperatures of the melt inclusions and from the isochores for the coexisting CO₂ inclusions.

It can be concluded that the anorthoclasite and trondhjemite xenoliths exhibit signatures of cumulate rocks and may thus perhaps represent final products of the fractional crystallization

of basaltic magma chambers related to a continental rift zone induced basaltic volcanism. The magma chambers seem to be emplaced at mid-crustal (11-13 km) and deep-crustal (21-22 km) levels. Uniform composition of the primary CO₂ inclusions, comparable to those reported in lherzolite xenoliths from this area, high Fe content in residual melts indicated by the presence of daughter Fe,Al-spinels in zircon-hosted melt inclusions and high homogenization temperatures of melt inclusions favour the presumption about initially mantle origin of the anorthoclase and trondhjemite xenoliths. The contrasting composition of the alkaline anorthoclases (containing abundant zircon, monazite and other REE and Nb-bearing minerals) and sub alkaline trondhjemites (depleted in accessory minerals), may be explained either by various degree of crustal contamination, or by diverse composition of the parental basaltic magma occurring in various isolated storages, which could have been fed either from upwelled asthenosphere, producing sub alkaline basalt, or from metasomatised lithospheric mantle, generating alkaline basalt to basanite.

Table I.

Sample	Anorthoclases				Trondhjemites		
	HP-3	PI-12	KP-9	PI-14	HP-2	KP-31	KP-30
<i>T_m</i> CO ₂ (°C)	-57.8 to -58.0	-57.3 to -58.5	-57.5 to -58.0	-57.5 to -58.1	-57.3 to -58.8	-57.3 to -58.7	-57.4 to -58.8
min. <i>T_h</i> CO ₂	5.4 (L)	8.9 (L)	27.1 (L)	27.8 (L)	9.9 (L)	8.2 (L)	26.1 (L)
CO ₂ density (g.cm ⁻³)	0.894	0.870	0.675	0.661	0.863	0.875	0.694
<i>T_h</i> of melt inclusions	?	?	> 1080	?	?	1260-1280	1140-1190
Pressure (kbar)			> 3.4			6.5-6.6	3.8-3.9
Depth (km/300 bar)			> 11.3			21.7-22.0	12.7-13.0
Remark							water-over-saturated

**FLUID - ABSENT AND CARBONIC FLUID GRANULITE METAMORPHISM
IN GRENVILLE PROVINCE, ADIRONDACK AND ONTARIO**

ISTRATE, G. & ALTHAUS, E.

Mineralogisches Institut, Universität Karlsruhe, FRG

The study of fluid inclusions and mineral equilibria is used to identify and to distinguish pre-metamorphic, peak- and post-metamorphic events and related magmatic processes. Estimates of metamorphic fluid speciation and fluid inclusion studies document the local complexity of fluids in the deep crustal rocks. The study of the physico-chemical characteristics of fluid inclusions, their densities and chronology in high-grade metamorphic rocks represent an important topic of metamorphic petrology. Detailed petrographic observations and textural analysis of the fluid inclusions in ancient terranes with high-grade rocks with complicated evolution is a difficult task but essential for a correct interpretation of the metamorphic processes.

The identification of high-density, almost pure CO₂-rich fluid inclusions in granulites world-wide attests the important role of the carbonic fluid in granulite genesis and suggests that the fluid inclusion data can be used to constrain the peak P-T conditions of metamorphism. In some cases the fluid inclusions observations have been used to demonstrate the incompatibility of CO₂-fluid with granulitic mineral assemblages by maintaining that even the fluid inclusions with primary characteristics (textural, high-density) have been captured or reequilibrated during the subsequent phases of the granulite evolution.

This study has been undertaken to document the occurrence of primary, high-density fluid inclusions, to determine the nature of fluids and to constrain the pressures and temperatures for a variety of granulitic rocks from Ontario and Adirondack, Grenville Province. Another goal of our study is to compare these data with published results, especially considering the following aspects: 1. fluid present vs. fluid absent conditions of metamorphism; 2. nature of peak-metamorphic fluid; 3. chronology of fluid inclusions; 4. the subsequent fluid/rock evolution, i.e. isobaric cooling vs. isothermal decompression. Detailed examination of the fluid inclusions in garnet, quartz, plagioclase, pyroxenes, cordierite, sillimanite and apatite confirmed the existence of primary, high-density inclusions, CO₂-rich, pure or with only small amounts (<5 mol-%) of other gases such as CH₄, H₂S and N₂; no immiscible aqueous solutions like a syngenetic fluid have been detected.

The selected garnet occurs as granoblasts in migmatitic metapelitic gneisses, felsic granulites and charnockites and contain different types of inclusions, as follows:

- a. fluid inclusions, CO₂-rich, high density;
- b. mineral inclusions: Qtz, Bi, Sill, Cc, Kfs, Plg, Spinel, Ap, Ru, Ilm, Mon, Py, commonly concentrated in the core along with a few, rare fluid inclusions, difficult to distinguish optically;

c. silicate-melt inclusions, glassy or partially recrystallized, with daughter crystals \pm gas.

The high-densities of the primary inclusions, typically 1,0 to 1,06 g/cm³, exceptionally 1,07 to 1,16 g/cm³, as well as the textural evidences suggest that CO₂-fluid was trapped at or close to peak-metamorphism (750-800°C and 6,5 to 8,0 kbar). The isochores intersect the peak P-T region derived from mineral thermobarometry.

The subsequent evolution of the rocks, documented by up to five fluid inclusions generations containing high- to low-density CO₂, (and a very rare, late, pure H₂O-fluid), started with a nearly isothermal decompression, followed by a regionally isobaric cooling which is more obvious in Adirondack. The observation that some rock types contain variable amounts of carbonic fluid, others are practicably fluid absent at the peak of metamorphism, support the idea that fluid-absent and fluid present processes may operate in close proximity and are controlled lithologically and by magmatic intrusion and partial melting processes.

FLUID EVOLUTION AT THE VYHNE-KLOKOC IRON SKARN DEPOSIT (WESTERN CARPATHIANS, SLOVAKIA)

KODERA, P.

Dionyz Stúr Institute of Geology, Mlynská dolina 1, 817 04 Bratislava, Slovakia

The magnetite skarn deposit Vyhne-Klokoc is the largest and the best known skarn locality in the Western Carpathians with economically interesting accumulation of magnetite ore (2.6 mil tones proved magnetite ore stock).

Skarn deposit Vyhne-Klokoc is situated in the NW part of the central zone of the Banská Stiavnica stratovolcano, where the deep erosion level has exposed the granodiorite intrusion and the basement rocks. The skarn is formed here by replacement of the Mesozoic dolomitic limestone of the basement by contact metasomatic processes induced by granodiorite intrusion (Kácer et al., 1993). The Vyhne-Klokoc deposit belongs to the iron-rich Ca-exoskarns and contains also accessory amounts of base metal mineralization. Based on detailed geological and mineralogical data it was possible to distinguish three basic evolution stages: isochemical magmatic, metasomatic and retrograde stage.

The skarn-forming process during the isochemical stage had mostly the character of thermal contact metamorphism. Recrystallisation has caused formation of non-hydrous silicates, especially zoned garnets (grossularite-andradite series) and more rare pyroxene (diopside-hedenbergite series). Later originated mineral assemblages with epidote, tremolite and with clinocllore in the marginal zones.

Metasomatic stage began by gradual increase of tectonic activity and penetrating Fe-enriched metasomatic fluids. Characteristic is the occurrence of epidote, tremolite and also the development of several garnet generations, especially andradite. Important is the origin of magnetite, replacing carbonate rocks and older skarn assemblages.

Retrograde stage is characteristic by non-equilibrium crystallisation under varying redox conditions. Zoned garnet, major hematite and minor magnetite (both accompanied by extensive mutual overprinting) were formed here, also together with lesser amounts of epidote, amphibole and chlorite (picnochlorite and pennine). Epidote-calcite substage represents transition between the skarn and hydrothermal meteoric system. Hydrothermal mineralization was formed during the five substages. The substages correspond to the tectonic processes, connected as a rule with the final cooling of the intrusion. The amounts of all the minerals, crystallising during these substages, is decreasing. More abundant is only the first, pyrite-chalcopryrite substage, responsible for the formation of the main pyrite mass at the deposit. Base metal substage (with galena, sphalerite, chalcopryrite, hematite and pyrite) is closely related to the garnet skarns. The last three substages (calcite-hematite, quartz-carbonate, chalcedony-opal) occur mostly in form of crack infillings and are thus relatively less important (Kodera and Chovan, 1994).

The fluid inclusion study and the preliminary thermocryometry measurements indicate decreasing salinity and temperature towards the later stages. Inclusions in earliest garnets and interstitial quartz contain daughter minerals, implying probably a magmatic origin of these fluids. Variable liquid-to-vapour ratios observed in selected garnet-hosted inclusions trails indicate local boiling of the mineral-forming fluids. Most intensive boiling, however, was observed in the hematite-quartz-calcite assemblage, what might account for non-equilibrium crystallisation in the retrograde stage. The retrograde stage must have been affected by the progressively increasing involvement of meteoric waters, which caused continual cooling and dilution of mineral-forming fluids. Homogenisation temperatures (T_h) from the latest garnet occurred at 320°C and salinity was about 10 wt % NaCl equiv. T_h 's of fluid inclusions trapped in interstitial calcite were 250-310°C and salinity about 2 wt % NaCl equiv. No signs of boiling were found in later hydrothermal substages. Therefore, the mineral precipitation in these substages was controlled by decreasing temperature driven by circulating meteoric fluids. Fluid inclusion measurements from hydrothermal calcite-pyrite mineralization showed pure water with T_h 's around 230°C.

T_h 's from fluid inclusions in interstitial calcite, which originated together with picnochlorite, showed values comparable to those obtained from independent chlorite geothermometer (Cathelineau, Nieva, 1985): 225-275°C.

References

- Cathelineau, M., Nieva, D., 1985: A chlorite solution geothermometer. The Los Azufres (Mexico) geothermal system. *Contr. Min. Petr.*, 91, p. 235-244.
- Kácer, S., Kódera, P., Hojstřicová, V., Lexa, J. (1993): Evaluation of Fe-skarn skarn mineralisation in the district of the central zone of the Banská Štiavnica stratovolcano. Internal report of D. Stúr Institute of Geol. Bratislava, 67 p. (in Slovak)
- Kódera, P., Chovan, M. (1994): Mineralogical-paragenetic relations in the Vyhne-Klokoc skarn deposit. *Mineralia Slovaca*, 26, p. 38-49 (in Slovak)

SILICATE MELTS IN ANORTHOCLASITIC MELTS AND TRONDHJEMITIC XENOLITHS HOSTED BY LATE TERTIARY ALKALI BASALTS

KONECNY, P.(1), SIMON, K.(2), HURAIJOVA, M.(3) & HURAI, V. (1)

(1) Dionyz Stúr Institute of Geology, 81704 Bratislava, Slovak Republic

(2) Geochemisches Institut, Georg-August Universität, Goldschmidtstr. 1, D-37077 Göttingen, Germany

(3) Dept. of Mineralogy and Petrology, Comenius University, 84215 Bratislava, Slovak Republic

Xenoliths with modal composition corresponding to anorthoclase and trondhjemite-tonalite series (further trondhjemite) have been found in the explosive equivalents of the Upper Tertiary (Pontian) basaltic volcanism.

The anorthoclase xenoliths are almost monomineral rocks composed of anorthoclase ($Ab_{46-57} An_{2-9} Or_{37-51}$). Euhedral zircon is also essential constituent of the rock. The zircon is exceptionally overgrown over chemically and optically decomposed olivine core. Identified were also some additional REE and Nb-bearing minerals: chevkinite (?), monazite, samarskite as well as accessory apatite.

Two types of melt have been observed in the anorthoclases: micro-scale primary inclusions trapped in anorthoclases and irregular pockets of intergranular melt that may constitute up to 3 vol. % of rock. The interstitial melt crystallizes Fe-Ti oxides whereas Fe-Al spinels have been found as daughter minerals directly precipitated from zircon-hosted melt inclusions.

Trondhjemite xenoliths are composed of three main phases: plagioclase ($Ab_{39-55} An_{37-58} Or_{2-7}$), quartz and interstitial melt that may form up to 35 vol. % of rock. The most latest minerals crystallizing from interstitial melt are orthopyroxene, ilmenite, and rutile. Amount of other accessory minerals is substantially suppressed with respect to anorthoclase xenoliths. Scarce but present mirmekitic structures in proximity of interstitial melt suggest abrupt simultaneous crystallization of quartz and acid plagioclase. OH-bearing minerals have not been detected.

REE-patterns of the anorthoclases and trondhjemites are characteristic of strong LREE-enrichment (up to 400 times relative to chondrite), negative Eu-anomaly in the interstitial melts and high positive Eu-anomaly in the rock-forming plagioclases, what is suggestive of cumulate origin of the rock-forming minerals.

Melt composition does not significantly vary within samples and even between rock types. The melt is enriched in Si, Fe, Ti, Mn as compared with feldspar. The Na/K ratio is approximately constant for the melt, although variable in feldspars. Increased Zr contents in melt may be attributed to dissolved zircon. The melt is also enriched in Cl (up to 1 wt. %).

Primary melt inclusions have been observed in all rock-forming minerals, as well as in apatite, zircon and monazite. The inclusions are closely associated with primary CO₂ inclusions (Huraiová et al., this volume). Melting and homogenization temperatures (T_h) of the melt can have been measured only in rock-forming quartz and anorthoclase, as the inclusions in accessory minerals have been too small to be measured. Onset of the melting (solidus) has been observed within the temperature interval between 850-870°C in the anorthoclase (KP-9), and between 905-

930°C in the trondhjemite (KP-31). The final melting (liquidus) occurred around 1070-1080°C in the anorthoclase KP-9. The ThEs for two trondhjemites (KP-30 and KP-31) were 1140-1190°C and between 1260-1280°C, respectively. The Th in melt inclusions hosted by plagioclases can have not been determined, because the inclusions always decrepitated prior to homogenization. Solidus temperatures of the inclusion melts are roughly consistent with the solidi in the water-absent and water-deficient haplogranitic melts (e.g. Keppler 1989). It cannot be ruled out that the homogenization temperatures are overestimated owing to high melt viscosity and by failing the CO₂-vapour to dissolve in the molten silicate phase.

Evidences for immiscibility of two silicate melts have been obtained from the fluid inclusions hosted by trondhjemitic xenoliths. Homogenization of these two coexisting melts has been reached at 1090°C.

Several lines of evidence (close association with gabbroic xenoliths, typical REE-patterns, high Fe-Ti contents of the interstitial and inclusion melts, high homogenization temperatures) suggest that the salic alkaline and sub-alkaline xenoliths might have been formed by fractional crystallization within chambers of basaltic magma. The host alkali basalts are the most reasonable candidates for the parental rocks. Densities of the coexisting CO₂-rich inclusions indicate that quartz and plagioclases must have crystallized at mid- (~ 11-13 km) and deep-crustal levels (~ 22 km).

References:

Keppler H. (1989) The influence of the fluid phase composition on the solidus temperatures in the haplogranite system NaAlSi₃O₈-KAlSi₃O₈-SiO₂-H₂O-CO₂. *Contrib. Mineral. Petrol.* 102, 321-327

CHEMISTRY OF FLUID INCLUSIONS IN THE WERRA (ZECHSTEIN, UPPER PERMIAN) HALITE OF NORTH POLAND

KOVALEVICH, V.M. (1), PERYT, T.M. (2)

(1) Institute of Geology and Geochemistry of Combustible Minerals, National Academy of Sciences of the Ukraine, Naukova 3a, 290053 L'viv, Ukraine

(2) Państwowy Instytut Geologiczny, Rakowiecka 4, 00-975 Warszawa, Poland

Study of fluid inclusions in sedimentary forms of halite crystals represented by chevron and hopper crystals is important for deciphering the composition of brines from which the halite precipitated. The applications of such a study are twofold: first, they may explain the evolution of ocean chemistry in time, and second, they are of use to predict the zones where potassium salts could be deposited.

We studied the Werra (Zechstein) halites occurring in North Poland. During the Zechstein there existed a gulf of the Zechstein Sea in the Peri-Baltic area and peripheral evaporite platform (shelf) developed there, with local thick sulphate platforms surrounded by halite basins which in places contain also potash salts.

One such platform was small (3 sq kms) Zdrada platform where sulphate deposits of the Lower Werra Anhydrite (>150 m thick) covered by thin (<50m) Oldest Halite deposits pass at the distance of one kilometer into thick (up to 200 m) Oldest Halite underlain by thin (<50 m) sulphates (Peryt, 1994). We studied halites in two wells: from the shoal (Zdrada IG3), and the slope of the sulphate platform (Zdrada IG6). In these wells, chevron crystals up to a few centimetres long have been found although the frequency of chevrons increases towards the shoal. These crystals contain fluid inclusions that are cubic in shape and follow the zones of crystal growth. The inclusions are a fraction of to 300 micrometres long, although exceptionally long (1 mm) inclusions occur. For the chemical analysis of brines that are contained in fluid inclusions, Petrichenko's (1973) method of glass capillars was applied.

It was found that the Werra brine is of Na-K-Mg-Cl-SO₄ type and is similar to recent concentrated ocean water considering ratios between particular ions although it differs in having slightly lower sulphate ion content (Fig. 1). There is some variability of total content of ions examined in the profiles although all results suggest that the degree of concentration corresponds to the beginning and middle stages of halite precipitation. This is also supported by other geochemical data (distribution of bromine).

The relations between K⁺, Mg²⁺ and SO₄²⁻ as found during this study are similar to those found during examination of other Permian halites (Kovalevich, 1990, 1992; Horita et al., 1991). Accordingly, these data indicate that Permian marine water was similar to recent one and differed only in slightly lower content of sulphate ion in the Permian.

The study was supported by the International Science Foundation grant no. UCM000 to VMK and by Komitet Badań Naukowych grant no. 9 S602 024 04 to TMP.

References:

Eugster, H.P., Harvie, C.E. & Weare J.H., 1980. Mineral equilibria

in the six-component seawater system, Na-K-Mg-Ca-SO₄-Cl-H₂O, at 25°C. Geochim. Cosmochim. Acta, 44: 1335-1347.

Horita, J., Friedman, T.J., Lazar, B. & Holland, H.D., 1991. The composition of Permian seawater. Geochim. Cosmochim. Acta, 55: 417-432.

Kovalevich, V.M., 1990. Galogenez i khimicheskaya evolucia okeana v fanerozoje. Naukova dumka, Kiev, 154 p.

Kowalewicz, W.M., 1992. Fizykochemiczne warunki powstawania czechsztyńskich utworów solnych regionu bałtyckiego. Przegląd Geologiczny, 40: 721-726.

Peryt, T.M., 1994. The anatomy of a sulphate platform and adjacent basin system in the Łeba sub-basin of the Lower Werra Anhydrite (Zechstein, Upper Permian), northern Poland. Sedimentology, 41: 83-113.

Petrichenko, O.I., 1973. Metodi doslidzhennya vkluchen' u mineralakh galogennikh porid. Naukova dumka, Kiev, 91 p.

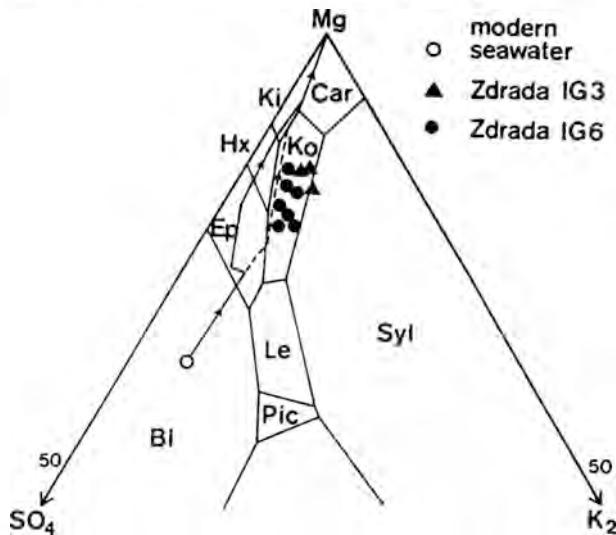


Fig. 1. Brine composition in the inclusions in the Werra halite of the Zdrada area plotted on the Jänecke projection in the quinary system Na-K-Mg-SO₄-Cl-H₂O saturated with respect to halite at 25°C (Eugster et al., 1980).

FLUID INCLUSIONS IN HALITE FROM PARATETHYS MIOCENE EVAPORITES AND THE PROBLEMS OF THEIR CHEMICAL COMPOSITION INTERPRETATION.

KOVALEVICH, V.M. & PETRICHENKO, O.Y.

Institute of Geology and Geochemistry of Combustible Minerals, Naukova st., 3a, 290053, L'viv, Ukraine.

Fluid inclusions in halite from Miocene marine evaporite deposits, distributed in submontane and intermontane depressions of Carpathians region on Ukraine, Poland, Romania and Slovakia area have been investigated. In Miocene stratigraphic column these evaporites belong to Eggenburgian, Carpathian, Badenian. For comparison there were used the published data and, in part, our data on Messinian evaporite formation of Italy (Sicilia) and Spain (Lorca). The laws of inclusions distribution in crystals, their shape, aggregate state and solutions chemical composition were studied. The analysis of inclusion solutions has been fulfilled by method of glass capillaries described earlier by Petrichenko O.Y.

The goal of investigation was: 1. To reveal the fluid inclusions that contain the reliable information about geological environment of salt sedimentation in ancient basins. 2. To determine the grade of another (besides the sea water) sources impact on basin supplying. 3. To elucidate the possibility of Miocene sea water composition reconstruction by inclusions in halite.

It has been determined that sedimentary forms (chevron and hopper crystals) preserved in halite of all studied evaporite formations. However, only inclusions from growth zones, those that are typical for these zones by sizes, shape and aggregate state and are not distorted by cracks, contain the most reliable information about chemical composition of basins brines.

The results of fluid inclusions in sedimentary halite analyses show that sea water was the main source of studied basins supplying. Solutions of these inclusions belong to Na-K-Mg-Cl SO_4 type and by ratio of major ions are close to modern sea water. All basins have some differences in solutions composition that, in our opinion, may be explained by differences in paleogeographic environment of salt accumulation. The obtained data do not consist with views about significant impact of continental run-off or endogenic sources.

For reconstruction of ocean water composition in Miocene we have calculated the average content of K^+ , Mg^{2+} , SO_4^{2-} ions in solutions from basins of Carpathians region for that moment when their concentration was correspondent to the beginning of halite precipitation. These values are accordingly 5,0; 15,5; 14,5 g/l, and are very close to the content in modern sea water, saturated to the same stage K^+ - 3,3; Mg^{2+} - 15,5; SO_4^{2-} - 21,0 (g/l). The main difference is that SO_4^{2-} is some lower. Thus, the obtained data testify that Miocene sea water, on whole, was close to the modern one by content of major components. We think that this conclusion is reliable, because accordingly to the current views, the residence time for most of major constituents

is comparable to or longer than absolute age of studied evaporites (10-20 mln years). On base of represented material the following conclusion may be done: the results of chemical analyses of inclusion solutions in sedimentary halite from evaporites of marine genesis permit to reconstruct precisely enough the composition of sea water in the past, but at that one must take into consideration the partly loss of SO_4^{2-} -ion directly in the basin conditions.

The research described in this publication was made possible in part by Grant # USM000 from the International Science Foundation.

TEMPERATURES OF CRYSTALLIZATION AND VOLATILES OF A-TYPE MAGMAS (ON INCLUSIONS IN MINERALS OF ALKALI GRANITES OF BRYANSKII MASSIF AND THEIR VOLCANIC COMAGMATITES, WEST TRANSBAIKALIA)

KUZMIN, D.V., TITOV, A.V. & CHUPIN, V.P.

Institute of Mineralogy and Petrography, Universitetsky pr.3,
630090 Novosibirsk, Russia

It is supposed that majority of A-type acidic magmas can be formed under the influence of volatiles derived from mantle alkaline basaltic magmas [1]. To investigate this problem, rocks of bimodal basalt-comendite series of the Tsagan-Khunthey member (Tsagan-Khurtey Ridge) were chosen. Alkaline granites of Bryanskii massif [2] and comagmatic to them volcanites of the Alentui and Tsagan-Khunthey members (West Transbaikalia) were studied also for comparison.

The main attention was paid to the determination of F, Cl and other volatiles contents in initial melts. F and Cl in glasses of melt inclusions were analyzed by electron microprobe. The composition of gas bubbles of melt and syngenetic fluid inclusions was determined by Raman-spectral and cryometrical procedure. The temperature regime of magma crystallization was established by means homogenization temperatures of primary melt inclusions (MI).

It is shown that liquidus temperatures was about 790-760°C and crystallization finished at 700-680°C. Under these conditions high F (1.5-1.7 wt.%) and Cl-contents (0.2-0.3 wt.%) were detected. H₂O-liquid-phase is visible only in syngenetic fluid inclusions from the late pegmatoids.

Volcanic and subvolcanic rocks of the Bryanskii massif framing comagmatic to alkaline granites can be subdivided into two groups according to their temperatures of formation and F and Cl contents. High-temperature (up to 990-960°C) and Cl-rich (up to 0.3-0.4 wt.%) melts fall into the first group. Low temperature (750-700°C), F-rich (1.75 wt.%) and probably water-rich melts are referred to second group. The study of gas bubbles of MI and essentially gaseous syngenetic inclusions allowed to establish that the main components of fluids along with H₂O were N₂ on early crystallization stages and CO₂ on the late stages.

The investigated trachyandesites of the Tsagan-Khunthey member are characterized by high liquidus temperatures (1200-1180°C), low Cl content (up to 0.11 wt.%) and the absence of F in an initial melt. Crystallization of acidic volcanites of the Tsagan-Khurtey Ridge occurred in wide temperature interval and initial melts had comendite-pantellerite composition. According to homogenization temperatures of MI these rocks may be also subdivided into two groups: high-temperature (1) melts (1110-1130°C) and low-temperature (2) melts (920-735°C). F-content in glasses of these inclusions are relatively high (0.4-0.9 wt.%) and approach to 1.5 wt.% in the low-temperature inclusions. Cl-content in the homogeneous glasses varies from 0.09 to 0.15 wt.%.

Inclusions in olivine phenocrysts from basalts are homogenized at T=1320-1280°C. Ti-augite and rhonite were found as daughter phases in these inclusions. Initial melt composition refers to subalkaline basalt. Some homogeneous glasses are rich in F (up to

0.64 wt.%) and poor in Cl. The residual glasses of the unheated inclusions correspond in composition to dacitic melts. In these glasses F is absent and Cl-content is slightly higher than in initial melts.

It is shown that fluid derived from basalt melts on the late stages of olivine crystallization contains mainly CO₂. The fluid pressure at this stage was equal to 0.8-1 kbar. N₂ predominated in the gas bubbles of glassy inclusions in both basalts, and acidic rocks.

Data obtained display that basaltic magma could be the source of F during formation of A-type acidic magmas. Formation of high-temperature, Cl-rich magmas could occur under the influence of trachyandesitic melts.

References

1. Litvinovsky B.A. (1990) Problem of magmatism and metamorphism of East Asia, Novosibirsk, Nauka : 151-163.
2. Litvinovsky B.A. et al. (1995) Doklady Academe Nauk, in press.

CONSTRAINTS ON TEMPERATURES OF QUARTZ AND CARBONATE CEMENTATION IN THE MIDDLE JURASSIC OSEBERG RESERVOIR (NORTHERN NORTH SEA) DERIVED FROM FLUID INCLUSIONS

LEGENDRE, O. & GIRARD, J.P.

BRGM, - BP 6009, 45060 Orléans cedex 02, FRANCE

The Oseberg oil and gas field is a major producer located in the northern part of the North Sea in the Norwegian sector. The main reservoir, i.e., the Oseberg formation, is a rather homogeneous sandstone which constitutes the bottommost unit of the Middle Jurassic BRENT succession. In the study area the Oseberg sandstone is 20 to 60 m thick and occurs at depths ranging from 2500 to 3200 m corresponding to present temperatures of 100 to 120°C. These coarse to medium-grained and immature sandstones are interpreted as representing proximal, marine-dominated delta fan deposits bracketed by alluvial deposits. The burial history of the reservoir is typical of many BRENT reservoirs in the North Sea and characterized by a initial period of slow subsidence or local uplift (late Jurassic to early Cretaceous) followed by a rapid subsidence (22 m/my) up to present day.

A detailed multidisciplinary study of the Oseberg formation was carried out in collaboration with Norsk Hydro (and Oseberg operating partners) in order to describe and reconstruct as precisely as possible the timing and conditions of diagenetic transformations occurring in the reservoir. Core samples from 13 different wells located throughout the study area were investigated.

The detrital mineral assemblage is essentially composed of quartz, feldspars, muscovite and lithic clay clasts. Integration of all petrographic observations yields a comprehensive diagenetic sequence generally applicable to the reservoir. The main successive events are as follows:

- early precipitation of minor siderite and pyrite in restricted areas,
- development of K-feldspar overgrowth, only in the northernmost part of the field,
- sporadic precipitation of ankerite cement,
- extensive and pervasive dissolution of detrital and diagenetic feldspars,
- ubiquitous crystallization of intergranular vermiform kaolinite together with discrete precipitation of quartz overgrowth,
- development of porosity-occluding, poikilotopic Fe-rich calcite, in areas which appear lens-like,
- and precipitation of dickite (recrystallization of kaolinite?) restricted to the water-filled part of the formation.

K-feldspar, quartz and carbonate cements were systematically investigated for fluid inclusions. However, two-phase inclusions suitable for microthermometric measurements were found in ankerite, quartz and calcite only. Observations under UV fluorescence microscope indicate that hydrocarbon-bearing inclusions are present in quartz and calcite in association with aqueous (non fluorescent) inclusions. Homogenization temperatures

were measured for both types of inclusions and yielded similar results for a given sample. Due to the very small size of most inclusions, only a few freezing temperature measurements could be performed.

Inclusions in ankerite were observed in one sample which comes from the southernmost well. Measured homogenization temperatures range from 66 to 76°C (av. 72°C).

Most fluid inclusions in quartz occur at the boundary between the detrital grain and the diagenetic rim. In a few instances inclusions were also found within the overgrowth but yielded identical homogenization temperatures. Inclusions were particularly studied in three wells aligned along a 12 km North-South trend in the central part of the field. Th values range from 91 to 107°C (av.=100°C) in the northernmost well, 91 to 95°C (av.=93°C) in the central well, and 84 to 92°C (av.=88°C) in the southernmost well. Although temperatures ranges overlap to a large extent, the results suggest that a positive temperature trend may have existed from South to North at the time the quartz cement formed. Alternatively, diagenetic quartz may have formed at slightly different times, i.e., different depths. Three measured freezing temperatures indicate salinities around 3-4 wt.% eq. NaCl.

Fluid-inclusion data for diagenetic calcite were obtained from three wells roughly aligned in a North-South direction at the northernmost end of the field. Distance between extreme wells is only 2 km. The fluid inclusions in calcite occur either as isolated, scattered inclusions or in small clusters. Th values range from 88 to 100°C (av.=92°C), 91 to 107°C (av.=97°C) and 101 to 112°C (av.=106°C), successively from North to South. Again, in spite of a significant overlap in the data, Th values seem to decrease progressively from North to South. This trend is opposite to that observed for quartz. Similarly, it may relate to different ages of calcite formation as well. Freezing temperatures indicate salinities on the order of 2 to 4 wt.% eq. NaCl.

Because Raman spectroscopy indicates unambiguously the presence of CH₄ in the vapor phase of a few aqueous inclusions and because the reservoir contains a gas cap, it is likely that the aqueous solution in the inclusions is methane-rich. As a consequence, Th values may be approximated as close representatives of trapping temperatures.

The results therefore indicate that ankerite formed at lower temperatures than quartz and calcite, i.e., earlier in the diagenetic sequence. This is in agreement with petrographic observations. Quartz formed at temperatures lower than calcite on average. Both quartz and calcite formed at temperatures either slightly lower or similar to present reservoir temperatures, in agreement with a late diagenetic precipitation. Combining fluid inclusion temperatures with the modeled burial-thermal history for the Oseberg reservoir indicates that ankerite most likely formed during early Tertiary times, while quartz and calcite did not formed before mid-Tertiary times.

FLUID PALAEOCIRCULATIONS IN A PASSIVE MARGIN OF THE SOUTH-EAST BASIN OF FRANCE. PRELIMINARY RESULTS OF FLUID INCLUSIONS AND STABLE ISOTOPES IN THE MORTE MERIE-1 BOREHOLE (ARDECHE).

LEOST, I., RAMBOZ, C.(1), MOSSMANN, J.R.(2) and BRIL, H.(3).

(1) CRSCM, 1A rue de la Férollerie, 45071 Orléans cedex 2, France.

(2) BRGM, BP n°6009, 45060 Orléans cedex 2, France.

(3) Université de Limoges, 123 av. Albert Thomas, 87060 Limoges, France.

As part of the Deep Geology of France program, the SE Basin Western Margin was selected to study the diagenetic reactions occurring in Triassic-Liassic sandstone and carbonate reservoirs and to characterize fluid circulations [1]. Two boreholes were thus drilled on both sides of the Uzer extensional basement-rooted fault (Ardèche). The first core, Balazuc-1 (BA-1) [2], was drilled in the eastern downfaulted block; the second one, Morte Mérie-1 (MM-1) [3], was drilled 1200m west, in the upfaulted block. Here we present preliminary fluid inclusions and stable isotope results from stratabound and fracture-filling minerals sampled in the Mesozoic part of MM-1. Thermometric data are discussed referring to the conditions established at BA-1: a palaeogradient of 35°C/km and a maximum thickness of the Mesozoic cover of 2200±500m reached before Eocene [4].

In stratabound Anisian-Carnian sandstones, carbonates and sulphate-bearing shales (Lower-Middle Trias), vein-fillings mostly consist of anhydrite or gypsum. In sulphate-bearing shales, fluid inclusions (FI) were studied at 4 levels. 342.39m: quartz replaces stratabound anhydrite. Both anhydrite and quartz contain numerous scattered primary FI. Homogenization temperatures (Th) measured in anhydrite are below 70°C and salinities range from 1 to 15wt%eq.NaCl [5]. Replacement quartz yields 83<Th<127°C and variable salinities from 14 to 23wt%eq.NaCl. 294.49m: mm-wide anhydrite veins contain associated monophase and two-phase FI along transgranular cracks. Salinities in monophase FI range from 0.5 to 6.5wt%eq.NaCl. Biphase FI show 169<Th<278°C and salinities from 0.5 to 8.5wt%eq.NaCl. 285.12m: stratabound anhydrite contains primary monophase (too small to be measured) and two-phase FI. The latter show 206<Th<295°C and salinities from 0.5 to 3wt%eq.NaCl (6 measurements) and 2 isolated measurements at 11.7 and 22wt%eq.NaCl. 295.10m: euhedral dolomite crystals along contact zones between shales and sulfate-bearing levels show primary FI which underline a growth aureole. Their Th and salinities range from 63 to 102°C and from 8.5 to 22wt%eq.NaCl respectively. Overlying sandstone and carbonate formations (Upper Trias to Hettangian) are essentially crosscut by carbonate veins (dolomite or calcite, depending on the wall-rock) and locally by barytes. Mm-wide dolomitic veins contain few primary FI. 191.58m: FI in a vertical crack yield 127<Th<146°C and salinities between 6 and 10wt%eq.NaCl. 130.63m: FI in a horizontal vein yield similar results (108<Th<140°C, salinity of 10.5wt%eq.NaCl) whereas FI data in the vertical crack are more scattered (103<Th<173°C and salinities from 1.5 to 16wt%eq.NaCl). Isotopic results are in table 1

Fluid circulations have been so far related to three stages.

1) Fluid circulations during the Triassic extension ("pré-rift stage) [6], as recorded by anhydrite. The $\delta^{34}\text{S}$ values of stratabound anhydrite suggest an authochthonous seawater sulfur source. In all

anhydrite samples however, most FI have salinities lower than the minimum concentration required to precipitate calcium sulphates from evaporated seawater (13wt%eq.NaCl) [7]. Moreover, the two-phase FI from levels 285.12 and 294.49m are interpreted as leaked monophase FI for the following reasons. (i) Both monophase and two-phase FI have similar salinities. (ii) The internal pressure in monophase FI at the maximum burial depth exceeded the lithostatic pressure by 400 bars, which is about the resistance pressure of anhydrite. These results thus suggest that anhydrite has extensively recrystallized in contact with cold diluted fluids of probable meteoric origin when the cover was less 1km. This percolation was favoured by long-duration fracturation movements at the pre-rift stage, when the porosity of rocks was still important.

2) Fluid circulations at a more advanced burial stage. In euhedral dolomite, the Th-increase of FI towards the edge of the crystal suggests fluid trapping during burial diagenesis. A maximum Th of 102°C implies a trapping temperature of 110°C along the geothermal gradient during maximum burial (pressure corrections assuming a hydrostatic regime [8]). Variable salinities indicate either fluid mixing or an evolution of the fluids with time.

By contrast, measured Th in replacement quartz and vertical dolomitic cracks are in excess of the maximum admitted diagenetic temperature, which suggests thermal disequilibrium between the fluid and the wall-rock. Salinities of trapped fluids in quartz suggest mixing, whereas those in dolomitic veins are in favour of a trapping of pulsating fluids with variable salinities. At level 130.63m, the $\delta^{13}\text{C}$ show a seawater origin of the carbonate carbon and the thermometric interpretation of $\delta^{18}\text{O}$ values are in good agreement with FI data. At level 191.58m, the $\delta^{13}\text{C}$ suggests an additional continental component to sea water and/or an organic one (indeed, the sandstones at 200m are oil-impregnated). The $\delta^{18}\text{O}$ value is in favour of an enriched-basinal fluid if the isotopic fractionation occurred at the FI-derived temperatures. The comparison between FI and isotopic results at levels 130.63 and 191.58m shows that although the fluids have the same temperatures and salinities they have not the same origin.

Replacement quartz and dolomitic cracks are considered to correspond to hydrothermal events contemporaneous with the extension by analogy with available datings of similar events in the Cévenole margin.

3) After the erosion of part of the sedimentary pile, fibrous gypsum crystallized in horizontal tension cracks at the favour of a compressive phase during alpine orogenesis (pyrenean phase?). No FI was measured in gypsum, but this mineral indicates $T \leq 50^\circ\text{C}$ [9]. $\delta^{18}\text{O}$ and $\delta^{34}\text{S}$ values suggest in situ remobilization of earlier-formed Triassic or Permian sulfates. These interpretations will be soon completed by Sr isotopic results.

Depth (m)	mineral	Deposit type	$\delta^{13}\text{C}\text{‰} \pm 0.1$ vs PDB	$\delta^{18}\text{O}\text{‰} \pm 0.1$ vs SMOW	$\delta^{34}\text{S}\text{‰} \pm 0.3$ vs CDT
130.63	dolomite	wall-rock	+1.8	+23.6	
130.63	dolomite	horizontal vein	-0.4	+17.0	
130.63	dolomite	horizontal vein	+0.7	+18.9	
191.58	dolomite	vertical vein	-5.1	+21.2	
278.72	fibrous gypsum	horizontal vein		+13.8	+13.6
285.12	anhydrite	stratabound		+13.4	+13.9
295.10	anhydrite	stratabound		+13.0	+13.9
355.07	fibrous gypsum	horizontal vein		+11.1	+14.3

Table 1.

Bibliography ;

- [1] GIOT D. et STEINBERG M., 1990. Doc. BRGM 200, 130p.
- [2] SUREAU J.F. et STEINBERG M., 1992. Doc. BRGM 218, 112p.
- [3] SUREAU J.F., 1993. Doc. BRGM 229, 153p.
- [4] DISNAR J.R., 1994. Chem. Geology, 118, 289-299; PAGEL M., 1994. 15^e RST Nancy, Soc. Geol. France, edit. Paris, p 44.
- [5] BODNAR R.J., 1993. Geochim. Cosmochim. Acta, 57, 683-684.
- [6] BERGERAT F. et MARTIN P., 1994. Bull.Soc.Geol.Fr., 165, 4, 307-315.
- [7] HERMANN A.G. et KNAKE D., 1973. Cont. Miner.Petrol., 40, 1-24.
- [8] ZHANG Y. et FRANTZ J.D., 1987. Chem. Geology, 64, 335-350.
- [9] BLOUNT C.W. et DICKSON F.W., 1973. Amer.Miner., 58, 323-331.

HIGH TEMPERATURE FTIR MEASUREMENTS OF SYNTHETIC H₂O-CO₂ FLUID INCLUSIONS IN THE ONE-PHASE FIELD

LINNEN, R.L. (1), KEPPLER, H. (1) & STERNER, S.M. (2)

(1) Bayerisches Geoinstitut, Universität Bayreuth, 95440 Bayreuth, Germany

(2) Battelle Pacific Northwest Laboratory Richland, WA 99352, USA

A major problem in the analysis of aqueous-carbonic fluid inclusions is the determination of their bulk composition and density. Normally, the molar volumes of the aqueous and carbonic phases at room temperature, together with the volume percentage of each phase are used to calculate these bulk parameters. Because fluid inclusions are three-dimensional objects, commonly with irregular shapes, large errors can be associated with estimating volume proportions, resulting in incorrect compositions, molar volumes and isochore extrapolation. In this study we present preliminary Fourier transform infra-red spectroscopic results for aqueous-carbonic inclusions with different compositions and molar volumes, determined at P-T conditions in the one phase field. The ultimate goal is to establish the effects of P-T-V-X on the H₂O and CO₂ extinction coefficients, which could provide the means for routine analysis of the composition of natural aqueous-carbonic fluid inclusions.

Synthetic H₂O-CO₂ fluid inclusions of known composition and density from the study of Sterner and Bodnar (1991) were analysed on a Bruker IFS 120 HR spectrometer equipped with a Bruker IR microscope, Globar source, CaF₂ beamsplitter and a MCT detector. The resolution is 4 cm⁻¹ and spectra typically consist of 20 to 100 scans (a few minutes of data collection). An adjustable rectangular aperture in the rear focal plane of a 15x Cassegranian objective (working distance 32 mm) was used to isolate the selected fluid inclusion from the surrounding quartz and the minimum inclusion size is approximately 15 µm in length.

A U.S.G.S.-type heating-stage has been adapted for use with the above equipment. All of the glass plates in the sample chamber have been removed, and are replaced by a single CaF₂ window (~1 mm thick) and a spacer ring in both the upper and lower chamber halves. The sample rests on an Inconel disk (~.015 mm thick) that contains a triangular hole. This setup changes the thermal character of the stage and consequently the thermocouple must be re-calibrated. However, thermal gradients were found to be < 2°C if the thermocouple tip was positioned <0.6 mm from the inclusion analysed, thus the accuracy and the precision of temperature measurements with the CaF₂ setup is comparable to that of the classic gas flow stage.

In Figure 1, a 22°C spectrum of the aqueous portion (~2.3 mol% dissolved CO₂) of an inclusion with a bulk composition of 12.5 mol% CO₂ is compared to the spectrum of the same inclusion in the one-phase field at 300°C (T_{H1}=289°C). The higher CO₂ content for the 300°C spectrum is reflected by an increase of the relative CO₂ peak height, and corresponding decrease for that of H₂O. There is also a peak shift to higher wavenumbers for H₂O at higher temperatures, related to a decrease in the hydrogen bond strength. The two

spectra in Figure 2 (scaled to equal H₂O peak heights) were collected at the same temperature (300°C) for inclusions with 12.5 and 25 mol% CO₂ (Th₁ 289° and 275°C, respectively). The CO₂ peak is as expected, higher for the 25 mol% CO₂ inclusion, and there is no apparent difference of the CO₂ and H₂O peak positions for the two samples (although there is only a small difference in the molar volumes of the two inclusions).

These results are encouraging for the development of a calibration curve for extinction coefficients in the system H₂O-CO₂ at high temperature, but a wide range of compositions and densities need to be examined.

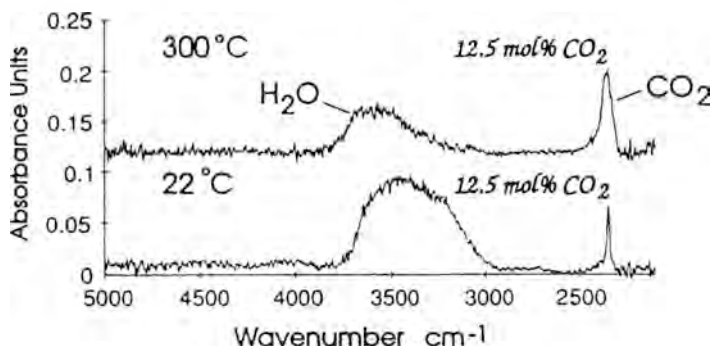
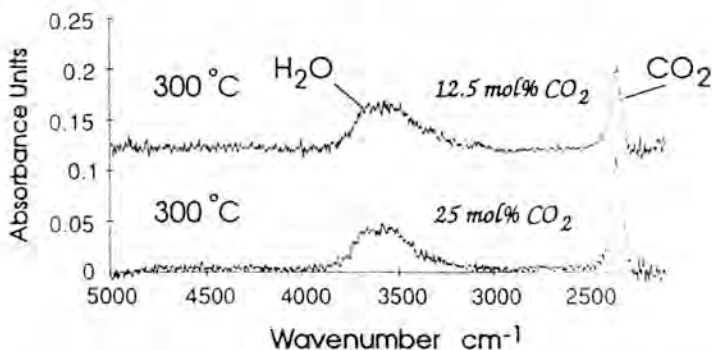


Figure 1. FTIR spectra of a 12.5 mol% CO₂ inclusion at 22° and 300° C. The room temperature spectrum was measured through the aqueous phase only.



FTIR spectra of 12.5 and 25 mol% CO₂ inclusions at 300°C

References

Sterner, S.M. and Bodnar, R.J., 1991, Synthetic fluid inclusions. X: Experimental determination of P-V-T-X properties in the CO₂-H₂O system to 6 kb and 700°C: Amer. J. Sci., v. 291, p. 1-54.

FLUID INCLUSION STUDIES ON SKARN HELVITES FROM CORDOBA PROVINCE, CENTRAL ARGENTINA.

LIRA, R. (1), MARTÍNEZ, E. (2) & GOMEZ, G.M. (1)

(1) CONICET, Instituto de Geología Aplicada, Secretaría de Minería de la Prov. de Córdoba, Celso Barrios s/nº, (5000) Córdoba, Argentina.

(2) CONICET, Departamento de Química, F.C.E.F. y N., Universidad Nacional de Córdoba, Velez Sarsfield 299, (5000) Córdoba, Argentina.

Helvite, the Mn-rich member and the most common of the helvite group $R_4Be_3(SiO_4)_3S$ [where $R=Mn^{2+}, Fe^{2+}, Zn$], is a relatively widespread mineral found associated with skarn paragenesis in several localities of the Sierras Pampeanas Orientales in Córdoba Province, central Argentina.

Helvite occurrences in this region are related to skarn associations developed in close proximity to pegmatite dykes. Samples selected for study are from the Chingolo mine (64°33'17" W long. and 31°13'42" S lat.), one of several in a large scheelite-skarn mining district. Here, helvite is found in a garnet-epidote skarn formed on both sides of a marble unit in contact with a granite pegmatite (Gay and Gordillo, 1979). Marble and amphibolite are interbedded with gneiss country rocks of Precambrian age and pegmatites are related to the lower Carboniferous Achala batholith granite intrusion.

Sample selection from the Chingolo mine was made based on the availability of superb crystals that occur in well-developed tetrahedra, sometimes larger than 15 cm edge size. Crystals are dark brown to reddish and hard to distinguish from associated garnet, other than by crystallographic habit.

Studied helvite is a late-forming mineral in the depositional sequence. Crystals normally occur partially included in garnet, lining cavities later filled with calcite, or sometimes with fluorite or quartz. Some crystals, like the ones from this study, have grown completely free in vugs and are found included in coarse spathic calcite. Associated late-stage phases are sphalerite, specularite, chlorite and ochraceous hematite derived from sulfide oxidation.

Helvite crystals are heavily loaded with fluid inclusions. Three distinctive types of fluid inclusions are identifiable from microscopic observation.

Type I fluid inclusions of primary and pseudosecondary origin are arranged in growth planes and microfractures, respectively. Type I inclusions represent boiling fluids with immiscibility evidences supported by phase volume relationships under microscopic examination and microthermometric behavior. Inclusions are primarily aqueous polyphase daughter crystal-rich with little amounts of CO_2 . The same population contains two-phase vapor-rich inclusions (V/L range: 0.4 - 1.0) mixed with polyphasic vapor-poor daughter crystal-rich and various intermediate phase ratios. Fluid inclusion sizes are extremely variable, most ranging between 3 and 15 μm up to 40 μm . Morphologies include tetrahedral negative crystals and irregular-shaped inclusions. Type I inclusions have total homogenization temperatures (T_h) that range from 345 up to 403 °C and final points of ice melting (T_m) distributed between two contrasting groups of values, one that ranges from -4.5 to -5.5 °C and the other from -15.2 to -23.8 °C. A (T_h) versus (T_m) plot shows a boiling liquid trend from higher T/lower salinities toward lower T/higher salinities. A gap separates the liquid trend from the low salinity high V/L-ratio inclusions. CO_2 -bearing inclusions of this type are rare, liquid-

rich, and have approximate clathrate melting values of -6.3 °C and CO_2 melting points of -56.9 °C. A few measurements of the eutectic point (not accurate) yield approximate melting temperatures in the range -35.0 to -33.5 °C. Daughter crystal-rich inclusions are very abundant. Solids identified by a combination of optical microscopy and SEM-ED analysis include the recurrent presence of an opaque mineral $(\text{Zn,Fe})\text{S}$ (sphalerite), a highly birefringent carbonate $(\text{Mn,Fe,Zn})\text{CO}_3$, possibly rhodochrosite, and a pure Si-mineral (quartz?).

Type II are vapor-rich, (V/L range: 0.6 to ≈ 1.0) CO_2 -rich fluid inclusions grouped in healed fractures of secondary origin that clearly cross-cut former Type I groups. This low density type is void of daughter crystals. Clathrate melting temperatures are around $+6.6$ °C. Homogenization mode is to the vapor phase between 340 and 350 °C. CO_2 homogenization temperature mean value is $+30.2$ °C and CO_2 melting temperatures are close to that of pure CO_2 . This low salinity type of fluid introduced in already crystallized helvite, is thought to be related to the deposition of later-stage spathic coarse crystals of vug-filling calcite.

Type III are two-phase or polyphase liquid-rich aqueous inclusions of secondary origin confined to microfractures of scarce distribution. Necking-down features characterize this group. Most are irregular-shaped, with variable V/L ratios, some only liquid-bearing. Homogenization temperatures are lower than Types I and II, ranging from 245 up to 325 °C. Some decrepitation temperatures have been recorded at ≈ 250 °C prior to homogenization and most will be decrepitated before 350 °C. Ice melting temperatures are low, within the range -2.0 to -5.5 °C.

Field occurrence, paragenetical relationships and microthermometric data suggest that helvite was formed during late stages of garnet-epidote skarn evolution, after the reaction between hydrothermal fluids (pegmatite related?) and dolomite-bearing host marbles. Helvite was deposited from aqueous-rich CO_2 -bearing fluids of moderate salinity. Fluids were boiling at the moment of trapping primary and pseudosecondary inclusions, hence homogenization temperatures within the range 345-403 °C are trapping temperatures. Eutectic point values suggest that components such as $\text{H}_2\text{O-MgCl}_2\text{-NaCl-FeCl}_2$ could be present in a mixed fluid. Sphalerite, as a daughter phase, suggests reducing conditions during helvite crystallization stage. Daughter phases also indicate that Mn, Fe, Zn and Si were important components of the fluids, especially Mn, which is a major constituent of helvite along with Fe and Zn, and is also concentrated in earlier paragenetic spessartine-rich garnet.

As already stated by Holser (1953) and noted by Gay and Gordillo (op. cit.), the role played by wallrock composition was decisive to precipitate helvite instead of beryl by the removal of excess Al_2O_3 from the fluid as garnet+epidote creating subaluminous conditions for helvite precipitation. The prevailing incidence of chemical conditions over P-T parameters and the fact that each skarn environment is more or less unique, does not allow extensive application of P-T-X conditions of helvite formation to other helvite-bearing skarns.

REFERENCES

- GAY, H.D. and GORDILLO, C.E. (1979) Hallazgo de helvita $(\text{Mn,Fe,Zn})_8 [\text{S}_2 | (\text{BeSiO}_4)_6]$ en la mina Chingolo, Cosquín, Córdoba. Bol. Acad. Nac. Ciencias, Córdoba, Tomo 53 (1-2), pp. 71-76.
- HOLSER, W.T. (1953) Beryllium minerals in the Victorio Mountains, Luna County, New Mexico. The American Mineralogist, Vol. 38 (7-8), pp. 599-611.

GEOCHEMISTRY AND SOURCES OF CO₂-BEARING HYDROTHERMAL FLUIDS AT THE PALEOZOIC BREWER GOLD HYDROTHERMAL SYSTEM, SOUTH CAROLINA, U.S.A.

LU, Ch.(1) and MISRA, K.C.(2)

(1) Jacobs Engineering Groups, Inc., Oak Ridge, Tennessee, U.S.A.

(2) Dept. Geol. Sci., Univ. of Tennessee, Knoxville, TN 37996, U.S.A.

Gold mineralization at the Brewer Mine, South Carolina, occurs in an intensely silicified zone composed primarily of multi-stage hydrothermal quartz-pyrite breccias, probably of hydromagmatic origin, in a hydrothermal system that extends over more than 2 km into the volcanic country rocks of the Carolina slate belt. Outward from the interior, the alteration pattern consists of concentric zones of silicic, advanced argillic, sericitic, and sporadically distributed propylitic alteration (Lu et al., 1993). Silicification is characterized by widespread occurrence of quartz as both pervasive replacement of, and cement to, breccia fragments. The inner part of the aluminosilicate hydrothermal system is predominantly an acid-sulfate alteration assemblage characterized by quartz, pyrite, alunite, enargite, topaz, and andalusite. Gold mineralization is confined almost exclusively to the multi-phase, eruptive breccia bodies or pipes in the central part of the alteration zone (Scheetz, 1991). The brecciation and hydrothermal alteration have produced abundant matrix quartz and quartz veins, often with pyrite, enargite, sericite, or pyrophyllite, in the mineralized zone and in the surrounding hydrothermally altered rhyolitic volcanic breccias, flows, and tuffs of the Carolina slate belt.

Most of the fluid inclusions in the quartz from the Brewer mine contain CO₂-bearing fluids, occurring in various modes: randomly isolated, 3-D randomly distributed, and along microfractures. The fluid inclusions are divisible into three groups: CO₂-rich; H₂O+CO₂; and H₂O-rich. Heterogeneous trapping was probably the dominant process that resulted in the variable CO₂:H₂O ratios in fluid inclusions, although limited episodic boiling could have played a role in the formation of CO₂-rich inclusions. Homogenization temperatures (T_h) of the fluid inclusions range from 160° to 330°C, reflecting repeated brecciation and hydrofracturing during mineralization. The temperature range obtained from the $\Delta^{34}\text{S}_{\text{alunite-pyrite}}$ values is 300°-500°C (Lu, 1994), but the fluid inclusion temperatures could be up to 100°C higher if relatively higher fluid pressure prevailed during mineralization. Further constraint on the temperature of the mineralizing fluids is obtained from the hydrothermal mineral assemblage of andalusite, diaspore, kaolinite, and pyrophyllite that suggests a temperature range of 250° to 400°C. The fluid pressure required for decrepitation of CO₂-rich inclusions, common in the Brewer samples, would probably be in excess of 1,000 bars.

The fluid inclusions exhibited complex phase changes during freezing-heating cycles and often developed as many as five phases -- aqueous liquid, ice, gas hydrates, solid CO₂, CO₂-rich liquid, and CO₂-rich vapor -- suggesting a complex chemical composition in a multi-component system. The CO₂ densities range from 0.95 to 0.51 g/cm³ from T_h-CO₂ temperature calculation. In general, CO₂-rich inclusions have higher densities. The bulk density of the fluid and the CO₂ content were calculated using volumetric property of H₂O-CO₂ phases, salt content in H₂O, and T_h-CO₂. The bulk densities of the fluid inclusions range from 0.68 to 1.08 g/cm³. The calculated X_{CO₂} values range from 0.275 for CO₂-rich inclusions to 1.00 for nearly pure CO₂ inclusions. The H₂O-CO₂ inclusions have X_{CO₂} from 0.02 to 0.177.

Calculated salinities vary from 0.02 to 14.77 for H₂O-CO₂ inclusions and from 1.16 to 14.98 for H₂O-rich inclusions. A general trend of inclusions with higher T_h having relatively lower T_m-ice and higher salinity may be attributed to the mixing of deeper hydrothermal fluid with cooler, less saline meteoric water during its ascent to the site of mineralization.

Laser Raman microprobe analysis revealed the presence of CO₂, SO₄²⁻, and possibly SO₂ and H₂S+HS⁻ in the Brewer fluid inclusions. CO₂ and SO₄²⁻ are the dominant components of the fluid inclusions. The SO₄²⁻ appears to be preferably concentrated in the H₂O phase.

Synchrotron x-ray fluorescence microprobe analysis of fluid inclusions has indicated the presence of S, Cl, K, Ca, Ti, Cr, Mn, Fe, Ni, Cu, Zn, As, and Br in a H₂O-rich, H₂O-CO₂ inclusion. On the other hand, a CO₂-rich 3-phase inclusion, which was probed on the CO₂ phase, had only low intensities of Mn, Fe and Ca (?) peaks and no Cl peak. The higher metal content in the H₂O phase compared to the CO₂ phase suggests that the metals and other constituents may have stayed preferentially in H₂O phase.

The fluid inclusion data suggest that the fluids related to the gold mineralization in the Brewer were moderately saline (<15 wt% NaCl= equiv), metal-rich, H₂O-CO₂ fluids with variable CO₂ contents. The fluids were probably SO₄²⁻-rich, at least during late stage of the mineralization, and relatively oxidized. Alternatively, the reduced sulfur may have been consumed to precipitate pyrite and other sulfides in the central part of the hydrothermal system (the mineralized breccia zone), leaving the fluid relatively enriched in SO₄²⁻. The lack of CO and CH₄ in the inclusion fluids may also be attributed to an relatively oxidized environment favoring CO₂.

Although the tectonic setting, hydrothermal alteration pattern, mineralization style, and alteration mineral assemblages indicate an epithermal acid-sulfate environment for the gold mineralization at Brewer, the fluid composition, with a high CO₂ content, is somewhat different from the typical Tertiary epithermal precious metal deposits. A deep-seated felsic magma (high aluminosilicate melt), which could release H₂O-CO₂ fluid, appears to be the most likely source of the heat and CO₂-bearing hydrothermal fluids for the Brewer mineralization as well as for the volcanic activity in the area either during or prior to the mineralization. The Brewer hydrothermal system may represent a slightly deeper environment than the typical epithermal system, but salinity-T_h relationship and the presence of mostly secondary H₂O-rich aqueous inclusion suggest the likely mixing of meteoric water with magmatic fluid, especially during the later stage of mineralization.

References:

- LU, C., 1994, Geochemical characterization of the Brewer Gold hydrothermal system in Carolina Slate Belt, Jefferson, South Carolina: Unpubl. Ph.D. diss., Univ. of Tennessee, Knoxville, 226p.
- LU, C., MISRA, K. C., STONEHOUSE, J. M., and ZWASCHKA, M. R., 1992, Geochemical signatures of alterations in Brewer gold mine, South Carolina: *South Carolina Geology*. v. 35, p. 37-54.
- SCHEETZ, J. W., 1991, The geology and alteration of the Brewer gold mine, Jefferson, South Carolina: Unpubl. M.S. Thesis, Univ. of North Carolina, Chapel Hill, 180p.

FLUID INCLUSION STUDIES IN WOLFRAMITE AND SULPHIDES- APPLICATIONS OF INFRA-RED MICROSCOPY.

LÜDERS, V. (1) & PFLUGBEIL, B. (2)

(1) GeoForschungsZentrum Potsdam PB.4.3 Lagerstättenbildung, Telegrafenberg A 50, D-14473 Potsdam.

(2) Technische Universität Berlin, FB Geowissenschaften Ernst-Reuter-Platz 1, D-10587 Berlin.

Infra-red microscopy allows the observation of fluid inclusions in very dark to opaque minerals such as black tourmaline, garnet, wolframite, tantalite or columbite. Also sulphidic ores sometimes appear transparent for near infra-red light (Fig.1). A general problem for fluid inclusion studies by IR-microscopy is the adaptation of a heating/freezing system with the microscope. The combination of the Olympus BHSM-IR microscope with an USGS gas-flow heating/freezing system allows the use of long working distance objectives (up to 80x) for infra-red light observation in the near infra-red spectrum (500-1800 nm) and measurements in the temperature range -195 to 600 °C. The infra-red image is transmitted to a monitor by a high-resolution infra-red TV camera with a detection capacity up to 2200 nm.

Fluid inclusions were studied in wolframite from Panasqueira (Portugal) and various occurrences of the Erzgebirge (Saxony, Germany). Additionally, inclusions in sulphides such as stibnite, bournonite and tetrahedrite from hydrothermal vein mineralizations of the Harz Mts./Germany and pyrites from the Murgul deposit (Turkey) were measured. The data obtained are compared with those of fluid inclusions in gangue quartz in order to prove paragenetic relationships.

It turned out that fluid inclusions in wolframite and quartz which are assumed to have formed from the same fluid differ strongly in salinity as well as in homogenization temperatures. Fluid inclusions in wolframite from all occurrences under investigation show higher salinities and lower homogenization temperatures than inclusions in coexisting quartz.

A cogenetic formation which is assumed for stibnite /sulfosalt mineralization on a vein structure of the Lower Harz Mts. can also be excluded due to the results of infra-red fluid inclusion studies in these minerals. Finally, it was possible for the first time to study fluid inclusions in euhedral pyrite crystals which yield homogenization temperatures of about 210 °C and indicate crystallization from KCl-rich fluids.



Primary two-phase inclusion in bournonite (Wolfsberg, Lower Harz Mts./Germany). Final melting at $-35.5\text{ }^{\circ}\text{C}$ indicates precipitation from a CaCl_2 - NaCl -rich fluid. The homogenization temperature was measured at $124.5\text{ }^{\circ}\text{C}$.



Two-phase fluid inclusions in pyrite (Murgul/Turkey) showing final melting temperatures of about $-3\text{ }^{\circ}\text{C}$ and homogenization temperatures in the range 206 - $215.5\text{ }^{\circ}\text{C}$.

**IMMISCIBILITY PHENOMENA IN THE GIGLIO ISLAND PLUTON
SOUTHERN TUSCANY ITALY.**

MAINERI, C.(1) and LATTANZI, P.(2)

(1)Dipartimento di Scienze della Terra, Università di Firenze, Italy

(2)Dipartimento di Scienze della Terra, Università di Cagliari, Italy

This is a preliminary report of an ongoing study on the magmatic to hydrothermal evolution at Isola del Giglio. The Isola del Giglio pluton is a 5 My old acidic S-type intrusive, and belongs to the collision-related rocks of the Tuscan Archipelago Granitoids (Poli, 1992). It is mainly composed of hypidiomorphic granular monzogranite - bearing biotite, plagioclase, orthoclase and quartz as major phases (Main Facies, MF). More mafic enclaves, showing a I-type affinity, are also present. Scattered throughout the stock, small miarolitic cavities and numerous aplitic and pegmatitic veins and pockets are found.

Twelve quartz specimen from MF, from pegmatitic veins and from miarolitic cavities were selected for fluid inclusion studies. The following inclusion types were observed in different proportions in the quartz samples:

I) Recrystallized silicate melt inclusions, corresponding to "magmatic remnants" (cf. Touret and Frezzotti, 1993);

II) Brine Inclusions (L+V+Hn+Sn), extremely chloride-rich, with minor carbonates;

III)Low density CO₂-rich gas inclusions.

On heating to high temperatures, type I inclusions (from MF quartz) exsolve, around 700 C, one or more (up to 6) small vapour bubbles and some solids. Raman analysis shows that the bubbles contain pure low density CO₂.

Type II Inclusions exhibit strong reequilibration textures, probably corresponding to implosion phenomena. Homogenisation to liquid was observed before dissolution of solids, at T = ca. 300 C. The same behaviour was observed for brines in pegmatitic and miarolitic quartz, the only difference being the dissolution of some solids before bubble disappearance.

Raman and microthermometric analysis of type III inclusions indicate a very constant composition of the low-density phase in all samples, that is 85% CO₂ and 15% CH₄.

Textural relationships and preliminary microthermometric and Raman data of studied inclusions suggest that at Isola del Giglio silicate melt/hydrosaline melt/ low density fluid immiscibility phenomena occurred at the magmatic stage. Further measurements are currently underway, and will be presented at the meeting.

References

POLI,G. (1992), Journal of Geology, vol.100, p.41-56.

TOURET J.L.R. & FREZZOTTI M.L. (1993), Bull. Soc. Geo. Fr., vol. 164,2, p.229-242.

GEOLOGICAL AND FLUID INCLUSION CHARACTERISTICS OF THE Zn-Pb CARBONATE HOSTED MINERALIZATIONS IN THE S.E. AREA OF PICOS DE EUROPA (NORTHERN SPAIN).

MANGAS, J. (1) & GOMEZ-FERNANDEZ, F. (2)

(1) Dpto. de Geología, Univ. de Las Palmas de G.C., Apdo.550, Campus Universitario de Tafira, 35080 Las Palmas de Gran Canaria, Spain.

(2) Apdo. 261, Torrelavega, 39300 Cantabria, Spain.

The Pb-Zn mineralizations object of the study are located within the Cordillera Cantábrica, in the SE edge of the Picos de Europa region. The stratigraphic sequence is basically constituted of several carboniferous limestone formations. From a tectonic point of view, it is to be noted that the existence of imbricate thrusts of limestones, are present in each one most of the carboniferous sequence. Another important tectonic characteristic is the existence of a system of subvertical faults in the strike N105-120E, which had its origin at the end of Hercynian orogeny. A process of epigenetic dolomitization which affected large volumes of rock in the lower structural units and smaller volumes in upper units occurred in the area under study, prior to the deposition of the Zn-Pb mineralizations.

Two types of mineralizations have been found in most of the deposits. Type I mineralization is formed by granular sphalerite, galena, dolomite and calcite, and in lower proportions, chalcopyrite, tetrahedrite and pyrite, which have abundant granular, laminated and botroidal textures. Type II mineralization is characterized by toffee-coloured sphalerite, galena and calcite, and in lower amounts dolomite, pyrite and quartz. The type II sphalerite and galena may show large size crystals. Associated to this type of mineralization, fluorite appears added to it. The mineralizations of the two types are accompanied by graphitoid matter with sericite, microcrystalline quartz and carbonate minerals, which are products of the alteration caused by hydrothermal solutions upon the host carbonate rocks. Type II mineralizations are later than type I. Subsequent to these two phases, late (dolomite, calcite, galena, pyrite and fluorite) and secondary (hydrozincite, azurite, malachite, chalcocite, aurichalcite, cinnabar and Fe oxides) minerals were deposited.

The study of the fluid inclusions by microthermometry and cryogenic scanning electron microscopy was carried out in two deposits: Aliva (AL) and Andara (AND) on samples of sphalerite I (AL36 and AL37) and II (AL200, AL222, AL227, and AND85), dolomite I (AL36 and AL37), calcite II (AL200, AL222 and AL227) and fluorite II (AL20, AL51a and AL51c). The Aliva samples have been selected in different exploitation levels, thus: samples AL 36, 37 and 227 belonged to 1° level (1.602 m.); AL 200 to 3° (1.552 m.); AL 222 and 20 to 4° (1527 m.) and, AL 51a and 51c to 6° (1467 m.).

The fluid inclusions are primary, pseudosecondary or secondary in character and these show generally two-phase (H_2O L + V) at room temperature in which the vapour bubble is below to 20% of the total inclusion volume. In addition, a smaller number of inclusions are one (H_2O L), two (H_2O L + mechanically trapped solids) or three (H_2O L + V + mechanically trapped solids) phases. Inclusion morphology and their abundance in samples are varied, and sizes are generally below 30 μm . More than 450 inclusions have been studied and

themicrothermometric results are summarized in the following Table.

The microthermometric results and the paragenetic data suggest that the fluid inclusions trapped in minerals of Aliva mine from different exploitation levels are evidence of discontinuous hydrothermal evolution. Thus, there are various stages of circulation and trapping of basement brines belonging to the system H₂O-NaCl and other salts, with spatial and temporal variations in salinity and temperature. The inclusion X-ray microanalyses in sphalerite I (sample AL37) confirm that the trapped solutions are mainly constituted by H₂O and ClNa, and the mechanically trapped crystals are calcite with small amounts of Fe and Mg, dolomite with small amounts of Fe, and clays.

For the Aliva mine a minimum depth of mineralization formation of 1050±50 m. can be considered and this depth is the difference of the height between the mine and the summit of Peña Vieja. Taking into account a representative mineralizing solution of these deposits (waters with salinity of 15 wt. % eq. NaCl and Th of 150°C), Th corrections would be of 20°C (170°C) for a hydrostatic pressure and of 50°C (200°C) for a lithostatic pressure. In these deposits, pressure has been high enough to prevent the boiling of the fluids.

In conclusion, these Pb-Zn mineralizations are epigenetic hydrothermals of moderate temperature associated with faults and limestones. The mineralizing fluids were possibly formation brines of the Pisuerga-Carrion Region sediments (S and O isotopic data show marine waters and that the sulphur is of crust origin). During the Permian, possibly within extension tectonic phases, these fluids moved towards Picos de Europa zone through late-hercynian fractures. Successive changes, sudden or continuous, in temperature, pressure, concentration, pH, among other factors, gave place to the mineral deposition when the mineralizing brines reacted with the wall rocks.

MINERAL	SAMPLE	N° I. F. STUDIED	T _{mice} (°C)	SALINITY (wt. % eq. NaCl)	MOLALITY in NaCl	Th (°C) in L
Sph I	Al 36	67	-4/-16.8	6.4/20.3	1.2/4.6	117/170
	Al 37	59	-7.1/-12	10.6/16	2.1/3.3	106/170
Dol I	Al 36	23	-8.5/-16	12.3/19.6	2.4/4.4	140/166
	Al 37	18	-13/-15.5	17/19.2	3.6/4.2	140/170
Sph II	Al 222	33	-9.2/10.2	13.1/14.2	2.6/2.9	150/156
	Al 200	12	-10.6/-12	14.6/16	3/3.3	133/155
	Al 227	13	-14.8/-18	18.6/21.2	4.1/4.9	154/172
Calc II	Al 222	53	-7.6/-21.3	11.2/23.6	2.2/5.7	95/174
	Al 200	32	-9/-15.2	12.9/19	2.6/4.2	110/155
	Al 227	31	-7/-15.8	10.5/19.5	2/4.3	125/156
Fl II	Al 51a	31	-12.2/-16.7	16.2/20.2	3.4/4.5	103/125
	Al 51c	52	-13/-16.4	17/20	3.6/4.5	95/133
	Al 20	40	-10.8/-16	14.8/19.6	3/4.4	80/135
Sph II	And 85	19	-18.5/-19.3	21.6/22.1	5/5.2	155/162

**FLUID-MINERAL EQUILIBRIUM IN ANTITAXIAL QUARTZ VEIN SYSTEM
IN MANGANESE-ORE FROM VAL GRAVEGLIA (NORTHERN APENNINES,
ITALY)**

MARESCOTTI, P.(1), GIORGETTI, G. (2)

(1) Dip.Scienze della Terra, C.so Europa 26, I-16132 Genova, Italy.

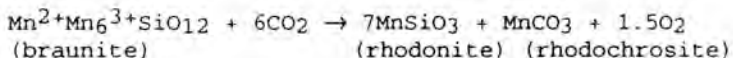
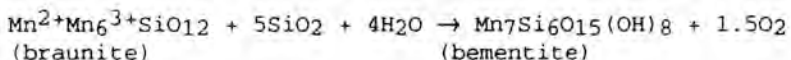
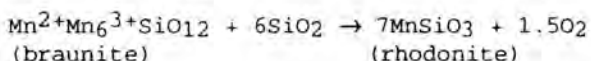
(2) Dip.Scienze della Terra, Via delle Cerchia 3, I-53100 Siena, Italy

The metacherts of "Diaspri di M.Alpe" formation often contain manganiferous levels near their stratigraphic bottom.

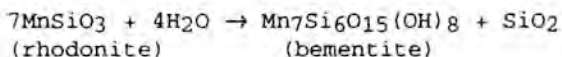
Mn-ores were partitioned from iron-rich siliceous muds and deposited at the base of the cherts, through turbiditic processes, during Middle Callovian stage (Abbate et al., 1986).

During Upper Cretaceous-Lower Cenozoic orogenic events, sedimentary-diagenetic Mn oxides and hydroxides (i.e. psilomelane, todorokite, pyrolusite and manganite) were completely replaced by braunite + quartz ± hematite assemblages, under prehnite-pumpellyite facies conditions (T= 275 ± 25°C; P= 2.5 ± 0.5 Kbars; Lucchetti et al. 1990). This main tectonic event induced mobilization of Mn and Si, and, mainly at the fold hinges, thickening of the mineralized layers up to some tens of meters.

During deformation, the mineralized layers underwent intense fracturation, or even cataclasis, especially at the fold hinges, where sigmoidal veins formed. At the vein walls a reaction rim developed and the rock-forming braunite + quartz assemblage was replaced by Mn-silicates (bementite ± rhodonite) and/or carbonates (rhodochrosite and Mn-calcite) through the following observed reactions (braunite and rhodonite are considered to be pure $Mn^{2+}Mn_6^{3+}SiO_{12}$ and $MnSiO_3$, respectively):



Rhodonite may be replaced by bementite through the following hydration reaction:



An antitaxial quartz + bementite vein was chosen to characterize the synmetamorphic fluids possibly trapped during the veining process.

The vein consists of fibrous quartz and, locally, of euhedral quartz crystals with well defined growth zones; bementite is present as thin symmetric rims in both vein walls and often surrounds the euhedral quartz crystals. In the fibrous quartz zone, a line of wall rock fragments runs near the central line of the vein.

Primary fluid inclusions, related to successive growth steps, were recognized and investigated in the large (up to 3 mm) euhedral quartz crystals and in the quartz fibres.

Such fluid inclusions can be divided in two compositionally distinct groups:

1) low-salinity, NaCl- KCl-bearing fluids (average salinity ≤ 1 wt% in NaCl_{eq}) occurring in all the growth zones of euhedral quartz, and in the fibres; ThL decrease from 180 to 140 °C.

2) high-salinity fluids (average salinity of 12 wt% in NaCl_{eq}), characterized by a different chemical system (eutectic temperature -35°C) and concentrated only in a narrow central part of large euhedral crystals; ThL are between 155 and 135 °C.

The density of the low-salinity fluids slightly increases from the core to the rim of the crystal (from 0.91 to 0.94 g/cm³); the high-salinity fluid shows an average density of 1 g/cm³.

Isochores of successively trapped fluids are all consistent with the estimated conditions for the metamorphic event. Their distribution indicates that the system was cooling nearly isobarically. These fluids were circulating during the tectono-metamorphic event and were in equilibrium with the system as it cooled.

The high-salinity fluid is related to a temporally defined episode recorded only in the large euhedral crystals: it probably bears a Mn chloride in solution, and its salinity may explain a relatively high pH in the system during the mineralizing events.

Thus, considering the P-T-x characteristics of this fluid, we hypothesize that it represents the "mineralizing" fluid (i.e. the fluid which triggered the observed reactions) producing the new mineralogical assemblage.

References

- ABBATE E., BORTOLOTTI V., CONTI M., MARCUCCI M., PRINCIPI G., PASSERINI P. and TREVES B. (1986). Appennines and Alps ophiolites and the evolution of the Western Tethys. *Mem. Soc. Geol. It.*, 31: 23-44.
- LUCCHETTI G., CABELLA R. and CORTESOGNO L. (1990). Pumpellyites and coexisting minerals in different low-grade metamorphic facies of Liguria, Italy. *J. metamorphic Geol.*, 8: 539-550.

RELATIONSHIPS BETWEEN FLUID MIGRATION AND REGIONAL STRESS FIELD IN MINERALIZED PEGMATITES: AN EXAMPLE FROM THE SPANISH CENTRAL SYSTEM

MARTIN-ROMERA, C. (1), VINDEL, E. (1), LOPEZ-G, J.A. (1) & CATHELINÉAU, M. (2)

(1) Dpto. de Cristalografía y Mineralogía. Univ. Complutense. 28040 Madrid, Spain

(2) CREGU, BP 23, 54501 Vandoeuvre-Les-Nancy, Cedex France.

Late magmatic activity in the granites from the Spanish Ventral System result in the formation of pegmatites and miarolitic cavities, and is followed by fluid circulation and water rock interactions at the origin of the W-bearing quartz veins and greisen. As most of these processes are structurally controlled, it has been attempted to relate fluid events and related mineral crystallization to the regional succession of deformational events. This has been carried out by a study of microdeformation (systematic measurements of microstructural marker orientations) together with a detailed study of inclusion fluids.

The pegmatites of Cabeza Lijar are $N65^{\circ}E \pm 10^{\circ}$ zoned veins, and cavities constituted by quartz (Q1, Q2 and Q3), K-Feldspar, plagioclase, phengite and fluorite. The border zone (1 cm thin) is constituted only by K-feldspar and fluorite and the central zone of quartz, K-feldspar and phengite as principal minerals.

Fluid characterization

Fluid inclusions were systematically studied in wafers of Q1 samples (0.5 to 1 cm of quartz grains located in the inner zone of the miarolitic cavities). All inclusions trapped in the miarolitic cavities are secondary inclusions. Three types of fluid inclusions have been distinguished on the basis of microthermometry and Raman analysis: i) Lw-s, containing brine, daughter phases and trapped minerals, Lw-s inclusions represent an early fluid of high temperature (400-450°C). ii) Lw-(c-m) inclusions contain aqueous-carbonic fluids of moderate salinity characterized by a volatile phase with dominant CO₂ and minor amounts of CH₄. They display moderate density (0.5 to 0.75) and homogenization temperatures ranging from 290° to 335°C. Lw inclusions contain aqueous liquids of variable salinity. They are later than the other types and are characterized by a moderate homogenization temperature, ranging from 150° to 250°C. Lw inclusions display irregular shapes. Dissolution processes, fractured borders and necking down were frequently recognized as resulting of reequilibration processes.

Microstructure characterization and geometry

The geometry of the orientations and textures in quartz grains were investigated using transmitted light microscopy on oriented thin sections and an interactive videographic analyzer (CRPG, Nancy, Lapique et al., 1988) which allows to get a statistical description (strike and dip of linear microstructural markers). Four main events are distinguished and may be classified in the following chronological order:

(i) most early structures are striking $N90-100^{\circ}E$ and subvertical: those acquired during the ductile deformation of quartz grains

(bands characterized by a specific extinction), the important early networks of healed FIP displaying Lw-(c-m) inclusions $N90^{\circ}E \pm 10^{\circ}$, as well as microfractures filled by phengites.


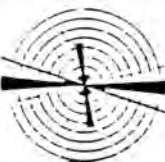



(ii) bands with a high density of aqueous fluid inclusions correspond to FIP with a low dip and large width. They develop mostly in a network constituted of $N90^{\circ}E$ and $N150^{\circ}E$ striking microfractures, with a dip in between 30 and 90° .

(iii) late fluid inclusions planes (FIP) with small size aqueous Lw inclusions striking $N40^{\circ}E \pm 10^{\circ}$, subvertical crosscut all other structures.

This study shows that the fluids linked to earliest stages (magmatic) associated with the formation of the cavities have been mostly lost during the succession of deformational events (deformed inclusions). Then a complex succession of microdeformation structures take place, with the trapping of aqueous fluids, the most represented being those in the fluid inclusion band networks. The main directions of the structural markers are summarized in fig.1). It can be noticed that there are some convergence between the observed preferred orientations in the microstructural study and the regional stress trajectories determined in the central part of the Spanish Central System (Capote et al., 1987). Thus, the latter work distinguishes at less two main stages: i) $N100^{\circ}E \pm 10^{\circ}$, the main brittle deformational stage related to the W-Sn neins and ii) an important late tectonic event in this area is characterized by the $N55^{\circ}E$ strike-slip faults.

Acknowledgements: This work has been carried out through the HCM network (CEE-DG XII-G) "Hydrothermal/metamorphic water rock interactions in crystalline rocks: A multidisciplinary approach based on paleofluid analysis"

Figure 1:

Shadow extinction in Quartz	Oriented phengites	Fluid Inclusion planes	Fluid inclusions bands	Empty Fractures
				
Directions $N100^{\circ}E$	Directions $N90^{\circ}E$ $N170^{\circ}E$	Directions $N90^{\circ}E$ $N150^{\circ}E$ $N40^{\circ}E$	Directions $N90^{\circ}E$ $N150^{\circ}E$	Directions $N140^{\circ}E$

UPPER CRUSTAL FLUID MIGRATION DURING AN OROGENIC CYCLE: AN EXAMPLE FROM THE VARISCIDES OF SOUTH WEST IRELAND.

MEERE, P.A. (1) and BANKS, D.A. (2).

(1) Department of Geology, University College, Cork, Ireland.

(2) Department of Earth Science, The University of Leeds, Leeds LS2 9JT.

Single generation fluids in quartz veins from two similar host lithologies located either side of the Irish Variscan front were investigated. The front marks the northern boundary of a distinctive cleavage developed under sub-greenschist facies conditions and coincides with the northern margin of a fault controlled inverted half graben, the Munster Basin.

The Munster Basin developed as Middle to Late Devonian half graben structure bound with Old Red Sandstone (ORS) basinal infill consisting of 5km of fine grained continental clastics. The northern margin of the basin, delineated by the Dingle Bay-Galtee fault zone fault zone, marked a dramatic facies divide with a marked attenuation of the continental clastic sequence to the south of this basin controlling structure. A maximum ORS thickness of 850m is recorded in the Inch area to the north. The end of the Devonian saw the onset of a major marine transgression across the area. This study is principally concerned with veining and crustal scale fluid movement associated with the Variscan orogenic event at the end of the Carboniferous. North of the cleavage front, in the Inch area, veining in the ORS is quite a rare deformational feature. Isolated veins are generally oriented orthogonal to the regional Slieve Mish fold axis, are steeply dipping and sub-planar. In contrast, quartz veining in the Allihies area, south of the cleavage front, dominates the outcrop. Veins are predominantly syn-compressional features, often centred on second order step folds on the main anticlinorial limbs. In addition, a number of normal faults clearly cross cut all pre-existing compressional features and are associated with late stage extension and orogenic collapse. Quartz is seen to fill dilational jogs along fault traces.

Single generation fluids trapped in Variscan veins north of the front have medium salinities (4-14 wt.%) and densities (0.97-1.08 g/cm³) generally compatible with the expected P-T conditions of deformation in the area. Fluids in veins south of the cleavage front can be grouped into those in (a) syn-compressional veins with moderate salinities (8-16 wt.%) and (b) late stage veins associated with post-orogenic extensional faults which have trapped high salinity fluids (22-27 wt.%). Again fluid densities for both vein types (0.87-1.12 g/cm³) are broadly compatible with estimated P-T conditions of both trapping events.

Crush-leach analyses (Banks & Yardley 1992) reveal that all the fluids analysed have Br/Cl ratios close to seawater, clearly indicating a marine origin. The moderate to high salinities observed had therefore to be produced by evaporation of sea water during the Late Palaeozoic marginal marine sedimentary history of the area (Figure 1a). Variations in I/Cl ratios indicate significant water/rock interaction for medium salinity fluids either side of the front. The cation content of the fluid also indicate that significant modifications to the composition of an evaporated sea

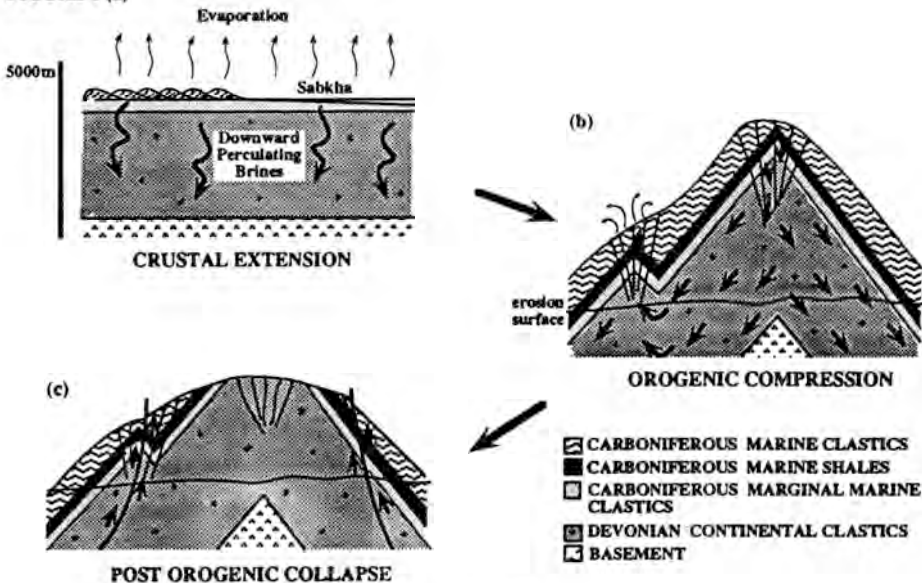
water have taken place. Na is depleted and K is elevated with respect to expected values. This can be ascribed to the destruction of K-feldspars by Na-rich fluids to produce albite which is present in quartz veins. As the concentration of K increases (representing increasing K-feldspar destruction) there are strong positive correlations with the trace elements Sr, Pb and Zn which are commonly found in feldspars, further supporting the argument that dissolution and reprecipitation of feldspars was a major control on fluid composition. Fluids from Inch are distinct from those of Allihies having an Fe/Mn ratio of approximately 0.5 compared with 0.9. This is consistent with the Inch beds being deposited on a more oxidising marginal horst block environment while fluids from the Allihies area originated in a more rapidly subsiding, reducing basinal environment (Bottrell & Yardley 1991).

The marked internal consistency in Br/Cl ratios from northern and southern fluids coupled with broad ranges of cation to chloride ratios suggests that an early homogenous fluid was subsequently modified by differing migration histories during the Late Palaeozoic tecto-sedimentary evolution of the area. It is contended that compressional tectonics and regional scale folding is associated with downward, gravity driven flow of meteoric surface waters with the resulting dilution of the high salinity formational waters (Figure 1b). Expulsion of supra-hydrostatically pressurised fluids is associated with late stage orogenic extension and collapse allowing these high salinity fluids to migrate upwards along normal faults with the minimum of water-rock reaction and dilution effects (Figure 1c).

References

- BANKS, D. A. & YARDLEY, B.W.D. 1992 Crush-leach analysis of fluid inclusions in small natural and synthetic samples. *Geochimica et Cosmochimica Acta*, 56, 245-248.
- BOTTRELL, S. H. & YARDLEY, B. W. D. 1991 The distribution of Fe and Mn between chlorite and fluid: Evidence from fluid inclusions. *Geochimica et Cosmochimica Acta*, 55, 241-244.

FIGURE 1 (a)



FLUID INCLUSION STUDIES ON THE PORPHYRY TYPE Cu-Mo(±Au) MINERALIZATION IN MARONIA AREA, THRACE COUNTY, GREECE.

MELFOS, V., & VAVELIDIS, M.

Aristotle University of Thessaloniki, Greece.

GEOLOGICAL SETTING

The Maronia area is located 35km south of Komotini (NE-Greece). It belongs to the Circum Rhodope Belt which in Thrace consists of the Makri and the Drymos-Melia Unit. According to Papadopoulos (1982) the Makri Unit (Triassic-Late Jurassic) overlies unconformably the crystalline basement of the Rhodope Massif and is divided into the Lower Metasedimentary Series (marbles, dolomites) and the Upper Metavolcanosedimentary Series (schists and quartzites). A plutonic rock of Tertiary age and a porphyry microgranite intersect the metamorphic rocks. Three alteration zones have been distinguished, the phyllic, argillic and propylitic zones. The present study refers to the microthermometric research of the mineralization, which is associated with the porphyry microgranite. It is hosted in quartz veins and silicified zones and occurs mainly as disseminations, veinlets or unregulated concentrations. Chemical analyses of the ore bodies showed contents in Cu, Mo and Au up to 5460ppm, 6900ppm and 12ppm respectively. The ore mineral assemblage consists of pyrite, chalcopyrite, cubanite, pyrrhotite, pentlandite, molybdenite, sphalerite, galena, bismuthinite, tetrahedrite-tennantite, zinkenite, chalcostibnite, famatanite, bournonite, boulanzerite and magnetite.

FLUID INCLUSION STUDIES

Most of the 400 studied fluid inclusions are situated in clusters or less frequently along trails, with sizes not exceeding 60µm. On the basis of phase assemblages at room temperature behaviour and during heating and freezing, four inclusion types were recognized. Type 1 inclusions contain a liquid water solution and a vapor bubble, which occupies 15 to 40% by volume. The temperatures of first melting (eutectic temperature) are approximately -21.4°C indicating that the dissolved salt in fluid inclusions is dominated by NaCl. Ice melting temperatures (-4.5 to -12.3°C) correspond to a salinity between 7 and 16.4wt% eq NaCl. The fluid inclusions show vapor homogenization into the liquid phase at temperatures mainly between 260 and 460°C, with two maximum values at 330 and 370°C. Type 2 contain a colorless isotropic solid cube, probably halite (NaCl) in addition to a liquid and a vapor phase not exceeding 40% of the total volume. Dissolution temperatures of halite ranges between 130 and 500°C indicating a salinity from 28 to 55wt% eq NaCl. The fluid inclusions homogenize into the liquid phase at temperatures mainly from 260 to 440°C with a distinct peak at 310°C. Two phases, a liquid and a vapor, have been observed in Type 3 fluid inclusions, with the vapor bubble occupying 50 to 90% by volume. The salinities derived from the melting temperatures (-3.4 to -10°C) are 5.5 to 14wt% eq NaCl. The homogenization takes place into the vapor phase and the dominant temperatures vary from 340 to 420°C, displaying a maximum at 380°C. Type 4 fluid inclusions were found rarely and consist of

a liquid phase, a vapor bubble (50 to 85% of the total volume) and a daughter mineral, probably halite. They homogenize into the vapor phase at temperatures from 307 to 444°C. Halite dissolves at temperatures between 315 and 450°C indicating a salinity of 38 to 51wt% eq NaCl. In many cases an accidental trapped opaque phase, possibly pyrite, were observed in type 1 and 2 fluid inclusions. Distribution histogram of homogenization temperatures of the different types of the fluid inclusions, displays dominant values from 260 to 440°C, with a distinct peak at 370°C.

DISCUSSION

The occurrence of highly saline liquid-rich inclusions (28 to 55wt% eq NaCl) coexisting with vapor-rich inclusions, homogenizing at the same temperature range, is evidence for boiling of a moderate saline aqueous solution (Nash and Theodore 1971, Roedder 1971). Figure 1 is a plot of the homogenization temperatures vs salinities obtained from the different types of fluid inclusions. Two distinct groups are distinguished, the high-salinity (28 to 55wt% eq NaCl) and the low- to moderate-salinity (5 to 16wt% eq NaCl) inclusions, with similar homogenization temperatures, indicating that two fluids, the high and the low- to moderate-salinity ones, participated simultaneously in the ore deposition. This is characteristic to the porphyry type ore deposits (Takenouchi 1984). The homogenization temperatures of the majority of the fluid inclusions (260 to 420°C, maximum at 370°C) represent the ore formation temperatures. The estimated trapping pressures range from 150 to 450 bars for the low-salinity inclusions and 160 to 510 bars for the high-salinity inclusions. The density of the highly saline fluids were $>0.85\text{gr/cm}^3$ and of the low- to moderate-salinity fluids $<0.95\text{gr/cm}^3$.

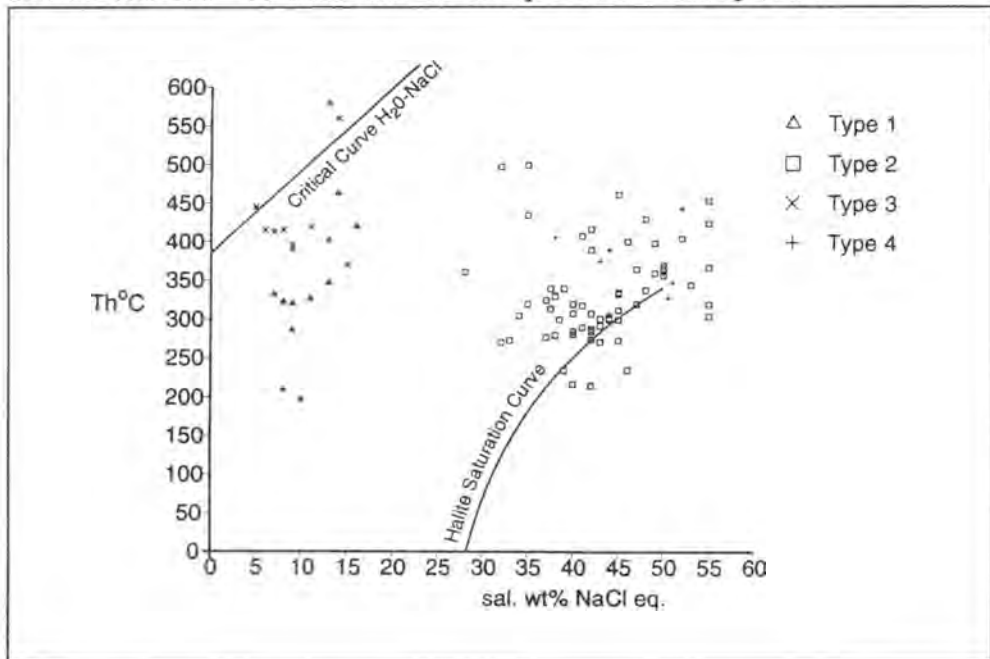


Fig. 1. Homogenization temperatures vs salinities diagram displaying two distinct groups.

CONCLUSIONS

Results of this study indicate that boiling was the main process for the formation of the investigated mineralization and that two types of fluids with very different salinities and densities participated simultaneously in the ore deposition. The fluids of high-salinity and high density are mainly of magmatic origin, whereas those of low- to moderate-salinity and lower density were formed by circulated meteoric water, possibly mixed with magmatic water. The temperature and pressure conditions during the ore deposition were the same for the two types of fluids and ranged from 260 to 420°C and 150 to 510bars respectively.

REFERENCES

- Nash, S.T. and Theodore, T.G. (1971). *Econ.Geol.*, 66, 385-399.
Papadopoulos, P. (1982). Geological Map, Sheet "Maronia", 1:50,000. IGME
Roedder, E. (1971). *Econ.Geol.*, 66, 98-120.
Takenouchi, S. (1984). In I.Sunagawa (ed), *Materials Science of the Earth's Interior*, 515-544.

FLUID INCLUSIONS STUDY IN QUARTZ RELATED TO THE AURIFEROUS GOLD MINERALIZATION OF LA GRUEBA, ASTURIAS, NORTHERN SPAIN.

MESA, M., LÓREDO, J. & GARCIA-IGLESIAS, J.

Departamento de Explotación y Prospección de Minas. Escuela de minas. Universidad de Oviedo. España.

The presence of gold occurrences, exploited many of them along the Roman occupation during the first and second centuries, are abundant in Asturias. They are related to different lithostratigraphic levels and they frequently appear close to igneous intrusions, without exist a specific affinity with the lithology of the sedimentary enclosing rocks. The old open works of La Grueba in Sierra del Courio, Belmonte de Miranda municipality, is one of the mining remains corresponding to the Roman times in northwestern Spain.

The As-Fe-Cu-Ag-Au mineralization of La Grueba is related to El Courio igneous stock, classified as leucogabro, which has given rise to a brecciated zone placed in the contact with the Barrios quartzite (ordovician). This subvertical breccia of 6-8 metres wide shows a brecciated mass with quartzite pebbles included in a matrix of massive quartz, which has sulphide remains. Immediately to breccia there is a 0.9 metres average thickness vein with milky quartz and sulphides.

According to observations in outcropping samples, arsenopyrite, pyrite and chalcopyrite are the main primary opaque minerals in the vein. Gold appears either as a non-visible gold in the arsenopyrite, either as visible particles lower than 10 microns mainly associated to arsenopyrite alteration (skorodite). The visible gold is scarce in the studied samples.

Quartz used for fluid inclusion studies corresponds to filling of fractures in arsenopyrite of the main vein (quartz I), and a late idiomorphic and geodic quartz in breccia with arsenopyrite remains (quartz II). First type of quartz seems to be lightly later and second one clearly later, than arsenopyrite.

All fluid inclusions are two-phase liquid-rich aqueous inclusions at room temperature (L + V) whose size ranges between 3 and 22 microns. Inclusions morphology is irregular but some negative crystal forms have been observed. Microthermometric analyses of primary fluid inclusions in quartz of veinlets in arsenopyrite (quartz I), reveal an homogenization in liquid phase and the maximum of the histogram of homogenization temperatures occur for the interval 300°C-320°C. They exhibit first melting below -25°C and last ice melting temperatures between 0 and -3°C, corresponding to salinities expressed in weight percent NaCl equivalent lower than 5. Fluid inclusions in geodic quartz (quartz II), later than most sulphides, show homogenization temperatures, in liquid phase, between 120°C and 280°C (mean= 150°C); and this order of temperature corresponds to values of secondary fluid inclusions in quartz of veinlets in arsenopyrite (quartz I).

The application of arsenopyrite geothermometer gives values of arsenopyrite crystallization between 395°C and 425°C. On the other hand, the analysis of pyrrothite in equilibrium with pyrite, both

included inside the igneous rocks in proximity to breccia, gives values of 46% Fe, corresponding to crystallization temperatures of pyrrhothite in the order of 600°C.

An estimation of maximum values of pressure during quartz I deposition may be obtained from the isochore of solutions trapped as primary fluid inclusions in quartz I (0.7 g/cc), considering 395°C as upper limit for quartz I deposition. An estimated pressure of 1 kbar is obtained on the basis of the before mentioned considerations.

In conclusion fluid inclusions data together with the application of arsenopyrite geothermometer suggest temperatures from 425°C to 220°C and estimated maximum pressures of 1 kbar, data in agreement with a mesothermal origen for the gold mineralization of La Grueba.

**ELEMENTAL ANALYSIS OF INDIVIDUAL AQUEOUS FLUID INCLUSIONS.
PART II: CALIBRATION STRATEGIES FOR THE OPTIMISATION OF LASER
ABLATION ICP-MS (LAMP-ICP-MS).**

MOISSETTE A. (1,2), SHEPHERD T.J. (2) and CHENERY S.R. (2)

(1) CREGU, B.P.23, 54501 Vandoeuvre les Nancy cedex, France

(2) British Geological Survey, Nicker Hill, Keyworth, Nottingham
NG12 5GG, U.K.

Using a combination of synthetic fluid inclusions, microvolume standard solutions and NIST glasses, elemental ratio calibration curves have been established for the laser ablation ICP-MS analysis of individual aqueous fluid inclusions. Synthetic fluid inclusions in halite were prepared by crystallization from oversaturated sodium chloride solution containing up to 13 major and minor cations from 100 to 1000 ppm (Li, Mg, K, Ca, Rb, Sr, Cs, Ba, Mn, Cu, Zn, Pb, B) for various Cl/Br ratios. The microvolume standards comprised small wells ($3 \times 3 \times 2 \text{ mm}^3$) drilled into perspex sheet, filled with a standard solution and hermetically sealed. To check the efficiency of laser ablation on inclusions and wells, standard NIST glasses were analysed under the same conditions. The three types of test material were characterized by calculating the relative standard deviation (RSD) for each element relative to strontium and this provided a measure of the analytical repeatability. Inspection of bi variate plots indicated that elemental ratios to Sr were linear over a wide range of responses. Synthetic inclusions from $20 \mu\text{m}$ to $80 \mu\text{m}$ in diameter at various depths ($10\text{--}80 \mu\text{m}$) were investigated. Whatever their size and depth, the inclusions gave similar elemental ratios. However, it was noted that for very flat inclusions (i.e. low total volumes) ICP-MS responses were poor due to small amount of material release for analysis.

The RSDs of elemental ratios for the synthetic fluid inclusions and microvolume 'wells' are generally better than 25%; those for Li, Mg, Ba and Rb being less than 15%. By comparison, RSD values for the glasses range between 5 and 10% for most elements. The latter are regarded as a repeatability reference for routine analysis using this particular laser-ICP-MS configuration. The well data not only confirm the results obtained with glasses and synthetic inclusions but also highlight potential matrix effects. In combination, the three types of standards tested provide ideal calibration curves for the study of natural fluid inclusions. Preliminary data will also be presented for in situ determination of Cl/Br ratios in single inclusions.

N.B. Our experience indicates that the process and manner of laser ablation remains a critical and as yet unconstrained parameter controlling the quality of single inclusion.

This work was carried out through the EU Human Mobility and Capital Network Programme (DG-XII-G) "Hydrothermal/metamorphic water-rock interactions in crystalline rocks: a multidisciplinary approach based on palaeofluid analysis."

A SUMMARY OF THE DOLOMITIZATION HISTORY OF THE PIKA AND ELDON FORMATIONS, YOHO NATIONAL PARK, B.C., CANADA

MOORE, S.L.O. & SPENCER, R.J.

The University of Calgary, Calgary, Alberta Canada.

The Pika and Eldon formations are Middle Cambrian in age and were deposited on a shallow carbonate platform west of the Kicking Horse Rim. Five types of dolomite are identified: 1) fine-grained, fabric preserving dolomite interbedded with limestone, 2) coarse-grained fabric preserving dolomite that forms pods, 3) massive coarse-grained, fabric destroying dolomite, 4) hydrothermal brecciation and 5) multiple fracture fills.

On the basis of petrographic evidence and geochemical data, dolomite type 1, the fine-grained fabric preserving dolomite, is interpreted to have formed at low temperatures from Middle Cambrian sea water. Dolomite type 1 is subdivided into dolomite type 1A, and dolomite type 1B. Dolomite type 1A is in muddy carbonate interbeds in ribbon rock. These interbeds contain small cloudy dolomite rhombs that float in a siliciclastic-rich limestone matrix. Dolomite type 1B is found in laminite beds. These beds are composed of laminated very-fine and fine-grained micrite, dolomicrite and dolomite microspar.

Dolomite type 2 is a coarse-grained fabric-preserving dolomite that occurs as pods. These pods cross-cut beds containing dolomite type 1. In ribbon rock, dolomite type 2 replaces the grainstone and overprints the mudstone (type 1A). In the laminite beds dolomite type 2 overprints the coarse-grained layers of dolomicrite and micrite (type 1B). Due to the fine-grained nature of dolomite types 1 and 2, no homogenization temperatures were measured.

Stable isotopes suggest that the fluid responsible for dolomite type 1 was different than that responsible for dolomite type 2. The fluid that formed dolomite type 2 is considered to be a hydrothermal fluid and is interpreted to be related to the events responsible for dolomite types 3 and 4.

Based on the petrography of the cements in dolomite types 3 and 4, a detailed crystallization history and model is formulated. This model incorporates the fluid composition and temperature changes that played a role in the formation of dolomite types 3 and 4.

Both dolomite types 3 and 4 contain a gray matrix dolomite and a white cement. In the gray matrix dolomite, homogenization temperatures range from 98 to 163°C with a salinity between 4.5 to 5.1m NaCl. In the white cement, homogenization temperatures range from 110 to 160°C with a salinity of 5.0m NaCl. From homogenization temperatures, the gray matrix and white cement co-precipitated during the majority of the dolomite formation.

During the second stage of crystallization some fractures penetrated the sediment water interface causing brecciation of a bed of sub-aqueous laminite. Field evidence of early brecciation includes the lack of stoping of overlying layers into the

brecciated zones and measurable thickening and thinning of the unbrecciated laminite into topographic lows at the brecciated surface; compensating for the irregularities on the depositional surface.

Petrographic examination of the early cements show that they are composed of an inner cloudy core surrounded by an rim of banded dolomite. Generally, the inner cloudy cores have lower homogenization temperature (95 to 125°C) than the outer clear/cloudy growth bands (125 to 160°C). The outer boundary of the inner cloudy core contains fluid inclusions with varying proportions of liquid and vapor. The presence of these types of inclusions is evidence for boiling (122.5°C). Using the relationship $P = \rho gh$ and a fluid of 5.0m NaCl, a depth of burial of 16.8m is determined. Therefore, fluid inclusion techniques and field observations indicate that the brecciation event and the initial forming of the underlying massive white dolomite began very early in the depositional history of the area. The brecciation event was short lived as laminite deposition resumed and proceeded to infill the topographic irregularities caused by the brecciation.

The fluids responsible for the white cement (cloudy cores and clear/cloudy bands) and brecciation evolved through time. As the temperature of the fluid increased so did the isotopic ratios of strontium and the isotopic ratios of oxygen decreased. The $\delta^{18}O$ of the water in equilibrium with the dolomite became slightly more enriched as temperatures increased. These $\delta^{18}O$ values of the fluid were within the range for evaporated Middle Cambrian sea water.

Dolomite continued to form for some period of time after brecciation. The fluids responsible for the later stages of crystallization had higher temperatures and lower salinity's (2.0m NaCl) than the previous fluids.

Multiple fracture fills is dolomite type 5. This type of dolomite is interpreted to represent the migrations pathways for the fluids responsible for the various generations of dolomitization described above.

FLUID EVOLUTION AND GOLD MINERALIZATION IN THE PRECAMBRIAN BASEMENT OF THE ZAGROS BELT AT MUTEH, ESFAHAN PROVINCE, IRAN

MORITZ, R. (1) and GHAZBAN, F. (2)

(1) Dép. Minéralogie, Université de Genève, rue des Maraîchers 13, 1211 Genève 4, Switzerland

(2) Dept. of Geology, University of Tehran, Iran

The Muteh mine, about 270 km SW of Teheran, is one the largest gold deposits of Iran. It is hosted by Precambrian metamorphic rocks within the NW-trending Sanandaj-Sirjan tectonic zone, that runs parallel between the Urumieh-Dokhtar Tertiary Volcanic Belt in the NE, and the Zagros Simply Folded Belt in the SW. The Muteh gold deposit consists mostly of silicified rocks enriched in gold and of some gold-bearing quartz-pyrite-carbonate veins. The alteration associated with the gold mineralization overprints the metamorphic assemblage of the host rocks. Silicification of the host rocks is accompanied by the development of white mica, chlorite, pyrite and late stage carbonate. Gold is typically associated with pyrite. The ore bodies are controlled by NW-oriented, steeply dipping normal faults, which are late brittle structures crosscutting the regional ductile pattern of the host rocks.

A microthermometric fluid inclusion study has been undertaken on (1) barren, regional syn-to late kinematic quartz veins remote from the gold deposits and (2) quartz veins and silicified rocks from the ore zones. The aim is to contrast regional fluids with respect to the ore-bearing fluids and to constrain possible genetic scenarios. Four fluid inclusion types are recognized (Table 1):

Type I are liquid-rich, two phase inclusions at room temperature. Salinities based on clathrate melting temperature range between 4.9 and 16.6 wt% NaCl equivalent (mode at 12 wt%). **Type II** are vapour-rich, one or two phase inclusions. Clathrate dissociation temperatures indicate salinities of 1.2 and 2.6 wt% NaCl equivalent. Melting temperatures of CO₂ are lower than -56.6°C in both type I and type II inclusions and indicate the presence of other dissolved gases. Type I and type II inclusions occur in the regional quartz veins that are unrelated to the gold occurrences. Both types occur as secondaries in separate trails or together in clusters.

Type III are liquid-rich, two phase inclusions at room temperature. Apart from total homogenization, only clathrate melting between 6.4 and 8.7°C could be observed. It indicates the presence of dissolved gases, most likely CO₂. No liquid CO₂ is visible in these inclusions. Assuming that the fluid in type III inclusions can be approximated by a H₂O-CO₂-NaCl mixture, it is concluded that the salinity ranges between 0 and 7 wt% NaCl equivalent, the density of CO₂ is less than 0.47 (g/cm³), and the mole fraction of CO₂ is less than 0.1. Type III inclusions are only present in late stage quartz-carbonate-pyrite veins and silicified rocks at the gold occurrences, as well as in some regional quartz veins in the direct neighbourhood of the ore bodies.

Type IV inclusions are liquid-rich, one to two phase inclusions. First ice melting temperatures are typically below -42°C and indicate the presence of additional cations besides Na⁺, such as Ca²⁺. Type IV inclusions occur as secondaries in both late-stage veins in the ore bodies and in regional quartz veins.

Table 1 - Microthermometric results

FI type	Occurrence	TmCO ₂	ThCO ₂	TmClat	TmIce	Th bulk
I	Regional quartz veins	-58.1;-56.9 (-57.0) n=6	8.3;23.6 (18.5) n=8	-0.9;7.5 (3.1) n=17	-12.9;-6.7 n=4	148;257 (208) n=14
	II	Regional quartz veins	-58.5;-57.2 (-57.3) n=12	-23.8;12.0 (-5.7) n=12	8.7;9.4 n=2	
	III	Late gold quartz veins and regional quartz near gold occurrences			6.4;8.7 (7.6) n=27	181;302 (221) n=28
IV	Late gold quartz veins and regional quartz veins				-26.9;-21.0 (-23.5) n=22	84;191 (122) n=33

First and second values = range; in brackets = mode; n = number of measurements; ThCO₂ and Th bulk are to the liquid; all values in °C.

Type I and type II inclusions may represent immiscibility of a saline CO₂-bearing aqueous fluid during the geological evolution of the Precambrian basement rocks. The high salinities of type I fluid inclusions can be explained by interaction of the fluids with evaporite-rich units or alternatively by fluid evolution during retrograde metamorphic reactions. The CO₂-rich nature of type I and type II inclusions most likely reflects decarbonation reactions of carbonate rocks that are present in the Precambrian basement.

Type III are the less saline fluids observed in the Precambrian basement rocks. These fluid inclusions are spatially confined to the gold ore bodies at Muteh and are likely related to the ore formation process. Two possible scenarios can be offered:

(1) Type I inclusions, from the regional quartz veins, and type III inclusions show a similar range of homogenization temperatures, but type I inclusions are typically more saline than type III inclusions. Such a trend may indicate that the fluid in the ore zones (Type III) is the diluted counterpart of the regional fluid. In this scenario, formation of the gold orebodies occurs during a regional fluid migration event in the Precambrian basement with local dilution of this fluid in the NW-oriented normal faults.

(2) The low salinities and low CO₂ contents of type III inclusions are similar to those reported from epithermal gold deposits. Based on structural observations, the NW-oriented faults hosting the gold orebodies in the Precambrian metamorphic rocks have a similar Tertiary age as magmatism in the Urumieh-Dokhtar belt that is about 35 km NE of the Muteh mine. Thus, it is possible that Tertiary intrusive activity associated with the Urumieh-Dokhtar belt generated the heat anomaly responsible for fluid circulation and ore formation at Muteh.

Type IV inclusions are late-stage, low temperature brines that have circulated in the Precambrian basement rocks following the ore formation stage at Muteh. The high salinities most certainly reflect the interaction of these fluids with evaporite-rich units.

Acknowledgments: The Ministry of Mines and Metals of Iran is gratefully acknowledged for access to and hospitality at the Muteh Mine. We would like to thank the staff of the Muteh Mine for guidance and help in the field. This study was supported by a travel grant for the field studies to R. Moritz from the Swiss Society for Natural Sciences (ASSN-SANW), with additional support from the Swiss National Science Foundation (Grant n° 21.33789.92 to L. Fontboté).

**FLUIDS FROM THE RUBANÉ AND FISSURAL ORES OF THE CORVO OREBODY,
NEVES-CORVO MINE, PORTUGAL**

MOURA, A.J. (1), NORONHA, F. (1) & FERREIRA, A. (2)

(1) Centro de Geologia, Faculdade de Ciências da Universidade do Porto, 4050 Porto, Portugal

(2) Somincor, Mina de Neves-Corvo, 7780 Castro Verde, Portugal

The Neves-Corvo mine is certainly one of the richest copper mines in the world, with proven and inferred reserves of over 30 Mt at 8 % copper. This mine is the first European producer of copper and tin since it was opened in 1988. Neves-Corvo is located in the Iberian Pyrite Belt (IPB).

Tectonically the IPB has suffered two main folding episodes of Carboniferous age. The regional metamorphism was of low-grade in the Neves-Corvo region.

The mineralization at Neves-Corvo consists of five lens-shaped bodies mainly of massive sulphides (CORVO, GRACA, NEVES, ZAMBUJAL and LOMBADOR), locally linked by "bridges" of thin continuous sulphide mineralization.

Several main types of mineralization can be recognized:

Massive Sulphides- The main orebodies consist of rocks that are 60-100 wt.% sulphides, which contains shale near the contacts and internal segregations of silica and silicates.

Rubané - Is a banded assemblage of chloritic shales, chert-carbonate breccias and thin lenses of massive sulphides with variable quantities of parallel sulphide layers crosscutting remobilized sulphide veinlets. In the Corvo orebody, it occurs in the hangingwall of the massive sulphides. There are two different types: rubané copper (RC) and rubané tin (RT). Deformation is much more evident in the RT than in the RC.

Fissural - The sulphide mineralization in the shales and acid tuffs of the footwall rocks occurs as thin sulphide venular disseminations that sometimes lie sub-parallel to the main lens contact. Often it may have a crosscutting veinlet fabric and is considered as a stockwork.

The Department of Geology of the mine has defined the following types of ores:

MS- Massive sulphides with more than 2%Cu and 1%Sn; MC- Massive sulphides with more than 2%Cu; RC- Rubané Copper (rubané with >2%Cu); RT- Rubané Tin (rubané with >1%Sn); FC- Fissural Copper (fissural with >2%Cu) and FT- Fissural tin (fissural with >1%Sn)

The general model for the formation of the massive sulphide deposits is precipitation at or near the coeval sea floor, either during the waning stages of local volcanic activity and/or shortly thereafter, from hot, reducing, slightly acidic metal-bearing solutions largely of sea-water derivation.

Petrographic studies have revealed the presence of three types of quartz in the studied types of ore: Q1, the oldest one, very deformed; Q2, poorly deformed and considered coeval with a main mineralized event; Q3, younger recrystallized quartz mainly derived from the two other types.

FLUID CHARACTERIZATION

Based on microthermometric studies and Raman analysis two main types of fluids have been distinguished in Q2:

Aquo-carbonic fluids

These fluids are represented as different types of primary fluid inclusions (FI): (i) H₂O-CO₂-NaCl-(CH₄) liquids (Lc-w or Vc-w) showing three-phase inclusions at room temperature with CO₂ homogenizing to liquid phase or vapour phase but with global homogenization on liquid phase; (ii) H₂O-NaCl-(CO₂-CH₄) liquids (Lw-(c-m)) occur as two-phase inclusions.

Aqueous fluids

This kind of fluids is dominantly aqueous with low salinity and are represented by secondary Lw two-phase inclusions in trails.

METALLOGENIC IMPLICATIONS

In general terms the fluid inclusions in RT are Lc-w, whilst in the the RC ore are Vc-w. The three types of aquo-carbonic FI can be frequently observed in the FC ore.

Microthermometric studies and Raman analysis have allowed to estimate the following global compositions (H₂O, CO₂, CH₄, NaCl on moles %):

RT- (92.6; 6.5; 0.0; 0.9); RC- (93.9; 5.3; 0.1; 0.7); FC- (90.5; 7.4; 1.1; 1.0).

A P-T reconstruction has been carried out using the V-X properties of FI, and isochores have been drawn.

Relatively high P-T conditions during the mineralizing stage is shown by the fluids trapped in Q2. The minimal trapping conditions are given by the Th-Ph pair as follows:

RT- Th 240°C and Ph above 150 Mpa; RC- Th 240°C and Ph above 140 Mpa; FC- Th 250 °C and Ph above 50 Mpa, but with data suggesting great pressure fluctuations in the FC case.

The mode of occurrence and the composition of the fluids present in Q2 coeval with cassiterite and sulphide remobilization (mainly chalcopyrite) suggest the crystallization of cassiterite from CO₂ richer fluids and the sulphides from CO₂-CH₄ bearing fluids and the importance of the metamorphic fluids, on the epigenetic ore evolution processes in a rock-dominated system. The regional geological history and the macroscopic observations (at all scales) support this statement.

Aknowledgements: This work has been carried out through the GEOMMINCOR project. All Raman analysis and data processing were performed at CREGU-Nancy; authors are grateful to M.C.Boiron and M.Cathelineau for their support.

GEOCHEMICAL CONSTRAINTS ON THE ORIGIN AND MIGRATION OF PALAEOFLUIDS AT THE NORTHERN MARGIN OF THE VARISCAN FORELAND, SOUTHERN BELGIUM.

MUCHEZ, PH.(1), SLOBODNIK, M. (1,2), VIAENE, W.A.(1) & KEPPENS, E.(3)

(1). Fysico-chemische geologie, K.U. Leuven, Celestijnenlaan 200C, B-3001 Leuven, Belgium.

(2). Department of Geology and Paleontology, Masaryk University, Kotlarska 2, CR-61137 Brno, Czech Republic.

(3). Faculteit Wetenschappen, V.U.B., Pleinlaan 2, B-1050 Brussels, Belgium.

The aim of this study is to investigate the importance of tectonism in the origin and migration of fluids. Fractures, filled with calcite, which formed during and after the Variscan deformation at the northern margin of the Variscan foreland in southern Belgium have been studied.

Volumetrically the most important fracture type is characterized by conjugated shear veins, sigmoidal en-echelon and extensional calcite veins which formed before and during the Variscan folding. These veins, and the surrounding limestones, have both a similar dull brown-orange luminescence and stable isotopic composition ($\delta^{18}\text{O} = -11$ to -8% PDB and $\delta^{13}\text{C} = 0$ to $+3\%$ PDB). This indicates precipitation of the calcite cement from a fluid buffered by the rock. In the area studied, only a limited amount of fluid migrated through the Dinantian during the main phase of Variscan compression. The Dinantian limestones in southern Belgium recrystallized and lithified in meteoric waters early in their diagenetic history, so the amount of fluid available for migration during Variscan deformation was limited. Measurable primary and secondary two-phase (liquid and vapour) fluid inclusions have only been found in a few samples. The homogenization temperature (T_h) of the inclusions varies between 115° and 150°C , corresponding to trapping temperatures (T_t) between 150° and 185°C . The salinity of the inclusions is between 2.0 and 7.8 eq. wt% NaCl. The lowest T_t is similar to the maximum burial temperature deduced from the conodont alteration index (150°C). The low salinity supports the interpretation that the ambient fluids had a meteoric origin.

Inclusions in distinctly recrystallized syn-Variscan veins contain besides a few low salinity fluids, numerous high salinity CaCl₂-NaCl-H₂O inclusions ($T_{fm} -52^\circ\text{C}$). The salinity of the inclusions is between 10.3 and 26.3 eq. wt% CaCl₂. The T_h values range between 130° and 170°C . So, the original trapping temperatures were higher than 170°C . This indicates that after the migration of relatively low salinity fluids, and therefore after the main period of Variscan deformation, high salinity fluids circulated upward through the fractures at a temperature higher than that of the surrounding limestones.

After the Variscan deformation, five successive iron-rich fracture-filling calcite generations occur associated with Mississippi Valley-type mineralisations in southern Belgium. Fluid inclusion evidence indicates that all the calcites formed from fluids with a salinity between 16.0 and 23.1 eq. wt% NaCl. The trapping temperature of the fluid inclusions decreases from $\sim 125^\circ\text{C}$ in the first two calcite generations to 50°C in the last two vein cements. The oxygen isotopic composition of the ambient fluids, calculated from the trapping temperature and the isotopic

composition of the calcites varies between -5.2 and +7.6‰ SMOW. The highly variable oxygen isotopic composition of the fluids, the low $\delta^{18}\text{O}$ value of -5.2‰ SMOW and the intense water-rock interaction necessary to leach metals indicate that the original fluids had a low $\delta^{18}\text{O}$, and that these fluids became enriched in ^{18}O by water-rock interaction. Flow of this water into the deeper subsurface was likely gravity-driven and took place from the uplifted parts of the Variscan orogen towards the foreland basin. Non-ferroan calcites filling transversal fractures, formed later during the Mesozoic or Tertiary. Two types of fluid inclusions have been distinguished in these calcites. The first type consists of $\text{NaCl-CaCl}_2\text{-H}_2\text{O}$ inclusions with a salinity between 11-28 eq. wt% CaCl_2 and a homogenization temperature between 42' and 55'C. Very high salinity NaCl-CaCl_2 fluids are very common at depths up to 10km and represent basement brines. Tentatively we propose that such brines have been intersected by the transversal fractures and faults. The second type of fluid inclusions contain pure H_2O or $\text{NaCl-H}_2\text{O}$ and have a salinity between 0 and 12.6 eq. wt% NaCl . The near zero salinities indicate meteoric water. The higher salinities are interpreted to be the result of the interaction between the meteoric water and the rocks. These fluids likely had a local gravity-driven origin, determined by fold and fault patterns.

**PT-TIME-PATH, FLUID EVOLUTION AND CRYSTAL GROWTH IN THE AAR-
AND GOTTHARD MASSIFS DURING LATE PLATE COLLISION AND
EXHUMATION OF THE CENTRAL ALPS**

MULLIS, J.

Mineralogisch-Petrographisches Institut, Bernoullistrasse 30, CH -
4056 Basel

Fluid inclusions in fissure quartz from Zinggenstock in the Aar Massif and La Fibbia in the Gotthard Massif were studied by microthermometry, Raman spectroscopy and sodium-potassium thermometry yielding composition, density, temperature and pressure of fluid trapping and crystal growth. Combining this knowledge with radiometric data from the vicinity, fluid evolution and crystal growth is approximately defined in space and time.

The mineralizing fluid was an aqueous chloride solution. Only the earliest growth stage from La Fibbia in the South of the Gotthard Massif crystallized in a CO₂-enriched environment. The main quartz precipitation occurred 20 to 15 Ma ago, between 430±20 and 220 °C and 350±50 and 180 MPa.

Assuming that P_{fluid} equals P_{lith} , the studied extensional veins opened at a depth of 14±2 km around 20 Ma ago. At this depth rocks were affected by compressional tectonics of the African and European plate close to the brittle-ductile transition. During further collision and thickening the Central Alps were discontinuously exhumed. Fluid composition evolved towards lower salinity and CO₂-content. Pressure and temperature decreased, leading to mineral precipitation in the fissure systems.

R.E.E. ICP-MS ANALYSES OF FLUID INCLUSIONS WITHIN FLUORITE FROM SOUTHWESTERN MASSIF CENTRAL (FRANCE); CONTRIBUTION TO THE CHARACTERIZATION OF BRINE EVOLUTION.

MUNOZ M.(1), NESBITT R.W.(2) and POLVE M.(1)

(1) Université Paul Sabatier, Laboratoire de Géochimie, 38 rue des 36 ponts 31400 Toulouse, France.

(2) University of Southampton, Department of Geology, Highfield, Southampton SO17 1BJ United Kingdom.

Fluorite samples from 4 vein deposits located in the Paleozoic basement of the southwestern Massif Central in France have been crushed and leached for conventional solution ICP-MS analyses. In three deposits (Mont-Roc, Le-Burc and Embournegade) the mineralization is F-dominated while in the other (Peyrebrune) it is Zn-dominated with the fluorite stage post-dating the Zn stage.

Microthermometry of fluid inclusions indicates in the four veins that mineralization has been deposited by an high salinity H₂O-NaCl-CaCl₂ fluid (20-24 wt.%eq NaCl) similar in composition to basinal formation waters.

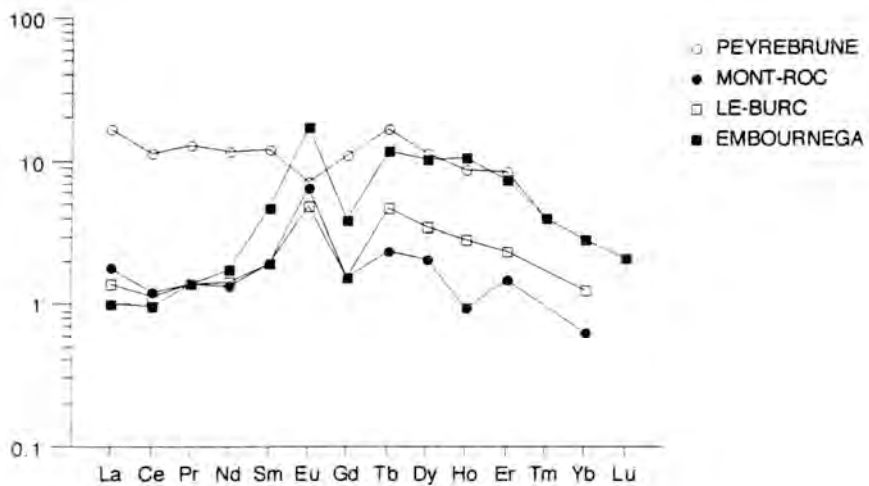
Sr, Rb and the whole serie of R.E.E. have been analysed in the leachate and in the fluorite residue. Sr and Rb have also been analysed in individual fluid inclusions (previously selected as primary inclusions) within fluorite using a Laser equipment attached to the ICP-MS. The Sr/Rb ratio obtained on individual fluid inclusions is similar to the Sr/Rb ratio obtained on fluid inclusion leachate from the same sample. This indicates that the leachate solution is representative of the same primary fluid inclusions population characterized by microthermometry.

R.E.E. data have been shales normalized (see figure). The Eu anomalies displayed by the fluorite are also displayed by the fluid inclusions, consequently they were already present in the mineralizing solution. Together with the presence of sulfides in the paragenesis of the Peyrebrune deposit, the negative anomaly is indicative of reducing conditions while the positive anomalies of the Mont-Roc, Le-Burc and Embournegade deposits are indicative of a change from reducing to more oxydizing conditions. This could be a major constraint for the deposits specialization sulfide/fluorite.

Fluid inclusions display a negative Gd anomaly which is not displayed by the mineral. An exceptional behavior of Gd has been observed in seawater where positive anomalies have been reported (KIM et al., 1991). A complementary negative anomaly can be expected in minerals precipitated from seawater, such as evaporites. With regard to the basinal origin of the mineralizing fluid suggested by the microthermometric data, this Gd anomaly would be consistent with an acquisition of the salinity by the fluid through evaporites dissolution rather than through concentration of elements in seawater during evaporite sequences formation.

References

- KIM, K.-H., BYRNE, R.H. and LEE, J.H. 1991. Gadolinium behavior in seawater : a molecular basis for gadolinium anomalies. *Mar. Chem.*, 36: 107-120.



OBSERVATIONS ON THE MELTING AND NUCLEATION BEHAVIOUR OF CLATHRATES IN MULTIVOLATILE FLUID INCLUSIONS

MURPHY, P.J., & ROBERTS, S.

Department of Geology, University of Southampton, SO17 1BJ, U.K.

Clathrates (solid gas hydrates) form by reaction between gases and water at low temperatures. In fluid inclusions the presence of these clathrates severely complicates the use of microthermometric data for the estimation of composition and density of aqueo-carbonic fluids. Numerous recent publications have presented modelling techniques, particularly statistical thermodynamics methods, for the prediction of clathrate composition and the estimation of salinity. Such techniques involve the measurement of final clathrate melting temperature, and assume equilibrium within the inclusion.

In most natural inclusions, clathrates are virtually invisible, and their presence must be inferred from the deformation of the vapour bubble. However, studies of synthetic CO₂-N₂-H₂O inclusions in clear quartz (courtesy of L.W. Diamond), in which the clathrate crystals are clearly visible, has allowed the detailed observation of clathrate melting and nucleation behaviour.

In these inclusions, clathrate melting occurs in two stages, as clathrate crystals within the vapour bubble always melt at a lower temperature than crystals within the aqueous part of the inclusion. The final crystals to melt are generally distant from the vapour bubble, and appear to be at equilibrium with the composition of dissolved gases in the water, rather than the composition of the vapour bubble. This observation is supported by low temperature laser Raman analyses, which show that the composition of the clathrate can vary considerably within the inclusion. In particular the clathrate which forms within the aqueous part of the inclusion will tend to be very rich in CO₂, due to the higher solubility of CO₂ in water relative to N₂ and CH₄, while the clathrate that forms in and around the vapour bubble will be mixed, containing all the gases present.

The most commonly used technique for the measurement of the final melting temperature of clathrate is temperature cycling, whereby the inclusion is heated until just below the expected melting point of clathrate, and then cooled rapidly by a few degrees. Any remaining crystals will grow, deforming the vapour bubble. When no crystal growth on cooling occurs, the final clathrate melting temperature has been passed, and clathrates should not be present until their nucleation at around -30°C. However, it has been observed that cooling may not immediately result in crystal growth. On cooling an inclusion from its apparent final melting temperature to -13°C, a clathrate crystal has been observed, attached to an impurity in the inclusion. On continued cooling, the crystal grows rapidly in the aqueous part of the inclusion. When the crystal touches the vapour bubble, an apparent renucleation takes place, forming large amounts of clathrate in and around the vapour bubble. The initial crystal appears to act as a seed crystal, allowing the renucleation of the clathrate. Such observations suggest a problem with the use of temperature cycling: clathrate melting and growth on cooling is not simple, and the clathrate crystals which grow in the water are not

in equilibrium with the vapour bubble.

Because of the problems of composition and density change associated with clathrate formation, where possible ThCO_2 is often measured in the so-called 'metastable absence' of clathrate, by cooling the inclusion to allow nucleation of separate liquid and vapour carbonic phases, without nucleating clathrate. However, analyses of an inclusion at low temperatures, but in the absence of clathrate, show a gas composition depleted in CO_2 , and the presence of CO_2 clathrate in the aqueous part of the inclusion. No clathrate was visible in the inclusion, and on reheating no evidence of clathrate melting could be detected.

It is likely that this clathrate is the result of prenucleation structures: the hydrogen-bonded water molecules become more structured, and although crystals do not nucleate small, short-lived clathrate lattice structures can form. This is predicted by nucleation theory: what is surprising is that there is sufficient gas involved to change the composition of the carbonic fluid, and to produce clathrate spectra. The measurement of ThCO_2 in the 'metastable absence' of clathrate will therefore produce erroneous results in terms of both composition and density.

It is obvious that the melting and nucleation behaviour of mixed-gas clathrates is not simple, and that a fluid inclusion in the presence of clathrates cannot be considered to be at equilibrium. This suggests problems in the use of predictive models which assume a single, homogeneous clathrate at equilibrium with the carbonic phase.

FLUID INCLUSION EVIDENCE FROM TWO GENERATIONS OF QUARTZ-VEINS IN THE ARCHAICAN GOLD-BEARING VENUS SHEAR ZONE OF THE ARCTURUS MINE, ZIMBABWE.

MUTEMERI, N. (1), BLENKINSOP, T. (2) & TOURET, J.L.R. (3)

(1) Institute of Mining Research, University of Zimbabwe, Harare, Zimbabwe

(2) Department of Geology, University of Zimbabwe, Harare, Zimbabwe

(3) Institute for Earth Sciences, Free University, Amsterdam, The Netherlands

Structural analysis, spatial distribution of some quartz veins, ore microscopy and fluid inclusion studies reveal part of the fluid evolution of the structurally controlled Venus Orebody in Archaean lode gold deposits of the Arcturus Mine in Zimbabwe.

Arcturus is the largest mine in the Enterprise part of the Archaean Harare Greenstone Belt, and consists of several sections based different ore-bodies of which the Venus is one. These ore-bodies are closely associated with shear zones. The present study focuses on the Venus Section; which consists of a shear zone (SE trend) defined by an area of more intense (ductile) deformation and greenschist retrograde metamorphism, containing several lens-shaped bodies of silicified biotite-actinolite schist (Brown, 1991). This shear zone is hosted by amphibolite grade, lightly deformed metabasaltic greenstones.

The main structure in the Venus section is a foliation in this biotite-actinolite schist that generally dips at 52° to the NNE but has considerable variation in strike. A later north-west trending planar fabric cross-cutting the earlier north-west trending mineral foliation is observed. The earlier fabric is associated with sinistral-reverse shear sense and the later north-west fabric has indications of dextral-normal shear sense. These fabrics must have controlled access and flow of the mineralising fluid.

The earlier fabric in silicified biotite-actinolite schist is associated with quartz lenses and veins; a result of localised brittle behaviour in an otherwise ductile deformational regime. The veins are concordant with this main foliation and represent the earlier generation associated with mineralisation. A later generation of quartz veining has been distinguished (there may be several others); it cuts across the foliation of the biotite-actinolite schist ore bodies and has an orientation similar to that the latter planar fabric.

The early phase of quartz veins are associated with pyrrhotite and arsenopyrite and the later one is richer in pyrrhotite and free gold. There is an intimate relationship between the sulphides and gold. In the earlier quartz, textural relationships between quartz and pyrrhotite show contemporaneity in deposition; however the pyrrhotite in the latter quartz veins appear to be remobilised.

Fluid inclusion study of the above mentioned two generations of

quartz veins reveals the presence of three types of inclusions, distinguished on the basis of composition, I-gaseous, II-aqueous and III-mixed (I+II). Several chronological populations have been distinguished, some as primary and others as secondary.

The mineralising fluids were silica-rich, low salinity (10 wt% NaCl) aqueous/gas-rich (CO_2/CH_4). The $\text{XCO}_2/(\text{XCO}_2+\text{XCH}_4)$ ratios estimated for the primary gas-rich inclusions are within the same range (0.38-0.7) for both generations of quartz, indicating that the primary source of the fluid is similar. Mineralisation which must have commenced post-peak metamorphism at P-T conditions ranging between 300°-400°C and 1-2 kbars, was probably due to immiscibility and produced sulphides intimately associated with gold (in solid solution). Oxygen fugacities were calculated by COHFLUID (Huizenga, 1995), for a fixed pressure and temperature of 1.5 kbars and 350°C and graphite activity of 1. These show that an increase in $f\text{O}_2$ can explain the variation in the $\text{XCO}_2/(\text{CO}_2+\text{XCH}_4)$. These calculations also demonstrate that XH_2O of the initial fluid must have been between 0.8 and 0.9. Later remobilisation by fluids recorded in the primary inclusions of the latter phase of quartz, deposited sulphides and discrete native gold grains. This is why greater silicification and higher gold values are expected where the two fabric trends intersect.

The molar volume of the primary inclusions indicated higher density fluids in the early generation of quartz veins (68-43 cm^3/mole) than in the later (78-90 cm^3/mole). This indicates a progressive decrease in P-T conditions in the shear zone. This information is also documented by successive generations of inclusions in the earlier phase of quartz, however, it was difficult to extract chronological evidence from microscopic observation. A retrograde path in the shear zone is also supported by the replacement of metamorphic hornblende by actinolite and biotite (also documented in one other Arcturus orebody, the Gladstone East Extension (GEE), Brown, 1991). Some of the secondary trails which show greater abundance of aqueous inclusions could have trapped meteoric water after uplift to higher crustal levels. Uplift is evidenced by decrepitated inclusions (Roedder, 1984).

REFERENCES

- Brown, I.J. (1991). Geology and geochemistry of Archaean gold mineralisation, Arcturus District, Zimbabwe. Ph.D. thesis, Oxford Polytechnic.
- Huizenga, J.M. (1995). Fluid evolution in shear zones from the late Archaean Harare-Shamva-Bindura Greenstone Belt (NE Zimbabwe): Thermodynamic calculations of the COH system applied to fluid inclusions.
- Roedder, E. (1984). Fluid Inclusions. Mineralogical Society of America. *Reviews in Mineralogy*, Volume 12.

FLUID INCLUSION AND STABLE ISOTOPE STUDIES OF EPITHERMAL PRECIOUS AND BASE METAL MINERALISATION, LESVOS ISLAND, GREECE.

NADEN, J. (1), LENG, M.L. (2), CHELIOTIS, Y. (3), ELIOPOULOS, D. (3)

(1) British Geological Survey, Nottingham, UK.

(2) NERC Geosciences Laboratory, Nottingham, UK.

(3) Institute of Geology and Mineral Exploration, Athens, Greece.

Lesvos Island is situated in the eastern part of the central Aegean Sea close to the mainland of Anatolia, Turkey. The oldest rocks comprise low grade metamorphic rocks. Mineralisation is hosted in Neogene calc-alkaline to shoshonitic volcanic rocks which make up a major part of the island.

Two regions of mineralisation, on the northern coast of Lesvos Island, are currently under examination. These are Therma and Katjilemonas. At Therma, mineralisation consists of a series of NW-SE to NNE-SSW trending mineralised faults, and is characterised by localised intense kaolinitisation and silicification of already propylitised wallrocks. Multiple generations of quartz fill the veins and locally quartz pseudomorphs barite. Sulphide mineralisation, at the surface, is sporadically distributed and gold grades are $\leq 4\text{g/ton}$. Generally, high concentrations of gold are associated with high elevations whilst base metal concentrations are greatest in the, topographically, lower parts of the deposit. The region is still geothermally active, and hot slightly saline springs discharge into the sea. Maximum temperatures, at depth, for the hot springs are between 133 and 155°C (Papastamataki and Leonis, 1982). Mineralisation at Katjilemonas is similar to that at Therma. However, Katjilemonas, is characterised by the presence of fluorite and generally poor gold values.

A suite of samples, including geothermal waters, was collected for fluid inclusion and stable isotope analysis. Analyses include: $\text{CO}_2, \text{N}_2, \text{CH}_4$ and δD on inclusion fluids; $\delta^{18}\text{O}$ on associated quartz; $\delta^{34}\text{S}$ on pyrite, galena and sulphate in the geothermal waters.

Preliminary geochemical and isotopic data indicate that the mineralising fluids are low in gas content ($\text{CO}_2, \text{N}_2, \text{CH}_4$). Generally, there is no correlation between gas contents of the fluid and gold grade. However, cumulative frequency plots indicate a bimodal distribution of $\text{CO}_2/\text{H}_2\text{O}$, at present the relationship between this distribution and mineralisation is not known. Stable isotope data suggest a complex history of fluid-rock interaction. Present day geothermal waters show a meteoric water signature ($\delta^{18}\text{O} = -5.9\%$; $\delta\text{D} = -36.2\%$). However, the sulphur isotope composition ($\delta^{34}\text{S} = 15.1\%$) of sulphate in present day geothermal fluids indicate an ancient source rather than present day seawater. The paleo-geothermal fluids responsible for mineralisation show a narrow range of $\delta^{18}\text{O}$ values (5.1 to 6.7%) and a slightly broader range of δD (-41 to -67%). These data plot close to the field for magmatic waters. This can, probably, be accounted for by fluid-rock reaction between meteoric water and the host volcanic rocks. Sulphur isotopes

suggest an igneous source for sulphur (-2.6 to -5.1% for pyrite, -4.5 to -6.6% for galena).

The data indicate an epithermal origin for the mineralisation.

REFERENCES:

PAPASTAMATAKI, A. and LEONIS, K., (1982). Geochemical research for geothermy, I-Lesbos area. *IGME Internal report.*

"PLANIF" A COMPUTER PROGRAM FOR THE STUDY OF FLUID INCLUSION PLANES

NOGUEIRA, P. & NORONHA, F.

(1) Centro de Geologia, Faculdade de Ciencias da Universidade do Porto, 4050 Porto, Portugal

Introduction

The study of the circulation of fluids in the crust until recent times was characterised by studies of meso and megascales. Recently some research has been carried in order to understand this phenomenon at microscopic scale (Cathelineau et al 1990; Lespinasse, 1990). These workers proved that fluid inclusion planes (FIP), namely the ones in quartz, are good structural markers of fluid circulation in granitic rocks. To completely characterise the FIP-network of a homogeneous rock mass one must quantify and characterise the FIP in fluid type, direction, dip, number/volume, length, opening.

The equipment developed at Centro de Geologia of Porto University aims to characterise all of these features. The version of the software here presented can analyse most features, the exception being the dip of the planes.

Equipment requirements

The study of FIP is performed in oriented thick sections, similar to those used in microthermometric studies. A microscope with a video camera attached to it are required equipment. This video camera produces images in the format NTSC or PAL and the signal is read by a video frame grabber attached to the main board of the computer. This board transforms the analogic signal into a digital signal interpreted by the computer as an image (the same as the observed in the microscope field). The user also needs to have a computer (IBM PC type) with Windows Version 3.0 or later.

Description of the operations

To the user the program (PLANIF) presents a screen with the image seen in the microscope field and two toolbars. The toolbar in the top part of the screen contains the buttons with the operations available at each moment. The bottom screen toolbar provides some information about the data being entered.

The user must previously study the thick section and define the fluid inclusion types found in the thick section. PLANIF can handle five different types (1 to 5). Following this study the user is ready to start the program, choose the appropriate objective and calibrate it, then indicate to the computer program which is the reference direction, by indicating in the computer screen two points of that direction.

In the next step the user finally inputs the data. Using the mouse the operator must indicate two precise points on the screen (the beginning and the end of the FIP). If the FIP is longer than what the screen can match PLANIF as got a specific command (button) to indicate this situation. The user can also indicate

the opening of the FIP by indicating the width of a fluid inclusion with a average size.

At any time during data entering the user can erase some bad data entered. The user can also visualise the data already entered as a rosegram plot (just push the proper button). Finally the user can save the data in 3 formats: a) sorted by type: Direction , number of FIP in direction, Total length of FIP in direction; b) sorted by type and classed in 10 degrees direction: Direction , number of FIP in direction, Total length of FIP in direction; c) sorted by type: X1,Y1,X2,Y2 -(relative co-ordinates on the screen), direction, length, opening

An example of application

In Godinhaços (North Portugal) the observation of colour alterations near fractures and veins in granitic rocks is due to mineralogical alterations of the rock. This process is normally limited to a small extension (< 20cm) near fractures and quartz veins. The circulation of fluids is the cause of this alteration. Since we are in a brittle deformation stage the main process for fluid circulation in rock is microfracturing. To prove this phenomenon and quantify the permeability were studied two thick sections of the granite, near a fracture: one in the altered zone and another in the non-altered zone. For the calculation of permeability the method described in Ayt Ougougdal (1989), was used.

The results clearly show that: for the early fluids (associated with the fracture formation) the permeability is identical; for the late fluids the permeability in the two neighbour zones is dramatically different (an order of magnitude change between the two zones). This results show that the quantification and signature of fluid circulation can be found using this method.

Conclusion

This computer program permites the user to acquire a more precise knowledge about the fluid circulation pathway at microscopic scale, obtaining reliable quantitative and qualitative data about it.

Acknowledgements

This work has been carried out through the HCM network (Hydrothermal/metamorphic water rock interactions in crystalline rocks: a multidisciplinary approach based on palaeofluid analyses). P. Nogueira's work is supported by a J.N.I.C.T. bursery - Programa Ciencia: BD-2028/92.

References

- Ayt Ougougdal, M. 1989 - Etude de la transition ductile fragile le lond d'une zone de cisaillement: l'exemple de la faille de la Marche (NW du massif central Francais). Mém. DEA, Université de Nancy. 62 pp.
- Cathelineau, M., Lespinasse, M., Bastoul, A., Bernard, C. et Leroy, J. 1990. Fluid migration during contact metamorphism: the use of oriented fluid inclusion trails for a time/space reconstruction. Mineralogical Magazine, V.54. pp 169-182.
- Lespinasse, M. 1999 - Les trainees d'inclusions fluides: marqueur microstructural des paleocontraintes et des migrations fluides. Memoire du CREGU n°19, Nancy. 251 pp.

FLUID EVOLUTION ASSOCIATED WITH W(Sn)-SULPHIDE-QUARTZ-VEIN IN THE IBERIAN PENINSULA.

NORONHA, F. (1); VINDEL, E. (2); LOPEZ, J.A. (2); DORIA, A. (1); BOIRON, M.C. (3) & CATHELINÉAU, M. (3)

(1) Centro de Geologia, Faculdade de Ciencias, 4050 PORTO, Portugal.

(2) Dpto de Cristalografía y Mineralogía. Univ. Complutense. 28040 Madrid, Spain

(3) CREGU, BP 23, 54501 Vandoeuvre-les-Nancy, Cedex France

The Sn-W metallogenic province of Iberian Peninsula is one of the most important of Europe. Thus, the W deposits were one of the leading European source of tungsten. The deposits are essentially located, in the Hesperic Massif, in Central-Iberian (CIZ) and in Galicia Tras-Os-Montes zones (GTMZ). Plutonic magmatism is essentially represented by two main groups of hercinian synorogenic granites. The first group of granites (two-mica granites) is considered as related to the peak of metamorphism, and synchronous of the collision and D3 deformation. The granitoids from the second group are essentially, post-metamorphic, post-collisional and late and post-tectonic biotitic granite intrusions related to late distensive stages. W (Sn) quartz veins, with W(Sn) in the contact zone and W in the exocontact zone, are dominantly related with the second group of granites.

A comparative study of P-V-T-X fluid evolution in different Iberian W deposits has been carried out using previous and new microthermometric studies and Raman data on the following deposits: Panasqueira, Borralha, Mirandela and Murçós (Portugal) and several deposits of Sierra del Guadarrama (SCS, Spain).

FLUID CHARACTERIZATION

Three types of fluid have been distinguished:

1) Magmatic hypersaline aqueous fluids

These fluids are represented by Lw (S) inclusions (three phase inclusions including one or more solid phase (dominantly halite and/or sylvine, and unknown trapped minerals) with global homogenization to the liquid). ranges from 250°C to 450°C and salinity from 40 to 50 wt% eq.NaCl. These fluids are only present in the Guadarrama examples.

2) Metamorphic aquo-carbonic fluids

This fluids is represented as different types of fluid inclusions: (i) H₂O-NaCl-CO₂(CH₄) liquids (Lc-w or Vc-w, density 0.5/0.7) showing two-phase or three fluid phase at room temperature. CO₂ homogenizes to the vapour phase in the range of -4 to 30°C, TmCO₂ in the range of -64°C to -57°C, TmCl in the range of 6 to 12°C and Th in the range of 250 and 350°C (to the liquid phase (L)); (ii) H₂O-NaCl-CO₂-(CH₄) vapours (Vc-w, density 0.2/0.3) with a dominant vapour phase; TmCO₂ is in the range of -62.0 to -60.0°C, Th in the range of 250 to 350°C (to V). They are only present when immiscibility process occurred and may be found associated to the precedent type; (iii) H₂O-NaCl-CH₄-(CO₂) liquids (Lw-(c-m), density 0.7/0.8) occur as two phase inclusions, with a low density volatile phase displaying strong fluctuation of the CH₄/CO₂ ratio, that could be rather high, explaining the high TmCl

(7/16°C) values. Global homogenization is in the range of 290-380°C.

3) Aqueous fluids

This kinds of fluids is represented in different types of fluid inclusions: (iv) Lw1 are two-phase aqueous inclusions (Flw 0.7-0.9) and with Tmice between -5.7 and -1.5°C corresponding to a salinity of 2.6 to 8.8 wt% eq.NaCl and moderate Th, ranging from 100-300°C; (v) Lw2 are small (<5-10µm) biphasic inclusions (Flw =0.9). They display higher Tmice than Lw1, with a range -2.7 to -0.2°C corresponding to a low salinity of 0.3 to 4,7 wt% eq.NaCl. Th is in the range 90-210°C.

METALLOGENIC IMPLICATIONS

The reconstruction of the P-V-T-X evolution in each deposit using fluid inclusion data and mineralogical constraints has been used to model the conditions of transport and deposition of the metals.

The first stage of W deposition is always characterized by the presence of aquo-carbonic fluids, which are probably fluids equilibrated with metamorphic host-rocks. It is clear that the early hypersaline fluids observed locally are not related to the main stage of W deposition. Progressive dilution of early fluids yield to fluids compositions displaying rather low volatile contents which is dominated by methane when the temperature is lower than 350-400°C. The transport of W is probably related to aquo-carbonic fluids at pressures ranging from 130 to 50 Mpa. Dilution and nearly isobaric temperature decrease, probably causing according to Dubessy et al (1987), an increase of the dielectric constant of the fluid, and correlatively the destabilization of neutral species may have caused the deposition of tungsten.

Presence of volatile characterize the whole evolution until the main sulphide stage. The spatial relationships between CH₄ bearing inclusions and the main sulphides, indicate a crystallization of these sulphides from CH₄ bearing fluids. This indicates that the sulphide stage is not disconnected from the whole evolution of the first hydrothermal cycle. The late aqueous fluids could be related to microfissure opening and produce the latest sulphide crystallization of replacement, but are not related to the main depositional stages.

Acknowledgements: This work has been carried out through the HCM network (CEE-DG XII-G) "Hydrothermal/metamorphic water rock interactions in crystalline rocks: A multidisciplinary approach based on paleofluid analysis". This work has also supported by the program "Action Intégrée PICASSO, France-Espagne"

**CHARACTERIZATION OF FLUID INCLUSIONS IN W-Sn-SULPHIDE
MINERALIZATION HOSTED BY CALEDONIAN MICROTONALITES ON THE SE MARGIN
OF THE LEINSTER GRANITE, IRELAND.**

O REILLY, C. (1), GALLAGHER, V. (2) and FEELY, M. (1)

(1) Dept. of Geology, University College, Galway

(2) Geological Survey of Ireland

Scheelite mineralized microtonalite dikes occur on the SE margin of the end-Caledonian Leinster Granite in SE Ireland. Scheelite, cassiterite and sulphides occur in veins in the microtonalites, disseminated throughout the greisenized microtonalite dikes and in the adjacent wallrocks. Two major vein types occur in the microtonalite dikes:

(1) Scheelite \pm arsenopyrite \pm pyrrhotite occur in quartz-fluorite veins with no muscovite selvage

(2) Cassiterite \pm sphalerite \pm stannite \pm chalcopyrite \pm pyrite \pm galena occur in quartz-fluorite veins with a coarse muscovite selvage and are often intergrown with the muscovite.

Quartz-hosted fluid inclusions were examined from representative samples of both vein types using petrographic, microthermometric and raman spectroscopic techniques. Three distinct types of fluid inclusions have been recognized. Primary, vapor rich Type 1 inclusions in quartz from the scheelite mineralized veins are of H₂O-CO₂-CH₄-N₂-NaCl composition (Fig. 1). These inclusions are noteworthy in that clathrate melting occurs after homogenization of the volatile-phase (Fig. 2). All such inclusions so far examined decrepitated between 300 ~ 400°C. Primary, liquid-rich Type 2 fluid inclusions in the cassiterite \pm sulphide mineralized veins are of H₂O-CH₄-N₂-H₂S-NaCl composition, (Fig. 1), homogenize to the liquid at ca. 260 ~ 350°C and occur as pseudosecondary and secondary inclusions in scheelite-mineralized veins. Secondary, dilute, low temperature, H₂O-NaCl fluid inclusions occur in cross-cutting planes in both vein and microtonalite quartz and may be related to a regional, retrograde alteration of the microtonalites and of the Leinster Granite.

FIGURE 1

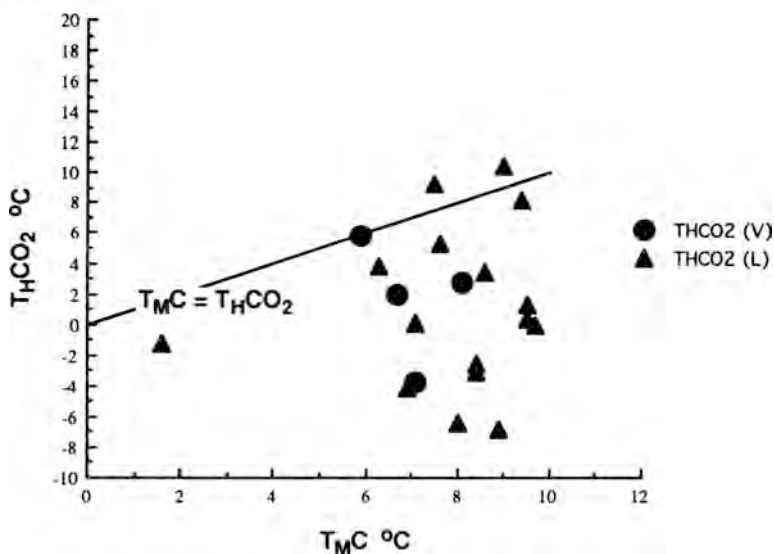


Figure 1 Microthermometric features of the Type 1 inclusions, showing that only two inclusions have $T_{HCO_2} > T_{MC}$.

FIGURE 2

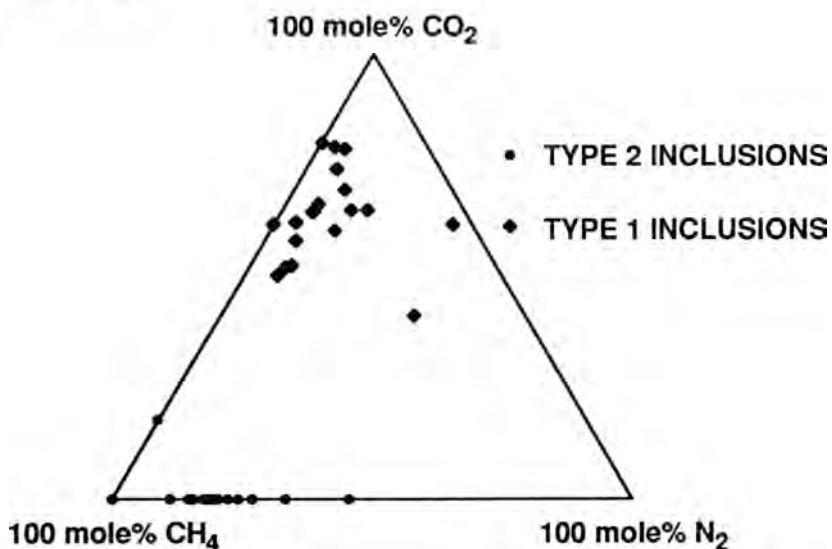


Figure 2 Composition of the non-aqueous volatile phase for vein-quartz hosted Type 1 and Type 2 inclusions.

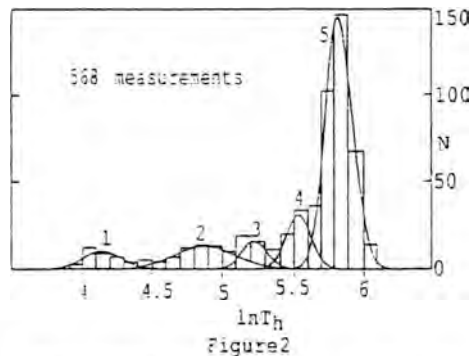
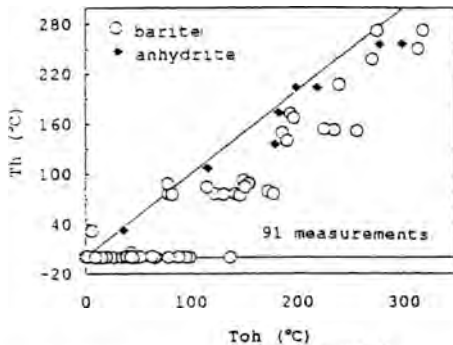
MECHANISM OF BARITE AND ANHYDRITE COPRECIPITATION AT TEMPERATURES AROUND 400°C IN THE SUBSEAFLOOR OF SW BASIN, ATLANTIS II DEEP (CENTRAL RED SEA)

ORPHANIDIS I. (1), PASCAL M.L. (1), RAMBOZ C. (1), OUDIN E. (2), THISSE Y. (2)

(1) CNRS-CRSCM, 1A, rue de la Ferrollerie, F 45071 ORLEANS CEDEX 2
 (2) BRGM, Avenue de Concy, BP 6009, F 45060 ORLEANS CEDEX 2

In the SW basin of Atlantis II deep, epigenetic sulfates (mostly anhydrite) are characteristic of geyser-type discharge areas [1,2]. The barite subfacies is most remarkable by its base and precious metal-content, and it is considered as a modern analog of the Meggen deposit [3]. In level 980 from core 268KS, barite and anhydrite which amount 48 and 6 wt.%, respectively, coprecipitate with sulfides and native gold [4,5]. Hydrothermal fluids discharge at the deep bottom into an anoxic brine pool, precluding the mixing with seawater as a mechanism of sulfate precipitation. Fluid inclusion (FI) and solubility measurements have been performed in order to ascertain the temperature and mechanism of sulfate coprecipitation in this subseafloor setting, and to precise the Ba-content of the hydrothermal fluid.

Fluid inclusion data. Barite and anhydrite crystals, less than 2mm-wide, from level 980, were studied without any previous preparation. *Evaluation of stretching problems.* FI in both sulfates were heated at a rate of 1.5°C/min and their homogenization temperature (T_h) was measured. These FI were then submitted to various degrees of overheating ($T_{oh}=T-T_h$). Figure 1 shows that FI can be overheated up to 30°C, without any significant modification of T_h .



Results. Barite: Primary (90%) and pseudosecondary (10%) FI were visually discriminated and studied. Ice melting temperatures (T_{mI}) in primary and pseudosecondary FI range from -21.2°C to -7° and -13°C, respectively. Hydrohalite melts after ice only in primary FI at temperatures between -15.4° and -1.2°C (T_{mhy}). The T_h to the liquid phase, of all FI measured in barite, vary from 53.7° to 425°C. Figure 2 shows that the T_h histogram can be interpreted in terms of the addition of five populations with a log-normal distribution.

Anhydrite: All FI in anhydrite appear to be primary. Ice melting temperatures vary from -21.2° to -6.3°C. In 50%

of the FI, hydrohalite melts after ice, between -5.2° and -0.3°C . All FI homogenize to the liquid phase between 55.7° and 393°C . *Interpretation.* Barite FI record both low T (populations 1 and 2) and high T processes (populations 3, 4 and 5), characterized by large and narrow standard deviations, respectively. Low T processes probably correspond to fluid circulations in the heated sediment around the vents, as confirmed by clay isotope geothermometry^[6]. High T processes mark the rapid cooling of the hydrothermal fluid. The T_h of population 5 over lap the two phase field boundary of the hydrothermal fluids at 220bar ($\approx 390^{\circ}\text{C}$ ^[7]). This, plus the lack of vapor homogenization and the absence of any oblique heterogeneous trapping trend in the T_h -X plane, demonstrate that barite repeatedly trapped metastable superheated fluids with salinities increasing from 18 to 23 wt.% NaCl. Anhydrite started to precipitate at and below $\approx 390^{\circ}\text{C}$, only when the fluid had reached a salinity of 23 wt.% NaCl, by isothermal boiling in the deep reservoir. Level 980 anhydrite records neither superheating nor significant boiling.

^{18}O isotopic constraints. Barite and anhydrite which have precipitated at the same temperature ($\approx 390^{\circ}\text{C}$), have similar ^{18}O isotopic compositions of $\approx 8.5\%$ ^[6]. This value contrasts with the calculated fluid-mineral ^{18}O isotopic fractionation factors, which differ greatly with temperature. Moreover, equilibrium temperatures calculated for, on the one hand, ^{34}S for the pair epigenetic sulfates-sulfide, and, on the other hand, ^{18}O for the pair epigenetic sulfate-lower brine sulfate, show a strong contrast, suggesting that the precipitated sulfate was not derived by oxydation of the hydrothermal fluid sulfide. It was more likely taken from the interstitial brine (460ppm^[9]), with a $\Delta^{18}\text{O}$ value taken similar to that of the lower brine: 7.5% ^[8]. Thus, the proposed mechanism of sulfate precipitation is the mixing of the hydrothermal end member with the interstitial brine. The low T circulations shown around the vents at level 980, have certainly contributed to bring about the large amount of sulfate required for the massive precipitation of barite and anhydrite observed.

Solubility data. The solubility of barite was measured by crystal weight loss at conditions relevant to those in level 980, and it was shown to be strongly prograde for salinities over 4m NaCl. Available anhydrite solubility data^[10] in the same conditions, show that its solubility is slightly retrograde. All these measurements permit to fix the molar Ca/Ba ration of the hydrothermal fluid when sulfates coprecipitate, at ≈ 30 . Assuming that the Ca-content of the hydrothermal fluid is similar to that of the lower brine, the Ba-content of the hydrothermal fluid is calculated at $\approx 600\text{ppm}$. This in turn, shows that mixing of 8 wt.% of interstitial brine with this fluid is required to precipitate barite. Such a mixing ratio is indeed below the detection limit of microthermometry.

References.

- [1]Bäcker and Richter 1973, Geol. Rundschau 62: 697,
- [2]Zierenberg and Shanks 1983, Econ. Geol. 78: 57,
- [3]Bäcker 1976, Geol. Jahrbuch D17: 151,
- [4]Oudin, Ramboz and Thisse 1984, Marine Geol. 5: 3,
- [5]Oudin 1987, Marine Minerals: 349,
- [6]Zierenberg and Shanks 1988, Canad. Mineral. 26: 737,
- [7]Ramboz, Oudin and Thisse 1988, Canad. Mineral. 26: 765,
- [8]Zierenberg and Shanks 1986, Geochim. Cosmochim. Acta 50: 2205,
- [9]Anschutz 1993, PhD Thesis, [10]Blount and Dickson 1969, Geochim. Cosmochim. Acta 33: 227

THE EPITHERMAL MANTO GOLD DEPOSITS FROM ANDACOLLO (CHILE)

ORTEGA, L., SIERRA, J., OYARZUN, R. & LUNAR, R.

Dept. Cristalografía y Mineralogía, Facultad de C.C. Geológicas,
Universidad Complutense
28040 Madrid, Spain.

Geology of the deposits

The Andacollo district (northern Chile; Müller, 1986; Reyes, 1991) comprises a variety of gold, copper, and mercury deposits. Central to the district is a porphyry copper of mid Cretaceous age (Andacollo porphyry; 98 ± 2 , 104 ± 3 Ma, whole rock K/Ar). Manto-type, epithermal gold deposits (91 ± 6 Ma, whole rock K/Ar) occur to the west of the porphyry while gold veins occur to the NW, W and SE. Dayton Chile has outlined some 29 Mt of 1.2 g/t Au in the mantos. The geology of the district is characterized by the presence of a mainly volcanic (andesitic-dacitic) formation of lower Cretaceous age (Quebrada Marquesa Formation; Aguirre and Egert, 1965). The manto-type mineralization is stratabound and largely confined to preferential rock types (andesite breccias and dacites) and the sites of strong fracturing. Three zones of mantos can be distinguished: Toro-Chisperos, Churumata and Tres Perlas, the latter being the nearest to the porphyry and Toro the farthest. These formed during the ascent of hydrothermal fluids along veins and fractures which deposited their metal load in zones where fracture-induced enhanced permeability allowed decompression and brecciation. The mantos are characterized by a relatively simple paragenesis including two generations of pyrite. The early one is barren and the second gold-bearing. The second stage also includes sphalerite, chalcopyrite and galena. Gangue minerals include calcite, chlorite and quartz. Ore grades range from 2 - 8 g/t Au. The veins have similar mineralogical characteristics even though the gangue is mostly composed of quartz. Gold grades (average) are in the range 5 - 6 g/t Au. Based on the alteration mineralogy the manto-type deposits of Andacollo can be ascribed to adularia-sericite type. Adularia represents an early alteration phase and is related to a very strong K metasomatism affecting the volcanics. This early phase of alteration was accompanied by calcite deposition, followed by sericite-kaolinite and a very late period of intense carbonate (microcrystalline calcite) deposition.

Fluid inclusion data

Fluid inclusion studies were carried out in quartz and calcite from Toro, Chisperos, Churumata and Tres Perlas. Composition of the fluids is mainly aqueous with dissolved salts. The absence of volatiles other than H₂O was checked by Raman analyses. Three main types of inclusions can be distinguished in the area:

- **Type A:** low to moderate salinity, two-phase (L+V) inclusions. Th \approx 150° - 330°C and salinities of \approx 3 - 11 % eq. NaCl. They are

present in all the mantos.

- **Type B:** saline, two-phase (L+V) inclusions, $T_h \approx 110^\circ - 310^\circ\text{C}$ and salinities of $\approx 12 - 17\%$ eq. NaCl. They are associated to quartz from manto Tres Perlas.

- **Type C:** very high salinity, both two-phase (L+V) and three-phase (S+L+V) halite-bearing inclusions. Total homogenization values occur between $\approx 110^\circ - 250^\circ\text{C}$. Salinities range between $\approx 20 - 30\%$ eq. NaCl. They have only been found in calcite samples from the manto Toro.

Modelling the hydrothermal system

The homogenization temperatures show a generalized decreasing trend for all the deposits. However, higher T_h values ($>290^\circ\text{C}$) are restricted to mantos Toro and Chisperos which are the most distant deposits from the Andacollo porphyry. This is in open contradiction with the classic model for Andacollo i.e. a porphyry-centered hydrothermal system. A major point to be considered is that mantos Toro and Chisperos are located within the lowest unit of Quebrada Marquesa Formation, thus suggesting a vertical rather than horizontal thermal gradient. Within such an scheme the actual heat source should be located stratigraphically beneath the manto zone. Structural and mineralogical data supports this model.

Mixing of fluids rather than boiling seems to be the most probable mechanism for ore deposition at Andacollo. The evolution trend (from low-, to high-salinity) may be indicating the sequential appearance of fluids with contrasting characteristics. It should be noted that meteoric waters circulating within the epithermal environment are expected to be very-low salinity (e.g. 1.6 % eq. NaCl in andesitic environments; Henley, 1985). A "typical" evolution trend for an epithermal system (e.g. Creed; Hayba et al., 1985) would imply progressive dilution of solutions due to increasing participation of meteoric waters. However, two facts must be considered in the Andacollo case: 1) the mantos formed within a relatively deep environment (≥ 2 km), and 2) the whole area was the site of massive intrusion of granitoids of batolithic dimensions from which a whole suite of shallow-seated intrusives was derived. Based on geologic and fluid inclusion evidence the following working hypothesis can be proposed. Fluid circulation would have been driven by a second porphyry or related intrusive type lying beneath the manto zone (e.g. Sillitoe, 1989). Fluid inclusions population A would have formed from the initial mixing of low-salinity meteoric waters with hot brines originated within the intrusive. Even if higher degrees of mixing were attained during the process (as shown by the "hybrid" population B), as the system evolved, the brine partially displaced the descending meteoric waters. This eventually would have led to formation of population C. Under these conditions, gold and sulphide precipitation can be explained in terms of progressive cooling and oxidation of the system during the interaction of descending (meteoric) and ascending (saline) fluids.

References

- Aguirre, L. and Egert, E. (1965): *Instituto de Investigaciones Geológicas* (Carta Geológica de Chile, 15, 92 p.).
- Hayba, D.O., Bethke, P.M., Heald, P. and Foley, N.K. (1985). *Reviews in Economic Geology*, 2: 129-168.
- Henley, R.W. (1985). *Reviews in Economic Geology*, 2: 1-24.
- Müller, R. (1986). *University of La Serena unpubl. rept.*, 61 p.
- Reyes, M. (1991): *Econ. Geol.*, 86: 1301-1316.
- Sillitoe, R.H. (1989). *Economic Geology Monograph*, 6: 274-291.

EPITHERMAL CARBONATE-HOSTED AU-CU-NI-CO MINERALIZATION AT THE VILLAMANIN AREA (CANTABRIAN ZONE, N SPAIN): FLUID INCLUSION STUDY VERSUS PARAGENETIC AND SULFUR ISOTOPIC DATA.

PANIAGUA, A. (1), LÓREDO, J. (2), GARCIA-IGLESIAS, J. (2)

(1)Depto. Geología. Universidad de Oviedo. E-33005 Oviedo, Spain.

(2)Depto. Explotación y Prospección de Minas. Universidad de Oviedo. E-33004 Oviedo, Spain.

The Cantabrian Zone is the outermost part of the Variscan belt in the NW of the Iberian Peninsula. In the Cantabrian Zone the post-Variscan geodynamic processes have been of little effect on its tectonostratigraphic whole, allowing preservation of the Permian paleotopographic surface in certain areas. This fact has contributed to keep several types of hydrothermal deposits related to late-Variscan deep faults, from gold-bearing skarn deposits as the deeper ones, to epithermal mercury deposits as the shallower ones. A number of these deposits can be regarded as carbonate-hosted epithermal Au deposits (Paniagua 1993, Paniagua et al. 1993). Among them, the Providencia and Profunda mines (Villamanin, NW Spain) display a remarkably high Ni, Co, Se and U contents. The Providencia mine is the type-locality of the mineral villamaninite, (Cu, Ni, Co, Fe)(S, Se)₂.

The deposits occur as veins and pods located at the intersection of E-W and NE-SW high-angle faults, within a brittle shear duplex. Host rocks are black, bituminous limestones of Namurian age, with evaporitic levels. Dolomitization and silicification are the most important alteration processes. The ore is mainly composed of Cu-Ni-Co-Fe sulfides, sulfarsenides and selenides, hematite and subordinate amounts of heavy metal selenides, native gold and uraninite in quartz-carbonate gangue. Among the carbonates, dolomite is the most common one. Significant Au concentrations with subordinate Ag-PGE anomalies have been detected. Au is present in a chemically bound state in villamaninite of the early mineralization (Friedl et al. 1991, Paniagua 1991), but also as native gold or electrum associated to Cu-Fe-Ni sulfides and selenides, and minor heavy metal selenides. The paragenetic sequence can be divided into three hypogenic stages and a supergenic one. The first stage is characterized by the presence of pyrite-type disulfides as major ore minerals. Among them, villamaninite is dominant at the shallower levels of the mineralization, but it disappears progressively at deeper level, being replaced by Fe-rich disulfides and Ni-Co sulfides and sulfarsenides. Late stages of mineralization are constituted by chalcopyrite-group minerals plus Ni-Co sulfides and sulfarsenides, selenides and native gold, among others. Among gangue minerals, dolomite is dominant at the shallower levels, whereas quartz increases with deep. Age dating of early uraninite grains by the U-Th-Pb method gives 273 ±11 m. y. (according to Bowles 1990), in agreement with the reported data for post-tectonic calc-alkaline granites present in this province (277-287 m. y.).

Fluid inclusions in quartz, dolomite, calcite and sphalerite of barren and ore zones have been studied. Microthermometric measurements on primary fluid inclusion give a high variation of

temperatures along the deposit (100-275°C) and salinities (2,5-25,0 wt. % NaCl equiv., with clear evidences of other ions, such as Ca and Mg, in the fluid). From a general point of view, salinity increases greatly in shallower, villamaninite-rich zones, whereas temperature decreases.

Several geothermometers based on the mineral assemblages present at the ore agree with the fluid inclusion homogenization temperatures. Among others, fractionation of Se in the system $Pb(Se,S)/CuFe(S,Se)_2$ gives temperatures close to 250°C at the deep levels, whereas the $Pb(Se,S)/Zn(S,Se)$ and $Zn(S,Se)/CuFe(S,Se)_2$ systems give a temperature range of 100-170°C (according to Bethke & Barton 1971) at shallower levels, in agreement with the upper stability limit of bravoite (137°C, Clark & Kullerud 1963) and talnakhite (186°C, Barton & Skinner 1979) associated to them. Sulfur isotopic data show ^{34}S ratios suggesting reduction of an evaporitic source. From these results a fluid-rock interaction between moderately saline hydrothermal fluids and the Namurian limestones (involving the hypersaline facies) can be inferred.

- BARTON, P. B. JR. & SKINNER, B. J. 1979. Sulfide mineral stabilities. In: Barnes, H. L. (Ed) *Geochemistry of hydrothermal ore deposits*. 2ed. John Wiley & Sons, New York. pp 278-403.
- BETHKE, P. M. & BARTON, P. B. 1971. Distribution of some minor elements between coexisting sulfide minerals. *Econ. Geology*, 66, pp 140-163.
- BOWLES, J. F. W. 1990. Age dating of individual grains of uraninite in rocks from electron microprobe analyses. *Chemical Geology*, 83, pp 47-53.
- CLARK, L. A. & KULLERUD, G. 1963. The sulfur-rich portion of the Fe-Ni-S system. *Econ. Geology*, 58, pp 853-885.
- FRIEDL, J., PANIAGUA, A. & WAGNER, F. E. 1991. Mössbauer study of gold-bearing villamaninite. *Neues Jahrb. Miner. Abh.*, 163 (2/3), pp 247-254.
- PANIAGUA, A. 1991. Trace elements in villamaninite and other pyrite-type disulfides of the Providencia mine, Leon, NW Spain. *Neues Jahrb. Miner. Abh.*, 163 (2/3), pp 241-247.
- PANIAGUA, A. 1993. Mineralizaciones asociadas a estructuras tardihercínicas en la Rama Sur de la Zona Cantábrica. Unpub. T. Doc. Univ. Oviedo, 337 pp (in spanish).
- PANIAGUA, A., FONTBOTÉ L., FENOLL HACH-ALÍ P., FALLICK A. E., MOREIRAS D. B., CORRETGÉ, L. G. 1993. Tectonic setting, mineralogical characteristics, geochemical signatures and age dating of a new type of epithermal, carbonate-hosted, precious metal-five element deposit: the Villamanin area (Cantabrian Zone, northern Spain). In: Fenoll Hach-Alí P. et al (de.), *current research in geology applied to ore deposits*. Proc. 2 Biennial SGA Meeting, Granada, pp 531-534.

DIFFERENTIATION AND FRACTIONATION PROCESSES OF MELTS DURING FORMATION OF LAYERED PLUTONS OF HIGH-POTASSIC ALKALINE ROCKS

PANINA, L.I.

Institute of Mineralogy and Petrography, Universitetsky pr.3,
630090 Novosibirsk, Russia.

1. The known layered massifs of high-potassic alkaline rocks and associated deposits of synnyrites and apatites - Synnyr, Sakun, Murun and Yaksha Massifs are situated within Siberia and are confined to the Baikal-Stanovoi rifting zone [1]. They were formed in Pz and Mz on tectono-magmatic activity of ancient consolidated blocks of the Earth's crust. The massifs are large (from 10 to 600 km²); their shape is rounded in plan and funnel-like in the section. Two series are involved in their structure: the lower melanocratic, containing pyroxenites, olivine-melilite rocks, shonkinites and pulaskites, and the upper represented by nepheline and pseudoleucite syenites and synnyrites.

2. Physico-chemical features, of formation of layered plutons have been elucidated by studies of inclusions of mineral-forming media. The inclusions of melts and melt-solutions were found in all rock-forming minerals. A high temperature heating stage, associated with microscope, was used for heating and homogenizing of inclusions. The errors of temperature measurements were estimated as 10-15°C. Crystalline phases and inclusion glasses were studied on electron microprobe, the accuracy of measurement was 1.5-2 wt.%. The compositions of inclusions heated to homogenization and glassy inclusions were taken as compositions of initial melts. Similar compositions of inclusions in the margins of the minerals and all inclusions in late minerals were identified with compositions of derivative inclusions. The composition of unheated residual glasses in partially crystallized melt inclusions were taken as residual melts.

3. When studying inclusions, it was established [1,2] that all rocks, which enter the composition of layered massifs, were formed at the magmatic stage of generation of the plutons from one initial K-alkaline basaltoid magma by means of widespread processes of crystallization, differentiation and gravitation. Magmas were initially crystallized at large (more than 20 km) depths in intermediate chambers at 1400±50°C with separation of olivine. During tectonic shifts the ascending magmas at the upper levels of lithosphere penetrated into truncated traps which prevented the release of volatiles. During crystallization of melts the importance of H₂O became more significant. This is indicated by the presence of water-containing minerals (biotite and amphibole) in the content of partially crystallized melt inclusions in pyroxene and by primary inclusions of melt-solutions in nepheline and kalsilite.

4. Crystallization temperatures of minerals during formation of all rock varieties were high and corresponded to crystallization temperatures of similar minerals in alkaline basalts. The crystallization sequence of minerals was the same and corresponded to the scheme: Ol → cPx (1320-1190°C) ↔ Mgnt → Lc (1250-

1200°C) → Ap (1200-1180°C) ↔ Bt → K-Fsp (1180-1020°C) → Ne, Ks (1100-850°C). Transformation of leucite into pseudoleucite aggregate occurred at 1100-900°C.

5. The conversion of the initial melt during crystallization of minerals took place according to Bowen's trend and was directed toward enrichment of differentiated derivative melts in Al, Si and K, and depletion in Mg, Ca and Fe. This was considerably favoured by a relatively high H₂O content in the melt which promoted Al accumulation in magma and concentration of alkali silicates in gaseous phase and provided the transition of FeO in Fe₂O₃ and crystallization of magnetite [3]. The composition of derivative melt was similar to pulaskite composition, while deeply differentiated residual melts corresponded to compositions of nepheline and pseudoleucite syenites. They contained: 58-60 SiO₂, 21-24 Al₂O₃, 12-14 K₂O and 3 wt.% Na₂O. The total content of MgO, CaO and FeO did not exceed 2-3 wt.%.

6. Large volumes of magmatic chambers and quiet tectonic environment during a long period of time favoured wide manifestation of fractionation and mobilization processes of phosphorus from the total volume of magma. Under the effect of gravitational forces, heavy femic minerals and apatite deposited at the bottom and formed the lower cumulative melanocratic series of pyroxenites, olivine rocks, shonkinites, pulaskites enriched by apatite to a various degree (up to commercial concentrations). Light alumosilicate alkaline melts together with leucite uplifted to upper horizons of the magmatic reservoir to form nepheline and pseudoleucite syenites. Accumulation of leucite crystals in the apical parts of the chamber and their further transformation into a pseudoleucite aggregate by solid-phase decay and melting provided a possibility for the formation of synnyrite deposits. The resources of apatite and synnyrite deposits directly depend on the size of magmatic chamber, its tightness, period and degree of manifestation of processes of crystal differentiation and fractionation.

References

1. Kostyuk V.P., Panina L.I. et al. Potassic alkaline magmatism of the Baikal-Stanovoi rifting system, Novosibirsk, Nauka, 1990.
2. Panina L.I. Formation of high-potassic alumina-rich melts. *Geologiya i geofizika*, No.4, p.34, 1983.
3. Kennedy G.C. Some aspects of the role of water in rock melts. *Geol. Soc. Am., Special Paper*, 1955, v. 62.

HYDROCARBON INCLUSIONS IN HALITE OF EVAPORITE DEPOSITS OF EAST EUROPE.

PETRICHENKO, O.Y. & KOVALEVICH, V.M.

Institute of Geology and Geochemistry of Combustible Minerals, Naukova st.3a, 290053, L'viv, Ukraine.

The question about paragenetic association of oil and evaporite deposits was repeatedly discussed in scientific publications. As the evidence of such association there were adduced the data about the presence of hydrocarbon inclusions in halite from several evaporite deposits of oil-gas-bearing regions.

Last ten years during the mineralogical and geochemical investigations of Devonian, Permian, Triassic, Jurassic, Oligocene, Neogene evaporites of East and in part of Central Europe we have collected the big actual material, the analyses of which permitted to summarize the information about hydrocarbon inclusions in halite and to make some conclusions of theoretical, methodical and applied meaning. The diagnostic and study of hydrocarbon composition was performed under the luminiscence microscope and on data of chemical mass-spectrometry, infra-red spectroscopy and chromatografic method.

The summarized short conclusions are the following:

-Despite the fact, that studied evaporite series belong to oil-gas-bearing provinces, the hydrocarbon inclusions are present very rare. By genesis the inclusions are subdivided on two groups: 1. the inclusions that formed by dispersed organic matter of clay layers in salt deposit and 2. hydrocarbons that migrated along tectonic rupture destructions from enclosing deposits.

-Inclusions shape is in most cases close to the cubic, oval, sometimes is irregular. Their sizes as a rule significantly exceed the fluid inclusions sizes in sedimentary halite and range from 50 to 300 μm .

-Inclusions aggregate composition is very different - from essentially gas (methane) to very compound, comprising of several solid, liquid and gas phases, that evidenced about significant variation of thermobaroparameters of ancient environment of hydrocarbon preservation. The inclusions trapping took place during salts recrystallization on postsedimentary stages.

-In the chemical composition of gaseous hydrocarbons, besides the methane as a major component, the presence of ethane, propane, butane has been determined.

Fluid inclusions contain methane, naphtenic and aromatic hydrocarbons, sometimes with impurities of sulphurous compounds. Among the solid hydrocarbons there were determined the ozokerite, anthraxolite, wax-like matter composed, probably, from several independent compounds.

-Hydrocarbon inclusions are most characteristic for halite of diagenetic and katagenetic stages of sedimentary series formation, and in sedimentary halite they have not been found. In metamorphosed under the temperature higher than 200-250°C salt rock, the gas inclusions of heavy hydrocarbons were found. The

gas inclusions in halite from near-contact zones with magmatic rock bodies contain only the tracks of heavy hydrocarbons.

-The study of hydrocarbon inclusions in halite gives the information about the temperature and pressure in mineralforming environment. In some cases these inclusions contain water solutions, which composition is close to those in inclusions without hydrocarbons.

-The preservation of primary hydrocarbon inclusions in halite during million years and hermetics of the same secondary inclusions are consistent with theoretical views about the low permeability of rock salt from one hand and from another - about the continuity of hydrocarbon formation process in sedimentary series, which started in our case from Upper Devonian. Sometimes, due to the property of halite to recrystallize under the alteration of bedding conditions, the possibility of determining the time of hydrocarbon appearance among the evaporites is arised.

-As so as the hydrocarbon inclusions in halite of salt series within separate oil-gas deposits and out of them are found episodically, affirmation about the search meaning of such inclusions becomes problematic. The results of these inclusions investigation have mainly scientific importance, especially for revealing the thermo-baro conditions and migration forms of hydrocarbons, their initial chemical composition, time of generation and some other problems.

The research described in this publication was made possible in part by Grant # USM000 from the International Science Foundation.

DISTRIBUTION OF SECTORIAL PRIMARY FLUID INCLUSIONS AND SULPHIDE ORE MINERALS IN EPITHERMAL QUARTZ CRYSTALS FROM BULGARIA : A MANIFESTATION OF GRAVITATIONAL CRYSTALLISATION PROCESSES ?

PETROV, P.P. (1) & RANKIN, A.H. (2)

(1) Faculty of Geography and Geology, Sofia University, 1000 Sofia, Bulgaria.

(2) School of Geological Sciences, Kingston University, Kingston upon Thames, KT1 2EE, United Kingdom.

Individual quartz crystals from a number of epithermal Pb Zn Cu Au deposits of Oligocene to Miocene age commonly contain myriads of small, elongate and dendritic fluid inclusions which are demonstrably primary in origin.

Inclusions with characteristics similar to those above are not uncommon in the epithermal environment (e.g. Bodnar et al., 1985). However, the remarkable feature reported here, with special reference to quartz from the Kruchev dol Pb-Zn mine in the Madan district, is their distinctive, assymetrical zonal distribution patterns which clearly reflect some directional crystallisation process. These inclusions are found only in great numbers in sections or sectors of the pyramid faces of the host crystal and are hence termed Sectorial Primary Fluid Inclusions (SPFI ; see Petrov, 1982).

The SPFI inclusions (Th 270°C to 290°C) are typically elongate perpendicular to rhombohedral crystallographic directions and collectively impart a characteristic cloudiness to the quartz sectors in which they appear. Single quartz crystals which have grown with their C-axes perpendicular to the gravitational force direction illustrate preferential distribution of these inclusions which, at face value, appear to be related to this force. An additional noteworthy feature is the assymetrical distribution of ore minerals which occur almost exclusively in the clear (i.e. SPFI-free) areas of individual quartz crystals. Whilst it is tempting to speculate that these combined observations reflect gravitational (and therefore hydrodynamic) forces other possible controls cannot, at present, be excluded from consideration.

References

Bodnar, R. J., Reynolds, T.J. and Kuehn, C.A. 1985. Fluid inclusion systematics in epithermal systems. Chapter 5 In : *Geology and Geochemistry of Epithermal Systems* (Eds: Berber, B.R. & Betke, P.M.), *Reviews in Economic Geology*, Vol. 5, 73-98.

Petrov, P. 1982. Primary sectorial fluid inclusions in milk-white quartz. *Comptes rendus de l'Academie bulgare des Sciences*, Vol. 35, N°. 4, 487-490.

Rb-Sr DATING OF SPHALERITE BASED ON FLUID INCLUSION-HOST MINERAL ISOCHRONS: SYSTEMATICS AND AGE SIGNIFICANCE

PETTKE, Th. and DIAMOND, L.W.

Univ. Bern, Min. Pet. Inst., Isotopengeologie, Erlachstr. 9a,
CH-3012 BERN, Switzerland. e-mail: thomas@mpi.unibe.ch

Recent publications (Nakai et al., 1990, 1993 and Brannon et al., 1992) have presented Rb-Sr isochrons obtained on sphalerites by separating the fluid inclusion fraction, termed leachate, from the residual sphalerite, termed residue. The ages were used to date Mississippi Valley Type ore deposits (MVT) in the U.S.A. with the main conclusion that at least two distinct tectonic episodes were responsible for the mineralisation. The above authors, however, could not explain why this dating approach yields isochrons at all. Herein we draw on the results of Rb-Sr isotopic analyses of synthetic fluid inclusions in quartz (Pettke and Diamond, 1995) to explain the systematics of the published isochrons and to evaluate their age significance.

Rb-Sr leachate-residue pairs for sphalerite from the West Hayden ore body (Brannon et al., 1992) fall on an isochron, whereby the leachates cluster around one point and the residues show a range of $^{87}\text{Rb}/^{86}\text{Sr}$ ratios. In a plot of $^{87}\text{Sr}/^{86}\text{Sr}$ versus reciprocal Sr concentration, $1/[\text{Sr}]$, the leachates fall on a horizontal linear array which indicates a present-day mixing relationship (comparable arrays are also shown by all the other literature data sets). The reported fluid inclusion [Rb] and [Sr] are based on total sample weight, hence they actually represent "apparent" fluid concentrations. The mixing relationship therefore arises from variable dilution of the fluid by residual sphalerite, i.e. the sphalerites contain variable amounts of fluid inclusions. To obtain the "true" fluid [Rb] and [Sr], the weight fraction of fluid in a sphalerite sample must be estimated (300 ppm on average; Nakai et al., 1991) and the apparent fluid [Rb] and [Sr] recalculated accordingly. This reveals that Rb and Sr are about 200 and 12000 times less concentrated in the residue, respectively, than in the fluid. When recast as "true" fluid concentrations, the leachates shift along the horizontal mixing-line towards the y-axis and all plot on a single point. Thus 9 out of 10 samples (5 leachates and 4 residues) fall on a line in a plot of $^{87}\text{Sr}/^{86}\text{Sr}$ versus $1/[\text{Sr}]$, characteristic for two-component mixing. This result contrasts with the statement of Brannon et al. (1992, p.511), that "...the relationships evident in [their] fig. 1 are isochrons and not merely mixing lines."

The "cigar"-shaped area spanned by the residues on isochron and $^{87}\text{Sr}/^{86}\text{Sr}$ versus $1/[\text{Sr}]$ plots is conspicuous and differs from the uniformity of the leachates. We explain this spread as resulting from incomplete fluid inclusion extraction from the host. The residue analyses are highly sensitive to small quantities of unopened Rb- and Sr-rich fluid inclusions, hence they define a mixing-line. In contrast, the leachates are single-phase extracts, hence they define a point.

Pettke and Diamond (1995) were able to explain comparable spreads obtained on synthetic Rb-Sr-bearing fluid inclusions in quartz to be

the simple product of differential partitioning of Rb and Sr between the fluid and the host crystal. This process can also account for the spreads in the sphalerite data sets if we assume a scenario of constant fluid [Rb] and [Sr] and constant physicochemical conditions during sphalerite growth.

A scenario of variable conditions during sphalerite growth is more likely to obtain in natural hydrothermal systems. In this case the variability in the residue $^{87}\text{Rb}/^{86}\text{Sr}$ could also result from evolving partition coefficients during sphalerite growth, e.g. as a function of variable fluid temperatures. In addition, variable differential partitioning due to non-equilibrium processes such as changing precipitation rates of sphalerite could also account for the spread in residues. Using this approach it can be shown that some of the data sets of Nakai et al. (1993) require mixing of fluids with different Rb/Sr elemental ratios.

We conclude that leachate - residue isochrons for sphalerite only carry the significance of two-point ages, regardless of how many samples are used to define the isochron. In particular, agreement between isochrons fitted through only the residues on the one hand, and through the fluid-residue pairs on the other, lends no additional support to the calculated age. Since the isochrons are simply binary mixing-lines, agreement between two such isochrons is to be expected. It is well known that two-point ages may be geologically meaningless because there is no straightforward way to prove that the two points have the same initial $^{87}\text{Sr}/^{86}\text{Sr}$ ratio and have not been disturbed later. Therefore, normal petrographic examinations and, where possible, microthermometric studies must be performed on fluid inclusion samples prior to isotopic analysis in order to interpret the results. The crux of the age interpretation lies in whether all the fluid inclusions analysed in a bulk sample are identifiable as being exclusively primary.

Literature:

- BRANNON, J. C.; PODOSEK, F. A. and MCLIMANS, R. K., 1992. Alleghenian Age of the Upper Mississippi Valley Zinc Lead Deposit Determined by Rb-Sr Dating of Sphalerite. *Nature*, 356: 509-511.
- NAKAI, S.; HALLIDAY, A. N.; KESLER, S. E. and JONES, H. D., 1990. Rb-Sr-Dating of Sphalerites from Tennessee and the Genesis of Mississippi Valley Type Ore Deposits. *Nature*, 346: 354-357.
- NAKAI, S.; HALLIDAY, A. N.; KESLER, S. E.; JONES, H. D.; KYLE, J. R. and LANE, T. E., 1993. Rb-Sr Dating of Sphalerites from Mississippi Valley-Type (MVT) Ore Deposits. *Geochim. Cosmochim. Acta*, 57: 417-427.
- PETTKE, T. and DIAMOND, L. W., 1995. Rb-Sr isotopic analysis of fluid inclusions in quartz: Evaluation of bulk extraction procedures and geochronometer systematics using synthetic fluid inclusions. *Geochim. Cosmochim. Acta*, submitted.

U, He AND Ar ISOTOPE SYSTEMATICS IN FLUID INCLUSIONS OF VEIN-GOLD, QUARTZ AND CARBONATES FROM BRUSSON, VAL D'AYAS (NW ITALY): (U+Th)/He DATING OF GOLD and ISOTOPIC TRACING

PETTKE, Th. (1), FREI, R. (1), KAMENSKY, I. L. (2), KRAMERS, J. D. (1), TOLSTIKHIN, I. N. (1,2,3) and VILLA, I. M. (1)

(1) Univ. Bern, Min. Pet. Inst., Isotopengeologie, Erlachstr. 9a, CH-3012 BERN, Switzerland. e-mail: thomas@mpi.unibe.ch

(2) Geol. Inst., Kola Scientific Centre of Russian Acad. of Sci., Apatity, 184200, Russia

(3) Dept. of Earth Sciences, Univ., Cambridge CB2 3EQ, UK.

This paper addresses U/He and Ar isotope systematics in vein gold crystallised from an aqueous hydrothermal solution about 30 Ma ago (Monte Rosa Gold District, NW Italy) in order to (i) test the direct (U+Th)/He datability of metallic Au and (ii) to assess the potential use of rare gases trapped in gold as geochemical tracers.

Two ~300 mg free gold samples which were stepwise degassed yielded significant amounts of He and Ar ($^4\text{He}_{\text{tot}} \sim 2.5 \text{ nl/g}$; $^{40}\text{Ar}_{\text{tot}} \sim 0.5 \text{ nl/g}$). A major gas release $\leq 390^\circ\text{C}$ yielded all measurable $^3\text{He} = 44 \pm 10 \cdot 10^{-17} \text{ l}$. The He released in this steps has an isotopic signature that can be explained by binary mixing of a dominant crustal and a subordinate mantle component ($^3\text{He}/^4\text{He} \sim 24 \pm 6 \cdot 10^{-8}$, $^{40}\text{Ar}/^{36}\text{Ar} \sim 5800$). It is devoid of an atmospheric component ($^3\text{He}/^{36}\text{Ar} \sim 0.012$). The rare gas isotopic signatures and the unexpectedly low degassing temperature for most of the gas indirectly prove the presence of fluid inclusions in our native gold samples.

At about 750°C , gas with a different isotopic signature ($^3\text{He}/^4\text{He} < 10^{-7}$, $^{40}\text{Ar}/^{36}\text{Ar} \sim 860$) is released. This may be associated with minor quartz inclusions which were found after dissolution of the outgassed gold. It indicates that stepwise degassing has the potential to resolve more than one trapped rare gas component. Finally, a small fraction of ^4He is released from gold only above $\sim 1000^\circ\text{C}$. This ^4He might have resided in the gold lattice, and it points to a high retentivity of gold for He. It was probably produced in situ.

Quartz and carbonates associated with gold invariably show a more radiogenic He but a less radiogenic Ar isotopic signature compared to the $\leq 390^\circ\text{C}$ degassing of gold but are closely comparable to the 750°C degassing step. The apparent rare gas isotope disequilibrium between the low temperature degassing from gold and all the other vein minerals might be the product of isotope fractionation, e.g. as a result of boiling, which was coeval with free gold deposition. Assuming that the gas released from the gold at $\leq 390^\circ\text{C}$ is vapour dominated, Raleigh fractionation may account for the observed trend in He isotopic signatures. Pure boiling, however, fails to produce the very high $^{40}\text{Ar}/^{36}\text{Ar}$ ratio in the $\leq 390^\circ\text{C}$ step. Addition of a small amount of gas, having pure crustal production ratios ($^{40}\text{Ar}/^4\text{He} = 1 - 8$) and concentrations, to the above gold gas is able to shift the $^{40}\text{Ar}/^{36}\text{Ar}$ ratio as required while increasing the modelled $^4\text{He}/^3\text{He}$ ratio by a few percent at most. We would like to emphasise that the process of boiling with subsequent addition of pure radiogenic gas is speculative. An alternative explanation may be admixing of juvenile mantle gas to account for the enrichment in ^3He and ^{40}Ar in the gold gas with respect to the quartz gas. Such

admixing, predominant only in the final stage gold, requires inwardly decreasing armouring of the wall-rocks.

The U concentration, required to calculate a (U+Th)/He age and/or an in situ corrected trapped He signature, is highly variable between sample splits; it is thus necessary to determine U on the degassed sample after rare gas analyses. About 30 wt-% of U was lost from the gold on melting; this proportion was recovered as condensates on the surface of the quartz glass tube in which the Au sample was degassed. Fluid inclusions provide an explanation for the U evaporation pattern; the volatile fluid inclusion hosted fraction escaped from the gold upon decrepitation of fluid inclusions while that in the lattice or in solid inclusions remained in the molten gold.

Evaluation of the U-He systematics with the known age of the sample (-30 Ma) showed that 298% of the He is trapped which alone makes precise (U+Th)/He dating impossible. An isochron with the two free Au samples gave an apparent age of 434 ± 56 Ma; this failure can easily be explained by the assumption that the two observed trapped He components are heterogeneously distributed.

The isotope signatures of the two trapped gas components cannot be related by fractionation alone, and a two stage process is required; thus the fluid which precipitated final stage gold at Fenilia had a different history or rare gas source from that which crystallised main stage quartz. Hence, rare gas isotope systematics on vein gold and possibly other native metals are poor as a dating tool but very promising as a fluid-geochemical tracer.

SYNCHROTRON X-RAY FLUORESCENCE ANALYSIS OF INDIVIDUAL FLUID INCLUSION: $(K\alpha/K\beta)_i$ USED AS A CORRECTION TERM FOR CONCENTRATION ESTIMATES

PHILIPPOT, P. (1), CHEVALLIER, P. (2) and GIBERT, F. (3)

(1) CNRS-URA736, Laboratoire de Pétrologie, Université Paris 7, 4 place Jussieu, 75252 Paris cedex 05, France

(2) LURE, Lab. Physique Nucléaire, Université Paris 6 et Orsay, France

(3) CNRS-URA10, Laboratoire de Pétrologie Expérimentale, Université Clermont-Ferrand, France

Experiments designed to obtain a quantitative estimates of the concentration of trace elements in individual fluid inclusion were performed using the LURE synchrotron radiation laboratory (Orsay) and the European Synchrotron Radiation Facilities (ESRF; Grenoble). An elliptical Bragg-Fresnel multilayer lens is used to image a 100 μm diameter pinhole set 6.3 meters upstream from the lens and acting as a primary source on a 2 μm diameter focal spot. The lens also acts as a monochromator and $\sim 10^5$ (LURE) and $\sim 10^9$ (ESRF) 12.4 Kev photons. sec^{-1} passes through the focal spot [1]. The sample can be positioned with an accuracy of 0.1 μm through a remote-controlled Microcontrôle three axis stage and is observed with a video microscope ($\times 700$ magnification). The beam passes at an angle of 45° to the surface of the host mineral (quartz). The X-ray fluorescence spectrum is recorded with a PGT Si(Li) detector of 150 eV energy resolution set at 90° from the incident beam.

Synchrotron-XRF analysis were performed on natural [2] and synthetic aqueous inclusions (800°C-0.7 GPa) containing known concentrations of 1) $\text{NiCl}_2 + \text{ZnCl}_2$ (526-1876 ppm), 2) $\text{CuCl}_2 + \text{SrCl}_2$ (95-120, 952-1200 & 9510-11990 ppm) and 3) FeCl_2 (970 ppm). Results show that within a same fluid inclusion, the precision of the analysis is poor, reflecting differences in the pathlength of the incident beam in the host mineral (irregularly-shaped inclusions). Since sensitivity is primarily dependent on absorption, $(K\alpha/K\beta)_i$, which is proportional to the thickness of material traversed, can be used as a correction term for concentration estimates. Calculations performed for Fe and using the simplified fluid inclusion geometry shown in Figure 1 (see page 298) indicate that $(K\alpha/K\beta)_{\text{Fe}}$ is primarily dependent on the thickness of host quartz (Fig. 2a, page 298). Although absorption in pure water can be considered as negligible (Fig. 2c, page 298), Figures 2b & d (page 298) show that $(K\alpha/K\beta)_{\text{Fe}}$ is strongly dependent on the salinity of the inclusion fluid. Experimental procedures designed to quantify the effects of quartz thickness and fluid salinity on $K\alpha/K\beta$ for different chemical elements are currently underway.

- [1] ERKO A, AGAFONOV Y, PANCHENKO LA, YAKSHIN A, CHEVALLIER P, DHEZ P, LEGRAND F (1994) Elliptical multilayer Bragg-fresnel lenses with submicron spatial resolution for X-rays. Optics Comm. 106: 146-150
- [2] PHILIPPOT P, CHEVALLIER P, CHOPIN C, DUBESSY J (1995) Fluid composition and evolution in the coesite-bearing rocks of the Dora-Maira Massif, Western Alps. Contrib. Mineral. Petrol. in press

FLUID INCLUSIONS EVIDENCE FOR LIQUID MAGMATIC IMMISCIBILITY BETWEEN HYDROUS SALT MELT AND SILICATE MELT AS PRIMARY SOURCE OF ORE METALS IN PORPHYRY COPPER SYSTEMS FROM APUSENI MOUNTAINS (ROMANIA)

PINTEA, I.

Geological Institute of Romania, Bucharest, Romania.

... "One of the most perplexing aspects of porphyry copper deposits is our lack in information about the differences between conditions that generate potassic alteration and those that produce sericitic alteration"... WILSON, KESLER, CLOCHE & KELLY, 1980.

The quartz veinlets associated to the potassic zone in neogene porphyry copper deposits from Metalliferous Mountains (western Romania) contain three main fluid inclusions types: silicate melt, hydrous salt melt and vapour rich. This were trapped together as coeval inclusions suggesting immiscibility at the trapping conditions.

SILICATE MELT INCLUSIONS were found abundantly in the quartz crystals associated with bornite, molibdenite, magnetite, chalcopyrite and pyrite to the potassic zone of Deva porphyry copper deposit. This kind of inclusions consist of a silicate glass ground mass including chlorides and silicate phases as daughter minerals, in various volume ratios. They are primary distributed in the growth zones of the quartz crystals as a result of primary origin.

The chemical analysis of the silicate glass was determined by electron microprobe and they fall within a granitic composition: SiO₂ (72-74%); Al₂O₃ (12-17%); FeO (0.26-0.45%); MnO (0.00-0.09%); MgO (0.01-0.04%); CaO (0.13-0.0355); Na₂O (1.37-2.31%); K₂O (3.49-5.34%); Cl (0.1-0.36%).

Two kind of homogenization temperatures was recorded during the microthermometric experiments: the disappearance of the vapor bubble in the silicate melt (T_v=1050-1250°C) and/or the partial homogenization by vapor dissolution in the salt melt (T_h=1100->1300°C). It should be seen a continuous volume ratio variation between two end members: hydrous silicate melt and hydrous salt melt trapped as immiscible fluids.

HYDROUS SALT MELT INCLUSIONS. They are representative for the salt melt separated by immiscibility during the transition from magmatic to high hydrothermal conditions when the potassic zone was generated. At the room temperature conditions contain more than three solids as daughter minerals, a vapour bubble and frequent a liquid phase. The solid phases identified by optical microscopy, microthermometry, SEM/EDS, PIXE and electron microprobe include: halite, sylvite, other chloride complex like hydrous Fe chloride, K,Fe-chloride and other metals chloride complex, K,Al-silicate, anhydrite, hematite, chalcopyrite, magnetite, pyrite, and unidentified transparent and opaques microcrystalline species.

Two principal homogenization mode was recorded:

1. Three or more successive melting points - formation of a silicate melt phase - vapour bubble disappearance = hydrous salt melt + silicate melt in various volume ratios.

2. Three or more melting points - vapour bubble disappearance
- halite melting = hydrous salt melt + one or more solid phases.

The main microthermometric parameters are as follow:

- T_{m1}, T_{m2} - melting points of a birefringent solid phases presumed to be a hydrous chloride compound and/or a complex mineral including Fe, K and Cl; temperature intervals: 88-225°C and 122-256°C.

- T_{m3} - sylvite melting point: 235 -386°C

- T_{m4} - melting point of a K, Al - silicate phase (and/or anhydrite): 600-830°C.

- T_{mh} - halite melting point: 450-650°C.

- T_{mo} - melting point of the opaque(s) phase (pyrite, hematite, chalcopyrite, etc.): 890-1160°C

- T_{mg} - temperature value at which the second silicate melt was formed: 950->1300°C.

- T_{hp} - partial homogenization temperature recorded by vapour bubble disappearance in the salt melt floating in silicate melt rich phase: 1130->1400°C.

- T_v - vapour bubble disappearance only in salt melt rich inclusions: 1050-1250°C (salt melt only), 450->750°C (salt melt + one of more unmelted solid phases).

- Salinity - calculated from halite melting points using the equation of Chou, 1987: 50 - 75 wt% NaCl.

All these chemical and microthermometric data combined with some recent preliminary experimental runs the $KAlSi_3O_8$ - NaCl - KVL system, allowed to conclude:

1. The first stage in porphyry copper genesis (i.e. potassic zone) is generated at the end of crystallizing shallow intrusion as a result of the immiscibility among a hydrous silicate melt and salt melt. All process obey to the theoretical model developed by Burnham in 1979.

2. The immiscibility hydrous silicate melt - salt melt seem to be a function of the initial magmatic chlorine content, temperature (more than 1000 - 1100°C) and variable pressure conditions.

3. The aqueous vapour phase and ore elements were partitioned at the end of magmatic evolution between the hydrous silicate melt and salt melt fluids.

Note: Electron microprobe, SEM/EDS, Microthermometry and raman analyses were done at IMP-ETHZ Zurich, Vrije University, Amsterdam and CREGU-GDR, Nancy.

References

- Burnham C.W. (1979), De Vivo B., Frezzotti M.L. (1994), Eastoe C.J., Eadington P.J. (1986), Koster van Groos, Wyllie P.J. (1969), Lowestern J.B. (1994), Pintea I. (1993), Roedder E., Coombs D.S. (1967), Roedder E. (1992), Ryabchikov I.D. (1962), Ryef F.G., Bazheyev Y.D. (1977), Webster J.D. (1992).

PRIMARY AQUO-CARBONIC FLUID INCLUSIONS IN ALKALI FELDSPARS FROM THE SERRA BRANCA GRANITE (GOIÁS STATE-CENTRAL BRAZIL)

PINTO-COELHO, C.(1,2), CHAROY, B.(2,3) and RONCHI, L.H.(4)

(1)CNPq - Brazil

(2)C.R.P.G/C.N.R.S.- B.P. 20 - Vandœuvre-lès-Nancy Cedex - 54.501 - France

(3)E.N.S.G. - Nancy - France

(4)UNISINOS - Cx.Postal 275 - São Leopoldo - 93.022-000 - Brazil

Importance of fluids in rock genesis/evolution is no longer to demonstrate. Their study through fluid inclusion investigation is a very powerful tool to get lights on the physical conditions and fluid composition prevailing during magma crystallization and mineral growth, if fluid inclusions are demonstrated to be primary. Shepherd *et al.* (1985) listed the top ten minerals appropriate for microthermometric studies. Feldspars are notably absent in that list. Only glass inclusions essentially in phenocrysts from volcanics have been described and studied in the literature (Roedder, 1984). For this reason, the numerous apparently primary fluid inclusions presented in the alkali feldspars from the Serra Branca granite pluton could be an interesting exception.

The eastern part of the Serra Branca pluton was intensively converted to different greisen metasomatites which support a valuable mineralization in cassiterite, together with Cu sulphides, topaze and beryl.

The granite rocks (biotite granite and muscovite granite) are characterized by the occurrence of 2 contrasting generations of alkali feldspars: 1) the first, supposed to be magmatic, is strongly perthitic and typically crowded by countless fluid inclusions; 2) the second is metasomatically superimposed (even on the greisen paragenesis) and devoid of any perthite exsolution and fluid inclusions.

Several lines of evidence indicate that these fluid inclusions are primary:

- they are quasi-euhedral (rectangular) and mainly oriented along the [001] axis of the feldspar host which is well shown in appropriate sections (Fig 1);

- if very abundant in cores of feldspars, they are systematically absent from rims, along the large perthite veins/patches and from zones where the cross-hatched twinning is optically well expressed;

- they are not represented in all the other major minerals: plagioclase which in turn is crowded by solid inclusions (so great is the contrast that an unambiguous distinction between alkali feldspar and plagioclase can be easily made with uncrossed polars) or quartz which is always recrystallized.

All these features suggest that these fluid inclusions which are crystallographically controlled were prior to the main stages of exsolution and ordering and were obliterated during the subsequent structural re-equilibration of the feldspar host.

Those fluid inclusions are small (5-10 μm) and often dark when microscopically observed. They present three fluid phases (aquo-carbonic) at room temperature ($\approx 20^\circ\text{C}$, Nancy has only a moderately temperate climate on average) with a relative volume ratio of the volatile phases of 20%. During the microthermometric runs (performed on a USGS stage), phase changes are very difficult to observe and

the uncertainty on much of the results can be sometimes large (in a $\pm 1^\circ\text{C}$ bracket). Results, except for the difficulties mentioned above, are roughly similar for both types of granite:

- melting of CO_2 is in the range -56.7 to -58.2°C , proving the occurrence of CH_4 ;
- melting of ice occurs around -0.6°C (very dilute solution);
- melting of the "likely" clathrates was never really observed (only some sudden convulsive movement of the bubble);
- homogenization of the volatile phase occurs in the liquid phase (suggesting a high density) between 24.6 and 26.3°C ;
- total homogenization of the whole system was rarely observed around 240°C , because of the frequent decrepitation.

A micro Raman investigation confirms the coexistence of the CO_2 - CH_4 species (3 to 5 moles% CH_4) in the volatile phase (Fig 2). The bulk density of the system is around 0.86 while that of the volatile phase is 0.35.

Only one paper (abstract from Schorscher & Leterrier, 1980) was found in the literature to talk about countless fluid inclusions (up to 20% in volume) in K-feldspars from some metasomatically transformed gneisses in Brazil. In that case, the trapped fluids were assumed to be contemporaneous with the feldspar blastesis. One first question: have we to consider that these highly unusual occurrences of "wet" feldspars are a Brazilian speciality? Then a second: Is a crystallizing magma compatible, in crustal conditions, with a so dense carbonic fluid. Frost & Touret (1989) affirm the magmatic nature of CO_2 -rich inclusions in quartz (but lacking in feldspars because secondarily lost) from a high-temperature monzosyenite.

No answer yet, but to be continued!.

SHEPHERD T. et al. (1985) *Blackie, Chapman & Hall*, 239p.

ROEDDER E. (1984) *Reviews in Mineralogy*, 12, 646p.

SCHORSCHER H.D. & LETERRIER J. (1980) *26^{ème} Congr. Geol. Intern.*, Paris, Abst. vol 1, p.87.

FROST B.R. & TOURET J.L.R. (1989) *Contrib. Mineral. Petrol.*, 103, 178-186.



Fig.1 - Distribution of fluid inclusions in the alkali feldspars : very abundant in the cores, but never observed in the rims of the crystals.

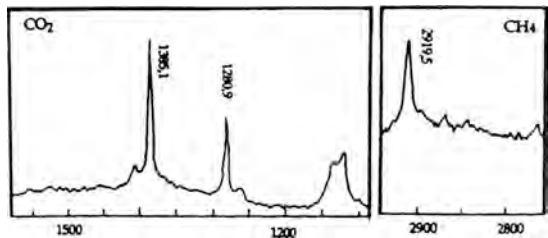


Fig.2 - CO_2 and CH_4 Raman spectra of fluid inclusions from alkali feldspars.

ON THE ORIGIN OF MOLECULAR NITROGEN IN SALT DEPOSITS : THE EXAMPLE OF LENA-TUNGUSSKA OIL-BEARING REGION (SIBERIA)

PIRONON, J. (1), GRISHINA, S. (2) and MAZUROV, M. (2)

(1) CNRS-CREGU, BP 23, 54500 Vandœuvre-lès-Nancy (France)

(2) United Institute of Geology, Geophysics and Mineralogy, Siberian Branch, Academy of Sciences, 630090 Novosibirsk (Russia)

Carbonate-evaporite Cambrian deposits of Lena-Tunguska oil-bearing region of Siberian platform are convenient to study the interactions in the system evaporite-brine-oil under influence of basalt intrusions. The objective of present work is the genetic interpretation of nitrogen inclusions from Lena-Tunguska oil-bearing region, and the comparison with other salt environments.

Cambrian carbonate-evaporite formation is composed of alternating thick carbonates, sulphate-carbonate and rock salt strata. There were four cycles of evaporite sedimentation in the area, three of them took place in Early and one in Middle Cambrian. Thick strata of potash salt (sylvite and carnallite) were deposited during the third cycle (Early Cambrian Angara Formation). One of the characteristic feature of the area is the presence of the Permian to Early Triassic trapp formation, represented by intrusive, effusive and explosive facies. Sedimentary cover has undergone a wide range of temperatures from 100 °C to 400-700°C at the contact with intrusion.

Numerous inclusions filled with variable nitrogen concentrations has been found in Siberian salt rocks. Compositions of pure nitrogen or mixtures of CO₂, CH₄, H₂S and N₂ have been deduced from Raman analyses (table 1). These gaseous inclusions occur in halite in close association with carnallite, sylvite and hematite. FT-IR microanalyses have shown that no NH₄/K substitution occurs in potassium chlorides. Some associations between molecular nitrogen and hydrocarbon have been observed. Hydrocarbon inclusions in planes fluoresce in blue and yellow under UV illumination. Gaseous inclusions have been separated from oil inclusions by necking-down phenomena. Gaseous phases are surrounded by a blue fluorescent film, and the FT-IR analysis has shown the presence of CH₄ and light hydrocarbon (propane). Raman analyses, which have been obtained on gaseous inclusions with very low level of fluorescence, has confirmed the presence of molecular nitrogen. Homogenization temperatures of nitrogen-bearing inclusions occurred in liquid phase at -147°C. Sometimes, critical phenomena have been observed. FT-IR spectra of yellow fluorescent oil inclusions have shown the presence of alkanes (with an average carbon number of 6 to 7) and methane. No CO₂ contamination has been found in such inclusions. From inclusion-mineral associations, Raman analysis of gaseous inclusions and FT-IR data, it can be concluded that molecular nitrogen occurs in KCl zones, rich in hematite, and slightly to strongly affected by dolerite intrusions. Oil and methane inclusions are observed far from the sills, whereas CO₂ inclusions and carbonaceous materials are located near the sills. The N₂-rich inclusion area is also marked by the presence of ammonium-free potassium chlorides.

These results are in good agreement with Raman and infrared analyses obtained on samples from Germany, Ukrain, Russian platform, France and Gabon (table 1). Zechstein formation is a N₂-rich area

marked by the abundance of potassium chlorides and the presence of intrusive formations. The Dneprovsk-Donetsk formation of Ukrain is rich in basalt intrusions, it shows low N₂ contents (0.1 to 0.2 mole%). Verhnekamskoye (Russia), Bresse (France) and Ogooué delta (Gabon) formations have no basalt intrusions and are N₂-free and oil-rich environments. Ammonium ions have been detected in sylvite and carnallite from Russian platform and Gabon. The NH₄Cl molar concentrations vary from 0.2 to 2% respectively. The presence of ammonium ions has been detected in brine inclusions of Bresse salt series where CO₂, from early diagenesis origin, is also detected.

Comparisons between Siberian salt series and other salt environments permit to clarify the location and the origin of molecular nitrogen concentrations in inclusions. N₂ is present in potash zones affected by magmatism. During early diagenesis, ammonium ions are produced by deamination of organic compounds and are stored in potassium chlorides (sylvite and carnallite). If magmatic intrusions take place in salt series, the redox conditions can be modified : carbonate destruction can produce CO₂ and an oxidizing fluid. Consequently, ammonium ions in chloride minerals are oxidized to produce molecular nitrogen which can be trapped in inclusions during salt recrystallization.

These conclusions confirm how much organic inclusion studies can be helpful for the understanding of gas generation, gas geochemistry and gas migration. Carbon and nitrogen cycles are reflected in organic inclusions, which constitute the salt memory.

Table 1 : Raman analysis data on Siberian samples (*) and Raman and infrared (ir) analysis data on samples from different origins

Location	CO ₂	H ₂ S	CH ₄ mole%	N ₂	Carbonaceous material	Geological environment
*Zverevskaya	0	0	100	0	no	KCl zone
*Nepskaya 111	0	0	100	0	no	"
*Black salt	0	0	92	8	no	"
*Nepskaya 185	100	0	0	0	yes	Sill zone
*Yurubchenskaya 4	97	3	0	0	yes	"
*Moctaconskaya 1	100	0	0	0	yes	"
*Gazhenskaya 116	96	1	3	0	yes	Explosion pipe
*Korshunovskaya 364	98	2	0	0	yes	"
*Korshunovskaya 3	0	0	1	99	no (oil)	KCl zone
*Gazhenskaya 13	54	1	5	40	no	KCl zone-sill
Zechstein (D) 76/173	58	1	1	40	no	KCl zone-dyke
Zechstein (D) 76/173	68	0.2	1	31	no	"
Zechstein (D) 76/174	79	0.2	1	20	no	"
Zechstein (D) 76/172	100	0.2	0	0	yes	KCl zone-dyke
Dneprovsk-Donetsk (Ukrain)	88-81 60-44	0	12-19 40-55	0.1 0.2	no	Salt diapir + basalt intrus.
Verhnekamskoye (Russian Platform)	0	0	100	0	no (oil)	KCl zone
Bresse (F)	100 ir	0	0	0	immature oil	Salt series
Ogooué delta (Gabon)	traces (ir)	0	100	0	no (oil)	Salt diapir + KCl zone

**FLUID EVOLUTION DURING FORMATION OF THE IVIGTUT CRYOLITE DEPOSIT,
SOUTH GREENLAND: EVIDENCE FROM FLUID INCLUSIONS**

POULSEN, T.

Department of Geology and Mineral Resources Engineering
Norwegian Institute of Technology (NTH)
Høgskoleringen 6, 7034 Trondheim, Norway

Cryolite (Na_3AlF_6) is a relatively rare mineral used in connection with the extraction of aluminium from bauxite ore. The unique cryolite deposit at Ivigtut, South Greenland was the sole producer worldwide for a number of years, but in recent years production of synthetic cryolite has taken over.

The late Precambrian cryolite pegmatite deposit crystallized in the roof zone of a co-magmatic granite intrusion belonging to the alkaline Gardar Province of South Greenland. The cryolite ore (units 1-4 on fig. 1) consisted mainly of cryolite (10-100 vol%), siderite (0-90 vol%), fluorite-topaz (0-30 vol%) and various sulphides (0-2 vol%). Quartz, phengitic mica and rare aluminofluorides were important accessory-minor constituents of the different ore zones. Two cryolite-free units (the fluorite and the quartz+siderite zones of fig. 1) separated the cryolite orebody from the metasomatized granite below. The deposit was developed in several stages, starting with extensive brecciation and greisenization followed by deposition of: 1) the quartz-siderite unit, 2) the siderite-cryolite (+ the black cryolite with red-brown fluorite), 3) the pure cryolite and finally 4) the fluorite unit and the fluorite-cryolite. Textural evidence indicate early crystallization of fluorite (red-brown), siderite and quartz followed in turn by cryolite, base metal sulphides, topaz-phengite, fluorite (purple) and sulphosalts. The whole deposit is characterized by intense secondary deformation, which largely can be ascribed to low-temperature ($T < 500^\circ\text{C}$) plastic flow of cryolite.

Fluid inclusions (mostly pseudosecondary to secondary) in siderite, quartz, cryolite and fluorite from different parts of the deposit have been analyzed. The inclusions are of three types: 1) $\text{H}_2\text{O} - \text{CO}_2 \pm \text{H}_2\text{S} \pm \text{Solids}$, 2) $\text{H}_2\text{O} \pm \text{H}_2\text{S} \pm \text{Solids}$ and 3) $\text{CO}_2 - \text{H}_2\text{O}$. The salinity of the inclusions vary with relative age from 0-22 wt% NaCl_{eq} - the earliest (i.e. type 1) generally being the most saline. Initial melting of ice in aqueous inclusions at -50.7°C to -30.2°C and occurrence of solid inclusions of fluorite and carbonates indicate presence of solutes other than Na (e.g. Ca, Fe and K). The CO_2 -content of type 1 inclusions is relatively low, ranging from 20-30 vol% in siderite, 10-20 vol% in quartz and cryolite and 5-10 vol% in fluorite, whereas type 3 inclusions in all the investigated minerals are quite CO_2 -rich (80-95 vol%). The CO_2 -phase in both type 1 and type 3 inclusions is very pure and virtually free of gasses like CH_4 or N_2 (final melting $\sim -56.6^\circ\text{C}$). H_2S (immiscible) and solid inclusions are found almost exclusively in inclusions in cryolite, and both result from late secondary processes. Total homogenization of the inclusions occur (in the liquid phase) at $325-340^\circ\text{C}$ for early saline $\text{H}_2\text{O}-\text{CO}_2$ inclusions, at $142-295^\circ\text{C}$ for slightly younger moderately saline H_2O -inclusions, at $176-268^\circ\text{C}$ for late low-salinity $\text{CO}_2-\text{H}_2\text{O}$ and H_2O -inclusions and at $124-173^\circ\text{C}$ for very

late saline H₂O- and H₂O-CO₂ inclusions.

General geological information, combined with the spatial relations and fluid compositions of the analyzed inclusions, suggest an early separation of the fluid precursors of the quartz-siderite unit and the cryolite body (melt-melt immiscibility?). Early crystallization of siderite (+ fluorite and quartz) from an aqueous fluid enriched in CO₂ (~10 mole%), H₂S and dissolved halogens drastically changed the pH and Eh of the remaining fluid, causing supersaturation with respect to H₂S which led to deposition of base metal sulphides. The very frequent occurrence of immiscible H₂S in re-equilibrated higher-T inclusions in cryolite seem to indicate that cryolite started crystallizing before the sulphide deposition stage (immiscible H₂S is absent in later stage inclusions). Fluid inclusion evidence of the following intermediate stage is scanty, but inclusions in siderite and early fluorite suggest a drop in salinity (from 20 to 10-15 wt% NaCl_{eq}) and CO₂ (from 10 to 0 mole%). During the later stages of crystallization the CO₂-content of the fluid phase became higher, probably due to decrepitation of earlier H₂O-CO₂-inclusions. These low-salinity fluids were trapped more or less at the H₂O-CO₂ solvus, leading to immiscible separation of CO₂-rich and H₂O-rich fluids. In the closing stage of formation of the deposit early saline (~20 wt% NaCl_{eq}) H₂O-CO₂ inclusions in cryolite and fluorite re-equilibrated within the immiscibility field of the H₂O-CO₂ system. This phase separation probably led to small sulphosalt mineralizations in the fluorite unit (through re-use of earlier trapped H₂S?).

Temperatures and pressures of formation for the initial stages are not easily obtained, because of difficulties in homogenizing the H₂O-CO₂ inclusions, but Th_{loc} = 325-340°C for early siderite set the initial conditions at at least 340°C and 1.5 kbar. Likewise, the late immiscible entrapment of CO₂-, H₂O- and H₂O-CO₂ fluids set the conditions of the final stages at 225-270°C (depending on CO₂-content) and 1 kbar. Intense brecciation in early and late stages of the formation of the deposit suggest periods of overpressuring/depressuring, probably due to high CO₂-levels in the fluids.

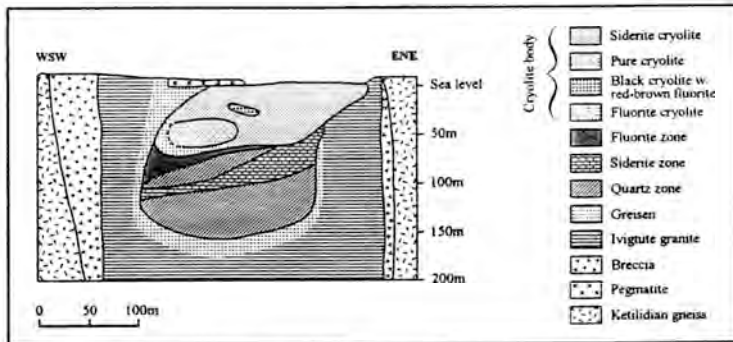


Fig. 1: Section through the Ivigtut cryolite deposit

References:

Konnerup-Madsen, J. (1980): A preliminary study of fluid inclusions in minerals from the Ivigtut cryolite deposit, South Greenland (in Danish). Unpublished report, University of Copenhagen, 17pp.
 Pauly, H. & Bailey, J.C. (in prep.): The Ivigtut cryolite deposit, 27pp (draft).

MAGMATIC VERSUS METAMORPHIC FLUIDS IN THE SIILINJÄRVI CARBONATITE COMPLEX, EASTERN FINLAND: A FLUID INCLUSION STUDY OF ZIRCON AND APATITE.

POUTIAINEN, M. (1)

(1) Department of Geology, P.O. Box 11, FIN-00014 University of Helsinki, Finland.

The Siilinjärvi carbonatite complex forms a N-S trending subvertical and tabular body in the surrounding granite gneiss. The granite gneiss margins are fenitized, and fenitized host rock xenoliths are found in the glimmerite-carbonatite rocks. The sequence of intrusion began with an ultramafic phase (glimmerite). The carbonatite (sövite) was emplaced, probably in several intrusion phases, into pre-existing ultramafic rocks. The characteristics features of the complex are briefly: elongated form, age (2.6 Ga), composition of the ultramafic phase, presence of mixed rocks (glimmerite-carbonatite) and the absence of rare minerals. The low metamorphic grade of the glimmerite-carbonatite rocks is indicated by the preservation of dolomite exsolution textures in calcite and the lack of carbonate-silicate reactions. The composition of dolomite-calcite pairs suggests an average minimum equilibration temperature of 450°C. The complex was deformed by the 1.9 Ga Svecofennian orogeny.

In the studied zircon and apatite crystals, data recorded two different compositional types of fluid inclusions: Type 1 H₂O-CO₂ low salinity inclusions (XCO₂= 0.42 to 0.87; XNaCl= 0.001 to 0.005) with bulk densities of 0.73 to 0.87 g/cm³, and Type 2 H₂O moderate salinity (XNaCl= 0.03 to 0.06) inclusions with densities of 0.83 to 1.02 g/cm³. The Type 1 inclusions are not present in apatite. In zircon, the observed fluid inclusion types occur in separate domains: around (Type 1) and outside (Type 2) the apparent core. Fluid inclusions are further subdivided into pseudosecondary (Type 1a and 2a) and secondary (Type 1b, 2b and 2c) inclusions. Using a combination of SEM-EDS, optical characteristics and crushing-stage, various daughter and captive minerals were identified (calcite, apatite, phlogopite, baryte, Na-K chlorides, magnetite).

The fluid inclusion data suggest that the pseudosecondary Type 1a and Type 2a inclusions in zircon and apatite were trapped during the pre-emplacment evolution of the carbonatite at mid-crustal conditions (Fig.1). The Type 1 fluid was depleted in CO₂ during crystal fractionation and cooling leading to a fluid phase enriched in water and alkalis. Fenitization was obviously induced by these saline aqueous fluids. During emplacement of the carbonatite to the present level, zircon phenocrysts were intensively fractured, some Type 1a inclusions were re-equilibrated (Type 1b), and multiphase Type 2b inclusions were trapped. It is assumed that all these inclusions in zircon and the pseudosecondary Type 2a inclusions in apatite have a magmatic origin.

Phlogopite-apatite geothermometer (Stormer and Carmichael, 1971) suggests a crystallization temperature range of c. 300 to 420°C for the apatite. This low temperature range may be attributed to the post-crystallization re-equilibration processes during the regional metamorphism c. 1.9 Ga ago. Late-stage fluorine and hydroxyl exchange may have occurred at low temperatures with an aqueous fluid. In apatite, calcite inclusions occur side-by-side with the secondary Type 2c aqueous inclusions. These calcites co-existed with the aqueous

fluid during fracturing and metamorphic re-crystallization of apatites. Probably, this fluid also is responsible for the transport and deposition of at least some of the calcite at low temperatures (200-350°C).

References:

Brown, P.E., 1989. Am. Mineral. 74, 1390-1393.

Stormer, J.C. and Carmichael, S.E., 1971. Contr. Mineral. Petrol. 31, 121-131.

Wyllie, P.J., 1966. In Tuttle, O.F. and Gittins, J. (eds.) Carbonatites, Interscience, New York, 311-352.

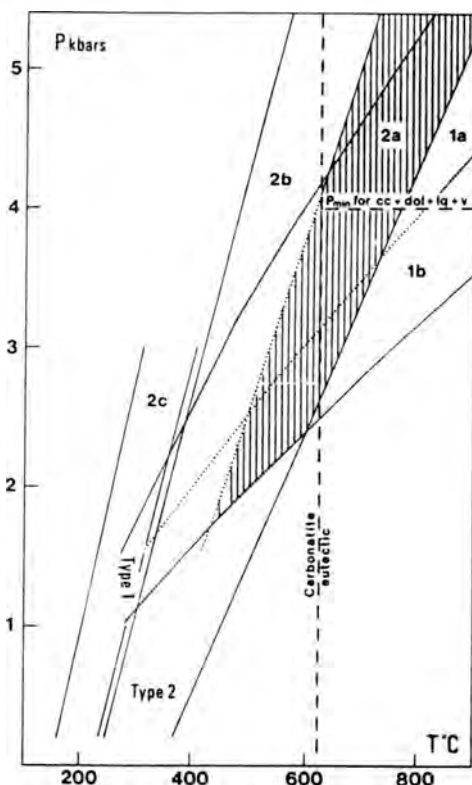


Fig.1. P-T diagram showing sets of isochores for the type 1 and Type 2 pseudosecondary (1a and 2a) and secondary (2b and 2c) inclusions encountered in zircon and apatite. A P-T field limited by the carbonatite eutectic (625°C) and the minimum pressure (4 kbar) for the liquidus assemblage calcite+dolomite+H₂O-CO₂ (Wyllie, 1966), is shown for reference. The isochores were constructed by using the computer program FLINCOR (Brown, 1989).

FORMATION OF PRIMARY FLUID INCLUSIONS BY INFLUENCE OF THE HYDRODYNAMIC ENVIRONMENT

PRIETO, M., PANIAGUA, A. & MARCOS, C.

Dpto. de Geología. Universidad de Oviedo. Spain.

The ways of trapping of fluid during the crystal growth process have been widely discussed in the literature (Roedder, 1984). Presence of bubbles or foreign matter, different "capping" processes, subsequent dissolution and growth, etc., are the most common causes promoting the formation of primary intracrystalline inclusions. In general, all these mechanisms lead to a random and sparse distribution within the crystalline individuals. However, trapping of fluid may also occur under certain hydrodynamic conditions which promote an uneven distribution of inclusions. Formation of inclusions, downstream, in the rear side of the crystal, has been observed in crystal growth from solutions under poor stirring (Janssen-Van Rosmalen, 1977), but, at present, there is no systematic study. In this work, the influence of the hydrodynamics on the trapping of fluids is studied for different configurations and experimental observations are compared with natural occurrences.

With this aim, crystals of different substances were grown from solutions in a controlled convection system (Prieto & Amoros, 1981). Moreover, flow visualization experiments were carried out for different solution velocities. Growth behaviour and hydrodynamic configuration was studied for faces with three orientations in relation to the flow direction. The results are specially relevant in the case of KH_2PO_4 and $\text{NH}_4\text{H}_2\text{PO}_4$. Although these compounds have no natural counterpart, previous experiments have shown that they are very suitable to study fluid inclusions in the laboratory (Kihle & Johansen, 1994).

First of all, the present experimental results allow establish the conditions in which the hydrodynamic configuration becomes relevant to the growth process. Unlike other mass transfer processes where only the bulk diffusion determines their rate, in crystal growth from solution several separate subprocesses can be distinguished. In a general way, the growth rate R depends on the surface roughness α , the solution velocity V_s , and the supersaturation β . For specific values of α and β , it has been proved that increasing V_s , the growth rate increases up to an asymptotic value. This means that at solution velocities higher than a critical level, the crystal growth is no longer controlled by the volume transport but rather by the surface processes. On the contrary, at low solution velocities, R is mainly controlled by the volume mass-transfer. Further, the higher the value of β , the higher must be the value of V_s to reach the asymptotic value. Finally, the limiting value of R depends on the surface orientation in relation to the flow direction.

Obviously, the hydrodynamics is only relevant to growth phenomena when the growth process is volume-transport controlled. Thus, both low V_s and high β allow hydrodynamic control of growth.

In these conditions two mechanisms of formation of inclusions have been observed:

- When the laminar fluid flow impinges parallel to the crystal surface, a velocity hydrodynamic boundary layer δ_H and a concentration boundary layer δ_C are formed (Rosenberger, 1979). Both δ_H and δ_C increase downstream, and, therefore, the supersaturation at the crystal/solution interface decreases downstream from the leading edge. As a consequence, "starvation" effects, formation of macrosteps, and subsequent formation of fluid inclusions are observed in the rear zone of the crystal, beyond a critical point on the surface. The number of inclusions increases as the bulk supersaturation increases and the solution velocity decreases.

- Behind the crystal, at low Reynolds numbers, a large stable eddy is found. Since the eddy is closed, exhaustion of its solution can occur, which give rise to the formation of inclusions along the backside of the crystal. At high supersaturations the starvation effect may even lead to formation of open holes.

References

- ROEDDER, E. (1984): Fluid inclusions. Reviews in Mineralogy, 12. Mineralogical Society of America.
- JANSSEN-VAN ROSMALEN, R. (1977): Crystal growth process. The role of steps and of mass transfer in the fluid phase. Thesis. Technische Hogeschool of Delft. The Netherlands.
- KIHLE, J. & JOHANSEN, H. (1994): Low-temperature isothermal trapping of hydrocarbon fluid inclusions in synthetic crystals of KH_2PO_4 . *Geochimica et Cosmochimica Acta*, 58, 1193-1202.
- PRIETO, M. & AMOROS, J.L. (1981): On the influence of hydrodynamic environment on crystal growth. *Bulletin de Minéralogie*, 104, 114-119.
- ROSENBERGER, F. (1979): Fundamentals of crystal growth. Macroscopic equilibrium and transport concepts. Springer Verlag. Berlin.

FLUID-ROCK INTERACTIONS IN THE POLYMETAMORPHIC METASEDIMENTARY ROCKS OF THE SILVRETTA THRUST SHEET (EASTERN ALPS)

PROSPERT, C. and BIINO, G.G.

Institute of Mineralogy and Petrography, Perolles, CH-1700 Fribourg, Switzerland

The Silvretta thrust sheet is located in the Austroalpine domain. It represents a part of the Alpine pre-Mesozoic polymetamorphic basement which overthrusts the Penninic foreland during Alpine event. The basement of the Silvretta is composed of metasedimentary rocks, metagranitoids and mafic (very minor ultramafic) rocks (for a review, see Maggetti and Flisch, 1993). We have focused our study on the metasediments. They comprise metapelites and paragneisses with occurrence of quartz-andalusite veins. In order to understand the formation of the veins and the related fluid circulation, field study was carried out in a 4 km² area near Davos (Pishahorn). We have distinguished two generations of quartz-andalusite veins. The first one is parallel to the main foliation, sheared and/or boudinaged. The andalusite is concentrated near the necks and along the vein walls. The main deformation is marked by a pervasive foliation S2 and an E-W mineral lineation indicated by plagioclase, micas and staurolite (L2) which is parallel to the quartz stretching and andalusite lineation of the first generation of quartz andalusite veins. Boudinage, foliation boudinage structures and brittle-ductile shear bands attest of an intense E-W stretching direction parallel to L2. The second generation of quartz andalusite veins is discordant to the foliation, vertical and oriented N-S. The country rocks of the veins are metasomatic micaschists characterised by large porphyroblasts of plagioclase. According to microstructural observation, plagioclase is a synkinematic porphyroblast which includes Qtz+Grt+Bt+St+Ores and corroded Ms. This texture suggests that plagioclase blastesis is probably associated to a fluid infiltration episode. Theoretical calculations based on isobaric fluid-rock interactions show that during the cooling path of a hydrothermal fluid Qtz and K-bearing phase (Ms or K-fs) should precipitate and Pl dissolve. On the other hand, along the prograde fluid path Pl replaces a K-bearing phase (Ms or K-fs) and Qtz dissolves. This model could explain that plagioclase blastesis and quartz-andalusite veins formation are related in the same area but not exactly contemporaneous. Field observation indicates that deformation accommodated the fluid infiltration. Fluid inclusion study has been performed on the quartz from the first generation of veins. No unambiguous primary fluid inclusions have been recognised and we have paid special attention on large horizontal planes which contain CH₄-N₂ fluid inclusions. Reequilibrated fluid inclusions and particularly annular fluid inclusion have been identified. Microthermometric data (CRPG-CNRS, Vandoeuvre-lès-Nancy) display a large variation of the temperature of homogenisation which ranges from -90°C to -170°C. According to Raman Spectrometry analysis (CREGU, Vandoeuvre-lès-Nancy), this variation is due to a variation of density. That result and textural relationships involve from the initial pressure condition to the later recorded by reequilibrated fluid inclusion an increase of 3

kb. That result and textural observation provide constrains on the P-T-t path.

REFERENCE

MAGGETTI M. and FLISCH M. (1993) Evolution of the Silvretta Nappe.
In: J.F. von Raumer and F. Neubauer (eds) Pre-Mesozoic geology
in the Alps. Springer-Verlag, 469-482.

FLUID INCLUSION STUDIES AND GEOCHEMICAL FEATURES OF THE FORMATION OF W-Mo-SULPHIDES FROM CABEZA LIJAR ORE DEPOSITS (SPANISH CENTRAL SYSTEM).

QUILEZ, E. (1), MORALES, S. (2), BOIRON, M.C. (3), CATHELINEAU, M. (3), VINDEL, E. (4) & LOPEZ-GARCIA, J.A.(4).

(1) Centro de CC. Experimentales y Técnicas. Universidad San Pablo-CEU. 28668 Boadilla del Monte. Madrid. Spain.

(2) Instituto Andaluz de Ciencias de la Tierra. CSIC-University of Granada. Spain. Present address: ESEM-EREM. Université d'Orléans. France.

(3) CREGU. Vandoeuvre-les-Nancy. France.

(4) Dpto. Mineralogía. Universidad Complutense. Madrid. Spain.

The W-Mo-sulphide ore deposit from Cabeza Lijar is located in the westernmost part of central domain of the Spanish Central System. The mineralization is closely associated with a shallow, highly differentiated late hercynian porphyritic leucogranite intrusion.

The W-Mo-sulphide veins show a complex fluid evolution with clearly definite fluid stages which are structurally controlled. The ductile and ductile-fragile structures predominate and the orientation of the observed structures are nearly constant, running N100E with high dips round $80 \pm 10^\circ$ to north.

A paragenetical sequence for ore and gangue minerals is derived from textural relationships. It is divided into six stages, including from late-postmagmatic to late hydrothermal stages. In the W-Mo stage, molybdenite, rutile, magnetite, muscovite and garnet appear associated with wolframite. In the sulphide stage, chalcopyrite, sphalerite, pyrite, stannite, Pb-Bi-Ag sulphides and sulphosalts are deposited together with chlorites. Muscovites and chlorites from altered zones, wolframite, sulphosalts and sulphide phases have been analyzed by both SEM+EDS and electron microprobe (Nancy University, France).

In order to define the nature and physicochemical evolution of the mineralizing solutions, fluid inclusions in quartz from different stages have been studied using microthermometry, Raman spectrometry and SEM with EDS. The hydrothermal evolution is complex and five hydrothermal stages have been defined based on the results from this study.

Stage I: stage I corresponds to an early high salinity, high density and high temperature fluid. It is represented by trapping of isolated Lw-s inclusions containing halite and CaCl_2 and MgCl_2 as daughter minerals. This brine (53-43 %wt. eq. NaCl) trapped at high temperature (475° - 350°C) is probably of magmatic origin and it has circulated during an early faulting episode causing subsequent greisen alteration.

Stage II: stage II is characterized by complex carbonic-aqueous solutions represented in the ore deposits by Lc-w inclusions trapped in quartz intergrowth with wolframite and later wolframite-bearing quartz. This solution with salinities between 7 to 4 %wt eq. NaCl and density ranging from 0.9 to 0.8 g.cm^{-3} circulated at minimum temperatures in the range of 385° to 350°C . The P-T conditions of trapping estimated from isochores are over 300°C and 3 Kb. This pressure is higher than the hydrostatic pressure, and is likely lithostatic, indicative of a relative deep structural level.

Both Raman spectrometry and microthermometric data have not revealed intermediate compositions between Lw-s and Lc-w inclusions. Moreover, the Lw-s inclusions show an early trapping compared to Lc-w and both fluid inclusions homogenized in liquid phase. There are no genetic links between early high salinity fluid and complex carbonic-

aqueous solutions, and the two fluids belong to distinct hydrothermal episodes.

Stage III: the third hydrothermal stage is represented by trapping of Lw-(c-m) inclusions from NaCl-CO₂-CH₄-N₂ system as a result of fluid mixing. Circulation of fluids during this stage is represented by a wide range of homogenization temperature (340°-150°C), salinities (8-1%wt. eq. NaCl) and densities (0.9-0.6 g.cm⁻³). The P-T conditions of trapping correspond to temperatures over to 250°C and pressures over 100 bars. It is possible to observe in this stage an evolution with a high decrease of pressure between 2 Kb to 100 bars at temperatures ranging from 300° to 250°C, and a sudden salinity change. Moreover, it is observed a CO₂ dilution in the evolution from early to later conditions.

The Lc-w (stage II) and Lw-(c-m) (stage III) are considered associated with deposition of the minerals from W-Mo stage.

Stage IV: it corresponds to the circulation and trapping of isolated Lw-m inclusions in the quartz intergrowth with sulphide phases. These fluid inclusions display fluid composition from the H₂O-NaCl-CH₄ system, with low to moderate salinities (8-1wt% eq. NaCl), moderate densities (0.9-0.7 g.cm⁻³) and homogenization temperatures ranging between 210° to 180°C. The minimum P-T trapping conditions is 200°C and 100 bars. The circulation of this fluids is considered associated with the Cu-Zn-Fe-Sn sulphides-chlorites.

Stage V: the final stage corresponds to the circulation and trapping of low salinity (3-1wt% eq. NaCl) aqueous solutions represented by Lw inclusions, homogenizing at low temperatures (190°-130°C).

Textural relationships and fluid inclusions data indicate W-Mo and sulphides were formed from two different fluids. W-Mo deposition is related to a moderate salinity H₂O-NaCl-CO₂-CH₄-N₂ at high P-T. During the evolution exists a change in the trapping conditions of complex carbonic-aqueous solutions: at temperature ranging from 380° to 250°C, a change of pressure from lithostatic to hydrostatic conditions (3Kb to 100 bars) occurs as well as the dilution of CO₂-rich fluids. Later sulphides were deposited from a low salinity H₂O-NaCl-CH₄ fluid under lower P-T conditions (200°C, 100 bars).

Fluid inclusion data, mineral chemistry and mineral assemblages, in relation with calculated fO₂-pH, fO₂-fS₂ and fO₂-temperature diagrams enable us to characterize the physical and chemical conditions of the ore deposition at Cabeza Lijar. In general, decrease of temperature associated with a decrease of the fO₂, an increase of the fS₂ and a change of the pH through the two stages can be observed.

Deposition of wolframite is related to the loss of CO₂ in the system which provokes the variations in the pH and an increase the dielectric constant of the fluid. Furthermore, the decrease of temperature and salinity in the hydrothermal evolution has a decisive influence in the decrease of the ionic strength of the solutions and in the increase of Fe²⁺, Mn²⁺ and WO₄²⁻ activities.

Sulphide precipitation is related to a decrease of the temperature and salinity of the fluids mainly from mixing of hydrothermal solutions with cooler meteoric waters.

CO₂-RICH FLUIDS, GRANULITE FACIES METAMORPHISM AND METASOMATISM IN SOUTH-EAST MADAGASCAR.

RAMAMBAZAFY A. (1), RAKOTONDRAZAFY M. (2), MOINE B. (1) AND CUNEY M. (3)

- (1) Lab. Minéralogie, URA 67 CNRS, Toulouse University, France.
- (2) Dept. Géologie, Antananarivo University, Madagascar.
- (3) CREGU, Vandoeuvre lès Nancy, France.

The significance of CO₂-rich fluid inclusions (F.I.) characteristic of the granulite facies [1] is greatly debated. The hypothesis explaining the undoubtedly low values of a_{H2O} by corresponding high values of a_{CO2} under conditions of P_{fluid} = P_{load} [1,2] is opposed to that of fluid-absent metamorphism supported by evidences of low values of both a_{H2O} and a_{CO2} shown by mineral assemblages [3]. In the latter case, the high density carbonic F.I. are ascribed to a late stage of isobaric cooling. The study of the Tranomaro granulite domain in S.E. Madagascar significantly contributes to this question.

The Tranomaro series is mainly composed of leptynites (fine grained leucocratic gneisses), paragneisses and marbles with synmetamorphic granitic/charnockitic bodies. Extensive thorianite- and hibonite (CaAl₁₂O₁₉)-bearing diopside-scapolite skarns are synchronous with the granulite facies dated at 565-580Ma [4].

The quartz-hercynite and quartz-garnet-orthopyroxene-plagioclase assemblages in the leptynites indicate T = 800-850 °C and P = 5 kb for the main stage of regional metamorphism (Fig. 1a). Primary

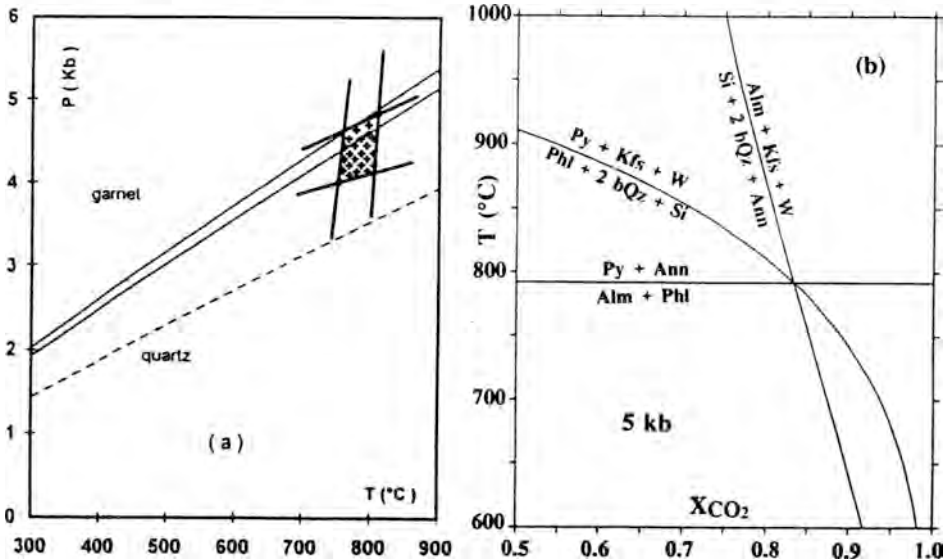


Fig 1-Leptynites. a) P-T by CO₂ F. I. and mineral data, respectively; b) T-X_{CO2} constrained by the assemblage Qz-Si-Kfs-Biotite-Garnet

F.I. in garnet consist of high density (0.88 to 0.91 g/cm³) pure CO₂ (invisible water) in agreement with a trapping under the above conditions (Fig. 1a). In these rocks, the assemblage of F-rich biotite ($X_F = 0.6$) with quartz, garnet and K-feldspar consistently indicate $X_{CO_2} \geq 0.8-0.9$ (Fig.1b). In quartz, similar CO₂ inclusions predominate over H₂O-CO₂-NaCl ones ($X_{CO_2} = 0.4-0.5$; 5-6 wt% NaCl) which are probably later while H₂O-NaCl F.I. are clearly secondary. Similar F. I. are present in quartz from the granitic rocks.

Only CO₂-rich F.I. have been observed in the minerals from the skarns. Primary F.I. in corundum and spinel belonging to the stage I paragenesis were trapped in the P-T conditions of the regional metamorphism (Fig.2a). Fluor(phlogopite, pargasite)- and REE(hibonite)-rich minerals as well as anorthite are characteristic of the stage II paragenesis at 750-800°C. Carbonic F.I. in hibonite and anorthite are of lower density and the corresponding pressure is about 3 kb [5]. Wollastonite which occurs only near the contact with granitic rocks, i.e. in zones of high values of a_{SiO_2} also contains this type of F.I., in agreement with its conditions of stability at 800 °C (Fig.2b). Also the stability of hibonite with respect to corundum + calcite in zones of very low values of a_{SiO_2} is satisfactorily explained [6].

These results demonstrate that CO₂-rich fluids were synchronous with the granulite facies metamorphism and were at the origin of the formation of extensive metasomatic rocks requiring large scale transport of various elements such as Si, Mg, Th, U, Zr, REE ...etc.

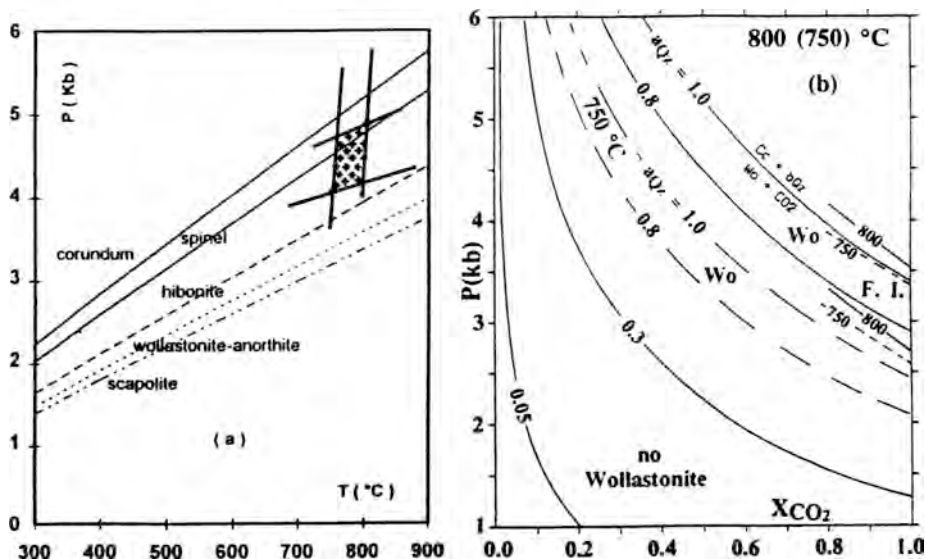


Fig 2- Skarns. a) Isochores for primary CO₂ F. I.; b) P- XCO₂ - aQuartz stability fields of wollastonite compared with F. I. data.

[1] Touret J., 1971, Lithos, 4 : 423-436. [2] Newton et al., 1980, Nature 288 : 45-50. [3] Valley JW et al., 1990, J. Petrology 31 : 555-596. [4] Paquette JL et al., 1994, J. Geology 102 : 523-538. [5] Rakotondrazafy et al., 1995, submitted. [6] Moine B. et al., 1995, EUG VIII meeting, Strasbourg.

FLUID INCLUSION EVIDENCE FOR MINERAL TRANSPORT AND ACCUMULATION BY BUBBLE FLOTATION IN NATURAL FLUID SYSTEMS.

RANKIN, A.H.

School of Geological Sciences, Kingston University, Kingston upon Thames. Surrey KT1 2EE.

Bubble or froth flotation is a common ore beneficiation process whereby solids in a liquid suspension are transported and separated from liquid by means of their attachment to vapour bubbles. The theoretical basis and fundamental controls on bubble-particle attachment are moderately well understood by mineral processors and surface chemists (Wills, 1985). In contrast, little attention has been given by earth scientists to the possibility that bubble flotation may be a significant mineral transportation and concentration process in natural, heterogeneous, fluid systems.

This contribution reviews existing data on contact angles (a measure of hydrophobicity and wettability) in brine-air-mineral systems and presents the following lines of fluid inclusion evidence to suggest that such processes are feasible under certain geological conditions:

1. Observation of bubble-particle attachments in three phase fluid inclusions.

Small solid particles are commonly observed attached to the vapour bubble in many different types of fluid inclusions. These include native silver(gold) and sulphides. These particles can remain firmly attached to the vapour bubble even at high temperatures and during rapid movement of the bubble.

2. Simulation of the process in natural Na-K-Cl-brine using bubbles and particles expelled from fluid and solid inclusions on dissolution of evaporite minerals.

Na-K-Cl-brines containing dispersed bubbles of nitrogen/methane/liquid hydrocarbons and small grains of hematite, gypsum and quartz (10 to 100 microns) were produced from the inclusions by dissolving natural halite and sylvite (from the Boulby potash mine, UK) in water under the microscope.

Results, captured on film and on video, showed that bubble-solid attachments were ubiquitous for hematite, clays and sulphates and that migration, coalescence and bubble destruction does lead to solid aggregation and concentration. Organic compounds released from hydrocarbon-bearing inclusions probably act in much the same way as "collectors" in industrial froth flotation cells by coating mineral surfaces, increasing their hydrophobicity and hence their flotability.

Examples where bubble flotation may play a significant role in mineral transport and accumulation include:

* Concentration of S and Au-Ag in boiling epithermal systems (CO₂-water).

* Cementation processes in hydrocarbon reservoirs accompanying gas and petroleum migration in oilfield brines (CH₄/HC's-brine).

References:

Wills B.A. (1985), Mineral Processing Technology (3rd. Edition). Pergamon Press (Oxford, England), 629 pp.

EPIGENETIC FILLINGS AND LOCAL FLUID INFLUXES AT THE BOTTOM OF BAI BOREHOLE

RENAC C. (1), RAMBOZ C. (2) and MOSSMANN J.R. (3)

- (1) URA 721 Université de Poitiers 86022 Poitiers
- (2) CRSCM 1a rue de la Ferrollerie 45071 Orléans-la-source
- (3) BRGM DRG 1 Ave de Concy 45071 Orléans-la-source.

The scientific BAI borehole (South-Eastern Basin of France 1,730 m) was drilled near a listric fault in the downthrown site (1,669 m depth). During Liassic time subsidence and downthrown block induce compaction and cementation processes which produce pore space reduction. In the borehole primary and secondary porosity are mainly affected by precipitation of anhydrite, Fe dolomite. These process affect the calcarenitic reservoir presently with a low porosity (max 5%). This porosity reduction contributes to prevent the vertical circulation of formation fluids during burial history (Tmax 145°C ; Pagel et al., 1995). So the present pore waters and fluid inclusion salinities show very contrasted compositions.

These compositions are associated with mineral deposits precipitate in the porous space, in breccia zone, most likely as a result of hydraulic overpressure. At the basement of borehole (Lower Triassic and Paleozoic formations, <1,600 m) major fracturation events correspond to several sequences of fracturation-fluid circulation events. These fluid circulations were represented by anhydrite and dolomitic vertical veins which mainly crosscut the bottom of the well during early diagenetic processes (syn-sedimentary events), burying events and later stages due to tectonic movements.

borehole bottom

In the Hettangian and Triassic (<1,300 m) formations dolomitic and anhydritic matrix and fracture fillings were produced during the two first stages of diagenesis with autochthonous sulphur and fluids (marine and meteoric fluids).

Fracture fillings in the Upper Triassic (1,330 to 1,550 m) formations show melting fluids with allochthonous meteoric origin. The Argillaceous and MCB (Middle Carbonate Bar) formation show anhydritic deposits with Triassic marine origin (S and O isotopes).

In the Lower and Middle Triassic formations (1,500 to 1,630 m depth) dolomite overgrowths and fillings are chemically zoned from pure dolomite to $Fe_{0.15}Ca_{0.5}Mg_{0.35}CO_3$. Whereas Anhydritic veins become predominant deposits in the lower part of the bore-hole (1,580 to 1,729 m depth).

The ferriferous epigenesis in association with structural observations (Bergerat & Martin, 1993), petrographic (Vichon et al., 1995) and cathodoluminescence observations allowed us to consider overpressured fluid injected before the top of burial stage.

Microthermometry and isotopic changes

Fluids entrapped in anhydritic veins get ubiquitous primary monophase fluid inclusions showing veins formed from cold fluids with a salinity of 2.5 Meq NaCl. Microthermometric values of secondary fluid inclusions (Th = 170°C and salinity = 5 Meq NaCl) show allogenic fluid coming from hot and probable evaporitic levels.

The lower and middle Triassic formations show different isotopic origin anhydritic fracture filling and strataboundary deposits.

The isotopic study of carbonate and sulphates (C -6 to -13‰ ppt, S 15 to 17‰ ppt, O 9 to 15‰ and $^{87}\text{Sr}/^{86}\text{Sr}$ = 0.712 to 0.715) at the bottom of the borehole. The largest scattering of O isotopic values could explain difference between strataboundary and fracture anhydrite, but the S value homogeneity of anhydritic veins denied this hypothesis. Moreover, S isotopes of sulphates fracture filling in Lower Triassic formation show non triassic marine sulphur and $^{87}\text{Sr}/^{86}\text{Sr}$ a continental fluid origin.

Sr ratio of stratabound deposits allowed us to identify continental fluid and Sulphur an autochthonous marine fluid. The scattering of oxygen values could indicate a reequilibration by burying or slight high temperatures.

Microthermometric and isotopic results of vertical veins light upon : meteoric water mixed marine fluids and fluid migrations.

An hypothesis, is fluid coming from Carboniferous formation with faulting activity. S, C and O isotopes of Carboniferous level show Sulphur with probable Stephanian origin, but Sr (0.710) allowed us to identify continental fluid or older Sr which has exchange with Sr matrix. Microthermometric data in dolomite and quartz show similar salinity of anhydrite (4 Meq NaCl) but slight low Th values 100 to 140 °C. Moreover, petrographic and Structural observations indicate later event probably during maximal burying stage.

These dolomitic and anhydritic deposition processes imply fluid overpressure linked up to non Triassic-Liassic reservoir during recurrent faulting of the margin. Changes of fluid compositions with depth between marine, evaporite and continental waters suggest several the fluid flow direction and discontinuity thermal events probably linked to faulting activity.

REFERENCES

- BERGERAT F. and MARTIN P. (1993) mise en évidence d'une tectonique distensive synsédimentaire et caractérisation du champ de contraintes au Trias inférieur-moyen sur la bordure vivaro-cévenole du bassin du Sud-Est de la France: La région de Largentière et le forage de Balazuc1 (programme Géologie Profonde de la France). C.R. Acad. Sci. Paris, 316. série II, p. 1279-1286.
- MOSSMANN J.R. (1995) Etude isotopique (C,O,S et Sr) des cimentations sulfatées et carbonatées des sédiments carottés à Balazuc (Lias inférieur-Carbonifère supérieur, forage BA1 Programme GPF-Ardèche, France) Rapport interne BRGM n 230.
- PAGEL M., BRAUN J.J., DISNAR J.R., MARTINEZ L., RENAC C. and VASEUR G. (1995) Thermal History constraints from organic matter, clay minerals, fluid inclusions, apatite fission tracks and stable isotopes studies at the Ardeche Paleao-Margin (Bal drill Hole, GPF program, France) 25p submitted to Marine petrology.
- VINCHON C., ARBEY F., CROS P., GIOT D. and JEANNETTE D. in press.(1995) Behavior of initial reservoirs during sedimentary burial and tectonic diagenesis, Balazuc 1 borehole, Ardeche, France, GPF program: Marine and Petroleum Geology.

GAS MIGRATION AND ACCUMULATION ALONG LINEAMENT STRUCTURES - LOWER SAXONY BASIN (NW GERMANY).

REUTEL, C. (1), LUDERS, V. (2), HOTH, P. (2) & IDIZ, E.F. (3)

- (1) GEOLINK Inc. Göttingen, Gervinusstr.5 D-37085 Göttingen
- (2) GeoForschungsZentrum Potsdam, Telegrafenberg D-14473 Potsdam
- (3) BEB Erdgas und Erdöl GmbH, Riethorst 12 D-30659 Hannover

The Lower Saxony Basin in NW Germany forms part of the Southern Permian Basin gas province in Central Europe. Commonly, methane-rich gas generated from Upper Carboniferous sediments and accumulated in Permian sandstones and carbonates. A locally different situation is given for some gas deposits along a NW-NNW/SE-SSE striking lineament. Due to Cretaceous inversion tectonics blocks of Carboniferous sediments were uplifted some hundreds of meters in wrench structures and gas is trapped in open fissures. Vitrinite reflectance data of drilled profiles within these horst structures in the depth range of 3000 to nearly 4000 m vary between 3 and 4.2% Rm and are anomalous high compared with reflectance data of 1.2-2.0% Rm from similar depth intervals of several boreholes outside the lineament structure.

Aqueous fluid inclusions in carbonate- and quartz-bearing fissure mineralization of the uplifted Carboniferous sediments are characterised by low T_e values and final ice melting temperatures mostly below the eutectic point of the system NaCl-H₂O. According to the observed T_e values the solution can be interpreted in terms of the NaCl-CaCl₂-H₂O system with salinities of about 20 wt.% NaCl-CaCl₂ equiv. In few cases clathrate melting can be observed with final melting temperatures up to 20°C, indicating a dissolved gaseous component (CH₄?). The homogenization temperatures of primary and pseudosecondary inclusions in carbonates and quartz range between 210-230°C and 180-240°C, respectively.

Based on the phase transitions of monophase gaseous inclusions in quartz, nearly pure CH₄ or varying mixtures of CH₄ and CO₂ can be deduced as main components. Laser-Raman spectroscopical analyses yield compositions of 71-100 mol% CH₄, 0-28 mol% CO₂ and in few cases 1 mol% N₂ or > 1 mol% H₂S.

In contrast, gaseous inclusions in calcites hosted by the overlying Zechstein carbonates always contain H₂S in addition to CH₄ and CO₂, with largely varying compositions of 14-25 mol% CO₂, 5-60 mol% CH₄ and 18-76 mol% H₂S. The H₂S content of these inclusions is probably due to partial thermochemical sulphate reduction within the Zechstein rocks.

Assuming CH₄ saturation of the aqueous fluids during entrapment the P-T conditions can be reconstructed. The isochoric P-T projection indicates a slight trend of increasing temperature with depth (Fig.1). However, this conclusion cannot be drawn for pressures. Pressure estimations derived from Fig.1 show only little correlation with the original sampling depth assuming conditions of lithostatic pressures. Most of the inclusions reveal much higher pressures, which may be due to overpressure phenomena.

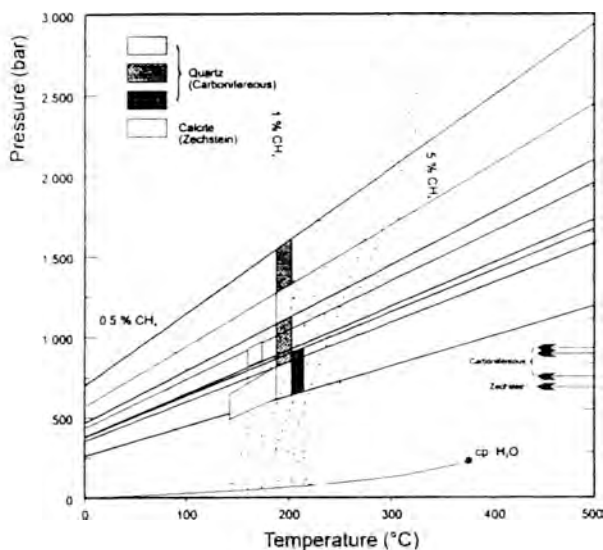
The geothermal gradient, which can be derived from homogenization temperatures of primary inclusions in fissure minerals from different levels of the wells, can be estimated between 58 and

64°C/km, indicating an enhanced heat-flow during fluid migration and entrapment. Further temperature estimates derived from vitrinite reflectance data and chlorite thermometry support the idea that the anomalous coalification history and the activity and evolution of hydrothermal fluids were influenced by a thermal event. Two explanations can be discussed:

coupling of an important erosion and a former higher geothermal gradient.

circulation of hydrothermal fluids in the tectonically activated area during uplift of the Carboniferous block

Taking in consideration the microthermometric results and important differences in the vitrinite reflectance as well as model temperatures of chlorites between boreholes which are only a few kilometres apart, the latter explanation must be favoured.



PT-diagram showing trapping conditions of primary cogenetic aqueous and CO₂-CH₄ ± H₂S inclusions from selected samples via isochore constructions. Isochores were calculated with FLINCOR[®] (dotted lines: aqueous inclusions, solid lines: CH₄-rich inclusions, fine dotted curves: saturation curves for 0.5, 1 and 5% CH₄). By assumption of CH₄ saturated H₂O at time of trapping, it can be concluded that homogenization temperatures of aqueous inclusions reflect original trapping temperatures (dashed vertical lines). Interception of these lines with methane rich inclusions approximate PT-conditions of trapping, shown as shaded areas for different inclusion arrangements from different samples.

MICROPROBE ANALYSIS OF SILICATE MELT INCLUSIONS IN QUARTZ FROM "STOCKSCHEIDER" PEGMATITE AT EHRENFRIEDERSDORF, ERZGEBIRGE, GERMANY

RHEDE, D. & THOMAS, R.

GeoForschungsZentrum, Telegrafenberg A50, D-14473 Potsdam, Germany

Silicate melt inclusions in rock-forming minerals may look very different at room temperature depending on the P-T-conditions of trapping and the cooling rate of the host rock. In many volcanic rocks, melt inclusions consist of glass (common, for example in quartz phenocrysts of rhyolite and in olivine or pyroxene phenocrysts of basalts). Due to the different thermal expansivities of melt and host crystal, such inclusions generally form a shrinkage bubble on cooling and closely resemble two-phase fluid inclusions under the microscope. Melt inclusions in slowly-cooled plutonic rocks on the other hand, are generally very small, average diameter less than 10 μm , and consist of crystallites of feldspar, micas and quartz; thus they are often overlooked or misidentified as solid inclusions. The fluid components of the melt inclusions, consisting mostly of H_2O and lesser CO_2 , are concentrated in the shrinkage bubble, the fluid sub-system.

The often extreme difficulties of studying melt inclusions in plutonic rocks are justified by the unique information they can provide. Intrusive rocks as exposed at the surface are the integrated products of a long and complex magmatic and, in some cases, postmagmatic development. Only in favorable cases will analysis of the solid rocks and minerals reflect the composition of the melt from which they formed. Thus the value of melt inclusions in igneous petrology cannot be overestimated. It is relatively straightforward to determine the solidus and liquidus temperatures, and to derive values of viscosity and equivalent water content of melt inclusions from heating and quenching experiments. Microprobe techniques are well-suited for chemical analysis of the melt inclusions but analyses are very difficult in practise. The purpose of this contribution is to discuss problems of analysing melt inclusions and give first results which show the promise of this approach.

Melt inclusions in plutonic rocks are multicrystalline at room temperature and volatile components are concentrated in the shrinkage bubble. Before analysis, therefore, the inclusions must be homogenized at liquidus temperature and quenched to a homogeneous glass. After quenching the sections are polished down until inclusions are exposed at the surface. The search for opened inclusions under the microprobe is best made with back-scatter electron images.

The homogenization and quenching procedure introduces several problems. First, excessive time and temperature of homogenization causes the inclusion walls to dissolve in the melt. Second, many inclusions decrepitate before complete homogenization; this problem can be avoided by heating under pressure. A further problem for the P- and F-rich compositions encountered in this

study (Table 1) is that some inclusions could not be quenched completely and skeletal crystals formed on cooling.

Table 1 shows the composition of several melt inclusion types found in pegmatitic quartz. These are attributed to different stages in pegmatite melt evolution and/or heterogeneity in the melt. Our analyses of more than 300 melt inclusions has shown that, at the time of trapping in quartz and feldspar, the melt was a suspension of a F- and P-rich silicate melt with minor immiscible phases of extremely P-rich melt, and crystals of quartz, feldspar, apatite, triplite, berlinite, topaz and other solids. Moreover, during crystallization, a KCl- and NaCl-rich fluid was exsolved, leading to coexisting melt- and fluid inclusions. The compositions of the melt inclusions from more simple granitic melt (1) to the highly-evolved pegmatitic composition (2, 3), extreme volatile-rich melt (4) and globules of immiscible P- and Fe-rich melt (5) are shown in the table.

Table 1. Composition of melt inclusions in quartz from the "stockscheider" pegmatite, melt(1)- granite (aplitic phase), melt (2) and(3)- pegmatitic phase, melt (4) - volatile-rich phase and melt (5)- globules of immiscible high - P glass

	melt (1) (n=8)	melt (2) (n=9)	melt (3) (n=28)	melt (4) (n=3)	melt (5) (n=3)
P ₂ O ₅	0,07	0,20	3,65	8,75	37,75
SiO ₂	72,82	72,14	69,98	57,83	1,00
TiO ₂	0,02	0,12	0,03	0,04	0,06
Al ₂ O ₃	13,79	17,65	15,69	21,65	3,16
FeO	1,02	2,21	0,38	0,54	43,34
MnO	0,06	0,16	0,05	0,10	5,28
MgO	0,08	0,02	0,01	0,00	0,00
CaO	0,13	0,03	0,06	0,16	0,57
Na ₂ O	2,84	2,34	2,66	2,31	4,91
K ₂ O	5,88	3,43	3,49	5,95	0,35
F	<0,02	1,04	3,44	2,01	2,02
Cl	<0,02	0,10	0,08	0,16	0,82
Total	96,71	99,44	99,52	99,50	98,74
O=F	0,00	-0,44	-1,45	-0,85	-0,85
O=Cl	0,00	-0,02	-0,02	-0,04	-0,18
Total	96,71	98,98	98,05	98,61	97,71

MAGMATIC PROCESSES AS VIEWED FROM FLUID INCLUSION STUDIES

ROEDDER, E.

Harvard University, Cambridge, MA 02138, USA

A brief review of the entire range of magmatic inclusion studies, gas, liquid, and glass, giving the present status of methods of study analysis. In particular, some of the newer analytical methods for trace elements in inclusions are helping in the solution of geological problems:

Rare earths in fluid inclusions by inductively coupled plasma mass spectrometry (ICP-MS). The REEs have been excellent tracers for the evolution of rocks in a host of problems in igneous petrology, and ICP-MS has been in use for years for the analysis of major constituents in fluid inclusions. But now it is possible to get valid REE patterns on the tiny amounts present in the fluid inclusions. The results provide valuable constraints on the source and evolution of the fluids.

Heavy metals in inclusions by synchrotron X-ray fluorescence (SXRF). This method also has been used in several groups for some years for semiquantitative results, and is being improved rapidly. At present the data look good for most heavy metals in the ppm range on individual <10 micrometer inclusions, and have proved particularly valuable in understanding the processes of ore transport and deposition. Measurement and corrections for individual inclusion parameters still provide the major hurdles for truly quantitative analysis.

Ca, Cl, K, Br, I, Se, Ba+Te, U, and isotopes of Ar, Kr, and Xe in inclusions, by laser microprobe noble gas mass spectrometry (LMNGMS). This has also been around for several years now, but the leader in the field, James Irwin of Scripps, has greatly improved the sensitivity and accuracy. It has a wide range of possible applications for tracing the source and evolution of the fluids present during various geological processes.

FLUID INCLUSIONS ASSOCIATED TO GOLD QUARTZ VEINS IN DIAMANTINA AND COSTA SENA, MINAS GERAIS, BRAZIL: A COMPARATIVE STUDY.

RONCHI, L.H. (1), FOGACA, A.C.C. (2), FUZIKAWA, K.(3), GIULIANI, G.(4) & PIMENTA, M.(5)

(1)-Universidade do Vale do Rio dos Sinos - UNISINOS, Depto de Geologia, Caixa. Postal 275, 93.022-000 Sao Leopoldo, RS, Brazil;

(2)-UFMG, Inst. Geociências, Belo Horizonte, Brazil;

(3)-CNEN/ CDTN, Supervis o de Técnicas Especiais, Belo Horizonte, MG, Brazil;

(4)-ORSTOM-CRPG, France;

(5)-UFMG, Depto Física, Belo Horizonte, MG, Brazil.

During the 17th and beginning of the 18th century Brazil, a colony of Portugal, was the world leading gold producer. Part of production came from Diamantina region, in Minas Gerais Province. Gold was present in sedimentary detrital deposits (conglomerates and recent placer deposits) and in quartz veins. Nowadays the production is small and the yield is due to garimpeiros (gold diggers). Ancient mines like Mil Oitavas, near Diamantina or new occurrences like Periquito, near Costa Sena village - 60km south of Diamantina - are from time-to-time reopened for diggings, producing some gold. A comparative study of these two mines reveals similarities in their paragenetic association and fluid inclusion characteristics. At the Mil Oitavas mine the quartz vein - average thickness of 20cm - are hosted by a grey altered phyllite with magnetite, sericite, chlorite and graphite in thin beds. These phyllites are considered to be of Proterozoic age. They present a compositional banding (S_0) paralel to the foliation S_1 and exhibiting crenulation. The quartz veins roughly follow the regional foliation (N10E, 40-45 SE). The mineral association includes specularite, magnetite and rutile. The U/Pb age in the latter mineral indicated 620 M.a. in spite of large analytical error (20%), and can be correlated to the Brasiliano cycle (Abreu et al., 1992). Native gold visible to the naked eye, is disseminated in fractures or associated with clays in boxworks.

The fluid inclusions are similar to those described at Costa Sena (Ronchi et al., 1991) and they have been classified in three main types of inclusions: Type C, Type L and Type M.

Type C - three phase, aquo-carbonic fluid inclusions. They occur either isolated (primary inclusions) or in leaked fractures in intracrystalline trails (pseudo-secondary inclusions) reaching 100mm in size. Calcite trapped in these inclusions can also be found as solid inclusions in quartz, reinforcing the criteria for primary origin. The degree of filling of the carbonic phase ranges from 5 and 30% and necking down is a frequent feature. Raman multichannel micro-spectrometry indicated pure CO₂ in the carbonic phase. The microthermometric data confirmed the Raman analysis and indicated salinity of 10-15 wt% eq. NaCl. The homogenization and decrepitation temperatures are in the range from 200 to 250°C.

Type L - Two phase, aqueous inclusions. They occur as fluid inclusions in intracrystalline healed fractures (probably pseudo-secondary) in 25µm to <100µm. The salinity is variable between 10 to 15 wt% eq. NaCl and homogenization temperatures are in the range 130 - 180°C.

Type C and type L inclusions may occur associated in the same healed fracture. Necking down is responsible for much of the scatter in microthermometric data.

Type M - one phase, aqueous inclusions. They are small (<1 μ m to 10 μ m), and all secondary in origin.

The results of fluid inclusion study of free gold-bearing quartz veins at Costa Sena (Ronchi et al., 1991) where aquo-carbonic (type C inclusions) and aqueous (type L inclusions) fluids were present have been repeated in the Diamantina district. The early stage aquo-carbonic fluid, represented by type C fluid inclusions, progressively mixed with an aqueous fluid, represented by type L fluid inclusions, at around 350°C and 2.0-2.5kb, by an aqueous fluid. The fO_2 of the aquo-carbonic fluid estimated by the presence of specularite/hematite and absence of sulphides in the veins, is closed to the Fe_3O_4 - Fe_2O_3 buffer. Deposition of gold is ascribed to the destabilisation of $AuCl_2^-$ complexes in the incoming fluid as a result of the dilutional process, leading to a pH increase of the fluid at a relatively constant fO_2 .

The similarity of fluid inclusions and their analytical results found in Costa Sena and Diamantina point out to similar parameters controlling the gold deposition in quartz veins in this whole area.

References

- ABREU, F.R., SANTOS, G.G.V. & SCHRANK, A. (1992) Estudo das mineralizações auríferas filoneanas da região da cidade de Diamantina/MG. In 37º Cong. Brasileiro de Geol., SBG/SP, Sao Paulo, SP. Boletim de resumos expandidos, vol. 1, p. 229.
- RONCHI, L.H., GIULIANI, G., BENY, C., FOGAÇA, A.C.C. (1991) Physico-Chemical evolution of the fluids associated to the Costa Sena gold quartz veins (MG - Brazil). ECROFI XI, Firenze, april, 1991, In: Plinius, Supplemento Italiano all'European Journal of Mineralogy, 5 : 185-186.

FLUID INCLUSIONS AND ISOTOPE DATA FROM A PHREATIC BRECCIA OF THE MONTEVERDI 5A WELL (LARDERELLO GEOTHERMAL FIELD, ITALY).

RUGGIERI, G. (1) & GIANELLI, G. (1)

(1) International Institute for Geothermal Research, Pisa, Italy

In the geothermal field of Larderello, a level of phreatic breccia was recently found at 1090 m below ground level (b.g.l.) in the well MV5A, drilled by the Italian National Electricity Board (Enel). Gianelli and Bertini (1993) estimated a minimum temperature of 325°C at its formation and assumed that the pressure evolved from lithostatic to hydrostatic after the hydraulic fracturing. In-hole temperature, at 1090 m b.g.l., is 160°C. Well MV5A produces super-heated steam from the bottomhole (3500 m b.g.l.). At Larderello, down-hole fluid sampling is greatly hindered by flashing phenomena. For this reason, few data are available on the characteristics of the liquid phase that it is presumed coexists with the vapour at depth.

Fluid inclusion studies and isotope analyses on the breccia cement were carried out in order to reconstruct the physico-chemical nature and the evolution of the fluid that circulated in the hydrothermally fractured zone of the well, and to compare it with the present geothermal fluids.

The breccia forms a 20 cm thick level in a 9 m core sample of a low-grade metamorphic sandstone of the Verrucano Formation (Upper Triassic), consisting of quartz, white mica and minor hematite. The breccia is constituted by angular to subangular millimetric to centimetric clasts of the sandstone in a cement consisting of calcite, chlorite, dolomite with minor amounts of quartz, anhydrite, albite, hematite and apatite. Textural relationships reveal three stages of hydrothermal deposition. Calcite, chlorite and minor apatite constitute the first stage assemblage. The second stage is characterized by the association of dolomite, quartz, albite and chlorite. The deposition of anhydrite characterizes the last hydrothermal stage.

Preliminary microthermometric measurements were carried out on fluid inclusions hosted in the calcite and in one anhydrite crystal. Three types of inclusions were identified in the calcite: 1) One-phase (vapour) or sometimes two-phase (liquid+vapour) vapour-rich inclusions (V). Many of the V inclusions were considered to be primary. At low temperature, few of the V inclusions showed the presence of solid CO₂, which dissolved between -62.0/-58.3°C; final ice melting temperature (T_{mic}) was observed in the range of -2.2/-1.2. Clathrate formation indicated that some CO₂ is present in most of the V inclusions. Clathrate melted between 4.6/6.3°C. No liquid CO₂ was observed. Homogenization temperature to the vapour (Th_v) varied from 225 to more than 300°C. The wide range of Th_v is probably due to heterogeneous trapping of some liquid together with vapour.

2) Two-phase (liquid+vapour), low-salinity liquid-rich inclusions (L1). Some L1 inclusions were primary and appeared to be contemporaneous with V inclusions. T_{mic} occurred between -3.3/-

1.5°C, giving a salinity of 2.5/5.3 wt% NaCl eq.. Homogenization temperatures to the liquid (T_{HL}) were between 203/240°C.

3) Two-phase (liquid+vapour) relatively high-salinity liquid-rich inclusions (L2). L2 inclusions were only observed along one secondary trail. They displayed T_{mice} between -4.7/-6.1°C, which correspond to a salinity of 7.4/9.3. wt% NaCl eq.; T_{HL} were in the range of 321/334°C.

Two types of inclusions were observed in the anhydrite:

1) One-phase (vapour) inclusions. Microthermometry was not performed on these inclusions because they were too small.

2) Two-phases (liquid+vapour) liquid-rich inclusions (L). Few L inclusions show primary features. T_{mice} occurred at around -3.0°C corresponding to a salinity of 4.5 wt% NaCl eq., T_{HL} were between 140/165°C. L inclusions appeared to coexist with V inclusions.

The occurrence of contemporaneous liquid-rich and vapour-rich inclusions in calcite and anhydrite indicate that these minerals crystallized from boiling fluids. The T_{HL} of the liquid-rich inclusions are thus equal to their trapping temperature. The above data indicate that a boiling two-phase fluid constituted by a liquid low-salinity (2.5/5.3 wt% NaCl equiv.) fluid and an aqueous, CO₂-bearing vapour phase were present in the hydrothermally fractured zone. A similar two-phase fluid can be present today in the reservoir. The hydrothermal fluid evolved from a temperature of about 325°C (breccia formation) to 200/240°C (carbonate deposition) to 140/165°C (anhydrite deposition). The latter temperature is consistent with the present day temperature (160°C). No change in salinity with time was evidenced in the studied inclusions. Sporadic inflow of high temperature, relatively high-salinity fluids at 1090 m was also recorded by secondary fluid inclusion. Recurrent inflow of hot fluids at a relatively shallow level can trigger hydraulic fracturing in zones of tectonic weakness and it is very important in maintaining the permeability of the reservoir rocks.

Isotope analysis on the carbonate cement showed that the $\delta^{13}C$ and $\delta^{18}O$ of the calcite are -7.00‰ PDB and 10.69‰ SMOW respectively. The computed values of $\delta^{13}C$ and the $\delta^{18}O$ for the CO₂ in equilibrium with calcite, for a temperature of 223°C (from the average T_{HL} of L1 inclusions), are -6.13‰ and +19.9‰ respectively. Similar $\delta^{13}C$ and $\delta^{18}O$ values were found in the CO₂ produced in the field, even if the $\delta^{13}C$ data falls close to the lower limit. The computed $\delta^{18}O$ value for H₂O (vapour) in equilibrium with calcite gives a value of 0.24‰, which is also consistent with the more positive values of the steam produced in the field. These data indicate that the carbonate cement was deposited by a fluid in equilibrium with a vapour phase similar to the present geothermal fluid.

References:

Gianelli G. and Bertini G. (1993). Natural hydraulic fracturing in the Larderello geothermal field: evidence from well MV5A. Boll. Soc. Geol. It., 112, 507-512.

DEVELOPMENT OF PIXE AND THE PROTON MICROPROBE AND THE NON-DESTRUCTIVE ANALYSIS OF FLUID INCLUSIONS IN MINERALS

RYAN, C.G.

CSIRO Exploration and Mining, PO Box 136, North Ryde NSW 2113, Australia

The study of ore forming fluids trapped as fluid inclusions in minerals is the key to understanding fluid flow paths at the time of ore formation and to predicting the location of ore bodies within large-scale magmatic hydrothermal systems. Large penetration depths and the predictable nature of MeV proton trajectories enables modelling of PIXE yields and the development of standardless quantitative methods. This permits microanalysis of minerals at ppm levels, and more recently has enabled the development of methods for quantitative trace-element imaging and quantitative, non-destructive analysis of individual fluid inclusions. This paper reports on recent developments in Proton Microprobe techniques with special emphasis on ore systems and fluid inclusion analysis.

Recent advances in fluid inclusion analysis at the CSIRO have come from improvements in modelling of PIXE yields from the complex 3D geometry of the inclusion in its host mineral (Ryan *et al.*, 1993), and from the use of beam-scanning to control the proton dose distribution across an inclusion (Ryan *et al.*, 1995). The method has been tested using synthetic fluid inclusions in quartz. Inclusions, 5-20 μm in diameter, were probed using 3 MeV protons, and the geometry of each inclusion was determined by optical microscopy, and the depth was inferred from the fit to the Cl Ka/Kb ratio. Expected X-ray yields per ppm were calculated with the GeoPIXE software (Ryan *et al.*, 1993,1995). The results demonstrate an accuracy of ~10-15% (Ryan *et al.*, 1995; Fig. 1).

Collaborative research at the CSIRO has focused on the analysis of ore elements in fluids and experiments to study chalcophile element partitioning between crystalline material and magmatic fluids (Ballhaus *et al.*, 1994). Much of this work is centred on the analysis of hydrothermal fluids associated with copper-gold deposits. A good example is the Kidston granite-related breccia gold-copper deposit in North Queensland, Australia. Brine and vapour inclusions showed strong partitioning of Cu into the vapour phase and the presence of S in the vapour (Heinrich *et al.*, 1993a; Fig. 2). A similar effect was observed in the Yankee Lode Sn deposit in Northern NSW (Heinrich *et al.*, 1993b) where it was concluded that brine-vapour segregation of trace metals, and transport in the vapour phase, plays an important role in Cu deposit formation. They argued that if a S complex is responsible for partitioning of Cu into the vapour, then Au is predicted to show a more extreme behaviour. This helps to understand the formation of deposits such as Kidston in terms of vapour transport of Cu and Au.

The detailed PIXE analyses of the more primitive brines, which are closely related to the fluid exsolved from the granite, also provide starting compositions for modelling the formation of ore

deposits. Modelling of progressive cooling of the brine composition, given by PIXE analysis of brine inclusions from Yankee Lode, with addition of meteoric water was used by Heinrich and Ryan (1992) to explain the detailed zonation of ore deposits in the Mole Granite. The model predicted the sequence of ore deposition from cassiterite, through arsenopyrite, chalcopyrite, galena and sphalerite, to pyrite in the country rock. This is in general agreement with the regional distribution of Sn, Ag and base metal deposits away from the Mole Granite (Heinrich and Ryan, 1992), and illustrates the usefulness of PIXE analysis in the study of hydrothermal processes.

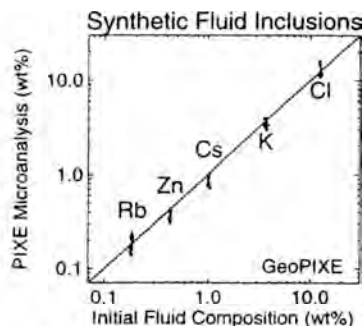


Fig. 1 Results of PIXE analysis of synthetic inclusions in quartz.

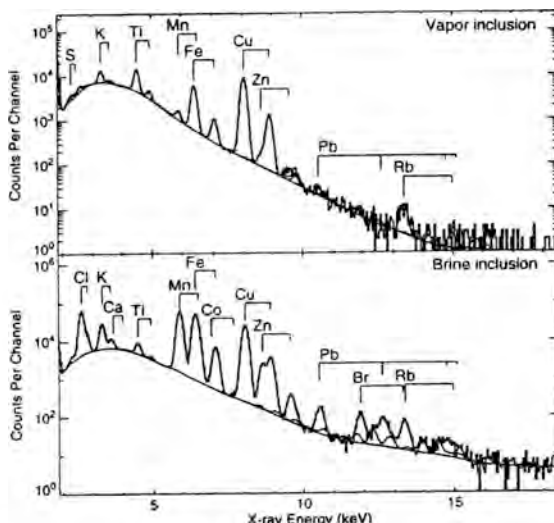


Fig. 2 PIXE spectra from vapour (top) and brine (bottom) fluid inclusions in quartz from the Kidston copper-gold deposit, Queensland, analyzed using a 3 MeV proton beam.

References:

- Ballhaus, C., C.G. Ryan, T.P. Mernagh and D.H. Green (1994), *Geochim. et Cosmochim. Acta* 58, 811-826.
 Heinrich, C.A., and C.G. Ryan (1992), in *Proc. 7th Int. Symp. on Water - Rock Interaction*, p. 1583-1587.
 Heinrich, C.A., C.G. Ryan and T.P. Mernagh (1993a), "Ore Metals in Magmatic Brine and Vapour: New Evidence from PIXE Micronalysis of Fluid Inclusions", Abstract, 'Specialist Group in Economic Geology' meeting, Armidale, 2-6 February 1993.
 Heinrich, C.A., C.G. Ryan, T.P. Mernagh and P.J. Eadington (1993b), *Economic Geology* 87, 1566-1583.
 Ryan, C.G., C.A. Heinrich and T.P. Mernagh (1993), *Nucl. Instr. Meth.* B77, 463-471.
 Ryan, C.G., Heinrich, C.A., Van Achterbergh, E., Ballhaus, C., and Mernagh, T.P., (1995), *Nucl. Instr. Meth. B*, in press.

HIGH-SALINITY BRINES IN ECLOGITIZED METABASITES AS THE RESULT OF ROCK HYDRATION DURING HIGH PRESSURE METAMORPHISM (MT. EMILIUS AUSTROALPINE UNIT, ITALIAN WESTERN ALPS).

SCAMBELLURI, M. (1), PHILIPPOT, P. (2) & PENNACCHIONI, G.(3)

- (1) Dipartimento di Scienze della Terra, Genova, Italy
(2) Laboratoire de Petrologie, CNRS-URA736, Paris, France
(3) Dipartimento di Geologia, Padova, Italia

Fluid-induced eclogitization of granulite-facies rocks has been described in a variety of high pressure terranes (Austrheim, 1987; Andersen et al., 1993). The fluids trapped in syn-metamorphic veins and in eclogitic minerals as primary fluid inclusions, can give information on the nature and chemistry of the high-pressure fluids, and on deep fluid-rock interaction processes. By means of a study of fluid inclusions from omphacite veins in the Mount Emilius crustal Austroalpine unit, we want to emphasize the control exerted by hydration processes at eclogite facies conditions on the composition of the coexisting fluid and on rock rheological behaviour.

The Mount Emilius unit consists of garnet + kyanite + chloritoid - to garnet + glaucophane - bearing micaschist, derived from Alpine eclogitic reequilibration (1.3 Gpa and 450-500°C) of precursor pre-Alpine paragneiss. Micaschists include numerous pods of two types of eclogitic metabasites: (1) garnet + omphacite + glaucophane + epidote + phengite + rutile banded eclogite; (2) garnet + clinopyroxene + tremolite + zoisite + sphene ± Mg-chlorite metabasite, deriving from pre-Alpine garnet + clinopyroxene + plagioclase + hornblende granulite. Bulk-rock compositions indicate that higher contents of Na₂O, SiO₂ and lower X_{Mg} and H₂O of the banded eclogite with respect to metagranulites control the different high-pressure parageneses, as well as the composition of clinopyroxenes (J/Q ratios are from 0.3 to 1 in metagranulite and from 0.8 to 1.7 in eclogites; J=2Na, Q=Ca+Mg+Fe). Omphacite-bearing veins developed in both types of metabasites: in eclogites the veins commonly postdate a stage of high pressure ductile deformation, whereas in eclogitized granulites the veining episode separates two distinct events of eclogitic ductile deformation. The vein clinopyroxenes (J/Q between 0.1 and 0.8 in metagranulite, and between 0.7 to 1.2 in eclogite) largely overlap the compositions of the pyroxenes of the host rocks. This suggests that the vein filling material is locally derived.

All veins contain abundant primary to pseudosecondary fluid inclusions trapped along the growth zones of sector-zoned omphacite, or disposed parallel to the long axis of pyroxene fibres in syntaxial stretched crystal type of veins. The fluid inclusions fall into two main categories: (1) type A two-phase aqueous inclusions (liquid + vapor; liquid/vapor ratios = 20-25% volume); (2) type B three phase inclusions (liquid + vapor + a salt cube). Most of these inclusions shows depression of the eutectic melting between -28 and -50°C, suggesting the presence, besides NaCl, of extra components such as CaCl₂ and MgCl₂. Average salinity estimates of type A inclusions is of 20-25 wt% salts. Inclusions with lower salinity (10-15 wt% NaCl equivalents) are

also present. Halite dissolution temperatures of type B inclusions indicate salinities between 33 to 46 wt% salts. CaCl_2 content of type B inclusions ranges from 1 to 4 wt%. No CO_2 , H_2S , CH_4 and N_2 have been detected using Raman techniques. These data indicate that the fluid populations filling the eclogitic veins in both the eclogite and metagranulite host rocks contain moderate to highly saline aqueous brines of similar composition. Eclogitization of the metagranulite is driven by infiltration of aqueous fluids dehydrating micaschists during high-pressure metamorphism. Compared to fresh mafic granulite of the Ivrea Zone (analogous to the Mt. Emilius granulite precursor) metagranulites display a bulk enrichment of 1 to 2 wt% H_2O . Eclogitic equilibration of metagranulite occurred through pervasive replacement of plagioclase and hornblende into finegrained hydrous mineralogy during early stages of fluid infiltration. This process favored strain softening and allowed ductile deformation to proceed. The effect was progressively counteracted by syn-kinematic growth of hydrous minerals along shear zones, which reduced the amount of fluids wetting the grain boundaries, led to strain hardening and finally to veining. The progressive water consumption during growth of hydrous phases, increased salinity of the metamorphic fluid and led to entrapment in the veins of a residual high-salinity brine. A similar mechanism may be proposed for the development of the foliation plane and of the veins observed in the banded eclogites.

References

- Austrheim H., 1987. Earth and Planet. Science Letters, 81, 221-232.
Andersen T., Austrheim H., Burke E., Elvevold S., 1993. Chemical Geology, 108, 113-132.

HIGH-PRESSURE VEINING AND FLUID INCLUSIONS IN AN ALPINE ECLOGITIZED PERIDOTITE: RECYCLING OF OCEANIC FLUIDS?

SCAMBELLURI, M., ROBBIANO, A., & PICCARDO, G.B.

Dipartimento di Scienze della Terra, Genova, Italy

The Erro-Tobbio peridotite is a slice of subcontinental mantle emplaced at the ocean floor during rifting and opening of the Ligurian Tethys. The peridotite was intruded by gabbroic and basaltic dikes. Sea-floor hydration of these rocks is followed by Cretaceous subduction to 75 km and 600°C leading to coeval formation of eclogitic assemblages in the mafic dikes and of olivine + antigorite + titanian clinohumite + chlorite ± diopside in the peridotite. The eclogitic event in the peridotite occurs through partial rock dehydration and formation of widespread vein systems containing olivine + titanian clinohumite + chlorite + diopside in variable modal proportion. Apatite is locally present in veins close to dikes of metagabbro. At high pressure the ultramafic rocks still contain a considerable amount of volatiles bounded in hydrous minerals and occurring as a free phase trapped in fluid inclusions within vein forming minerals. Aim of our study is to define the composition of pre-eclogitic minerals and of the fluid inclusions trapped in the high pressure veins.

Early ocean floor and prograde assemblages are still preserved in the low strain domains of the peridotite body, where the mantle assemblage (orthopyroxene + clinopyroxene + spinel ± plagioclase ± amphibole) is statically overgrown by several generations of serpentine and chlorite. The earliest assemblages include chlorite, serpentine, brucite and a fillosilicate consisting of mixed chlorite/biotite layers. Serpentine and brucite may contain up to 0.35 wt% chlorine, and the mixed chlorite/biotite layers show up to 5 wt% K₂O and 0.3 wt% chlorine. These features denote interaction of the mantle peridotite with seawater presumably occurred at ocean floor environments. The high pressure phases antigorite, chlorite, olivine and titanian clinohumite do not contain any of the above elements.

The fluid inclusions analyzed are from high pressure veins within the peridotite. In some high strain domains, the veins are stretched and transposed along olivine shear band systems related to the high pressure event. The fluid inclusions mainly occur within diopside as clusters of tubular fluid inclusion parallel to the {010} face of pyroxene. The inclusion tubes are not disposed along fractures and never cut the grain boundaries. When diopside is dissected by the syn-eclogitic olivine shear bands, the inclusion clusters also change orientation, following that of pyroxene and do not cut the subgrain boundaries of deformed clinopyroxene. Such textures testify that inclusion entrapment predates the eclogitic deformation and is related to crystallization of diopside during an early eclogite stage of veining. The primary inclusions (5 to 30 microns) are mostly three phase (liquid+vapor+halite) and may contain additional solid phases consisting of magnetite, ilmenite and locally quartz. The

three phase inclusions may be associated with two phase inclusions showing a liquid + vapor assemblage at room temperature. During freezing the two phase inclusions usually precipitate a salt cube, suggesting that their salinity is close to halite saturation (about 20 wt% NaCl equivalents). In all analyzed inclusions, the total range of initial melting recorded extends from -39 to -26°C, which can be taken to imply the presence of MgCl₂ and probably KCl in the fluid. Halite dissolution temperatures in the three phase inclusions (315 to 380°C) point to salinities of 40 to 45 wt% NaCl equivalents. These data testify for an aqueous saline brine containing 20 to 45 wt% dissolved NaCl, KCl and MgCl₂. SEM analyses on thin section plates polished with a petroleum distillate (to avoid salt dissolution during sample preparation) have been made on the daughter salts of three phase inclusions, and on some naturally decrepitated two phase inclusion. Due to the small size (a few microns) of the daughter salts and of the salt rims surrounding the decrepitated inclusions, the analyses done mainly represent the host vein mineral (olivine, titanian clinohumite and diopside), but are characterized by significant amounts of Cl, Na₂O, K₂O. MgO contents significantly higher than those usually measured in the host minerals attest the presence of Mg in the daughter chloride. The SEM qualitative data thus confirm that the daughter salts are mixtures of NaCl, KCl and MgCl₂.

The fluid inclusion analysis demonstrates that saline aqueous fluids containing Na, K and Mg chlorides were present in the peridotite at an early stage of eclogite-facies metamorphism. Alkalies, chlorine and water were incorporated in serpentine and chlorite at the seafloor; breakdown of such minerals thus influences the composition of the fluid released at high pressure. Rock control on the fluid composition is also suggested by the presence of magnesium chloride in the peridotite fluid. The presence of apatite in veins opening close to gabbroic dikes further confirms that the fluid composition is locally controlled by rock variabilities. The deposition of high pressure veins containing hydrous assemblages determines consumption of water from the aqueous fluid and may result in increase in the bulk fluid salinity.

FLUID INCLUSION STUDIES IN EPITHERMAL AURIFEROUS-QUARTZ DEPOSITS OF MACIZO DEL DESEADO, SANTA CRUZ, ARGENTINA.

SCHALAMUK, I.A. (1), RIOS, F.J. (2), FUZIKAWA, K. (2), PIMENTA, M.A. (3)

- (1) UNLP-CONICET, La Plata, Argentina.
- (2) CNEN-CDTN, Belo Horizonte, MG, Brasil.
- (3) UFMG-ICEX, Belo Horizonte, MG, Brasil.

Fluid inclusion (FI) studies were carried out on samples from five localities in the Macizo Del Deseado, Santa Cruz Province. They consisted of microscopy, microthermometry and microRaman spectroscopy. Figure 1 is the histogram for all Th obtained in this study.

The Macizo del Deseado became an area of high exploration interest following the discovery of important Au/Ag-bearing quartz veins. They are of the low sulphur epithermal adularia-sericite mineralization type. The Bajo Pobre and Dorado/Monserrat veins are hosted by andesites and basalts of the mid-Jurassic age whereas the Cerro Vanguardia and Manantial Espejo veins are in a volcano-piroclastic complex of middle to upper Jurassic age (Chon Aike Formation). The latter has an extensive areal distribution consisting basically of ignimbrites and piroclastic breccias of rhyolitic composition. The El Macanudo siliceous vents are lateral exposures of sinter crusts deposited on ignimbrite covers. In the El Macanudo area four thin sections from different concentric vent layers showed a dominance of chalcedony with quartz in limited areas. The few FI detected were primary, small (< 5µm), and always monophasic. Freezing studies were unable to show noticeable phase changes or nucleation of vapor phases pointing to a very low FI formation temperature (<70°C).

Samples from Bajo Pobre area presented many FI in growth zones (primary) of quartz crystals. One phase FI dominate over the two phase ones. The aqueous fluid indicated almost pure water (0.18-0.35 wt% NaCl equiv.). The measured Th may be somewhat lower than the highest values (~230°C, Fig. 1) as necking down is a common feature. In the Manantial Espejo area, Rios et al. (1994) indicated low salinity (4 wt% NaCl equiv.) aqueous FI in quartz from Veta Maria. A sample from a breccia pipe indicated higher salinity (5.0-6.6 wt% NaCl equiv.). Quartz crystals from both samples present growth zones with decreasing Th: from 300 to 180°C in the vein and from 240 to <160°C in the breccia.

In the Dorado/Monserrat area barite which is of late stage paragenesis presented only one phase FI of fairly large size (~15 µm), with $T_{mice} = -1.0^{\circ}C$ (1.74 wt% NaCl equiv.). Common occurrence of superheated ice metastability precluded further measurements. FI in quartz indicated salinities of 0.71-1.4 wt % NaCl equiv. and Th in the range of 190-280°C.

At Cerro Vanguardia deposit quartz from Atila vein presented fairly good FI related to growth zones. The T_{mice} all fell in the narrow range of -0.2 to 0.0°C (0.35 wt% NaCl equiv.). The T_h were between 200 and 310°C, the highest T_h found in this study.

The obtained composition and temperatures of fluids fit well within the values known for veins in volcanics of epithermal Au deposits (Roedder, 1984 - Table 15-4). They are also consistent

with studies on conditions of Au deposition in these environments (Berger and Henley, 1989). If the temperature is one of key factors in Au precipitation as is suggested by these authors (Fig.2) it fits well in our case: Cerro Vanguardia, Manantial Espejo, and Dorado/Monserrat which presented the highest T_h values are the areas with richer Au mineralization. Mineralization is poor or non existent at Bajo Pobre and El Macanudo where the T_h is below 200-220°C. In these areas, deeper levels where the temperatures reach values equivalents to Cerro Vanguardia and Manantial Espejo, may prove to be the places with Au precipitation. The correlation between Au mineralization and T_h of FI in quartz is a prospecting tool worth further testing in Chon Aike formation quartz veins.

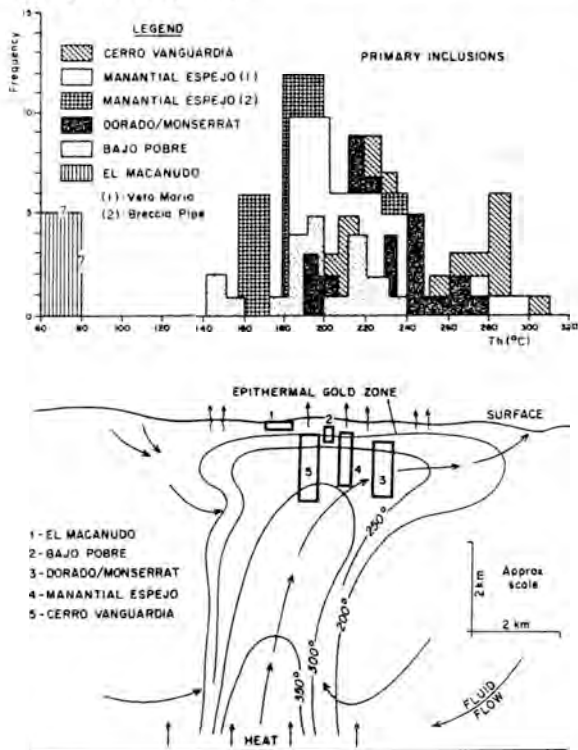


Fig. 1: Composed histogram of aqueous two-phase FI homogenization temperatures from the studied areas.

Fig. 2: Cross section showing isotherms of a geothermal system to indicate levels of FI entrapment in the studied areas. (adapted from Berger and Henley, 1989).

References

BERGER, B.R. and HENLEY, R.W., 1989. Economic Geology Monograph 6, 405-423.
 RIOS, F.J., FUZIKAWA, K., SCHALAMUK, I., PIMENTA, M.A., 1994. II Reun. de Min. y Metalog., Publ. del INREMI, UNLP, n° 3, 345-351.
 ROEDDER, E., 1984. Fluid Inclusions. Min. Soc. America, Reviews in Mineralogy 12, 644p.

GOLD MINERALIZATION AND REGIONAL FLUID MOBILIZATION DURING THE EBURNEAN CRUSTAL CONSOLIDATION IN GHANA, WEST AFRICA

SCHMIDT MUMM, A. (1),, BLENKINSOP, T. (2) & OBERTHÜR, T.

(1) Institut für Geologische Wissenschaften, Domstr. 5, D-06108 Halle

(2) Geology Department, University of Zimbabwe, P.O. Box MP 167, Harare, Zimbabwe

(3) Bundesanstalt für Geowissenschaften und Rohstoffe, Stilleweg 2, D-30655 Hannover

The Ashanti Belt in Ghana, striking in NE-SW direction over more than 250km, hosts numerous epigenetic gold deposits, which formed during the Eburnean tectonothermal event at ca. 2100Ma. Gold mineralization, hosted by greenschist metamorphic Birimian and Tarkwaian sediments, volcanics and also late kinematic granitoids is commonly associated with quartz veins or sulfide bearing strata with auriferous arsenopyrite and pyrite. High gold concentrations are found in:

a) quartz reefs within major transcrustal shear zones and dispersed in the adjacent wallrock. Gold is mostly free gold. Locally a selvage enrichment (e.g. Ashanti, Konongo, Prestea) may carry significant amounts of gold in sulfides; notable is also an intense graphitization in the sheared wallrock units.

b) stockwork in impregnated, carbonatized granite (Ayanfuri) in close spacial association with a mineralized shear zone, and

c) gold in stockwork and disseminated in the country rock, associated with silicification in an anticlinal position, e.g. Abosso-Damang.

The ore mineral paragenesis varies but is dominated by free gold and gold in arsenopyrite and pyrite. Galena, chalcopyrite and sphalerite are rare accessories. Structural investigations in the Ashanti, Konongo and Prestea deposits show that Birimian and Tarkwaian rocks were deformed jointly during a single episode of the progressive Eburnean deformation. Mineralization hosting shear zones are developed in positions of axial planar S0 (bedding) and S1 (foliation). Kinetic analyses of structural data by Blenkinsop et al (1994) reveal a NW-SE compression and subvertical extension. The structural control of the shear zone hosted mineralizations is further evidenced by the paralleling of ore shoots with the regional trend of fold axes. The intensely carbonatized granite at Ayanfuri shows multiple sets of steeply dipping quartz veins witnessing the intense fluid penetration. High gold grades are found in the altered granite rather than in the quartz veins. The Abosso-Damang mineralization is hosted by jointly deformed Birimian and Tarkwaian units in an anticlinal position. High gold grades are found in stockwork impregnation and disseminated in Birimian and Tarkwaian units.

Fluid inclusions in samples from these deposits were investigated in order to determine the physicochemical characteristics of the mineralizing conditions. The fluid inclusion assemblage in the Ashanti gold deposit is dominated by CO₂>>N₂>CH₄-rich fluids of sometimes high density (>1g/cm³). Inclusions containing aqueous phases are extremely rare and, if present, are mostly secondary. In the Konongo and Prestea mineralizations, aqueous inclusions are more abundant and of

variable, rather high salinity. However, $\text{CO}_2 \gg \text{N}_2 > \text{CH}_4$ -rich fluids are still predominant. For the Ayanfuri granite-hosted mineralization the trend of fluid evolution can be reconstructed. Early primary inclusions contain low saline aqueous fluids. Later generations contain increasing gas contents and have higher salinity. Intense carbonatization of the granite evidences a strong participation of CO_2 -rich fluids. The disseminated and stockwork mineralization in Birimian and Tarkwaian sedimentary rocks of the Abosso-Damang area contains abundant gaseous of rather low density and only few aqueous inclusions. Primary, gas-rich inclusions were also determined in quartz clasts from the palaeoplacer deposit of Tarkwa and are suggested to be inherited from the primary source of the alluvial gold deposit to the west, in the Kibi-Winneba belt (KLEMD et al. 1993).

Konservative P-T estimates based on fluid inclusion data indicate a depth interval of at least 15km within which gold deposition from these $\text{CO}_2 \gg \text{N}_2 > \text{CH}_4$ -rich fluids took place. For Ashanti and Prestea the high densities of fluids in inclusions point to 15 to 20km depositional depth, the mineralization of the Ayanfuri granite took place at rather shallow 5 to 8 km depth at temperatures around 330 to 340°C. The Abosso Damang mineralization is inferred to have occurred at a similar depth but considerably lower temperatures of 180 to 270°C.

The near absence of aqueous fluid inclusions bears some problems with respect to the composition of the mineralizing fluids. A yet unknown process of selective trapping of the gaseous components is in conflict with the abundant CO_2 - H_2O inclusions at Ayanfuri. If secondary selective leaching had extracted the aqueous phase from initially mixed inclusions, this process must have been very effective over 250km along strike and at least 15km to depth - still, the Ayanfuri mineralization was left out. Can we envisage these fluids as potential mineralizing agents in crustal processes? Very little is known of the physical and chemical characteristics or the solvent properties of these volatile-rich fluids at the considered P-T conditions.

The mobilization and migration of the $\text{CO}_2 \gg \text{N}_2 > \text{CH}_4$ -rich fluids and associated gold mineralization was a regional process, traceable for 250km along strike of the Ashanti belt, and diachronously to the west in the Kibi-Winneba area. The source of these fluids is not finally cleared. Stable isotope ratios of O, C and S suggest metamorphic mobilization from the sedimentary country rock (Oberthür et al. 1994). The high content of gaseous ($\text{CO}_2 + \text{N}_2 + \text{CH}_4$) components in the fluid inclusions appears to be of regional significance for the process of gold enrichment in the Ashanti belt and may serve as a pathfinder for exploration.

References:

- Blenkinsop, T.G., Schmidt Mumm, A., Kumi, R. & Sangmor, S., 1994: Structural Geology of the Ashanti Gold Mine, Geol. Jahrbuch, D100. 131-153
- Klemd, R., Hirdes, W., Olesch, M. & Oberthür, T., 1993: Fluid inclusions in quartz-pebbles of the gold bearing Tarkwaian conglomerate of Ghana as guides to their provenance area. Min. Dep. 28, 334-343
- Oberthür, T., Vetter, U., Schmidt Mumm, A., Weiser, T., Amanor, J.A., Gyapong, W.A., Kumi, R. & Blenkinsop, T.G. 1994: The Ashanti gold mine at Obuasi in Ghana: mineralogical, geochemical, stable isotope and fluid inclusion studies on the metallogenesis of the deposit. Geol. Jb., D100. 31-130

THE MINERALIZATION AT THE VICEROY GOLD MINE, HARARE-BINDURA GREENSTONE BELT, ZIBABWE

SCHMIDT MUMM, A. (1), BLENKINSOP, T. (2), OBERTHÜR, T. & WEISER, T (3)

(1) Institut für Geologische Wissenschaften, Domstr. 5, D-06108 Halle

(2) Geology Department, University of Zimbabwe, P.O. Box MP 167, Harare, Zimbabwe

(3) Bundesanstalt für Geowissenschaften und Rohstoff, Stilleweg 2, D-30655 Hannover

The Viceroy gold mine lies in an E-W trending arm of the Harare-Bindura greenstone belt, Zimbabwe, hosted by amphibolite facies metamorphic basalts with intercalated dacitic (guinea-fowl rock) and garnetiferous felsitic rocks (Teviotdale porphyry) of the Upper Bulawayan Arcturus Formation. Two main phases of folding both with E-W axial traces can be identified in the greenstone belt, accompanied and followed by several phases of shearing and faulting. Mineralization in the Viceroy mine occurs in two subvertical quartz veins namely the "Main reef", striking N-S, and the "Diagonal reef", striking NE-SW. The ore mineral assemblage is characterized by a number of unusual -and one so far unknown- components of the system Au-Bi-S-Te. The upper temperature stability limit 241°C for Maldonite in the presence of Bi and 271.5°C for native Bi marks an upper limit for the temperature of mineral deposition. Subhorizontal mineral stretching lineations strongly suggest that the Main and Diagonal reefs are located in a strike-slip fault. The mineralized quartz veins cut across or are cut by NW-SE striking, vertical quartz-calcite veins. In close vicinity of the mineralized veins is a zone of hydrothermal brecciation, consisting of metabasaltic clasts in a matrix of quartz-calcite. Two phases of alteration can be distinguished: the first one, which somewhat postdates the amphibolite grade metamorphism has caused local biotitization of the basaltic country rock in the vicinity of the shear. The second phase mainly resulted in epidotization and formation of chlorite. It is notable that the shear evidently was active during both episodes. Carbon isotope compositions of calcite ($\delta^{13}\text{C}$ in ‰, PDB) range from -9.8 to -5.6‰, (mean -6.8) in the mineralization and -3.4 to -3.6‰, in the hydrothermal breccia. Oxygen isotope compositions ($\delta^{18}\text{O}$ in ‰, SMOW) of calcite range from 9.4 to 10.7‰, and of quartz from 11.6 to 12.2‰. From this the isotopic composition of the fluid can be calculated (Table 1). Together with δD values of fluid inclusions in quartz of -51 and -31‰, a surficial affinity of the mineralizing fluids may be inferred. Sulfur isotope composition ($\delta^{34}\text{S}$ in ‰, CDT) of sulfides (arsenopyrite) ranges from 1.9 to 3.3‰, which is compatible with a derivation of the sulfur from magmatic rocks.

Fluid inclusion studies revealed a complex pattern of fluid systems. Primary and secondary generations of aqueous inclusions associated with the gold mineralization are of low but complex salinity (T_m : mostly 0 to -7°C, sometimes as low as -22.7°C, T_e : mostly -20 to -35°C, sometimes as low as -55°C) and homogenize over a wide range from 150 to 317°C. The higher homogenization temperatures were measured on inclusions which also showed clathrate melting or even a separate gas (CO_2) phase. Secondary inclusions on intersecting secondary fracture planes may have mixed salinities at or near the intersection line. Closely

associated with the aqueous inclusions are gaseous, CO₂-rich inclusions which may locally contain additional CH₄. Evidence for phase separation is present but not unequivocal. In the wallrock of the mineralized shear zones inclusions in small quartz carbonate segregates are aqueous and of high, complex salinity; homogenisation temperatures are 150 to 190°C. Fluid inclusions were also analyzed in the carbonate breccia pipe. Here aqueous inclusions have moderate but complex salinities (T_e: -55 to -65°C, T_m: -10 to -18°C) and homogenize over 180 to 280°C. The abundant gaseous inclusions in the breccia pipe carbonate show strong evidence for the presence of increased CH₄ contents (T_m: -184 to -172°C, T_h: -84 to -77°C).

Petrographic, structural as well as fluid inclusion data point to a very complex evolution of the shear zones and mineralization at the Viceroy mine. At least two episodes of mineral deposition can be distinguished: the first one postdates metamorphism but clearly occurred at increased temperatures to cause biotitization of the country rock. Field relations also suggest that the carbonate breccia pipe originates from this event. The second mineralizing system, which led to the Viceroy deposit was active at a later stage and at considerably lower temperatures. Fluid inclusion and the ore mineral paragenesis provide evidence for a hydrothermal system at shallow depth which may have interacted with meteoric waters in the course of this second episode. Regional structural interpretation even raises the possibility of a Proterozoic origin of this second mineralizing system.

References:

Matsuhisa, Y., Goldsmith, J.R. & Clayton, R.N., 1979: Oxygen isotope fractionation in the system quartz-albite-anorthite-water. Geochim. Cosmochim. Acta, 43, 1131-1140.
 O'Neil, J.R., 1977: Stable isotopes in mineralogy, Phys. Chem. Mineral. 2, 105.

	δ ¹⁸ O mineral	δ ¹⁸ O H ₂ O at Temperature:	
		250°C	300°C
‰ δ ¹⁸ O calcite	9.4-10.7	2.7-3.2	4.7-5.3
‰ δ ¹⁸ O quartz	11.5-12.2	4.3-4.9	6.0-6.6

Table 1: δ¹⁸O (‰ rel. SMOW) of calcite and quartz and calculated isotopic composition of the mineralizing fluid (calculated after: Matsuhisa et al. 1979 (quartz), O'Neil 1977 (calcite)).

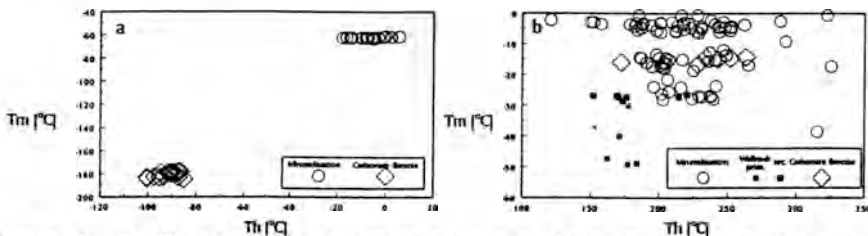


Figure 1: T_m/T_h plot of microthermometric data on gaseous (a) and aqueous (b) inclusions. a: T_m = final melting of the CO₂-CH₄ solid phase, T_h final homogenization of the CO₂-CH₄ liquid and vapour phases (in all cases homogenization to the liquid); b: T_m = melting of ice, T_h = final homogenization.

GAS ANALYSIS IN FLUID INCLUSIONS BY NIR FT RAMAN SPECTROSCOPY

SCHMIDT MUMM, A.(1), LEHNER, C.(2), SAWATZKI, J.(2) & IDIZ, E.(3)

(1) Institut für Geologische Wissenschaften und Geiseltalmuseum, Domstr. 5, D-06108 Halle

(2) Bruker Analytische Meßtechnik GmbH, Wikingerstr. 13, D-76189 Karlsruhe

(3) Erdem Idiz, BEB Erdgas und Erdöl GmbH, Riethorst 12, D-30659 Hannover

Raman spectroscopic analysis has developed into a standard method for the semiquantitative determination of the relative composition of gaseous components (e.g. CO₂, CH₄, N₂, H₂, H₂S, etc.) or aqueous solutions in fluid inclusions (Pasteris & Seitz 1988, Pironon et al. 1991). In the conventional dispersive Raman microprobe, an Ar laser (514nm) is used for the excitation of molecular vibrations. The use of the high energy laser beam has the advantage of producing relatively strong Raman signals from the considered species. However, Raman spectroscopy may not be suitable for samples with inclusions of higher hydrocarbons or organic impurities due to effects of fluorescence: the high energy Ar laser beam may induce electronic transitions and in the return of the electron to lower energy levels a light quantum is emitted. This fluorescence in the range of approximately 400 to 700nm may cover most of the spectral range of the much weaker Raman signals and thus inhibit the analysis. The problem of fluorescence can be substantially reduced by the use of near IR excited FT-Raman techniques. The long wavelength/low energy excitation (1064nm) avoids the effects of fluorescence as well as local heating. Fluorescent materials would thus be accessible for Raman microprobing. For the investigation of microscopic samples an FT-Raman microscope coupled to the bench of an FT-Raman spectrometer was used. The excitation source was a diode-pumped NIR Nd:YAG laser of 1064nm, providing a power of 100mW at the sample location. Pironon et al (1991) and Kihle and Johansen (1994) successfully analysed hydrocarbon inclusions with a similar instrumental setup.

Fluid inclusions of 5 to 12µm diameter were analysed in calcite from a calcitesphalerite vein in the Upper permian Zechstein. Initial microthermometric analyses provided strong indications for the presence of CH₄ and in some cases also N₂ through melting temperatures of -196.3 to -171.4°C and homogenisation temperatures of -117.2 to -81.2°C. The attempt to subsequently analyse these inclusion by conventional dispersive Raman spectroscopy using a laser excitation of 514nm was unsuccessful because of an intense fluorescence of the hosting carbonate, which was several orders of magnitude stronger than the expected Raman signals. In order to avoid the interfering effects of fluorescence, samples were then analysed by FT-Raman with NIR excitation at 1064nm. For the first time FT-Raman spectra of CH₄ and N₂ in natural fluid inclusions in calcite could be obtained using the BRUKER NIR FT-Ramanscope. An example of the obtained spectra is given in Fig. 1. Methane is the dominant hydrocarbon phase with a well developed peak at 2912cm⁻¹. The relatively wide base of this peak may be indicative for further hydrocarbon components as the CH stretching vibrations fall in the range of

approximately 2850 to 3100 cm^{-1} . The peak for N_2 at 2329 cm^{-1} is much smaller, but may still represent significant amounts of N_2 in the inclusion as the Raman scattering cross section of N_2 is several times smaller than for CH_4 . However, calibration measurements of inclusions of known composition are needed for a quantification of the results.

Instrumental development of the NIR FT-Raman spectrometers, mainly in spectral stabilisation of the laser source and optimisation of the detectors has led to an improvement of the detection limits and also spot size for the application as a method for non-destructive microanalysis. Analysis of gaseous components in natural fluid inclusions by NIR FT-Raman is at present the only method when fluorescence inhibits the use of the high energy excitation from Ar lasers. This may be especially useful for fluid inclusion studies related to generation, migration and fixation of hydrocarbons.

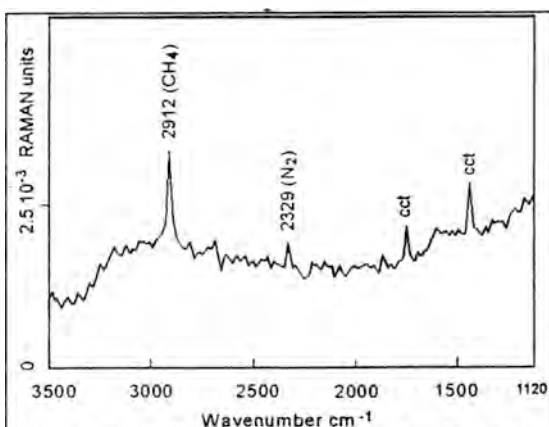


Figure 1: FT-Raman spectrum of a CH_4 - N_2 inclusion in calcite. Spectral resolution 12 cm^{-1} , scan accumulations 20000, laser power 100mW, objective 40x numerical aperture 0.65. cct = calcite

References

- Kihle, J. & Johansen, H., 1994: Low-temperature trapping of hydrocarbon fluid inclusions in synthetic crystals of KH_2PO_4 . *Geochim. Cosmochim. Acta*, 58, 1193-1202
- Pasteris, J.D., Wopenka, B. & Seitz, J.C., 1988: Practical aspects of quantitative laser Raman microprobe spectroscopy for the study of fluid inclusions. *Geochim. Cosmochim. Acta*, 52 979-988.
- Pironon, J., Sawatzki, J. & Dubessy, J., 1991: NIR FT-Raman microspectroscopy of fluid inclusions: Comparison with VIS Raman and FT-IR microspectroscopies. *Geochim. Cosmochim. Acta*, 55, 3885-3891.

FLUID EVOLUTION IN A MINERALIZED SHEAR-ZONE: GOLD DEPOSITS OF TIREK AND AMESMESSA (HOGGAR, ALGERIA)

SEMIANI, A. (1), BOIRON, M.C. (2) and MARIGNAC, CH. (3)

- (1) ORGM, Boumerdes, Algeria
- (2) CREGU, Nancy, France
- (3) CRPG-CNRS, Nancy, France

INTRODUCTION

In the W Hoggar, the East-Ouzzal shear-zone (EOSZ) is a dextral transcurrent N-S ductile fault 900 km long, separating a granulite complex (In Ouzzal block), to the W, from a Middle Proterozoic unit, to the E. The EOSZ was active during the late Panafrican.

The EOSZ is the host for numerous Au-bearing quartz veins, upon a length of 100 km, from the deposit of Amesmessa to the S to the one at Tirek to the N (Ferkous & Leblanc, 1993).

A three-stage evolution is recorded: (i) alternations of hydrothermal alteration under brittle conditions (hydraulic fracturing) and of ductile deformation; quartz veins were subjected first to mylonitization, then to cataclasis, at the ductile to brittle transition; (ii) brittle microfracturing: sealed microfractures (planes of fluid inclusions and quartz veinlets), overprinting porphyroclastic and cataclastic textures; (iii) mineralization (sulphides and gold) as veinlets and disseminated droplets along intergranular joints. The micropermeability inherited from the cataclasis stage was enlarged by quartz dissolution prior to mineral deposition.

FLUID INCLUSIONS

Quartz porphyroclasts are clouded of small fluid inclusions, which could not be studied. Measurable fluid inclusions (f.i.) are later and were found:

- in sealed "E-W" microfractures of stage (ii), where are observed 2-phase inclusions (Lw1) filled with brines (Te <-40°C; Tmi in the -16.5°C to -26°C range) and exhibiting variable Th (127°C to 380°C);

- in "cleaned" strips, along joints between porphyroclastic quartz; these strips are closely associated with mineralization, but distinctly earlier; they overprint Lw1 planes. Two kinds of inclusions are observed:

- 3-phase and 2-phase (carbonic) inclusions (Lc-w and Cl), with a few non-CO₂ volatile component (TmCO₂: -58.8°C to -56.6°C), moderate to low salinity (Tmcl around 8°C, ranging from 3°C to 10°C) and density (ThCO₂: 19°C to 32°C for most f.i., in the liquid phase for both Lc-w and Cl); the homogenization temperatures are around 300°C, some Lc-w f.i. decrepitating at 320°C, before homogenization.

- 2-phase inclusions (Lw-c) exhibiting clathrates, with Tmcl around 9°C and moderate Th (220°-270°C).

- 2-phase (aqueous) inclusions (Lw2), overprinting the carbonic f.i.; they show low to moderate Tmi (-26°C to -5°C) and variable Th (150°-380°C).

- in clear quartz, rimming sulphides and gold crystals and overprinting all previous f.i., where are seen rare 2-phase

inclusions (Lw3), with moderate to low salinities (Tmi: -6.6°C to -0.2°C) and low Th in the 140°C- 380°C range.

It must be emphasized that the nature of the fluid inclusions and the microthermometric parameters are very similar in the two deposits of Tirek and Amesmesa, although they are distant from more than 50 km.

FLUID COMPOSITION

From Raman analysis and interpretation of Tmcl and Th-Tmi data, it is deduced that five kinds of fluid components were involved in fluid circulation along the EOSZ, two (aqueous)-carbonic (Ca,b) and three aqueous (Wa, Wb, Wc) (table 1).

Kind of fluid	Composition
(aqueous)carbonic fluids { Ca Cb	CO ₂ -(H ₂ O?) CO ₂ -N ₂ -(H ₂ O?) (up to 5 mole % N ₂)
aqueous fluids { Wa Wb Wc	H ₂ O-NaCl-R ²⁺ Cl ₂ (≥25% wt eq. NaCl) H ₂ O-NaCl (5 to 7 % wt eq.NaCl) H ₂ O-(NaCl)

Table 1. Kinds of fluids involved in circulation along the EOSZ

These basic types were variously mixed :

- mixture of Wa and Wb to produce fluids trapped in Lw1 and Lw2 f.i.
- mixture of Ca, Cb and Wb to produce fluids trapped in the Lc-w, Lc and Lw-c f.i.
- mixture of Wa and Wc, then of Wa, Wb and Wc, to produce fluids trapped in the Lw3 f.i.; it is precisely the mixing of these three aqueous fluids which caused ore deposition in the quartz veins of the EOSZ.

P-T-t PATH

Combining isochore computation and external constraints derived from mineral composition and geological data, it was possible to reconstruct P-T conditions prior to and during ore deposition:

- early brines (Lw1) circulated under a lithostatic pressure of 1.3 kbar (ca. 5 km), at high temperatures (up to 400°C), decreasing down to 250°C.
- aqueous-carbonic fluids (Lc-w) circulated under the same pressure, at temperatures up to 300°C, i.e. after reheating.
- late aqueous fluids (Lw2 and Lw3) circulated after a pressure drop, down to 0.5 kbar (lithostatic-hydrostatic transition) and deposited gold and sulphides at a rather low (ca. 200°C) temperature.

REFERENCES

- FERKOUS, K. & LEBLANC, M. 1993. Gold-bearing quartz veins in a lithospheric shear zone (SW Hoggar, Algeria). *Current Research in Geology Applied to Ore Deposits, Fenoll Hach-Ali, Torres-Ruiz & Gervilla (eds): 445-448.*

CRYSTALLIZATION CONDITIONS OF HAUYNE PHONOLITES OF LAAHER SEE VOLCANO (E.EIFEL, W.GERMANY)

SHARYGIN, V.V.

Institute of Mineralogy and Petrography, Universitetsky pr.3, 630090 Novosibirsk, Russia.

Three series of phonolites have been distinguished due to the detailed mineralogical-geochemical investigations of the Laaheer See Tephra: LLST - lower, MLST - middle, ULST - upper [2,4]. The ULST hauyne phonolites, which are most enriched in phenocrysts (up to 30-40 vol.%) among the rocks of three series, were used for fluid inclusion study.

These porphyritic rocks contain phenocrysts of nine minerals (sanidine, plagioclase, hauyne, clinopyroxene, amphibole, sphene, Ti-magnetite, apatite, and occasionally biotite), while leucocratic minerals predominate over melanocratic ones (~75:25). Greenish-gray groundmass is commonly fine-crystallized and composed of sanidine, blue hauyne, clinopyroxene and magnetite. Fresh glass with a few amounts of gas bubbles is usually present around mafic phenocryst cumulates. The approximate crystallization sequence, deduced from mineral relationships, is: hauyne -> apatite, magnetite, sphene -> pyroxene, amphibole, plagioclase -> sanidine for phenocrysts and hauyne, magnetite -> pyroxene -> sanidine, glass for groundmass.

The primary melt inclusions have been found in all mineral phenocrysts (excepting biotite). Mono- and two-phase inclusions (glass + gas) with $T_{hom}=1080-1150^{\circ}C$ are most common of the earliest phenocrysts (hauyne, apatite, sphene). Pyroxene- and amphibole-hosted inclusions ($T_{hom}=1030-1120^{\circ}C$) consist of glass + some gas bubbles, sometimes carbonate occurs as a daughter phase. Some glassy inclusions in the latest phenocrysts (plagioclase and sanidine) contains also the cavity with fine-devitrified salt aggregates (salt melt?) in glass and/or salt crystalline phases in gas bubble. The melting of the salt phases proceeded at $780-900^{\circ}C$. Complete homogenization of these inclusions are $950-1050$ and $980-1120^{\circ}C$ (for sanidine and plagioclase, respectively [1]). The inclusions hosted by plagioclase are characterized by different extent of crystallization: from glassy (glass + gas) to partly crystallized (glass + daughter phases + gas), while latter corresponds to the rock groundmass in modal composition.

The electron microprobe analysis of melt inclusions in the ULST phenocrysts has shown that initial glasses in the earliest minerals (hauyne -> sphene) correspond to bulk rock composition, while residual glasses in later minerals (pyroxene -> sanidine) are close to groundmass glass. This tendency is clearly seen on the inclusions hosted by plagioclase, crystallizing during long temperature interval: from glassy to most crystallized inclusions the glasses became richer in SiO_2 , alkalis (mainly, K_2O), BaO and poorer in the femic components, Cl , SO_3 . In general, composition of the final derivatives during crystallization of melt initial of the ULST phonolites is close to alkali trachytes (essentially K-feldspar rock).

The preliminary Raman investigation of gas bubbles in melt inclusions from the ULST phonolites has shown that only bubbles of hauyne-hosted inclusions contains high concentration of CO₂ (89 mol.% versus 11 mol.% N₂). The presence of CO₂ is also detected in bubbles of sanidine-hosted inclusions (57 mol.% versus 43 mol.% N₂). The bubbles of the partly crystallized melt inclusions in other phenocrysts and groundmass bubble contain N₂ only. The same distribution of carbon dioxide seems to depend on extent of inclusion devitrification. In partly crystallized inclusions CO₂ partitioned between glass, bubble and daughter phases (for example, due to carbonate formation)

According to mathematical modeling, a possible magma, parent for the Laaer See Tephra phonolites, might be basanitic liquid during common fractionation processes [3]: basanite (1100°C) -> 70% fractional crystallization -> mafic phonolite -> 20% fractional crystallization -> erupted phonolites of three series (880-800°C). Fluid inclusion study of basanite and leucite tephrite related to the phonolites confirms these conclusions [1]. The secondary melt inclusions in basanite and tephrite pyroxenes contain up to 60% femic daughter phases in an inclusion volume, and their residual glasses correspond to the phonolites (mainly, ULST rocks). Thus, basanitic melt might be parent for the ULST phonolites during widespread processes of crystal fractionation under conditions of shallow-deep magmatic chamber.

References

- [1] Sharygin V.V. (1993). Russian Geol. and Geophys., 34(6):84-95.
- [2] W rner G. and Schmincke H.-U. (1984). J.Petrol., 25: 805-835.
- [3] W rner G. and Schmincke H.-U. (1984). J.Petrol., 25: 836-851.
- [4] W rner G. et al. (1983). Contrib.Mineral.Petrol., 84: 152-173.

ZR-TI-BEARING DISILICATES FROM INCLUSIONS IN MINERALS OF PEGMATOID VENANZITE (PIAN DI CELLE VOLCANO, SAN VENANZO, ITALY)

SHARYGIN, V.V. (1) & STOPPA, F. (2)

(1) Institute of Mineralogy and Petrography, Universitetsky pr.3, 630090 Novosibirsk, Russia.

(2) Dipartimento di Scienze della Terra, Piazza dell'Università, 06100 Perugia, Italy.

Rare diorthosilicates (götzenite, cuspidine, khibinskite) have been found during fluid inclusion study of the Pian di Celle rocks. They occur as trapped/daughter phases of the inclusions hosted by minerals of pegmatoid venanzites. These rocks form dykelet swarm in the NE flow-front of porphyritic olivine-leucite melilitites (normal venanzites) and are late-crystallizing products of the activity of the Pian di Celle volcano [1,3,4].

Melilite (up to 5 cm), olivine and leucite form a large frame with numerous cavities in pegmatoid venanzites. Interstices between these minerals are filled by a fine-grained groundmass consisting of Ti-magnetite, F-apatite, F-phlogopite, nepheline, kalsilite, clinopyroxene, gôtzenite, delhayelite-like mineral, sulphides, carbonates, and dark brown or green glass, listed in order of the approximate crystallization sequence.

Zr-Ti-rich disilicates were observed in polycrystal, silicate-melt and combined (polycrystal assemblage plus adhered glass and/or gas) inclusions (10-100 μm) hosted by olivine and melilite of the pegmatoid venanzite. All inclusions are confined to healed micro-fractures in the host minerals and seem to be secondary in origin. Other minerals of the rock also contain fluid inclusions, but no Zr-Ti-disilicates are found in them.

Cuspidine has been identified only in melilite-hosted inclusions. It forms euhedral colorless crystals (up to 40 μm), sometimes with pronounced zoning. Its composition strongly varies in CaO (58.2-44 wt.%), Na₂O (0.5-3.6 wt.%), F (10.1-8.5 wt.%) and ZrO₂ (0.2-10.5 wt.%) from the core to rim of the crystals. The considerable variations in these components suggest the existence of limited solid solution between cuspidine Ca₄[Si₂O₇]F₂ and hiortdahlite NaCa₂Zr[Si₂O₇]OF (probably, hiortdahlite-2, [2]) due to possible combined substitution $2\text{Ca}^{2+} + \text{F}^- \rightleftharpoons \text{Na}^+ + \text{Zr}^{4+} + \text{O}^{2-}$. Maximum content of ideal hiortdahlite end-member in the Pian di Celle cuspidines may be up to 33 mol %.

Three varieties of gôtzenite (Ca,Na)_{3.5}(Ti,Zr)_{0.5}[Si₂O₇](O,F)₂ are found in the inclusions: pure Ti-gôtzenite (10.2 wt.% TiO₂), Zr-rich (6.9-7.3 wt.% TiO₂, 5.8-8.3 wt.% ZrO₂) and REE-rich (7.8 wt.% TiO₂, 2 wt.% ZrO₂, 5.5 wt.% TR₂O₃) gôtzenites. Earlier, only Zr-gôtzenite were reported as inclusion in melilite of pegmatoid facies of venanzites [1]. Our data show that Ti-variety is typical of the melilite-hosted inclusions, while Zr-gôtzenite occurs in both melilite- and olivine-hosted inclusions. REE-rich variety has been observed in olivine-hosted inclusions only and is compositionally close to the groundmass gôtzenite.

Khibinskite K₂ZrSi₂O₇ has been observed only in an olivine-hosted polycrystal inclusion together with phlogopite, perovskite, FeS and kalsilite. It contains up to 1.15 wt.% Na₂O and 0.8 wt.%

FeO. Relationships of khibinskite with F-disilicates are not yet clear, as no inclusions were found, where these minerals coexist.

According to mineral relationships, the approximate crystallization sequence in melilite- and olivine-hosted inclusions may be as follows: Ti-magnetite, apatite -> phlogopite -> Zr-götzenite, cuspidine -> clinopyroxene, kalsilite -> Ti and REE-götzenites, perovskite, khibinskite -> sulphide -> glass, that are similar to those of the pegmatoid venanzite groundmass.

Preliminary microthermometric investigations of the secondary melt inclusions hosted by olivine and melilite of pegmatoid venanzites have shown that silicate glass began to melt at 680-720°C during heating. The colorless daughter phases (kalsilite, cuspidine and g g tzenite), which are optically indistinguishable in the inclusions, fused at 770-860°C. Decreasing of gas bubble fixed up to 850-900°C. Unfortunately, neither olivine-hosted nor melilite-hosted inclusions failed to homogenize due to possible leakage. Only heating experiments with the primary melt inclusions in kalsilite were successful (Thom - 835-840°C).

According to previous studies on the Pian di Celle rocks [3,4], pegmatoid venanzites are essentially richer in CaO, FeO_t, TiO₂, F, some trace elements (Zr, Sr, REE) and poorer in Al₂O₃, MgO than normal venanzites. Agpaitic index of about 0.9 and Ca predomination over alkalis (18 wt.% versus 8 wt.%) are typical of the pegmatoid venanzite. Electron microprobe analysis has shown that residual glasses of olivine-, melilite-hosted inclusions and groundmass glass of the rock are enriched in alkalis (15 and 10 wt.%, respectively), FeO_t (up to 17-22 wt.%), BaO (0.5-2 wt.%), F (1-2 wt.%), SO₃ (0.7-1.8 wt.%), Cl (0.4-0.1 wt.%), ZrO₂ (0.1-0.7 wt.%) and depleted in Al₂O₃ (1-3 wt.%), CaO (6-2 wt.%), MgO (3-1 wt.%), and so have ultraagpaitic composition (9.3-5.3). Thus, high abundances of CaO (up to 18 wt.%), TiO₂ (up to 3.3 wt.%), F (up to 0.5 wt.%) and Zr (>1000 ppm) in melt initial of pegmatoid venanzites and agpaitic character of its crystallization under low pressures were responsible for the appearance of cuspidine and g tzenite on the intermediate and late stages. Khibinskite seems to be crystallized at the latest stages, when melt was rich in alkalis, Zr and poor in F.

References

- [1] Cundari A. and Ferguson A.K. (1991). Contrib. Mineral. Petrol., 107: 343-357.
- [2] Merlino S. and Perchiazzi N. (1988). Can. Mineral., 26: 933-944.
- [3] Mittempergher M. (1965). Bull.Volcanol., 28: 85-94
- [4] Stoppa F. and Lavecchia G. (1992). J. Volcanol. Geotherm. Res., 52: 277-293.

LASER ABLATION ICP-MS ANALYSIS OF SINGLE INCLUSIONS IN EVAPORITE MINERALS

SHEPHERD, T.J., CHENERY, S.R. and MOISSETTE, A.

British Geological Survey
Nicker Hill, Keyworth
Nottingham NG12 5GG, U.K.

Natural variation in the size, shape, abundance and populations of fluid inclusions in rocks and minerals presents a major problem for determining the geochemistry of palaeofluids. High spatial resolution laser ablation ICP-MS (LAMP-ICP-MS) using a 266nm UV laser microprobe marks an important breakthrough in the acquisition of elemental data for aqueous inclusions. Though simple in concept, establishing a working protocol has proved more difficult. By redesigning the ablation cell to incorporate variable temperature control of the sample, and using synthetic fluid inclusion standards, factors limiting analytical reproducibility have been identified and successfully minimised. Detection limits are related to the volume of the inclusion (i.e. the mass of fluid released). For a 20µm diameter inclusion, detection limits for Cu and Zn are estimated to be approximately 10-25ppm. Reproducibility for the major and minor cations is generally better than 25%. Significant progress has also been made in the measurement of Cl/Br ratios. To test these improvements on naturally occurring inclusions, samples of inclusion-rich halite have been analysed from the Cheshire Basin, UK and Lorca Basin, Spain.

In common with other European, intracratonic, rift-related Permo-Triassic basins, the Cheshire Basin displays a synergy between evaporites and 'red bed' copper deposits. LAMP-ICP-MS data for aqueous inclusions in the evaporite units demonstrates that the brines present during late stage halite precipitation and burial diagenesis were highly enriched in Mg, K, Ca, Rb, Pb (up to 80ppm) and Ba. At least 2 chemically distinctive fluids can be identified. Leaching of iron oxide cements further enriched the fluids in Cu (up to 100ppm) and Mn (Fe not analysed). Cu-Pb mineralization in the stratigraphically lower sandstone units is interpreted as a product of density driven, downward circulation of metalliferous, evaporite brines and their mixing with upwelling reduced fluids from the basement Carboniferous.

For the Miocene Lorca Basin evaporites, halite samples provided the opportunity to compare LAMP-ICP-MS data and Mg, K and Na analyses obtained by cryogenic XRF. Agreement is generally good and confirms the added value and desirability of using integrated techniques for the analysis of single.

This work was carried out through the EU Human Mobility and Capital Network Programme (DG-XIII-G) "Hydrothermal/metamorphic water-rock interactions in crystalline rocks: a multidisciplinary approach based on palaeofluid analysis".

INVESTIGATION OF SYNTHETIC FLUID INCLUSIONS IN HYDROTHERMAL ANALCIMES

SLABY, E. (1), KOZŁOWSKI, A.(1), CZERWOSZ, E (2), DIDUSZKO (2) & BANERJEE, A. (3)

(1) Institute of Geochemistry, Mineralogy and Petrology, University of Warsaw (Poland)

(2) Institute of Vacuum Technology, Warsaw (Poland);

(3) Institute of Geosciences, Mainz University (Germany)

Analcime crystals appear in a number of different environments. They are divided, correspondingly to their formation conditions, into five groups: P-type (primary analcimes), H-type (hydrothermal analcimes), S-type (sedimentary analcimes), M-type (metamorphic analcimes), L-type (formed by exchange conversion of leucite). One can suppose that inclusions in analcimes could be a good indicator of their origin. Nevertheless inclusions trapped in analcimes are seldom investigated due to "leakage", which in turn may be caused by likely interaction between framework water and the water from fluid inclusions.

The aim of the experiment, we have conducted, was to crystallise H - analcimes under various kinetic conditions and to investigate inclusions trapped in them. The experiment was performed in a standard cold seal vessels. Crystals of H - analcimes were products of oligoclase decay reaction in carbonate solution. The runs were performed for $T = 300^{\circ}\text{C}$ and $P = 2$ kbars. The first run (R-1) series lasted 8 days, leading to complete oligoclase dissolution and with the reaction not approaching equilibrium. Analcimes are accompanied there by small amount of cancrinite. The second run (R-2) series lasted 40 days - giving the same products, but the reaction was approaching equilibrium.

Although crystallisation time was so different, analcime crystals from both experiments (R-1 and R-2) possess identical three kinds of inclusions:

* inclusions A - single phase fluid inclusions,

* inclusions B - two fluid phases inclusions with very small bubbles (3-5 vol.%),

* inclusions C - two fluid phases inclusions with big bubbles (25-30 vol.%).

Inclusions trapped in crystals from the first series (R-1) are very fine: 1-2 mm, those from (R-2) much more bigger i.e. > 5 mm. Types A and B occur deeply inside crystals. Type C occupies area near the crystals' surface. Cryometric measurements have given the equivalent of NaCl value respectively 8 wt% for A and B type, 5 wt% for C type.

During the heating, inclusions A were decrepitating at various temperatures, or bubbles were formed in them at $T = 130-250^{\circ}\text{C}$, which did not disappear during further temperature increase. Inclusions B homogenised at $T = 110-120^{\circ}\text{C}$, when the heating process proceeded quickly. Along with slow heating the bubbles were growing in the inclusions without any homogenisation. Inclusions C manifested similar behaviour. Fast heating was causing their homogenisation at $T = 310-370^{\circ}\text{C}$. During the slow heating they were not becoming homogenised. The bubbles volume in them was constantly increasing reaching 70 vol% of the total volume of inclusions.

Sodium concentration obtained by means of cryometric method from the A and B-type inclusions fits exactly to the maximum sodium contents in the solution after full plagioclase release. Also the sodium value from inclusions C, though much more higher than that in the post-reaction solution, could deliver valuable information about analcime crystallisation process. This is because the Na profiles through analcime crystals show remarkable decrease in sodium contents, what in turn is a consequence of crystallisation in a closed system. We believe that actual crystal composition and the trapped fluid reflect the alkalis decrease in the solution during crystallisation, due to sodium incorporation into crystallising phase.

Knowing the Tt and Pt we could evaluate the Th data. Quick homogenisation of the B-type prevents the inclusion from leaking. Moving the Th value along 10 wt% NaCl isochore we receive, at 2 kbars, almost exactly Tt = 285-295°C. Slow homogenisation causes visible leakage, more pronounced in the C-type inclusion than in the A and B-types. Analcime are minerals with zeolitic structure. They can easily incorporate additional water molecules and retain them in two types of channels. The channels are, however, more closed than in other zeolites. One could expect therefore, that leakage in analcimes will be slower, comparing with other zeolite behaviour. Similarly water diffusion in analcime channels is very slow, in comparison to other zeolites structure (Dyer & Molyneux, 1968). Kinetics of the water escaping from an inclusion into structure depends on sodium site position. Sodium cations occupy two positions in analcime structure Na(1) and Na(2). The second one is practically empty (Mazzi & Galli, 1978, Ferraris et al, 1972). The empty sodium polyhedron is large enough to accumulate additional water molecule. Because of the irregular and slightly zoned sodium distribution in investigated analcimes, the leakage is more visible in inclusion C and less in inclusion A and B. Fluid inclusions behave similarly in both the R-1 and R-2 samples since analcime structures resemble each other. Duration of the initial crystallisation influences reaction kinetics but not the resulting crystal structure.

The H-analcime more than any other zeolite can be used in fluid inclusion research. The fluid inclusions trapped in the analcime crystals may give proper information about solution composition and the crystallisation path. Quick homogenisation of two phase inclusion prevents the inclusion from leaking and allow us to use the Th for further consideration. Knowledge about analcime structure, especially about sodium and water order-disorder, is needed to calculate the amount of water, which can be additionally incorporated into channels.

References:

- Dyer, A., Molyneux, A. (1968): The mobility of water in zeolites - I. Self-diffusion of water in analcime. *J. Inorg. Nucl. Chem.*, 30, 829-837.
- Ferraris, G., Jones, D.W., Yerkess, J. (1972): A neutron-diffraction study of the crystal structure of analcime, NaAlSi₂O₆·H₂O. *Zeitschr. Kristallogr.*, 135, 240-252.
- Mazzi, F., Galli, E. (1978): Is each analcime different, *Amer. Miner.*, 63, 448-460.

MODELLING OF FLUID EVOLUTION ON THE BASIS OF CRUSH LEACH ANALYSES OF FLUID INCLUSIONS FROM THE CLIGGA HEAD GREISEN RELATED Sn-W DEPOSIT, S.W.ENGLAND.

SMITH, M.P.

Department of Earth Sciences, University of Leeds, Leeds, LS2 9JT, U.K.

INTRODUCTION.

Recent work on the Sn-W deposits of S.W. England has suggested that the ore fluids were magmatic in source. Oxygen isotope data from vein quartz and hydrogen isotope data from fluid inclusions from the Cligga Head greisen related Sn-W deposit support this view (analyses carried out by A.Boyce), and are consistent with re-equilibration of aqueous fluids with granite at temperatures ranging from $\approx 500^{\circ}\text{C}$ to 400°C . In order to test this hypothesis the composition of fluid inclusion leachates from greisen related quartz-tourmaline veins from Cligga Head has been determined using the procedure described in Bottrell et al (1988). The analyses were then compared with models of fluids equilibrated with granite mineral assemblages using a version of the EQ3NR computer program of Wolery (1983) modified by A.Komninou to perform calculations at temperatures up to 600°C for a pressure of 1 kb using data from Berman (1988).

ANALYTICAL RESULTS.

Fluid inclusions from the Cligga Head Sn-W deposit have been studied both microthermometrically and using crush leach analysis. The Cligga Head hydrothermal fluid had salinities from 5 to 12 wt % NaCl eq. and was dominated by Na-K-Fe-Ca chloride brines, with significant F, B and SO_4 contents. The ratios of Br to Cl in the fluids are comparable to those of modern volcanic fumarole gases (Bohlke and Irwin, 1992). The molal Na/K ratio varies from ≈ 4 to 10. The ratios of Ca and Fe to K also show some variation, showing a slight increase with the Na/K ratio.

MODELLING.

The composition of fluids in equilibrium with a model granite assemblage was calculated from 600 to 300°C and 1kbar pressure, and the composition of fluid in equilibrium with model greisen was calculated from 400 to 300°C . The granite assemblage was taken to be plagioclase (ab0.8;an0.2), K-feldspar, andalusite and fluorite at 600°C , and the two feldspars, sericite, and fluormuscovite at other temperatures. The greisen assemblage was taken to be sericite, the stable aluminosilicate phase (andalusite, pyrophyllite and kaolinite at 400°C , 350°C and 300°C respectively), fluorite and fluormuscovite. Quartz, hematite and magnetite were present in all assemblages.

The modelled fluid compositions in terms of Na-K-Fe are compared with the composition of fluid inclusion leachates in figure 1. It can be seen that the ratios of Na/K in the fluid inclusions are comparable with those from the model. The Fe contents are higher in the fluid inclusions than in the modelled fluids at temperatures below 600°C , but not as high as those predicted from a greisen mineral assemblage. The Ca contents of all the inclusion fluids are higher than any of the modelled fluid compositions.

DISCUSSION.

The variation in the analysed Na/K ratio of the fluid inclusions is consistent with a model of fluid re-equilibration with granite at progressively lower temperatures. The model predicts that high-T magmatic fluids will be rich in Fe and have high K/Na. The effect of wall-rock interaction at progressively lower temperatures will be to remove K and Fe from the fluid in exchange for Na (and probably Ca). The fluid inclusion compositions display precisely this trend, although Fe levels are higher than predicted. The predicted gains and losses of components in the fluid also match losses and gains of components in the rock during conversion of granite to greisen.

High Ca levels in the fluid inclusion analyses may reflect either mixing of the granite derived fluid with cooler, basinal fluids, or the inclusion of secondary fluid inclusions in the populations analysed using the bulk crush leach method.

CONCLUSIONS.

This study has demonstrated the value of crush leach analyses of fluid inclusions for examining the evolution of hydrothermal fluids, and the utility of thermodynamic modelling for predicting the chemistry of such fluids. The re-equilibration of an aqueous chloride bearing fluid with the granite at progressively lower temperatures can explain the cation composition of fluid inclusions from greisen related quartz veins at Cligga Head if mixing between fluids of different degrees of re-equilibration occurred. The anion content of the crush leach analyses of quartz from Cligga Head is consistent with resurgent boiling of granite as source for the fluid salinity.

REFERENCES.

- BERMAN, R.G. (1988) *J. Petrol.* v29, pp445-522.
 BOHLKE, J.K. and IRWIN, J.J. (1992) *Geochim. Cosmochim. Acta*, v56, pp203-226.
 BOTTRELL S.H, YARDLEY B.W.D. and BUCKLEY, F.(1988) *Bull. Mineral.* v111, pp279-20.
 WOLERY, T.J.(1983) EQ3NR. A computer program for aqueous speciation-solubility calculations:User's guide and documentation. Lawrence Livermore National Laboratory.

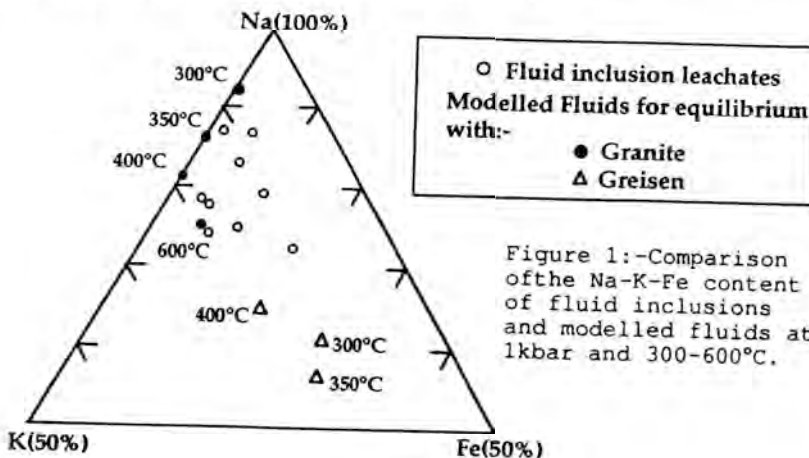


Figure 1:-Comparison of the Na-K-Fe content of fluid inclusions and modelled fluids at 1kbar and 300-600°C.

PALEOCLIMATE DATA FROM FLUID INCLUSIONS IN SALT: EXAMPLES FROM THE Qaidam Basin, China, and Death Valley, United States.

SPENCER, R.J., ROBERTS, S.M. & YANG, W.

Department of Geology and Geophysics, The University of Calgary, Calgary, Alberta, Canada T2N 1N4

Salt deposits hold great potential to supply unique data for the interpretation of past climate. One of the most exciting developments in paleoclimate research is the analysis of trapped atmospheric gases in polar ice allowing records of climate and climate forcings, based on analyses of stable isotopes and atmospheric gases, to be obtained from the same samples (Genthon et al., 1987; Lorius et al., 1990). Because of this, ice cores are now considered to contain some of the best paleoclimate records available. However, ice cores are limited to polar regions and a few high elevation mid- to high-latitude areas and extend in time only a few hundred ka.

Like ice, salt deposits contain direct samples of the ancient hydrosphere and atmosphere as fluid inclusions in evaporite minerals. Ancient surface brines trapped as fluid inclusions in halite crystals are petrographically distinct (Lowenstein & Hardie, 1985). Such fluid inclusions preserve a record of the major element and stable isotope composition of surface brines. Halite crystals and rafts which grow at the air-brine interface also trap atmospheric gases in some fluid inclusions. Salt deposits therefore carry a similar record to that found in ice. Further, fluid inclusions in salt also record the temperature at which the salt grew, allowing direct measurement of ancient surface brine temperatures. Salt deposits are also widely distributed, occur at high, mid- and low-latitudes, and are present from every geologic period.

A late Pleistocene/Holocene mid-latitude paleoclimate record is presented for the high elevation Qaidam Basin on the Qinghai-Tibet Plateau. Major element and stable isotope compositions of surface brines, preserved, along with atmospheric gases, as fluid inclusions in salt, are used to construct the record which covers the last 54 ka. Preliminary data from a core through Death Valley, California, covering the last 200 ka are also presented.

References:

- Genthon, C.; Barnola, J.M.; Raynaud, D.; Lorius, C.; Jouzel, J.; Barkov, N.I.; Korotkevich, Y.S. & Kotlyakov, V.M. (1987): *Nature* 329, 414-418.
- Lorius, C.; Jouzel, J.; Raynaud, D.; Hansen, J. & Le Treut, H. (1990): The ice core record: climate sensitivity and future greenhouse warming. *Nature* 347, 139-145.
- Lowenstein, T.K. & Hardie, L.A. (1985): Criteria for the recognition of salt pan evaporites. *Sedimentology* 32, 627-644.

CARBON DIOXIDE, SILICATE MELT AND SULFIDE MELT INCLUSIONS IN MANTLE METASOMATIZED PERIDOTITE XENOLITHS FROM THE NÓGRÁD-GÓMÖR VOLCANIC FIELD, NORTHERN HUNGARY/SOUTHERN SLOVAKIA

SZABÓ, CS. (1, 2) and BODNAR, R. J. (1)

(1) Fluids Research Laboratory, Department of Geological Sciences, Virginia Tech, Blacksburg, VA 24061, USA

(2) Department of Petrology and Geochemistry, Eötvös University, Budapest, Múzeum Krt. 4/A, 1880, Hungary

Extensive studies of upper mantle peridotite xenoliths have shown that much of the upper mantle is chemically heterogeneous over a wide range of spatial and temporal scales. It is now widely accepted that these heterogeneities are related to mantle metasomatic alteration associated with fluids of variable composition. Cr-diopside peridotite xenoliths hosted in alkaline basalts from the Nógrád-Gömör Volcanic Field (NGVF) of northern Hungary/southern Slovakia are excellent materials to study mantle metasomatic fluids and the products of the metasomatic event. Based on chemistry and texture, NGVF Cr-diopside xenoliths can be divided into two groups: (1) protogranular to porphyroclastic and equigranular spinel lherzolite - spinel websterite \pm amphibole, and (2) secondary recrystallized dunite - spinel lherzolite \pm minor phlogopite. Textural and chemical features indicate that both xenolith groups underwent modal and cryptic metasomatism, as evidenced by the presence of volatile-bearing minerals (amphibole and phlogopite) and LREE enrichment.

Both xenolith groups contain various types of fluid inclusions, including CO₂, sulfide melt, and silicate melt inclusions. The silicate melt inclusions are composed of glass + CO₂ \pm silicate, oxide, apatite and sulfide daughter minerals. Textural and chemical evidence suggests that the majority of these fluid inclusions represent mantle metasomatic agent(s) that were trapped in the mantle and preserved during transport to the surface.

CO₂ inclusions provide a minimum trapping pressure of 6.5 to 7.5 kbar (depth of 22-25 km) at an assumed trapping temperature of 1,250°C. This depth range approximates the crust/mantle boundary (MOHO) beneath the NGVF. Below the MOHO the ascent rate of the lavas was relatively slow, but probably increased considerably at shallower depths as a result of "boiling" of the melts to generate immiscible volatiles which increased melt buoyancy.

Sulfide assemblages from NGVF xenoliths provide an opportunity to address several questions related to the origin of sulfides commonly observed in upper mantle peridotites. Bulk compositions of multiphase sulfides were compared to Ni-poor monosulfide solid solutions that are clearly of metasomatic origin. The majority of the multiphase blebs are Ni-rich sulfides interpreted to have formed by immiscibility related to partial melting in the mantle. Other multiphase sulfides which are enriched in Fe developed their compositions during the mantle metasomatic process.

Based on the chemistry of the multiphase silicate melt inclusions, two types of silicate melts (andesitic and basaltic) are proposed as potential metasomatic agents beneath the Nógrád-Gömör Volcanic Field. Both melt compositions are characterized by high concentrations of alkalis, Al₂O₃, CO₂, halogens (F, Cl), high mg# (around 80), and probably elevated H₂O contents. The andesitic melt

was probably derived from the same mantle source as the Mio-Pliocene subduction-related magmas that occur within the Nógrád-Gömör Volcanic Field. This melt is probably also responsible for formation of mantle metasomatic minerals such as amphibole and phlogopite. The basaltic melt that occurs only in one peridotite xenolith likely has the same source as the host alkaline basalt magmas that transported the xenoliths to the surface.

FLUID COMPONENT IN YAKUTIAN DIAMONDS OF DIFFERENT PARAGENESIS

TALNIKOVA, S. (1), BARASHLOV, Y. (2) & PANKOV, V. (3)

(1,2) Institute of Geosciences, Yakutsk, Russia

(3) Yakut Committee for Precious Metals and Gemstones, Russia

For the first time, the authors found out compositions and concentrations of gases in diamonds of established paragenesis (Talnikova et al., 1991). Gases in the studied diamonds are mainly represented by six components: N_2 , H_2 , CO_2 , H_2O , CO and CH_4 , there-by corresponding to fluids of the system H-O-C-N (Table). Oxidation-reduction potential of the crystallization environment can hardly be calculated due to a generally multi-component composition of the studied fluids and highly varying concentrations of some components from diamond to diamond. Comparison of the available data with equilibrium compositions of ideal mixtures of the simplified system H-O-C-N (Nikolsky, 1987) shows that none of the discovered compositions corresponds to an equilibrium one because of high CO_2 and CO contents. The non-equilibrium composition of the volatile components appears to be due to the fact that they reflect bulk compositions of gases from different in time growth zones in diamond. Calculation of compositions of gases in equilibrium with diamond shows strong dependence of their molar fractions on the oxygen fugacity characterized by values an order of magnitude lower than fO_2 of the QFM buffer up to fO_2 of the WI buffer (Ryabchikov, 1980).

Analysis of the diagram for compositions of fluids from diamond (Fig.) shows that:

1) diamonds of eclogitic paragenesis fall into two groups in terms of gas composition: primarily carbon dioxide and carbon dioxide-aqueous;

2) carbon dioxide-aqueous fluid in diamonds of eclogitic paragenesis is more oxidized than that in diamonds of ultrabasic association.

Study of a gaseous component in diamonds of known paragenesis will make it possible to obtain new information about a fluid regime of the diamond crystallization environment.

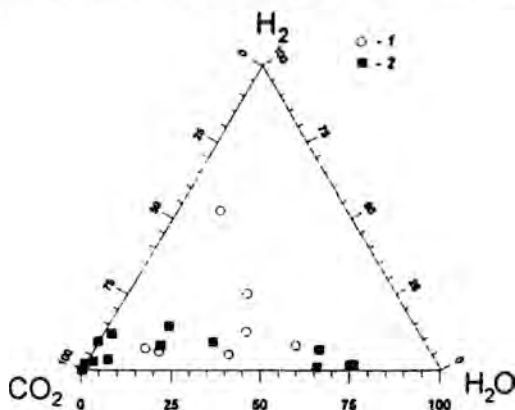


Fig. Gas composition in diamonds of ultrabasic (1) and eclogitic (2) paragenesis projected onto the CO₂ - H₂O - H₂ plane from the apex of the CH₄ tetrahedron.

Compositions of gases in Yakutian diamonds

N	N	H ₂	N ₂	CO ₂	H ₂ O	CH ₄
n/n	образца					
1	3207	0.032	1.414	2.851	0.943	0.007
2	3557	0.03	1.42	7.102	2.018	0.018
3	3600	0.004	0.131	0.301	0.078	0.109
4	3625	0.015	4.413	8.944	0.616	0.09
5	3659	0.021	2.369	1.917	1.218	0.092
6	3689(1)	0.06	0.086	1.055	-	-
7	3689(2)	0.008	0.291	2.138	-	-
8	198	0.038	3.344	5.887	0.071	0.071
9	1164(1)	0.008	1.546	3.843	0.768	0.021
10	1164(2)	0.015	1.739	4.098	0.741	0.012
11	1169(1)	0.029	1.153	2.99	0.308	0.01
12	1169(2)	0.035	4.356	36.104	-	0.116
13	3027	1.574	358.0	325.40	-	-
14	3031	0.061	11.489	12.184	1.209	0.037
15	3037(1)	0.01	0.395	5.494	0.131	0.021
16	3037(2)	0.019	4.047	13.637	0.112	0.027
17	3038	0.067	3.074	19.988	23.932	0.233
18	3165	0.091	7525	94.364	79.977	-
19	3640	0.032	8.778	3.091	2.654	-
20	3662	0.114	11.924	15.538	3.477	0.166

Note: Gas contents given in g/g of a crystal 10⁻⁶. Samples 8-12 from pipe Mir, 13-20 from pipe Udachnaya. CO identify at the 3600 - 0.173; 3689(1) - 0.223; 3689(2) - 0.36; 1169(1) - 3.345; 3037(1) - 2.126; 3037(2) - 7.044; C₂H₆ - 3600 - 0.018; 3625 - 0.073; 3659 - 0.018; 198 - 0.015; 3031 - 0.184; 3038 - 0.405; C₃H₈ - 3625 - 0.149; 3659 - 0.028; 198 - 0.029. NN 1-7 - diamonds of ultrabasic paragenesis, NN 8-20 - diamonds of eclogitic paragenesis.

References

Talnicova et al (1991) Composition and concentration of gases in diamonds of eclogitic and ultrabasic paragenesis. Doklady AN SSSR, vol. 321, N 1, p.194-197.
 N.S.Nikolsky (1987). Fluid regime of endogenous mineral formation. Moscow, Nauka, 198 p.
 I.D.Ryabchikov (1980). Nature of kimberlite magmas. Geology of ore deposits, v.XXII, no.6, p.18-25.

CRYOMETRIC STUDIES OF FLUID INCLUSIONS IN NATURAL DIAMONDS.

TOMILENKO, A.A., CHEPUROV, A.I. & SHEBANIN, A.P.

Institute of Mineralogy and Petrography, Universitetsky pr.3,
630090 Novosibirsk, Russia.

Series of monophasic transparent inclusions have been found during optical studies of flat-parallel plates made of single-crystals of natural diamonds from the placers of northeastern Siberian Platform. They are located in healed cracks, which are not exposed at the crystal surface. The inclusions are flattened and have the shape of isometric plates with the elements of diamond cutting mainly of faces (111). The size of inclusions range from a few to 35 μm .

The optical, cryometric and Raman-spectroscopic investigations allowed us to establish 3 types of liquid inclusions in diamonds. On cooling, a solid phase (phase A) is frozen out at temperature below -50°C in the I type inclusions, which turns into a thin isometric plate. Cooling up to -120°C of the liquid, left after freezing out of phase A, results in precipitation of one more or several solid phases (phase B). On slight heating they rather quickly recrystallize into one crystal. Phase B may occupy up to 20-30% vacuole volume of inclusions. Further cooling up to -196°C of the residual liquid does not lead to its heterogenization or other changes in inclusions. Slow heating of the sample results in the beginning of melting first of phase B, which is already observed at about -75°C . The final melting temperature of phase B is -66°C . Further heating leads to gradual melting of phase A, whose final melting temperature is -42°C . Similar values of melting temperatures of phase B and triple point for pure CO_2 ($-56,6^{\circ}\text{C}$) and peculiar features of its behavior on cooling and heating allowed an assumption that phase B is most likely a solid CO_2 . Melting of phase B at lower temperature as compared to the temperature of triple point for pure CO_2 seems to be affected by nitrogen. The presence of nitrogen in the I type inclusions was confirmed by Raman spectroscopy. The melting temperature (-42°C) and peculiar features of behavior of phase A at low temperatures allowed us to suggest the presence of some amount of hydrocarbons along with carbon dioxide and nitrogen in the I type inclusions. The fluid inclusions of the II and III types are similar in appearance to the I type inclusions and are localized within one healed crack. On cooling to temperatures -120°C one or a few solid phases precipitate in the II type inclusions, which are similar to phase B of the I type inclusions. According to the results of cryometric and Raman-spectroscopy analyses, the composition of the II type inclusions is represented by a mixture of carbon dioxide and nitrogen.

On cooling to -110°C , in the III type inclusions only one solid phase is precipitated, which commonly occupies up to 75-80% of vacuole volume of inclusions. Further cooling up to -196°C does not result in any changes in inclusions. On heating, gradual melting of solid phase occurs in the temperature range from -58 to

-36°C. No vibrational lines of Raman spectra typical of N₂, CO, CH₄ and heavier, than CH₄ hydrocarbons, which have vibrational lines in subregions 800-1200, 1400-1600 and 2800-3200 cm⁻¹, were observed. In terms of cryometric characteristics, this is solid phase similar to phase A of I type of inclusions, whose lower melting temperature in the I type inclusions seems to be affected by carbon dioxide and nitrogen. The results of cryometric and Raman-spectroscopic studies allow us to suggest that the composition of the III type inclusions contains mainly hydrocarbons (?), whose Raman-activity is extremely low.

The presence of the II and III types of inclusions within one crack suggest, that these inclusions were most likely formed as a result of necking down of the I type of inclusions.

The observed fluid inclusions are located in the cracks and their preservation occurred after crystallization of diamonds. At the same time, the healed character of cracks undoubtedly indicates that during preservation of inclusions there existed conditions (temperature, pressure and composition of medium) required for crystallization of diamonds. The latter is confirmed by the presence of a negative diamond cutting in the appearance of inclusions, their necking down and recrystallization of diamond sites around inclusions.

INTERACTION OF MELT INCLUSION SUBSTANCE AND HOST SYNTHETIC PERICLASE ON HEATING

TOMILENKO, A.A. & KOVYAZIN, S.V.

Institute of Mineralogy and Petrography, Universitetsky pr.3, 630090 Novosibirsk, Russia.

A series of experiments on heating of melt inclusions in synthetic periclase to various temperatures allowed an establishment of the phenomenon of diffusive exchange of components between inclusions and host mineral of constant composition. For the experiments we used commercially synthesized periclase produced by fusion-arc melting of natural magnesite. Periclase composition was macrochemically homogeneous in the crystal. The content of MgO amounts to 99.9 wt.%; the total amount of impurities does not typically exceed 0.05-0.25 wt.%. The iron content in terms of FeO in periclase ranges from 0.01 to 0.06 wt.%. Several groups of glassy and crystallized silicate-melt inclusions with ore phase (more than 80 inclusions) were selected for the experiments. The inclusions were similar in composition and size. Their main components are CaO (38-46 wt.%), SiO₂ (36-42 wt.%), MgO (15-20 wt.%), Al₂O₃ (2-11 wt.%) and FeO (about 2.6 wt.%). Spherical ore phase is nearly totally composed of iron (Fe up to 96.28 wt.%). Some ore phases of inclusions are enriched in Si (up to 5.21 wt.%) and P (up to 2.62 wt.%). The start of melting of crystalline phases and glass is observed at temperature about 1250°C. During heating of glassy inclusions a non-equilibrium retrograde crystallization occurs in them long before softening and melting of glass at about 950°C. Heating of inclusions is accompanied also by melting of ore phase, the beginning of which (in the case of rapid heating) is registered at about 1400°C. Within the range of temperatures 1400-1480°C the immiscibility of ore and silicate melts was observed. Dissolution of ore melt drop takes place at slight increase in temperature above 1480°C. Complete melting of all solid phases in the inclusions occurs to temperature 1500°C. The sizes of inclusions do not vary even at heating up to 2200°C.

Electron microprobe analysis along profiles through unheated inclusions and the host mineral showed that boundary between inclusions and matrix is very distinct, without any concentration zoning in the matrix around inclusions. Periclase samples, heated to 900°C and kept during 10 hours at this temperatures, are also characterized by a drastic alteration of the composition of media at the interface inclusion/matrix (the inclusion has reduced magnesium content and elevated contents of iron, calcium, silicon, aluminum, and phosphorus). At 1000°C (exposed during 8.5 hours) the variation of FeO concentration in the matrix at the boundary with inclusions is not so drastic, which indicates diffusion of iron from inclusions into the host periclase. The diffusion of iron from inclusion into matrix at 1100°C begins at shorter time of exposure (3.5 hours). When the first portion of the melt appears in inclusions, the rate of iron diffusion into the matrix considerably increases and continues to grow regularly with

increasing temperature of heating. Thus, at 1350°C and one-minute exposure, the FeO content in the matrix near the interface inclusion/host mineral is 0.58 wt.%, while at the same time exposure but 1400 and 1500°C, it increases from 1.38 to 2.05 wt.%, respectively. The size of diffusion zone around inclusions in the matrix at temperature 1350°C and 1-2 minute exposure attains 6 μm , while at 1400 and 1500°C and the same exposure - 12 and 50 μm , respectively. At longer exposure (1 hour at 1350, 1400 and 1500°C), the diffusion zone of iron in the matrix considerably increases (up to 20, 48, and 70 μm , respectively). The iron content in inclusions appreciably decreases (down to 0.22 wt.%), as compared with unheated (about 2.6 wt.%) and heated inclusions but with 1-2 minute exposure (1.62 wt.%). Two-hour exposure at temperatures 1350, 1400, and 1500°C results in widening of the diffusion zone of iron in the matrix respectively to 40, 60, and 80 μm and more. The iron content in the inclusions and in the matrix within this zone become practically similar (0.17 wt.% in the inclusion and 0.13 wt.% in the matrix 60 μm apart from the interface inclusion/matrix). The samples heated at temperatures below the beginning of melting of solid phases in the matrix around inclusions display a distinct asymmetry in the iron distribution in matrix around inclusions, if the ore phase in these inclusions is located near to the boundary with the matrix. More intensive diffusion of iron into the matrix occurs on this kind of sites where ore sphere is adjacent to periclase. At high temperature this asymmetry in iron distribution in the mineral around inclusions disappears.

Thus, the investigation performed show that during experiments on homogenization of melt inclusions, a diffusion exchange of components between inclusions and host mineral may occur. This may start at considerably lower temperatures than temperature of the beginning of the solid phase melting in inclusions. The diffusion process is essentially accelerated when new portions of melt appear in inclusions. Use of melt inclusions heated in laboratory experiments or under natural conditions (melt inclusions in mineral from deep-seated xenoliths uplifted by basalt or kimberlite melts) for estimating chemical composition of initial magmas without regard of this factor may lead to errors. Hence, it is very important to obtain quantitative values of possible alteration of melt composition depending on the property of host mineral, its chemical composition, sizes and properties of inclusions, etc.

CaCl₂-RICH FLUID INCLUSIONS IN THE GARNET BEARING GNEISS OF THE KO-HEGY QUARRY, SOPRON (W-HUNGARY)

TOROK, K

Eötvös L. Univ. H-1088 Budapest Múzeum krt. 4/A, Hungary

The metamorphic complex near Sopron (W-Hungary) is the eastern outcropping part of the Grogneiss series of the Austroalpine nappe system. The area is built up by medium and low grade micaschists and subordinate amphibolites, and low grade orthogneisses. The studied garnet bearing gneiss from the Ko-hegy quarry belongs to the low grade orthogneiss group, which suffered Alpine metamorphism. The rock consists of potash feldspar, almost pure albite (anorthite content less than 4%), quartz, phengitic muscovite, biotite, grosularite and almandine-rich garnet and accessory zircon and apatite. Quartz veins either parallel with foliation or crosscutting it are abundant.

Two phase, liquid and rich aqueous inclusions were measured from the matrix albite and the quartz vein cutting the foliation. Inclusions in the quartz vein trapped along healed fractures. These healed fractures can be followed through the entire thin section in a 5-6 mm wide track. These inclusions can be grouped in three types:

- Type I. Primary inclusions occurring in core of matrix albite together with solid inclusions of phengitic muscovite. Solid and fluid inclusions are absent from the clear rim of the albite. The inclusions contain medium salinity (10.9 - 12.4 NaCl eqv. wt%) aqueous solution with homogenisation temperature from 178.4 to 217.2 °C (Fig.1). Though the inclusions are quite small (less than 8-10 microns) some eutectic temperatures (between -28 and -35.4°C) show the presence of other cations than Na⁺ (possibly Ca²⁺).

-Type II. Inclusions of this type occur along healed fractures in quartz veins and contain low to medium salinity brine (7.1-12.4 NaCl eqv. wt%). Homogenisation temperatures range from 85.4 to 176.0°C (Fig.1).

- Type III. Inclusions occur along healed fractures in quartz veins and contain concentrated CaCl₂-NaCl-H₂O brine as it can be deduced from the low first melting points (between -65.6 and -45.5°C) and ice melting temperatures (-40 - -17.2°C). The calculated salinity is between 20 and 28 CaCl₂ eqv. wt% (Linke, 1965). Homogenisation temperatures are similar to those of the type II inclusions, range between 60.7 and 170.8°C (Fig.1).

One phase aqueous inclusions can be also observed in the quartz vein, associated with type II and III inclusions. These inclusions fail to heterogenize even at freezing down to -150°C. This phenomenon can be attributed either to metastability or show that trapping of inclusions continued at low temperatures as well.

Type II and III inclusions occur together in the same textural position or along parallel healed fractures which suggest that these two distinct fluids may have been coeval and existed

together without mixing for a long time. Mixing of the two fluids can be recorded only at low temperatures (Fig.1).

Mineral equilibria and phengite geobarometry indicate peak metamorphic conditions of about 8-10 kbar pressure at about 500°C temperature. The isochores of the Type I primary inclusions in the matrix albite indicate lower pressure, 5-6 kbar at 500°C. Type II and III inclusions in quartz vein crosscutting the foliation may belong to the retrograde phase.

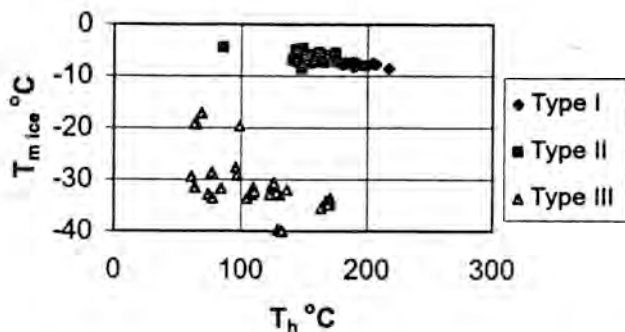


Fig. 1. T_h , versus T_{mice} for the measured inclusions in the Kő-hegy gneiss.

References

Linke, W.F. (1965). Solubilities of inorganic and metal-inorganic compounds. 2 Am. Chem. Soc., Washington D.C., 4th ed. 1914 p.

BRINES IN GRANULITES: THE OTHER FLUID.

TOURET, J.L.R.

Department of Petrology and Isotope Geology, Free University, De
Boelelaan 1085, 1081HV Amsterdam, The Netherlands.
E-mail: touj@geo.vu.nl

At world scale, metamorphic and igneous granulites are characterized by the occurrence of high-density, CO₂-rich fluid inclusions (carbonic fluids), CO₂ being sometimes mixed with other gaseous components (N₂ and, to a much lesser extent, hydrocarbons). In many cases, the density of these carbonic inclusions has been reequilibrated during the post-metamorphic evolution (retrograde P-T path), but with only limited movements of the fluid masses and nearly in-situ "transposition" of the inclusions, at the scale of the host-mineral or the hand specimen. It can then be demonstrated that the initial delivery of the gaseous fluid in the rock system has occurred during peak metamorphism (Touret, 1992). CO₂ (as well as N₂) has been transported from mantle depth (e.g. Van den Kerkhof et al., 1994) by various kinds of deep-seated, synmetamorphic intrusives.

Carbonic fluids, however, are not the only fluid remnants preserved in granulites. Traces of high-salinity, NaCl-rich brines have also been observed in inclusions from a great number of granulite occurrences. These are much less obvious than CO₂-rich inclusions and they can easily remain unnoticed if not systematically searched for: because of the steep slope of any brine isochore, the internal pressure in an inclusion occurring at peak conditions will be systematically much lower than external pressure during most retrograde regional P-T paths. The inclusion will collapse, leaving only a small aggregate of microcrystals within an irregular, squeezed cavity.

Many examples of these brine inclusions have been observed in different regions, some Archean, many Proterozoic, e.g. in Southern Norway (Touret, 1985). They occur in various lithologies, but mostly in pre-metamorphic, supracrustal remnants which have remained perfectly preserved despite the high metamorphic grade and a most complicated history. At least 3 major types of preferred environments have been identified:

1) Detrital sediments, essentially quartzites and metapelites. Brine inclusions are especially spectacular in and near tourmaline-apatite-cordierite-plagioclase lenses, pegmatitic in appearance, which in Southern Norway could represent remnants of former evaporites (Bjordammen near Kragero, Bamble sector).

2) Various lithologies, such as cordierite-antophyllite rocks, which could derive from hydrothermal, sea-floor type hydrothermal alteration of basaltic lavas. This type of environment includes the well-known skarns occurring in the vicinity of Arendal (Southern Norway), in which the diagenetic isotopic signature has been preserved (Broekmans et al., 1994). It can even be suggested that metasomatism leading to skarnification did already occur during the sedimentation, well before the peak of metamorphism. Skarns would then be the product of isochemical recrystallization of hydrothermally altered sea-floor carbonates.

3) Acid volcanics (metarhyolites) and shallow intrusives, high grade equivalents in the Bamble sector of some of the low-grade Telemark supracrustals (Norway).

The striking relationship between the brine inclusions and these different supracrustal lithologies show without any ambiguity that the brines are remnants from pre-metamorphic fluids, still present despite the most complicated regional P-T evolution. It is also obvious that fluids presently trapped in inclusions represent only a small fraction of the fluids which have been present in the rocks since their deposition at the Earth's surface. During prograde, peak and retrograde metamorphism, most of the brines have been remobilized and transported on various distances, either locally (evidenced in Southern Norway by extensive scapolitisation in and around some gabbroic intrusions) or regionally, along all the shear-zones which occur systematically in high-grade complexes (Huizenga, 1995). These brines must play an important role in controlling the chemical potential of alkalies during granulite metamorphism. They are the best candidates for explaining the complexities of LILE-element behaviour at the boundary of granulite metamorphism: either depletion (regional scale) or, on the contrary, increase (LILE-repletion) during the metasomatic transformation of metapelite into charnockite in the so-called "incipient charnockites" of Southern India and Sri-Lanka (Perchuk et al., 1994).

References

- BROEKMANS, A.T.M., NIJLAND, T.G. & JANSSEN, J.B.H., 1994, Are stable isotopic trends in amphibolite to granulite facies transitions metamorphic or diagenetic? An answer for the Arendal area (Bamble sector, SE Norway) from Mid-Proterozoic, carbon-bearing rocks. *Am. J. Science*, vol. 294-9, p. 1135-1165.
- HUIZENGA, J.M., 1995, Fluid evolution in shear zones from the late Archean Harare-Shamva-Bindura greenstone belt (NE Zimbabwe). Ph.D. Thesis, VUA (Free University Amsterdam), 146p.
- VAN DEN KERKHOF, A.M., TOURET, J.L.R. & KREULEN, R., 1994, Juvenile CO₂ in enderbites of Tromøy near Arendal, Southern Norway: a fluid inclusion and stable isotope study. *J. metamorphic Geol.*, vol. 12, p. 301-310.
- PERCHUK, L.L., GERYA, T.V. & KORSMAN, K., 1994, A model for charnockitization of gneissic complexes, *Petrology*, vol. 2, n° 5, p. 395-423.
- TOURET, J.L.R., 1985, Fluid regime in Southern Norway: the record of fluid inclusions, p. 517-550 in Tobi, A.C. and Touret, J.L.R. (eds) *The deep Proterozoic crust in the North Atlantic Provinces*, NATO ASI Series, C 158, D. Reidel Pub., 603p.
- TOURET, J.L.R., 1992, CO₂ transfer between the upper mantle and the atmosphere: temporary storage in the lower continental crust, *Terra Nova*, vol. 4, p. 87-98.

EVAPORITE-RELATED FLUIDS AND ORE DEPOSITION DURING MESOZOIC RIFTING IN EASTERN AND NORTHEASTERN SPAIN.

TRITLLA, J.(1,2), CANALS, A. (2), BANKS, D.(1),CARDELLACH, E. (3)

- (1)Earth Sciences Department. The University of Leeds. U.K.
(2)Departament de Cristal·lografia, Mineralogia i Diposits Minerals. Facultat de Geologia. Universitat de Barcelona, Spain.
(3)Departament de Geologia. Facultat de Ciències. Universitat Autònoma de Barcelona, Bellaterra, Spain.

Three Mesozoic rifting zones, located in E and NE Spain, formed during the breakup of Pangea have been studied: Pyrenees, Catalanian Coastal Ranges and Iberian Ranges. Along these rifts zones the presence of extensional faults and the anomalously high geothermal gradient caused the mobilization of hydrothermal solutions and the formation of a large number of low temperature ore deposits.

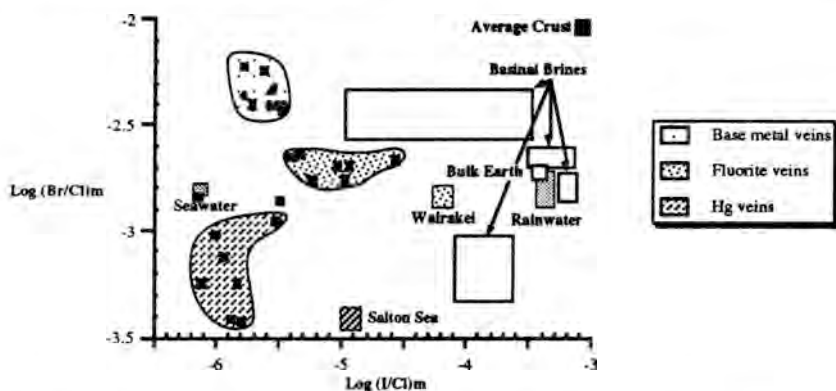
Low temperature veins in the Pyrenees and the Catalanian Coastal Ranges are hosted by Palaeozoic lithologies, tardihercynian granitoids and, occasionally, the Triassic basal levels. Mineralogical composition is variable, ranging from Pb-Zn-(Ba) rich veins (Atrevida, Cierco) to fluorite rich veins (Rigros, Berta), with variable amounts of barite. All these deposits have a low temperature of formation (between 75 and 200°C), the presence of complex polysaline fluids (NaCl-CaCl₂-KCl-(MgCl₂)) with salinities between 12 to 22 wt% eq NaCl, and a clear relationship with the pretriassic paleosurface (Cardellach et al, 1990; Canals et al, 1992). Similar ore deposits are also found in the Eastern part of the Iberian Ranges, (Sierra de Espadán) exclusively hosted by Triassic sediments (Buntsandstein sandstones and Muschelkalk dolostones) In these deposits, the base-metal paragenesis is replaced by mercury sulfides and sulfosalts (cinnabar and Hg-tetrahydrite; Tritlla, 1994). The solutions associated are polysaline (NaCl-CaCl₂-KCl), with temperatures of formation between 230 and 280°C and salinities ranging from 18 to 35wt% eq NaCl.

Halogen crush-leach analyses were performed in the fluid inclusions laboratory of the Earth Sciences Department of the of University Leeds, using the method of Yardley et al (1993). The total chloride concentration was derived from the estimates of the salinity of the inclusions obtained from microthermometry. Halogen ratios have been determined in quartz, calcite, dolomite, sphalerite and fluorite samples.

Base-metal and barite vein fluids have Br/Cl and I/Cl ratios greater than those of seawater but lie close to the seawater evaporation line. Deviations from this line, in terms of the iodide content, could quite easily be due to analytical uncertainties in the analysed data, where discrepancies of a factor of 2 or 3 would not be unreasonable at these low levels. Of greater importance is the Br/Cl ratio which shows that these fluids are similar to brines where the fluid is the "bittern" remaining after halite has precipitated from evaporated seawater.

Br/Cl ratios in fluorite veins are slightly higher than the seawater mean ratio, suggesting that these waters were marine waters that suffered some degree of evaporation before entering in the hydrothermal system. I/Cl ratios are also higher than seawater and can be explained by the circulation of these solutions through rocks rich in I as, for example, the enclosing granitic rocks.

Fluids trapped in dolomite and quartz from the carbonate-hosted mercury veins have Br/Cl ratios lower than and I/Cl ratios similar to sea water. These data suggest that the solutions can be related either with magmatic brines, even though the low iodine concentration in these fluids is not compatible with this hypothesis, or with secondary brines produced by leaching of halite-bearing evaporites. Both the very high salinity of the fluid inclusions (33% NaCl eq.) and the presence of Triassic evaporite layers, with gypsum and halite pseudomorphs, within the upper Buntsandstein facies and the basal levels of the Muschelkalk facies, support the latter hypothesis



Stable isotope data, such the sulfur isotopic composition of the barites and sulfides, and fluid inclusion studies show that these veins formed by the mixing of subsurface, metal rich brines with surficial waters either marine (Catalonian Coastal Ranges deposits) or that had interacted with evaporites (Pyrenees and Espadán deposits). The ultimate source for the subsurface brines would be evolved basinal brines that had interacted with the basement lithologies.

So, there is a common main mechanism of formation for these ore deposits, which is related with deep crustal circulation of fluids beneath subsiding basins in Mesozoic times. The differences between deposits are due to the importance of the regional geothermal anomaly and the local availability of one or another element.

References

- CANALS, A.; CARDELLACH, E.; RYE, D.M. and AYORA, C. (1992): Origin of the Atrevida vein (Catalonian Coastal Ranges, Spain): Mineralogic, Fluid Inclusion and Stable Isotope study. *Econ. Geol.*, 87, 142-153.
- CARDELLACH, E.; CANALS, A. and TRITLLA, J. (1990): Late and post-hercynian low temperature veins in the Catalonian Coastal Ranges. *Acta Geol. Hisp.*, 25, 75-81.
- TRITLLA, J. (1994): Geología y Metalogenia de las mineralizaciones de Ba-Hg de la Sierra de Espadán (Provincia de Castellon). Unpublished Ph.D. Thesis, Universitat Autònoma de Barcelona.
- YARDLEY, B.W.D.; BANKS, D.A.; BOTTRELL, S.H. and DIAMOND, L.W. (1993): Post-metamorphic gold-quartz veins from N.W. Italy: the composition and origin of the ore fluid. *Min. Mag.*, vol. 57, 407-422.

THE CHARNOCKITIZATION AT NICHOLSON'S POINT, NATAL METAMORPHIC PROVINCE, SOUTH AFRICA: THE ROLE OF FLUIDS

VAN DEN KERKHOF, A.M. (1) & GRANTHAM, G.H. (2)

(1) Institute of Geology and Dynamics of the Lithosphere, University of Göttingen (Germany)

(2) Department of Geology, University of Pretoria (South Africa)

In the Port Edward area (Proterozoic of southern Natal, South Africa) charnockitic aureoles up to ~4 m in width are developed adjacent to contacts with the Port Edward enderbite (opx-cpx-plag-Kfsp-qtz-bi (apatite (ilmenite (zircon) which intruded the Nicholson's Point granite. The non-charnockitized granite contains significant garnet, biotite and accessory pyrite and ilmenite; the charnockitic parts contain increased myrmekite, very little biotite and pyrite is replaced by pyrrhotite.

The garnetiferous and charnockitic granite have similar major element chemistry. Lower Rb, Th, Nb and Y contents in the charnockite suggest that these elements have been locally depleted during charnockitization. In the charnockitic granite the light REE are weakly depleted whereas the heavy REE show greater depletion compared to the garnetiferous granite. The depletions in REE are thought to be related to the breakdown of garnet. Eu is enriched or unchanged in the charnockite relative to the garnetiferous granite.

Two-pyroxene thermometry on the Port Edward enderbite suggests that it intruded at temperatures of ~1000-1100°C (Lindsley, 1983). These temperatures are consistent with the high P₂O₅ contents and the megacrystic textures in the enderbite. Hypersthene-ilmenite thermometry from the charnockitic Nicholson's Point granite suggests temperatures >1000-1100°C (Babich et al. 1994). Being higher than the solidus for dry granite however they do conform a high temperature environment. The composition of the hypersthene in the charnockite is ~Fe₇₅, which is stable at >~5 kbar at 1000°C. (Bohlen & Boettcher, 1983). The reaction of garnet + quartz formed from hypersthene + plag is typical of an isobaric cooling path (Harley, 1989). Thermobarometry suggests a pressure of ~5 kbar at ~950°C (Powell & Holland 1988). Higher temperatures in the aureole are also suggested by the formation of pyrrhotite (46% atomic Fe suggesting formation at >~700°C).

The Port Edward enderbite is characterized by dense CO₂ and CO₂-N₂ inclusions and N₂ inclusions with minor CH₄ (V=46-53 cm³/mole with a maximum at 46-48 cm³/mole). The restriction of these inclusions to the enderbite and their absence from the country rock (low salinity water, low density N₂) suggests that they may be primary in composition. CO₂ was probably introduced during emplacement of the enderbitic magma at granulite-facies conditions as also suggested for other examples of syn-metamorphic enderbitic intrusions (Bamble sector-Norway, Kerkhof et al. 1994; Magondi Mobile Belt-Zimbabwe, Munyanyiwa et al., 1993). The fluid inclusion morphology suggests that the inclusions are secondary or they have decrepitated (imploded) during isobaric cooling path recognized in Natal (Grantham et al., in press). The garnet-bearing country rock (Nicholson's Point Granite) is characterized

dominantly by aqueous saline inclusions showing secondary or decrepitated inclusion morphologies. Eutectic temperatures (around -35°C) and SEM analysis indicate the predominance of sulphate solutions. The charnockitic aureole is dominated by low salinity aqueous inclusions showing secondary or strong decrepitated morphologies.

SEM-CL observations of samples in the charnockitic aureoles (LB2 Leisure Bay) show some CL textures which can be related with fluid-rock interaction processes. Remarkable is the extensive development of zones which are indicative for alteration along the grain boundaries (dark contrast) in a regime of plastic deformation. In the same zones a pattern of darkly contrasting spots related with micropores can be observed (after longer radiation times). These textures are thought to be indicative for quartz with high contents of structural water. Superimposed on this pattern, fluid inclusions > -2 µm show irregular darkly CL-contrasting halos related with healed microcracks. These may indicate late transformation of the fluid inclusions by quartz dissolution-precipitation at conditions of semi-brittle deformation.

The charnockitization adjacent to the Port Edward enderbite appears to have been thermally driven. The lack of CO₂ in the aureole is surprising. A possible reason for the low salinity water-rich inclusions in the charnockite is that water, released during thermally induced dehydration of biotite + quartz (opx + Kfsp + water, was trapped during the intrusion of the enderbite. The few N₂ inclusions in the charnockite could similarly have been derived from intrusion of the enderbite. Subsequent cooling along an isobaric cooling path would result in decrepitation of the inclusions causing secondary morphologies. Assuming cooling towards a stable geothermal gradient of 30°C/km, the crustal thickness at 500-600 Ma would have been -8-9 km or pressures of 2-3 kbar, consistent with the entrapment/decrepitation conditions suggested for the higher and lower salinity aqueous inclusions in the garnetiferous and charnockitic granites respectively.

Whereas the genesis of charnockite in other localities has been attributed to high CO₂ fluids (e.g. Southern India, Srikantappa et al.,1992) in the Nicholson's Point Granite, charnockitization adjacent to the Port Edward enderbite appears to have been largely controlled by temperature.

References

- Babich YV, Green DH & Sobolev (1994) Abstracts 16th IMA meeting, Pisa, p. 22-23.
Bohlen SR & Boettcher AL (1983) *American Mineralogist*, 66, 951-64.
Grantham GH, Thomas RJ & Mendonidis P (1995, in press) *J. African Earth Sci.*
Harley SL (1989) *Geol. Magazine*, 126, 215-247.
Kerkhof AM van den, Touret JLR & Kreulen R (1994) *J. metamorphic Geol.*, 12, 301-310.
Lindsley DH (1983) *American Mineralogist*, 68, 477-493.
Powell R & Holland TJB (1988) *J. metamorphic Geol.*, 6, 311-332.
Srikantappa C, Raith M & Touret JLR (1992) *J. Petrology*, 33, 733-760.

FLUID INCLUSION EVOLUTION IN UPPER MANTLE XENOLITHS FROM PATAGONIA, ARGENTINA

VARELA, M.E. (1,2), BJERG, E.A. (1) & LABUDIA, C.H. (1)

(1) Departamento de Geología, Universidad Nacional del Sur, San Juan 670, (8000) Bahía Blanca, Argentina.

(2) Present address: Groupe des Sciences de la Terre, Laboratoire Pierre Sûe, CEN Saclay, 91191 France.

Fluid inclusions in ultramafic xenoliths hosted by Pliocene-Pleistocene alkaline basalts from the Somuncura Massif, Northern Patagonia, provide an estimation of the depth/pressure at which they were captured by the hosting alkaline basalts and their ascent history.

The main unit of the Somuncura Massif consists of low grade metamorphic rocks, Permocarboniferous-Triassic plutonic-volcanic cycle, Upper Triassic-Jurassic andesites and rhyolites. Pyroclastic and fluvial deposits interbedded with basaltic flows give rise, during Oligocene to Miocene, to the Somuncura Plateau. The Pliocene-Pleistocene time is represented by alkaline basalts with ultramafic nodules, controlled by a NW-SE and E-W faulting.

Basic petrographic and fluid inclusion data on these xenoliths allow a first attempt in the P-T estimation of their regional evolution based on a W-E regional profile of approximately 200 km long. In all the sampled localities (Fig. 1), the alkaline basalts host xenoliths of different sizes. They were classified as spinel lherzolites and harzburgites with protogranular and porphyroclastic textures.

Fluid inclusions were classified according to their occurrence, shapes and homogenization temperatures as "early" and "late" CO₂ inclusions. Different amounts of these inclusions are present in olivine, orthopyroxene and clinopyroxene. Because olivine is easily plastically deformed during eruption, a phenomenon that leads to incorrect density and pressure estimations (Kirby and Green, 1980.), thermometric analyses were done only when these minerals showed only minor deformation. All the studied fluid inclusions showed type H3 microthermometric behaviour (Kerkhof 1990), where $L+V>L$ or $L+V<V$ are the final phase transitions having initial melting (Ti) and final melting (Tm) at or close to the same temperature (-56.6°C) which is characteristic of pure CO₂ inclusions. This allows the fluid density determination using molar volume-temperature data on the two phase regions of pure CO₂ (Roedder 1984).

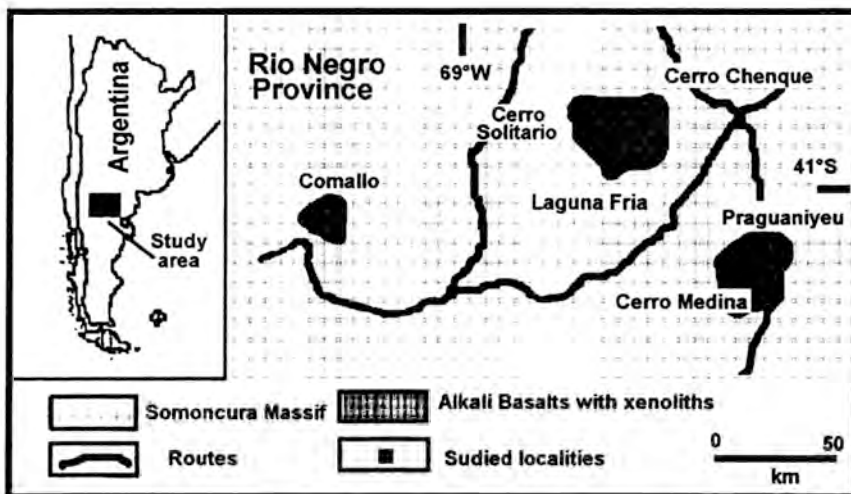
Early CO₂ fluid inclusions have liquid homogenization temperature (Thl) varying from -35°C to 0°C. Late CO₂ inclusions homogenize to a liquid phase between 12°C and 23°C and to a vapor phase within a narrow range: 21°C-25°C. The melting temperature values (Tm) of 140 inclusions range from -56.6°C to -59.2°C, with a mean value of -57.1°C.

Glass+CO₂ inclusions in olivine and clinopyroxene crystals exhibit melting temperatures at -57 °C and no other transition phases were observed up to room temperature due to a continue and progressive darkening of the bubble. This phenomenon impeded the visualization of the homogenization temperature. Trapping pressure

was calculated assuming a trapping temperature of about 1200°C (Roedder, 1984; Schiano and Clocchiatti, 1994) and analytical and experimental data for pure CO₂ systems (Kennedy, 1954 and Holloway, 1981). Trapping pressures for early CO₂ inclusions varies from 6.8 Kbs to 11.6 Kbs (ρ CO₂ 0.9 g/cm³-1.09 g/cm³). For late inclusions trapping pressures varies from 4 Kbs to 5.4 kbs (ρ CO₂ 0.74 g/cm³-0.84 g/cm³) and 0.65 kbs to 0.8 kbs (ρ CO₂ 0.20 g/cm³-0.24 g/cm³). The CO₂ density distribution for early inclusions indicates a minimum depth of origin for the studied xenoliths in the range 21 km-35km. The observed difference in CO₂ densities in late inclusions may indicate two stages in the ascent of these nodules. One episode occurred in the range 14-17 km and the second one, indicated by late CO₂ fluid inclusions that homogenize to the vapor phase, took place in the range 2.4-3 km. Taking into account that these processes were registered in all the studied xenoliths of this area, it is suggested that this evolution is valid on a regional scale in the central part of northern Patagonia.

References

Holloway, J. R., 1981. "Short Course in Fluid Inclusions", L.S. Hollister and M.L. Crawford, ed. Min. Assoc. of Canada, Vol. 6, 13-38.
 Kennedy, G.C., 1954. Am. J. Sci., 252:225-241.
 Kerkhof, A.M. van den, 1990. Geochim. Cosmochim. Acta, 54: 621-629.
 Kirby, S.H. and Green, H.W., 1980. Amer. Journ. Sci., 280-A: 550-575.
 Roedder, E., 1984. Mineral. Soc. Am., Reviews in Mineralogy, 12:1-644.
 Schiano, P. and Clocchiatti, R., 1994. Nature, 368:621-624.



**FLUID CIRCULATION PATH IN A VOLCANIC-HOSTED POLYMETALLIC DEPOSITS,
ANGELA MINE ARGENTINA**

VARELA, M.E. (1,2) & GREGORI, D.A. (1)

(1) Universidad Nacional del Sur, Departamento de Geología-CONICET. San Juan 670 (8000) Bahía Blanca Argentina.

(2) Present address: Groupe des Sciences de la Terre, Laboratoire Pierre Sûte, CEN Saclay, 91191 France.

The Angela Deposit is located in the Somuncura Massif, Patagonia, Argentina. Three main veins, Susana Beatriz, Cobre and Platífero and secondary veins, Dominó, Caldén, Buitre, etc. with a general strike N30-42°E conform this deposit. The area is characterised by an Upper Jurassic-Lower Cretaceous volcaniclastic complex. It is conformed by sedimentary, pyroclastic and volcanic facies of andesitic composition. During Late Cretaceous-Early Tertiary times this complex was intruded by rhyolitic dykes. In this deposit the ore veins and rhyolitic intrusions show a pattern along a NE direction, controlled by faulting and fracturing.

The mineralization is present in two forms: a) disseminated as in the San Jose area and b) in veins as in Susana Beatriz, Cobre, and Platífero. It consists of pyrite, sphalerite, galena, chalcopyrite, tetrahedrite and pyrrhotite. According to Wiechowski et al. (1990) gold, silver, electrum, enargite, boulangierite, bournonite and various undetermined sulfosalts are accessory minerals. Three types of quartz crystals are recognized: a: Coarse-grained euhedral quartz, with well developed growth banding zones and open-space textures, b: Medium euhedral quartz with smaller growth banding zones and c: Fine-grained subhedral quartz. Gold is present as small blebs in quartz.

Fluid inclusion studies were carried out on quartz and sphalerite. Three main types of fluid inclusions are present: Type I: Two-phase liquid-rich inclusions. Type II: Two-phase vapour rich inclusions. Type III: Polyphase inclusions with liquid, vapour bubble and daughter minerals. In them, the daughter mineral/fluid inclusion volumen ratio varies markedly. Towards upper levels the abundance of type III inclusions increase gradually, suggesting that mineralizing solutions could be enriched in carbonates, silica, aluminium, sodium and probably potassium. Type I fluid inclusion abundances in ore shoots duplicate or triplicate those in poorly mineralized zones. Type II fluid inclusions are more abundant in ore shoots, their presence is constant throughout them from deeper levels towards surface. The coexistence of primary or pseudosecondary liquid rich and vapour rich inclusions in the different levels of the Angela Mine could be considered a strong evidence of two-phase conditions due to boiling at the time of trapping (Roedder, 1984). Filling temperatures and salinity data of fluid inclusions are summarised in Table 1. The analysis of these data suggests a depth of formation fluctuating between 1200 and 1500 m.

Notwithstanding that towards surface type I fluid inclusions outnumber type II fluid inclusions, boiling process also occurred. The fluid inclusion studies indicate that boiling may be considered as the principal ore depositional mechanism. Salinity and homogenization temperatures diminish from deeper levels (105-

120) to the level 60 and increase from this level towards surface. An important feature to be noted is the absence of evidence for boiling at the level 60. The homogenization temperature isotherms of

Susana Beatriz and Cobre sectors indicate the appearance of minimum temperatures restricted to intermediate levels. The homogenization temperature data of primary fluid inclusions of the veins are similar to those homogenization temperatures of the secondary fluid inclusions in the quartz phenocrysts of the rhyolitic dykes.

These data indicate that the hydrothermal fluids have maintained broadly the same characteristics during the intrusion of rhyolitic dykes and deposition of ores. Notwithstanding that faulting was an important factor during vein's emplacement fluid circulation paths appears to be more complex. The temperature isotherm designs indicate the existence of a minimum located in or near to the level 60 and maximum temperature areas below and above this level.

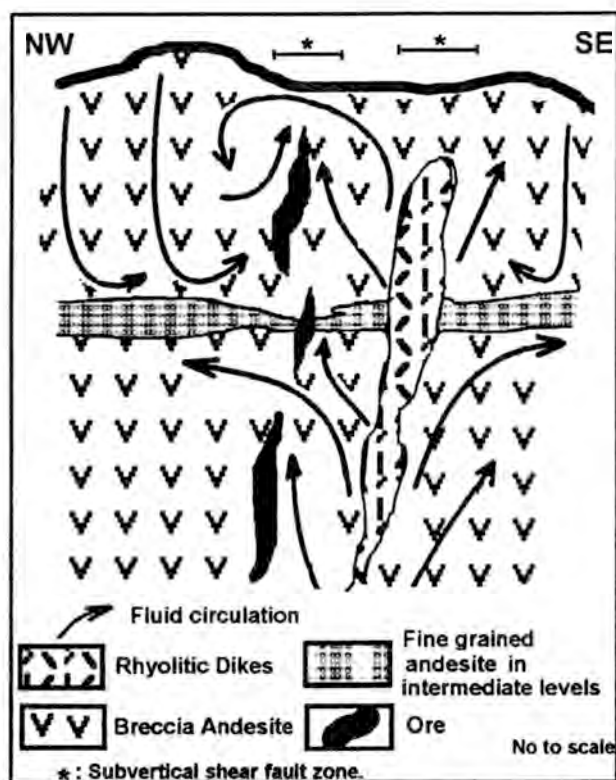
The different lines of evidences show that the fine grained andesite at the intermediate levels acted as an semipermeable media changing the fluid evolution and therefore variation in mineral deposition. In this contribution a speculative model for the fluid circulation path (Figure 1) is proposed considering that the hypersaline fluids released from an oversaturated water rhyolitic magma contributed directly to the formation of this deposit (Varela, 1994). Above intermediate levels mineralizing fluids were mixed and diluted with lower temperatures fluids. Below this level, the presence of the higher temperatures and salinities indicate that mixing and dilution were more restricted.

References

- Roedder, E. (1984), *Rev. Mineralogy*, 12, 646 p.
Varela, M.E. (1994), *Eur. J Mineral.* 6: 837-854.
Wiechowski, A.; Arizmendi, A. and Brodtkorb, M.K. (1990), *Asoc. Arg. Geol. Econ. Special Publication.* 41-43. (Spanish).

TABLE 1: Average thermometric (°C) and Salinity data NaCl (wt% eq.)

Sector	Level	n	NaCl wt% eq.	Th type	
				Ia	II
Susana Beatriz	105	100	5.68	338*	389
	60	100	3.66	308	-
	0	60	-	313	395.5
	Surface	40	4.2	315	387
Cobre	120	150	4.4	311	389.5
	90	170	3.7	308	385.2
	60	40	3.5	301	-
	30	40	3.3	307	378
	0	40	3.9	310	n.d.
Platifero	120	40	4.3	312	n.d.
	70	40	4.6	294	n.d.
	20	40	4.1	288	376



MICROTHERMOMETRIC INVESTIGATIONS IN THE Bi-Te-Ag BEARING Cu-MINERALIZATION OF PANAGIA AREA, THASOS ISLAND, GREECE.

VAVELIDIS, M. (1), SCHMIDT-MUMM, A. (2) & MELFOS, V. (1)

(1) Aristotle University of Thessaloniki, Greece.

(2) University of Halle, Germany

GEOLOGICAL SETTING

The island of Thasos is located at the northern Aegean Sea. It belongs geologically to the Rhodope massif and consists of metamorphic rocks (mainly marbles, schists and gneisses). Mineral parageneses of the Thasos crystalline complex indicate mainly a low grade stage of metamorphism and partly medium and high grade conditions (Vavelidis et al. 1987/1988). A series of Fe-Mn, Pb-Zn-Ag and Au deposits on the island have been intensively mined during antiquity (Vavelidis 1984). The present study refers to the microthermometric research of the Bi-Te-Ag bearing Cu-mineralization with framboidal pyrite, found at the northeastern part of the island, close to Panagia village. The mineralization is hosted in quartz veins and segregations which crosscut the schistosity in the lower part of the crystalline complex. The thickness of the ore bearing bodies reaches up to 1.20m (veins) and up to 30m (segregations). The ore mineral assemblage consists of chalcopyrite, pyrrhotite, pyrite and framboidal pyrite, fahlore, gersdorffite, tetradymite and hessite and is especially of interest for Ag prospecting.

MICROTHERMOMETRIC RESULTS

The microthermometric measurements were carried out on polished wafers of the mineralized quartz. Samples that have been examined for fluid inclusions contain undeformed, inclusion rich transparent quartz (Q1). A younger, clearer quartz generation (Q2) may be present locally which carries only few inclusions. Inclusions in Q1 are randomly distributed throughout. Based on their phase proportions at room temperature, three types can be distinguished. The first type (G1) is three phase and contains $\text{CO}_2(\text{g})-\text{CO}_2(\text{l})-\text{H}_2\text{O}(\text{l})$; maximum diameter is 20 μm . The vapor phase makes up 60-70vol.%. The second type of inclusions (G2) is less common and occurs only locally in isolated clusters. This type consist of liquid rich two-phase inclusions ($\text{H}_2\text{O}(\text{g})-\text{H}_2\text{O}(\text{l})$) with a maximum diameter of 18 μm . The third group of fluid inclusions (G3) is made up by large (<200 μm) irregularly shaped cavities, which often appear empty. Freezing of these inclusions showed, that they contain CO_2 . All types of inclusions have to be classified primary with respect to their host mineral on petrographic grounds. Secondary trails of inclusions have not been observed. Type G1 inclusions freeze at -45°C (aqueous phase) and -100°C (CO_2 phase). Melting temperatures of the CO_2 vary from -56.7 to -56.6°C near the triple point of CO_2 . Melting of ice was observed from -7.6 to -7.2°C . CO_2 clathrate melting occurs between $+7.8$ and $+8.9^\circ\text{C}$ (mainly $+8.2^\circ\text{C}$). This corresponds to a total salinity of 3.7 to 6.5 wt% NaCl equiv. The CO_2 phase homogenizes at temperatures from $+23.6$ to $+31.1^\circ\text{C}$ to the liquid or vapor phase. Final homogenization of the mixed inclusions occurs from 313 and 360°C with a maximum at 320 to 330°C . The fluid inclusions of the second type (G2) freeze at about -45°C

and the first melting temperatures range from -24 to -18°C, which indicates that the solution contained mainly NaCl. The ice melting temperatures (-1.9 to -2.0°C) correspond to a salinity of 3.5wt% NaCl equiv. The homogenization temperatures of these fluid inclusions vary between 229 and 305°C, with a maximum at 290 to 300°C. In only two cases we observed temperatures at 190°C. Only some freezing measurements were possible for the third type fluid inclusions (G3). Melting temperatures (-56.6°C) revealed a pure CO₂ phase. The homogenization were achieved at temperatures between +27.3 and +31.5°C in the liquid or the vapor phase. Fluid inclusion measurements from Q2 showed similar results with those from Q1.

DISCUSSION

According to our microscopic and microthermometric study of the investigated mineralization, the first type fluid inclusions (G1) represent the main mineral forming fluid. These fluids were rich in H₂O and CO₂ having low salinities (3.7 to 6.5 wt% eq. NaCl). The phase proportions at room temperature remain constant, from 60 to 70% of the total volume. The second type H₂O-rich fluid inclusions (G2) could be generated through phase separation in the H₂O-CO₂-NaCl system. This phase separation is further evidenced by the presence of the G3 inclusions and implies gas saturation of the H₂O-CO₂-salt inclusions. Under these conditions the temperatures of formation of the investigated mineralization can be reliably estimated from the homogenization temperatures of the CO₂-H₂O inclusions. Applying the Bowers & Helgeson (1985) equation of state to the microthermometric data of the H₂O-CO₂-NaCl inclusions, the isochores for the system were calculated. The derived pressure estimation is 500 bars. This is in good agreement with the estimate derived from intersection of the isochores of G2 and G3 inclusions, which reveals 340 to 360°C and 500 to 700bars. Temperatures of trapping of the CO₂-H₂O-salt inclusions range from 320 to 340°C, which is in good agreement with the formation of framboidal pyrite during the early stages of mineralization. The highest temperatures of formation of framboidal pyrite are 300 to 315°C (Sunagawa et al. 1971, Hannington et al. 1986). Metamorphism in the NE part of Thasos island, is characterized by medium and partly high grade conditions, which indicates temperatures from 400 to >600°C and pressures higher than 3kb. According to our field-work and microscopic investigations the quartz veins and segregations, which host the mineralization, crosscut the schistosity of the metamorphic rocks and is probably of hydrothermal origin. The mineralization were formed later than the last metamorphic event and this is in agreement with the microscopic study which shows that the investigated quartz is undeformed.

REFERENCES

- Bowers, T.S. & Helgeson, H.C. (1985). *Computers Geosci.*, 11: 203-213.
Hannington, M.D., Peter, J.M. & Scott, S.D. (1986). *Econ. Geol.* 81: 1867-1883.
Sunagawa, I., Endo, Y. & Nakai, N. (1971). *Soc. Min. Geol. Jp. Spec. Issue.* 2: 10-14.
Vavelidis, M. (1984). PhD Thesis, University of Heidelberg, 546p.
Vavelidis, M., Eleftheriadis, G. and Kassoli-Fournaraki, A. (1987/1988). *Ann. Geol. Pays Hellen.* 33: 203-216.

METAMORPHIC HYDROTHERMAL FLUIDS IN TONALITE-HOSTED COPPER-GOLD VEIN MINERALIZATION. MINA SULTANA (CALA, HUELVA, SPAIN)

VELASCO, F. (1), TORNOS, F. (2), PESQUERA, A. (1), and PEÑA, A. (1).

(1) Departamento de Mineralogía y Petrología, Universidad País Vasco. 48080 Bilbao (Spain).

(2) Instituto Tecnológico Geominero de España. Ríos Rosas, 23. 28003 Madrid (Spain).

The Sultana Cu-Au deposit is located in the Ossa Morena Zone, SW Spain. It consists of a N160°E trending vein hosted by the tonalites of the Santa Olalla pluton (363±26 Ma; Casquet & Galindo, pers. com.). Ore shoots, with up to 8% Cu and 105 gr/t Au are located in flat and thick bodies connected by more vertical and thin veins in an echelon structure. The hydrothermal assemblage is composed by an early fine grained and tectonized quartz ± pyrite assemblage followed by comb quartz grown on open spaces which is associated with ankerite, chalcopyrite and minor pyrothite. Bismuthinite, native bismuth and gold also occur as late minerals. Galena, sphalerite, arsenopyrite and löellingite are more sporadic phases. The host tonalites show a pervasive silicification, ankeritization, sericitization, chloritization as well as local tourmalinization.

Fluid inclusions in the late quartz related with the Cu-Bi-Au-rich mineral assemblage are likely primary ones. Three apparently synchronous types can be recognized. Type I fluid inclusions consist of an aqueous solution with up to two daughter minerals, halite and sylvite. Type II fluid inclusions also include CO₂-rich, liquid and vapor, phases. Type III fluid inclusions are CO₂-rich, locally with a subordinate aqueous phase (±daughter crystals).

Microthermometric results are shown in the Table 1. Most of the phase changes are difficult to recognize, but several modifications could be recorded. First melting temperatures (T_{1f}) range between -54.1 and -21.2°C, suggesting that the aqueous phase belongs to the H₂O-CaCl₂-NaCl±KCl system. The melting temperature of hydrohalite (T_{mhh}) suggest salinities between 9.6 and 19.2 wt % CaCl₂ eq., calculated from the data of Davis et al. (1990). Minimum NaCl salinities range between 8.1 and 18.8 wt%, but the temperature of halite dissolution indicate NaCl contents of up to 50 wt% and total salinities between 18 and 70 wt%. However, preliminary Cryo-SEM-EDS analysis (Ayora & Fontarnau, 1990) show that the CaCl₂ content is significantly lower than expected by microthermometric results, close to 0.5 wt%. Recalculated salinities are thus between 8 and 51 wt%, K/Na ratios are very low (<0.07) and the presence of daughter crystals of sylvite can be due to a salting-out effect. Appreciable amounts of MgCl₂ and FeCl₂ were not detected. The discrepancies between microthermometric and analytical data suggest a high degree of metastability in these complex Ca-bearing fluid inclusions, as has been recorded by Davis et al. (1990) or Oakes et al. (1992).

The CO₂ melting and homogenization temperatures of the CO₂-bearing fluid inclusions (T_{mCO₂}, T_{hCO₂}) show that CH₄ and/or N₂ are present in important amounts. Microthermometric measurements suggest that XCO₂/XCH₄ ratios range from 0.04 to 0.12 in type II and III inclusions. Guessed XCO₂ values are 0.10-0.23 for type II and 0.30-0.70 for type III inclusions. Clathrate melting temperatures are

hardly seen and the observed values are probably influenced by other gasses. Most fluid inclusions decrepitate before final homogenization, but the mode of recorded temperatures ranges from 310 to 380°C. Mass spectrometry of bulk samples (Shepherd & Miller, 1988) show that CH₄/CO₂ ratios are higher than measured ones in the range of 0.13-0.22. CO and H₂ are present in significant proportions, whereas XN₂ is negligible.

Table 1. Synthesis of microthermometric data

Type		TmCO ₂	Tlf	Tmhh	Tmcl	ThCO ₂	Tdh	Tds	Th
I [n=22]	mean		-36.4	-10.4			254	148	292
	min		-27.0	-18.9			140	126	226
	max		-41.0	-4.6			370	163	380
II [n=150]	mean	-58.5	-41.0	-12.7	7.5	22.8	315	151	346
	min	-64.4	-54.1	-23.3	3.9	8.5	210	97	143
	max	-55.6	-21.6	-7.1	16.5	31.8	450	273	419
III [n=8]	mean	-58.5	-47.4	-11.7	9.6	21.5	225	137	324
	min	-61.5	-52.3	-16.3		5.0			300
	max	-57.5	-42.5	-6.3		26.1			384

As a whole, the coexistence of the three types of fluid inclusions is consistent with the presence of an immiscibility process related to the vein opening. Homogenization temperatures and independent geothermometers agree with the H₂O-CO₂-salt solvus for pressures close to 1-1.5 Kbar. For the measured XCO₂, fluid immiscibility would produce a CO₂-poor salt-rich brine and a CO₂-phase with more than 70% molar CO₂ (Bowers & Helgeson, 1983). Nevertheless, the fluid inclusion interpretation is not straightforward. Extreme members of the immiscibility process are the type-I and the more vapor-rich type-III fluid inclusions. However, type-II inclusions can represent the original and unmixed fluid, but also trap different proportions of unmixed fluids. The same holds true for the more water-rich type III inclusions. The fluid composition, the P-T conditions of trapping, the geologic setting and the available stable isotope data suggest that hydrothermal fluids are equilibrated with nearby metamorphic rocks, probably the Precambrian black shales, which invaded the system after the emplacement of the Santa Olalla pluton. Fluid unmixing produce an alkalization of the system and dramatic lowering of the fS₂, leading to the precipitation of metals transported by thiosulphide or weak acid complexes, but inhibiting the precipitation of metals transported as chloride complexes. These veins share many of the characteristics of mesothermal gold deposits, but are developed in a postorogenic and extensional setting.

Acknowledgements: To Drs Javier García Veigas and Tom Shepherd their help in the fluid inclusion analysis and interpretation. Funded by the CICYT project MB-92-0918-CO2-02.

References:

- AYORA, C., FONTARNAU, R. (1990): *Chemical Geology*, 89, 135-148
 BOWERS, T.S., HELGESON, H.C. (1983): *Geoch. Cosm. Acta*, 47, 1247-1275
 DAVIS, D., LOWENSTEIN, T. SPENCER, R. (1990): *Geoch. Cosm. Acta*, 54, 591-601
 OAKES, C.S., SHEERS, R.W., BODNAR, R.J. (1992): *Abstracts PACROFIIV*, 128-132
 SHEPHERD, T.J. MILLER, M. (1988): In 'Mineral deposits within the European Community', Boissonas & Omenetto, eds.

EXPERIMENTAL RE-EQUILIBRATION OF SYNTHETIC FLUID INCLUSIONS: POTENTIAL EFFECTS OF TIME AND LOADING RATES

VITYK, M. and BODNAR, R. J.

Fluids Research Laboratory, Department of Geological Sciences, Virginia Polytechnic Institute & State University, Blacksburg, VA, U.S.A., 24061

The most important question concerning any experimental simulations of fluid inclusion re-equilibration phenomenon is whether laboratory-induced data can be used to infer P-T histories of natural samples. In order to effectively apply the experimental results to geologic problems, potential effects of loading rates and time must be considered.

Although we can never simulate in the lab the slow natural loading rates, we attempt to minimize the occurrence of "shock-induced" re-equilibration by changing the confining pressure in our experiments in small increments over several weeks to months duration. With this approach, we trap water-rich synthetic fluid inclusions in quartz at elevated P and T, and then re-equilibrate the inclusions by gradually changing (0.7 kbar week⁻¹) the confining pressure without quenching to room P-T conditions between steps. After the experiment, we found that a large percentage (about 40%) of aqueous synthetic inclusions maintained 2 kbar of internal overpressure for 7 days without changing volume. These results differ from experiments, which involve rapid application of the differential pressure over about 20-30 min (instantaneous loading) under the same re-equilibration conditions as the experiment with "slow" loading rates, where inclusions maintaining their original density have not been found. Note that instantaneous loading has been used in most of previous laboratory simulations of inclusion re-equilibration.

We have also initiated experiments to examine the effect of time on inclusion re-equilibration at elevated P and T. Four quartz samples containing synthetic water-rich inclusions formed at 700°C and 5 kbar were taken along identical decompressional P-T paths to simulate retrograde P-T conditions in high-grade metamorphic environments. The final conditions resulted in a cumulative overpressure of about 2.1 kbar relative to the original internal pressure. At the final conditions (625°C and 2 kbar) the samples were held for 7, 30, 90 and 180 days, respectively. After each experiments, about 160 randomly selected fluid inclusions were measured to monitor their density modification.

After all the experiments were completed, the following observations have been made. The most dramatic changes of fluid inclusion density occur some time between 7 - 30 days (Fig.1). Additional time has little effect on the mean histogram values, suggesting that some state of volumetric equilibrium had been achieved by most fluid inclusions after about 30 days under conditions of about 1.3 kbar of internal overpressure. All the experimentally simulated histograms of inclusion homogenization temperatures showed different spread, or variability, about the mean: the shorter duration of experiment the higher the variability (variance) of measurements (Fig. 1, insert). Thus, the 7 days

experiment produces a highly skewed Th histogram with high variance. On the other hand, the 180 days experiment produces a distribution with low variance. The mean and median values calculated for inclusions from the 180 days experiment are in a good agreement. Accordingly, it can be suggested that a final product of decompressional re-equilibration of fluid inclusions will be a symmetrical mound-shaped histogram. The mode, mean, and median for this histogram will all be the same.

Our data further indicate that after the long term experiments, a small percentage of aqueous synthetic inclusions preserve their original density (even when subjected to internal overpressures of about 2 kbar for as long as 180 days). Most homogenization temperature histograms reported in the literature for inclusions in quartz from high grade decompressional metamorphic terranes also show a characteristic pattern manifested as a broad range in homogenization temperatures with a characteristic gap between the minimum homogenization temperature and the main body of homogenization temperature values, similar to that reproduced in the lab. As in our experiment, inclusions with minimum homogenization temperature values (highest density) are the rare exception rather than the rule (only about 1-2 % of all inclusions measured).

Summarizing, our results suggest that by using synthetic inclusions it is feasible to develop standard characteristics of homogenization temperature histograms for naturally re-equilibrated inclusion populations in the form of numerical parameters (e.g., mean, mode, variance, range and extreme values). These parameters combined with other available geological information may be used to estimate the magnitude of departure of the inclusion P-T path from the original isochoric.

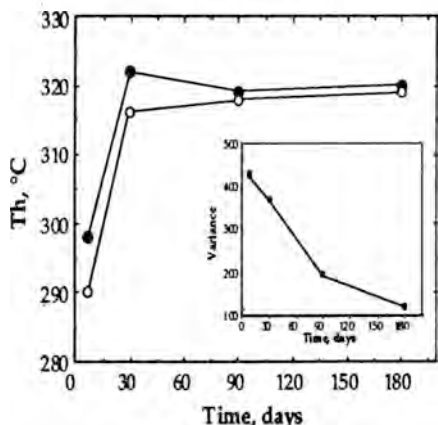


Figure 1. Evolution of the mean (arithmetic average - filled circles), median (histogram central value - open circles), and variance (sum of squared deviations of a set of measurements n divided by $n-1$ - squares) of homogenization temperature histograms during experimental decompressional re-equilibration of 10 wt. % NaCl-H₂O synthetic inclusions in natural quartz. The inclusions were formed at 700°C and 5 kbar for 7 days and then re-equilibrated at 625°C and 2 kbar for 7, 30, 90, and 180 days, respectively. The original isochore for the inclusions corresponds to 284°C; the final re-equilibration isochore corresponds to 380°C.

HEALED MICROCRACKS IN GRANITES FROM THE HDR DRILLHOLE EPS-1, SOULTZ-SOUS-FOR TS. - PALEOSTRESS DIRECTIONS, PALEOFLUIDS AND CRACK-RELATED VP-ANISOTROPY

VOLLBRECHT, A. (1), SCHILD, M. (1), REUTEL, Ch. (1), SIEGESMUND, S. (1), CHLUPAC, T (2) & WEIß, T. (1)

(1) Institut für Geologie u. Dynamik der Lithosphäre, Universität Göttingen

(2) Academy of Sciences of the Czech Republic, Prague

Complete 3D analyses of microcrack orientations were carried out by U-stage microscopy using three mutually perpendicular thin sections from reoriented core samples. The crack population is dominated by healed cracks in quartz forming an orthogonal pattern of three sets with strong preferred orientation (Fig. 1). The microstructural characteristics point to thermal contraction during cooling and uplift of the granites to be the main driving force for crack propagation. According to this model (Vollbrecht et al. 1991), the two steep crack sets formed simultaneously and indicate a NE-SW direction of ρ_H (max. horizontal normal stress) of the related paleostress field.

Fluid inclusion petrography reveals that different paleofluids can be related to certain crack generations (inter- and intra-granular cracks, grainboundary cracks). As indicated by higher degrees of fill the subhorizontal cracks formed at lower temperatures as compared with the steep sets. Accordingly, the subhorizontal cracks can be related to a later stage of uplift. Microthermometric investigations, which are in progress, will yield data for P/T estimates of crack-healing. Finally, a correlation of the resultant isochores with suitable paleo-geothermal gradients or P/T paths will enable a rough dating of the related stress field.

The distribution of P-wave velocities (V_p) was measured by using the pulse transmission technique in 132 independent propagation directions on a vacuum dried spherical sample with a diameter of 50mm (+/-0.5mm) under hydrostatic pressures up to 200 Mpa (Siegesmund et al. 1993). The strong geometric relationship between the V_p -diagram (Fig.2) and the crack pole figure (Fig.1) indicates that the V_p -anisotropy is mainly caused by the observed crack fabric. For the macroscopically isotropic granite lacking any foliation or lineation a texture related influence on the V_p -anisotropy can be excluded. The same holds for cleavage cracks in mica and feldspars, which display a random orientation. The present study points out that fluid inclusion data should be directly related to microfabrics which makes a more detailed reconstruction of the tectonothermal history possible. Moreover, it can be concluded that in shape- and texture-isotropic rocks V_p -measurements are a suitable tool to detect prominent crack patterns. These cracks may outline planes of mechanical weakness which must be considered during hydrofrac-experiment and HDR modelling.

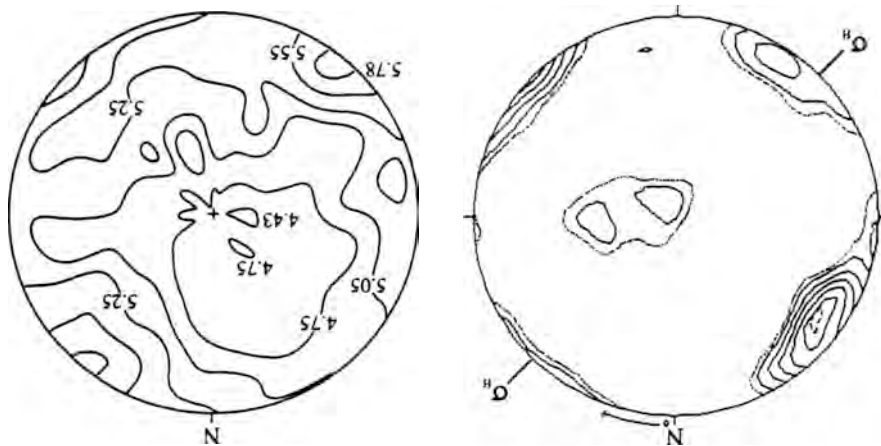


Fig.1: Pole figure of healed microcracks in quartz (Schmidt net, lower hemisphere, $n=799$) and inferred direction of σ_H .
Fig.2: V_p -velocities at 0.1 Mpa confining pressure measured on a spherical sample, isolines in km/sec represented in a Schmidt net (lower hemisphere). In contrast, for crack-free samples V_p -velocities between 6.4 and 6.8 km/sec can be assumed.

References

- Siegesmund, S. et al. (1993): *Tectonophysics*, 225: 477-492.
Vollbrecht, A. et al. (1991): *J. Struct. Geol.*, 13: 787-799.

ICP-AES ANALYSIS OF FLUID INCLUSIONS I: RECENT DEVELOPMENTS AND APPLICATIONS

WILKINSON, J.J., GLEESON, S.A. & COLES, B.

Fluid Processes Research Group, department of Geology, Imperial College of Science, Technology and Medicine, Prince Consort Road, London SW 7 2BP, U.K.

The primary goals in the analysis of solutes in fluid inclusions are to determine an ever wider range of elements which may be of geological interest, and to obtain these data from smaller and smaller samples, the ultimate resolution being the analysis of individual inclusions. For the last 15 years, inductively-coupled plasma atomic emission spectrometry (ICP-AES) has proved a reliable method for the determination of alkali, alkali-earth and transition metals in fluid inclusions, initially by bulk sampling methods: decrepitation or crush-leach (Rankin et al., 1993); and more recently single inclusion analysis by laser-ablation (Ramsey et al., 1992; Wilkinson et al., 1994). Despite the increasing availability of ICP-mass spectrometry, the application of this technique to inclusion analysis is still in its early stages and ICP-AES analysis remains a valuable tool in the study of natural fluid processes.

Recent advances in processing methodology (Coles et al., in press) have improved the detection limit for ICP-AES analysis of decrepitates by up to two orders of magnitude, for laser-ablation analysis by one order of magnitude and for standard solution nebulisation (e.g. leachate) by several hundred percent. This is achieved by the use of Correlated Background Correction (CBC), which uses the high degree of correlation between the relative fluctuations in the spectral background at different wavelengths to effectively predict the background emission under transient analyte peaks. The procedure substantially reduces both systematic and random fluctuations in background emissions and makes viable the analysis of smaller samples or samples containing more dilute fluid inclusions. It has also highlighted certain analytical problems such as the fact that background suppression, probably due to plasma cooling, is unavoidable during analysis of most samples and can result in the introduction of bias of several percent in the element ratios determined.

These developments are illustrated with a range of applications including analysis of synthetic inclusion standards which provide controls on analytical accuracy and precision; and natural samples where the use of CBC has demonstrated that small-scale (spatial and temporal) variations in hydrothermal fluid chemistry can be resolved.

References: COLES, B.J., GLEESON, S.A., WILKINSON, J.J. & RAMSEY, M.H. (in press) *The Analyst*. RAMSEY, M.H., COLES, B.J., RANKIN, A.H. & WILKINSON, J.J. (1992) *J. Analytical Atomic Spectrometry*, **7**, 587-594. RANKIN, A.H., RAMSEY, M.H., HERRINGTON, R.J., JONES, E., COLES, B. & CHRISTOULA, M. (1993) in: Maurice, Y, ed., Proc. 8th Quadrennial IAGOD Symposium, E. Schweizerbart'sche Verlagsbuchhandlung (Nägele u. Obermiller), D-7000 Stuttgart, 183-198. WILKINSON, J.J., RANKIN, A.H., MULSHAW, S.C., NOLAN, J. & RAMSEY, M.H. (1994) *Geochim. Cosmochim. Acta*, **58**, 1133-1146.

FLUID CHARACTERISTICS OF VARISCAN PORPHYRY GOLD SYSTEM: AN EXAMPLE FROM BOHEMIAN MASSIF, CZECH REPUBLIC

ZACHARIAS, J. (1), PUDILOVA, M. (1), PERTOLD, Z. (1), PERTOLDOVA, J. (2), BENDL, J. (3) & WILKINSON, J. (4)

- (1) Charles Univ., Albertov 6, 128 43 Prague 2, Czech Rep.
- (2) GMS a.s., Prístavní 24, 170 04 Prague 7, Czech Rep.
- (3) Analytika Co. Ltd., U elektry 650, 189 00 Prague 9, Czech R.
- (4) Imperial College, SW7 2BP, London, UK

Porphyry-Au deposits (PAuD) were predicted and later described by Sillitoe (1979, 1991) and Villa et al. (1991) from Tertiary terrains in South America. Exploration by GMS Co. in the Bohemian Massif discovered the "Petržckova hora" deposit of supposedly porphyry type (Morávek & Studnicná 1992). After further structural, geochemical and fluid inclusion research we conclude that the deposit is closely connected with its magmatic host and is of porphyry type.

The deposit is related to a small (0.16km²) granodiorite stock, which intruded into Cambrian metasedimentary and volcanosedimentary rocks. Stock is composed of two facies of biotite - hornblende granodiorite and accompanied by dykes of granodiorite porphyries. The two granodiorite facies has been dated by Rb-Sr at 344+/-18 and 398+/-46 Ma. Four deformation phases occurred from the Cambrian to the Carboniferous and now make difficult all isotope and fluid inclusions interpretations.

Mineralisation (Au+/-W,Bi,Cu) is related to a stockwork of thin quartz veins and veinlets (0.X-15cm). Five types of Au-bearing veins have been distinguished (Tab 1.). The Q2 veins are most common. The ore is represented by native gold (960/1000), scheelite and minor sulphide mineralisation (chalcopyrite >> arsenopyrite, pyrite > pyrotine and Bi-Te minerals.) Ore assemblages indicate lower fugacities of S, Te, O than typical for hydrothermal (Afifi et al., 1988) and PAuD (Villa et al., 1991).

Hydrothermal alterations - compare to the Caenozoic porphyry deposits - are present only in small volumes. K-feldspar alteration and silicification prevail, phyllic and propylitic alterations are absent.

Oxygen isotope studies of cogenetic minerals from Q veins (Tab 1.) revealed high temperature character (550-450°C) and relatively constant fluid composition (6-7% δ^{18}). Isotopic temperatures for K-alterations (530-610°C) are identical with that of granodiorite (530-640°C) and composition of alteration and magmatic fluids (5.5-6.5 δ^{18}) is similar to that of Au-Q-veins. The estimated δ^{18} whole rock value for granodiorite (4.6 ‰) is lower than typical values for igneous rocks (Taylor, 1978).

Fluid inclusions (FI) have been studied in Q2,3,5 vein types. Observations are difficult due to small size of FI (<10 μ m) and ductile deformation of all vein types at greenschist facies conditions. No significant differences in fluid inclusion characteristic between individual vein types were found (Tab 1.). Most of the FI are 2 phase liquid rich (4-23 wt.% eq. NaCl, TFM: -23,5 to -22°C and T_H(L):230-360°C), minor type represent polyphase inclusions with 2-3 daughter minerals (NaCl and KCl). The estimated KCl/NaCl ratio (1.4) is higher than in most porphyry

copper deposits. Increase in salinities together with decrease in TH (Fig. 1) indicate possible boiling of fluids. However no vapour rich FI have been found to confirm this suggestion.

Using the isotopic temperature of Q vein formation (530-450°C) FI isochores indicate possible trapping pressures of 1-2.8kbar. This does not correlate with a supposedly shallow subvolcanic character of intrusion.

Some fluid characteristics of the 'Petráckova hora' deposit (high T, low f_{O_2} , f_S , f_{Te} , presence of scheelite and Bi-min.) are similar to Precambrian porphyry style deposits (Boddington in Australia, Young-Davidson in Ontario) and different from Tertiary deposits in South America.

Tab 1. Selected characteristics of gold bearing (Q_{1-4}) and barren (Q_x) quartz veins.

Vein type	∅Au (ppm)	Other minerals	Alterations	δO^{18} Quartz	Estim. T (°C)	δO^{18} Fluid	Fluid incl. wt. % eq. NaCl
Q ₁	0-10	Hb, Sph	K-fsp	7,7-9,4	530-570	5,7-6,7	-
Q ₂	20-80	Sch	-	7,8-9,5	?	?	4-23
Q ₃	20	Sch	-	8,7-10,3	450-490	6,3-7,2	10-18,46-50*
Q ₄	0-10	Sch	-	8,4	?	?	
Q ₅	0-5	-	-	11,0	?	?	6-19
Q _x	0	-	-	13,3	?	?	-

Abrev.: Hb = Hornblende, Sph = Sphene, Sch = Scheelite

*salinity: 46-50 wt. % of NaCl+KCl

References:

- Afifi A.M. et al. (1988): *Econ. Geol.*, 83, 377-404.
 Morávek P., Studnicná B. (1992): Porphyry-gold deposits also in Bohemian region? (in Czech). - *Geologicky pruzkum*, 1, 11-15, Prague.
 Sillitoe R.H. (1979): *Mineralium Deposita*, 14, 161-174.
 Sillitoe R.H. (1991): In: *Gold Metallogeny and Exploration* (ed. R.P. Foster), 165-209, Blackie, London.
 Taylor H.P., Jr. (1978): *Earth Planet. Sci. Letters*, 38, 177-210.
 Villa T. et al. (1991): *Econ. Geol.*, 86, 1271-1286.

GEOLOGY AND FLUID INCLUSION MICROTHERMOMETRY OF GRANITIC PEGMATITES IN MYANMAR: RELATIONSHIPS WITH W-Sn VEIN MINERALISATION

ZAW, K. (1*)

(1) Applied Geology Department, Yangon University, Yangon, Myanmar
*Present address: Centre for Ore Deposit and Exploration Studies, Geology Department, University of Tasmania, GPO Box 252C, Hobart, Tasmania, Australia 7001
Phone +61 02 20 2787 Fax +61 02 23 2547
e-mail: zaw@postoffice.utas.edu.au

Pegmatites commonly occur in a 1500 km N-S trending, tungsten-tin bearing granitoid belt in Myanmar (Fig. 1) (Khin Zaw, 1990). Pegmatites are emplaced as veins and dykes that cut granitoid, migmatite, granitoid gneiss, gneiss and schist. They are mostly 2 to 5m wide and 30 to 150m long, and some traceable over a distance of 300m. Components of pegmatite include: quartz, orthoclase, albite, microcline, microperthite, and muscovite with minor biotite, tourmaline, beryl, garnet, topaz, lepidolite, magnetite, wolframite, cassiterite, and rarely columbite. Zonation is common, feldspars and muscovite being abundant in the center; quartz more prevalent at the margin. Zoning is also distinct where tourmaline is present. Light-coloured, felsic minerals are confined to the core zone; and dark-coloured, tourmaline crystals to the outer zone.

Numerous fluid inclusions have been found in quartz, topaz and beryl. Most of the inclusions are rounded to elliptical with a variable degree of liquid filling. All inclusions are aqueous, two-phase (liquid and vapour) inclusions with no daughter minerals. Homogenization temperatures of 173 fluid inclusions were measured in this study. Frequency-temperature distribution for the fluid inclusions in quartz and topaz from the Sakangyi pegmatite have yielded a narrow homogenization temperature range of 290°-320°C. Quartz from the Sakangyi pegmatite gave a homogenization temperature range of 315°-318°C, whereas topaz from the same pegmatite yielded 300°-315°C. Quartz from the Gu Taung pegmatite gave a homogenization temperature range of 241°-389°C with a bimodal distribution and modes at 250°C and 370°C. Similar bimodal distribution with modes at 270°C and 410°C was also recorded for the quartz and beryl from the Taunggwa pegmatite. Fluid inclusions in beryl from the Taunggwa pegmatite gave a homogenization temperature range from 266° to 410°C, whereas those inclusions in quartz from the same pegmatite yielded a lower homogenization temperature range of 231°-360°C. Homogenization temperatures of quartz from the Sinmakhwa pegmatite range from 273° to 307°C with a mode of 290°C.

Geothermometric studies indicate that the pegmatites were formed over a homogenization temperature range of 230° to 410°C. Salinities of fluid inclusions in pegmatite minerals ranged from 1.0 to 10.8 NaCl equiv. wt %. Topaz and quartz single crystals of several cm's across from the Sakangyi pegmatite provide an opportunity to extract the fluid inclusions trapped in these minerals. The Na/K ratio of the fluid inclusions in two topaz samples were 3.0 to 4.9, and that of two quartz samples were 2.9 to 10.5 suggesting an involvement of potassium in the pegmatite-forming fluids. Evidence for phase separation of the pegmatite-forming fluids was not observed.

Tungsten-tin ore veins in Myanmar formed under a homogenization temperature range of 140°-360°C and salinities of ~1-10 NaCl equiv. wt %. No unequivocal fluid inclusion evidence for boiling was recorded for the tungsten-tin deposits in Myanmar (Khin Zaw and Khin Myo Thet,

1983; Khin Zaw, 1984). Present fluid inclusion characteristics and geothermometry suggest that pegmatite emplacement occurred under post-magmatic conditions at 200°-400°C and salinities of -1-10 NaCl equiv. wt %, and that extensive vein-type tungsten-tin mineralization along the same central granitoid belt occurred at lower temperatures (150°-350°C) but with similar salinities and under non-boiling conditions. The post-magmatic, hydrothermal fluids responsible for the both pegmatites and tungsten-tin ore veins was probably from the cooling 'S' type granitoids that they are spatially associated with.

References:

- KHIN ZAW (1984): Geology and geothermometry of vein-type tungsten-tin deposits at Pennaichaung and Yetkantzintung prospects, Tavoy township, southern Burma. Mineral. Deposita, 19, 138-144.
- KHIN ZAW (1990): Geological, petrological and geochemical characteristics of granitoid rocks in Burma: with special reference to the associated W-Sn mineralization and their tectonic setting. Jour. SE Asian Earth Sci. 4, 293-335.
- KHIN ZAW & KHIN MYO THET (1983): A note on fluid inclusion study of tin-tungsten mineralization at Mawchi Mine, Kayah State, Burma. Econ. Geol., 78, 530-534.

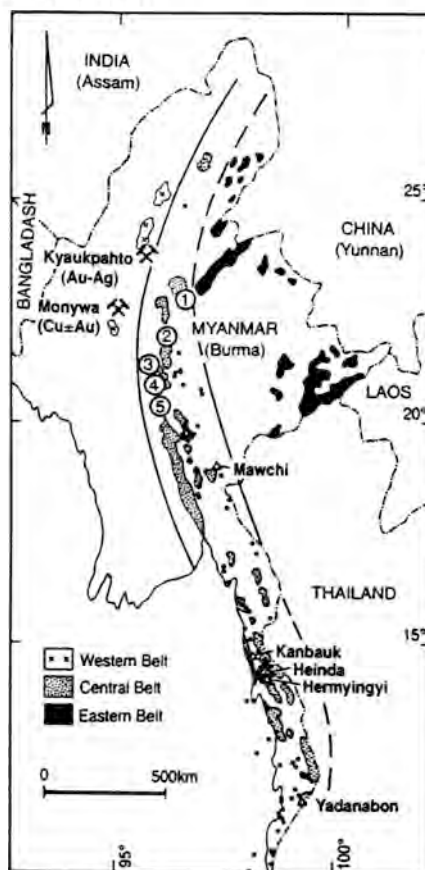


Fig. 1. Granitoid belts of Myanmar (Burma) and location of selected granitic pegmatites. 1. Sakangyi, 2. Gu Taung, 3. Payangazu, 4. Taunggwa and 5. Sinmahwa. Solid dots are tungsten-tin occurrences in central granitoid belt and open triangles are major tungsten-tin deposits.

THERMOBAROMETRIC AND MICRO-RAMAN INVESTIGATIONS ON FLUID AND MELT INCLUSIONS IN SILLIMANITE FROM REINBOLT HILL / EAST-ANTARCTICA

ZIEMANN, M. (1) & THOMAS, R. (2)

(1) University of Potsdam, Institute of Geosciences, Germany
(2) GeoForschungsZentrum Potsdam, Germany

Sillimanite of gemstone quality was studied from a pegmatite of the Reinbolt Hill locality in the east-antarctic granulite province (Hofmann, 1978; Grew, 1980). The samples contain primary elongate silicate melt inclusions with gaseous parts and syngenetic nearly isometric fluid inclusions. High density CO₂ and N₂ with various contents were detected in the gaseous phases with the Raman-spectroscopy. From these and micro-thermometric investigations (Thomas et al., 1992) the conditions of the sillimanite crystallization from the melt were estimated: solidus: 719 °C, 6,1 kbar and liquidus: 747 °C, 6,3 kbar.

The investigations show, that during growth of this sillimanite and inclusion formation the fluid composition changed considerably. Because of the absence of secondary inclusions the results are quite definite. In case of several inclusion generations this could cause false interpretations.

Possible reasons for formation of these gaseous inclusions with different density values (from 0,98 up to 1,06 g/cm³) and N₂-contents (from 20 to 40 Mole-%) were discussed.

References

- Grew E.S. (1980): *Journ. of Petrology* 21, p. 39-68
Hofmann J. (1978): *Freiberger Forschungshefte*, C335, p. 7-110
Thomas R., Ziemann M. and Hofmann J. (1992): *Mitt. Osterr.Mineral. Ges.*, 137, p. 73-82

FLUID INCLUSION ANALYSIS OF HALITE FROM THE SOLAR SALTWORK OF INAGUA, BAHAMAS

ZIMMERMANN, H.

Institut für Geologie und Dynamik der Lithosphäre, Universität Göttingen, Goldschmidtstr, 3D-37077, Göttingen

Microextraction and chemical analysis of single fluid inclusions (> 0.2 mm) in evaporites can give us information on the history of sea water composition, and on secondary processes occurring in salt deposits due to brines. The interpretation of fluid inclusion data observed in fossil evaporites seems to be limited. Therefore we study the recent process of trapping brine in halite from solar saltworks. Inagua is a good place to look at evaporation and trapping processes under natural but controlled conditions, since we find halite crystals of the size of 2 to 6 cm containing comparatively large fluid inclusions. The chemical compositions of the evaporating brine, the halite precipitating from this brine and the fluid trapped in halite during precipitation are analysed. Major components (Na, K, Mg, Ca, Cl, SO₄) and minor components (Li, F, Br) of brine, halite and inclusion are determined by Ion Chromatography (IC); Rb, Sr, Cs, I, and B in the evaporating brine (reservoirs, crystallizers) by ICP-MS. The element distribution between the different liquid and solid phases is studied.

**FLUID INCLUSION STUDIES OF MESSINIAN EVAPORITES FROM SICILY -
PRELIMINARY RESULTS**

ZIMMERMANN, H.

Institut für Geologie und Dynamik der Lithosphäre, Universität
Göttingen, Goldschmidtstr, 3D-37077, Göttingen

The Sicilian salt deposits are of Miocene age and can be divided into unit A, B, C, and D, with unit B containing up to 10 kainite horizons. The Br distribution of halite and kainite shows possibly primary patterns. Fluid inclusions (> 0.2 mm) in vertical and lateral profiles of halite are extracted and analysed (Na, K, Mg, Ca, Li; Cl, SO₄, F, Br) by Ion Chromatography (IC) in order to reconstruct brine compositions during the process of precipitation.

QADRUPOLAR MASS SPECTROMETRIC STUDY OF FLUIDS IN GEMS: AN APPLICATION TO COLOMBIAN EMERALDS.

ZIMMERMANN, J.L.(1), GIULIANI, G.(1,2) and CHEILLETZ, A.(1,3)

- (1) CRPG, CNRS, BP.20, 54501 Vandoeuvre-lès-Nancy Cedex.
- (2) ORSTOM, Département TOA, 213 rue Lafayette, 75480 Paris.
- (3) ENSG, BP 452, 54001 Nancy Cedex.

Beryl minerals have a structure with hexagonal rings of six linked Si-O tetrahedra stacked one above another, giving a series of open channels parallels to the c axis of the mineral (Deer et al. 1986). These channels are wide enough to incorporate fluids such as H₂O, CO₂, N₂ as well as inert gases (Rayleigh 1933, Damon & Kulp 1958).

In the present work, we study fluids in Cr-bearing beryls (emerald variety), from Eastern and Western Cordillera, incorporated in inclusions as well as in channels, whose an hydrothermal sedimentary origin has been recently demonstrated (Giuliani et al 1992, Cheilletz et al 1994).

Fluids were extracted by heating under vacuum and analysed by means of a BALZERS QMG 420 quadrupolar mass spectrometer. Continuous heating analyses allow to follow the release of each fluid. The corresponding curves give the liberation rates according to temperatures. Bending points and maximum of curves correspond to temperatures of gases desorption, inclusions decrepitation and channel opening. In a second series of analyses, gases are extracted by incremental heating. At each step, temperature stays constant until fluids pressure levels off to an asymptotical value. Fluids are separated into several fractions, using cold traps, oxidation and reduction processes. Pressure in the line, of known volume, is measured with a capacitance manometer before the gas analysis through the quadrupolar mass spectrometer. Quantities and compositions of fluids released at each step are so determined. Continuous liberation curves (from ambient temperature to 1200°C) of each gas show three domains corresponding to fluid locations in beryls. Adsorbed gases are liberated from 100°C to 200°C, the temperatures of maximum rate for inclusions decrepitation are between 450°C and 500°C and the ones for the release of fluids in channels are between 880°C and 1000°C. These results confirms those on beryls from different origins and ages, in granites or in pegmatites precambrian and hercynian beryls (Zimmermann 1972). Fluids are essentially located in channels and their contents are higher in Western beryls than in Eastern ones. Their liberation curves are similar to the ones of water, except in some cases for CO₂ whose a part is the result of Ca carbonates dissociation; such inclusions are frequent in these emeralds so called emerald gardens. For step heating analyses, the temperature steps were selected from the results of previous continuous heating analyses: 400°C, 550°C, 720°C, 900°C, 1000°C and 1150°C. Composition of the whole fluid phase is this one: H₂O (80 to 92%), N₂ (3 to 10%), CO₂ (2.5 to 5%), H₂ (< 5%), CO (< 1.5%), CH₄ (< 0.5%), organic compounds (dissociation mass) and inert gases: He, Ar, Ne. The first two steps correspond to fluids in inclusions, about 1 to 7%, depending on samples. The largest part located in channels is released at 720°C and especially at 900°C steps. Western beryls contains more water

than Eastern beryls, about 20% (an average of $980.10 \cdot 10^{-6}$ mole/g against $765.10 \cdot 10^{-6}$ mole/g).

Only one sample has a largest CO₂ content, released at 550°C and 720°C steps and originated from carbonate dissociation ($72.10 \cdot 10^{-6}$ mole/g). Except this sample, the mean contents of CO₂ in inclusions are respectively 5.9 and $3.9 \cdot 10^{-6}$ mole/g whereas they are : $41 \pm 8 \cdot 10^{-6}$ mole/g in Western beryl channels and $32 \pm 8 \cdot 10^{-6}$ mole/g in Eastern ones.

Concerning Nitrogen, mean values in inclusions are approximately the same in Western and Eastern samples ($5.2 - 5.35 \cdot 10^{-6}$ mole/g) and a little different in the channels (62.5 in Western and $56.10 \cdot 10^{-6}$ mole/g in Eastern).

Methane and Organic compounds are found in all samples, quantities are however too low to distinguish between Western and Eastern beryls (average 0.07 and $0.035 \cdot 10^{-6}$ mole/g in inclusions); there are from 15 to 35 times more in channels than in inclusions. Only one sample contains twice more CH₄ ($2.2 \cdot 10^{-6}$ mole/g in channels) than the others; it has also more Hydrogen ($80.5 \cdot 10^{-6}$ mole/g) and Nitrogen ($91 \cdot 10^{-6}$ mole/g).

Hydrogen appears also in all beryls, its mean content is $0.44 \cdot 10^{-6}$ mole/g in Western beryls inclusions and 0.2.

10^{-6} mole/g in Eastern beryls; they are respectively $33 \cdot 10^{-6}$ mole/g against $20 \cdot 10^{-6}$ mole/g in the channels (except for G.89).

Inert gases, He, Ne, Ar, are trapped in all samples, inclusions and channels (He < 0.06%, Ne < 0.006%, Ar < 0.02%). The channels contain sensibly more Helium than inclusions; however for Argon and Neon, the contents are close in inclusions and in channels and it is not possible to differentiate Western beryls from Eastern ones.

The ternary diagram (H₂O-CO₂-N₂) shows an aquacarbonic fluid phase, rich in water, with CO₂/N₂ ratios near one (0.8- 0.84 in inclusions, 1- 1.3 in channels).

These results confirm and define the data obtained by microthermometry and by Raman Spectrometry on fluids inclusions.

Water released from the structural channels represents the original water of formation which may be characterized by its D/H ratio. Preliminary studies on H, C, O isotopes (Giuliani et al 1992) show evidence the basinal waters signature of the mineralizing fluids associated to carbonates, quartz and emeralds. Sulphur isotopes studies indicates (Giuliani et al 1995) that sulphur has an evaporitic origin.

All these data constrained an hydrothermal-sedimentary model which allow us to conclude that water kept by emerald in its ring-structure has a basinal origin. Following this model, the present study shows that the quantity of water induced in the development of the hydrothermal system and emeralds formation was more consequent (20% in addition) in Western emerald zone than in Eastern one.

REFERENCES:

- DAMON, P.E. & KULP, J.L. (1958): *Am. Miner.* 43, 433-459.
CHEILLETZ, A., FÉRAUD, G., GIULIANI, G. AND RODRIGUEZ, C.T. (1994): *Econ. Geology* 89, 362-380.
DEER, W.A., HOWIE, R.A. & ZUSSMAN, J. (1986): *Rock Forming Minerals*. Longman, London.
GIULIANI, G., SHEPPARD, S.M.F., CHEILLETZ, A. (1992): *C.R. Acad. Sci. Paris* 314, II, 269-274;
GIULIANI, G., CHEILLETZ, A., ARBOLEDA, C., CARRILLO, V., RUEDA, F. & BAKER, J., (1995): *Eur. J. Miner.* 7, 151-165.
RAYLEIGH, J.W.S. (1933): The helium in beryls of varied geologic ages. *Proc. Roy. Soc. London* A 142, 370-381;
ZIMMERMANN, J.L. (1972): L'eau et les gaz dans les principales familles de silicates. *Science de la Terre Mem.* 22, 188p.

THE VOLATILES IN MINERAL-FORMING FLUIDS OF MYKYTIVKA Sb-Hg DEPOSIT

ZINCHUK I.M., BAGATAJEV R.M., VISHTALIUK S.D. & SVOREN' J.M.

Institute of Geology and Geochemistry of Combustible Minerals of National Academy of Sciences, L'viv, Ukraine.

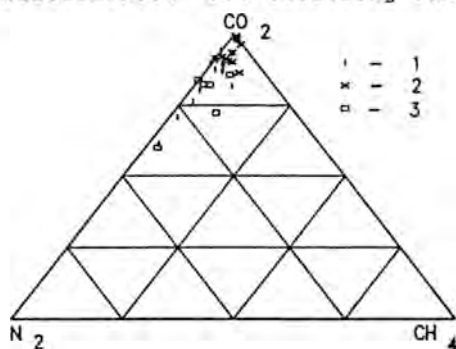
Mykytivka Sb-Hg deposit is localized in an arch of Gorlivska anticline, which is a western part of Main anticline of Donets Basin. The ores are localized in Middle Carboniferous sandstones and argillites of suites $C_2^2-C_2^4$ and make metasomatic beds in sandstones and veins in argillites. The ores of main stage consist of cinnabar, antimonite, arsenopyrite, quartz and dickite. Preore Fe-Mg carbonates with bournonite, sphalerite, Pb-Sb sulfosalts and postore quartz-dickite veinlets are less common.

The ores was formed from CO_2 -saturated heterogeneous water solutions at 200-150 ° C (preore stage), 160-110 ° C (main stage) and from undersaturated by CO_2 homogeneous solutions at 110-80 ° C (postore stage).

There exist three main genetic conceptions of Mykytivka deposit. - The first assumes the connection of ore forming with katagenesis of sedimentary rocks; the second assumes a migration of ore-forming fluids from deep-seated levels with participation of mantle derivatives; the third provides the possibility of supply of mercury with migrating waters from oil-bearing strata of Dniepr-Donets basin.

This work is the first attempt of research of volatile components of fluid inclusions in minerals of Mykytivka's ores as possible genetic indicators. The gases were analyzed by mass spectrometric method. Releasing of gases from inclusions was realized by crushing of specimens in vacuum without heating. Analytical results are adduced as volume ratios, put in standard conditions.

The gases of inclusions in quartz, cinnabar, antimonite and silicificated ore-enclosing sandstones were analyzed.



The analytical results display, that among volatile components carbon dioxide prevails over nitrogen and methane is presented as minor admixture. In some quartz samples ethane was found (up to 1.7%).

The sulphides - both cinnabar and antimonite - show very uniform composition of gases with prevailing CO_2 (86.5-99.3%) and minor N_2 (0-6.9%) and CH_4 (0.7-7.9%) contents.

The quartzes was divided into two groups.

Fig.1. The composition of volatile components of fluid inclusions in minerals of Mykytivka Sb-Hg deposit. 1 - quartz; 2 - cinnabar, antimonite; 3 - silicificated enclosing sandstones.

Synore quartzes show maximum contents of CO₂ (average 92.5%) similarly to sulphides. Preore quartzes differ from synore ones by increased N₂ contents (average 16.9%) and decreased CH₄ (less than 2.5%).

The metasomatites (silicificated sandstones) have volatiles

similar to those in preore quartzes. The gases from inclusions have moderated concentration of CO₂ (60.0-85.6%) and relatively high N₂ (8.0-37.0%). The methane concentration is 0-9.8%.

The data obtained show, that the composition of gases does not corresponds with composition of volatiles of katagenetic fluids (see the paper in this issue) because of very low concentration of methane and may does not correspond with oil waters from the same reason. The conception of migration of ore-forming fluids from deep-seated sources is in a better agreement with data obtained.

THE PARAMETERS OF MIGRATION OF HYDROCARBONS IN LVIV-VOLYN COAL BASIN OF UKRAINE

ZINCHUK I.M., KALYUZHNY V.A., PLATONOVA E.L., & MUROMTSEVA A.O.

Institute of Geology and Geochemistry of Combustible Minerals of National Academy of Sciences, Lviv, Ukraine.

The Devonian and Carboniferous formations of Lviv-Volyn coal basin contain numerous small oil and gas shows, oil and gas seeps at the surface and in boreholes. Macroscopic fractures in limestones and argillites contain numerous calcite and quartz-calcite veins with barite, celestite and anhydrite. These same veins often contain tar and oil filled openings or accumulations of hard bitumen. Five phases of vein forming are established; frequently in samples up to three systems of veinlets are presented. The most frequent vein system is confined to deep faults which are subparallel to main fold structures of region. The calcite veins often contain elongated along L3 quartz crystals up to 16 mm with evidences of skeletal growth. The early zones of crystals are dark red-brown coloured. The late zones are smoky or colourless and form isometric subindivides on dark prismatic quartz.

Both quartz and calcite contain numerous primary and secondary coexisting inclusions of water solution and organic fluid. This fact is an evidence for heterogeneous two-phase state of mineral-forming system; in some samples we found evidences for three-phase heterogeneous state of system, in which water phase coexisted with two liquid organic phases.

The concentration of water solutions in inclusions does not exceed 10-12 wt.%; the presence on minute NaCl crystals in some oil inclusions suggests episodic increasing of concentration of solutions. Microthermometric analyses of oil and water inclusions indicate, that the vein minerals was precipitated at 110-200° C.

The organic inclusions may be divided based on optical characteristics and behaviour during freezing into several types:

Type I. The most abundant type of inclusions, which contains colourless light oil or condensate with blue fluorescence under UV illumination. Often contain droplets of dark brown (bituminous?) substance. May be subdivided into two subtypes:

I-a. The two-phase inclusions L1+G (L1=80-85%) display almost full crystallization of liquid during freezing. During heating homogenize to the liquid at 70-128° C.

I-b. The one-phase inclusions L1 (G) which heterogenize at low temperatures by condensing of liquid or by appearing of gas bubble due to a density of fluid. The liquid phase display partial crystallization; inclusions homogenize at -20 - +18° C.

Type II. The one-phase inclusions with white-blue fluorescence, which heterogenize at low temperature by condensing of liquid or by appearing of gas bubble due to a density of fluid without appearing of crystals. Homogenize at -(60-30)° C. The fluid of these inclusions consist of mixture of light hydrocarbons.

II-b. Essentially methane inclusions without fluorescence. During freezing display crystallization of minute crystal of CO₂, which during heating dissolves in liquid at -(90-75)° C. Homogenization

appears at $-(80-65)^{\circ}$ C. This type of inclusions is rare and is present in quartz veinlets in south-eastern vicinity of region.

Type III. Colourless one or two-phase at room temperature inclusions with blue or rarely light yellow fluorescence, which display the coexistence of two liquids.

III-a. The more abundant type of inclusions, which consist of

two liquids L1+L2. During freezing the small gas bubble appears. The volume ratios of liquids L1 and L2 are very changeable during freezing due to changes of density of phases and redistribution of components among them. After deep cooling the crystallization of one of liquids appears. The gradual melting takes place at $-(120-122)^{\circ}$ C. The partial homogenization L1+L2+G - L1+L2 appears at $-(53-39)^{\circ}$ C, and full homogenization from -26 to $+53^{\circ}$ C in different inclusions. -

III-b. The rare type of inclusions, which are filled at room temperature by the dense fluid, which after cooling is divided to two liquids L1+L2 (L1 = 5%) and then gas bubble appears. The main peculiarity of inclusions behaviour is the existence of L1 in restricted temperature interval from -64 to $+4^{\circ}$ C. Out of this interval L1 is fully dissolved in L2. After cooling lower than -106° C the minute crystal appears in L2.

Type IV. This type of inclusions is relatively rare. The two- or three-phase L3+G; L3+L1+G inclusions contain 10-80 % of dark red-brown or yellow-brown liquid L3 with red-brown fluorescence. In polarized light this substance has a marked birefringence.

The composition of above-mentioned types of inclusions is discussed on the basis of mass-spectrometric analysis.

Two trends of evolution of composition of hydrocarbon systems in inclusions were determined. For veinlets formed on progressive stage of catagenetic processes the evolution from oil-like mixtures to more light essentially methane fluids is typical.

The reverse trend was determined for veins formed on regressive stage of basin history, including veins in zones of deep faults. The hydrocarbon phase of fluid changed its composition in time; migrating fluid lost light components, especially methane being transformed to oil-like mixture. This process was accompanied by destruction of part of components and forming of bitumen-like liquids and solid anthraxolite-type substances at shallow levels.

For some boreholes the temperature of fluid exceeded minimum values, determined by inclusions ($70-100^{\circ}$ C); it decreased during vertical migration by $15-20^{\circ}$ per 100 m with regional geothermal gradient 2° per 100 m. Such discrepancy probably is caused by fast fluid inflow along deep faults from more heated levels.

THE GASES OF INCLUSIONS IN SANDSTONES MINERALS OF DONETS BASIN

ZINCHUK I.M., & VISHTALIUK S.D.

Institute of Geology and Geochemistry of Combustible Minerals of National Academy of Sciences, L'viv, Ukraine

Diagenetic and katagenetic transformation of rocks of coal-bearing series of Donets basin was accompanied by releasing of considerable quality of volatile products, enriched with C, N, S compounds. Owing to this process fluid-rock system was formed. We have found numerous inclusions of heterogeneous methane-water fluids in growth rims of quartz grains in sandstones, as well as in recrystallized clastic grains and newly formed minerals. In this paper we describe a composition of volatiles of such inclusions.

The sandstones were chosen as an object of investigation so far as this essentially quartz rocks remain katagenetic inclusions better, than argillaceous ones. In addition, sandstones have significantly minor sorptive capacity, thus adsorbed gases of various origin exert minimal contamination on gas of inclusions. It must be taken into account, that we obtain the mixed gas from inclusions of various origin and composition during analysis. The inclusions in minerals of cement of sandstones are related with katagenetic processes and partly with later history of rocks, but in detrital grains the relict inclusions, corresponding to processes of forming of magmatic, metamorphic and other source rocks, can remain. Therefore, with the purpose of increasing of informativity of obtained data, we made separate analyses of gases, released from whole rock and from clastic grains of rock. The sand fractions, free from cement minerals, were obtained by means of chemical, mechanical and U-sound disintegration of rocks. Gases was released from inclusions by crushing of specimens in vacuum without heating and analyzed by mass spectrometric method. Analytical results are adduced as volume ratios, put in standard conditions.

Analyses of gases were made for Middle Carboniferous sandstones from Chervonoarmijsky, Donets-Makiivsky, Central and Almas-Marjivsky geologic-industrial districts of Donets basin. The compositions of gases in detrital grains and whole rock are obtained. Within Chervonoarmijsky district all specimens of essentially quartz sandstones with argillaceous, rarely argilloalcalcareous cement were picked out from suites $C_2^5-C_2^6$ in Stahanov coal mine. Clastic quartz fractions had a small admixture of feldspars, apatite, garnet and carbonificated plant detritus. The results of analyses of gas components display wide dispersion of compositions of gas. Even within one stratum of sandstone L₁sl₁ four specimens of sandstone displayed range of CH₄ contents 7,6-50,1 %. On diagram (fig. 1) the compositions are dispersed within wide field being attracted to average composition 50%CA₂+30%CH₄+20%N₂. The lesser dispersion of data was found for detrital fractions of sandstones (fig. 2). There is no correlation among gas composition for whole rock and its detrital fraction.

Considerably lesser dispersion of analytical data was found for Donets-Makiivsky (suite C_2^7) and Almas-Marjivsky districts (suites $C_2^5-C_2^6$). Methane is prevailing component (>65,5 %) and concentrations

of nitrogen and carbon dioxide are low. There is no difference among composition of gases for sandstones and their clastic fractions (fig.1, 2). The sandstones of Central district (suite C₂⁵) have uniform composition of gas components of inclusions. The main component of gas is CH₄; CA₂ content is increased up

to 20-32%, much greater comparing with sandstones of neighbouring districts.

Besides sandstones the gases of inclusions in minerals from veinlets in Carboniferous rocks were analyzed. The specimens were picked out from suites C₂⁵-C₂⁶ along sections of deep boreholes and in Vergelivska coal mine in Almas-Marjivsky district. Calcite and quartz-calcite veinlets in sandstones, rarely in limestones and argillites frequently have an admixture of dickite, sphalerite, galenite, chalcopryrite. Inclusions have very uniform composition of gas components. All compositions are very closely attracted to average composition 3%CA₂+94%CH₄+3%N₂. Only coarse-grained smoky calcite from septarian veinlets in siderite concretion from suite C₂⁵ has high concentration of CO₂ - 17,8%, that is close to sandstones of enclosing series. One can say about evolution trend of gas composition of fluids in the direction to decreasing of relative concentration of CO₂ and N₂ in essentially methane gas.

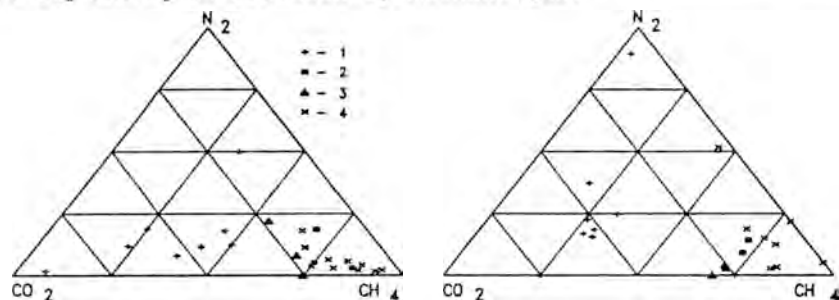


Fig. 1. The composition of gases of fluid inclusions in minerals of sandstones. Geologic-industrial districts: 1 - Chervonoarmijsky; 2 - Donets-Makiivsky; 3 - Central; 4 - Almas-Marjivsky.

Fig. 2. The composition of gases of fluid inclusions in minerals of sand fractions of sandstones.

The results of analyses display, that there are two groups of rocks with different features of gas composition. The first group, to which belong sandstones of Chervonoarmijsky district, is characterized by variable concentrations of main components and by relatively high concentrations of nitrogen and carbon dioxide. The gases of inclusions in clastic fractions of rocks have higher than those in whole rock concentration of carbon dioxide and especially nitrogen that are partly associated with relict prekatagenetic inclusions. On the level of individual samples there was not found correlation among gas composition in whole rock and its clastic part. The second group of rocks to which belong sandstones of Donets-Makiivsky, Central and Almas-Marjivsky districts, is characterized by essentially methane gases of inclusions in minerals and uniform concentrations of minor components. The compositions of gases in clastic part and cement of rocks are practically identical. The differences among this two groups of rocks in our opinion are caused by different level of recrystallization of clastic quartz during katagenesis. The rocks of Central, Donets-Makiivsky and Almas-

Marjivsky districts display high level of recrystallization and regeneration of quartz, close intergrowth of quartz and cementing minerals. Due to this, inclusions characterizing the previous history of quartz are almost completely replaced by katagenetic ones. On the other hand the quartz of sandstones of Chervonoarmijsky district partly remain roundness due to weak regeneration processes; thus relict inclusions was remained.

FLUID INCLUSION STUDIES IN MEXICAN GEOTHERMAL FIELDS: AN UNDERESTIMATED MATTER.

VIGGIANO, J.C. (1)

(1) Esc. de Ing. Civil UMSNH, Ciudad Universitaria, Morelia, Mich, Mexico.

Practical application of fluid inclusion interpreting data in active geothermal fields has been widely emphasized in many papers (Browne, 1990; Hedenquist et al., 1992). Yet this task requires a rather accurate and systematic study with a consequent reliable interpretation in the study field. Fluid inclusions are often formed during mineral growth in hydrothermal systems and are hosted predominantly by quartz crystals but calcite and other minerals also host them less commonly. Therefore the trapped bubbles keep the thermal history of the system which is very useful in planning new exploration and exploitation strategies. The next list is, as far as I can judge the best guide for exploration and exploitation geothermal systems on fluid inclusions.

a) Fluid types and their relation to the processes of boiling and mixing.

b) Compositional variations of chloride fluids.

c) Interpretation of Th data: thermal history.

d) Boiling points constraints on temperature profiles.

The table below displays the advances reached so far in mexican geothermal systems under the above scheme.

Type of interpretation

GEOTHERMAL SYSTEM	a	b	c	d
Cerro Prieto			.	
Los Azufres			.	
Los Humeros			.	
La Primavera			.	
Las Tres Vírgenes *
El Ceboruco *			.	
Araró *	.	.	.	

* Exploration zones.

Sources: CFE's unpublished data.

As seen above, fluid inclusion studies carried out in mexican geothermal systems have been performed unsystematically and of an underestimated way. This means that it remains a fertile field especially in exploitation system in terms of fluid inclusions studies.

References:

Hedenquist, J.W., Reyes. A.G., Simmons, S.F., and Taguchi, S. (1992). The thermal and geochemical structure of geothermal and epithermal systems: A framework for interpreting fluid inclusion data. *Eur. J. Miner.*, 4 989-1015.

P.R.L., Browne (1990) Hydrothermal alteration and geothermal systems. Geothermal Institute, University of Auckland, 86.102.

SHEAR RELATED GOLD MINERALIZATION DURING RETROGRESSION OF THE NILGIRI GRANULITES, SOUTH INDIA.

SRIKANTAPPA, C. (1), LAKSHMEESHA, B. (1), RAITH, M. (2)

(1) Department of Geology, Manasagangotri, University of Mysore 570 006, India.

(2) Institute for Mineralogy and Petrology, University of Bonn, Poppelsdorfer Schloss, 53115 Bonn, Germany.

The late Archaean Nilgiri Granulite (NG) terrain in South India is composed mainly of enderbitic granulites with enclaves of basic granulites, pyroxenites and rare metasediments like kyanite-quartzite and banded magnetite quartzite. Granulite facies metamorphism affected all the lithologies about 2.5 b.y. ago. A regional gradient of near peak metamorphic conditions from 750°C/9-10 Kb in the north to 730°C/ < 7 Kb in southwestern part of the massif has been documented (Raith et al., 1990) which indicates a strong differential uplift of the NG.

The NG is bounded by the E-W trending Moyar Shear Zone (MSZ) in the north and N 60°E trending Bhavani Shear Zone (BSZ) in the south. Field and petrographic information reveal extensive retrogression of the NG along these shear zones at epidote-amphibolite facies conditions (Srikantappa et al., 1988).

Numerous gold-quartz veins occur within the MSZ and towards the western part of the NG. These veins are hosted by retrogressed enderbites and basic granulites viz., hornblende gneiss (qtz+plag+epi+hbl+opaq with relict gt+opx), biotite gneiss (qtz+plag+bio+kfs+opaq+carb+seri with relict gt) and amphibolites (plag+hbl+gt+epi+bio+carb+opaq). The gold-quartz veins trend NE-SW to E-W and intersect the regional foliation of the NG at low angles. They developed within a ductile to brittle regime.

In the NG, gold is associated with the primary sulphide phases pyrrhotite and chalcopyrite in basic granulites. It occurs as disseminated grains as well as invisible gold locked in pyrrhotite. In the retrogressed granulites within the MSZ, pyrrhotite is altered to pyrite and a second generation of chalcopyrite is formed, indicating the increased value of sulphur fugacity.

During the retrogression, pore fluids trapped in the granulites evolved from a near peak metamorphic high density CO₂ fluids (1.15 to 1.08 g/cc) to a late low density CO₂ fluids in the intensely retrogressed rocks (0.88 to 0.86 g/cc) within the MSZ. In the gold-quartz veins, in contrast to the high density CO₂ fluids in the granulites, mixed CO₂-H₂O and low density CO₂ (0.90 to 0.86 g/cc) fluids predominate.

Geochemical data of the retrogressed rocks and their granulite equivalents indicate element mobility with increase in SiO₂, Al₂O₃, FeO, CaO and K/Rb ratio (Srikantappa et al., 1992). Trace elements with geochemical affinity to gold i.e. Cu Zn and Co are enriched where as Cr and Zr are depleted.

Based on structural and petrographic observations, the ore assemblages as well as the chronology and compositional characteristics of fluid inclusions, it is envisaged that the transport and deposition of gold took place during the shear deformation of the NG. The Au mineralization occurred at a late stage (2-3 Kb and 280 to 340°)

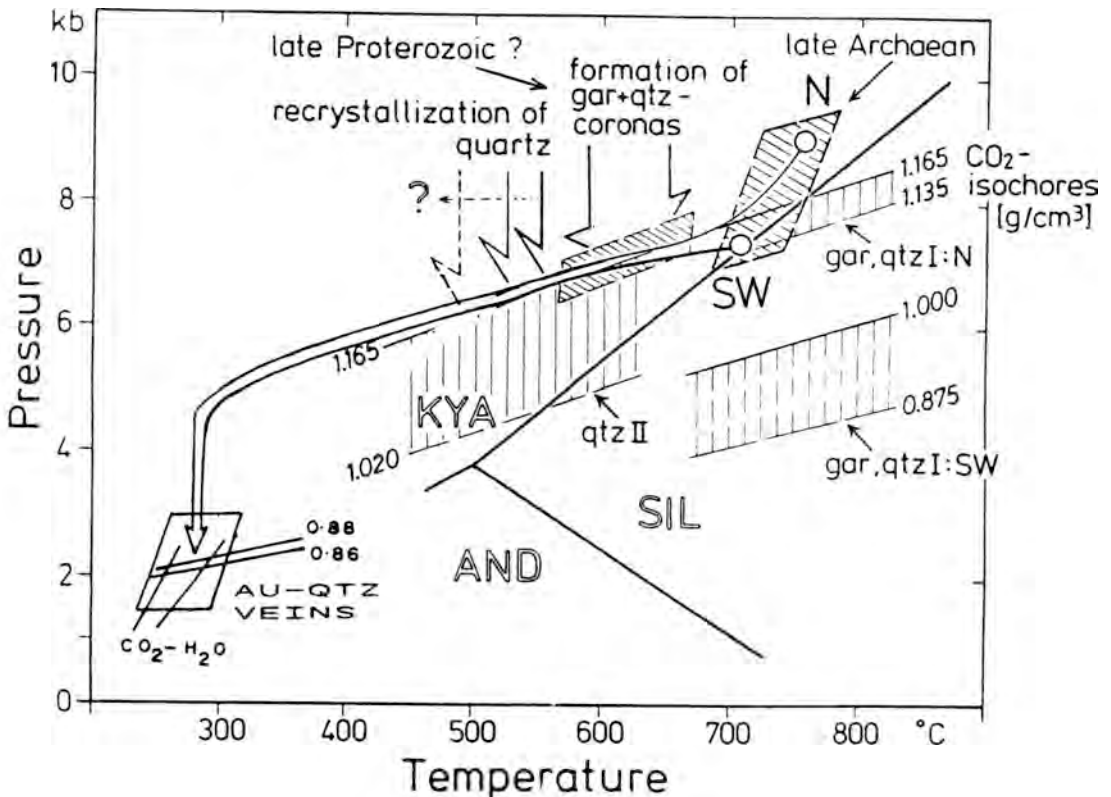
Following the uplift and cooling of the NG along an early IBC subsequent ITD path (Fig.1).

References:

Raith, M., Srikantappa, C., Ashamanjeri, K.G., Spiering, B., 1990. The Granulite terrane of the Nilgiri Hills (Southern India): Characterization of high grad metamorphism. In: Vielzeuf, D. & Vidal, Ph (eds.) Granulite and Crustal Evolution. NATO ASI Ser. C 311, Dordrecht: Kluwer, 339-365.

Srikantappa, C., Prakash Narasimha, K.N., Raith, M. 1988. Retrograde charnockite-gneiss relations in southern India. *J. Geol. Soc. India* 31, 147-148.

Srikantappa, C., Prakash Narasimha, K.N., 1992. The Moyar Shear Zone: A Tectonic suture separating the Archaean Dharwar Craton and the early Proterozoic Niligiri Granulites in South India. Abs. IGCP 304. Lower Crustal Processes, Adirondack Mountains, New York, May 16-22.



THE RELATIONSHIP BETWEEN DIAPIR AND PERIDIAPIRIC ORE DEPOSITS, IN TUNISIA, AS DEDUCED FROM FLUID INCLUSIONS STUDIES.

CHAREF, A. (1) & SHEPPARD, S.M.F. (2)

(1) I.N.R.S.T.B.P. 95-2050 Hammam-Lif- Tunisie.

(2) E.N.S. Lyon Allée d'Italie- 69364 Lyon Cedex 07 - France.

In the North Africa, the triassic series are often in place and not associated to metallic deposits.

Nevertheless, in North Tunisia and East Algeria, the trias outcrop as diapirs. This extrusions materials are gypsum with carbonate, clay, sandstones and automorphic minerals called triassic neoformation minerals (TNM). These salt domes are associated with, economically, peridiapiric ore deposits.

The diapiric sediments are proposed as the main sulphur and Zn-Pb reservoir of Fedj-El-Adoum (FH) and Bou Grine (BG) peridiapiric ore deposits.

To look for the possible relationship between the tunisian diapirs and the peridiapiric mines, we tried to compare the composition, the physical and chemical parameters of trapped fluids both in triassic neoformation minerals and in sphalerite and carbonate hosted minerals of peridiapiric FH and BG ore deposits.

The mineralogical and geochemical results of automorphic minerals studies have permitted one chronological classification of mineral crystallization which is Magnesite-Dolomite 1 (Ca/Mg ~ 1) - Dolomite 2 (Ca/mg > 1) - Quartz and Siderite.

The microthermometric and isotopic results are recapitulated in Table 1.

Table 1: Fluid inclusions results of Triassic Minerals.

Generation	Trapping Mineral	Fluid composition	TH °C	Salinity eq wt %	Origin CO ₂	δD fluid, ‰
I	Magnesite Dolomite 1	NaCl, H ₂ O,CO ₂	280-380	12-23 NaCl	Deep	-27 to -15
II	Dolomite 1 Dolomite 2 Quartz	NaCl, KCl, H ₂ O, CO ₂ , N ₂	120-370	->43% NaCl >38%KCl	Mixing (org.+ Deep)	- 52 to 16
III	Magnesite Dolomite 1 and Dolomite 2 Quartz	NaCl, H ₂ O, CO ₂	50-160	18 - 23 NaCl	Organic	- 80 to - 63

The Table 2 recapitulate the microthermometric and isotopic fluid inclusions results of FH and BG ore deposits.

Table 2: Fluid inclusions results of peridiapiric mineralizations.

Generation	Trapping Mineral	Fluid composition	TH °C	Salinity eq. wt %	Origin CO ₂	δD fluid, ‰
<u>Fedj-El-Adoum</u>						
I	Celstine	NaCl, H ₂ O.	120-280	21-23	Organic	- 45 to
	Calcite	CO ₂ , N ₂		NaCl		- 40
II	Sphalerite	NaCl, H ₂ O.	50-160	13-23	Organic	- 60 to
	Calcite	CO ₂		NaCl		- 58
	Dolomite					
<u>Bou Grine</u>						
I	Sphalerite	NaCl, H ₂ O.	55-230	18-32	Organic	- 75 to
	Calcite	CO ₂		NaCl		- 56
II	Calcite	NaCl, H ₂ O	< 50	< 7		- - 40

The comparison of the physical and chemical characteristics of different fluids (Table 1 and 2) show:

- The I and II generation fluid inclusions (F.I.) of TNM, and the I generation of FH are comparable.
- The III fluid generation of TNM is comparable to the second of F.H. and the first of BG.

In addition

- The TH histograms of secondary TNM fluid inclusions and of II fluid generation of FH and of I generation of BG represent each one three pulsating hydrothermal system.

- The diagrams TH - TM_{ICE} of these last fluid inclusions generations of TNM, FH and BG show that if the TH is relatively high there are one little salinity variation. But when the TH decrease, we remark one wide salinity variation.

These distinctions and these likeness of fluids characteristics between the TNM and Fedj-El-Adoum and Bou Grine minerals permitted to suggest that all Triassic neof ormation minerals have crystallised along the first evolution period of diapirs rising. The late region fracturation (and TNM) have facilitate the mineralization fluids migration by the contact zone diapirs -wall rock. These fluid types are trapping at the same time in the sphalerite (of the ore deposits) and in the late fracture of TNM.

So, the diapir play only an indirect role in the genesis of peridiapiric ore deposits.

THE EVOLUTION OF POLYSALINE FLUIDS DURING THE ORE GENESIS OF THE HYDROTHERMAL DEPOSITS AT AGUILAS-SIERRA ALMAGRERA (SE SPAIN)

MORALES, S. (1,3), QUILEZ, E. (2) & FENOLL HACH-ALÍ, P. (3).

(1) Instituto Andaluz de Ciencias de la Tierra and Departamento de Mineralogía-Petrología. CSIC-Universidad de Granada. Fuentenueva s/n, 18002 Granada, SPAIN.

(2) Centro de CC. Experimentales y Técnicas. Universidad San Pablo-CEU. Boadilla del Monte, Madrid, SPAIN.

(3) Present address: URA n°1366 CNRS, ESEM-EREM, Université d'Orléans, 45072 Orléans Cedex 2, France.

The aim of this work has been to study the fluids involved in the mineralization of the base-metal deposits in the Aguilas region (El Charcón, Ermita de la Cuesta de Gos y Reina del Cielo) and the Sierra Almagrera (El Arteal and El Jaroso). Morales (1994) and Morales et al. (1995) have made a detailed study of the geological setting, the paragenesis and the mineral chemistry of these ore deposits.

This study has been based on a microthermometric analysis of the fluid inclusions in the quartz at Aguilas and in the barite at Sierra Almagrera. In none of the samples studied are the fluid inclusions very abundant; they are of primary nature and randomly distributed. They vary in size from 5µm to 40µm and appear in various geometrical shapes, although their predominant form is more-or-less regularly oval or ellipsoid. At room temperature, the inclusions comprise aqueous liquid and H₂O vapour in the typical two phase forms with a volumetric ratio, Vg/Vt, ranging between 10% and 50%.

On freezing to -100°C the inclusions become dark and opaque and tend to contract, disappearing completely on occasions, compressed by ice. Later we allowed them to return to room temperature and watched the changes in phase which took place (ice first melting, hydrohalite melting and ice last melting crystals) and the temperature at which these occurred (Table 1). The first ice melting occurred between -55°C and < -21°C. The low eutectic temperatures indicate the presence of a polysaline system (NaCl-KCl-MgCl₂-CaCl₂-H₂O) of relatively variable proportions at El Charcón I, El Charcón II, Ermita de la Cuesta de Gos and Reina del Cielo. The exceptions to this are the inclusions with lower temperature of homogenization at El Charcón II, which show eutectic temperatures of around -21°C. The melting point of the hydrohalite is difficult to note due to its similarity to the ice and the small size of fluid inclusions. Nevertheless, all the inclusions have been subjected to progressive cooling cycles (Mashedier et al., 1988), which have allowed the hydrohalite crystals to aggregate and grow sufficiently to observe their melting point; this turns out to be at between -22°C and -33°C. This temperature interval shows that the ratios of NaCl/CaCl₂ vary and are always greater than unity, according to the estimates made on Borisenko's graph (1977). The ice last melting always takes place after the melting of the hydrohalite in a different temperature range (and consequently salinity range) for every outcrops.

Once the samples had returned to room temperature we heated them to see at what temperature they homogenized. This always occurred for the liquid phase and within a wide range of temperatures depending on which outcrops they came from (Table 1).

Our microthermal studies have distinguished four different types of fluid inclusion: in El Charcón we have found two fluids (El Charcón I

and El Charcón II), El Charcón I being higher in temperature, salinity and pressure than El Charcón II. Both fluids are polysaline with different proportions of salts. At El Charcón II we have observed a trend towards lower-temperature NaCl-H₂O compositions, something which is not to be seen at El Charcón I. At Ermita de la Cuesta de Gos (Ermita), on the other hand, there is a polysaline fluid that was generated throughout a wide range of temperatures and salinities, whilst at Reina del Cielo (Reina) there is only one fluid, which is polysaline but very restricted in the variations in its salinity.

In general we can say that two extreme types of fluid exist: on the one hand El Carcón I and Reina del Cielo, with high salinity and on the other El Charcón II, with low salinity. Between these Ermita de la Cuesta de Gos fluid exists. We propose a magmatic origin for the fluids of El Charcón I and Reina del cielo whilst we suggest that the fluids of El Charcón II and Ermita de la Cuesta de Gos derive from a mixture of magmatic and marine/meteoric sources.

The absence of significative hydrothermal alterations between the veins and host rock contacts might be explained by a very fast circulation of fluids through the fractures. Fractures put shallow zones in contact with deeper zones and they establish a hydraulic gradient so that the fluids have not sufficient time to react with the host rocks. The low reactive nature of the host rocks also help to explain this lack of alteration.

This study of fluid inclusions has lead us to the parameters necessary for gauging the thermodynamic conditions (temperature, pH, fO₂, fS₂, fH₂S) under which the transport and precipitation of the metals in question took place, and also the predominance of each species in the fluid (ZnCl₂, CuCl, FeCl₂, PbCl). We propose the cooling of the system and, to a lesser extent, the small fluctuations in salinity as being the principal factors responsible for precipitating the metals.

Table 1. Microthermometric data from freezing/heating study. System: NaCl-KCl-MgCl₂-CaCl₂-H₂O

Phases	Topic	Remarks	CharcónI	CharcónII	Ermita	Reina
L+V	Room Temperature	Start freezing cycle	always biphasic at room temperature			
I+(V)	Freezing	No CO ₂ or CH ₄ vapours				
I+H+L+V	First melting ice	Na, Mg, K...chlorides	-55 to -45	-50 to -30	-55 to -45	-55 to -48
I+L+V	Hydrohalite melting	Changeable ratios of salts	—	-29 to -22	-33 to -22	-32 to -23
L+V	Last melting ice	Different salinity	13 to 19	1 to 5	1 to 19	10 to 19
L+V	Room temperature	Start heating cycle				
L	Stage II homogenization	Always to liquid phase		160 to 310	203 to 402	180 to 320
L	Stage I homogenization	Always to liquid phase	405 to 508			
Salinity			17 to 22	2 to 8	2 to 22	14 to 22
Density			0.9 to 1.1	0.7 to 0.8	0.7 to 1.0	0.9 to 1.0

References

- Borishenko, A. (1977). Soviet Geol. & Geophys. 18, 11-19.
 Mashedor, R. and Rankin, A.H. (1988). Mineral. Magazine, 52, 473-482.
 Morales, S. (1994). Doctoral Thesis. University of Granada. 257p.
 Morales, S., Fenoll Hach-Alfí, P. and Both, R. (1995) Procceding 3th SGA Meeting, Prague (in press).

THE STRATABOUND Zn-Pb-(Ge-F) CERRO DEL TORO ORE DEPOSIT (ALPUJARRIDE CARBONATE FORMATION, BETIC CORDILLERA, SOUTHERN SPAIN): MINERALOGY AND FLUID INCLUSIONS STUDIES.

MORALES, S. (1&2), BARBANSON, L. (2), FENOLL HACH-ALÍ, P. (1), TOURAY, J.C. (2)

(1) Instituto Andaluz de Ciencias de la Tierra and Departamento de Mineralogía-Petrología. CSIC-Universidad de Granada, Fuentenueva s/n, 18002 Granada, SPAIN.

(2) URA n°1366 CNRS, ESEM, Université d'Orléans, 45072 Orléans Cedex 2, FRANCE.

Numerous strata-bound F-Pb-Zn-(Ba) ore deposits occur within the Alpujarride Carbonate Formation of the Betic Cordillera, Southern Spain (Fenoll Hach-Alí, 1987; Martín et al., 1987). They are linked to defined stratigraphic positions within the Anisian and at the Ladinian/Carnian transition. They occur at the transition from predominant terrigenous-continental and/or coastal-sedimentation to marine carbonate sedimentation (Anisian ore deposits) and, viceversa (Ladinian/Carnian ore deposits). The geostructural history of the area during Alpine orogeny was complex. Apparently most of the ore deposits are older than deformation and the associated polyphase metamorphism (Martín et al., 1987). During a general reappraisal of ore deposits from the Alpujarrides, special attention has been given to the sulphide-rich and fluorite-poor deposits of Cerro del Toro. The Cerro del Toro mine is hosted by lagoonal fine-grained dolomites from the Alpujarride Carbonate Formation (Anisian), (Higueras et al., 1981). It was mined by the SMMP from 1975 to 1979 for Zn (production: 250.000 tonnes, 5-6% of the ore) and it is presently closed.

Mineralogy

The mineralogical study was carried out using optical microscopy, SEM+EDS and Electron Microprobe. Mineral assemblages found in the Cerro del Toro ores contain dominant sphalerite, with galena, pyrite, chalcopyrite, fahlore, Ge-bearing sulphides, dolomite, fluorite and chlorite. Sphalerite occurs as massive aggregates (up to 2 cm), coloured red to dark brown, or yellow. The composition of sphalerite does not change with colour: Fe= 0.21-0.64% at. and no trace elements were detected by electron microprobe analysis. Galena is also massive and intergrown with sphalerite or fahlore. Microprobe analyses reveal only small amount of Bi (0.00-0.41% at.) Pyrite and Chalcopyrite occur as small grains disseminated into sphalerite or galena. Fahlore was found with galena or as small crystals disseminated into sphalerite. No compositional differences has been observed between both varieties is close to the Zn-Fe-bearing tenantite end-member* (As= 3.81-3.94; Sb= 0.02-0.11; As/As+Sb= 0.97-0.99; Cu= 9.78-10.04; Zn= 1.05-1.44; Fe= 0.60-1.08; Ag= 0.00-0.41). Briartite is the dominant Ge-bearing mineral, and occasionally Renierite is also found. Microprobe analyses of briartite show a wide range of composition* (S= 3.72-4.07; Cu= 1.30-2.11; Ge= 0.27-1.10; Zn 0.67-2.19; Fe= 0.15-0.83). EDS images show variable compositions within crystals, the cores having higher Ge and Zn contents (and lower Cu and Fe) than the rims. Dolomite occurs as massive aggregates in relation with sulphides and sometimes displays rhombohedral morphology. Fluorite is scarce, massive and

light coloured. Fibrous Chlorite is intergrown with dolomite or sphalerite. It belongs to the chamosite-clinoclone type' (Si=5.28-5.69; Al^{IV}= 2.31-2.72; Al^{VI}= 2.00-2.66; Mg= 9.16-9.64).

Fluid inclusions

Microthermometric analyses of fluid inclusions were carried out on sphalerite. They were performed in doubly polished wafers by optical microthermometry using a Chaimeca heating/freezing stage. Most of the studied fluid inclusions are primary (isolated inclusions, random disseminations or outlining growth zones in sphalerite). Some flat large sized inclusions could be representative of healed cleavages. Abundant small sized secondary fluid inclusions are present but they could not be studied because of elevated refraction index of sphalerite. Fluid inclusions have a maximum size of 30µm. They are often negative crystal-shaped or spheroidal. At 25°C, they have two phases (dominant liquid and gas) with minor trapped solids (sulphides?) occurring occasionally. Filling coefficients are 0.8 to 0.9. From microcryoscopic data, inclusion fluids can be dispatched within two types: (1) H₂O-CO₂-(CH₄?) -NaCl and (2) H₂O-NaCl-CaCl₂.

(1) H₂O-CO₂-(CH₄?) -NaCl: Fluid inclusions are two-phase at room temperature (CO₂ gas+ aqueous liquid). During freezing runs, a phase transition is firstly noticed (CO₂ gas + liquid CO₂ + aqueous solution) at about +10°C. At lower temperatures, three other transitions are characteristics of this type of inclusions: (a) between -30 and -40°C, a volume reduction with deformation of the gaseous fraction due to clathrate formation, (b) between -50 and -65°C, a reduction of the gas bubble due to ice formation, and (c) between -100 and -115°C, a overgrowth of small crystals on bubbles (with major concentration at the interface gas-ice); sometime the bubble is divided in two parts: a bright-yellow one (solid CO₂) and a dark-grey part (gas CO₂); on reheating, these small crystals join to from larger ones, permitting good observations of CO₂ melting, at temperatures ranging from -60.1 to -57.7°C. Eutectic temperatures (-22± 1°C) fall close to the eutectic for the NaCl-H₂O system. Final ice melting temperatures range from -12.9 to -5.0°C. At higher temperatures, a progressive melting of clathrates is noticed. Melting of the last crystal of clathrate is very difficult to see, but characteristic strong movements and sudden morphological changes of the bubbles can be recognized. The melting of the last clathrate crystal scatters between +7.7 and +9.9°C. Some tenth of degree later, inclusions become three-phase. The CO₂-rich phase homogenizes to vapour with Th CO₂ ranging between +11.2 and +12.9°C. Characteristics for the H₂O-CO₂-(CH₄?) -NaCl fluid calculated from freezing data are as following: salinity (using equation from Collins, 1979): 0.5 to 4.5 wt. % NaCl; estimated "equivalent" CH₄/CO₂: 0.18 to 0.43 (Heyen et al., 1982), density of the gas phase: 0.15 gr/cm³. Raman microprobe investigations are currently in progress for improvement of these data.

(2) H₂O-NaCl-CaCl₂: Fluid inclusions belonging to this family are two-phase at room temperature. During freezing runs, only a reduction of the bubble size is observed between -80 and -110°C. Thus, no significant volatile amounts are supposed present within this type of fluid inclusions. The low eutectic temperatures (between -55 to -49°C) indicate the presence of CaCl₂, and possibly MgCl₂. Hydrohalite melting was observed -40 and -33°C, probably under metastable conditions. Melting of the last crystal of ice ranges from -24.9 to -11.0°C, corresponding to an equivalent salinity between 15.0 and 25.9 wt% NaCl.

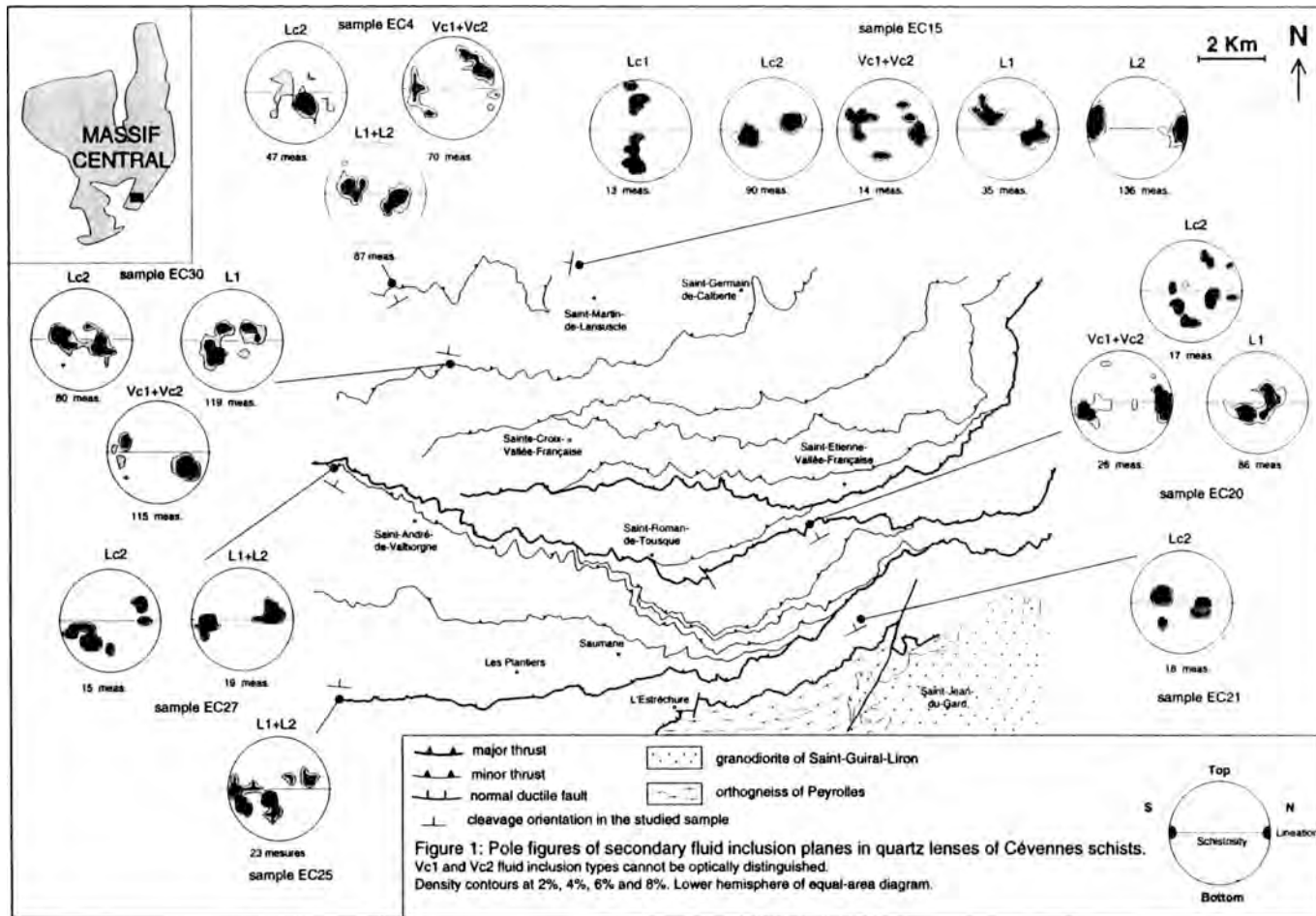
Concluding remarks

At a regional scale, Cerro del Toro is the first occurrence of germanium minerals described within stratabound F-Pb-Zn(Ba) deposits of Betic Cordillera. Ge occurs within small crystals of Ge-bearing sulphides (briartite and minor renierite) disseminated in sphalerite. At local scale, apparently, two "incompatible" ore forming solutions have been characterized. One is comparable to MVT-forming brines with elevated CaCl_2 (or MgCl_2) while the other is Ca^{2+} poor; in addition the former does not contain any detectable CO_2 in contrast with the latter.

The exact nature of the chronological and genetic relationships between these "incompatible" solutions remains to define. Both, apparently, are found within primary cavities. The refilling by late CO_2 -rich solutions of a part of a population of cavities initially containing "MVT brines" is a possible explanation.

Bibliography:

- Collins, P. (1979). *Econ. Geol.*, 74, 1435-1444.
Fenoll Hach-Alí, P. (1987). "Los yacimientos de F-Pb-Zn-Ba del Sector Central de la Cordillera Bética". Universidad de Granada 127 pp. ISBN:84-338-0689-0.
Heyen, G., Ramboz, C. and Dubessy, A. (1982). *C.R. Acad. Sci. Paris*, 294, 203-206.
Higuera, P., Fenoll Hach-Alí, P. and Rodríguez Gordillo, J. (1981). *Tecniterrae*, VII, 44, 65-76.
Martín, J., Torres-Ruiz, J. and Fontboté, L. (1987). *Mineralium Deposita*, 22, 216-226.



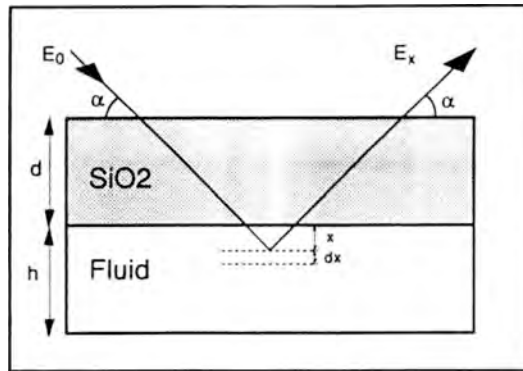


Figure 1. Simplified geometry used to calculate absorption in XRF-measurements

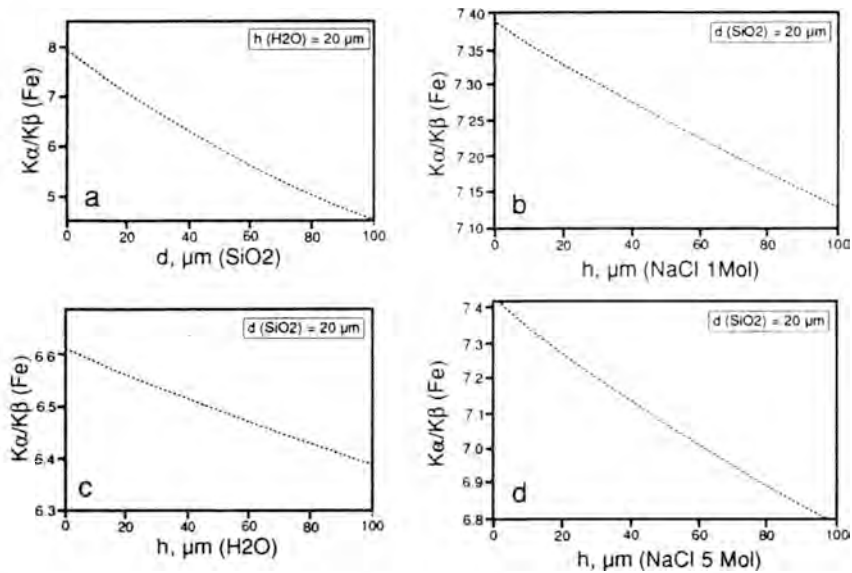


Figure 2. Variations of $K\alpha/K\beta$ (Fe) as a function of quartz-wall thickness (a) and fluid inclusion thickness and salinity (b, c & d).

Autor Index

- AISSA, M. 1
ALDERTON, D. 50
ALFONSO, P. 4
ALLERTON, S. 41
ALTHAUS, E. 104
ANDERSEN, T. 7
APPEL, P. 99
ARCOS, D. 8
ARNAUD, F. 10
AYT OUGOUGDAL, M. 13,34
AYORA, C. 11,86
BAGATAJEV, R.M. 279
BAKKER, R.J. 15,66
BANERJEE, A.18,235
BANKS, D. 13,20,22,28,34,
137,235
BARAKAT, A. 22
BARASHLOV, Y. 242
BARBANSON, L. 73,294
BEHR, H.J. 97
BENLD, J. 270
BENCHEKROUN, F. 24
BENY, C. 1,43
BIINO, G. 196
BJERG, E.A. 256
BLENKINSOP, T. 158,222,224
BODNAR, R. 26,240,265
BOIRON, M.C.13,22,28,34,68,
78,84,164,198,228
BOULLIER, A.M. 10,78
BRIL, H. 118
BROWN, P.E. 30,32
BURG, J.P. 10
BURKE, E.A.J. 7,80
CANALS, A. 252
CANALS, M. 22
CARDELLACH, E. 252
CAROSI, R. 88
CATHELINEAU, M. 13,22,34,52
62,135,164,198
CHAREF, A. 290
CHAROY, B. 186
CHEILLETZ, A. 20,277
CHELIOTIS, Y. 160
CHEPUROV, A.I. 244
CHENERY, S.R. 144,234
CHEVALIER, P. 183
CHLUPAC, T. 267
CHOI, C.G. 70
CHUPIN, V.P. 36,38,39,114
CHUPIN, S.V. 36
CLINE, J.S. 41
COELHO, C.E.S. 43
COETZEE, D.S. 46,48
COLES, B. 269
CORDON, S. 93
COX, W. 50
CRISPINI, L. 52
CUNNEY, M. 200
CZERWOSZ, E. 235
DELGADO, J. 8
DE VIVO, B. 54
DIAMOND, L. 56, 178
DIDUSZKO, 235
DOBES, P. 58,60
DORIA, A. 62,164
DOUMBIA, S. 64
DUBESSY, J. 28,58,60,66
DURAND, C. 93
DURISOVA, J. 22,68
EDON, M. 70
ELIOPOULOS, D. 160
ENACIRI, A. 72
FANLO, I. 76
FEELY, M. 166
FENOLL HACH-ALI, P.292,294
FERNANDEZ-NIETO, C. 76
FERREIRA, A. 149
FIRDAOUS, K. 78
FOGACA, A.C.C. 210
FRANTZ, J. 66
FREI, R. 181
FREZZOTTI, M.L. 52,80,88
FUERTES, M. 82
FUZIKAWA, K. 210,220
GAGNY, C. 64
GALLAGHER, V. 166
GARCIA, E. 84
GARCIA-IGLESIAS, J. 142,172
GARCIA-VEIGAS, J. 11,86
GEERTSEN, C. 28
GHAZBAN, F. 147
GHEZZO, C. 80
GIANELLI, G. 212
GIBERT, F. 183
GIORGETTI, G.88, 133
GIRARD, J.P. 116
GIULIANI, G. 20,210,277
GLEESON, S. 90,269
GOMEZ, G.M. 123
GOMEZ-FERNANDEZ, 131
GRANTHAM, G.H. 254
GREGORY, D.A. 258
GRISHINA, S. 91,188
GUILHAMOU, N. 93
GUMIEL, P. 95
HAGEMANN, S.G. 30,32
HÉBERT, R. 95
HEIN, U.F. 97
HERMS, P. 99
HOFSTRA, A.H. 41
HOTH, P. 205
HURAI, V. 101,102,108
HURAIIOVA, M. 102,108
IDIZ, E.F. 205,226
ISABELLE, D. 70

ISTRATE, G. 104
 KALBSKOPF, S. 46
 KALYUZHNY, V.A. 281
 KAMENSKY, I.L. 181
 KEPPENS, E. 151
 KEPPLER, H. 121
 KNIPPING, B.J. 91
 KODERA, P. 106
 KONECNY, P. 102,108
 KOTKOVA, J. 60
 KOVALEVICH, V.M. 110,112,176
 KOVYAZIN, S.V. 246
 KOZLOWSKI, A. 235
 KRAMERS, J.D. 181
 KUZMIN, D. 38,114
 LABUDIA, C.H. 256
 LACOUR, J.L. 28
 LAKSHMEESHA, B. 288
 LANDIS, G.P. 41
 LATTANZI, P. 130
 LEGENDRE, O. 116
 LEHNER, C. 226
 LENG, M.L. 160
 LEOST, I. 118
 LESPINASSE, M. 34
 LIMA, A. 54
 LINNEN, R. 121
 LIRA, R. 123
 LOPEZ-GARCIA, J.A. 84,135,
 164,198
 LOREDO, J. 142,172
 LU, Ch. 125
 LUDERS, V. 128,205
 LUGLI, S. 86
 LUNAR, R. 170
 MAINERI, C. 130
 MANGAS, J. 82,131
 MARCOS, C. 194
 MARESCOTTI, P. 133
 MARIIGNAC, Ch. 64,228
 MARTIN-IZAR, A. 82
 MARTIN-ROMERA, C. 135
 MARTINEZ, E. 123
 MAUCHIEN, P. 28
 MAZUROV, M. 188
 MECCHERI, M. 88
 MEERE, P. 137
 MELFOS, V. 139,261
 MELGAREJO, J.C. 4
 MESA, M. 142
 MISRA, K.C. 125
 MOINE, B. 24,200
 MOISSETTE, A. 28,144,234
 MÖLLER, A. 99
 MOORE, S.L.O. 145
 MORALES, S. 198,292,294
 MORITZ, R. 147
 MOSSMANN, J.R. 118,203
 MOURA, A.J. 149
 MUCHEZ, Ph. 151
 MULLIS, J. 153
 MUNOZ, M. 154
 MUROMTSEVA, A.O. 281
 MURPHY, P. 156
 MUTEMERI, N. 158
 NADEN, J. 160
 NESBITT, R.W. 154
 NOGUEIRA, P.M. 62,162
 NORONHA, F. 62,149,162,164
 OBERTHÜR, T. 222,224
 O'REILLY, C. 166
 ORPHANDIS, I. 168
 ORTEGA, L. 170
 ORTI, F. 11,86
 OUDIN, E. 168
 OYARZUN, R. 170
 PANIAGUA, A. 172,194
 PANINA, L. 174
 PANKOV, V. 242
 PASCAL, M.L. 1,168
 PENNACCHIONI, G. 216
 PEÑA, A. 263
 PERTOLD, Z. 68,270
 PERTOLDOVA, J. 270
 PERYT, T.M. 110
 PESQUERA, A. 263
 PETROV, P.P. 178
 PETRICHENKO, O.Y. 112,176
 PETTKE, T. 178,181
 PFLUGBEIL, B. 128
 PHILIPPOT, P. 183,216
 PICCARDO, G.B. 218
 PIMENTA, M. 210,220
 PINTEA, I. 184
 PINTO-COELHO, C. 186
 PIRONON, J. 13,188
 PLATONOVA, E.L. 281
 POLVE, M. 154
 POTY, B. 34
 POULSEN, T. 190
 POUTAINEN, M. 192
 PRIETO, J.L. 28
 PRIETO, M. 194
 PROSPERT, C. 196
 PUDILOVA, M. 270
 QUILLEZ, E. 198,292
 RAITH, M. 288
 RAKOTONDRAZAFY, M. 200
 RAMAMBAZAFY, A. 200
 RAMBOZ, C. 1,43,70,118,
 168,203
 RANKIN, A.H. 50,178,200
 RENAC, Ch. 203
 REUTEL, Ch. 205,267
 RHEDE, D. 207
 RIOS, F.J. 220

ROBBIANO, A. 218
 ROBERT, F. 78
 ROBERTS, S. 95,156
 ROBERTS, S.M. 239
 ROEDDER, E. 209
 RONCHI, L.H. 186,210
 ROSELL, L. 11,86
 ROUCHY, J.M. 86
 RUEDA, F. 20
 RUGGIERI, G. 212
 RYAN, C. 214
 SANDERSON, D.J. 95
 SAWATZKI, J. 226
 SCAMBELLURI, M. 216,218
 SCHALAMUK, I.A. 220
 SCHENK, V. 99
 SCHILD, M. 267
 SCHOTTLER, T. 97
 SCHMIDT-MUMM, A. 222,224,
 226,261
 SEMIANI, A. 228
 SHARYNGIN, V.V. 230,232
 SHEBANIN, A.P. 244
 SHEPHERD, T.J. 144,234
 SHEPPARD, S.M.F. 290
 SIEGESMUND, S. 267
 SIERRA, J. 170
 SIMON, K. 101,108
 SLABY, E. 235
 SLOBODNIK, M. 151
 SMIRNOV, S.Z. 38
 SMITH, M. 237
 SOLDEVILA, J. 95
 SOLER, A. 8
 SOMMER, F. 93
 SPENCER, R. 145,239
 SRIKANTAPPA, C. 288
 STERNER, M. 121
 STOPPA, F. 232
 STRNAD, L. 68
 SVOREN, J.M. 279
 SZABÓ, C. 240
 TALNIKOVA, S. 242
 THISSE, Y. 168
 THOMAS, R. 207,274
 TITOV, A.V. 38,114
 TOLSTIKHIN, I.N. 181
 TOMILENKO, A.A. 39,244,246
 TOROK, K. 54,248
 TORNOS, F. 263
 TOURAY, J.C. 73,294
 TOURET, J. 88,158,250
 TRITLLA, J. 252
 VAN DER KERKHOFF, A.M.48,254
 VARELA, M.E. 256,258
 VAVEDELIS, M. 139,258
 VELASCO, F. 263
 VIAENE, W.A. 151
 VIGGIANO, J.C. 286
 VILLA, I.M. 181
 VINDEL, E. 84,135,164,198
 VISHTALIUK, S.D. 279,283
 VITYK, M. 265
 VOLFINGER, M. 70
 VOLLBRECHT, A. 267
 WILKINSON, J. 90,269,270
 WEIB, T. 267
 WEISER, T. 224
 YANG, W. 239
 YARDLEY, B.W.D. 13
 ZACHARIAS, J. 270
 ZAW, K. 272
 ZHANG, Y. 66
 ZIEMANN, M. 274
 ZIMMERMANN, H. 275,276
 ZIMMERMANN, J.L. 277
 ZINCHUK, I.M. 279,281,283

Instrucciones a los Autores para la presentación de manuscritos

El Boletín de la Sociedad Española de Mineralogía publica trabajos originales, revisión de artículos y notas cortas relacionadas con mineralogía, petrología, geoquímica, cristalografía, yacimientos minerales y mineralogía aplicada.

Los manuscritos deberán estar escritos en español o en inglés.

De cada manuscrito (texto y figuras) se enviarán **Tres Copias** a la Dirección del Comité de Redacción. Dos copias serán revisadas por especialistas elegidos por el Comité Editorial, y sólo se publicaran los manuscritos que hayan sido informados favorablemente.

Cada manuscrito deberá estar preparado según las siguientes normas. Si no se cumplen le será devuelto a los autores.

I- Trabajos originales y revisión de artículos

- 1./ Planificación
- 2./ Título
- 3./ Título abreviado
- 4./ Nombre(s) de autor(es) y nombre(s) y dirección(es) de la(s) institución(es)
- 5./ Resumen - Abstract
- 6./ Palabras Clave - Key Words
- 7./ Texto
- 8./ Referencias
- 9./ Tablas
- 10./ Figuras
- 11./ Leyenda de Tablas y Leyenda de Figuras

Si el manuscrito no está escrito en español, el título y las leyendas de tablas y figuras deberán estar también traducidas al español.

1./ Planificación

El plan indica el orden de los diferentes apartados del manuscrito. No sera publicado.

2./ Título

Deberá ser conciso, preciso y con palabras que reflejen el contenido del trabajo

3./ Título abreviado

No contendrá más de 60 caracteres, con objeto de poderlo imprimir en la parte superior de cada página impar del Boletín.

4./ Nombre(s) de autor(es)

Deberá incluirse el primer nombre completo y la inicial del segundo (si es compuesto) y los apellidos de cada autor, así como la dirección(es) completa(s) del Centro de trabajo de cada uno. Cualquier correspondencia se dirigirá al primer autor si no existen indicaciones en contra.

5./ Resumen - Abstract

Ambos deberán presentar los resultados principales del trabajo, con datos cuantitativos. Extensión máxima de 150-200 palabras.

6./ Palabras clave - Key Words

A continuación del Resumen y del Abstract se añadirán ocho palabras, como máximo, que caractericen el contenido, las técnicas y los resultados. Siempre que sea posible se elegirán de las contenidas en el Index publicado en cooperación con las Sociedades Mineralógicas Europeas o en el "Multilingual Thesaurus of Geosciences", Ed. Pergamon.

7./ Texto

- Deberá ser claro y conciso, con una extensión total que no exceda de las 15 páginas mecanografiadas a doble espacio en tamaño DIN A4, incluyendo referencias, tablas y figuras.

- Las referencias en el texto deberán aparecer como sigue:

(Arribas, 1978; Fontboté & Amstutz, 1981)

o

según Arribas (1978) y Fontboté & Amstutz (1981)

o, si son más de dos autores:

(Velasco et al., 1988)

Si en la lista de referencias hay varias para un mismo autor con el mismo año de publicación, deberán distinguirse entre sí añadiéndole una letra tal como se indica:

(Puga 1987a; Brindley & Robinson, 1947a y b)

Los nombres de los autores de las referencias se escriban siempre con minúsculas.

- Las figuras (independientemente de que sean gráficos o fotos) y las tablas se numerarán separadamente, usando números arábigos, así:

(Fig. 3) (Tabla 2)

- Para obtener palabras impresas :

. en *itálica*, deberán ir así: *itálica*

. en **negrita**, deberán ir así: **negrita**.

- Para facilitar los trabajos de impresión se aconseja que los autores envíen una copia del texto (una vez aprobado por el Comité de Redacción) registrada en disquete, en lenguaje Wordperfect o Word para compatibles PC.

8./ Referencias

Las referencias deberán presentarse en un listado final ordenado alfabéticamente tal como sigue:

Bliss, N.W. & MacLean, W.H. (1975): The paragenesis of zoned chromite from central Manitoba. *Geochim. Cosmochim. Acta* 39, 973-990.

Frenzel, G., Ottemann, J., Kurtze, W. (1973): Über Cu-haltigen Bleiglanz und Pb-haltigen Covellin von Boarezzo (Varese) und ihre Sulfidparagenese. *Schweiz. Mineral. Petrog. Mitt.* 53, 217-229.

Guinier, A. (1956): *Théorie et technique de la radiocristallographie*. Dunod ed., Paris, 736 p

McLaren, A.C. (1974): Transmission electron microscopy of the feldspars. in "The Feldspars", W.S. MacKenzie and J. Zussman, eds. Manchester University Press, 379-423.

- Spry, P.G. (1978): The geochemistry of garnet-rich lithologies associated with the Broken Hill Orebody, N.S.W., Australia. M.S. Thesis, Univ. Adelaide, Adelaide, Australia.
- ____ & Scott, S.D. (1986a): The stability of zincian spinels in sulfide systems and their potencial as exploration guides for metamorphosed massive sulfide deposits. *Econ. Geol.* **81**, 1446-1463.
- ____ & ____ (1986b): Zincian spinel and staurolite as guides to ore in the Appalachians and Scandinavian Caledonides. *Can. Mineral.* **24**, 147-163

9./Tablas

Todas las tablas se reproducirán reduciendo un 50% y por tanto deberán estar escritas con especial cuidado y nitidez.

Se sugiere un espaciado de uno y medio y un número limitado de líneas horizontales o verticales. Si hay demasiados espacios desaprovechados se devolverán a los autores para su reimpresión.

La anchura de las tablas será de 13,5 cm (para reducir a una columna) o de 28 cm (para reducir a dos columnas).

10./ Figuras

- El tamaño máximo de los originales será de 21 x 29,7 cm. En ellos deberá figurar, escrito a lápiz en la parte posterior, el nombre del autor y el número de orden.

- Dibujos y gráficos: han de ser originales, preferiblemente delineados sobre papel blanco o vegetal, con grosor de líneas y tamaño de letras adecuados para ser legibles una vez reducidos; así, en una figura de 13,5 cm de ancho (para reducir a una columna) las letras deberán ser de 5 mm.

- Fotografías: **4 máximo**. Deberán tener un buen contraste y la escala irá incluida en cada una de ellas. Si las fotos están agrupadas en una lámina, se enviarán también un duplicado de las fotos separadas.

11./ Leyendas

Todas las figuras y tablas llevarán una leyenda suficientemente explicativa. Dichas leyendas se escribirán en una hoja aparte.

II - Notas cortas

El Boletín de la Sociedad Española de Mineralogía podrá publicar también los resultados más importantes de un trabajo en forma condensada; la totalidad de los resultados podrán ser presentados posteriormente en un trabajo más extenso.

Dichas notas deberán presentarse como los artículos pero serán más cortas: con un pequeño abstract, un texto de 1000 a 1500 palabras y no más de dos tablas o figuras.

La decisión para su publicación la dará la dirección del Boletín o un miembro de la Comisión Editorial.

Los manuscritos originales y las ilustraciones se destruirán dos meses después de su publicación.

SOCIEDAD ESPAÑOLA DE MINERALOGIA

C/ Alenza, 1 (D-201), 28003-MADRID.

Tfno.: (91) 441.71.38 (L, Mi, de 18h a 21h)

Ficha de Inscripción

Nombre Apellidos

Domicilio, Código Postal

Fecha y Lugar de Nacimiento

Teléfono part.: Teléfono trabajo: Profesión

Fax: Correo Electrónico

Dirección del Centro de Trabajo, Código Postal

Tipo de socio (marcar con una X): ordinario ; estudiante ; colectivo ; protector ; vitalicio ;
Interesado en los siguientes temas: Cristalografía ; Mineralogía ; Petrología ; Geoquímica ; Yacimientos ;
Inclusiones Fluídas ; Coleccionismo ; Otros

Firmas de 2 socios avalistas

Fdo.:

Fdo.:

Cuotas vigentes para el año 1995

Socio ordinario	6.000 Ptas.	Socio estudiante	3.000 Ptas. (adjuntar documento acreditativo)
Socio Protector	25.000 Ptas.	Socio Colectivo	12.000 Ptas. (Empresas, Bibliotecas, etc.)
Socio Vitalicio	80.000 Ptas.	Honorario:	Exento

La cuota del año de ingreso debe abonarse en metálico, mediante cheque o transferencia bancaria a nombre de la Sociedad Española de Mineralogía. Las de años sucesivos se efectuarán por domiciliación bancaria, cumplimentando estos datos:

X

Sr. Tesorero de la Sociedad Española de Mineralogía
Alenza 1, Despacho 201, 28003 MADRID

Muy Sr. mío:

Le ruego tramite el cobro de las cuotas anuales de la Sociedad Española de Mineralogía, con cargo a la cuenta que poseo en la entidad:

BANCO/CAJA DE AHORROS Código

Sucursal/Agencia Código Población

Número de cuenta (20 dígitos)

Domicilio entidad

Atentamente,

Firma

Nombre y Domicilio

X

Sr. Director del Banco/Caja de Ahorros

Sucursal y dirección

Muy Sr. mío:

Le ruego atienda el cobro de las cuotas anuales de la Sociedad Española de Mineralogía, con cargo a la cuenta que poseo en esa entidad.

Atentamente,

Firma

Firmado: Sr. D.

Domicilio:

Nº Cuenta completo (20 dígitos)